SYNTHETIC AND STRUCTURAL INVESTIGATIONS ON SCHIFF BASE COMPLEXES OF IRON AND VANADIUM

A THESIS SUBMITTED TO ASSAM UNIVERSITY, SILCHAR

IN PARTIAL FULFILMENT OF THE REQUIREMENT FOR THE DEGREE OF

DOCTOR OF PHILOSOPHY IN CHEMISTRY

BY

PANKAJ GOSWAMI

(Ph.D. Registration Number. Ph.D./120/2002 dt. 26.11.2002)

DEPARTMENT OF CHEMISTRY

SCHOOL OF PHYSICAL SCIENCES

ASSAM UNIVERSITY

SILCHAR-788011, INDIA

2010

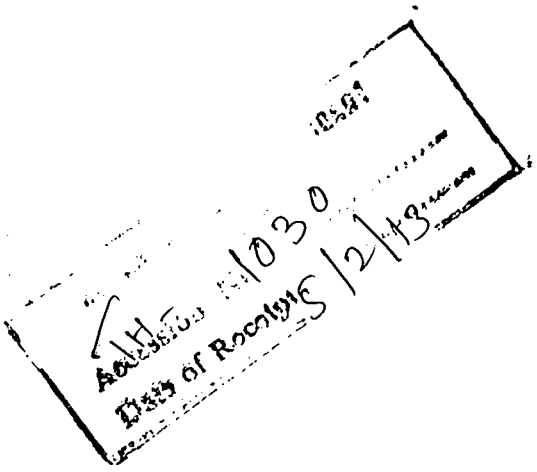

Dedicated

to

my father

Late Prabhat Ranjan Goswami

असम विश्वविद्यालय
(संसद के अधिनियम तेरह वर्ष 1989 के अन्तर्गत स्थापित एक केन्द्रीय विश्वविद्यालय)
शिलचर - असम, भारत
ASSAM UNIVERSITY, SILCHAR
(A CENTRAL UNIVERSITY CONSTITUTED UNDER ACT XIII OF 1989)
Silchar - 788 011, Assam, India

Dr. Chira R Bhattacharjee
Email: crbhattacharjee@rediffmail.com

15th May, 2010

CERTIFICATE

Certified that the thesis entitled "**Synthetic and structural investigations on Schiff base complexes of iron and vanadium**" submitted by **Pankaj Goswami** for award of the Degree of **Doctor of Philosophy in Chemistry** is a bonafide research work. This work has not been submitted previously for any other degree of this or any other university. It is further certified that the candidate has complied with all the formalities as per requirements of the Assam University. I recommend that the thesis may be placed before the examiners for consideration of award of the degree of this university.

Dr. Chira R Bhattacharjee
Supervisor
Department of Chemistry
Assam University

DECLARATION

I, **Pankaj Goswami** bearing Registration Number **Ph.D./120/2002** dated **26.11.2002** hereby declare that the thesis entitled "**Synthetic and structural investigations on Schiff base complexes of iron and vanadium**" is the record of work done by me and that the contents of this thesis did not form the basis for award of any degree to me or to anybody else to the best of my knowledge. The thesis has not been submitted to any other university / Institute.

The thesis is being submitted to Assam University for the degree of Doctor of Philosophy in Chemistry.

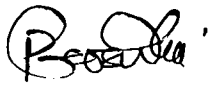

Place: Silchar
Date: 15-05-2010

Pankaj Goswami

ACKNOWLEDGEMENT

With a deep sense of gratitude, I express my indebtedness to my esteemed Supervisor Dr. Chira R Bhattacharjee, Department of Chemistry, Assam University, Silchar under whose guidance this thesis has been prepared. His constructive suggestions and healthy criticisms was a continuous source of inspirations to me during the entire course of the work.

I am grateful to Prof. N. V. S. Rao, Head of the Department of Chemistry, for his invaluable advice. I am thankful to Prof. M. R. Islam for his many words of encouragement. I would like to render my sincere thanks to Dr. S.B. Paul for his valuable support and generous help. My heartfelt thanks goes to Dr. P.C. Paul, Dr. Sk. Jasimuddin and Dr. D. Sengupta, Dr. H. Acharya and Dr. S. Ghosh for encouragement.

My sincere thanks goes to Dr. P. Mondal and Dr. M.K. Pal for their extensive cooperatation in carrying out DFT and POM studies.

With great demureness, I express my gratitude to Dr. Mahuya Sengupta, Department of Biotechnology, Assam University for her valuable guidance in carrying out antimicrobial screening of the synthesised compounds.

I am thankful to Prof Debajyoti Biswas, Dean of the School of Physical Sciences, Assam University for his sustained support in my work.

I also take this opportunity of thanking Gobinda Das, Sankar Neogi, Debraj Dhar Purkayastha, Abhijit Nath, Bishop Dev Gupta, Harun All Rashid Pramanik, Rajdeep Deb, Tirup Dutta Choudhury, Rahul Deb, Saptarshi Dhibar and all research scholars of the department whose help and suggestions stood by me in difficult times during the course of my work.

I also sincerely acknowledge the support extended by P. R. Ramesh, Suman Bhattacharjee, Biswajit Nath, Alom Barbhuiya and Rajib Kurmi during the tenure of my research.

I would like to place on record my sincere acknowledgement to Sri Nikhil Ranjan Choudhury, Principal, Silchar Polytechnic for his manifold help and guidance in difficult times. My heartfelt thanks goes to Department of Higher and Technical Education, Govt. of Assam for allowing me to continue my higher studies on part time basis.

Analytical and instrumental facilities provided by SAIF, NEHU, Shillong ; SAIF, CDRI, Lucknow ; STIC, Kochi ; IIT, Guwahati ; Department of Chemistry, Assam University and Department of Biotechnology, Assam University is gratefully acknowledged.

Last but not least, I am ever obliged to my family members for their continuous support and inspirations that helped me a lot to accomplish the work.

Date: 15-05-2010 Pankaj Goswami

Place: Silchar

CONTENTS

LIST OF TABLES

LIST OF FIGURES

ABSTRACT

The present research work is aimed at synthesis of newer multidentate Schiff base ligands and to devise appropriate synthetic strategy to access mononuclear and binuclear VO(IV) and Fe(III) complexes. Spectral characterization and investigation of magnetic, mesogenic, electrochemical, thermal and antimicrobial properties of synthesized compounds is the focal theme of the work undertaken for the present Ph.D. thesis. The structure optimization of few selected compounds by DFT method (Gaussian 03) is also carried out the in present research programme. The content of the thesis is distributed over six chapters followed by conclusions, references, figures and graphs. Each chapter is virtually complete in itself including references.

The **Chapter 1** portrays an introductory overview highlighting the significance and explaining the motive of undertaking the present work.

Chapter 2 deals with review of literature. The current status vis-a-vis the historical developments in the field of metal-Schiff base complexes with special reference to iron(III) and vanadyl(IV) complexes have been highlighted in this chapter.

Chapter 3 presents a description of experimental methods, chemicals and materials, and details of equipment used for physical measurements.

Chapter 4 describes the synthetic route to various types of Schiff bases. An account of synthesis various types of Schiff base ligands with different denticity (di, tri and tetra) are included in this chapter. The strategy to functionalise the ligand with long alkoxy chain to create mesogenicity has been demonstrated in select cases. The ligands possessing N / O donor coordinating sites were primarily accessed from the condensation of salicyldehydes, diketones, benzoin, furfuraldehyde with different types of amines.

Chapter 5 describes the complexation of the Schiff base ligands with iron(III) and oxovanadium(IV). Different strategies adopted to devise synthesis of mono- and dinuclear compounds have been reported herein. Ligand exchange reactions with loosely coordinated solvent molecules to access newer mixed-ligand Schiff base complexes have been dealt with in this chapter. The complexes accessed are of the types **$[Fe(L)_2(NO_3)_2]NO_3$** and **$[VO(L)_2]SO_4.H_2O$** (L=N, N donor bidentate Schiff bases obtained from condensation of benzil with *p*-anisidine or *p*-toludine) ; **$[FeLCl]_2$** and **$[VOL]_2$** (L=O, N, O donor tridentate Schiff bases obtained from condensation of 4-n-alkoxy salicyldehyde with 2-aminophenol) ; **$[Fe(L)Cl]_2$, $[Fe(L)ClX]$, $[Fe(L)(H_2O)_2]_2$** and **$[VOL]_2.H_2O$, $Na[VO_2L]$** (L=O, N, O donor tridentate Schiff bases obtained from condensation of acetylacetone with 2-aminophenol and X=Im or PPh_3) ; **$[Fe(L)Cl]$** and **$[VO(L)(H_2O)].H_2O$** (L=O, N, O donor tridentate Schiff bases obtained from condensation of acetylacetone with 2-aminobenzoic acid) ; **$[FeL(acac)(EtOH)]$** (L=O, N, O donor tridentate Schiff bases obtained from condensation of 2-hydroxy-1-napthaldehyde with 2-aminophenol or 2-aminobenzoic acid) ; **$[Fe(L)(H_2O)_2]NO_3$, $[Fe(L)(H_2O)(NO_3)]$, $[Fe(L_9)(H_2O)_2]$, $A[Fe(L_9)X_2]$ ($A=NH_4$, X=F, NCS; A=Na, $X=N_3$), $[Fe(L)X_2]NO_3$ (X=Im or Py)** and **$[VO(L)].H_2O$** (L=N_2O_2 donor tetradentate Schiff bases obtained from condensation of acetylacetone, 2-hydroxy-1-napthaldehyde and benzoin with ethylenediamine or *ortho*-phenylenediamine) ; **$[FeLCl_2]Cl$** and **$[VOL]SO_4.H_2O$** (L=tetraimine macrocyclic Schiff bases obtained from condensation of benzil with ethylenediamine or *ortho*-phenylenediamine) ; **$[Fe(L)(H_2O)_2](NO_3)_3$** and **$[VOL].SO_4.H_2O$** (L= N_2O_2 donor neutral tetradentate Schiff bases obtained from condensation of furfuraldehyde with hydrazine).

Chapter 6 of the thesis deals with results and discussion pertaining to the work. Herein, is described the characterization of the synthesized compounds using elemental

analysis, IR, UV-VIS, NMR and Mass spectroscopy. Single crystal XRD analysis of one of the ligands is also discussed in this chapter. Besides structural characterization, the mesogenic, electrochemical, thermal and magnetic behaviour of the compounds is described in this chapter. A description of the results of antimicrobial activity of some select compounds towards some microbial strains is included herein. Structure optimization and computation of geometrical parameters by DFT using GAUSSIAN 03 package is also incorporated in this chapter.

Conclusions provided at the end highlight the salient findings of the research work.

Part of the work described in the thesis has been published or under communication (as detailed below) with the rest being processed for publication.

Published / Accepted

1. C. R. Bhattacharjee, **P. Goswami,** S. Neogi and S. Dhibar. *Transition metal complexes of a neutral [N_2O_2] donor Schiff base derived from furfuraldehyde and hydrazine hydrate : Synthesis, characterization and redox behaviour*. **Assam Univ. J. Sc. Tech.** 2010, **5**, 81.
2. C. R. Bhattacharjee, **P. Goswami** and P. Mondal. *Synthesis, structural characterization and DFT studies of new mixed ligand iron(III) Schiff base complexes.* **J. Coord. Chem.** 2010, Accepted.
3. C. R. Bhattacharjee, **P. Goswami** and P. Mondal. *Synthesis, spectroscopic characterization and dft studies of mixed ligand coordination complexes of iron (III) with a tetradentate [NNOO] donor Schiff base ligand incorporating aquo, fluoro, thiocyanato and azido group.* **Procedings on International Conference on Coordination and Organic Chemistry**, Bharatiar University, Coimbatore, India, 18-20 March, 2009.

4. C. R. Bhattacharjee, **P. Goswami,** M. Sengupta and B. Chakraborty. *Synthesis and antimicrobial activity of a new binuclear vanadyl complex of a tridentate [ONO] donor Schiff base.* **Proceedings on National Conference on Recent Progresses in Physical Sciences,** Karimganj College, Karimganj, India, 20-21 December, 2008.

Communicated

1. C. R. Bhattacharjee, **P. Goswami** and M. Sengupta. *Mono and binuclear iron(III) and oxovanadium(IV) complexes of [ONO] donor tridentate Schiff base ligands – synthesis, electrochemical and antimicrobial studies.* **J. Coord. Chem.** (Communicated).
2. C. R. Bhattacharjee and **P. Goswami.** *Synthesis, characterization, electrochemical and magnetic studies of 12-membered tetraimine macrocyclic Schiff base ligands and their iron(III) and oxovanadium(IV) complexes.* **J. Chem. Sci.** (communicated)
3. C. R. Bhattacharjee, **P. Goswami,** H. A. R. Pramanik and P. Mondal. *Reactivity of tris (acetylacetonato) iron(III), [Fe(acac)$_3$] as an access to new mixed-ligand tridentate [ONO]- donor Schiff base Complexes.* **Inorg. Chem. Commun.** (communicated).

CHAPTER - 1

GENERAL INTRODUCTION

1.1. Schiff base: Definition and concepts

Compounds containing an azomethine (-CH=N-) group are known as Schiff bases. They are usually formed by condensation of primary amine with a carbonyl compound according to the following scheme.

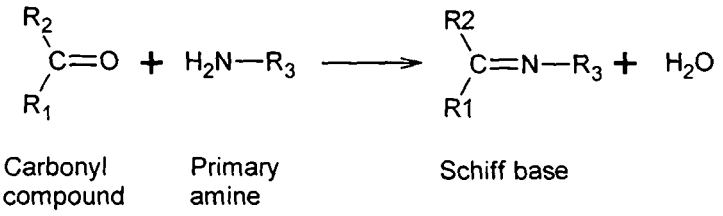

where R_1, R_2 and R_3 may be an alkyl or aryl groups. Hugo Schiff described for the first time the condensation between an aldehyde and an amine leading to a Schiff base in the year 1864 [1] and hence the compounds are named after him. Schiff bases of aliphatic aldehydes are relatively unstable and readily polymerize [2-3] while those of aromatic aldehydes having an effective conjugation system, are more stable [4-5]. Schiff bases

obtained from aromatic amines are known as anils. The mechanism of Schiff base formation is an acid catalysed nucleophilic addition of an amine to a carbonyl compound forming a hemiaminal, followed by dehydration to generate an imine.

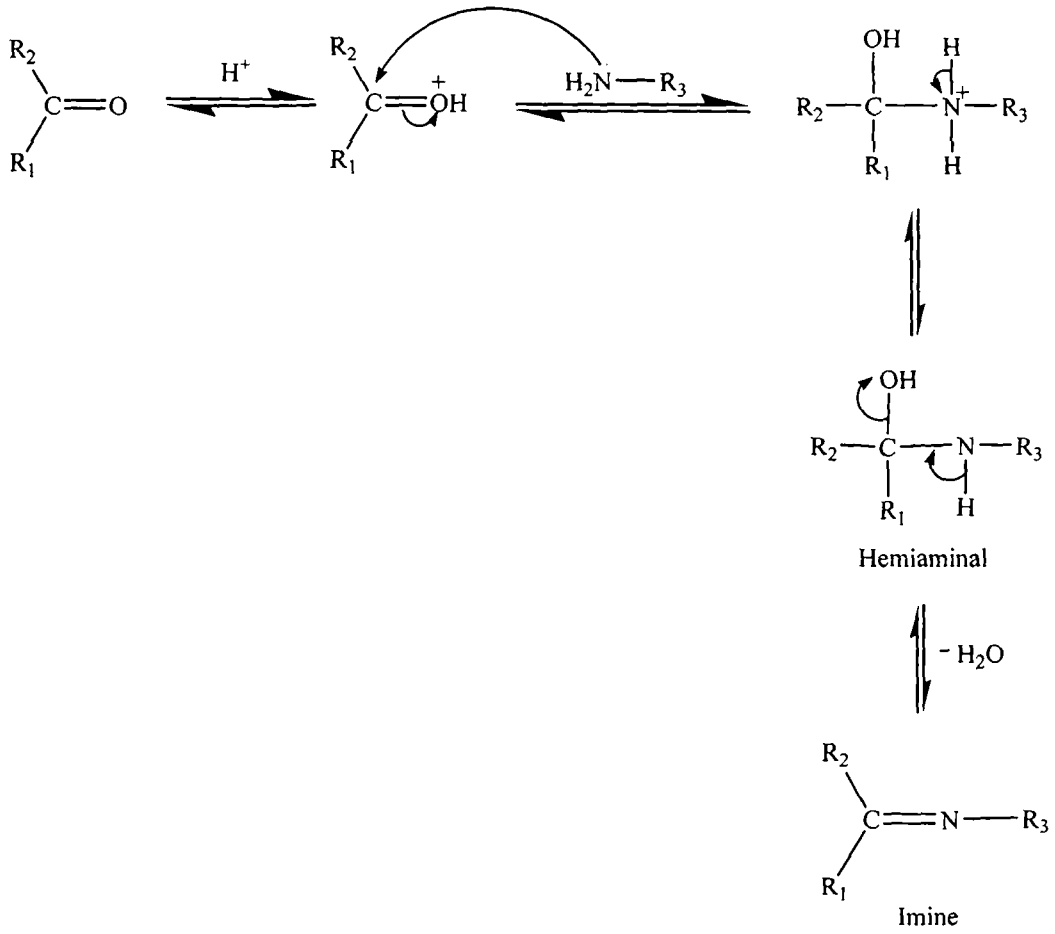

Condensation of amines with aldehydes and ketones find numerous applications that include preparative use, identification, detection and determination of aldehydes and ketones, purification of carbonyl compounds or amines or protection of these groups during complex or sensitive reactions. In chemistry, Schiff bases find versatile use [6-8]; some serve as basic units in certain dyes, some exhibit liquid crystalinity whereas some are fluorescent. Schiff bases that have solvent dependent UV/VIS spectra (solvatochromicity) are suitable for NLO (non linear optical) active materials [9]. These

are also useful materials in solid phase extraction [10] and synthesis of ion selective electrodes for determination of anions in analytical samples [11-14]. They are also useful in enantioselective [15-16] and regioselective [17] ring opening of epoxides, enentioselective epoxidation of alkenes [18] and asymmetric oxidation of methyl phenyl sulphide [19].

1.2. Biological importance of Schiff bases

Schiff bases play an important role in many biological processes involving amino acids and keto acids, including trans-amination, decarboxylation, condensation, β-elimination, and racimization, which may involve Schiff base intermediates [20]. A large number of enzymatic reactions are known that involve Schiff base intermediates. One of the most prevalent types of catalytic mechanism in biochemical processes involves condensation of primary amine in an enzyme, usually that of a lysine residue, with a carbonyl group of the substrate to form an imine or Schiff base. Schiff bases derived from pyridoxal (the active form of vitamin B_6) and amino acids are considered as very important ligands from biological point of view. Transition metal complexes of such ligands are important enzyme models. Many biologically important Schiff bases have been reported in literature possessing antibacterial [21, 22], antifungal [23-25] antimicrobial [26-29], anticonvulsant [30], anti-HIV [31], anti-inflammatory [32] and antitumor [33] activities. Certain polymeric Schiff bases are also reported to possess antitumor or activity [34]. The biosynthesis of porphyrin, for which glycine is a precursor, is another important pathway that involves the intermediate formation of Schiff base between keto group of one molecule of δ-amino levulinic acid and ε-amino group of lysine residue of an enzyme. Another important role of Schiff base is in transamination [35]. Transamination reactions are catalysed by a class enzyme called transaminases or aminotransferases. Transaminases are found in mitochondria and cytosal of eukaryotic

cells. All the transaminases appear to have same prosthetic group, i.e. pyridoxal phosphate, which is covalently attached to them via an imine or Schiff base linkage. Schiff bases formation is also involved in chemistry of vision, where the reaction occurs between the aldehyde function of 11-cis retinal and amino group of the protein (opsin) [36].

1.3. Schiff base transition metal complexes

Schiff bases are generally bi, tri or polydentate ligands capable of forming very stable mononuclear, binuclear and polynuclear complexes with transition metals. Schiff base ligands are able to coordinate metals through imine nitrogen and another group, usually linked to the aldehyde. Modern chemists still prepare Schiff bases, and nowadays active and well-designed Schiff base ligands are considered ''privileged ligands''. In fact, Schiff bases are able to stabilize many different metals in various oxidation states, controlling the performance of metals in a large variety of useful catalytic transformations. Metal complexes of Schiff base have occupied a central place in development of coordination chemistry after the work of Jorgensen and Werner [37]. Schiff prepared complexes of metal salicyldehyde with primary amines [38]. Subsequently he prepared complexes from the condensates of urea and salicylddehyde [39]. Delepine prepared complexes by reacting metal acetates, salicyldehydes and a primary amine in alcohol and showed a 2:1 stoichiometry [40]. However, there was no comprehensive and systematic study until the preparative work of Pfeiffer and associates [41]. Pfeiffer and his co-workers prepared a series of complexes derived from Schiff bases of salicyldehyde and its substitution products [42]. The activity of trace metals in biological system is attained through the formation of complexes with different bio-ligands and the thermodynamic or kinetic properties of the complexes govern the mode of biological action. It is worthwhile to mention that the antitumor

activity of some Schiff bases has been attributed to their ability to chelate with trace transition metals [43, 44]. The coordination chemistry of Schiff bases as multidentate ligands gained importance because of their use as models in biological systems, in catalysis and in material chemistry. The presence of both nitrogen and oxygen donor atoms permits coordination with a wide range of transition and non-transition metals yielding stable and intensely coloured metal complexes, some of which have interesting physico-chemical [45, 46] and potentially beneficial chemotherapeutic properties [47-52]. In the past two decades synthesis, structure and properties of Schiff base complexes have stimulated much interest for their noteworthy contributions in the field of photoluminescence, magnetism, molecular architecture, material science, corrosion inhibitors, sensor design and catalysis of many reactions like carbonylation, hydroformylation, reduction, oxidation, epoxidation and hydrolysis etc. [53-58]. The flexibility of disposition of different donor sites is the secret behind their successful performances in mimicking peculiar geometries around the metal centres, leading to very interesting spectroscopic properties with varied magnetic activities [59].

1.4. Coordination chemistry of iron-Schiff base complexes

The common oxidation states of iron are +2 and +3. The relative stability of the two oxidation states in aqueous solution is defined by the standard electrode potential of +0.77 V for the Fe^{3+}/Fe^{2+} couple. The chemistry of iron, including its importance in biology is closely associated with the ready interconversion of these two oxidation states and with the dependence of redox potential on the ligand environment. The versatility of the chemistry of iron is reflected by the variety of roles it plays in biological system where it is frequently found at the active centers involved in processes such as oxygen and electron transport in nitrogenase, many oxidases and in metalloenzymes such as hydrogenases and reductases.

The Fe^{III} ion has a d^5 electron configuration showing a high spin (S=5/2) in most of its complexes. However, there is a possibility of stabilization of low spin (S=1/2) ground states in strong octahedral field such as generated by CN ion and many bi or polydentate ligands containing unsaturated nitrogen. In addition, intermediate spin (S=3/2) states may also be produced in fields of lower symmetry. The commonest coordination number of iron is six but a range of other coordination numbers three, four, five, seven and eight are also established.

Condensation reactions between carbonyl compounds and primary amines have provided one of the most important and widely studied class of chelating ligand which vary in denticity, flexibility, nature of the donor atoms and in electronic properties. A wide diversity in coordination geometries and magnetic behaviour has also been found.

The bidentate [N, O] donor schiff bases like N-substituted salicylaldimines (**1**) form complexes of stoichiometry $[Fe(L)_2X]$ (**2**) where X=Cl or Br and L=ligand which have a high spin (S=5/2) monomeric five coordinated structures [60]. An X-ray investigation of the compound indicated a stereochemistry intermediate between trigonal bipyramidal and square pyramidal [61].

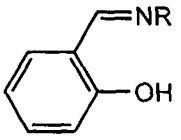

1

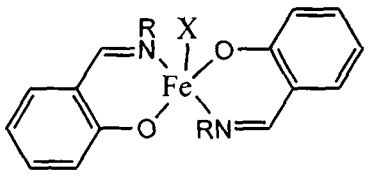

2

The [ONO] donor tridentate dianionic ligand (L) of the type (**3**) form a five coordinated dimeric complexes of stoichiometry $[Fe(L)Cl_2]_2$ (**4**). The iron atom of the dimer are bridged by the alkoxide oxygens to form a four membered ring with the Fe-O distances of 1.983 and 1.934 Å and angles 75.9 and 104.1^0 at iron-oxygen, respectively. The geometry of the complex is distorted square pyramidal, the basal plane being made up

of the donors of tridentate ligand and the bridging alkoxide oxygen with the chlorine atom in apical position. The magnetic behaviour of the complex accords with the occurrence of antiferromagnetic super exchange interaction mediated by the dialkoxy bridge. The μ_{eff} having a reduced value of 4.52 B.M. at room temperature and falling further to 2.37 B.M. at liquid nitrogen temperature.

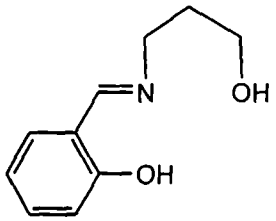

3

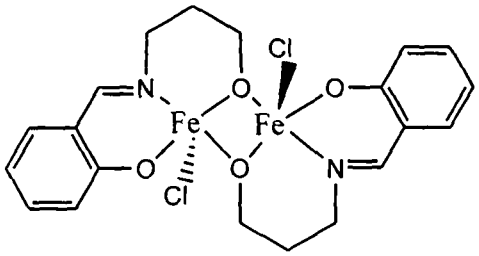

4

Condensations of two equivalent of salicyldehyde with a diprimary amine, commonly 1,2-diaminoethane (en), provide a convenient route to $[N_2O_2]$ donor tetradentate Schiff base ligands of the type (**5**). Complexation with iron(III) yields monomeric form (**6**) and dimeric form (7) depending upon the methods of preparation or isolation [62].

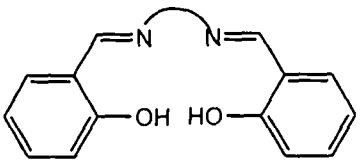

5

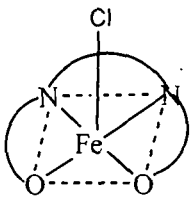

6

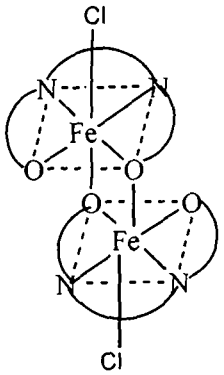

7

The monomeric form is obtained from recrystallisation of the dimeric form from nitromethane, containing a molecule of solvent in the lattice and has a square pyramidal geometry with the metal atom sitting about 0.46 Å above the plane defined by the N_2O_2 donor set of the tetradentate ligand, in the direction of the apical chlorine atom [63]. In the dimer, isolated from acetone solution, two molecules of monomer each share one

oxygen atom from each ligand to give an overall octahedral environment for each metal atom [64].

The monomers have magnetic moments at room temperature close to the spin only value of 5.92 B.M. and obey the Curie-Weiss law with small Weiss constant. The dimers, on the other hand, have subnormal room temperature moments which reduced further on lowering the temperature, thereby describing the antiferromagnetic superexchange interaction between the pair of iron atoms.

Spin–crossover phenomenon has also been encountered in several examples of iron(III) complexes with tridentate and hexadentate Schiff base ligands.

$$Fe^{III}(t_{2g}^{5}) \rightleftharpoons Fe^{III}(t_{2g}^{3}e_{g}^{2})$$

These complexes may be high spin or low spin depending on nature and position of substituents, counterions, lattice solvents and even geometrical isomerism.

Iron(III) complexes of tetradentate macrocyclic Schiff base ligands having N_4 donor set are generally five coordinated or six coordinated having square pyramidal or nearly octahedral geometry. These complexes may be high spin (S=5/2), intermediate spin (S=3/2) or low spin (S=1/2) depending upon nature of the macrocyclic ligand i.e. size and degree of unsaturation and on the number of the axial ligands.

Mixed ligand Fe(II)-bis-Schiff base complexes (**10** and **11**) of tetradentate ligand bis(o-vanillin)-o-phenylenediimine (**8**) or bis(o-vanillin)-2,3-naphthalenediimine (**9**) and pyrazine are reported with their crystal structures and magnetic property. Compound **10** shows a two-step spin cross over behavior while **11** shows high spin at all the temperature range measured [65].

The macrocyclic complexes of the type, $[FeLCl_2]Cl$ [**13**] have been prepared by reacting iron(III) chloride with a novel Schiff base tetraimine macrocyclic ligand, (L): 5,6,11,12-

dibenzophenone-2,3,8,9-tetraphenyl-1,4,7,10-tetraazacyclo-dodeca-1,3,7,9-tetraene (**12**). The ligand was obtained from [2+2] condensation between 3, 4-diamino benzophenone and benzil.

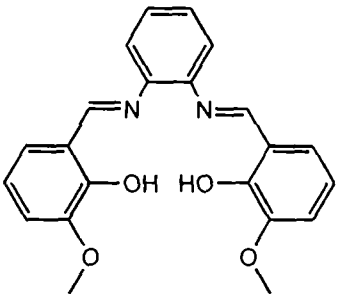

8

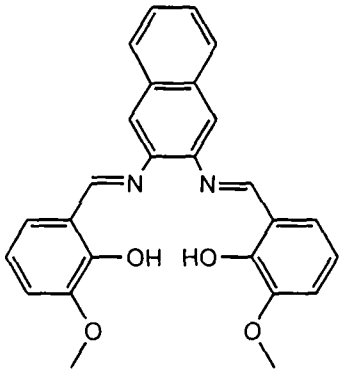

9

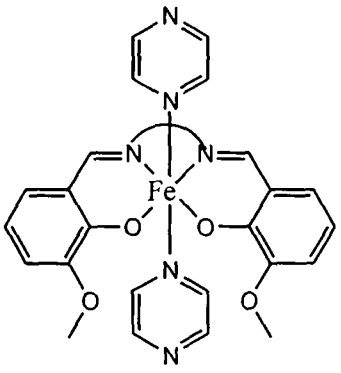

10

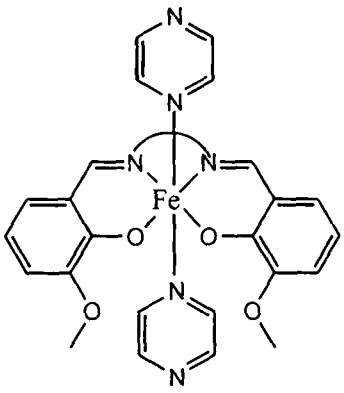

11

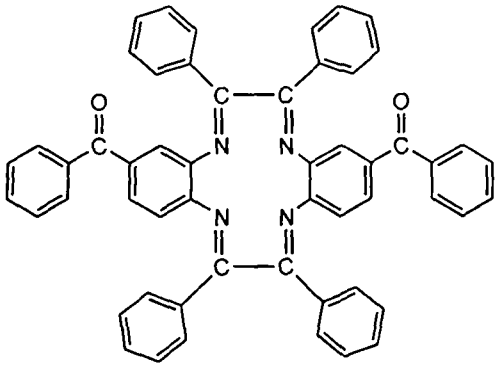

12

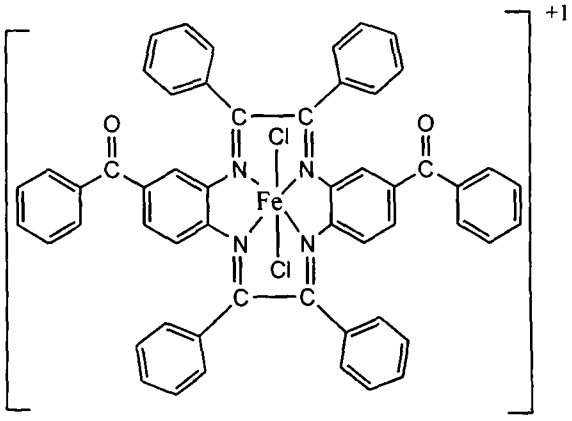

13

1.5. Coordination chemistry of vanadium-Schiff base complexes

Vanadium may exhibit formal oxidation states from –3 to +5 with the exception of –2. Under ordinary conditions, the most stable states are +4 and +5. The coordination chemistry of vanadium is strongly influenced by the oxidizing/reducing properties of the metallic center, and the chemistry of vanadium ions in aqueous solution is limited to oxidation states +2, +3, +4 and +5.

Vanadium easily switches between the oxidation states V and IV, which alongwith III are the oxidation states of naturally occurring vanadium compounds. The redox potential at pH 7, for the couple $H_2VO_4^- + 4H^+ + e \rightarrow VO^{2+} + 3H_2O$ amounts to -0.341V and so, it is the range where vanadyl(VO^{2+}) is oxidized to vanadate under aerobic conditions, and vanadate is reduced to vanadyl by cellular components such as cysteine containing peptides (glutathione) and proteins, ascorbate, NADH and phenolic compounds [66]. The main species present under physiological aerobic conditions is the acid–base pair $H_2VO_4^- \rightarrow HVO_4^{2-} + H^+$ (pKa 8.1) [67]. Cationic V^V species such as VO^{3+} or VO_2^+ are stable in solution around pH 7 only when coordinated to sufficiently strong ligands, which prevent precipitation of hydroxides.

The +4 oxidation state is the most stable under ordinary conditions and the majority of the vanadium(IV) compounds contain VO^{2+} unit (Vanadyl ion). It forms stable anionic, cationic, and neutral complexes with all type of ligands and has one coordination position occupied by the vanadyl oxygen.

The complexes are typically square pyramidal (**14**) or bipyramidal (**15**) with the vanadyl oxygen apical and the vanadium atom lying above the plane defined by the equatorial ligands. Trigonal bipyramidal complexes (**16**) are also known. Many vanadium(V) compounds are known to exist as oxo complexes containing the VO^{3+} or

the VO^{2+} entity and the cis geometry in dioxo complexes has been confirmed by structure determinations.

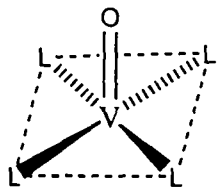

14

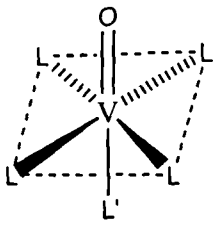

15

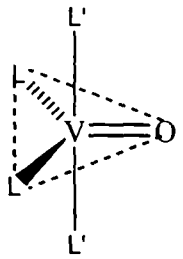

16

The V=O stretching frequency is an important characteristics of oxovanadium(IV) complexes, generally observed at 985±50 cm^{-1}. Ligands that increase the electron density reduce V-O multiple bond character and hence the stretching frequency. For complexes $VOL_4^{n\pm}$, $\nu_{(V=O)}$ falls in the order $L=H_2O>NCS^->CN^->F^-$. Reduction in V=O frequency from 950-1000 to 800-850 cm^{-1} indicate polymerization or VO---VO----VO interactions.

Oxovanadium(IV) complexes with [N,O] donor bidentate Schiff bases derived from diamines and salicyldehydes (**17**) or β-diketones (**18**) normally have a monomeric structure with 1:1 stoichiometry having magnetic moment of 1.78 B.M. at 295 K and it obeys Curie-Weiss law over the range 95-295 K.

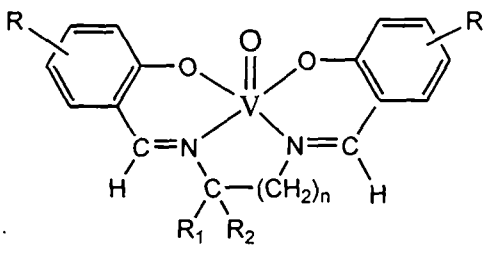

17

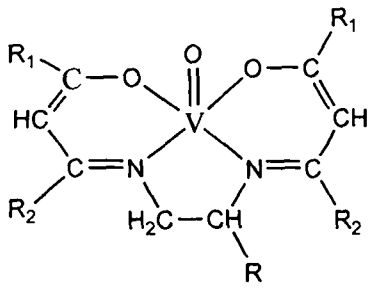

18

With various types of tridentate Schiff bases having [N, O, O] donor set (**19-22**) the complexes are very often found to be dimeric. It is presumed that the dibasic character of the ligands forces the VO^{2+} ion to dimerize (**23-24**) leading to anomalous magnetic

properties. The subnormal magnetic moment of the complexes decrease considerably as the temperature is lowered and this phenomenon is the characteristics of intramolecular antiferromagnetic exchange [68].

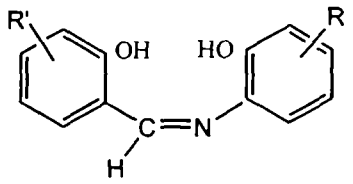

19

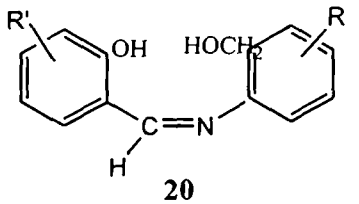

20

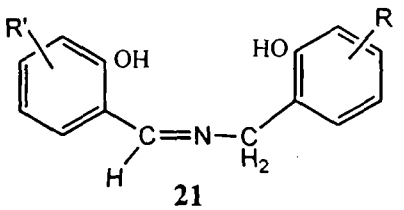

21

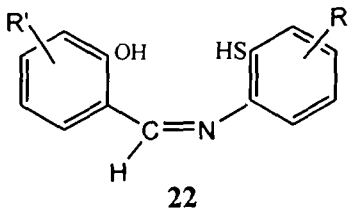

22

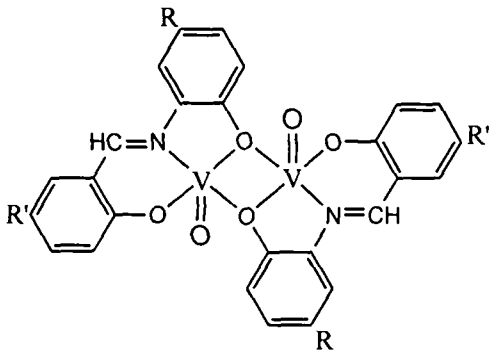

23

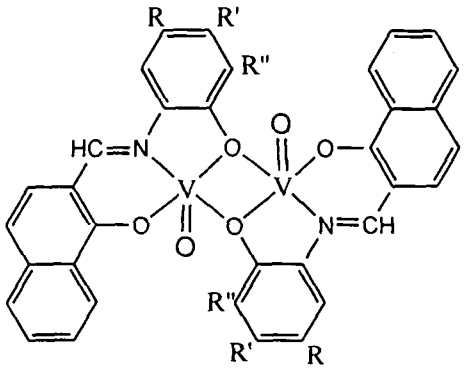

24

The complex **23** on treatment with a strong chelating agent such as phen, the dimer is broken with the formation of a mononuclear mixed ligand complex [VO(SB)(phen)] [69]. The dimeric structure is also broken on treatment of the complex with pyridine; a monopyridine adduct forms which obeys the Curie-Weiss law with θ=2K and μ_{eff}=1.75 B.M [70].

Schiff bases derived from 2-hydroxynapthaldehyde and o-aminophenol and some substituted derivative also formed a subnormal dimeric VO^{2+} complexes (**24**). Like **23**,

treatment of the complex **24** with phen, the dimmer is broken and a mixed ligand complex is obtained.

Several VO^{2+} complexes were prepared with the ligand **20** and **21**. High melting or decomposition temperature and insolubility in common noncoordinating solvents suggest a dimeric or polymeric nature. $\nu_{V=O}$ occurs at 910-985 cm^{-1} for complexes of **20** and at 900-910 cm^{-1} for those of **21**; this argues against the presence of a V=O·····V=O polymeric chain structure. The μ_{eff} values of the complexes were shown to be remarkably less than the spin only values and the magnetic moments decrease significantly as the temperature is lowered, suggesting antiferromagnetic exchange interaction of neighbouring VO^{2+} ions.

Oxovanadium(IV) complexes with Schiff bases **25** and **26** derived from alkyl aminoalcohols and salicyldehyde or o-hydroxyacetophenone (and substituted derivative) respectively, have been prepared by adding an alcoholic solution of Schiff base to alcoholic solution of vanadyl acetate. The compounds obtained have been formulated as $[VOL]_2$ with structure **27**. This structural feature is supported by IR spectra and magnetic properties. They have subnormal μ_{eff} and the dependence of χ_M^{corr} on temperature is characteristics of antiferromagnetic exchange.

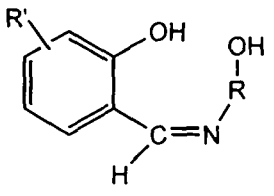

25

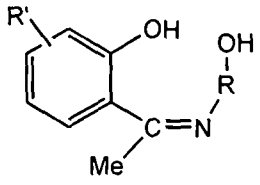

26

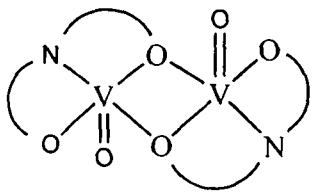

27

The electronic spectra of such complexes with tridentate Schiff bases of the type (**25-26**) generally exhibit three ligand field bands: (i) ca. 715-770, (ii) ca. 625 and (iii) ca. 500-550 nm, assigned to d-d transitions according to the Vanquickenborne and Gray

McGlynn MO scheme [71]. Some of these bands are not well developed and this gave rise to ambiguity in their assignment. No band characteristics of VO^{2+}-VO^{2+} interaction has been observed in complexes with these Schiff bases.

Several VO^{2+} complexes were prepared with Schiff bases **28** and **29** derived from dibenzoyl methane or pyrol-2-carboxaldehyde and several amines (taurine, anthranilic acids, β-alanine). These Schiff bases also behave as tridentate ligands and the complexes were formulated as $[VO(SB)(H_2O)_2]$ [72]. The monomeric structure was confirmed on the basis of μ_{eff} and ebulliometric measurements in dioxane.

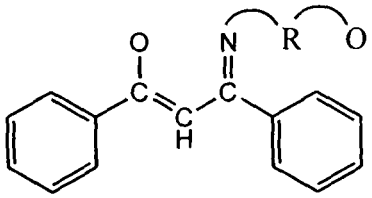

28

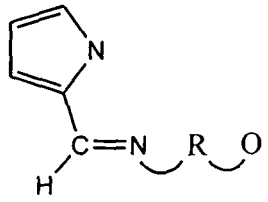

29

Oxovvanadium(IV) complexes with tetradentate Schiff bases (**30**) obtained from the reaction of two moles of benzoyl hydrazide with acetylacetone was monomeric square pyramidal (**31**) with ν(V=O) at 995 cm^{-1} and μ_{eff} of 1.7 B.M [73].

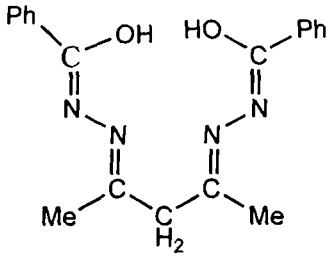

30

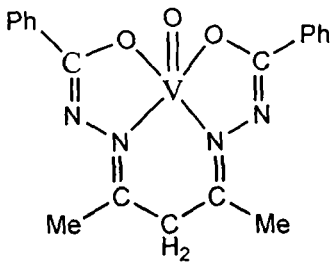

31

Mixed-ligand oxovanadium(IV) and oxovanadium(V) complexes with a tridentate dinegative ONO donor Schiff base ligand derived from acetylacetone and benzoyl hydrazine[viz.,4-(1-hydroxybenzylidenehydrazono)-2-penten-2-ol (H_2L)] and bidentate NN [viz., 2,2'-bipyridine (bipy) and 1,10-phenanthroline (phen): complexes (**32**) and

(**33**), respectively] or OO) [viz., ethylene glycol (H2gol), salicylaldehyde (Hsal) and vanillin (Hvan): complexes (**34-36**), respectively] donor ligands have been prepared and characterized. The complexes with NN donor ligands are one electron paramagnetic, displaying axial EPR spectra and exhibiting two ligand-field transitions in the visible region, whereas the complexes with OO donor ligands are diamagnetic and display only LMCT bands. The pentavalent complexes (**35**) and (**36**) exist in two isomeric forms [74].

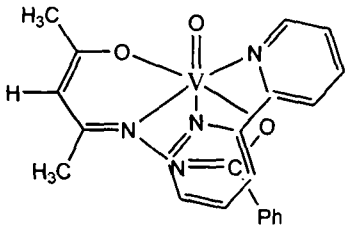

32

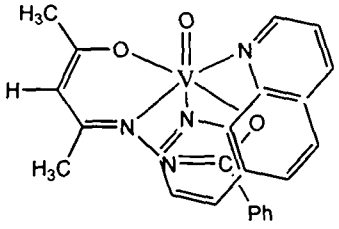

33

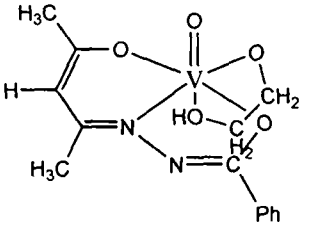

34

Reaction of $VOSO_4$ with the tridentate ONO donor ligand derived from the condensation of acetylhydrazide with either 2-hydroxybenzaldehyde (H_2L^1) or 2-hydroxyacetophenone (H_2L^2) in an equimolar ratio in the presence of two equivalents of sodium acetate in aqueous-methanolic medium in air produces yellow dioxovanadium(V) complexes of the type, $[V^VO_2(H^+\text{-}L)]$, (**37**) and (**38**) in good yield [75].

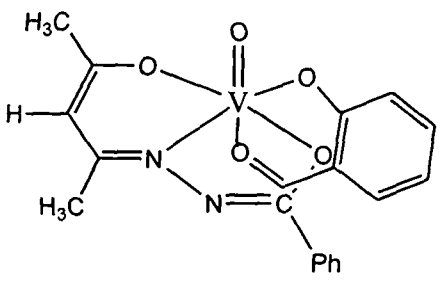

35

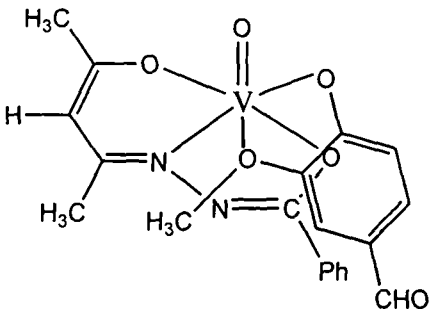

36

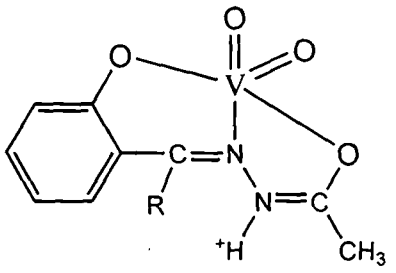

R	Complex
H	**37**
CH_3	**38**

Vanadyl complexes of N_2O_2 donor tetradentate Schiff base ligands, derived from aromatic aldehydes and aliphatic diamine (2, 2'-Dimethylpropanediamine) assumes a square pyramidal structure (**39**). The compound showed excellent selectivity for epoxidation of cyclooctene and good selectivity for styrene [76].

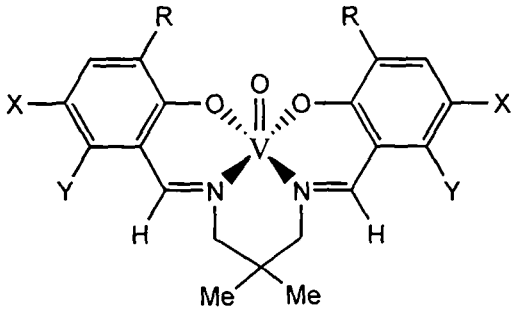

39

1.6. Goal

Set in this backdrop and also based on review of literature (Chapter 2) pertaining to the chosen area of research it was thought worthwhile to undertake investigation on synthesis, physicochemical characterization, reactivity and antimicrobial activity of some Schiff base ligands of different denticity and their complexes of iron (II, III) and vanadyl (IV).

Specifically the objectives of the present Ph.D. research are detailed as follows.

(i) To synthesize low molecular mass mesogenic Schiff bases from simple amines and to study the effects of complexation on mesogenicity.

(ii) To design newer multidentate Schiff base ligands and to devise appropriate synthetic strategy to access mononuclear and binuclear VO(IV) and Fe(III) complexes.

(iii) To synthesize and characterize mixed ligand Fe(III) complexes of Schiff bases.

(iv) To synthesize and characterize macrocyclic Schiff bases derived from benzil and diamines and their complexes with iron(III) and oxovanadium(IV).

(v) To carry out ligand exchange reactions of the solvated complexes with neutral or anionic donor ligands to afford newer mixed ligand complexes.

(vi) To investigate mesogenic, magnetic, electrochemical and thermal behaviour of the complexes.

(vii) To explore antimicrobial activities of the selected synthesized compounds against various microbial strains.

(viii) DFT studies on selected compounds to ascertain optimised geometry, single point energy and vibrational frequencies using GAUSSIAN 03 program.

CHAPTER-2

REVIEW OF LITERATURE

Schiff bases are versatile ligands for many transition metals. The field of Schiff base complexes was fast developing on account of the wide diversity of structures of the ligands and a little variation in the structure markedly affected the activity of the compounds. Metal-Schiff base complexes have continued to enjoy extensive interest owing to their synthetic proclivity, structural diversity and potential application in agriculture, industrial and pharmaceutical chemistry.

A review article on metal complexes of Schiff base and β-ketoamines [77] discussed various approaches for synthesis of Schiff base complexes.

2.1. Preparation of Schiff bases

Condensation between aldehydes and amines is carried out in different reaction conditions and in different solvents to produce Schiff bases. The presence of dehydrating agents normally favours the formation of Schiff bases.

2.2. Complexation of Schiff bases: different routes

Generally three synthetic procedures were employed for salicylaldimine complexes.

(a) Reaction of metal ion and Schiff base in alcohol or aqueous-alcohol medium in presence of a base like acetate or hydroxide.

(b) Reaction of primary amine with bis or tris(salicyldehyde) metal complex.

(c) Template reactions: Reaction of salicyldehyde with an aqueous solution of tetrakisethylenediamine-μ-dichloro nickel(II) chloride containing a few drops of pyridine results in the formation of Ni(sal)en in good yield.

2.3. Application of Schiff bases and their metal complexes

Schiff base and their metal complexes are used as catalyst in various biological systems, polymers and dyes, besides some uses as antifertility and enzymatic agents.

2.3.1. Catalytic activities

Aromatic Schiff bases or their metal complexes catalyze reactions like oxygenations [78], hydrolysis [79], electro-reduction [80] and decomposition [81]. Four coordinated cobalt(II) Schiff base chelate complexes show catalytic activity in oxygenation of alkene [78]. Synthetic iron(II) Schiff base complex exhibits catalytic activity towards electro-reduction of oxygen [80]. Use of iron-Schiff base complexes in different catalytic reactions have been dealt with in some recent works [82]. Recent studies showed iron(III) tridentate Schiff base complex as efficient catalyst for oxidation of sulfides to sulfoxides by urea hydrogen peroxide [83]. Similarly, $[N_2O_2]$ donor Schiff base complexes of palladium(II) have been used as catalyst for reduction of organic substrates under mild conditions [84]. Some metal complexes of a polymer bound Schiff base show catalytic activity on decomposition of hydrogen peroxide and oxidation of ascorbic acid. Copper(II) complexes of Schiff base ligands derived from 2,2′-dimethyl propanediamine catalyze the oxidation of cyclooctene and styrene using

tert-butylhydroperoxide as oxidant in good yield [85]. The polymer anchored N, N/-bis (o-hydroxyacetophenone) ethylenediamine Schiff base complexes of Fe(III), Co(II) and Ni(II) showed catalytic activity in oxidation of phenol [86]. Oxovanadium(V) complex of a tridentate Schiff base ligand derived from condensation of 1,2-propylenediamine and 2/-hydroxy-4/-methoxy acetophenone was found to be an efficient catalyst for selective epoxidation of cyclooctene [87].

2.3.2 Antimicrobial activities

Schiff base derived from furyl glyoxal and para-toludine [88] show antibacterial against Escherichia coli, Staphylococcus aureus, Bacillus subtilis and Proteus vulgaris. Complexes of thallium (I) with benzothiazolines show antimicrobial activity against pathogenic bacteria [89]. Tridentate Schiff bases and their metal complexes show antibacterial activities against *E.coli*, *S. aureus*, *B. subtilis* and *B. pumpilis* [90]. Isatin derived Schiff bases possess anti-HIV activity and antibacterial activity [92]. Schiff bases containing thiazole and cyclobutane ring show antimicrobial activity [93]. Schiff bases of pyrolidione, pyridine with ortho-phenylenediamine and their metal complexes show antibacterial activity [94]. N-chloro salicylidiene tauriene Schiff base and its copper, nickel complexes show antibacterial activities to Colibacillus and Pseudomonas aeriginosa [95]. Schiff base conjugates of p-amino salicylic acid enhance antimyco-bacterium activity against Mycobacterium smegmatis and M. lovis BCG [95].

2.3.3. Antifungal activities

Thiazole and benzothiazole Schiff bases posses effective antifungal activities [96]. Presence of methoxy, halogen and napthyl groups enhance fungicidal activity towards Curvularia [97]. Pyrandione Schiff bases show physiological activity against *A. niger* [97]. Some Schiff bases of quinazolinones show antifungal activity against *Canadia albicans*, *Trichophytons rubrum*, *T. mentagrophytes*, *A. niger* and *Micosporum gypseum*

[98]. Schiff bases and their metal complexes formed between furan and furylglycoxal with various amines show antifungal activity against *Helminthosporium gramineum* (causing stripe disease in barley), *Syncephalostrum racemosus* (causing fruit rot in tomato) and *C. capsici* (causing dieback diseases in chillies) [99]. Moreover, ligand hydrazine and carbothioamide and their metal complexes show antifungal activity against *A. alternate* and *H. graminicum* [99]. Tridentate Schiff bases and their metal complexes show biocidal activities [101]. Schiff base of salicyldehyde and O, O-dimethyl thiophospharamide and their complexes with Cu(II), Ni(II) and Zn(II) are effective chemicals to kill *Tetranychus bimaculatus* [102]. Transition metal complexes of Schiff base obtained from condensation of 4-aminoantipyrene and 2-aminobenzoic acid showed potent antibacterial activities against *E. coli*, *P.-aeruginosa*, *S. pyrogones* and *canadia* [103].

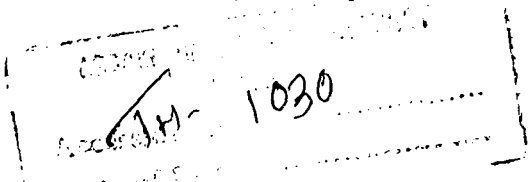

2.3.4 Antiviral activities

Schiff bases of gossypol show high antiviral activity [104]. Silver(I) complexes of glycine salicyldehyde Schiff bases gave effective results towards *Cucumber mosaic* virus [105]. Schiff bases of isoniazid also showed high levels of antitubercular activities against *Mycobacterium tuberculosis* [106].

2.3.5. Synergistic action on insectides

Schiff base derived from sulfane thiadizole and salicylaldehyde or thiophene-2-aldehydes and their complexes show toxicity against insects [107]. Fluorination on aldehyde part of the Schiff base enhances insectoacracicidal activity [108]. Schiff bases (thiadiazole derivatives with salicylaldehyde or vanillin) and their complexes with Mo(IV) show insecticidal activities against bollworm and cell survival rate of mung bean sproutsn [109].

2.3.6. Plant growth regulator

Schiff bases of esters and carboxylic acids show remarkable activities as plant growth hormone [110]. Schiff base of thiodiazole have good plant growth regulator activity towards auxin and cytokin [111].

2.3.7. Other therapeutic activities

Several Schiff bases posses anti-inflammatory, allergic inhibitors reducing activity, radical scavenging, analgesic and anti oxidative action [112-114]. Thiazole derived Schiff bases show analgesic and anti inflammatory activity [115]. Schiff bases N, N′-(Z-allylediene-1,3-diyl) bis amino acid methyl esters possess therapeutic actions for chronic pain and anti-inflamation [116]. Schiff bases of chitosan and carboxymethyl chitosan shows anti oxidant activity such as super oxide and hydroxyl scavenging [117]. Furan semicarbazone metal complexes exhibited significant anthelmintic and analgesic activities [118]. Hydroxy substituted Schiff bases obtained from corresponding aromatic aldehyde and aniline showed antioxidant effects against galvinoxyl radical and antiproleferative activities on human hepatoma HePG2 cells [119]. Iron(III) Schiff base complexes of arginine and lysine as netropsin mimics showing AT-selective DNA binding and photonuclease activity [120]. Oxovanadium(IV) complex of 2-(2-hydroxybenzylidene amino) phenol having phenanthroline bases was found to show DNA photo cleavage activity in near IR light and significant visible light induced induced phytotoxicity in human cervical cancer HeLa cells [121]. Oxovanadium(IV) complex with symmetrical tetradentate Schiff base obtained from the condensation of 2-hydroxybenzophenone with ethylenediamine or diethylenetriamine significantly increase glucose uptake when compared to basal glucose uptake in transformed and sensitized C1C12 cells, but not at the same level of insulin [122].

2.3.8. Antitumor and cytotoxic activities

Salicylediene anthranilic acid possess antiulcer activity [123] and complexation with copper enhances the same [124]. Some Schiff bases and their metal complexes containing Cu, Ni, Zn and Co were synthesized from salicylaldehyde, 2,4-dihydroxy benzaldehyde, glycine and L-alanine possess anti tumor activity and the order of reactivity is Ni>Cu.Zn>Co [125]. Amino acid Schiff bases derived from aromatic and heterocyclic amine possess high activity against human tumor cell lines [126]. Schiff base of indole-2-carboxaldehyde show inhibitor activities to K B Cell lines [127]. Complexes of rare earth ions with o-phenanthroline and Schiff base salicyldehyde L-phenylalanine could inhibit K562 tumor cells growth, generation and induce apoptosis [128].

2.3.9. Polymers

Photochemical degdration of natural rubber yield amine terminated liquid natural rubber (ATNR) when carried out in solution, in presence of ethylenediamine [128]. ATNR on reaction with glyoxal yield poly Schiff base which improves ageing resistance [128]. Organocobalt complexes with tridentate Schiff base act as initiator of emulsion polymerization and copolymerization of dienyl and vinyl monomers [129]. Vanillin Schiff bases have been proved to be an efficient thermal stabilizers and co-stabilizers for rigid polyvinyl chloride (PVC) [130]. The stabilizing efficiency of vanillinis attributed to the replacement of labile chlorine atom on PVC chain by a relatively more stable moiety of the organic stabilizer.

2.3.10. Dyes

Azo groups containing metal complexes are used for dying cellulose polyester textiles [131]. Cobalt complex of a Schiff base (salicylaldehyde with diamine) has excellent

light resistance and storage ability and does not degrade even in acidic gases. Tetradentate Schiff base acts as a chromogenic reagent for determination of Ni in some natural food samples [132].

2.3.11. Antifertility and enzymatic activity

Schiff bases of hydrazine carboxoamide and hydrazine and metal complexes of dioxo Mo(IV) and Mn(II) might alter reproductive physiology [133]. Schiff base linkage with pyridoxal 5-phosphate from lysine to alanine or histidine abolishes enzyme activity in protein [134].

2.4. Transition metal Schiff base complexes with particular reference to iron and vanadium

Transition metal complexes of Schiff base are becoming increasingly important as biochemical, analytical and antimicrobial reagents. Use of Schiff Bases as Fluorimetric analytical reagent is reported [134]. A colorimetric anion sensor was developed using the Schiff base obtained from the condensation of salicyldehyde and 2-amino-4-nitrophenol under micrpwave irradiation [135]. Binapthyl derived salicylidene Schiff base could be used as colorimetric naked eye and fluorescent chemosensor for detection of Cu^{2+} and Zn^{2+} ions [136]. Non-ionic Schiff base amphiphilies of p-aminobenzoic acid could serve as effective corrosion inhibitors for aluminium in acidic medium [137]. The design, synthesis and characterization of iron complexes with Schiff base ligand, however, play a relevant role in the coordination chemistry of iron due to their importance as synthetic models for the iron containing enzymes [138], oxidation catalysts [139-141] and bistable molecular materials based on temperature, pressure or light induced spin crossover behaviour [142]. Considerable attention has been devoted in recent years to the study of mixed-ligand complexes of transition metals containing nitrogen donor ligands [143, 144]. Their potential applications like separation materials,

catalysis precursors, potential models of the catalyse enzymes and their interesting structures has spurred extensive research in this field [145-148]. The mixed-ligand complexes containing N, O, and/or S donor atoms are important owing to their significant antifungal, antibacterial, and anticancer activity [149]. Schiff base metal complexes, prepared *in situ* or isolated as stable compounds are considered as simple and suitable candidate for catalytic application. Use of iron-Schiff base complexes in different catalytic reactions have been dealt with in some recent works [150-152]. Iron complex with a tridentate Schiff base, accessed *in situ* from $[Fe(acac)_3]$ has been shown to act as catalyst for enantioselective oxidation of sulfides to sulfoxides [153]. Synthesis of a mixed-ligand unsymmetrical tridentate Schiff base donor complex of iron(III), $[FeL(acac)(C_2H_5OH)]$ has recently been accomplished from the reaction of $[Fe(acac)_3]$ with the corresponding Schiff base and the performance of this complex in sulfide oxidation catalysis has also been assessed [154]. Reactions of $[Fe(acac)_3]$ with hydrogen halide (HX) to access newer mixed halo acctylacetonato iron(III) complexes have also been documented [155]. Solvent molecules usually bound to metal acetylacetonates are readily exchanged with neutral N-donor molecules such as ammonia, pyridine, imidazole, etc. to yield complexes of interesting structural and chemical properties [156].

The coordination chemistry of vanadium has attracted considerable attention of bioinorganic and coordination chemists because of the discovery of enzymatic [157] and physiological activities [158] of its compounds. EXAFS measurements on a vanadium containing enzyme bromoperoxidase, obtained from the marine brown alga Ascophyllum nodosum suggest that the catalytically active center contains a mononuclear oxovanadium(V) species coordinated by six O/N atoms [159]. The potential catalytic ability of vanadium compounds has lead to an increasing interest in

vanadium coordination chemistry [160]. A variety of oxovanadium complexes with Schiff base have been shown to catalyze the oxidation of sulfides [161], alcohols [162] and alkenes [163-165] by several oxidant, such as dioxygen (O_2), hydrogenperoxide (H_2O_2), and tert-butylhydroperoxide (TBHP). Further, oxovanadium (IV)-[N_2O_2] Schiff base complexes have been shown to exhibit insulin-mimetic activity [166].

[$VO(acac)_2$] serves as a good precursor in the synthesis of Schiff base complexes and undergoes ligand exchange reactions where one or both acetylacetonato groups can easily be exchanged with organic ligands having coordinating atoms of different potentialities. Depending upon reaction conditions, solvents and ligands used the complexes may adopt $[VO]^{2+}$, $[VO]^{3+}$, $[VO_2]^{+}$ or $[V_2O_3]^{4+}$ core with different structures. Other precursors such as the vanadate ion are only suitable for water soluble ligands and thus prevents its use in non-aqueous solvents while $VOSO_4$ can be used in aqueous as well as non-aqueous medium [167, 168]. $VO(OEt)_3$ or $VO(OiPr)_3$ requires their in situ generation and use under anhydrous condition in absolute alcohol [169, 170]. A review article by M.R. Maurya [171], rather exhaustively discussed the synthesis, structure, reactivity and coordination chemistry of oxovanadium(IV) and dioxovanadium(V) complexes developed through bis(acetylacetonato) oxovanadium(IV), [$VO(acac)_2$].

2.5. Complexes of macrocyclic Schiff bases

Macrocyclic Schiff base complexes are extensively studied from the viewpoint of molecular recognition, artificial catalyst and supramolecular structures [172] and there is continued interest in macrocyclic complexes because of their potential applications in fundamental and applied sciences [173] and importance in the area of coordination chemistry. Macrocyclic ligands form metal complexes, which in general are more stable than the complexes with analogous open chain ligands [174]. Such ligands have long

been employed as selective host for a wide variety of guest molecules and ions. The recognition of a metal ion by a macrocyclic ligand and modification of the properties of resulting complex is closely related to metal ion size compatibility with the ligand cavity. The high selectivity and strong coordination ability of the macrocyclic ligand towards transition metal ion have attracted considerable attention because of the wide range of applications as biomimmetic models for metalloprotiens [175] and metalloenzymes, as electron carriers in redox reactions [176], as dioxygen carriers [177], as ionophores in a number of biochemical processes [178], as antitumour drugs [179], as MRI contrast agents [180] and in radiopharmaceutical chemistry [181]. Condensation between dicarbonyl and diamine has played a vital role in the development of synthetic macrocyclic ligands, which have been proved to be a fruitful source of tetraazamacrocycles [182].

2.6. Synthetic importance of Schiff bases

Besides potential applications in the field of catalysis and pharmaceuticals, Schiff bases have various synthetic uses in organic chemistry. Acylation of Schiff bases [183] by acid anhydrides, acid chlorides and acyl cyanide leads to net addition of the acylating agent to the carbon-nitrogen double bond. Reactions of this type have been put to good use in natural product synthesis. The base catalysed condensation of acetyl chlorides (bearing an electron withdrawing group and at least one hydrogen atom at the α-position) with N-arylaldimines occurs by initial acylation at the nitrogen atom leading to formation β-lactum, which is of interest in penicillin chemistry (Scheme 2.1).

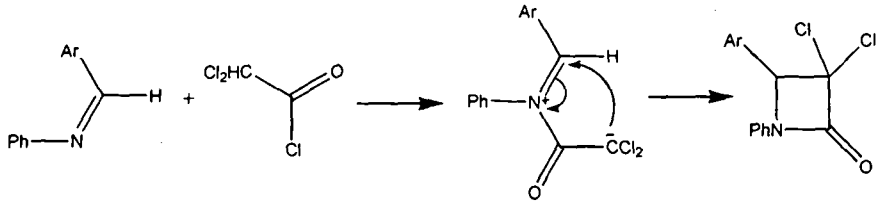

Scheme 2.1

Alkoxides add to schiff bases giving corresponding α-alkoxy amino compounds. This type of addition provides the key step in an elegant 'one-pot' stereospecific synthesis of penicillin intermediates that can be further elaborated to new cephalosporin derivatives [184].

Reaction of Schiff bases with primary amines results in adducts which tends to decompose to a new imine and primary amine, the overall process corresponding to imine exchange [185]. The rate of imine exchange increases with increase in the basicity of primary amine. Iminium salts also readily add primary, secondary and tertiary amines with the formation of aminals (gem- diamino compounds) or their quarternary salts [186].

Schiff bases react in general with ethereal solutions of chloramines in few hours at room temperature to give moderate to high yields of diaziridines (Scheme 2.2). This formal cycloaddition reaction has wide scope and is applicable to a variety of Schiff bases derived from aldehydes and cyclic or acyclic ketones. Diazidine formation is believed to result from initial nucleophilic addition to the carbon-nitrogen double bond followed by eliminative ring closure.

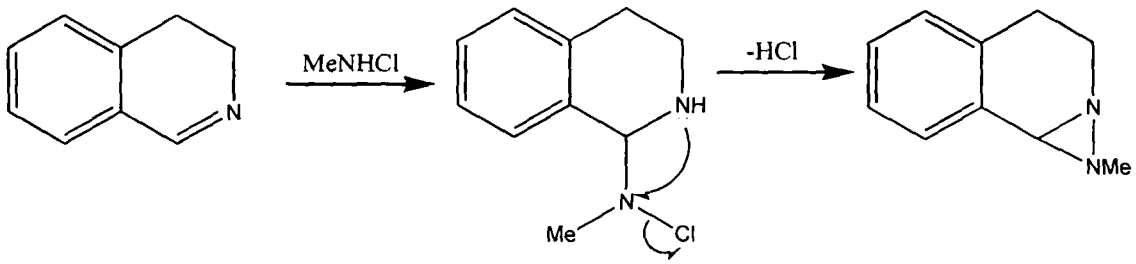

Scheme 2.2

The addition of hydrogen cyanides to schiff bases occurs readily and provides a viable route to α-aminonitriles, which can in turn be used as the precursors for the synthesis of amino acids (Strecker synthesis) [187]. This reaction is usually carried out using anhydrous hydrogen cyanide in inert solvents such as ether or benzene. Now a days

trimethyl silyl cyanide has been recommended as a safer alternative to hydrogen cyanide in the Strecker synthesis.

Schiff bases lacking hydrogen atom at the α-position to the carbon-nitrogen double bond react with Grignard or organolithium reagents analogously to carbonyl compounds forming adducts which on hydrolysis produce secondary amines in excellent yield (Scheme 2.3). Reactions occur best with arylaldimines and provided the general methods for the synthesis of secondary amines.

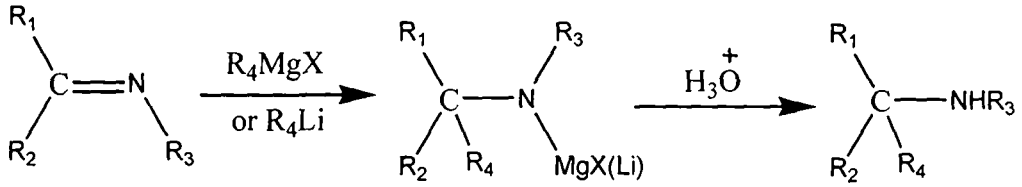

Scheme 2.3

Schiff bases incapable of enolization (i.e. lacking α-hydrogen atoms) also reacts with Reformatsky reagents with stereospecific addition to the carbon-nitrogen double bond to give erythro-β-amino esters which can be isolated at low temperature (-10^{0}C) but otherwise spontaneously cyclize, providing a useful synthetic route to β-lactams [188].

The carbon-nitrogen double bond of the Schiff bases like carbon-oxygen double bond, readily participates in condensation reaction of the Aldol type. Schiff bases in general, and N-substituted arylaldimines react readily with active methylene compounds under a variety of conditions to give adducts that leads to formation of corresponding alkenes (Scheme 2.4).

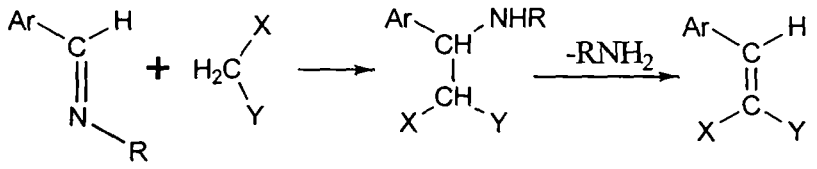

Scheme 2.4

Reactions of anils with carbonyls stabilised sulphonium ylides also provide a useful method for the synthesis of β-aminoalkenyl carbonyl compounds [189]. These reactions involve initial nucleophilic addition followed by ring closure and subsequent ring opening of an aziridine intermediates.

[1+2] cycloaddition reactions of carbenes and carbenoids to Schiff bases are well documented [190] and constitute the useful method for the synthesis of aziridines. In its simplest form this type of cycloaddition is exemplified by the reaction of benzylideneaniline with dichlorocarbene to give 2,2-dichloro-1,3-diphenylaziridine (Scheme 2.5). The technique of phase transfer catalysis has been successfully applied to such reactions and it has been demonstrated that dichlorocarbene is 1.65 times more reactive towards a carbon-nitrogen double bond than a comparable carbon-carbon double bond.

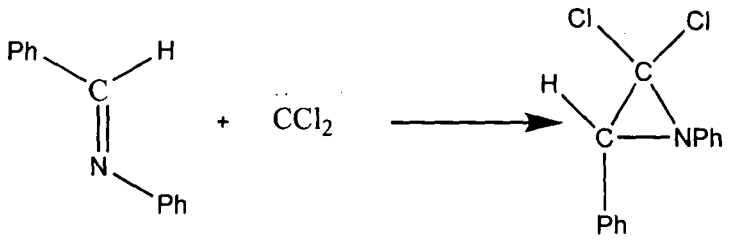

Scheme 2.5

Cycloaddition of Schiff bases to ketenes is highly stereoselective [191] implying a concerted process. However, a two step mechanism involving a dipolar intermediate (Scheme 2.6) adequately accounts for the observed stereoselectivity and is strongly supported by mechanistic studies of β-lactum formation from Schiff bases and ketenes [192].

Schiff bases react readily with diazoalkanes in presence of catalytic amounts of methanol or water to afford Δ^2-1,2,3-triazolines (Scheme 2.7). Electron withdrawing

groups on the Schiff base promote this cycloaddition while electron donating groups hinder it [193].

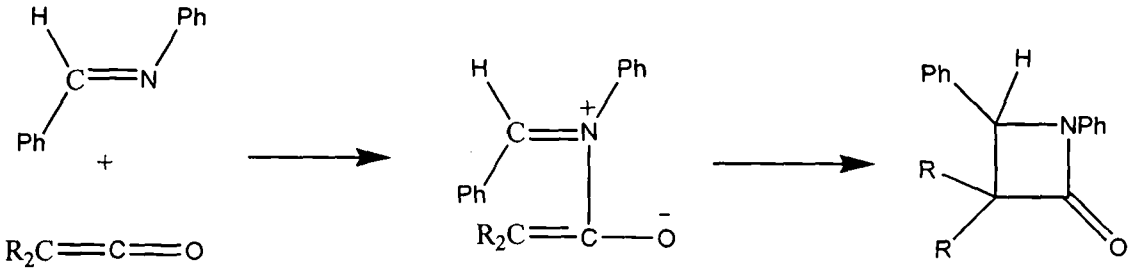

Scheme 2.6

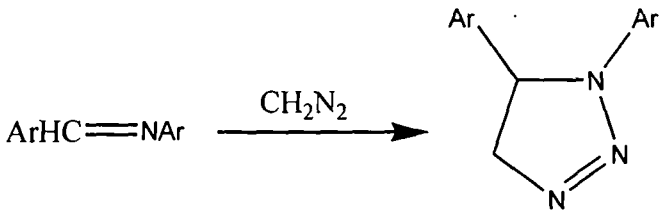

Scheme 2.7

The uncontrolled oxidation of Schiff base with peroxy acid results in cleavage of carbon-nitrogen double bond to give a carbonyl compound and a nitroso compound respectively [183]. On the other hand, oxidation using peroxy acid at low temperature affords an excellent synthetic route to oxaziridines (Scheme 2.8) [183, 194].

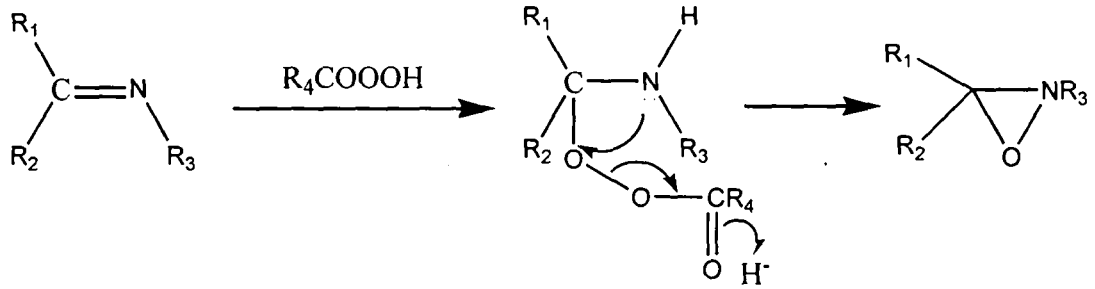

Scheme 2.8

Peroxy acid oxidation of Schiff base (derived from primary amine and heterocyclic aldehyde) to an oxaziridine followed by base catalysed rearrangement has been shown to provide a model (Scheme 2.9) for the pyridoxal pyrophosphate mediated enzymatic

oxidative deamination of α-amino acids to pyruvic acids, which find analogy in the well known double bond transposition of allylic alcohols via oxiran intermediates [195].

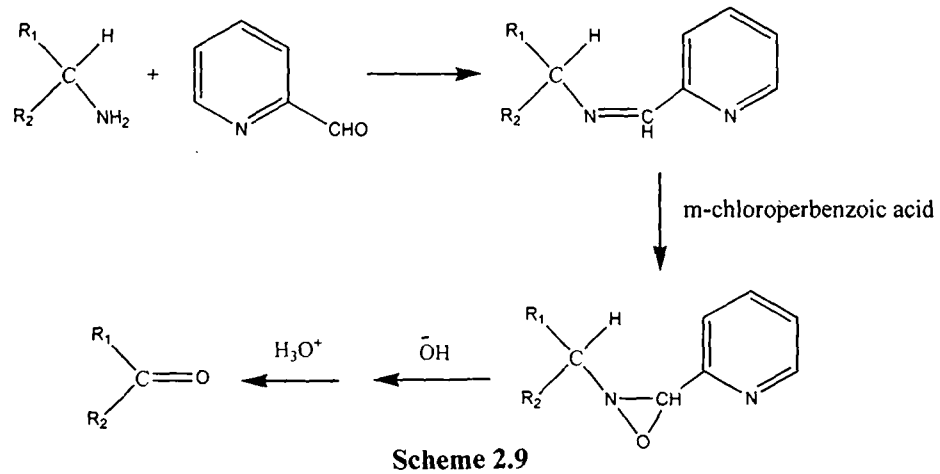

Scheme 2.9

The oxidation of Schiff bases (simple anils) by lead tetra acetate (LTA) results formation of aldehyde, arylamine and the corresponding azobenzene derivative [196]. Formation of amine and the azobenzene derivative has been attributed to the involvement of a nitrene intermediate produced by ionic breakdown of an initially formed lead derivative. Schiff bases having a hydroxyl or an amino group at the ortho position of the N-aryl ring leads to formation of heterocycle upon LTA oxidation (Scheme 2.10) [197].

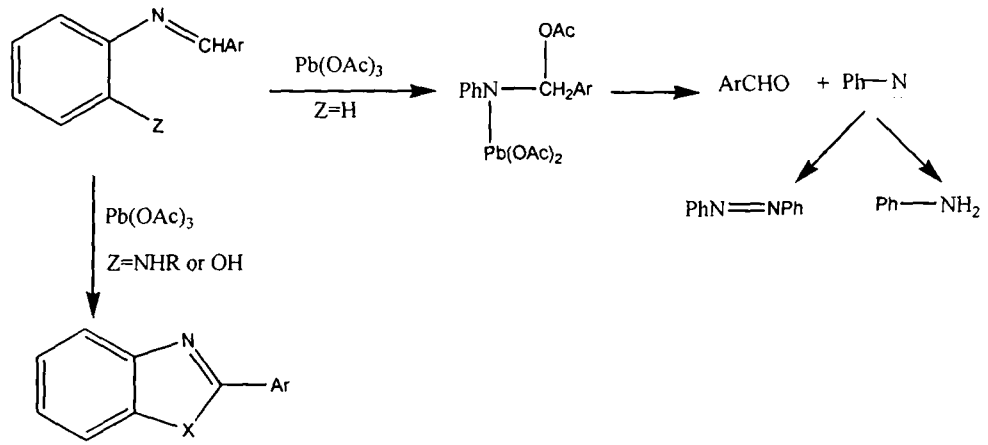

Scheme 2.10

The reactivity of carbon-nitrogen double bond towards a reducing agent is similar to that of a carbon-oxygen double bond. Reducing agents like sodium, sodium amalgam,

magnesium, aluminium in ethanol, zinc in acetic acid smoothly reduce Schiff bases to the corresponding amines [183]. Like carbon-oxygen double bond, the carbon-nitrogen double bonds of the Schiff bases are also readily hydrolysed by complex metal hydrides [198]. Thus lithium aluminium hydride in THF at room temperature reduces Schiff bases to secondary amines. Sodium borohydride is an equally effective reducing agent and is preferred over lithium aluminium hydride because of its inertness to a wider range of solvents and greater specificity. An even more effective reducing agent of this type is sodium cyanoborohydride ($NaBH_3CN$).

Schiff bases are readily reduced to amines by hydrogenation over nickel, platinum and chromium catalysts [183, 199]. Thus anils are reduced to secondary amines in essentially quantitative yield by hydrogenation over a platinum catalyst at 60^0C. Asymmetric induction has also been observed in catalytic hydrogenation of schiff bases and leads to chiral amines in good yield [200]. A new method for the efficient conversion of Schiff bases into amines under mild conditions involve reduction with alkyl silanes in presence of transition metal catalysts such as $PdCl_2$, $(Ph_3P)_3RhCl$ etc. [201].

A lot of current literature addresses rather exhaustively several aspects of metal-Schiff base complexes [202-208].

CHAPTER 3

EXPERIMENTAL

3.1. Chemicals and materials

1. 2,4-dihydroxybenzaldehyde, 2-hydroxy-1-napthaldehyde, 1-bromododecane and 1-bromotetradecane were obtained from Aldrich Chemical Company and used without further purification.
2. 2-aminophenol, 2-aminobenzoic acid, *o*-phenylenediamine and benzil were obtained from Qualigens fine chemicals, India and recrystallized before use.
3. Acetylacetone and furfuraldehyde were purchased from E-Merck, India and distilled before use.
4. Ethylenediamine, ammonium thiocyanate, sodium azide, ammonium bifluoride, triphenyl phosphine, imidazole, benzimidazole and pyridine is procured from Sd-fine chemicals and used as received.

5. *p*-Anisidine, *p*-toludine and benzoin were purchased from Fischer Scientific and recrystallised before use.
6. Anhydrous ferric chloride ($FeCl_3$), hydrated ferric nitrate [$Fe(NO_3)_3.9H_2O$] and vanadyl sulphate pentahydrate ($VOSO_4.5H_2O$) were obtained from S.D. fine chemicals and used as metal source for complexation with iron(III) and vanadyl(IV). Iron acetylacetonate [$Fe(acac)_3$] and vanadyl acetylacetonate [$VO(acac)_2$] were prepared following literature method [209] and also used for complexation with Schiff base ligands.
7. Ethanol and methanol used as solvent were purified by standard process.
8. Silica gel [(60–120 mesh) was used for chromatographic separation. Silica gel G [E-Merck (India)] was used for TLC.
10. Micobial ATCC strains for *Klebsiella pneumoniae, Staphylococcus aureus, Pseudomonas aeroginosa, Escherichia coli, Bacillus subtilis* and *Proteus vulgaris* were obtained from the Biotechnology Department of Assam University and these were cultured on agar agar medium.

3.2. Physical measurements and equipments used

1. Elemental analysis

Micro analytical (C, H, N) data were obtained with a Perkin-Elmer Model 240C elemental analyzer, from Central Drug Research Institute, Lucknow.

2. FT-IR

Infrared spectra of the ligands and complexes were recorded on a spectrum BX series FT-IR spectrophotometer / PERKIN ELMER spectrum RX1 spectrophotometer by using KBr pellets in the region 400-4000 cm^{-1}.

3. UV-VISIBLE

Electronic spectra of the ligands and complexes (10^{-4} M solution) were recorded on a Shimadzu 1601 PC UV-VIS spectrophotometer in 200-800 nm range.

4. NMR

The ^{1}H and ^{13}C NMR spectra of the ligands were acquired from Bruker Advance 300 MHz FT NMR Spectrometer using TMS as internal standard.

5. Mass spectra

Mass spectra were recorded on a ZQMS 4000 LC-MS spectrometer / JEOL SX-102 Mass spectrometers with ESI / fast atom bombardment (FAB).

6. Single crystal XRD study

A light yellowish crystal of the Schiff base L_9 was obtained when the methanolic solution was allowed to slowly evaporate for a few weeks. The X-ray data of the crystal was collected with a BRUKER SMART CCD diffractometer equipped with a normal focus, 2.4 KW sealed tube X-ray source with graphite monochromated Mo-$K\alpha$ radiation (λ = 0.71073 Å) operating at 50 kV and 30 mA at 295 K.

7. Thermal microscopy and differential scanning calorimetry

The textures of the mesophases were studied with NIKON ECLIPSE LV 100 POLARIZING OPTICAL MICROSCOPE fitted with hot stage. The enthalpy changes associated with the phase transition were recorded on a PERKIN ELMER PYRIS 1 DIFFERENTIAL SCANNING CALORIMETR.

8. Antimicrobial studies

Selected compounds were screened for their *invitro* antimicrobial activities against various microbial strains viz. *Klebsiella pneumoniae, Staphylococcus aureus, Pseudomonas aeroginosa, Escherichia coli, Bacillus subtilis* and

Proteus vulgaris by **Kirby-Bauer disc diffusion method** using ethanol as solvent as well as control and tetracycline as standard drug. To obtain bacteria in the mid-logarithmic phase 100 µl of an overnight culture made in nutrient broth was added to 10 ml of nutrient broth and incubated for 5 hours at 37^0C with orbital shaking for each strain. The strains were separately plated on nutrient agar media by pour plate method. The test samples were then dissolved in ethanol at a concentration of 50 µg/ml and adsorbed on the sterile paper discs. The discs were placed on the agar medium and the plates were incubated at 37^0C for 24 hours. The resulting inhibition zones on the plates were measured after 24 hours. The tests were carried out in triplicate and the results were expressed as mean.

9. Electrochemical behavior

Electrochemical behaviour of the representative compounds were studied by Cyclic Voltammetric technique at room temperature in acetonitrile for ca.

1X 10^{-3} mol dm^{-3} using n-Bu_4NClO_4 as supporting electrolyte under a dry N_2 atmosphere on a PC controlled CHI model 660C electrochemistry system. A Pt disk, a Pt wire auxiliary electrode and an aqueous saturated calomel electrode (SCE) were used in a three electrode configuration.

10 .Thermal investigations

T.G.A., D.T.G. and D.T.A. data were recorded on a PYRIS DIAMOND thermal analyzer under a dynamic flow of nitrogen (100 ml/min) and heating rate of 10^0C/min from ambient temperature to 1000^0C. The number of decomposition steps was identified with d,t,g.

11. Magnetic susceptibility measurements

Magnetic susceptibility of the complexes were measured at room temperature by employing a Lakeshore 7407 Vibrating Sample Magnetometer. The magnetization vs magnetic field were measured in the range −20000 to +20000 Gauss.

12. DFT (Density Functional Theory) STUDIES

Optimised geometry, single point energy and vibrational frequencies of the selected compounds were computed theoretically at B3LYP level by DFT method using 6-31G* basis set with the help of GAUSSIAN 03 program.

CHAPTER 4

SYNTHESIS OF LIGANDS

The general route for synthesis of Schiff base ligands involve condensation of aldehydic compounds with primary amines in presence of catalytic amounts of acetic acid. Variation in the structure of the aldehydic compounds and amines produce various kinds of Schiff bases that differ in their denticity, redox behaviour, catalytic ability etc. Depending upon the nature and substituent of the carbonyl compounds or amines, Schiff bases may be of bidentate, tridentate, tetradentate, pentadentate, hexadentate etc. Some of the Schiff bases may behave like a binucleating ligands.

This chapter describes the synthetic route to various types of Schiff bases. The aldehydes or ketones used for synthesising the ligands:

1. Benzil
2. 2,4-dihydroxy benzaldehyde
3. Acetylacetone
4. 2-hydroxy-1-napthaldehyde

5. Benzoin
6. Furfuraldehyde

Primary amines used for preparation of Schiff bases are-

1. *p*-anisidine
2. *p*-toludine
3. *o*-aminophenol
4. *o*-aminobenzoic acid
5. *o*-phenylenediamine
6. ethylenediamine

4.1 Synthesis of bidentate Schiff base ligands derived from Benzil (L_1 and L_2).

[N, N] donor bidentate Schiff base ligands were obtained from condensation of benzil and *p*-anisidine or *p*-toludine (Scheme 4.1)

p-anisidine (10 mmol, 1.23 g) or *p*-toludine (10 mmol, 1.07 g) was dissolved in dry ethanol and then added to an ethanolic solution of benzil (5 mmol, 1.05 g) containing few drops of acetic acid and the mixture was refluxed for 4 hours. The solvent was then removed on rotary evaporator and the residue crystallized at room temperature. The yellow crystals so obtained were recrystallized from ethanol. Yield ~75%.

4.2 Synthesis of chiral mesogenic Schiff base ligands (L_3 and L_4).

[ONO] donor tridentate mesogenic Schiff base ligands were prepared from condensation of 4-alkoxysalicyldehyde and 2-aminophenol. The methodology for the synthesis of the compounds are depicted in Scheme 4.2.

Synthesis of 4-alkoxysalicyldehyde

4-alkoxysalicyldehyde derivatives were prepared following the general methods reported in literature [210]. 2,4-Dihydroxybenzaldehyde (10 mmmol, 1.38g), $KHCO_3$ (10 mmol, 1.00g), KI (catalytic amount) and 1-Bromododecane (10 mmmol, 2.49g) or

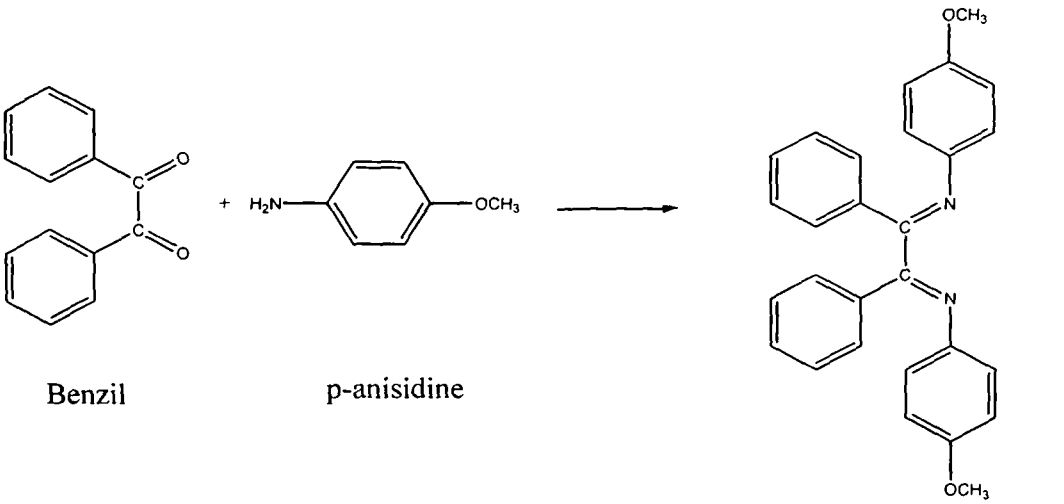

Benzil p-anisidine

Schiff base (L_1)

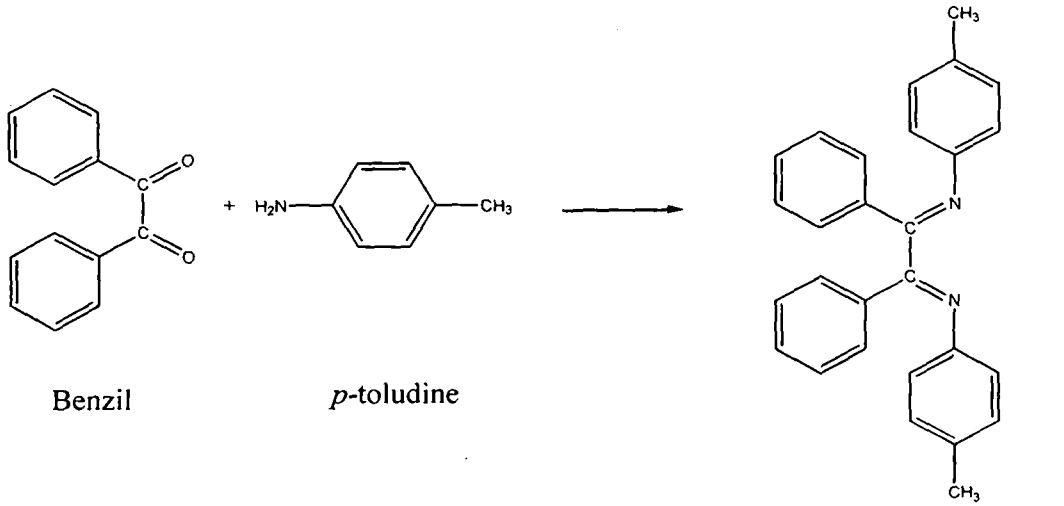

Benzil *p*-toludine

Schiff base (L_2)

Scheme 4.1

1-Bromotetradecane (10 mmol, 2.77g) were mixed in 250 ml of dried acetone under a nitrogen atmosphere. The mixture was heated under reflux for 24 hours, then filtered while hot to remove insoluble solids. Dilute HCl was then added to neutralize the warm solution, which was then extracted twice with chloroform (100 ml). The combined chloroform extracts were concentrated to give a purple solid. The solid was purified by

column chromatography eluting with a mixture of chloroform and hexane (V/V, 1/1). Evaporation of the solvents gave the product as a white solid.

Synthesis of N-(2-hydroxyphenyl)-4-alkoxysalicylaldimine

2-aminophenol (1.09 g, 10 mmol) in 10 ml of dried ethanol was added drop by drop to a warm solution of 4-dodecanoxy salicyldehyde (3.06 g, 10 mmol) or 4-tetradecanoxy salicyldehyde (3.34 g, 10 mmol) containing few drops of acetic acid. The reaction mixture was heated under reflux for 3 hours. The yellow product so obtained was collected and recrystallised from ethanol. Yield ~ 70%.

A similar kind of Schiff base (L_3' and L_4') was prepared from condensation of aniline with 4-dodecanoxy salicyldehyde and 4-tetradecanoxy salicyldehyde in ~ 70% yield.

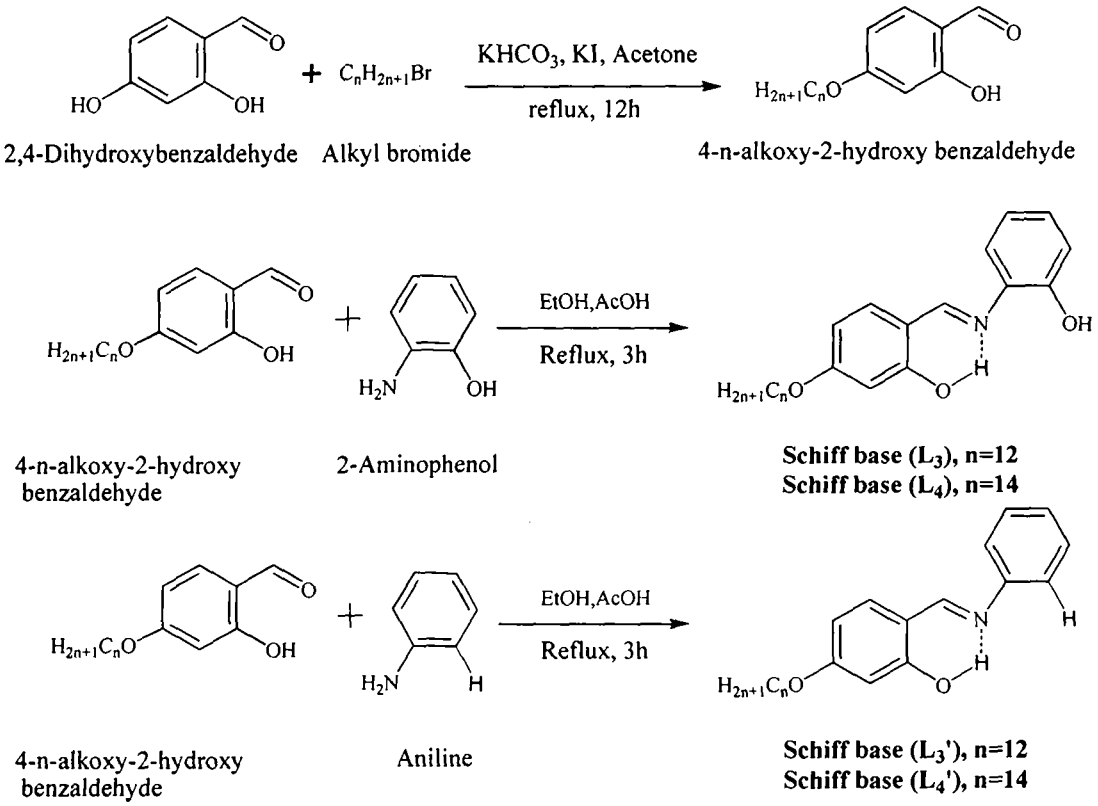

Scheme 4.2

4.3. Synthesis of [ONO] donor tridentate Schiff base ligand.

(a) *Derived from acetylacetone and 2-aminophenol or 2-aminobenzoic acid (**L_5** and **L_6**).*

2-aminophenol (10 mmol, 1.09 g) or 2-aminobenzoic acid (10 mmmol, 1.37 g) was dissolved in dry ethanol and then added to an ethanolic solution of acetylacetone (10 mmol, 1.00 g) containing few drops of acetic acid and the mixture was refluxed for 4 hours. The solvent was then removed on rotary evaporator and the residue crystallized at room temperature. The yellow crystals so obtained were recrystallised from methanol (Scheme 4.3). Yield ~ 70%.

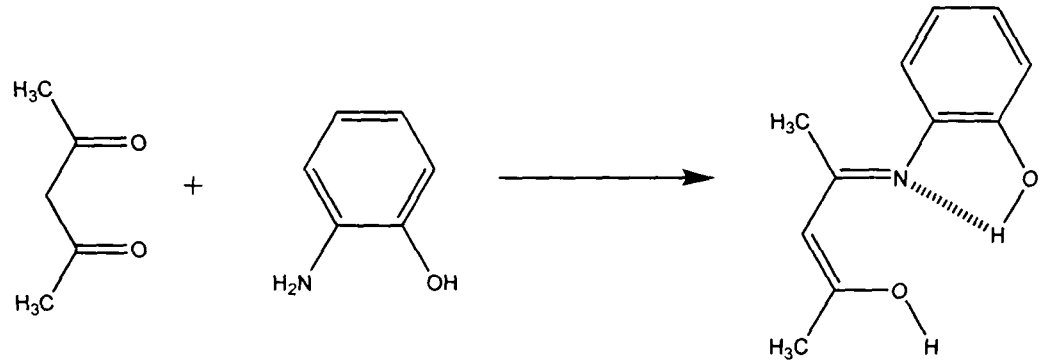

Acetylacetone 2-Aminophenol **Schiff base (L_5)**

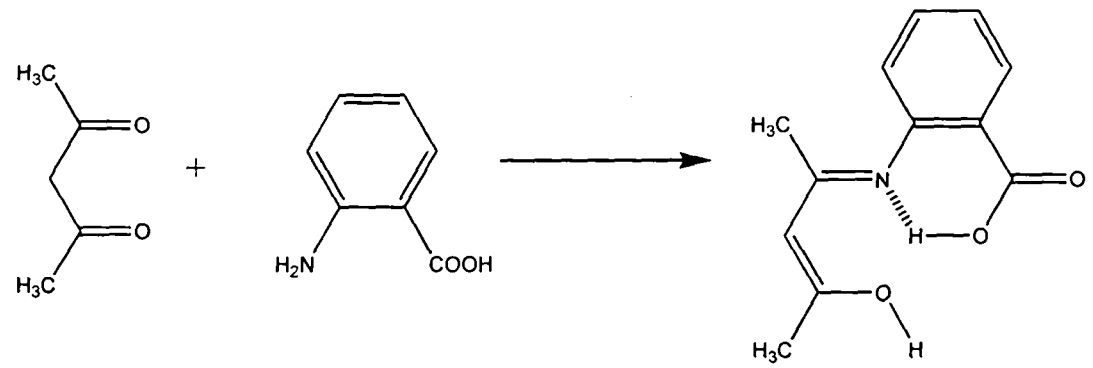

Acetylacetone 2-Aminobenzoic acid **Schiff base(L_6)**

Scheme 4.3

(b) *Derived from 2-hydroxy-1-napthaldehyde and 2-aminophenol or 2-aminobenzoic acid (**L_7 and L_8**).*

2-aminophenol (10 mmol, 1.09 g) or 2-aminobenzoic acid (10 mmol, 1.37 g) was dissolved in dry ethanol and then added to an ethanolic solution of 2-hydroxy-1-napthaldehyde (10 mmol, 1.72 g) containing few drops of acetic acid and the mixture was refluxed for 4 hours. The solvent was then removed on rotary evaporator and the residue crystallized at room temperature. The orange (L_7) or yellow (L_8) crystals so obtained were recrystallised from methanol (Scheme 4.4). Yield ~ 75%

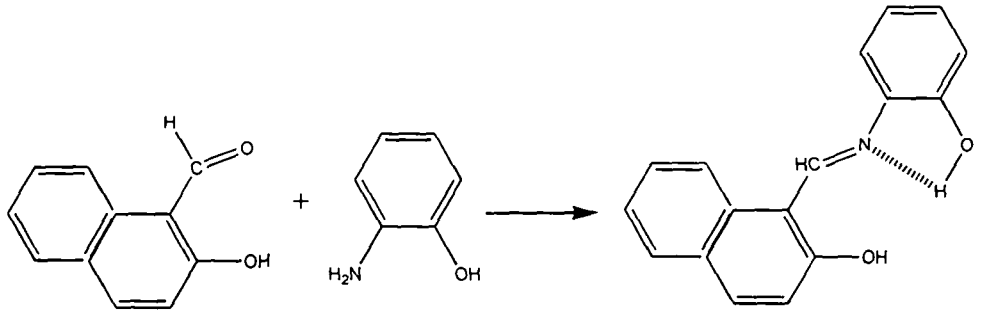

2-Hydroxy-1-napthaldehyde 2-Aminophenol **Schiff base (L_7)**

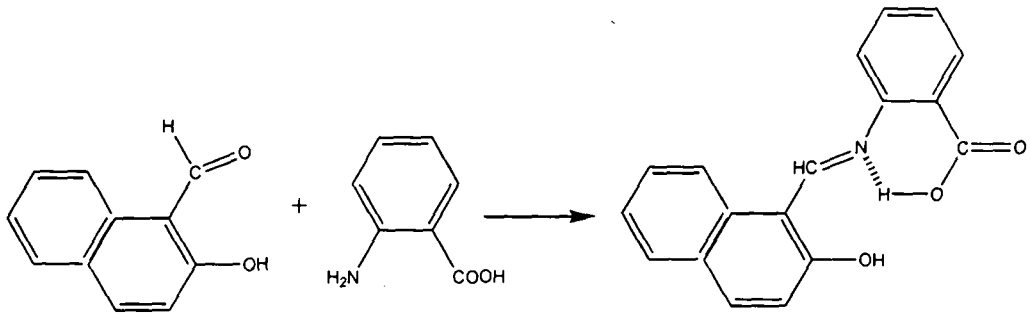

2-Hydroxy-1-napthaldehyde 2-Aminobenzoic acid **Schiff base (L_8)**

Scheme 4.4

4.4. Synthesis of [NNOO] donor tetradentate Schiff base ligand.

(a) *Derived from acetylacetone and ethylenediamine (L_9).*

Tetradentate Schiff base ligand bis(acetylacetonato)ethylenediamine (L_9) was obtained by the reaction of acetylacetone and ethylenediamine following the methods reported in literature [211]. Acetylacetone (20 mmol, 2.00 g) and ethylenediamine (10 mmol, 0.6 g) in 60 cm^3 dry ethanol were refluxed for two hours in presence of few drops of acetic acid and cooled in a refrigerator. The resulting yellowish compound was precipitated, filtered and recrystallized from methanol (Scheme 4.5). Yield ~ 65%.

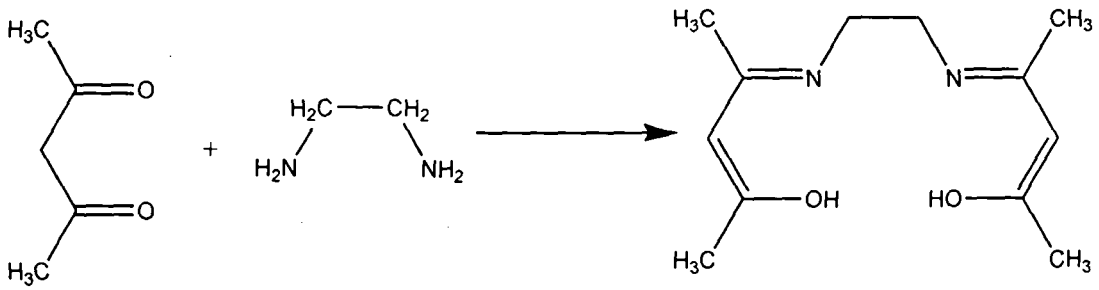

Acetylacetone Ethylenediamine Schiff base (L_9)

Scheme 4.5

(b) *Derived from furfuraldehyde and hydrazine (L_{10}).*

Hydrazine hydrate (10 mmol, 0.50 g) was dissolved in dry ethanol and then added to an ethanolic solution of furfuraldehyde (20 mmol, 1.92 g) containing few drops of acetic acid and the mixture was refluxed for 4 hours. The solvent was then removed on rotary evaporator and the residue crystallized at room temperature. The yellow crystals so obtained were recrystallised from ethanol (Scheme 4.6). Yield ~ 70%.

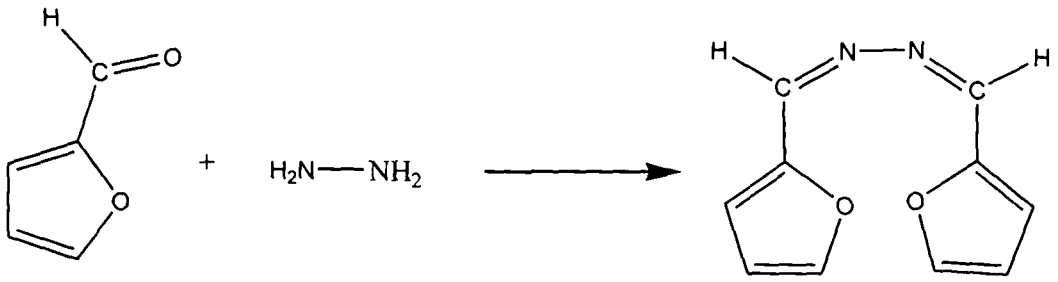

Furfuraldehyde Hydrazine Schiff base (L_{10})

Scheme 4.6

(c) Derived from 2-hydroxy-1-napthaldehyde and o-phenylenediamine or ethylenediamine (L_{11} and L_{12}).

A solution of *o*-phenylenediamine (10 mmol, 1.08 g) or ethylenediamine (10 mmol, 0.60 g) in dry ethanol is added to an ethanolic solution of 2-hydroxy-1-napthaldehyde (20 mmol, 3.74 g) containing few drops of acetic acid and the mixture was refluxed for 4 hours. The solvent was then removed on rotary evaporator and the residue crystallized at room temperature. The orange (L_{11}) or yellow (L_{12}) crystals so obtained were recrystallised from methanol (Scheme 4.7). Yield ~ 70%.

(d) Derived from benzoin and ethylenediamine or o-phenylenediamine (L_{13} and L_{14}).

A solution of *o*-phenylenediamine (10 mmol, 1.08 g) or ethylenediamine (10 mmol, 0.60 g) in dry ethanol is added to an ethanolic solution of benzoin (20 mmol, 4.24 g) containing few drops of acetic acid and the mixture was refluxed for 4 hours. The solvent was then removed on rotary evaporator and the residue crystallized at room temperature. The yellowish crystals so obtained were recrystallised from methanol (Scheme 4.8). Yield ~ 70%.

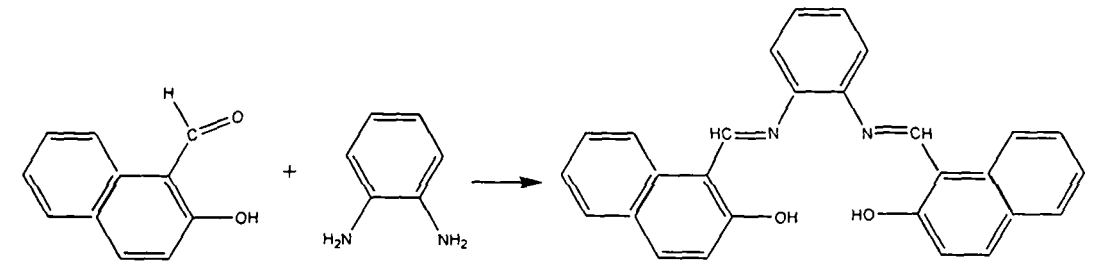

2-Hydroxy-1-napthaldehyde *o*-phenylenediamine **Schiff base (L_{11})**

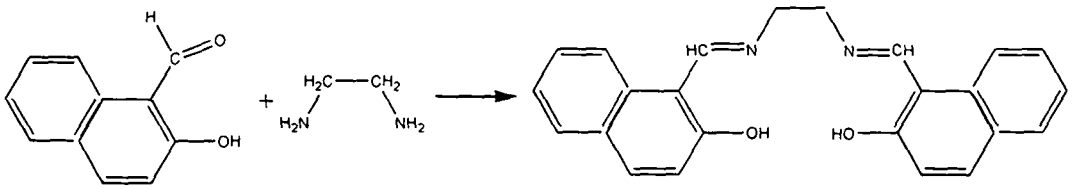

2-Hydroxy-1-napthaldehyde Ethylenediamine **Schiff base (L_{12})**

Scheme 4.7

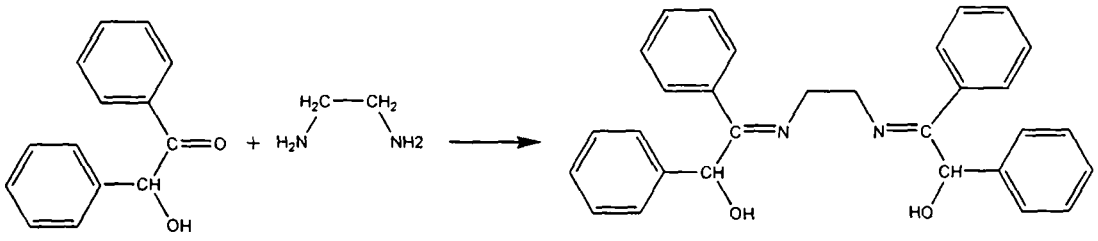

Benzoin Ethylenediamine Schiff base (L_{13})

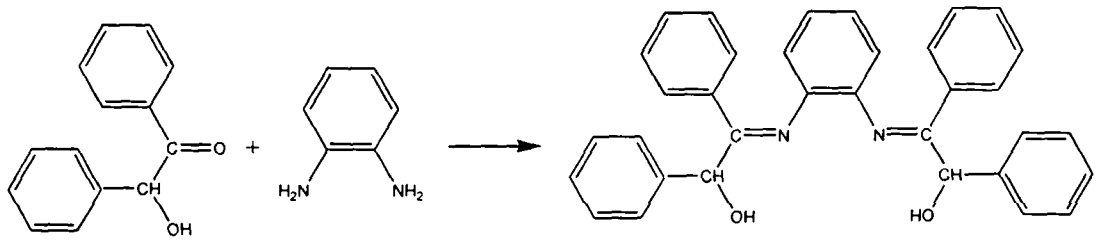

Benzoin *o*-phenylenediamine Schiff base (L_{14})

Scheme 4.8

4.5. Synthesis of 12-membered tetraimine macrocyclic Schiff base ligand (L_{15} and L_{16}).

Two tetraimine Schiff base macrocyclic ligands were prepared by the condensation of benzil and ethylenediamine or *o*-phenylenediamine in 1:1 molar ratio in methanolic medium as shown in Scheme 4.9. A methanolic solution (25 cm^3) of ethylenediamine (10 mmol, 0.60 g) or *o*-phenylenediamine (10 mmol, 1.08 g) was slowly added to a solution of benzil (10 mmol, 2.10 g) dissolved in 25 cm^3 of methanol with constant stirring in a 1:1 molar ratio. The solution was refluxed for 6 hours. The reaction mixture was then cooled resulting in a yellow solid product. The product was filtered, washed several times with methanol, recrystallized and dried in vacuum. Yield ~75%.

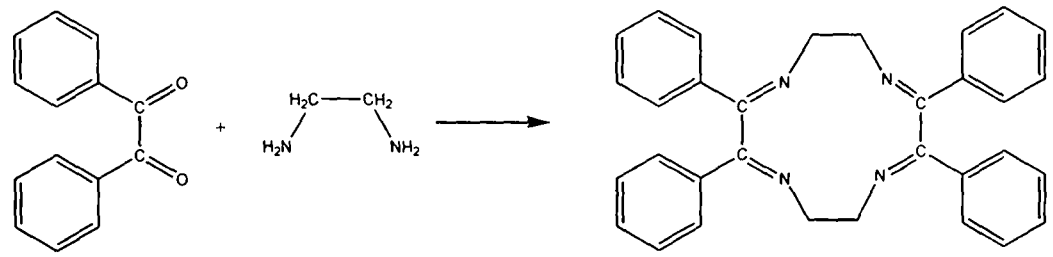

Benzil Ethylenediamine Schiff base (L_{15})

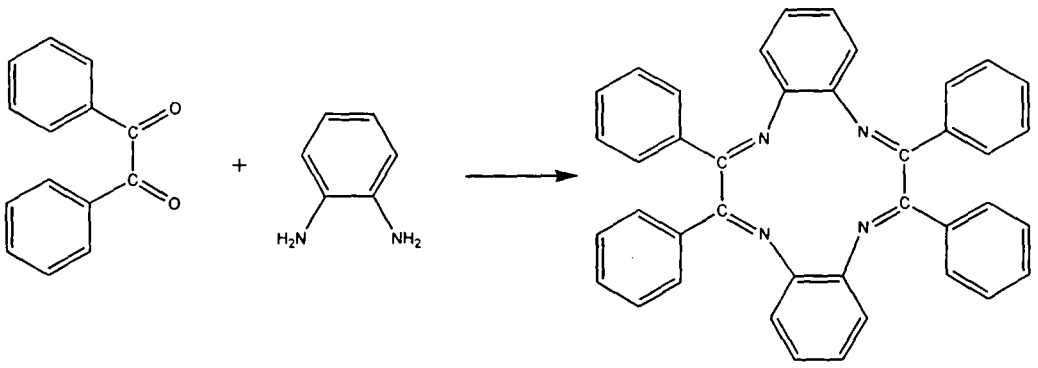

Benzil o-phenylenediamine Schiff base (L_{16})

Scheme 4.9

CHAPTER 5

SYNTHESIS OF COMPLEXES

This chapter describes the complexation of the Schiff base ligands with iron(II, III) and oxovanadium(IV, V). The general route for complexation involves reaction of the ligands with metal chloride, metal nitrate, metal sulphate and metal acetylacetonates. Complexation with iron was achieved using $FeSO_4.7H_2O$, anhydrous $FeCl_3$, hydrated $Fe(NO_3)_3$ or $[Fe(acac)_3]$ as metal source while oxovanadium(IV) complexes were prepared using $VO(acac)_2$ or $VOSO_4.5H_2O$.

5.1. Complexation of bidentate Schiff base ligands

5.1.1. Preparation of Fe(III) complexes, **$[Fe(L)_2(NO_3)_2]NO_3$ ($L=L_1$ or L_2; 1, 2)** with bidentate Schiff base ligands L_1 and L_2.

The ligand, $\mathbf{L_1}$ (1 mmol, 0.420 g) or $\mathbf{L_2}$ (1 mmol, 0.388 g) was dissolved in methanol (10 mL) and was added to a methanol solution (10 mL) of $[Fe(NO_3)_3].9H_2O$ (1 mmol, 0.404 g) and the mixture was refluxed for 4 h. After cooling, a dark brown microcrystalline solid was collected, washed with cold absolute ethanol, recrystallised and then dried at air (Scheme 5.1.a). Yield ~ 60%.

5.1.2. Preparation of VO(IV) complexes, **$[VO(L)_2]SO_4.H_2O$ (L=L_1 or L_2; 3, 4)** with bidentate Schiff base ligands L_1 and L_2.

A hot methanolic solution of $VOSO_4.5H_2O$ (1 mmol, 0.253 g) was added to a solution of the ligand **L_1** (1 mmol, 0.420 g) or **L_2** (1 mmol, 0.388 g) in dry ethanol and refluxed for 1 hour. The precipitated green complexes were filtered off, washed with cold ethanol, recrystallized and dried *in vacuo* (Scheme 5.1.b).Yield ~ 60%.

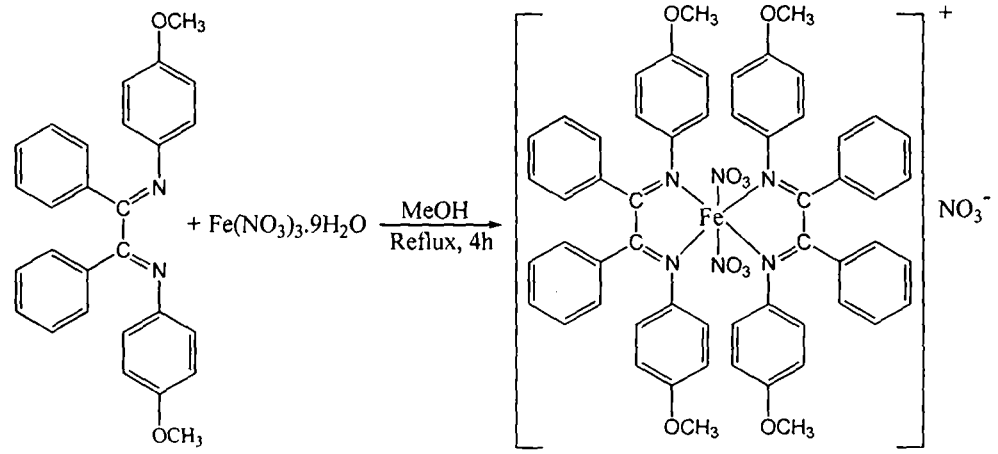

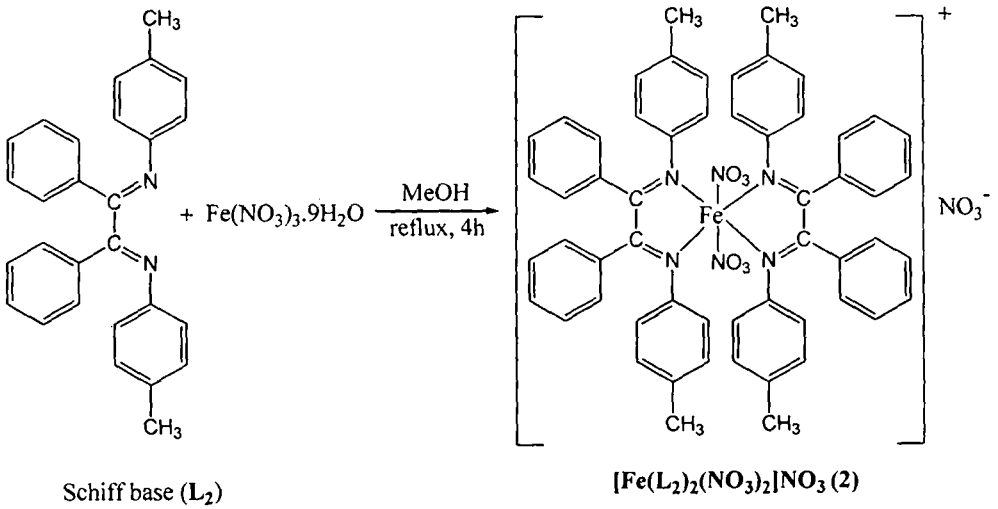

Scheme 5.1.a

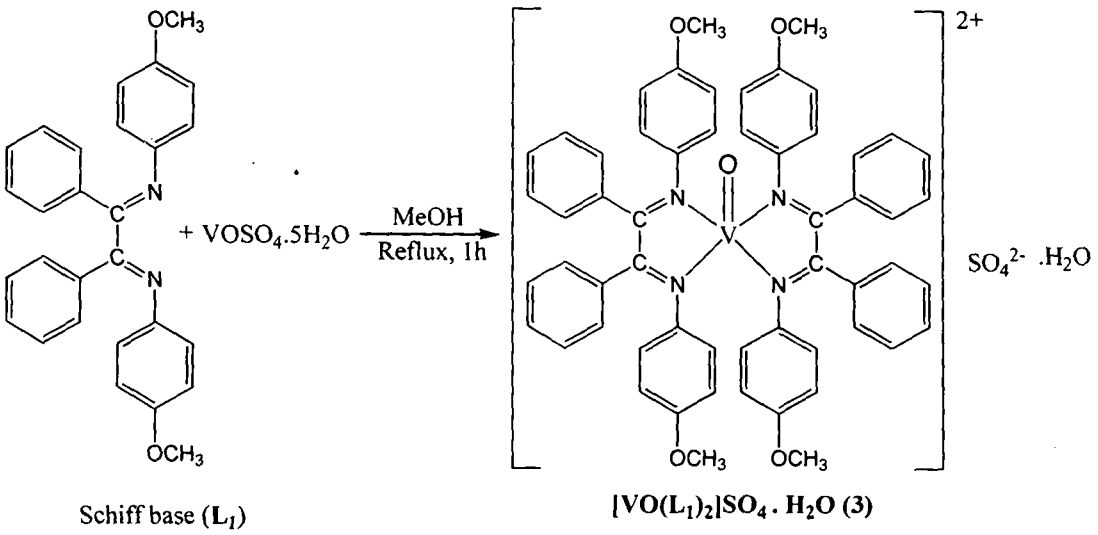

Schiff base (L_1)

$[VO(L_1)_2]SO_4 . H_2O$ (3)

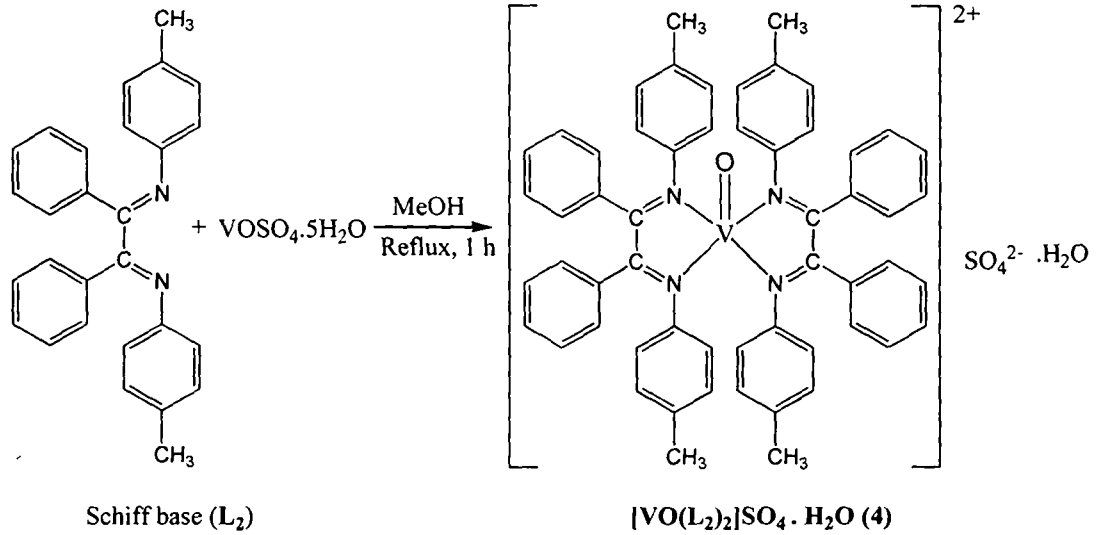

Schiff base (L_2)

$[VO(L_2)_2]SO_4 . H_2O$ (4)

Scheme 5.1.b

5.2. Complexation of tridentate Schiff base ligands

5.2.1. Preparation of binuclear Fe(III) complexes, **$[FeLCl]_2$ (L=L_3 or L_4; 5, 6)** with chiral mesogenic Schiff base ligands (L_3 and L_4).

An ethanolic solution of anhydrous $FeCl_3$ (1 mmol, 0.162 g) was added to a solution of the ligand **L_3** (1 mmol, 0.397 g) or **L_4** (1 mmol, 0.425 g) and refluxed over water bath for 3 hours. The precipitated brown complexes

were filtered off, washed with cold ethanol, recrystallized and dried *in vacuo* (Scheme 5.2.a). Yield ~ 60%.

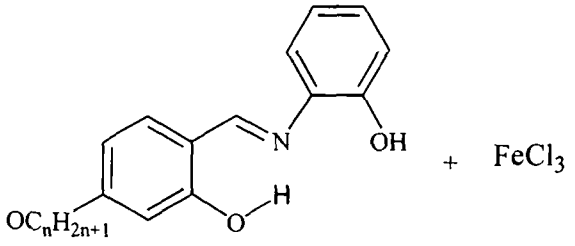

Schiff base (L_3), n=12
Schiff base (L_4), n=14

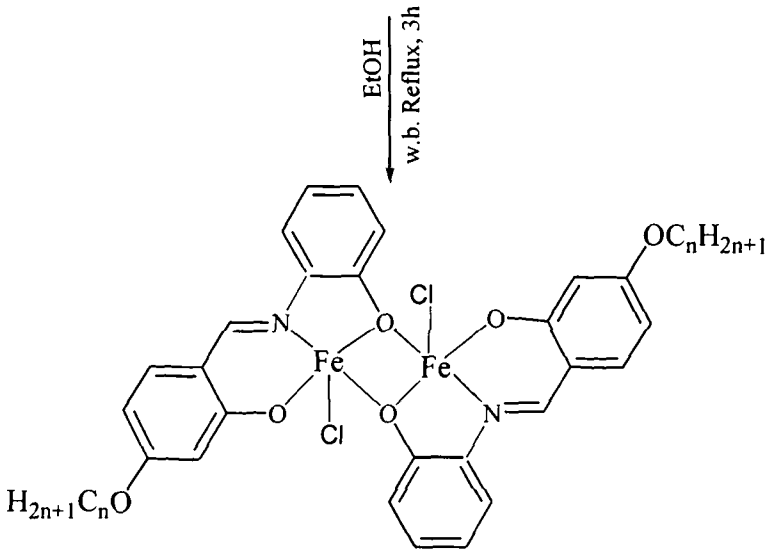

$[Fe(L)Cl]_2$ (L=L_3 or L_4; 5, 6)

Scheme 5.2.a

5.2.2. Preparation of binuclear VO(IV) complexes, **$[VOL]_2$ (L=L_3 or L_4; 7, 8)** with chiral mesogenic Schiff base ligands (L_3 and L_4).

An ethanolic solution of vanadyl acetylacetonate (1 mmol, 0.263 g) was added to a solution of the ligand L_3 (1 mmol, 0.397 g) or L_4 (1 mmol, 0.425 g) in ethanol and refluxed for 2 hours. The precipitated pale green complexes were filtered off, washed with cold ethanol, recrystallized and dried *in vacuo* (Scheme 5.2.b). Yield ~ 60%.

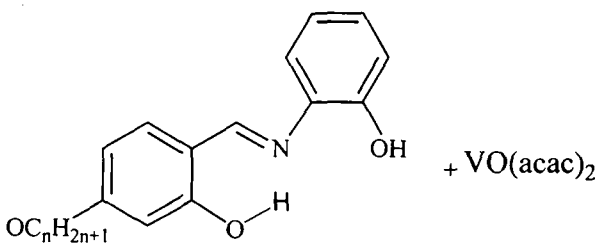

Schiff base **(L_3), n=12**
Schiff base **(L_4), n=14**

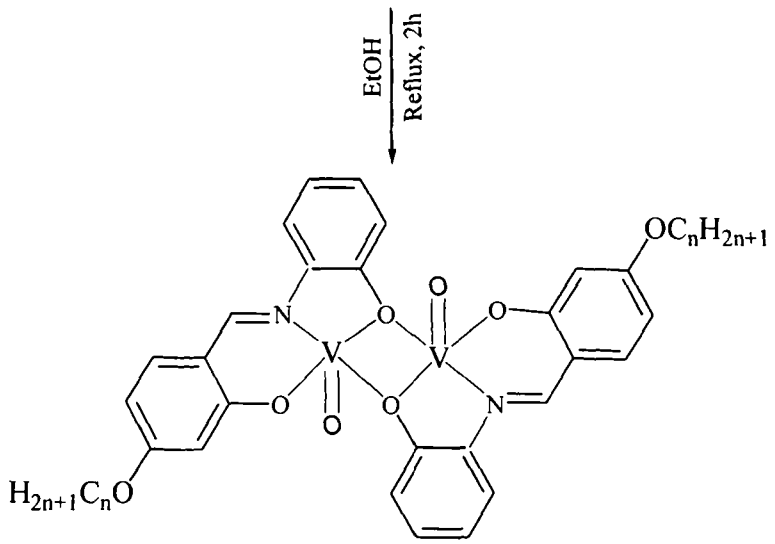

$[VO(L)]_2$ (7, 8)

Scheme 5.2.b

*5.2.3. Preparation of binuclear Fe(III) complex, **$[Fe(L_5)Cl]_2$ (9)** with [ONO] donor tridentate Schiff base ligand (L_5)

An ethanolic solution of anhydrous $FeCl_3$ (1 mmol, 0.162 g) was added to a solution of the ligand **L_5** (1 mmol, 0.191 g) and refluxed for 3 hours. On standing overnight, the dark black coloured complexes so precipitated was filtered off, washed with cold ethanol, recrystallized and dried in air (Scheme 5.2.c). Yield ~ 58%.

* The work described in the section 5.2.3 and 5.2.4 is communicated to the 'Journal of Coordination Chemistry'.

5.2.4. Preparation of binuclear VO(IV) complex, **$[VOL_5]_2.H_2O$ (10)** with [ONO] donor tridentate Schiff base ligand (L_5)

A hot methanolic solution of $VOSO_4.5H_2O$ (1 mmol, 0.253 g) was added to a solution of the ligand L_5 (1 mmol, 0.191g) in dry ethanol and refluxed for 2 hours. The dark green complex so formed was filtered off, washed with cold ethanol, recrystallized and dried *in vacuo* (Scheme 5.2.d). Yield ~ 65%.

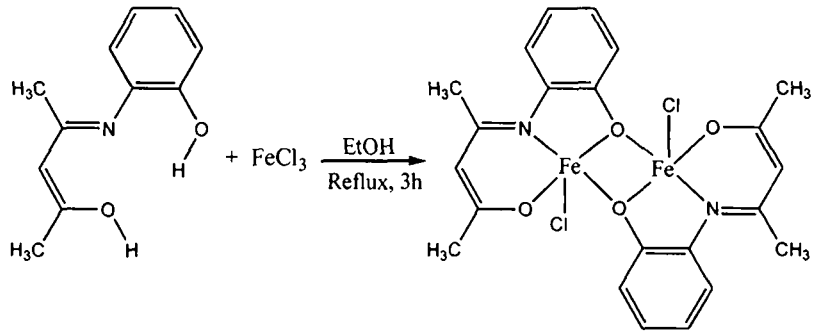

Schiff base (L_5) **$[Fe(L_5)Cl]_2$ (9)**

Scheme 5.2.c

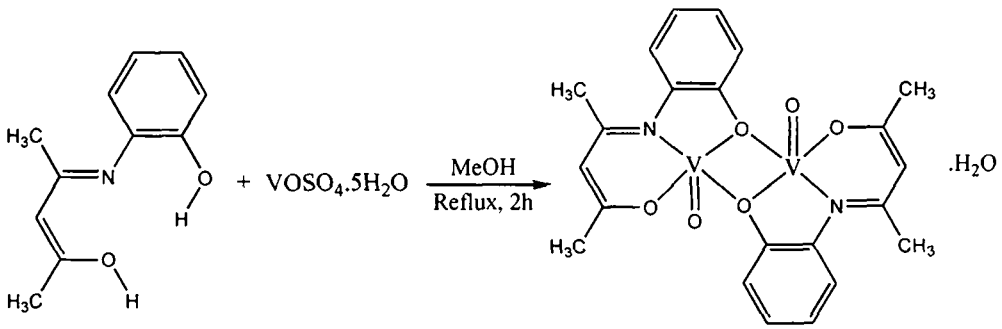

Schiff base (L_5) **$[VOL_5]_2.H_2O$ (10)**

Scheme 5.2.d

5.2.5. Synthesis of mixed ligand Fe(III) complex, **$[Fe(L_5)ClX]$ (X=PPh_3, Im) (11, 12)** using $[Fe(L_5)Cl]_2$ as starting material.

To a solution of the complex **$[Fe(L_5)Cl]_2$** in ethanol (0.1 mmol, 0.0561g) was added an ethanolic solution of imidazole (0.2 mmol, 0.0138g) or triphenylphosphine (0.2 mmol, 0.0524g) dropwise with continuous stiring

and then gently refluxed for 2 hours. On standing overnight the brownish complexes so precipitated were filtered off, washed with cold ethanol, recrystallized and dried in air (Scheme 5.2.e). Yield ~ 50%.

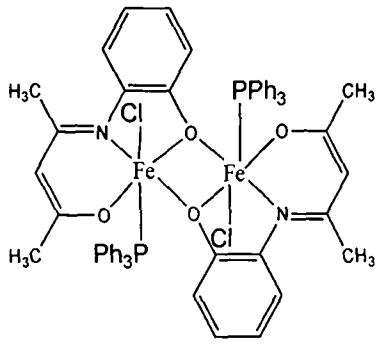

$[Fe(L_5)Cl(PPh_3)]_2$ (11)

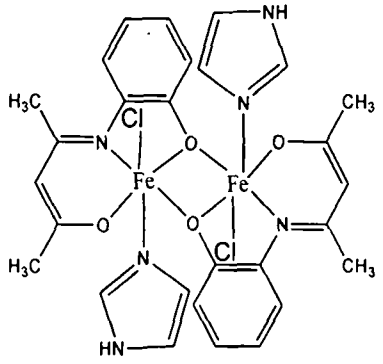

$[Fe(L_5)Cl(Im)]_2$ (12)

Scheme 5.2.e

5.2.6. Synthesis of Fe(II) complex, $[Fe(L_5)(H_2O)_2]_2$ **(13)** with [ONO] donor tridentate Schiff base ligands (L_5).

An ethanolic solution of $FeSO_4.7H_2O$ (1 mmol, 0.278 g) was added to a solution of the ligand L_5 (1 mmol, 0.191 g) and refluxed for 2 hours. The precipitated orange coloured complexes was filtered off, washed with cold ethanol, recrystallized and dried in air (Scheme 5.2.f). Yield ~ 50%.

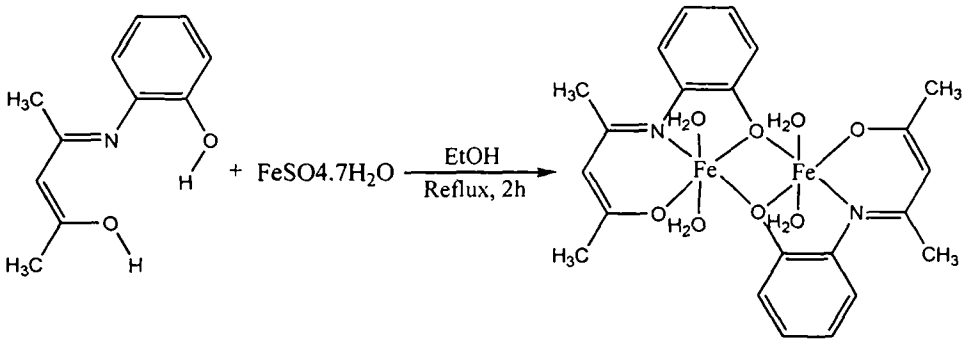

Schiff base (L_5)

$[Fe(L_5)(H_2O)_2]_2$ (13)

Scheme 5.2.f

5.2.7. Synthesis of VO(V) complex, **$Na[VO_2L_5]$ (14)** with [ONO] donor tridentate Schiff base ligands (L_5).

Vanadium pentoxide (0.05 mmol, 0.091g) was dissolved in minimum volume of aqueous sodium hydroxide solution (pH~ 8) and then warmed in a water bath with an ethanolic solution of the ligand L_5 (1 mmol, 0.191g). The green complexes so formed was filtered, washed with water-ethanol mixture and dried in air (Scheme 5.2.g). Yield ~ 55%.

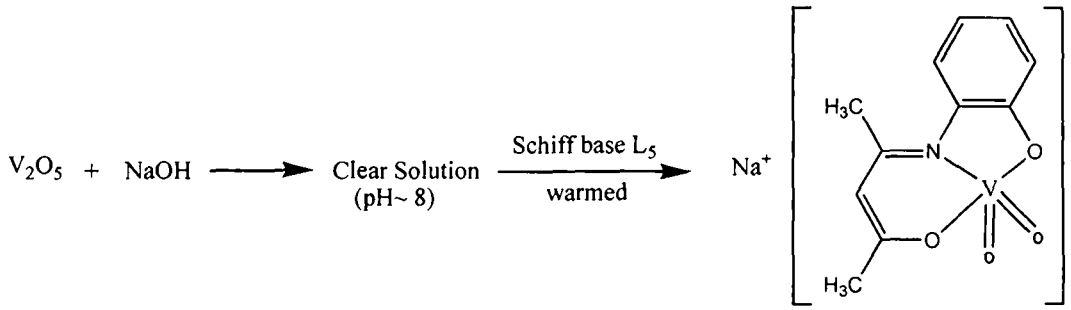

$Na[VO_2(L_5)]$ (14)

Scheme 5.2.g

5.2. 8. Synthesis of Fe(III) complex, **$[Fe(L_6)Cl]$ (15)** with [ONO] donor tridentate Schiff base ligands (L_6).

An ethanolic solution of anhydrous $FeCl_3$ (1 mmol, 0.162 g) was added to an ethanolic solution of the ligand **L_6** (1 mmol, 0.219 g) and refluxed for 3 hours. On standing overnight, the dark brown complexes so precipitated was filtered off, washed with cold ethanol, recrystallized and dried in air (Scheme 5.2.h). Yield ~ 55%.

5.2.9. Synthesis of VO(IV) complex, **$[VO(L_6)(H_2O)].H_2O$ (16)** with [ONO] donor tridentate Schiff base ligands (L_6).

A hot methanolic solution of $VOSO_4.5H_2O$ (1 mmol, 0.253 g) was added to a solution of the ligand **L_6** (1 mmol, 0.219 g) in dry ethanol and refluxed for

3 hours. The precipitated green complex was filtered off, washed with cold ethanol, recrystallized and dried *in vacuo* (Scheme 5.2.i). Yield 50%.

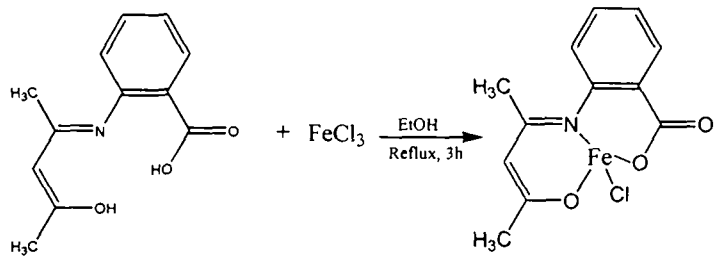

Schiff base(L_6) **[Fe(L_6)Cl] (15)**

Scheme 5.2.h

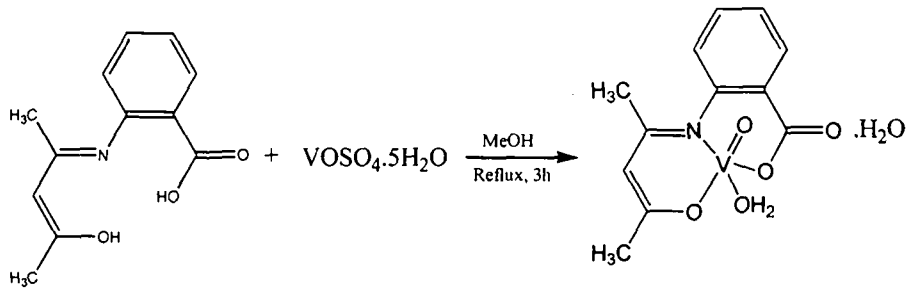

Schiff base(L_6) **[VO(L_6)(H_2O)]. H_2O (16)**

Scheme 5.2.i

*5.2.10. Synthesis of Fe(III) complex, **[FeL(acac)(EtOH)] (L=L_7 or L_8; 17, 18)** with [ONO] donor tridentate Schiff base ligands (L_7 and L_8).

The ligand, L_7 (1 mmol, 0.263g) or L_8 (1 mmol, 0.295g) was dissolved in absolute ethanol (10 mL) and was added to a ethanol solution (10 mL) of [$Fe(acac)_3$] (1mmol, 0.353g) and the mixture was gently refluxed for 4 h. After cooling, a dark brown microcrystalline solid was collected, and washed with cold absolute ethanol, recrystallised and then dried at air (Scheme 5.2.j). Yield: ~ 55%.

* The work described in section 5.2.10 is communicated to the journal 'Inorganic Chemistry Communications'.

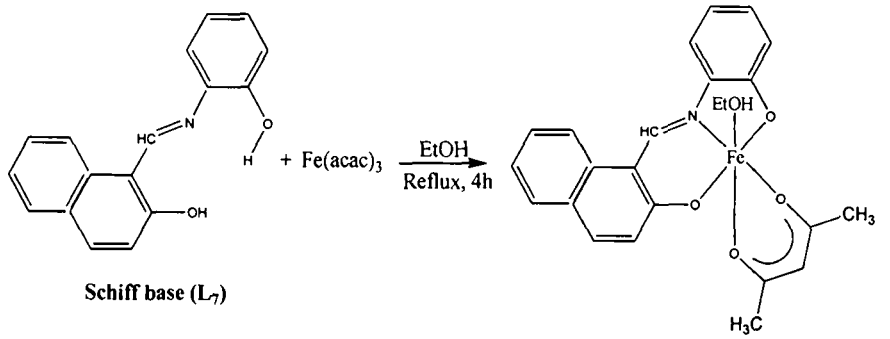

Schiff base (L_7)

$[Fe(L_7)(acac)(EtOH)]$ (17)

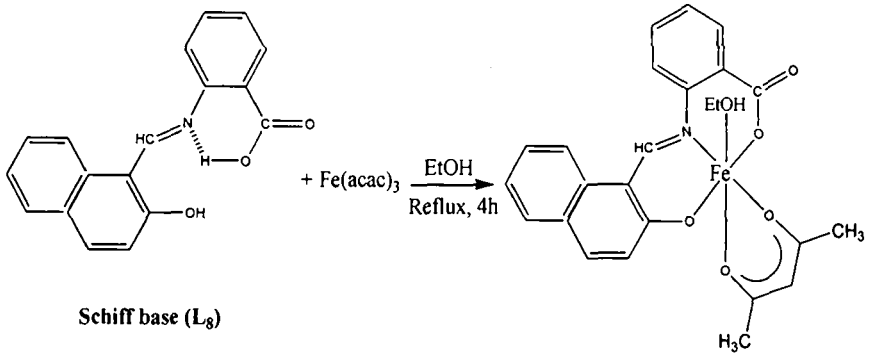

Schiff base (L_8)

$[Fe(L_8)(acac)(EtOH)]$ (18)

Scheme 5.2.j

5.3. Complexation of tetradentate Schiff base ligands

5.3.1. Synthesis of mixed ligand Fe(III) complexes, **$[Fe(L)(H_2O)_2]NO_3$ ($L=L_9$, L_{11}, L_{12}; 19-21** and **$[Fe(L)(H_2O)(NO_3)]$ ($L=L_{13}$, L_{14}; 22, 23)** with $[N_2O_2]$ donor tetradentate Schiff base ligands (L_9, L_{11}, L_{12}, $L_{13}$and L_{14}).

The ligand, L_9(5 mmol, 1.12g) or L_{11}(5 mmol, 2.08g) or L_{12}(5 mmol, 1.84g) or L_{13}(5 mmol, 2.24g) or L_{14}(5 mmol,2.48g) was dissolved in methanol (20 mL) and was added to a methanol solution (20 mL) of $[Fe(NO_3)_3].9H_2O$ (5 mmol, 2.02g) and the mixture was stirred for 4 h. After cooling, a dark coloured microcrystalline solid was collected, washed with cold absolute ethanol, recrystallised and then dried in air (Scheme 5.3.a).

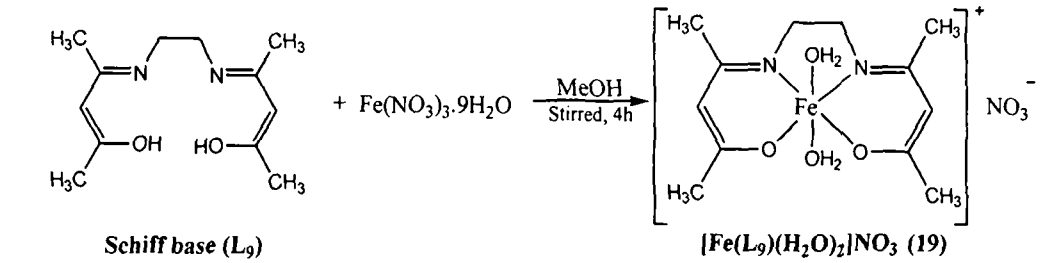

Schiff base (L_9) **$[Fe(L_9)(H_2O)_2]NO_3$ (19)**

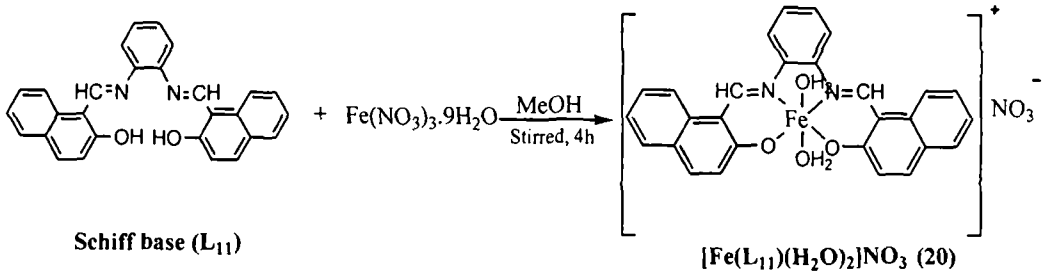

Schiff base (L_{11}) **$[Fe(L_{11})(H_2O)_2]NO_3$ (20)**

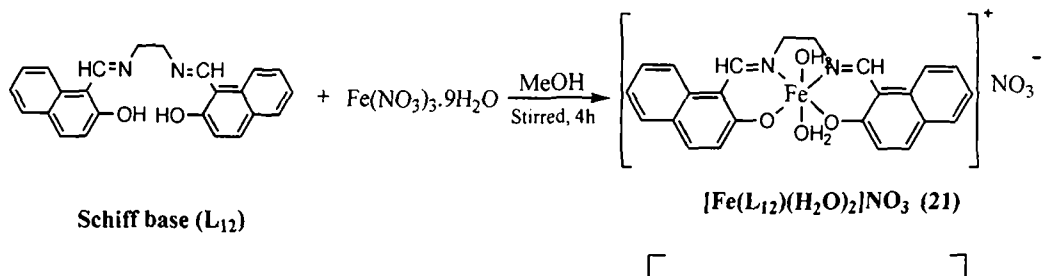

Schiff base (L_{12}) **$[Fe(L_{12})(H_2O)_2]NO_3$ (21)**

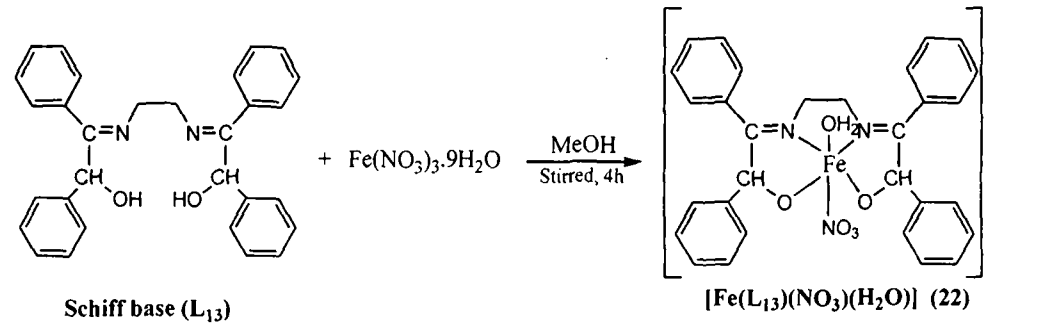

Schiff base (L_{13}) **$[Fe(L_{13})(NO_3)(H_2O)]$ (22)**

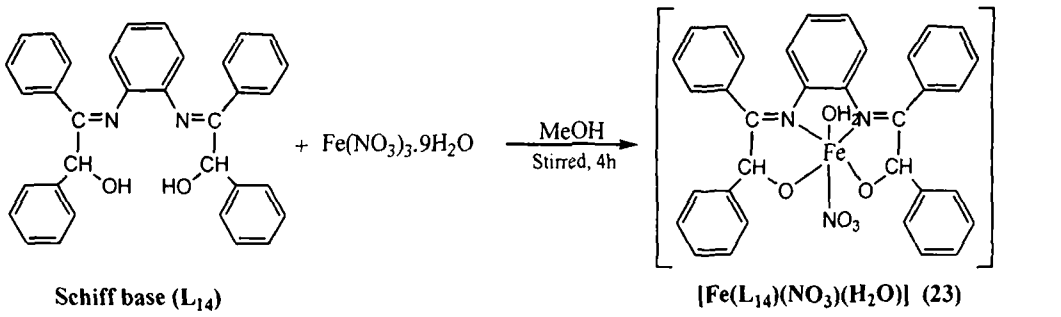

Schiff base (L_{14}) **$[Fe(L_{14})(NO_3)(H_2O)]$ (23)**

Scheme 5.3.a

*5.3.2. Synthesis of mixed ligand Fe(III) complexes, **$A[Fe(L_9)X_2]$ ($A=NH_4$, X=F, NCS; A=Na, $X=N_3$)** using $[Fe(L_9)(H_2O)_2]NO_3$ as starting material (Scheme 5.3.b)

(i) **$NH_4[Fe(L_9)(F)_2]$ (24)**

The complex $[Fe(L_9)(H_2O)_2]NO_3$ (1 mmol, 0.377g) was dissolved in 10 ml of methanol and to this a methanolic solution (10 ml) of $NH_4F{\cdot}HF$ (2mmol, 0.114g) was added with continuous stirring and the mixture was stirred further for 3 h. On standing overnight the compound so precipitated was collected, washed with ethanol and then dried in open air. Yield ~ 50%.

(ii) **$NH_4[Fe(L_9)(NCS)_2]$ (25)**

A similar procedure as described in the synthesis of $NH_4[Fe(L_9)(F)_2]$ was followed with the difference that in stead of $NH_4F{\cdot}HF$, NH_4SCN was added. Yield ~ 60%.

(iii) **$Na[Fe(L_9)(N_3)_2]$ (26)**

A similar procedure as described in the synthesis of $NH_4[Fe(L_9)(F)_2]$ was followed with the difference that in stead of $NH_4F{\cdot}HF$, NaN_3 was added. Yield ~ 60%.

5.3.3. Synthesis of mixed ligand Fe(III) complexes, **$[Fe(L_{12})X_2]NO_3$ (X=Im or Py)** using $[Fe(L_{12})(H_2O)_2]NO_3$ as starting material (Scheme 5.3.c)

(i) $[Fe(L_{12})(Im)_2]NO_3$ (27)

The complex $[Fe(L_{12})(H_2O)_2]NO_3$ (1 mmol, 0.520g) was dissolved in 10 ml of methanol and to this a methanolic solution (10 ml) of imidazole (2mmol, 0.136g) was added with continuous stirring and the mixture was refluxed

* The work described in section 5.3.2. is accepted for publication in the 'Journal of Coordination Chemistry', 2010.

further for 1 h. On standing overnight the reddish compound so precipitated was collected, washed with ethanol and then dried in open air. Yield 50%.

(ii) $[Fe(L_{12})(Py)_2]NO_3$ (28)

A similar procedure as described in the section **5.3.3.(i)** was followed with the difference that instead of imidazole, 2 mmol (0.158g) of pyridine was added. Yield 55%.

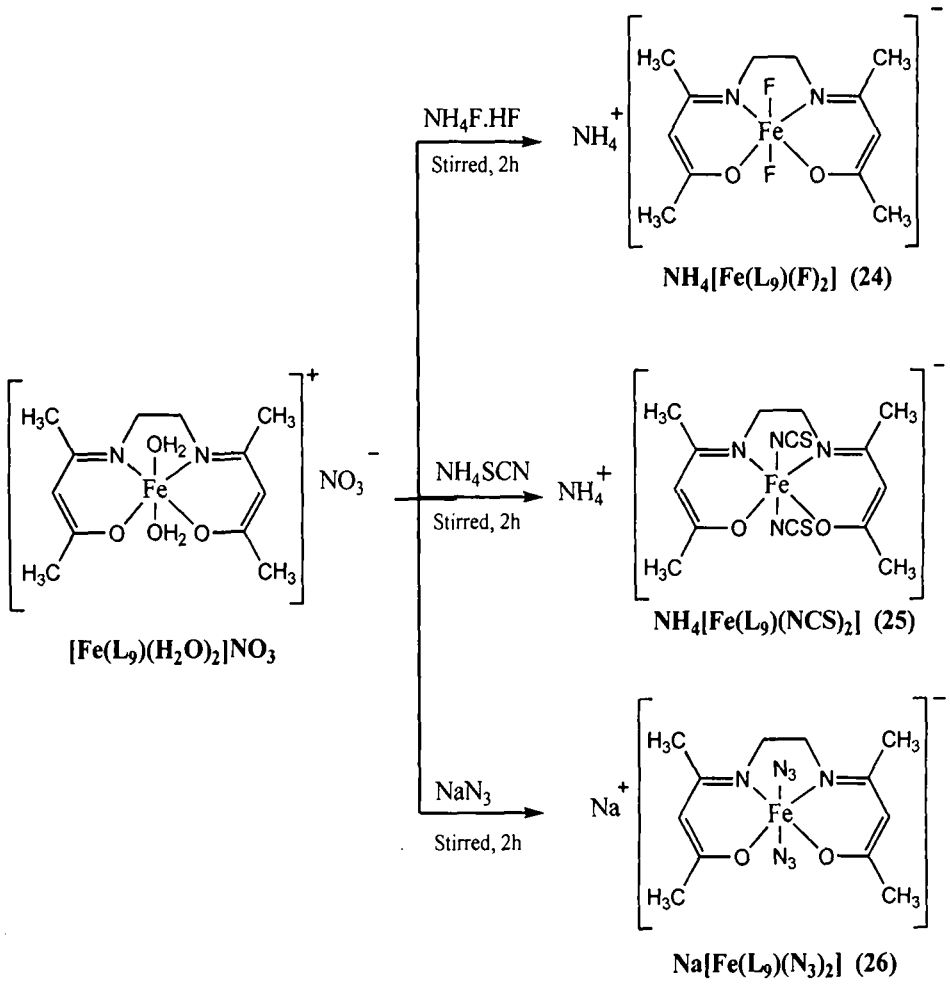

Scheme 5.3.b

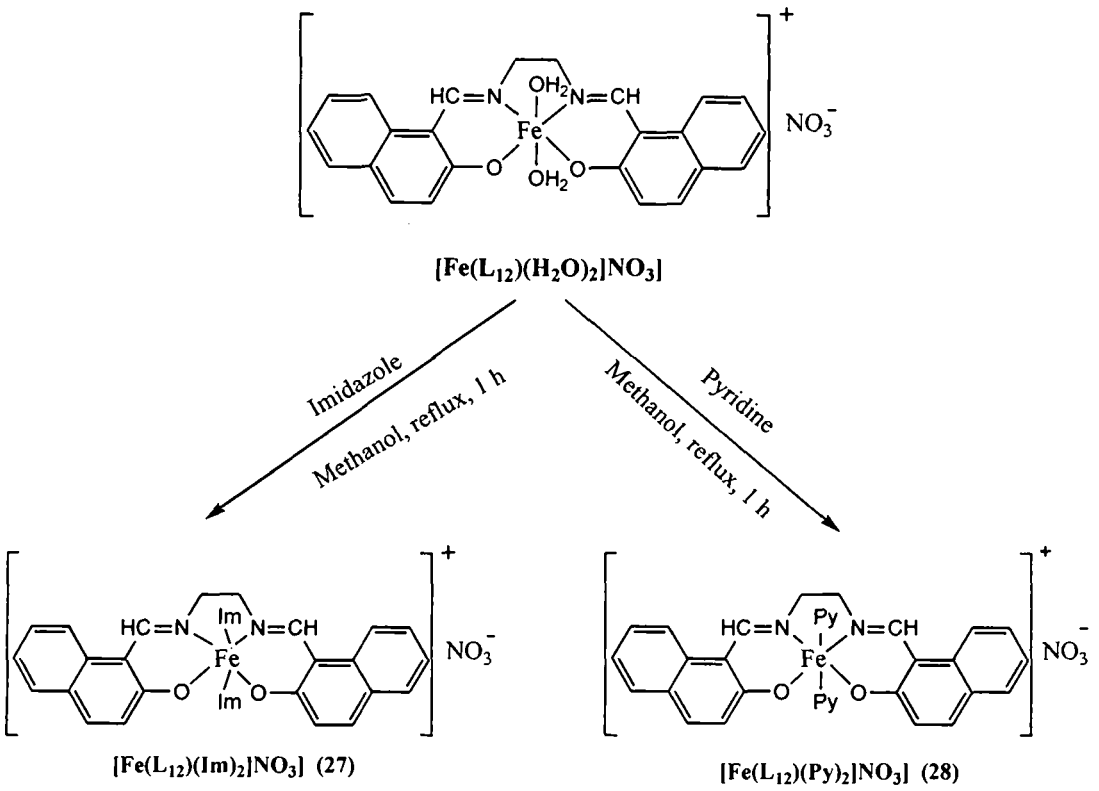

Scheme 5.3.c

5.3.4. Synthesis of VO(IV) complexes, **[VO(L)].H_2O (L=L_9, L_{11}-L_{14}; 29-33)** with $[N_2O_2]$ donor tetradentate Schiff base ligands (L_9, L_{11}, L_{12}, $L_{13}$and L_{14}).

A hot methanolic solution of $VOSO_4.5H_2O$ (1 mmol, 0.253 g) was added to a solution of the ligand L_9(1 mmol, 0.224g) or L_{11}(1 mmol, 0.416g) or L_{12}(1 mmol, 0.368g) or L_{13}(1 mmol, 0.448g) or L_{14}(1 mmol, 0.496g) in dry ethanol and refluxed for 3 hours. The precipitated green coloured complexes was filtered off, washed with cold ethanol, recrystallized and dried *in vacuo* (Scheme 5.3.d). Yield ~ 55%.

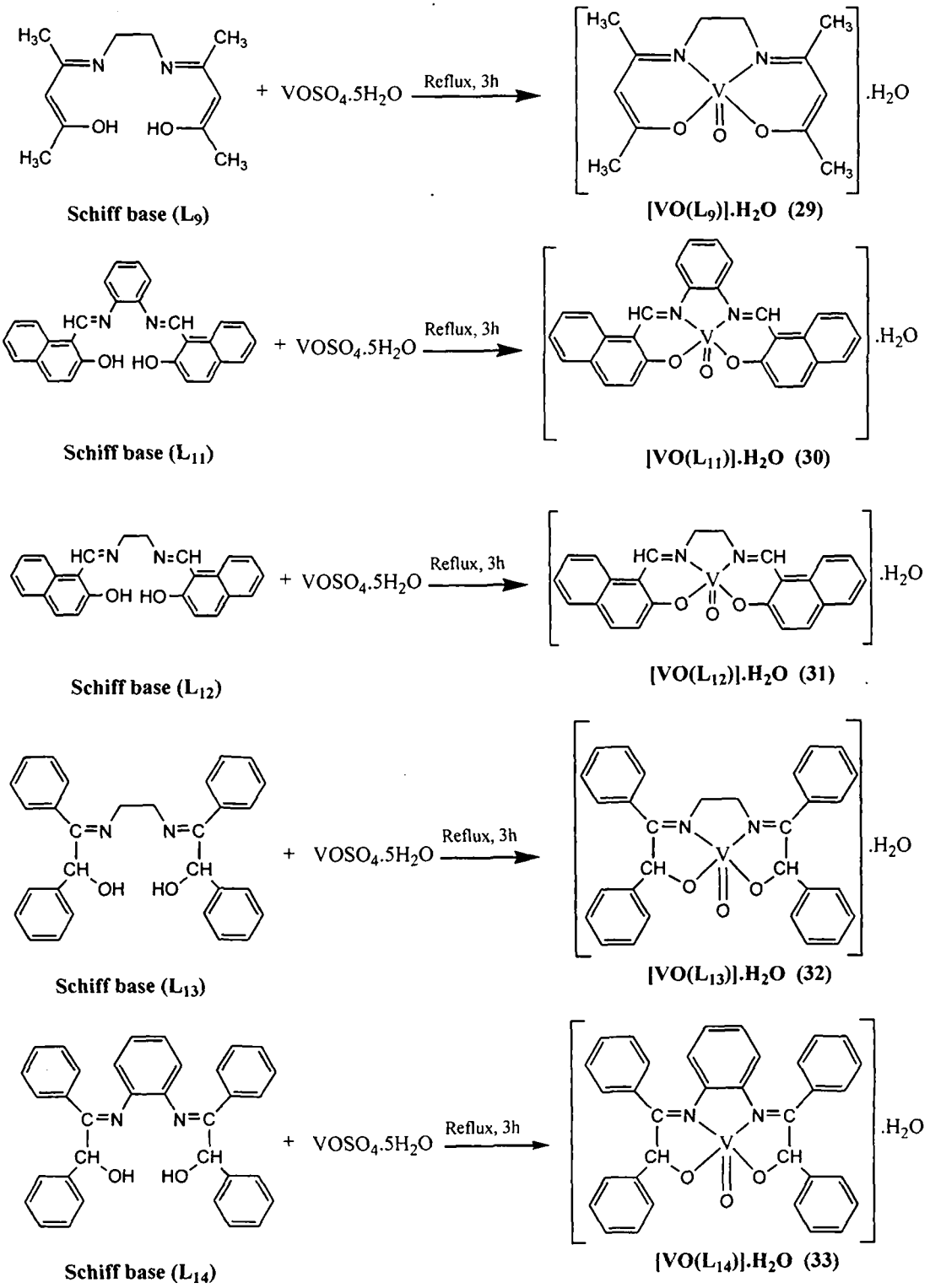
Schiff base (L_9)
+ $VOSO_4.5H_2O$
Reflux, 3h
$[VO(L_9)].H_2O$ (29)
Schiff base (L_{11})
+ $VOSO_4.5H_2O$
Reflux, 3h
$[VO(L_{11})].H_2O$ (30)
Schiff base (L_{12})
+ $VOSO_4.5H_2O$
Reflux, 3h
$[VO(L_{12})].H_2O$ (31)
Schiff base (L_{13})
+ $VOSO_4.5H_2O$
Reflux, 3h
$[VO(L_{13})].H_2O$ (32)
Schiff base (L_{14})
+ $VOSO_4.5H_2O$
Reflux, 3h
$[VO(L_{14})].H_2O$ (33)

Scheme 5.3.d

*5.4. Complexes of macrocyclic Schiff base ligands

5.4.1. Synthesis of Fe(III) complexes, **[FeLCl$_2$]Cl (L=L$_{15}$, L$_{16}$; 34, 35)** with 12-membered tetraimine macrocyclic Schiff base ligand (L$_{15}$ and L$_{16}$).

Equimolar amounts of $FeCl_3$ anhydrous (1 mmol, 0.162g) in MeOH (25 cm3) and the ligand, L$_{15}$ (1 mmol, 0.468g) or L$_{16}$ (1 mmol, 0.564g) taken in MeOH (25 cm^3) were reacted under refluxed conditions followed by stirring for ca.4 h. The reaction mixture thus obtained was continually evaporated leading to the isolation of wine red microcrystalline products. The product thus formed was filtered, washed several times with methanol and dried *in vacuo* (Scheme 5.4.a). Yield ~ 65%.

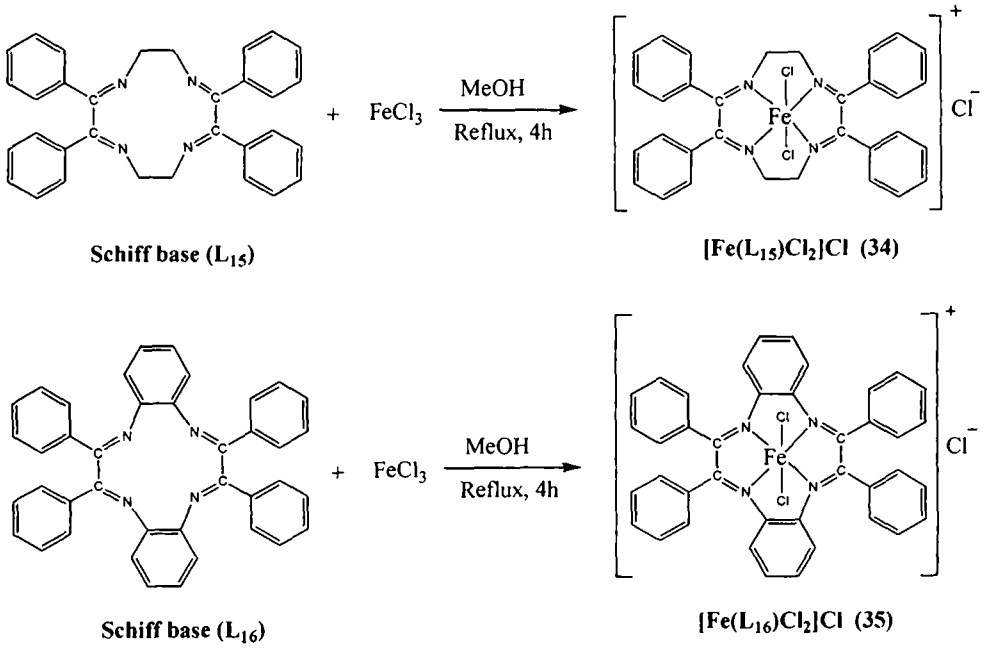

Schiff base (L$_{15}$) — [Fe(L$_{15}$)Cl$_2$]Cl (34)

Schiff base (L$_{16}$) — [Fe(L$_{16}$)Cl$_2$]Cl (35)

Scheme 5.4.a

5.4.2. Synthesis of VO(IV) complexes, **[VOL]SO$_4$.H$_2$O (L=L$_{15}$, L$_{16}$; 36, 37)** with 12-membered tetraimine macrocyclic Schiff base ligand (L$_{15}$ and L$_{16}$).

Equimolar amounts of $VOSO_4.5H_2O$ (1 mmol, 0.253g) in MeOH (25 cm3) and the ligand, L$_{15}$ (1 mmol, 0.468g) or L$_{16}$ (1 mmol, 0.564g) taken in

* The work described in the section 5.4 is communicated to 'Journal of Chemical Sciences'.

MeOH (25 cm3) were refluxed for 6 hours. The reaction mixture thus obtained was continually evaporated leading to the isolation of dark green complexes. The product thus formed was filtered, washed several times with methanol and dried in vacuo (scheme 5.4.b). Yield ~ 60%.

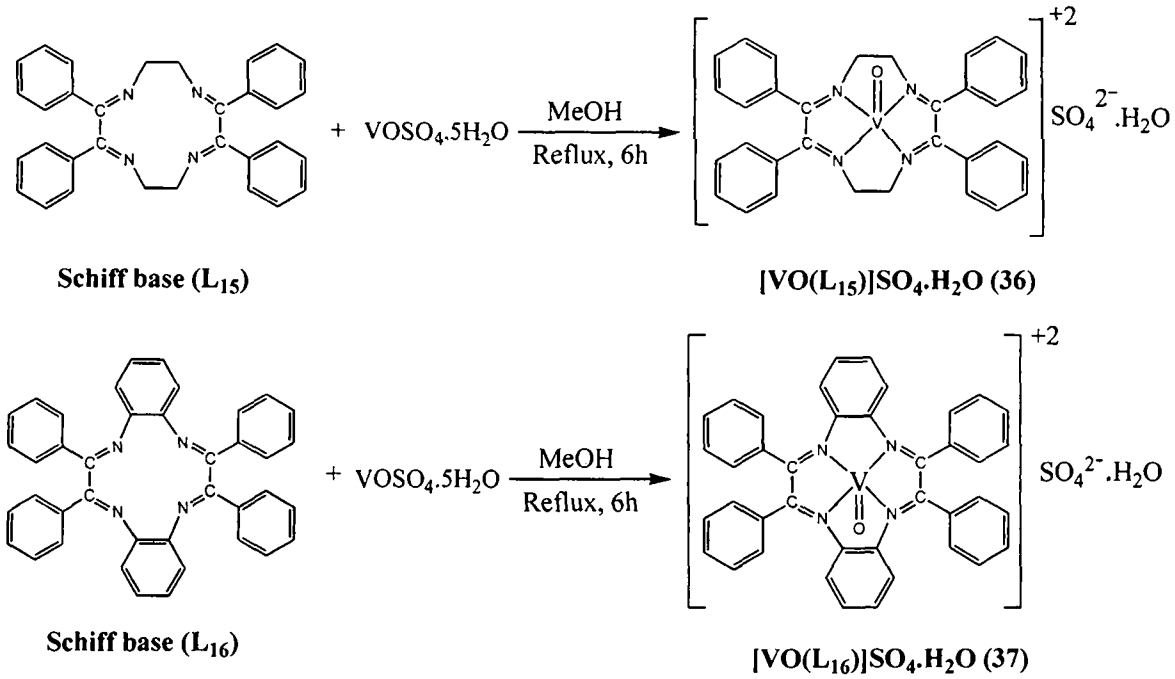

Scheme 5.4.b

*5.5. Complexation of $[N_2O_2]$ donor neutral tetradentate Schiff base ligands.

5.5.1. Synthesis of Fe(III) complex, **$[Fe(L_{10})(H_2O)_2](NO_3)_3$ (38)** with tetradentate Schiff base L_{10}.

To a solution of the $Fe(NO_3)_3.9H_2O$ (1 mmol, 0.404 g) in ethanol was added an ethanolic solution of the ligand L_{10} (1 mmol, 0.110 g) and refluxed for 2 h. On cooling the solution to room temperature the reddish compound so precipitated was filtered, washed with ethanol, recrystallised and dried *in vacuo* (Scheme 5.5.a). Yield 60%.

* The work described tn the section 5.5.1 and 5.5.2 is published in AUJ Sci. Tech. 2010, 5, 81.

5.5.2. Synthesis of VO(IV) complex, $[VOL_{10}].SO_4.H_2O$ with tetradentate Schiff base L_{10}.

Hot methanolic solution of vanadyl sulphate pentahydrate (1 mmol, 0.253 g) was slowly added to a solution of the ligand L_{10} (1 mmol, 0.110 g) and refluxed for 2 h. The resulting solution was concentrated when green complexes precipitated out. The product was filtered, washed with cold ethanol, recrystallised and dried *in vacuo* (Scheme 5.5.b). Yield 55%.

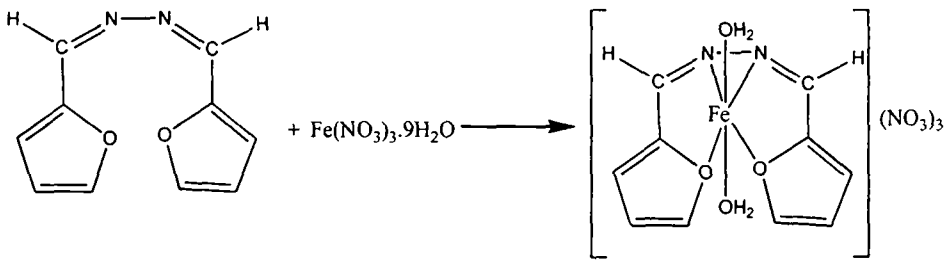

Schiff base (L_{10}) $[Fe(L_{10})(H_2O)_2](NO_3)_3$ (38)

Scheme 5.5.a

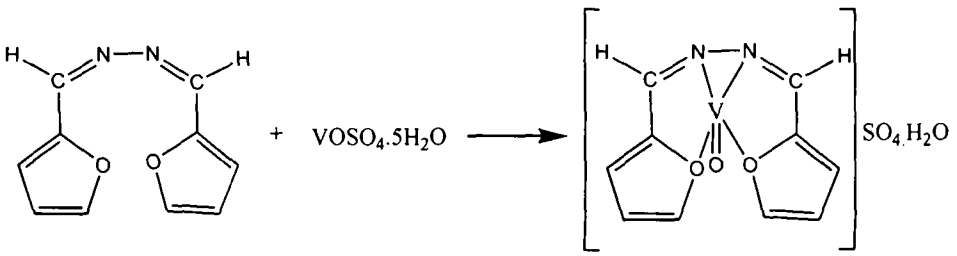

Schiff base (L_{10}) $[VO(L_{10})]SO_4.H_2O$ (39)

Scheme 5.5.b

5.6. Synthesis of Fe(II) complex, $[Fe(L_9)(H_2O)_2]$ with tetradentate Schiff base L_9.

An ethanolic solution of $FeSO_4.7H_2O$ (1 mmol, 0.278 g) was added to a solution of the ligand **L_9** (1 mmol, 0.224 g) and refluxed for 2 hours. The precipitated green complexes was filtered off, washed with cold ethanol, recrystallized and dried in air (Scheme 5.6). Yield 60%.

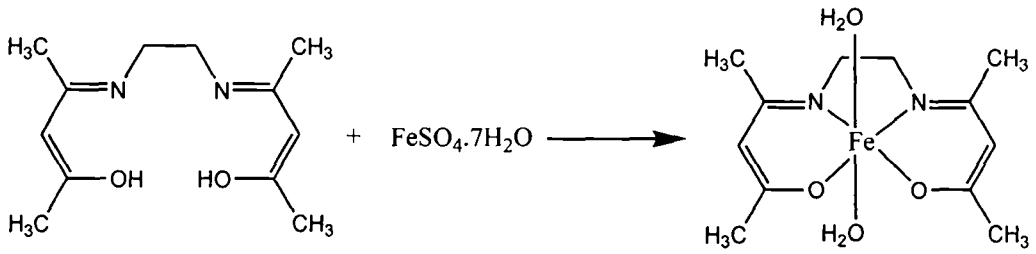

Schiff base (L_9) **$Fe(L_9)(H_2O)_2$ (40)**

Scheme 5.6

CHAPTER 6

RESULTS AND DISCUSSION

This chapter provides an account of the synthesis, characterisation of the synthesised compounds and correlation of results. The characterisation are based on elemental analysis, IR, UV-VIS, ^{1}H and ^{13}C NMR, mass spectroscopic technique, single crystal X-ray diffraction experiment. Magnetic susceptibility measurement, electrochemical behaviour, thermal microscopy, differential scanning calorimetry, thermogravimetric analysis, DFT computation and antimicrobial activity studies of the selected compounds are also incorporated herein.

6.1. Synthesis

Metal-Schiff base complexes since their discovery in 1840 [38] have continued to occupy a coveted position in the development of coordination chemistry. A large diversity of stable complex species has been synthesised containing both transition and non-transition metals and multifarious ligand systems. Direct reaction of metal ions with preformed Schiff base in the presence of added base such as acetate or hydroxide is a popularly employed synthetic technique. Reaction of amines with metal-aldehyde complexes, originally discovered by Schiff [38] also is considered as extremely convenient general preparative route. Extensive use of such synthetic method was made

by Pfeiffer [42]. Another approach to the synthesis of metal–Schiff base complexes is the template based reaction of metal-amines with aldehydes. Hydrolysis caused by traces of water from the organic solvents or other sources often complicate synthesis of Schiff base ligands or its complexes. The size of the metal ions, nature of substitient on the side aromatic ring, steric constraints, presence of other linking group such as azo or ester in the ligand, the type or number of donor sites greately imfluence the stability of metal-Schiff base complexes. In a way such variations also offer suitable scope for tuning physical properties of the complexes to achieve desired materials.

6.2. Elemental analysis

The analytical data for the ligand and complexes together with some physical properties are summarized in **Table-1**. The experimentally found percentages of C, H and N are consistent with those of calculated values based on the proposed formula of the compounds.

6.3. IR spectra

Structurally significant IR spectral data of the ligands and complexes (Appendix 1) are listed in **Table-2**. All the free ligands ($\mathbf{L_1}$-$\mathbf{L_{16}}$) showed bands resulting from azomethine (-CH=N-) stretching in the region 1600-1640 cm^{-1}. Appearance of broad band in the range 3414-3447 cm^{-1} in all the ligands except $\mathbf{L_1}$, $\mathbf{L_2}$, $\mathbf{L_{10}}$, $\mathbf{L_{15}}$ and $\mathbf{L_{16}}$ is attributed to O-H stretching. Characteristics C-O stretching vibrations in these ligands appeared in the range 1215-1351 and 1143-1249 cm^{-1} owing to phenolic and alcoholic OH groups, respectively. The formation of tetraimine macrocyclic Schiff base ligand $\mathbf{L_{15}}$ and $\mathbf{L_{16}}$ was confirmed by the appearance of ν(C=N) band at 1637 and 1610 cm^{-1}, respectively. The ligand $\mathbf{L_{10}}$ also showed characteristics C=N stretching at ca 1640 cm^{-1}. Further the absence of symmetric and asymmetric N-H stretching mode confirms

TABLE-1. Physical and analytical data of the compounds

Compounds	Molecular composition	Colour	Yield (%)	Found (Calcd) (%)		
				C	H	N
Schiff base (L_1)	$C_{28}H_{24}N_2O_2$ MW=420	Yellow	73	80.6(80.5)	5.4(5.7)	7.0(6.6)
Schiff base (L_2)	$C_{28}H_{24}N_2$ MW=388	Yellow	76	86.2(86.6)	6.5(6.2)	7.0(7.2)
Schiff base (L_3)	$C_{25}H_{35}NO_3$ MW=397	Yellow	74	75.1(75.6)	8.4(8.8)	4.1(3.5)
Schiff base (L_4)	$C_{27}H_{39}NO_3$ MW=425	Yellow	71	77.0(76.2)	9.0(9.2)	3.7(3.3)
Schiff base(L_3')	$C_{25}H_{35}NO_2$ MW=381	Yellow	68	78.5(78.7)	9.5(9.2)	4.0(3.7)
Schiff base(L_4')	$C_{27}H_{39}NO_2$ MW=409	Yellow	70	79.6(79.2)	9.2(9.5)	3.7(3.4)
Schiff base (L_5)	$C_{11}H_{13}NO_2$ MW=191	Yellow	69	68.8(69.1)	7.0(6.8)	7.3(7.3)
Schiff base (L_6)	$C_{12}H_{13}NO_3$ MW=219	Yellow	68	65.3(65.8)	5.8(5.9)	6.8(6.4)

Compounds	Molecular composition	Colour	Yield (%)	Found (Calcd) (%)		
				C	H	N
Schiff base (L_7)	$C_{17}H_{13}NO_2$ MW=263	Orange	70	77.4(77.6)	4.8(4.9)	5.8(5.3)
Schiff base (L_8)	$C_{18}H_{13}NO_3$ MW=291	Yellow	70	74.6(74.2)	4.2(4.5)	5.2(4.8)
Schiff base (L_9)	$C_{12}H_{20}N_2O_2$ MW=224	Pale yellow	68	64.2(64.3)	9.3(8.9)	12.3(12.5)
Schiff base(L_{10})	$C_{10}H_8N_2O_2$ MW=188	Yellow	71	63.5(63.8)	4.4(4.3)	15.2(14.9)
Schiff base(L_{11})	$C_{28}H_{20}N_2O_2$ MW=416	Orange	68	80.9(80.8)	4.5(4.8)	6.9(6.7)
Schiff base(L_{12})	$C_{24}H_{20}N_2O_2$ MW=368	Yellow	72	78.7(78.3)	5.2(5.4)	7.5(7.6)
Schiff base(L_{13})	$C_{30}H_{28}N_2O_2$ MW=448	Yellowish	73	80.6(80.4)	6.7(6.3)	6.2(6.3)
Schiff base(L_{14})	$C_{34}H_{28}N_2O_2$ MW=496	Yellowish	70	82.0(82.3)	5.3(5.6)	5.9(5.6)
Schiff base(L_{15})	$C_{32}H_{28}N_4$ MW=468	Yellow	69	82.4(82.1)	6.1(5.9)	11.8(12.0)

Compounds	Molecular composition	Colour	Yield (%)	Found (Calcd) (%)		
				C	H	N
Schiff base($\mathbf{L_{16}}$)	$C_{40}H_{28}N_4$ MW=564	Yellow	76	85.4(85.1)	4.8(4.9)	10.2(10.0)
$[Fe(L_1)_2(NO_3)_2]NO_3$ (**1**)	$FeC_{56}H_{48}N_7O_{13}$ MW=1082	Dark brown	64	62.6(62.1)	4.7(4.4)	8.9(9.1)
$[Fe(L_2)_2(NO_3)_2]NO_3$ (**2**)	$FeC_{56}H_{48}N_7O_9$ MW=1018	Dark brown	61	66.2(66.0)	4.4(4.7)	9.3(9.6)
$[VO(L_1)_2]SO_4.H_2O$ (**3**)	$VC_{56}H_{50}N_4O_{10}S$ MW=1021	Green	62	66.1(65.8)	5.1(4.9)	5.2(5.5)
$[VO(L_2)_2]SO_4.H_2O$ (**4**)	$VC_{56}H_{50}N_4O_6S$ MW=957	Green	59	70.0(70.2)	5.1(5.2)	6.3(5.9)
$[FeL_3Cl]_2$ (**5**)	$Fe_2C_{50}H_{66}N_2O_6Cl_2$ MW=973	Brown	61	62.0(61.7)	7.0(6.8)	3.2(2.9)
$[FeL_4Cl]_2$ (**6**)	$Fe_2C_{54}H_{74}N_2O_6Cl_2$ MW=1029	Brown	62	63.3(63.0)	7.5(7.2)	2.6(2.8)
$[VOL_3]_2$ (**7**)	$V_2C_{50}H_{66}N_2O_8$ MW=924	Pale green	63	65.2(64.9)	6.8(7.1)	3.3(3.0)
$[VOL_4]_2$ (**8**)	$V_2C_{54}H_{74}N_2O_8$ MW=980	Pale green	58	66.5(66.1)	7.8(7.6)	3.2(2.9)

Compounds	Molecular composition	Colour	Yield (%)	Found (Calcd) (%)		
				C	H	N
$[FeL_5Cl]_2$ (**9**)	$Fe_2C_{22}H_{22}N_2O_4Cl_2$ MW=561	black	58	47.4(47.1)	3.6(3.9)	5.3(5.0)
$[VOL_5]_2.H_2O$ (**10**)	$V_2C_{22}H_{24}N_2O_7$ MW=530	Dark green	63	49.5(49.8)	4.8(4.5)	5.7(5.3)
$[FeL_5Cl(PPh_3)]_2$ (**11**)	$Fe_2C_{58}H_{52}N_2O_4Cl_2P_2$ MW=1085	Brownish	51	24.5(24.3)	1.9(2.0)	2.8(2.6)
$[FeL_5Cl\ Im]_2$ (**12**)	$Fe_2C_{28}H_{30}N_6O_4Cl_2$ MW=697	Brownish	52	48.4(48.2)	4.2(4.3)	12.4(12.1)
$[FeL_5(H_2O)_2]_2$ (**13**)	$Fe_2C_{22}H_{30}N_2O_8$ MW=562	Orange	51	47.0(46.8)	5.4(5.3)	4.8(5.0)
$Na[VO_2L_5]$ (**14**)	$NaVC_{11}H_{11}NO_4$ MW=295	Green	54	44.6(44.8)	3.6(3.7)	4.9(4.7)
$[FeL_6Cl]$ (**15**)	$FeC_{12}H_{11}NO_3Cl$ MW=308.5	Dark brown	55	46.4(46.7)	3.8(3.6)	4.4(4.5)
$[VOL_6(H_2O)].H_2O$ (**16**) .	$VC_{12}H_{15}NO_6$ MW=320	Green	55	45.2(45.0)	4.6(4.7)	4.2(4.4)
$[FeL_7(acac)(EtOH)]$ (**17**)	$FeC_{24}H_{24}NO_5$ MW=462	Dark brown	60	62.4(62.3)	5.0(5.2)	3.3(3.0)

Compounds	Molecular composition	Colour	Yield (%)	Found (Calcd) (%)		
				C	H	N
$[FeL_8(acac)(EtOH)]$ (**18**)	$FeC_{25}H_{24}NO_6$ MW=490	Dark brown	56	61.3(61.2)	5.1(4.9)	2.7(2.9)
$[FeL_9(H_2O)_2]NO_3$ (**19**)	$FeC_{12}H_{22}N_3O_7$ MW=376	Brown	62	38.0(38.3)	6.2(5.9)	11.0(11.2)
$[FeL_{11}(H_2O)_2]NO_3$ (**20**)	$FeC_{28}H_{22}N_3O_7$ MW=568	Red	64	59.0(59.2)	4.0(3.9)	7.7(7.4)
$[FeL_{12}(H_2O)_2]NO_3$ (**21**)	$FeC_{24}H_{22}N_3O_7$ MW=520	Red	63	55.2(55.4)	4.5(4.2)	8.0(8.1)
$[FeL_{13}NO_3H_2O]$ (**22**)	$FeC_{30}H_{28}N_3O_6$ MW=582	Black	67	61.7(61.9)	4.9(4.8)	7.5(7.2)
$[FeL_{14}NO_3H_2O]$ (**23**)	$FeC_{34}H_{28}N_3O_6$ MW=630	Black	58	65.0(64.8)	4.1(4.4)	6.8(6.7)
$NH_4[FeL_9F_2]$ (**24**)	$C_{12}H_{22}N_3O_2F_2Fe$ MW=334	Orange	53	43.2(43.1)	6.7(6.6)	12.4(12.6)
$NH_4[FeL_9(NCS)_2]$ (**25**)	$C_{14}H_{22}N_5O_2S_2Fe$ MW=412	Violet	60	41.0(40.8)	5.2(5.3)	17.3(17.0)
$Na[FeL_9(N_3)_2]$ (**26**)	$NaFeC_{12}H_{18}N_8O_2$ MW=385	Green	58	37.2(37.4)	4.6(4.7)	29.4(29.1)

Compounds	Molecular composition	Colour	Yield (%)	Found (Calcd) (%)		
				C	H	N
$[FeL_{12}(Im)_2]NO_3$ (**27**)	$FeC_{30}H_{26}N_7O_5$ MW=620	Brown	52	58.4(58.1)	4.2(4.2)	15.6(15.8)
$[FeL_{12}(Py)_2]NO_3$ (**28**)	$FeC_{34}H_{28}N_5O_5$ MW=642	Dark brown	55	63.7(63.6)	4.2(4.4)	11.2(10.9)
$[VOL_9]H_2O$ (**29**)	$VC_{12}H_{20}N_2O_4$ MW=307	Dark green	59	46.8(47.0)	6.6(6.5)	9.4(9.1)
$[VOL_{11}]H_2O$ (**30**)	$VC_{28}H_{20}N_2O_4$ MW=499	Dark green	61	67.4(67.3)	4.3(4.0)	5.5(5.6)
$[VOL_{12}]H_2O$ (**31**)	$VC_{24}H_{20}N_2O_4$ MW=451	Dark green	62	63.6(63.9)	4.2(4.4)	6.5(6.2)
$[VOL_{13}]H_2O$ (**32**)	$VC_{30}H_{28}N_2O_4$ MW=531	Dark green	55	67.7(67.8)	5.5(5.3)	5.1(5.3)
$[VOL_{14}]H_2O$ (**33**)	$VC_{34}H_{28}N_2O_4$ MW=579	Dark green	56	70.3(70.5)	5.0(4.8)	5.2(4.8)
$[FeL_{15}Cl_2]Cl$ (**34**)	$FeC_{32}H_{28}N_4Cl_3$ MW=630.5	Wine red	66	61.3(60.9)	4.6(4.4)	8.7(8.9)
$[FeL_{16}Cl_2]Cl$ (**35**)	$FeC_{40}H_{28}N_4Cl_3$ MW=726.5	Wine red	62	65.9(66.1)	4.0(3.9)	7.5(7.7)
$[VOL_{15}]SO_4.H_2O$ (**36**)	$VC_{32}H_{30}N_4O_6S$ MW=649	Dark grren	56	59.5(59.2)	4.8(4.6)	8.3(8.6)
$[VOL_{16}]SO_4.H_2O$ (**37**)	$VC_{40}H_{30}N_4O_6S$ MW=745	Dark grren	60	64.7(64.4)	4.1(4.0)	7.6(7.5)

Compounds	Molecular composition	Colour	Yield (%)	Found (Calcd) (%)		
				C	H	N
$FeL_{10}(H_2O)_2](NO_3)_3$ (**38**)	$FeC_{10}H_{12}N_5O_{13}$ MW=466	Dark brown	61	26.0(25.8)	2.7(2.6)	14.9(15.0)
$[VOL_{10}]SO_4.H_2O$ (**39**)	$VC_{10}H_{10}N_2O_2S$ MW=369	Green	61	32.1(32.5)	2.9(2.7)	7.4(7.6)
$[Fe(L_9)(H_2O)_2]$ (**40**)	$FeC_{12}H_{22}N_2O_4$ MW=314	Green	57	46.2(45.8)	6.8(7.0)	9.3 (8.9)

condensation of both the NH_2 group of hydrazine forming a neutral quadridentate N_2O_2 donor Schiff base ligand.

The bonding of the ligands to metals were investigated by comparing the IR spectra of complexes with those of the free ligands. The bands appearing in the free ligands due to azomethine linkage shifted to lower wave numbers on complexation, indicating the coordination of the azomethine nitrogen atom to the central metal ion [212, 213]. The broad band assigned to ν(O-H) in the Schiff bases (**L_3-L_9** and **L_{11}-L_{14}**), was absent in the spectra of complexes, indicating coordination of the ligand in the deprotonated form. Moreover, two weak bands in the low energy region (400-600 cm^{-1}) assignable to ν(M–N) and ν(M–O) provide compelling evidence for the coordinated metal ion in the ligand framework [214, 215]. The oxo-vanadium(IV) complexes showed strong bands at *ca* 990 cm^{-1} attributed to the stretching vibration of the vanadyl (V=O) core [216]. The nature and position of the peak clearly suggest absence of any intermolecular V=O·····V=O interactions [216]. The presence of coordinated water molecules in the complexes **13, 16, 19-23, 38 and 40** was confirmed by the appearance of a broad band around 3360-3480 cm^{-1} for ν(O-H) together with a weak band at *ca* 590-660 and 830-940 cm^{-1} attributable to wagging and rocking modes of coordinated water, respectively [217]. However, the complexes **3, 4, 10, 29-33, 36-39** showed ν(O-H) band assignable to lattice water. The nitrato complexes **1, 2, 22, 23** showed bands at *ca* 1440, 1320 and 1030 cm^{-1} assignable to νNO_3^- of unidentate O-bonded nitrato ligand [218]. Sharp band appearing at *ca* 1385 cm^{-1} in the complexes **1, 2, 19-21, 27, 28, 38** corresponds to $\nu NO_{(asy)}$ of free nitrate ion [218]. The complexes **3, 4, 36, 37** and **39** showed peak at *ca* 1100 cm^{-1} that corresponds to ν_{SO} free sulphate ion. A strong doublet band at 2049 and 2073 cm^{-1} alongwith a medium intensity band at ca 770 cm^{-1} in the complex **25** corresponds to ν(C-N) and ν(N-C-S) indicating the presence of terminally nitrogen

TABLE-2. Structurally significant IR spectral bands of the compounds

Compounds	IR bands (cm^{-1})												
	$\nu_{C=N}$	ν_{O-H}	ν_{C-O}	$\nu_{C=C}$	ν_{M-N}	ν_{M-O}	$\nu_{V=O}$	ν_{NO} asy (free NO_3^-)	ν NO_3^- (coord. NO_3^-)	ν_{O-H} (H_2O)	ρ_{rock} (H_2O)	ρ_{wagg} (H_2O)	other
Schiff base (L_1)	1618	-	-	-	-	-	-	-	-	-	-	-	-
Schiff base (L_2)	1619	-	-	-	-	-	-	-	-	-	-	-	
Schiff base (L_3)	1636	3431 2953	1270 1158	-	-	-	-	-	-	-	-	-	-
Schiff base (L_4)	1636	3446 2956	1270 1159	-	-	-	-	-	-	-	-	-	-
Schiff base(L_3')	1626	2990	1258 1165	-	-	-	-	-	-	-	-	-	-
Schiff base(L_4')	1628	2995	1258 1160	-	-	-	-	-	-	-	--	-	-
Schiff base (L_5)	1614	3451 3071	1315 1166	1548	-	-	-	-	-	-	-	-	-
Schiff base (L_6)	1599	3414	1215 1166	1538	-	-	-	-	-	-	-	-	-

Compounds	IR bands (cm^{-1})												
	$\nu_{C=N}$	ν_{O-H}	ν_{C-O}	$\nu_{C=C}$	ν_{M-N}	ν_{M-O}	$\nu_{V=O}$	ν_{NO} asy (free NO_3^-)	ν NO_3^- (coord. NO_3^-)	ν_{O-H} (H_2O)	ρ_{rock} (H_2O)	ρ_{wagg} (H_2O)	other
Schiff base (L_7)	1615	3415 2924	1304 1249	-	-	-	-	-	-	-	-	-	-
Schiff base (L_8)	1612	3425	1317 1249	-	-	-	-	-	-	-	-	-	-
Schiff base (L_9)	1617	3447	1143	1520	-	-	-	-	-	-	-	-	-
Schiff base(L_{10})	1641		-	-	-	-	-	-	-	-	-	-	-
Schiff base(L_{11})	1629	3428	1319	-	-	-	-	-	-	-	-	-	-
Schiff base(L_{12})	1617	3428	1327	-	-	-	-	-	-	-	-	-	-
Schiff base(L_{13})	1626	3422	1145	-	-	-	-	-	-	-	-	-	-
Schiff base(L_{14})	1610	3429	1178	-	-	-	-	-	-	-	-	-	-
Schiff base(L_{15})	1637	-	-	-	-	-	-	-	-	-	-	-	-
Schiff base(L_{16})	1610	-	-	-	-	-	-	-	-	-	-	-	-
$[Fe(L_1)_2(NO_3)_2]NO_3$ (**1**)	1590	-	-	-	490	-	-	1383	1447 1321 1026	-	-	-	-
$[Fe(L_2)_2(NO_3)_2]NO_3$ (**2**)	1590	-	-	-	489	-	-	1383	1447 1321 1071	-	-	-	-

Compounds	IR bands (cm^{-1})												
	$\nu_{C=N}$	ν_{O-H}	ν_{C-O}	$\nu_{C=C}$	ν_{M-N}	ν_{M-O}	$\nu_{V=O}$	ν_{NO} asy (free NO_3^-)	ν NO_3^- (coord. NO_3^-)	ν_{O-H} (H_2O)	ρ_{rock} (H_2O)	ρ_{wagg} (H_2O)	other
$[VO(L_1)_2]SO_4.H_2O$ (**3**)	1590	-	-	-	462	-	937	-	-	3431	-	-	1111(ν_{as}) free SO_4^{2-}
$[VO(L_2)_2]SO_4.H_2O$ (**4**)	1595	-	-	-	467	-	985	-	-	3427	-	-	1111(ν_{as}) free SO_4^{2-}
$[FeL_3Cl]_2$ (**5**)	1607	-	1305	-	505	480	-	-	-	-	-	-	-
$[FeL_4Cl]_2$ (**6**)	1607	-	1300	-	505	480	-	-	-	-	-	-	-
$[VOL_3]_2$ (**7**)	1600	-	1305	-	480	429	990	-	-	-	-	-	-
$[VOL_4]_2$ (**8**)	1601	-	1305	-	530	510	990	-	-	-	-	-	-
$[FeL_5Cl]_2$ (**9**)	1604	-	1315 1218	-	546	443	-	-	-	-	-	-	-
$[VOL_5]_2.H_2O$ (**10**)	1596	-	1319 1212	-	530	460	966	-	-	3403	-	-	-
$[FeL_5Cl(PPh_3)]_2$ (**11**)	1617	-	1384 1158	-	541	477	-	-	-	-	-	-	1120(ν_{P-C}), 723, 667
$[FeL_5Cl\ Im]_2$ (**12**)	1617	-	1305 1145	-	481	408	-	-	-	-	-	-	3412(ν_{N-H}), 3110(ν_{C-H}), 1533, 1460, 1399

Compounds	IR bands (cm^{-1})												
	$\nu_{C=N}$	ν_{O-H}	ν_{C-O}	$\nu_{C=C}$	ν_{M-N}	ν_{M-O}	$\nu_{V=O}$	ν_{NO} asy (free NO_3^-)	ν NO_3^- (coord. NO_3^-)	ν_{O-H} (H_2O)	ρ_{rock} (H_2O)	ρ_{wagg} (H_2O)	other
$[FeL_5(H_2O)_2]_2$ (**13**)	1606	-	1378 1229	-	533	462	-	-	-	3406	835	657	-
$Na[VO_2L_5]$ (**14**)	1561	-	1416 1274	-	536	465	918	-	-	-	-	-	-
$[FeL_6Cl]$ (**15**)	1578	-	1301 1255	-	528	483	-	-	-	-	-	-	-
$[VOL_6(H_2O)].H_2O$ (**16**)	1586	-	1303 1242	-	539	488	976	-	-	3364	906	656	-
$[FeL_7(acac)(EtOH)]$ (**17**)	1601	-	1361 1277	-	550	495	-	-	-	-	-	-	3447(ν_{O-H}) (ethanol)
$[FeL_8(acac)(EtOH)]$ (**18**)	1597	-	1340 1252	-	502	458	-	-	-	-	-	-	3446(ν_{O-H}) (ethanol)
$[FeL_9(H_2O)_2]NO_3$ (**19**)	1573	-	1274	-	453	435	-	1385	-	3419	930	654	-
$[FeL_{11}(H_2O)_2]NO_3$ (**20**)	1597	-	1338	-	553	499	-	1378	-	3418	853	617	-
$[FeL_{12}(H_2O)_2]NO_3$ (**21**)	1605	-	1339	-	565	515	-	1384	-	3434	869	604	-
$[FeL_{13}(NO_3)H_2O]$ (**22**)	1597	-	1173	-	595	467	-	-	1433 1318 1026	3466	875	642	-

Compounds	IR bands (cm^{-1})												
	$\nu_{C=N}$	ν_{O-H}	ν_{C-O}	$\nu_{C=C}$	ν_{M-N}	ν_{M-O}	$\nu_{V=O}$	ν_{NO} asy (free NO_3^-)	ν NO_3^- (coord. NO_3^-)	ν_{O-H} (H_2O)	ρ_{rock} (H_2O)	ρ_{wagg} (H_2O)	other
$[FeL_{14}(NO_3)H_2O]$ (**23**)	1597	-	1211	-	518	463	-	-	1454 1306 1026	3434	937	640	-
$NH_4[FeL_9F_2]$ (**24**)	1627	-	1508	-	484	431	-	-	-	-	-	-	652(ν_{Fe-F})
$NH_4[FeL_9(NCS)_2]$ (**25**)	1569	-	1420	-	483	435	-	-	-	-	-	-	2073, 2049 (ν_{C-N}) 771 (ν_{C-S}) 483 (ν_{NCS}) 414(ν_{Fe-NCS})
$Na[FeL_9(N_3)_2]$ (**26**)	1624	-	1260	-	486	435	-	-	-	-	-	-	2366, 2344 (ν_{N-N-N})
$[FeL_{12}(Im)_2]NO_3$ (**27**)	1617	-	1341	-	505	477	-	1384	-	-	-	-	3431(ν_{N-H}), 3112(ν_{C-H}), 1541, 1457, 1360
$[FeL_{12}(Py)_2]NO_3$ (**28**)	1598	-	1295	-	561	520	-	-	-	-	-	-	1573, 1436, 639, 473
$[VOL_9]H_2O$ (**29**)	1527	-	1286	-	461	424	996	-	-	3420	-	-	-

Compounds	IR bands (cm^{-1})												
	$\nu_{C=N}$	ν_{O-H}	ν_{C-O}	$\nu_{C=C}$	ν_{M-N}	ν_{M-O}	$\nu_{V=O}$	ν_{NO} asy (free NO_3^-)	ν NO_3^- (coord. NO_3^-)	ν_{O-H} (H_2O)	ρ_{rock} (H_2O)	ρ_{wagg} (H_2O)	other
$[VOL_{11}]H_2O$ (**30**)	1610	-	1330	-	552	445	938	-	-	-	-	-	-
$[VOL_{12}]H_2O$ (**31**)	1606	-	1341	-	529	504	987	-	-	3418	-	-	-
$[VOL_{13}]H_2O$ (**32**)	1614	-	1163	-	478	443	983	-	-	3423	-	-	-
$[VOL_{14}]H_2O$ (**33**)	1591	-	1171	-	516	462	953	-	-	3317	-	-	-
$[FeL_{15}Cl_2]Cl$ (**34**)	1590	-	-	-	553	-	-	-	-	-	-	-	461 (ν_{Fe-Cl})
$[FeL_{16}Cl_2]Cl$ (**35**)	1624	-	-	-	512	-	-	-	-	-	-	-	455 (ν_{Fe-F})
$[VOL_{15}]SO_4.H_2O$ (**36**)	1556	-	-	-	454	-	988	-	-	3447	-	-	1111(ν_{as}) free SO_4^{2-}
$[VOL_{16}]SO_4.H_2O$ (**37**)	1635	-	-	-	498	-	978	-	-	3443	-	-	1058(ν_{as}) free SO_4^{2}
$[Fe(L_{10})(H_2O)_2](NO_3)_3$ (**38**)	1617	-	-	-	530	486	-	1382	-	3367	882	591	-
$[VO(L_{10})]SO_4.H_2O$ (**39**)	1626	-	-	-	470	434	978	-	-	3425	-	-	1120(ν_{as}) free SO_4^{2}
$[Fe(L_9)(H_2O)_2]$ (**40**)	1609	-	1232	-	586	542	-	-	-	3430	859	630	-

bound NCS^- group [219]. The peaks at 2044 and 2066 cm^{-1} in the complex **26** are attributable to the characteristics vibration of azido group. Coordinated triphenylphosphine in the complex **11** is confirmed by the appearance of P-C stretching at 1120 cm^{-1}. This is supported by strong out of plane ring vibration at 690 cm^{-1} and C-H out of plane bending vibration at 723 cm^{-1}. Mixed ligand imidazole complexes **12** and **27** showed characteristics C-H and N-H stretching at *ca* 3100 and 3400 cm^{-1} alongwith ring vibrations of coordinated imidazole (sp^2-N bonded) in the range 1600-1300 cm^{-1}. Two strong bands observed near 640 and 470 cm^{-1} in the complex **28** is attributable to in plane ring deformation and out of plane ring deformation of coordinated pyridine. Further characteristic ring vibration of coordinated pyridine is observed in the range 1600-1400 cm^{-1}. The other absorption peaks corresponding to aromatic ν(C–H) and ν(C=C) vibrational modes appear at expected positions.

6.4. Electronic spectra

The electronic spectra of the ligands and complexes (Appendix 2) were obtained in dichloromethane solution and the most significant data are presented in Table-3. The spectra of all the ligands exhibited two bands between 231-261 and 306-368 *nm* assigned to $\pi\rightarrow\pi^*$ and $n\rightarrow\pi^*$ transitions, respectively, originating from (-C=N-) chromophore of the Schiff base. Further, the ligands $\mathbf{L_3}$, $\mathbf{L_4}$, $\mathbf{L_7}$, $\mathbf{L_8}$ and $\mathbf{L_{13}}$ showed an additional $\pi\rightarrow\pi^*$ transition in 274-288 nm region. The peaks at 350-376 and 404-453 nm in the ligands $\mathbf{L_{11}}$ and $\mathbf{L_{12}}$ is also assignable to $\pi\rightarrow\pi^*$ and $n\rightarrow\pi^*$ electronic transitions. The electronic spectra of iron(III) complexes **1, 2, 11, 12, 17-28, 34, 35** and **38** showed bands in 482-517 nm that may be assigned to spin and parity forbidden $^6A_{1g}\rightarrow{}^4T_{2g}$ transition and suggested distorted octahedral geometry around the Fe(III) ions. The complexes **5, 6** and **9**, however, showed a very weak peak around 508 and 717 nm and were tentatively assigned to d-d transition in a square pyramidal ligand field or

TABLE-3. Electronic spectral bands of ligands and their complexes

Compounds	Bands (λ_{max}, nm)	Molar extinction coefficient (ε, $M^{-1}cm^{-1}$)	Assignments	Geometry
Schiff base (L_1)	337	2730	n→π*	-
	258	27990	π →π*	
Schiff base (L_2)	341	2050	n→π*	-
	261	33250	π →π*	
Schiff base (L_3)	360	23170	n→π*	-
	287	14200	π →π*	
	257	24550	π →π*	
Schiff base (L_4)	361	25400	n→π*	-
	288	14800	π →π*	
	260	11232	π →π*	
Schiff base (L_5)	312	32320	n→π*	-
	235	11460	π →π*	
Schiff base (L_6)	341	15300	n→π*	-
	247	20060	π →π*	
Schiff base (L_7)	340	18880	n→π*	-
	306	15700	n→π*	
	274	6100	π →π*	
	246	59400	π →π*	
Schiff base (L_8)	340	15600	n→π*	-
	306	13300	n→π*	
	277	2800	π →π*	
	246	49600	π →π*	
Schiff base (L_9)	317	35240	n→π*	-
	231	3600	π →π*	
Schiff base(L_{10})	337	20300	n→π*	-
	259	1800	π →π*	
Schiff base(L_{11})	454	11320	n→π*	-
	376	18700	π →π*	
	322	17820	n→π*	
	244	43580	π →π*	

Compounds	Bands (λ_{max}, nm)	Molar extinction coefficient (ε, $M^{-1}cm^{-1}$)	Assignments	Geometry
Schiff base(L_{12})	404	11100	n→π*	-
	350	12800	π →π*	
	313	17000	n→π*	
	241	49700	π →π*	
Schiff base(L_{13})	368	19400	n→π*	-
	286	16010	π →π*	
	261	15510	n→π*	
	244	17380	π →π*	
Schiff base(L_{14})	340	14400	n→π*	-
	246	61500	π →π*	
Schiff base(L_{15})	364	15400	n→π*	-
	260	16180	π →π*	
	234	27130	π →π*	
Schiff base(L_{16})	342	13100	n→π*	-
	244	44120	π →π*	
$[Fe(L_1)_2(NO_3)_2]NO_3$ (1)	501	540	$^6A_{1g}\rightarrow{}^4T_{2g}$	Octahedral
	363	940	LMCT	
	343	960	Intraligand	
	262	17700	Intraligand	
$[Fe(L_2)_2(NO_3)_2]NO_3$ (2)	513	120	$^6A_{1g}\rightarrow{}^4T_{2g}$	Octahedral
	380	540	LMCT	
	363	560	Intraligand	
	261	39580	Intraligand	
$[VO(L_1)_2]SO_4.H_2O$ (3)	451	769	$^2B_2\rightarrow{}^2A_1$	Square pyramidal
	418	766	LMCT	
	297	-	Intraligand	
	276	3957	Intraligand	
	271	-	Intraligand	
	261	-	Intraligand	
	250	-	Intraligand	
	237	-	Intraligand	

Compounds	Bands (λ_{max}, nm)	Molar extinction coefficient (ε, $M^{-1}cm^{-1}$)	Assignments	Geometry
$[VO(L_2)_2]SO_4.H_2O$ (**4**)	513 261 242 227	150 35100 44850 -	$^2B_2 \rightarrow {}^2A_1$ Intraligand Intraligand Intraligand	Square pyramidal
$[FeL_3Cl]_2$ (**5**)	374 272	15060 30440	LMCT Intraligand	Binuclear square pyramidal
$[FeL_4Cl]_2$ (**6**)	508 315 280 248	200 18160 43160 -	$^6A_{1g} \rightarrow {}^4T_{2g}$ Intraligand Intraligand Intraligand	Binuclear square pyramidal
$[VOL_3]_2$ (**7**)	411 406 341 249 244 224	500 490 510 - 5630 7650	$^2B_2 \rightarrow {}^2A_1$ - Intraligand Intraligand Intraligand Intraligand	Binuclear square pyramidal
$[VOL_4]_2$ (**8**)	414 356 323	24450 20150 20800	$^2B_2 \rightarrow {}^2A_1$ Intraligand Intraligand	Binuclear square pyramidal
$[FeL_5Cl]_2$ (**9**)	717 462 441 364 315 250 240	220 16210 16550 20340 17530 - -	$^6A_{1g} \rightarrow {}^4T_{1g}$ $^6A_{1g} \rightarrow {}^4T_{2g}$ $^6A_{1g} \rightarrow {}^4A_{1g}$ LMCT Intraligand Intraligand -	Binuclear square pyramidal
$[VOL_5]_2.H_2O$ (**10**)	410 231	7250 -	LMCT Intraligand	Binuclear square pyramidal

Compounds	Bands (λ_{max}, nm)	Molar extinction coefficient (ε, $M^{-1}cm^{-1}$)	Assignments	Geometry
$[FeL_5Cl(PPh_3)]_2$ (**11**)	365	2590	LMCT	Octahedral
	231	13800	Intraligand	
$[FeL_5Cl\ (Im)]_2$ (**12**)	503	930	$^6A_{1g}\rightarrow{}^4T_{2g}$	Octahedral
	466	1145	$^6A_{1g}\rightarrow{}^4A_{1g}$	
	364	2630	LMCT	
	311	2810	Intraligand	
	244	6620	Intraligand	
$[FeL_5(H_2O)_2]_2$ (**13**)	420	5980	LMCT	Octahedral
	306	29140	Intraligand	
	231	18940	Intraligand	
$Na[VO_2L_5]$ (**14**)	418	20700	LMCT	Square pyramidal
	242	25140	Intraligand	
$[FeL_6Cl]$ (**15**)	493	250	$^6A_{1g}\rightarrow{}^4T_{2g}$	Distorted square planer
	334	10000	Intraligand	
	247	18250	Intraligand	
	230	20650	Intraligand	
$[VOL_6(H_2O)].H_2O$ (**16**)	493	200	$^2B_2\rightarrow{}^2A_1$	Distorted square planer
	299	35400	Intraligand	
	276	28400	Intraligand	
	254	29400	Intraligand	
$[FeL_7(acac)(EtOH)]$ (**17**)	415	800	$^6A_{1g}\rightarrow{}^4T_{2g}$	Octahedral
	405	1200	$^6A_{1g}\rightarrow{}^4A_{1g}$	
	368	2200	Intraligand	
	340	17000	Intraligand	
	306	14200	Intraligand	
	246	51200	Intraligand	
$[FeL_8(acac)(EtOH)]$ (**18**)	415	700	$^6A_{1g}\rightarrow{}^4A_{1g}$	Octahedral
	368	1300	Intraligand	
	340	8250	Intraligand	
	306	6850	Intraligand	
	246	24950	Intraligand	
	233	-	Intraligand	

Compounds	Bands (λ_{max}, nm)	Molar extinction coefficient (ε, $M^{-1}cm^{-1}$)	Assignments	Geometry
$[FeL_9(H_2O)_2]NO_3$ (**19**)	482	300	$^6A_{1g} \rightarrow {}^4T_{2g}$	Octahedral
	410	500	$^6A_{1g} \rightarrow {}^4A_{1g}$	
	323	20500	Intraligand	
	278	8550	Intraligand	
$[FeL_{11}(H_2O)_2]NO_3$ (**20**)	513	1500	$^6A_{1g} \rightarrow {}^4T_{2g}$	Octahedral
	342	8200	Intraligand	
	248	11800	Intraligand	
$[FeL_{12}(H_2O)_2]NO_3$ (**21**)	517	400	$^6A_{1g} \rightarrow {}^4T_{2g}$	Octahedral
	473	420	$^6A_{1g} \rightarrow {}^4A_{1g}$	
	359	8130	Intraligand	
	319	12060	Intraligand	
	244	21110	Intraligand	
$[FeL_{13}NO_3H_2O]$ (**22**)	422	880	$^6A_{1g} \rightarrow {}^4T_{2g}$	Octahedral
	386	1800	Intraligand	
	262	19420	Intraligand	
	236	-	Intraligand	
$[FeL_{14}NO_3H_2O]$ (**23**)	415	220	$^6A_{1g} \rightarrow {}^4A_{1g}$	Octahedral
	340	3640	Intraligand	
	262	33360	Intraligand	
	246	32600	Intraligand	
$NH_4[FeL_9F_2]$ (**24**)	365	60	$^6A_{1g} \rightarrow {}^4A_{1g}$	Octahedral
	323	25220	Intraligand	
	204	52040	Intraligand	
$NH_4[FeL_9(NCS)_2]$ (**25**)	482	2600	$^6A_{1g} \rightarrow {}^4T_{2g}$	Octahedral
	361	1170	$^6A_{1g} \rightarrow {}^4A_{1g}$	
	303	6490	Intraligand	
	251	5810	Intraligand	
$Na[FeL_9(N_3)_2]$ (**26**)	429	1800	$^6A_{1g} \rightarrow {}^4A_{1g}$	Octahedral
	320	19460	Intraligand	
	276	24220	Intraligand	

Compounds	Bands (λ_{max}, nm)	Molar extinction coefficient (ε, $M^{-1}cm^{-1}$)	Assignments	Geometry
$[FeL_{12}(Im)_2]NO_3$ (**27**)	535	1085	$^6A_{1g} \rightarrow {}^4T_{2g}$	Octahedral
	519	1030	$^6A_{1g} \rightarrow {}^4A_{1g}$	
	309	13065	Intraligand	
	257	-	Intraligand	
	237	-	Intraligand	
$[FeL_{12}(Py)_2]NO_3$ (**28**)	381	6580	LMCT	Octahedral
	340	8940	LMCT	
	318	7240	Intraligand	
	256	18000	Intraligand	
	250	18300	Intraligand	
	231	22600	Intraligand	
$[VOL_9]H_2O$ (**29**)	481	140	$^2B_2 \rightarrow {}^2A_1$	Square pyramidal
	319	34120	Intraligand	
	227	13180	Intraligand	
$[VOL_{11}]H_2O$ (**30**)	425	17200	Intraligand	Square pyramidal
	353	17700	Intraligand	
	315	15300	Intraligand	
	302	14800	Intraligand	
	246	59400	Intraligand	
$[VOL_{12}]H_2O$ (**31**)	772	200	$^2B_2 \rightarrow {}^2E$	Square pyramidal
	513	400	$^2B_2 \rightarrow {}^2A_1$	
	386	16400	LMCT	
	334	28800	Intraligand	
	245	75700	Intraligand	
	235	-	Intraligand	
$[VOL_{13}]H_2O$ (**32**)	524	200	Intraligand	Square pyramidal
	415	1100	$^2B_2 \rightarrow {}^2A_1$	
	368	1400	LMCT	
	340	18300	Intraligand	
	306	23500	Intraligand	
	246	64500	Intraligand	
	238	-	Intraligand	

Compounds	Bands (λ_{max}, nm)	Molar extinction coefficient (ε, $M^{-1}cm^{-1}$)	Assignments	Geometry
$[VOL_{14}]H_2O$ (**33**)	415 363 340 262 246	140 170 1930 10420 12710	$^2B_2 \rightarrow {}^2A_1$ LMCT Intraligand Intraligand Intraligand	Square pyramidal
$[FeL_{15}Cl_2]Cl$ (**34**)	490 365 261 230	150 750 49150 34500	$^6A_{1g} \rightarrow {}^4T_{2g}$ Intraligand Intraligand Intraligand	Octahedral
$[FeL_{16}Cl_2]Cl$ (**35**)	343 245	8660 27370	Intraligand Intraligand	Octahedral
$[VOL_{15}]SO_4.H_2O$ (**36**)	490 262 229	200 28600 45800	$^2B_2 \rightarrow {}^2A_1$ Intraligand Intraligand	Square pyramidal
$[VOL_{16}]SO_4.H_2O$ (**37**)	490 414 342 245	300 500 11370 39570	$^2B_2 \rightarrow {}^2A_1$ LMCT Intraligand Intraligand	Square pyramidal
$[Fe(L_{10})(H_2O)_2](NO_3)_3$ (**38**)	505 338 259 235	- 25760 3960 -	$^6A_{1g} \rightarrow {}^4T_{2g}$ Intraligand Intraligand Intraligand	Octahedral
$[VO(L_{10})]SO_4.H_2O$ (**39**)	596 337 253 234	60 27370 3130 18510	$^2B_2 \rightarrow {}^2A_1$ Intraligand Intraligand Intraligand	Square pyramidal
$[Fe(L_9)(H_2O)_2]$ (**40**)	437 354 274	2740 2990 22410	LMCT Intraligand Intraligand	Octahedral

to the charge transfer spectra extending to the visible region. The oxovanadium(IV) complexes **3**, **7**, **8**, **10**, **31** and **33** exhibited a very weak intensity band in 410-451 nm region assignable to $^2B_2 \rightarrow {}^2A_1$ transition, which is characteristics of VO(IV) ion in a square pyramidal geometry. The other oxovanadium complexes, however, showed similar transition in relatively lower energy region around 500 nm. In addition, some of the complexes exhibited intense bands in the 363-418 nm regions, which are attributed to a ligand to metal charge transfer (LMCT) transition [220]. The intense higher-energy bands in the region 230-360 nm in all the complexes can be attributed to intraligand $\pi \rightarrow \pi^*$ and $n \rightarrow \pi^*$ transitions [221]. A rather high ε value some Fe(III) and VO(IV) complexes suggest substantial distortion of the octahedral/square pyramidal structure. In most cases, only two d-d bands were observed for Fe(III) complexes instead of three bands as would be expected for Fe(III) complexes in octahedral ligand field. A similar situation was observed in VO(IV) complexes where one d-d band was noted instead of two d-d bands.

6.5. NMR spectra

The ^{1}H NMR spectral data of ligands (Appendix 3) are summerised in **Table-4** and structurally relevant features are discussed herein. The ^{1}H NMR spectrum of the free ligand $\mathbf{L_1}$ and $\mathbf{L_2}$ displayed a sharp singlet at 3.67 and 2.22 δ, which are attributable to the $-OCH_3$ and $-CH_3$ groups, respectively. Schiff bases $\mathbf{L_3}$ and $\mathbf{L_4}$ exhibited the absorption of OH proton at 12.65 and 12.94 δ, respectively, as a singlet. The triplet at 0.88 δ, multiplet at 1.00-1.83 δ, triplet at 4.0 δ in the ligands $\mathbf{L_3}$ and $\mathbf{L_4}$ is due to protons of the $-CH_3$, $-(CH_2)_n$, $-OCH_2$ groups presents in alkoxy side chain, respectively. The singlet at 11.72, 12.97, 15.580 and 10.845 δ in the Schiff base $\mathbf{L_5}$, $\mathbf{L_6}$, $\mathbf{L_7}$ and $\mathbf{L_8}$, respectively, are attributable to the phenolic OH group present in 2-aminophenol moiety.

TABLE-4. ^{1}H NMR spectral data of Schiff base ligands

Compounds	Absorption (δ, ppm)	Type of proton	Multiplicity and coupling constant
Schiff base (L_1)	3.677	$-OCH_3$	Singlet
	6.650-7.531	Benzene ring H	Multiplet
Schiff base (L_2)	2.228	$-CH_3$	Singlet
	6.769-7.879	Benzene ring H	Multiplet
Schiff base (L_3)	0.882	$-CH_3$	Triplet, 4.5 Hz
	1.005-1.835	$-(CH_2)_{10}-$	Multiplet
	4.001	$-OCH_2-$	Triplet, 5.1 Hz
	6.314-7.309	Benzene ring H	Multiplet
	8.564	-CH=N-	Singlet
	12.658	-OH	Singlet
Schiff base (L_4)	0.880	$-CH_3$	Triplet, 4.8 Hz
	1.003-1.825	$-(CH_2)_{12}-$	Multiplet
	3.982	$-OCH_2-$	Triplet, 5.1 Hz
	6.480-7.282	Benzene ring H	Multiplet
	8.532	-CH=N-	Singlet
	12.94	-OH	Singlet
Schiff base (L_5)	1.845	$-CH_3$	Singlet
	2.069	$-CH_3$	Singlet
	5.171	-CH=C<	Singlet
	6.828-7.194	Benzene ring H	Multiplet
	11.725 (aromatic C-OH)	-OH	Singlet
	9.009 (enolic OH)	-OH	Singlet
Schiff base (L_6)	1.252	$-CH_3$	Singlet
	1.677	$-CH_3$	Singlet
	5.269	-CH=C<	Singlet
	6.637-8.045	Benzene ring H	Multiplet
	12.970	-OH	Singlet
Schiff base (L_7)	6.893-7.723	Benzene ring H	Multiplet
	8.041	-CH=N-	Singlet
	15.580	-OH	Singlet
	15.599	-OH	Singlet

Compounds	Absorption (δ, ppm)	Type of proton	Multiplicity and coupling constant
Schiff base (L_8)	6.564-7.841	Benzene ring H	Multiplet
	8.459	-CH=N-	Singlet
	10.845	-OH	Singlet
	13.041	-OH	Singlet
Schiff base (L_9)	1.913	$-CH_3$	Singlet
	2.003	$-CH_3$	Singlet
	3.429	$-CH_2-$	Triplet, 2.4 Hz
	5.001	-CH=C<	Singlet
	10.895	-OH (enol)	Singlet
Schiff base(L_{10})	6.548-6.917	Furan ring H	Multiplet
	8.541	-CH=N-	Singlet
Schiff base(L_{11})	6.836-8.442	Benzene ring H	Multiplet
	9.463	-CH=N-	Singlet
	15.053	-OH	Singlet
	15.269	-OH	Singlet
Schiff base(L_{12})	Very poor solubility in $CDCl_3$ and DMSO		
Schiff base(L_{13})	3.692	$-CH_2-$	Singlet
	4.601	-OH	Singlet
	5.957	-CH<	Singlet
	7.240-7.921	Benzene ring H	Multiplet
Schiff base(L_{14})	4.587	-OH	Doublet, 4.5 Hz
	5.959	-CH<	Doublet, 4.2 Hz
	7.258-7.925	Benzene ring H	Multiplet
Schiff base(L_{15})	3.537-3.753	$-CH_2-$	Multiplet
	7.084-7.404	Benzene ring H	Multiplet
Schiff base(L_{16})	7.166-8.179	Benzene ring H	Multiplet

The appearance of a singlet at 5.17 and 5.26 δ in $\mathbf{L_5}$ and $\mathbf{L_6}$ assignable to olefinic proton provides a compelling evidence that the ligands exist in enol form. The absorption corresponding to other protons appeared at their normal position. The spectra of the ligand $\mathbf{L_9}$ revealed a singlet at 10.89 ppm, attributed to the proton of the enolic OH

group. The methylene protons (-N-CH_2-CH_2-N-), olefinic proton (-CH=C<) and methyl protons (-CH_3) showed their resonances at 3.42, 5.00 and 1.91-2.00 ppm, respectively. Schiff bases ($\mathbf{L_{11}}$-$\mathbf{L_{16}}$), registered absorption of the characteristic protons at usual position. The azomethine protons (-HC=N-) of the Schiff bases ($\mathbf{L_3}$, $\mathbf{L_4}$, $\mathbf{L_7}$, $\mathbf{L_8}$, $\mathbf{L_{10}}$-$\mathbf{L_{12}}$) appeared as singlets at δ 8.53-9.46 while the protons of the benzenoid ring in all the Schiff bases appeared as a multiplet at δ 6.31-8.44. In the Schiff base $\mathbf{L_{10}}$, the protons of furfuraldehyde ring appeared at 6.54-6.91 δ as multiplet.

The ^{13}C NMR spectral data of the Schiff base ligands (Appendix 4) are displayed in **Table-5**. The azomethine carbon atom of all the ligands is observed at 162.82 – 198.92 ppm along with other peaks of structural significance and thus confirming the ^1H NMR results.

TABLE-5. ^{13}C NMR spectral data of Schiff base ligands

Compounds	Prominent peaks (δ, ppm)
Schiff base (L_1)	55.22, 113.89, 122.21, 128.82, 129.23, 131.37, 132.96, 142.29, 156.99, 165.36
Schiff base (L_2)	20.78, 120.49, 128.99, 129.26, 129.86, 131.46, 132.95, 135.21, 146.57, 165.77
Schiff base (L_3)	14.13, 22.54, 22.69, 25.97, 29.03, 29.35, 29.56, 29.59, 29.64, 29.66, 31.92, 68.36, 101.52, 108.13, 113.00, 115.67, 118.14, 120.91, 128.03, 134.03, 135.82, 149.68, 162.79, 163.52, 164.12
Schiff base (L_4)	14.14, 22.70, 25.97, 29.04, 29.37, 29.56, 29.60, 29.66, 29.68, 29.70, 31.93, 68.36, 101.55, 108.10, 113.01, 115.74, 118.22, 120.87, 128.00, 134.01, 135.78, 149.71, 162.68, 163.65, 164.11
Schiff base (L_5)	19.61, 28.61, 97.35, 117.26, 120.13, 125.37, 128.00, 128.74, 152.44, 163.46, 196.23

Schiff base (L_6)	20.54, 24.86, 99.95, 116.38, 124.60, 125.27, 132.09, 135.80, 151.04, 162.82, 168.50, 196.65
Schiff base (L_7)	107.34, 116.01, 116.84, 117.90, 119.41, 122.53, 124.42, 125.75, 126.25, 127.56, 128.62, 133.27, 137.23, 148.47, 149.03, 176.72
Schiff base (L_8)	114.89, 115.84, 116.94, 118.32, 124.32, 126.14, 127.73, 128.54, 128.65, 131.01, 131.42, 132.06, 132.98, 133.10, 137.99, 138.48, 150.32, 192.84
Schiff base (L_9)	18.69, 28.86, 43.49, 96.15, 162.91, 195.53
Schiff base(L_{10})	112.32, 116.92, 145.85, 149.38, 150.98
Schiff base(L_{11})	39.21, 39.49, 39.77, 40.04, 40.35, 118.79, 121.51, 123.30, 127.14, 127.79, 128.98, 136.25, 155.96, 168.48
Schiff base(L_{12})	Very poor solubility in $CDCl_3$ and DMSO
Schiff base(L_{13})	45.78, 127.78, 127.92, 128.14, 128.60, 129.15, 129.16, 133.44, 133.94, 138.99, 198.95
Schiff base(L_{14})	76.19, 76.58, 77.00, 77.42, 127.73, 128.22, 128.53, 128.64, 129.09, 129.81, 133.47, 133.85, 138.97, 198.92
Schiff base(L_{15})	45.76, 127.89, 128.12, 129.65, 137.69, 160.33
Schiff base(L_{16})	128.27, 128.80, 129.18, 129.82, 129.97, 139.04, 141.21, 153.47

6.6. Mass spectra

The mass spectra of selected ligands and complexes have been recorded in ESI^+/FAB^+ ionization mode (Appendix 5). The m/z values of the peaks are listed in **Table-6**. The peaks corresponding to molecular ions $[M]^+$ was observed in all the ligands and complexes. In few compounds the peaks due to $[M+H]^+$ has also been observed [222].

TABLE-6. Mass spectral data of the selected ligands and complexes.

Compounds	m/z
Schiff base (L_2)	388$[M]^+$, 194, 91, 103
Schiff base (L_3)	400.7, 399.7, 398.6, 396.6$[M]^+$, 228, 185
Schiff base (L_4)	427.4, 426.5, 229.6
Schiff base (L_5)	191.9$[M]^+$, 173.9, 133.8
Schiff base (L_6)	219.7$[M]^+$, 201.9, 162.8, 161.7
Schiff base (L_7)	263.1$[M]^+$
Schiff base (L_8)	291.1$[M]^+$, 292.1, 293.1
Schiff base (L_9)	226, 225, 166.8, 125.8, 83.8, 57.9, 44
Schiff base(L_{10})	190.1, 189.1, 188.1$[M]^+$, 161.1
Schiff base(L_{12})	370.1, 369.1, 368.1$[M]^+$, 225.1, 215.1
Schiff base(L_{13})	449, 225, 210, 105, 107
Schiff base(L_{15})	468$[M]^+$, 235, 206, 131.8, 129.8, 117.8, 103.8,
Schiff base(L_{16})	283.1, 204.9,
$[VO(L_1)_2]SO_4.H_2O$ (**3**)	1021$[M]^+$, 420
$[FeL_4Cl]_2$ (**6**)	1029$[M]^+$, 994, 958, 514, 479, 387, 282
$[VOL_3]_2$ (**7**)	926$[M]^+$, 755, 616, 463, 398, 370, 294, 278
$[FeL_5Cl]_2$ (**9**)	561$[M]^+$, 489, 281, 191
$[VOL_5]_2.H_2O$ (**10**)	529$[M]^+$, 512, 254, 191
$[FeL_7(acac)(EtOH)]$ (**17**)	464.1$[M]^+$
$[FeL_8(acac)(EtOH)]$ (**18**)	489$[M]^+$, 443
$[FeL_9(H_2O)_2]NO_3$ (**19**)	378$[M]^+$, 390, 340, 278, 263
$[FeL_{13}NO_3H_2O]$ (**22**)	578, 520
$NH_4[FeL_9(NCS)_2]$ (**25**)	413, 393, 278, 248

Compounds	m/z
$Na[FeL_9(N_3)_2]$ (**26**)	386, 364, 320
$[VOL_9]H_2O$ (**29**)	307, 289
$[VOL_{11}]H_2O$ (**30**)	498.2$[M]^+$
$[VOL_{13}]H_2O$ (**32**)	531$[M]^+$, 514
$[VOL_{14}]H_2O$ (**33**)	561, 409, 254
$[VOL_{15}]SO_4.H_2O$ (**36**)	648$[M]^+$
$[VOL_{16}]SO_4.H_2O$ (**37**)	744$[M]^+$, 669
$[Fe(L_{10})(H_2O)_2](NO_3)_3$ (**38**)	466$[M]^+$, 432
$[VO(L_{10})]SO_4.H_2O$ (**39**)	369, 351.1
$[Fe(L_9)(H_2O)_2]$ (**40**)	314$[M]^+$, 278$[M-2H_2O]$

In addition to molecular ion peaks, the spectra exhibited peaks assignable to various fragments. The probable fragmentation patterns are as follows.

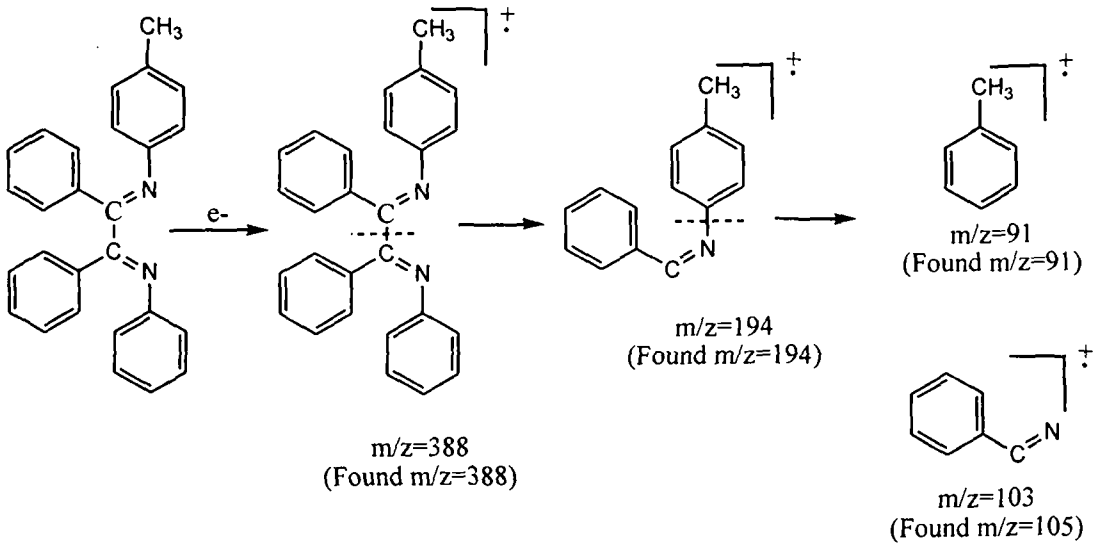

Fragmentation pattern of the Schiff base L_2

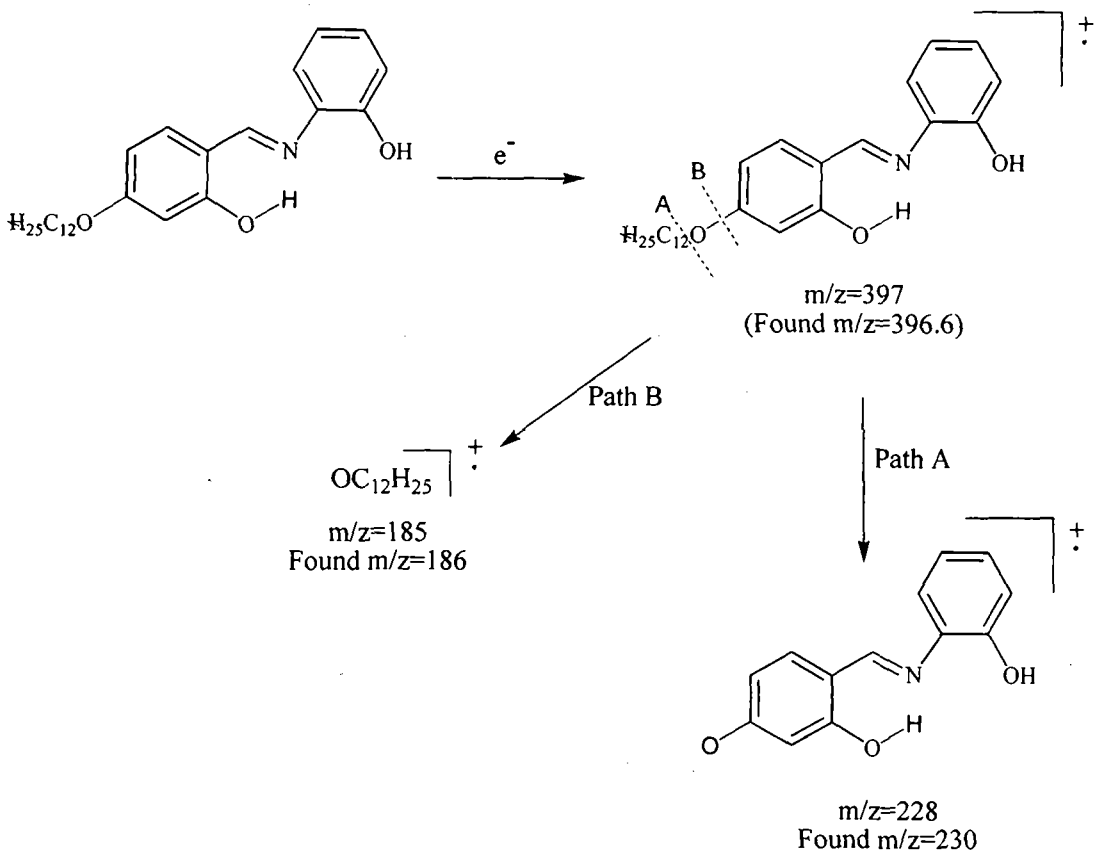

Fragmentation pattern of Schiff base L_3

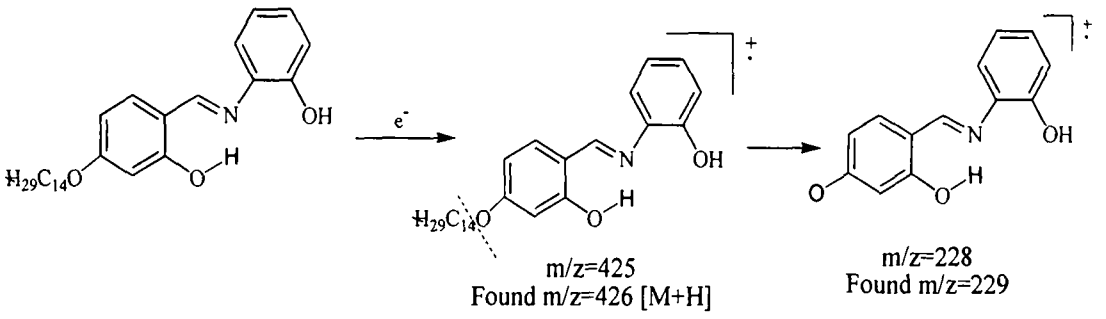

Fragmentation pattern of Schiff base L_4

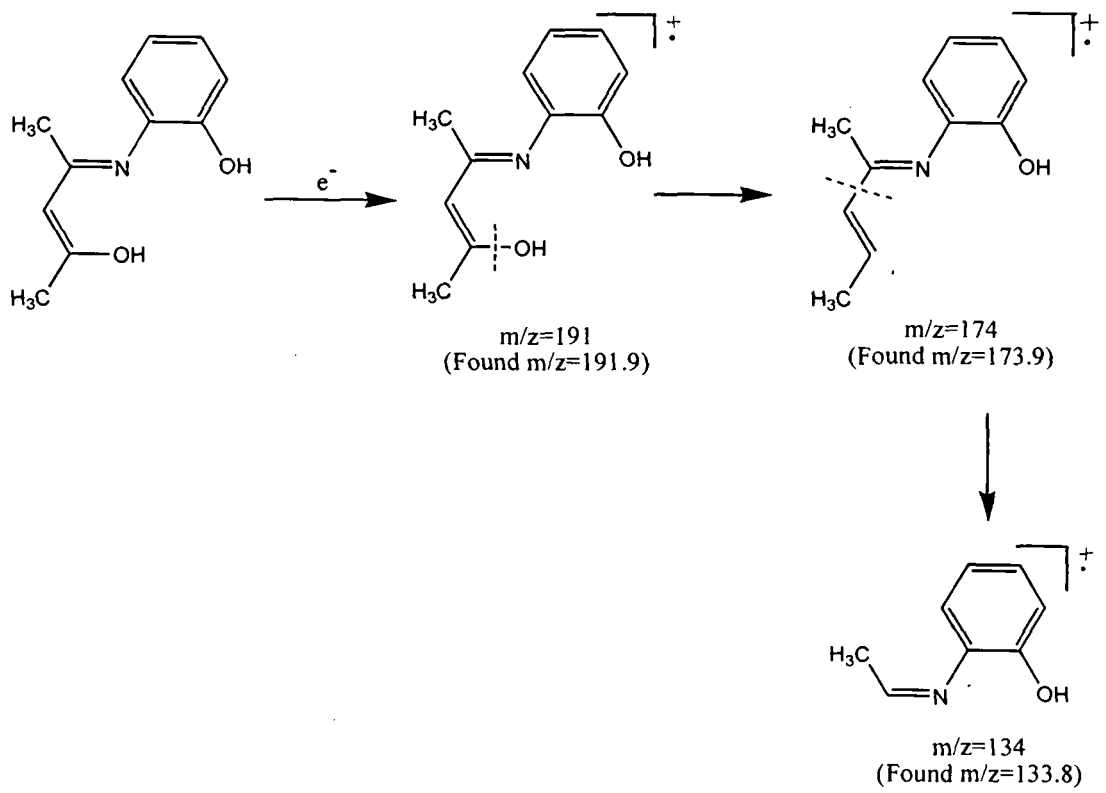

Fragmentation pattern of Schiff base L_5

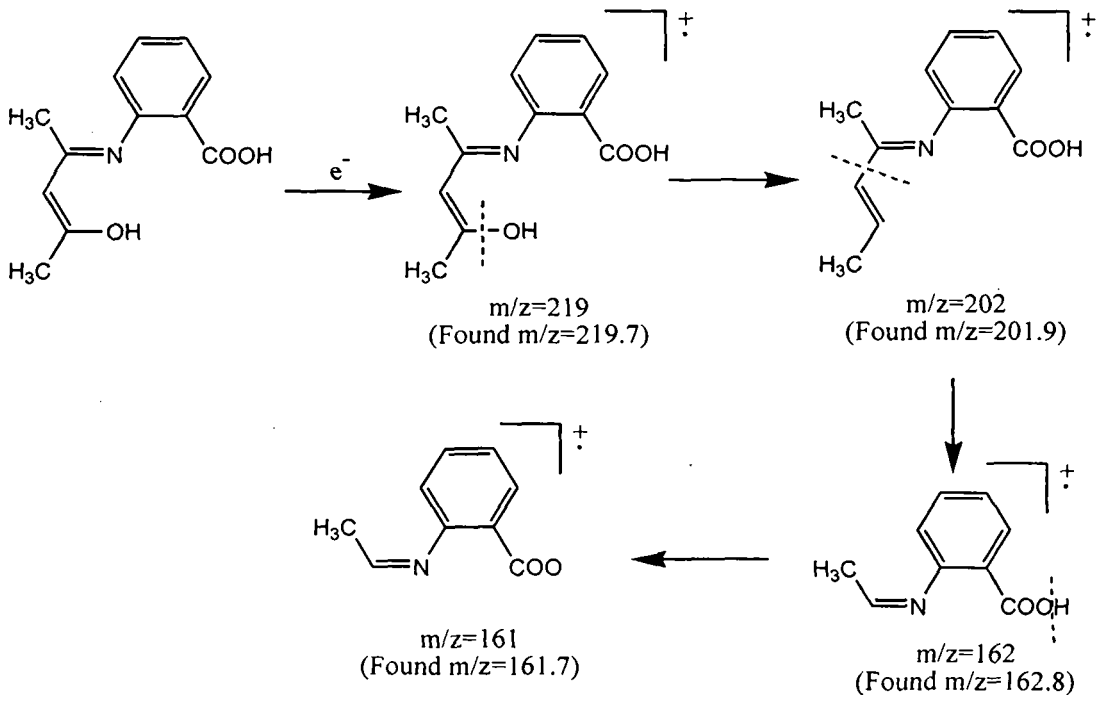

Fragmentation pattern of Schiff base L_6

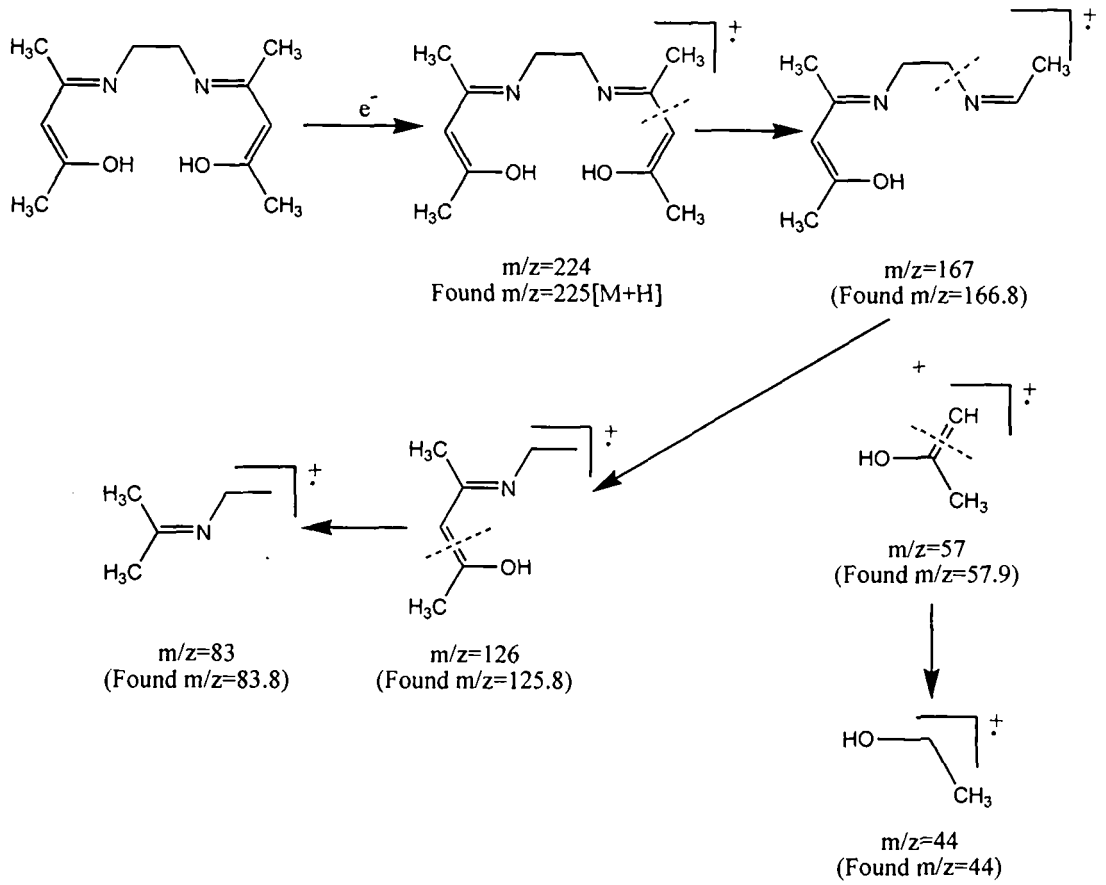

Fragmentation pattern of Schiff base L_9

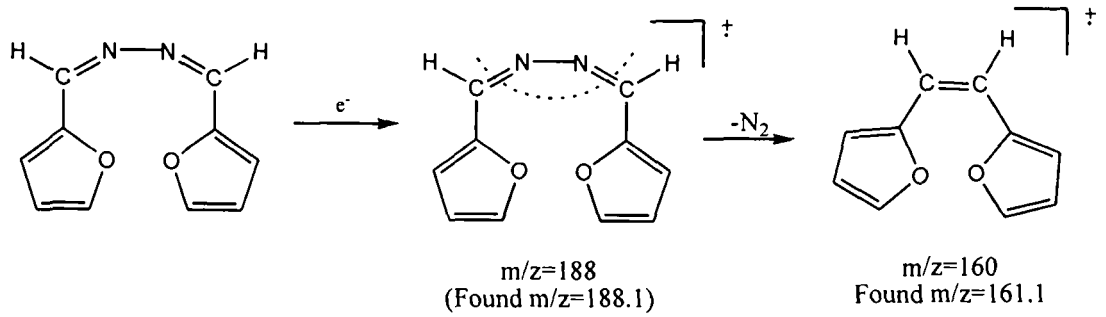

Fragmentation pattern of Schiff base L_{10}

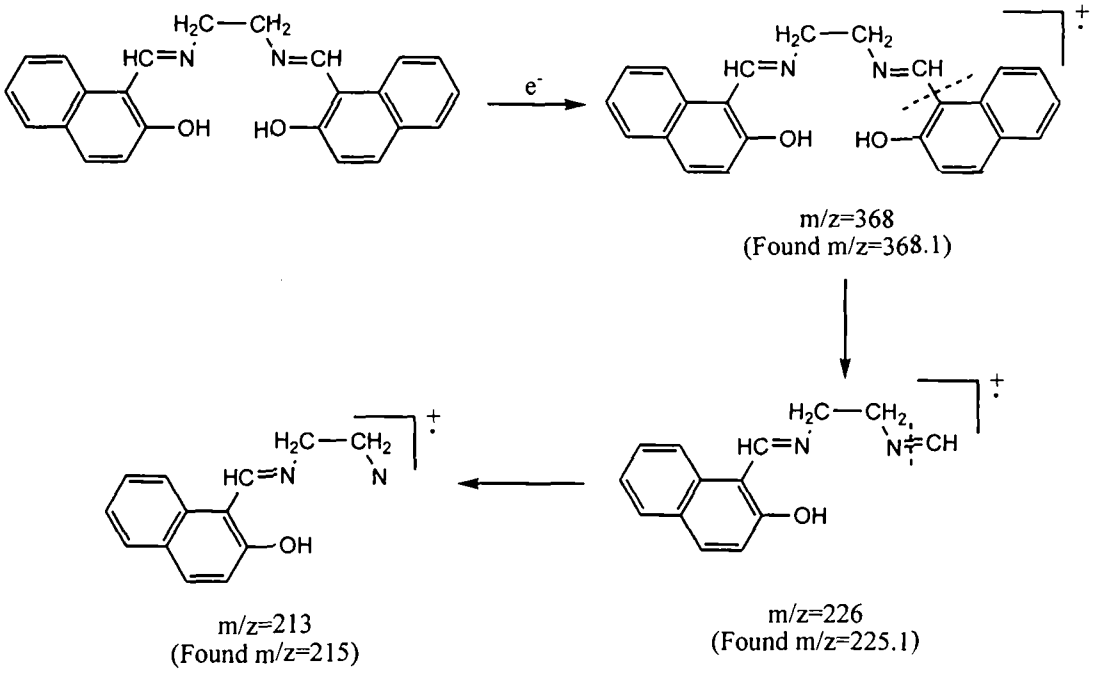

Fragmentation pattern of the Schiff base L_{12}

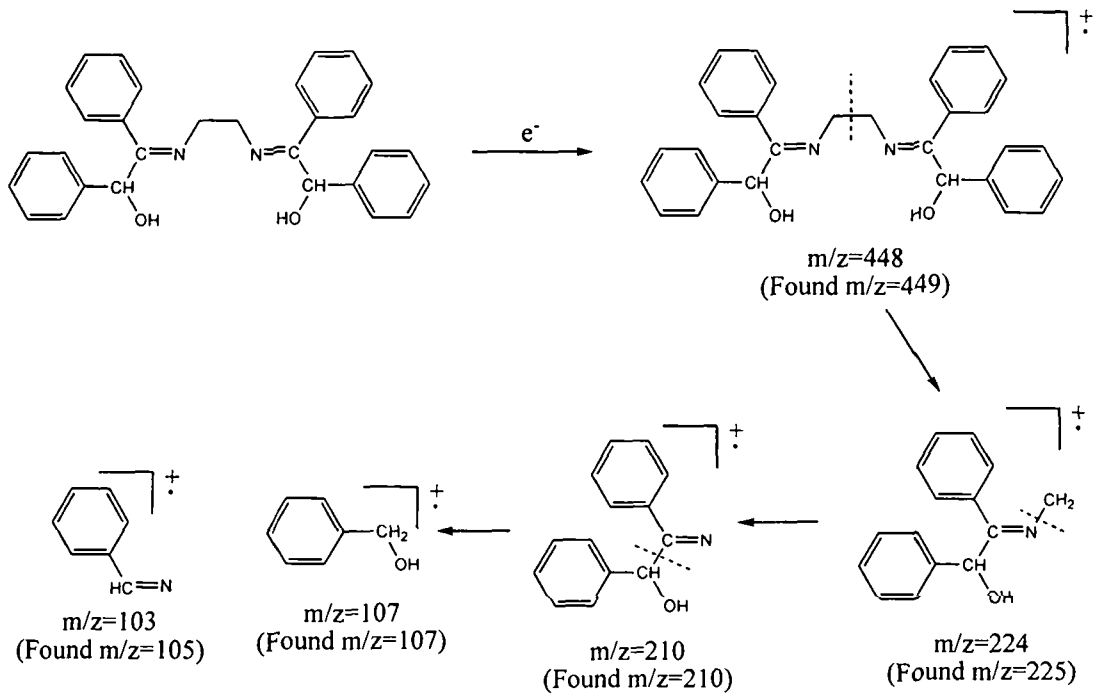

Fragmentation pattern of the Schiff base L_{13}

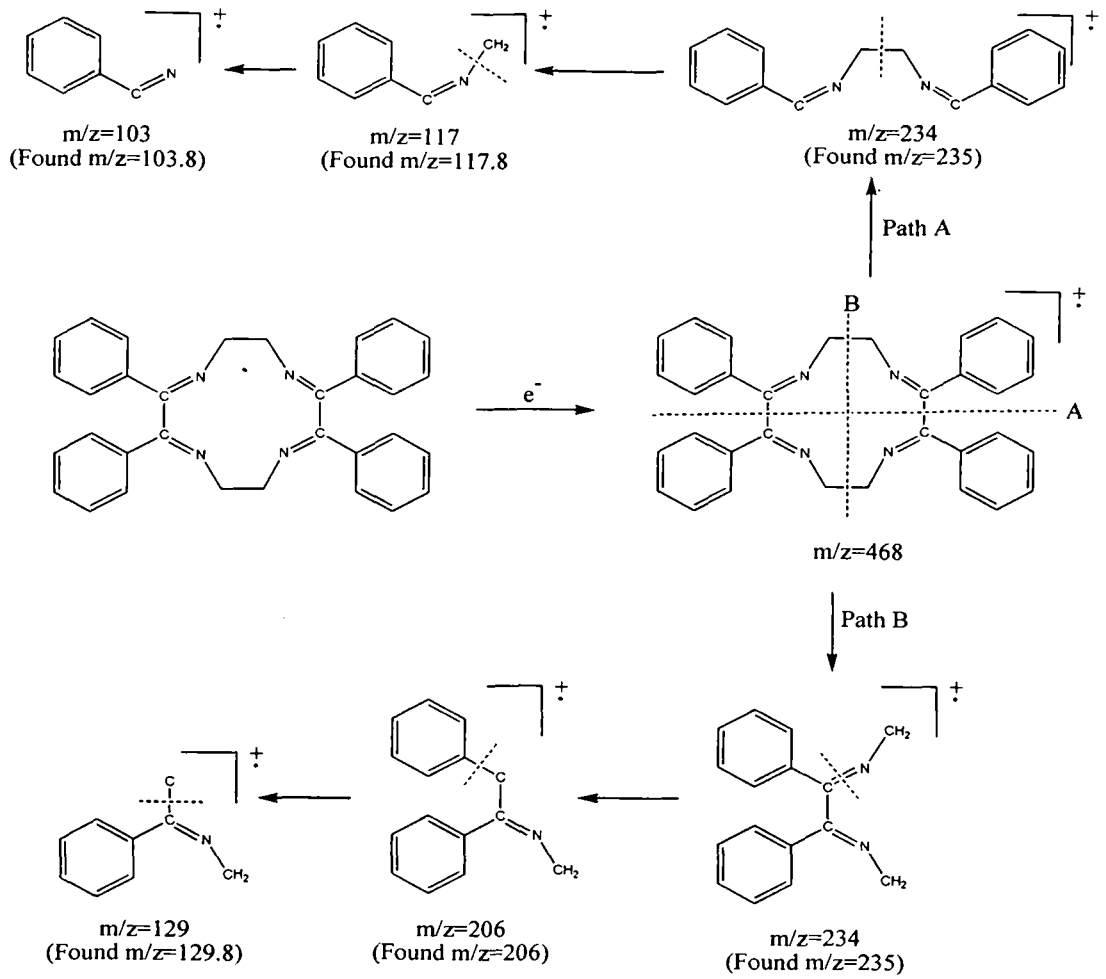

Fragmentation pattern of Schiff base L_{15}

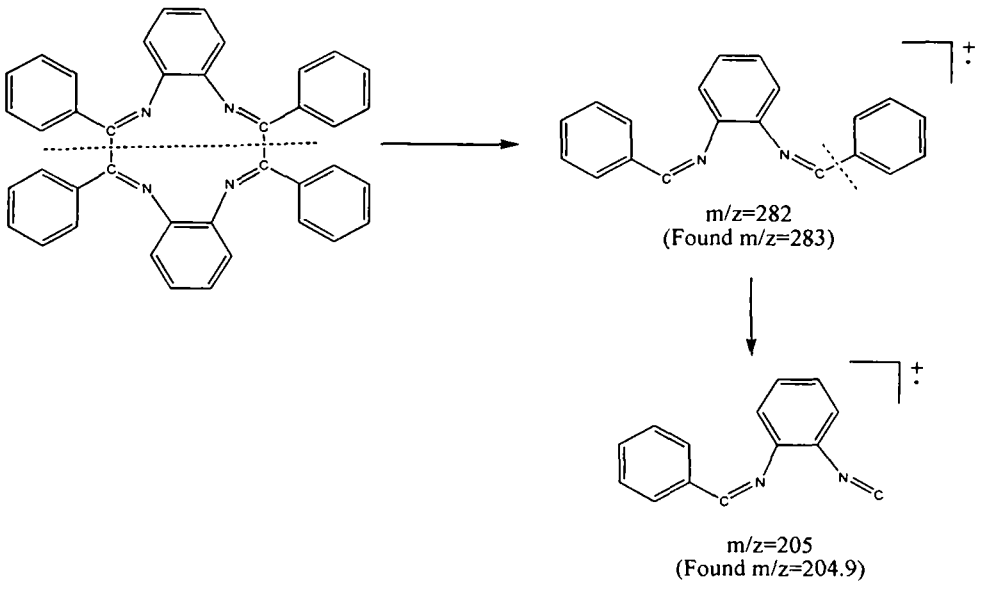

Fragmentation pattern of Schiff base L_{16}

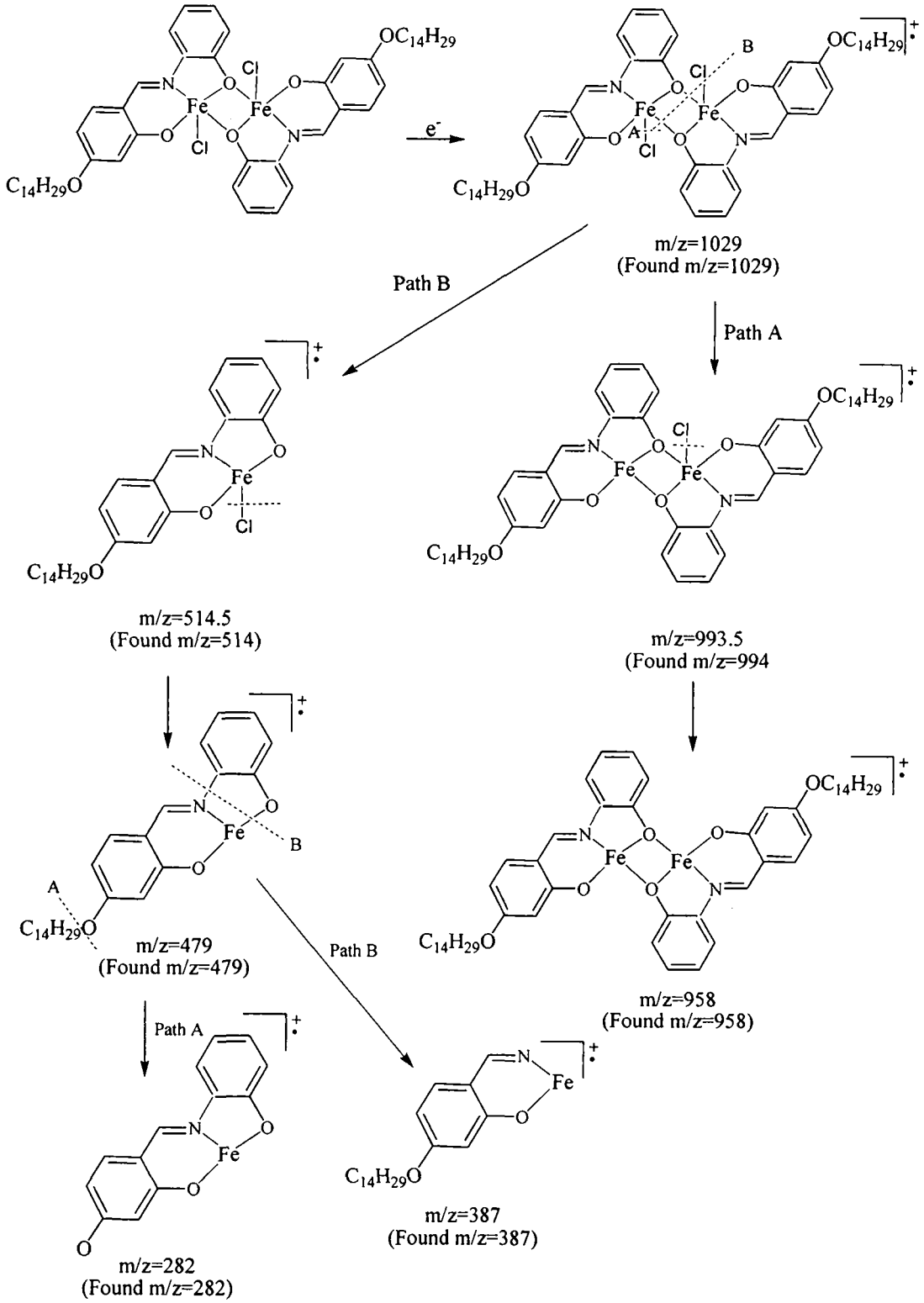

Fragmentation pattern of the complex $[FeL_4Cl]_2$

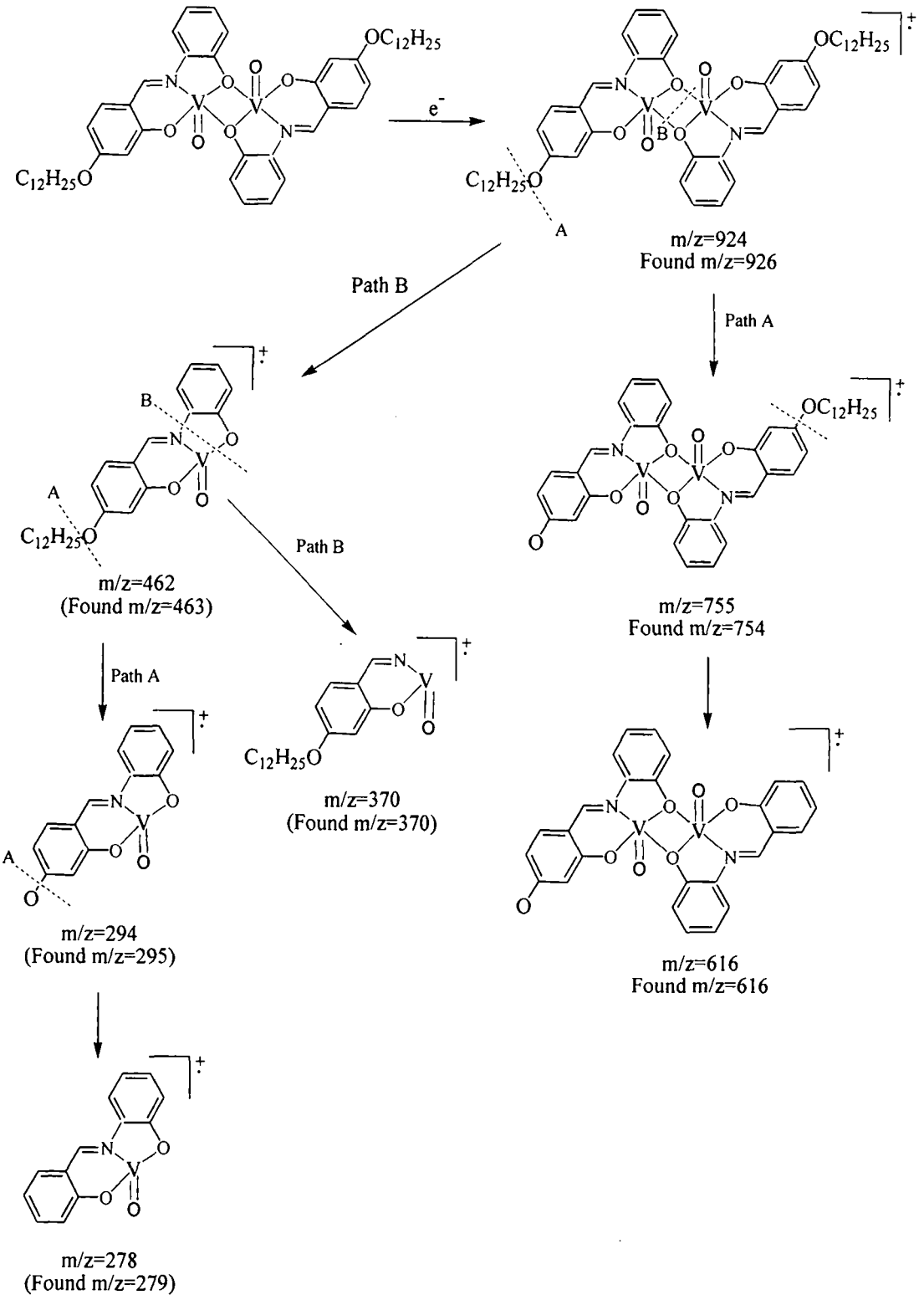

Fragmentation pattern of the complex $[VOL_3]_2$

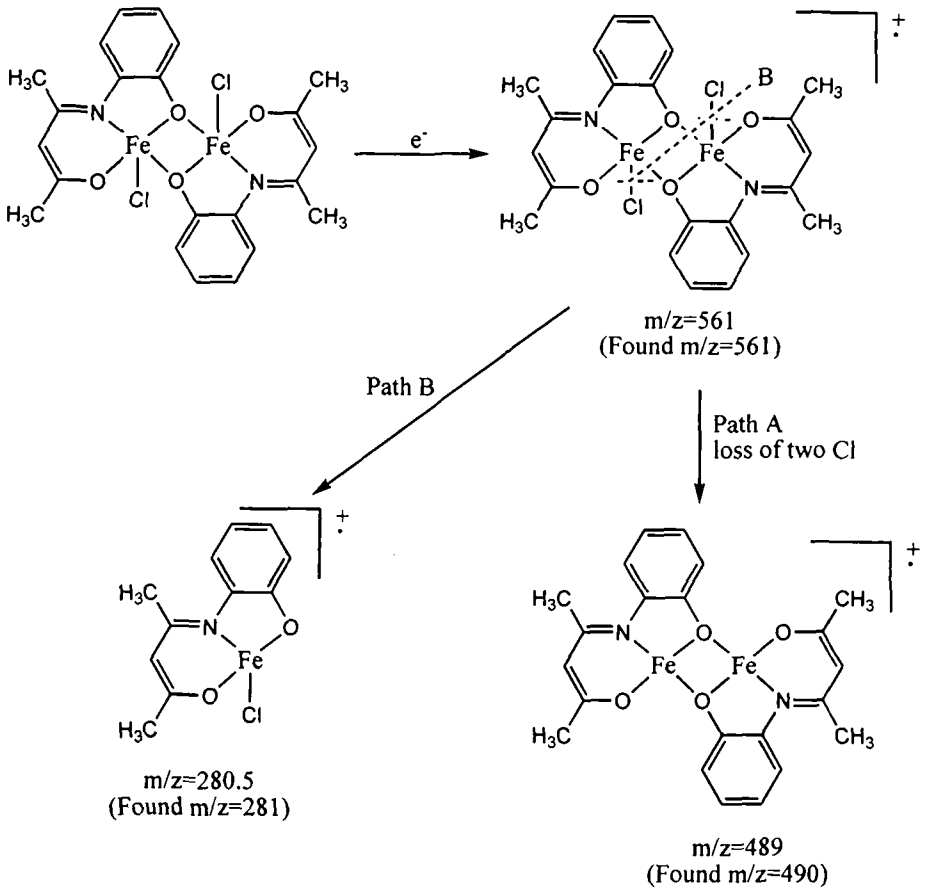

Fragmentation pattern of the complex $[FeL_5Cl]_2$

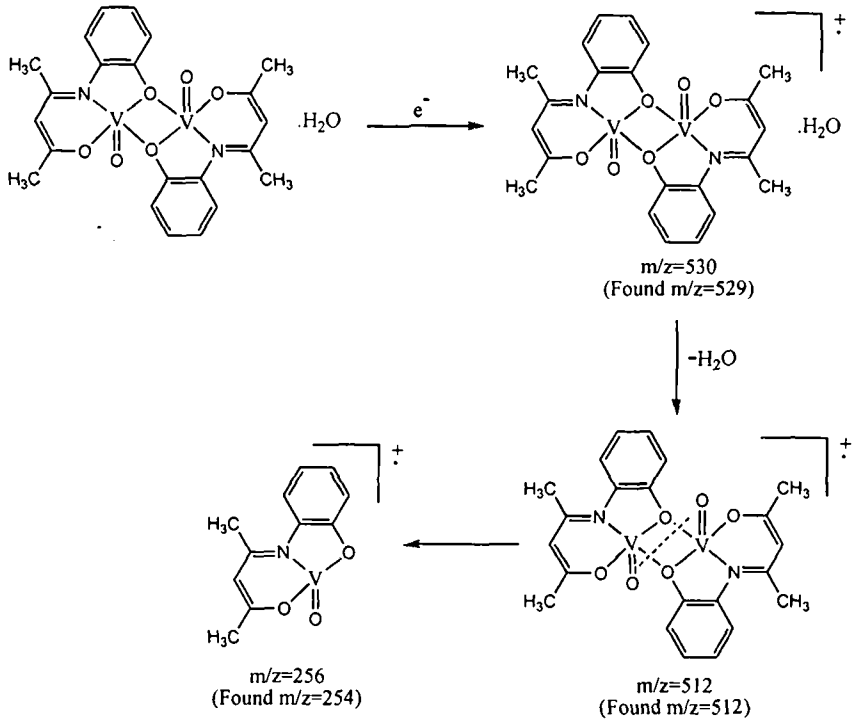

Fragmentation pattern of the complex $[VOL_5]_2.H_2O$

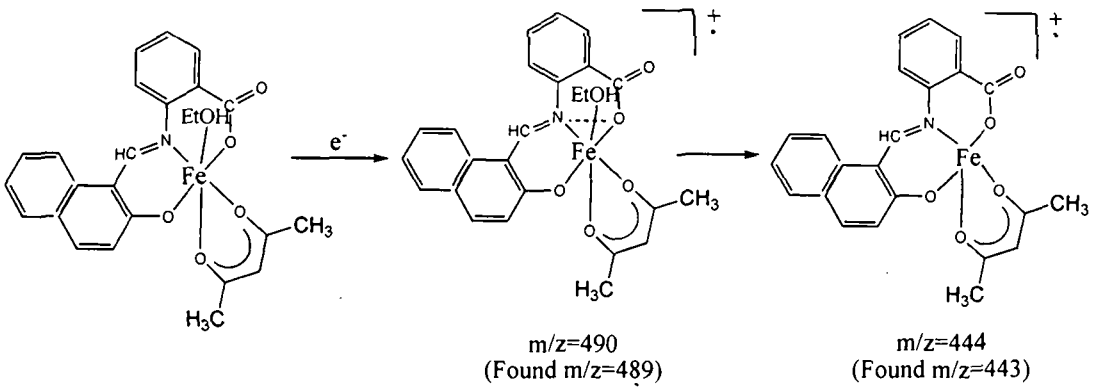

Fragmentation pattern of the complex [Fe(L_8)(EtOH)(acac)

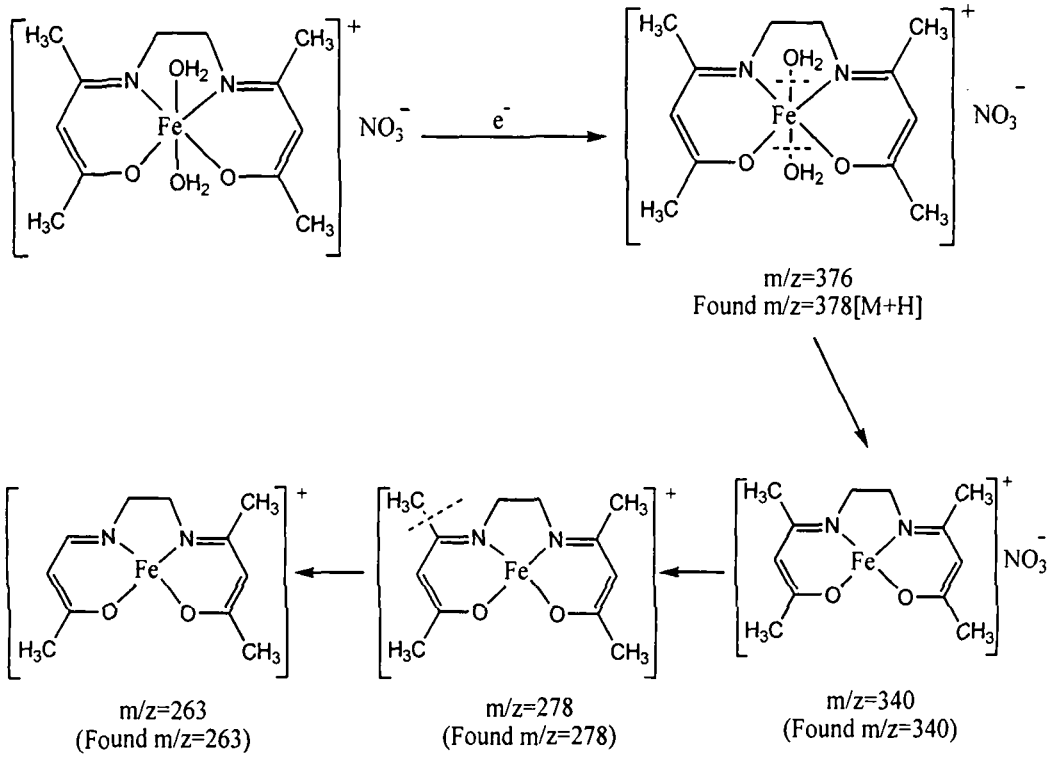

Fragmentation pattern of the complex [$FeL_9(H_2O)_2$]NO_3

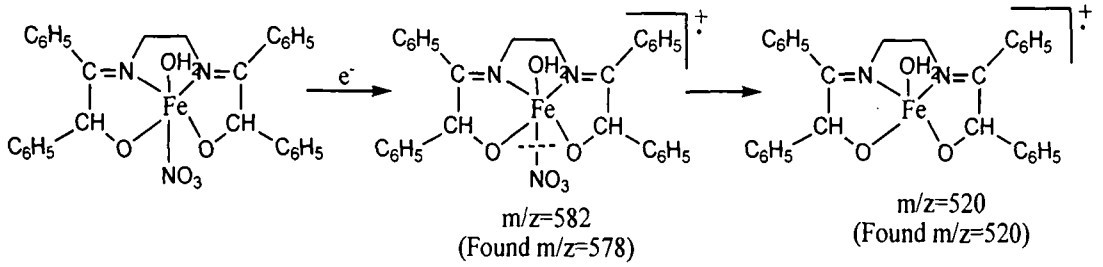

Fragmentation pattern of the complex $[Fe(L_{13})(NO_3)(H_2O)]$

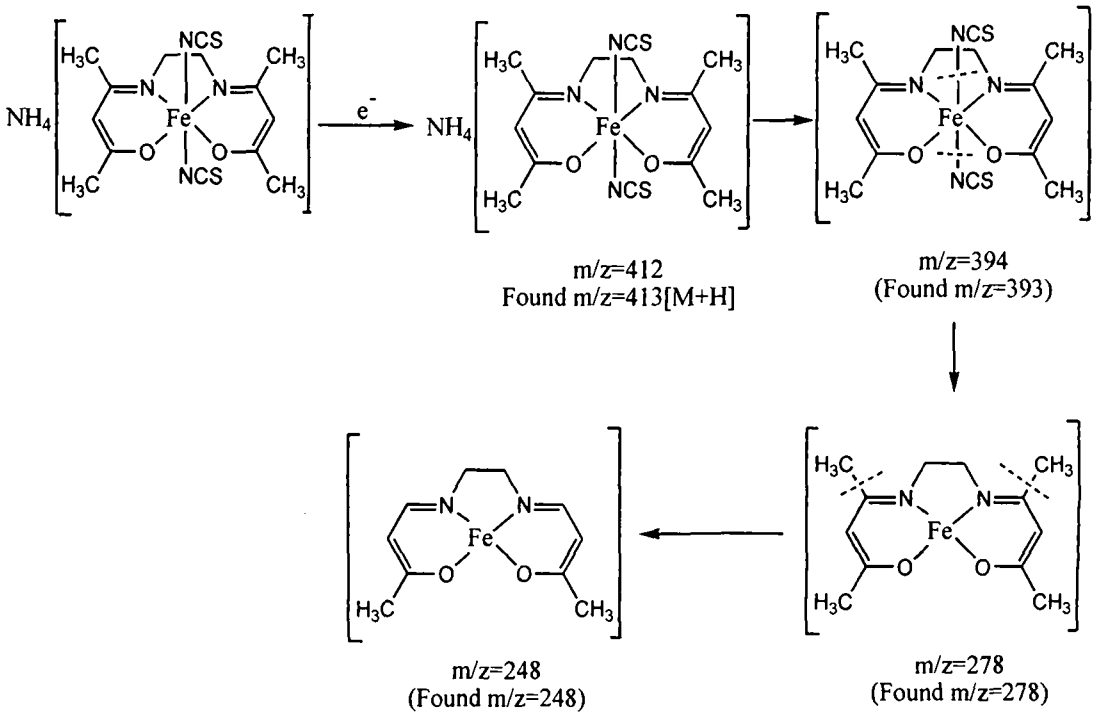

Fragmentation pattern of the complex $NH_4[Fe(L_9)(NCS)_2]$

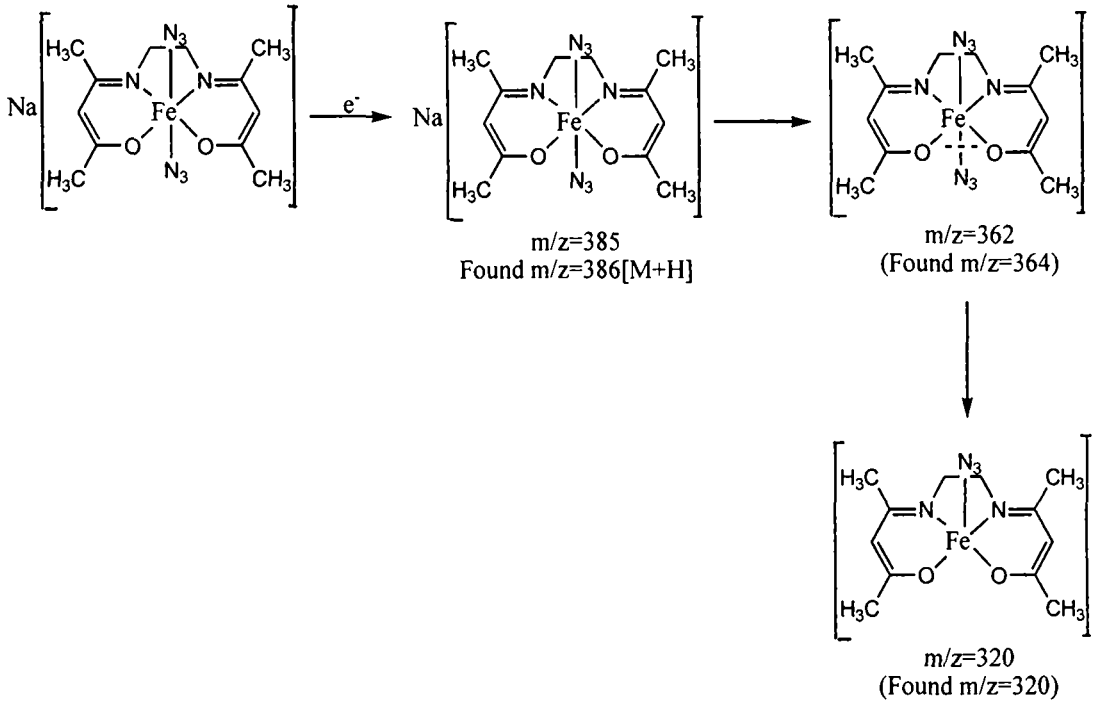

Fragmentation pattern of the complex $Na[Fe(L_9)(N_3)_2]$

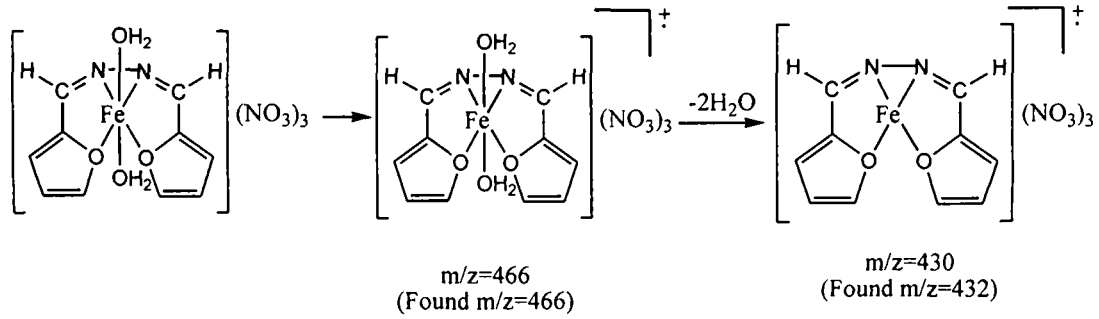

Fragmentation pattern of the complex $[Fe(L_{10})(H_2O)_2](NO_3)_3$

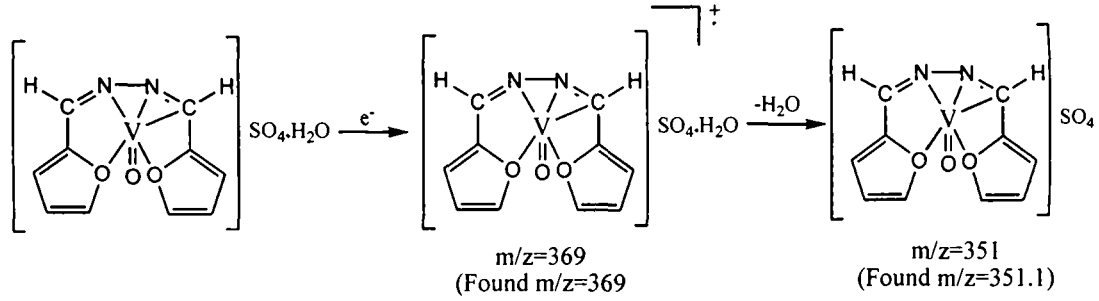

Fragmentation pattern of the complex $[VO(L_{10})]SO_4.H_2O$

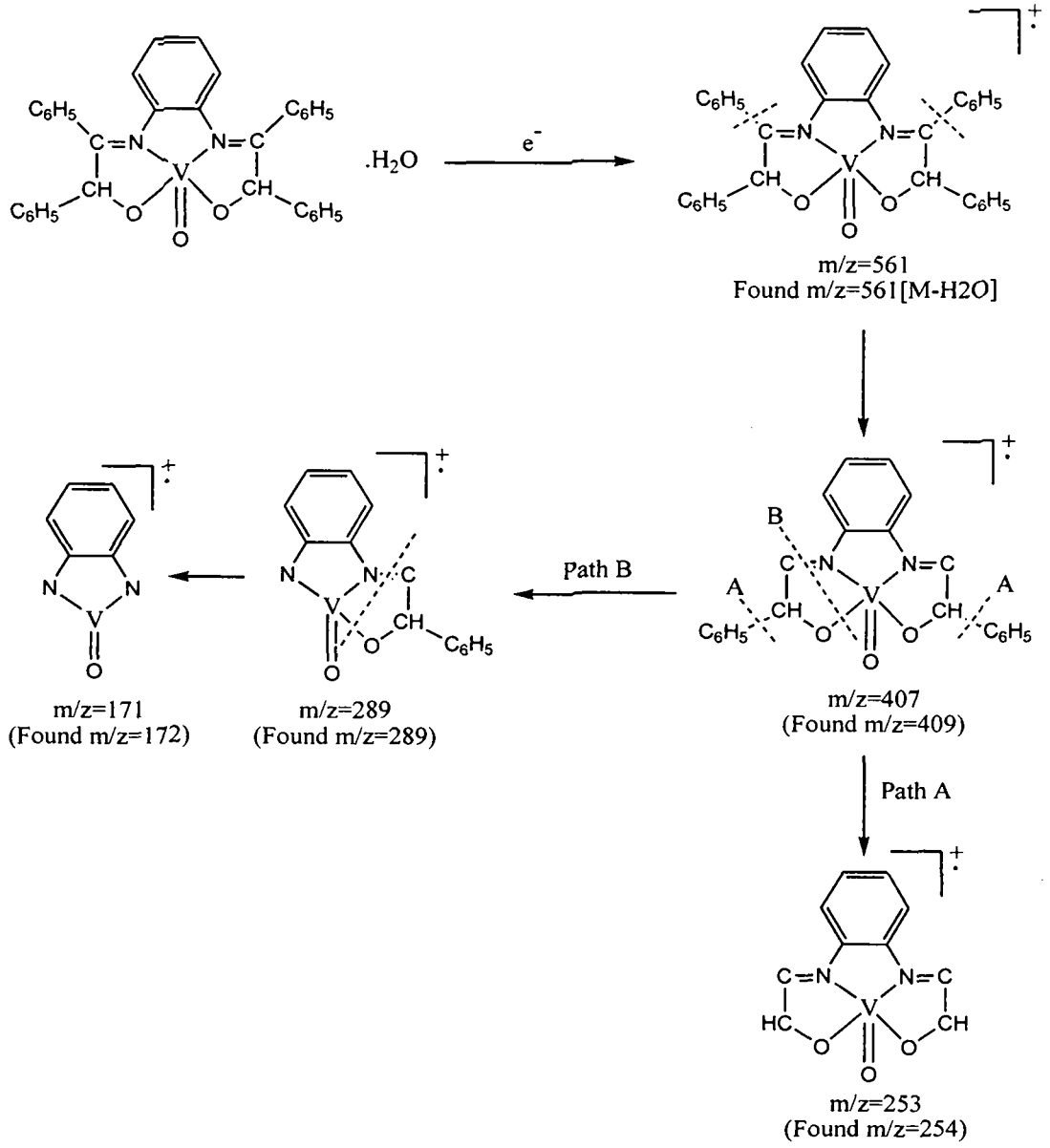

Fragmentation pattern of the complex $[VO(L_{14})].H_2O$

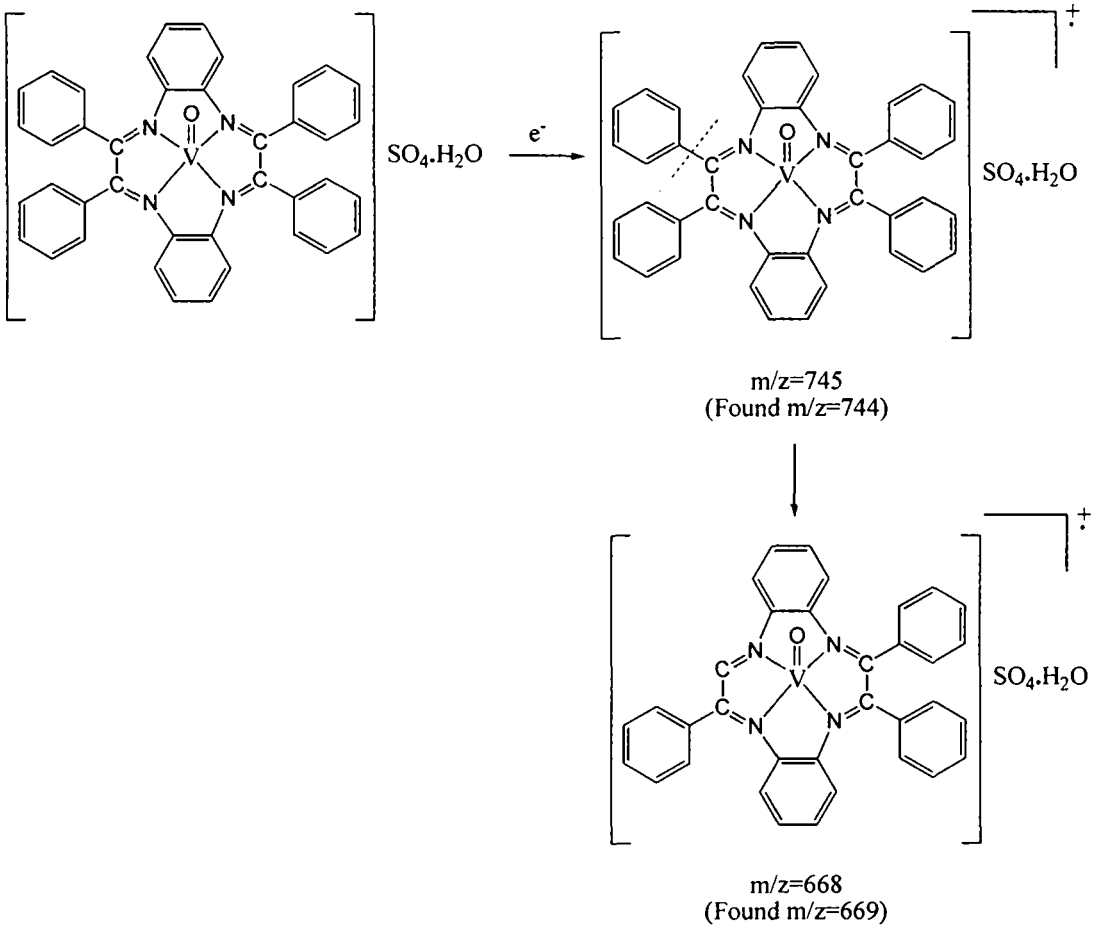

Fragmentation pattern of the complex $[VO(L_{16})SO_4.H_2O$

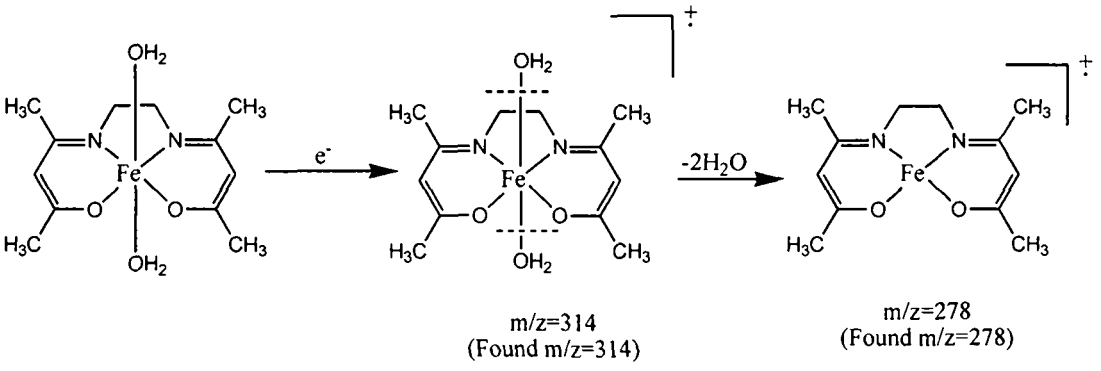

Fragmentation pattern of the complex $[Fe(L_9)(H_2O)_2]$

Scrutiny of the fragmentation pattern not only confirmed the molecular mass as per proposed formulae but also attested the bridging nature of the ligands in the dinuclear complexes.

6.7. Single crystal X-ray diffraction study: Data collection and structure refinement

Suitable single crystal of Schiff base L_9 (size 0.06X0.60X0.80 mm) was mounted on a thin glass fibre with commercially available super glue. The X-ray data were collected with a BRUKER SMART CCD diffractometer using graphite monochromated Mo Kα radiation λ=0.71073 Å, at 295(2) K. The programme SAINT was used for integration of diffraction profiles and absorption correction was made with SADABS programme. The structure was solved by direct methods (SIR-92) [223] and refined with the full matrix least squares method on F^2 with the use of SHELXL-97 program package [224]. The non-hydrogen atoms were refined anisotropically. All hydrogen atoms were located by Fourier analysis. All calculations were carried out using SHELXL 97[224], PLATON 99 [225], SHELXS 97 [227] and WinGX system, Ver 1.70.01.[227]. A summery of crystallographic data and structure refinement parameters are given in **Table-7**. Refinement converged satisfactorily to give R=0.0842 and R_w=0.2622 with residual electron density minimum and maximum of −0.23 and 0.37 respectively.

TABLE-7. Crystal data and structure refinement for the ligand L_9.

Empirical formula	$C_{12}H_{20}N_2O_2$	Absorption coeff. (μ)	0.076 mm^{-1}
Formula weight	224.30	F(000)	244
Temperature (K)	295(2)	$\theta(^0)$	2.2 to 27.5
Wavelength, $\lambda_{Mo\text{-}K\alpha}$	0.71073 Å	Index ranges	$-9 \leq h \leq 9$
Crystal system	Triclinic		$-13 \leq k \leq 13$
Space group	P-1 (No.2)		$-13 \leq l \leq 13$
a(Å)	7.1158(5)	Total data	9496
b(Å)	10.4490(8)	Unique data	3057
c(Å)	10.4810(8)	$I>2\sigma(I)$	1079

$\alpha(^0)$	62.589(5)	R(Int)	0.091
$\beta(^0)$	78.531(6)	Weighing scheme, W	$[\sigma^2(F_0)^2+(0.1218P)^2]^{-1}$
$\gamma(^0)$	75.900(6)		$P=(\|F0\|^2+2\|Fc\|^2)/3$
Volume($Å^3$)	667.55(9)	Final R indices	$R=0.0842, wR_2=0.2622$
Z	2	Goodness of fit on F^2	S=0.94
Density(gcm^{-3})	1.116	Min. and max. residual electron density(e. $Å^{-3}$)	−0.23, 0.37

The crystal structure of the Schiff base is shown in figure 6.6 using ORTEP 3v2 molecular graphic tools. and selected bond lengths and bond angles are summarized in **Table-8.**

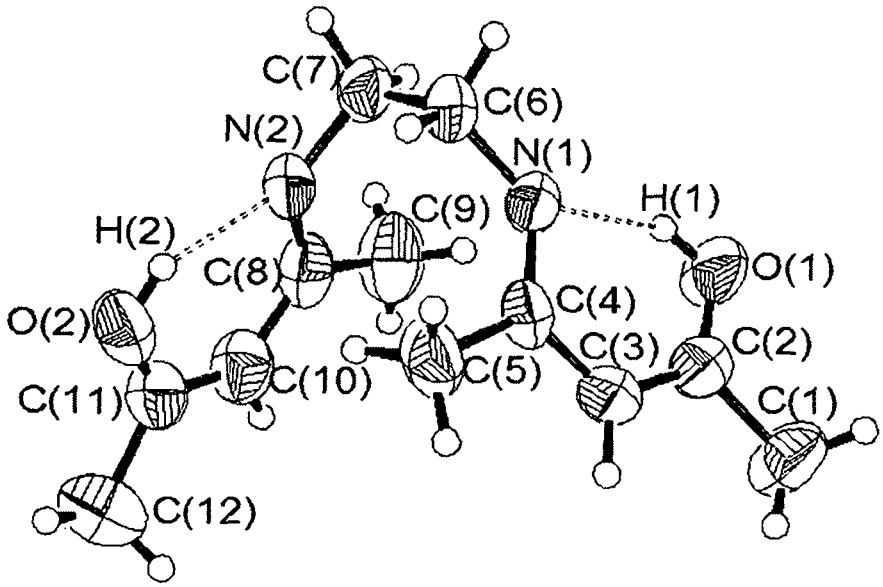

Figure 6.6. Crystal structure of the Schiff base L_9.

TABLE-8. Selected bond lengths and bond angles for the compounds L_9.

Bond lengths	(Å)	Bond angles	(^{0})
O1-H1	0.820(3)	H1-O1-C2	109.5(4)
O1-C2	1.240(6)	H2-O2-C11	109.5(4)
O2-H2	0.821(4)	C7-N2-C8	125.8(4)
O2-C11	1.233(6)	C6-N1-C4	126.4(3)
N2-C7	1.454(6)	N1-C6-C7	112.7(3)
N2-C8	1.330(6)	N2-C7-C6	112.1(3)
N1-C6	1.459(5)	O2-C11-C10	123.3(4)
N1-C4	1.324(6)	N1-C4-C3	121.0(4)
		C11-C10-C8	125.3(5)
		C4-C3-C2	124.7(4)
		N2-C8-C10	120.7(4)
		O1-C2-C3	120.4(4)
		N1-C6-C7-N2 (torsional angles)	66.4(4)

The crystal structure confirms the existence of the ligand in enol form. Further the presence of intramolecular hydrogen bonding between the pair of atoms O1–H1----N1 and O2–H2----N2 is seen. The two C–N bonds (C6-N1 and C7-N2) are not lying in the same plane making a torsional angle of 66.4^0. The two OH groups are oriented away from each other presumably due to the presence of intermolecular hydrogen bonds between the pair of atoms O1-N1 and N1-O1.

6.8. Thermal microscopy and Phase Behavior

The phase transitions of the compounds were measured using differential scanning calorimetry (DSC) at 10^0C min^{-1} heating rate. The transition temperatures along with associated enthalpies and entropies are shown in **Table-9**. The thermogram (**Figure**

6.7.1 and 6.7.2) showed three transitions in heating cycle and two in cooling cycle for compound L_3. That its higher homologue (compound L_4) showed only one transition both in heating and cooling cycle is noteworthy. Cr→SmB and SmB→SmX phase transition in compound L_4 could not be detected by DSC even at 5^0C/min rate of heating or cooling and with a sample of 10 mg (the capacity of cup used in DSC pyris1 system). However, those transitions were observed on cooling at a very slow rate by thermal microscopy.

TABLE- 9. Phase transition temperatures (^{0}C) along with associated enthalpies ΔH (KJmol^{-1}) and entropies ΔS (Jmol^{-1}K^{-1}).

Compound	Heating cycle				Cooling Cycle			
	Transition	T(^{0}C)	ΔH	ΔS	Transition	T(^{0}C)	ΔH	ΔS
Schiff base (L_3)	Cr→SmB	66.3	0.7	2.06	Iso→SmX	115.2	20.5	52.80
	SmB→SmX	97.0	8.6	23.24	SmX→SmB	84.1	1.2	3.36
	SmX→Iso	149.1	36.1	85.52	-	-	-	-
Schiff base (L_4)	Cr→Iso	143.5	24.3	58.34	Iso→Cr	127.6	28.0	69.89

Textural analysis was done with the help of a Polarizing Optical Microscope (POM). On slow cooling from isotropic liquid, a high birefringent mosaic texture (**Fig 6.7.3.a** and **6.7.3.b**) appeared at 162.1^{0}C. On further cooling, a low birefringent smectic X phase with grainy like texture appeared at 146.2 ^{0}C in compound L_1 (**Fig 6.7.3.d**) and at 145.9 ^{0}C in compound L_2 (**Fig 6.7.3.g**). The texture looks uniform between crossed polarizer, however, the formation of two distinct chiral domains were recognised by decrossing the polarizers as bright and dark domains. The brightness of these domains was interchanged by decrossing the analyzer in the opposite sense (**Fig. 6.7.3.c** and **6.7.3.e ; 6.7.3.f and 6.7.3.h**). Considering the fact that the brightness of two domains

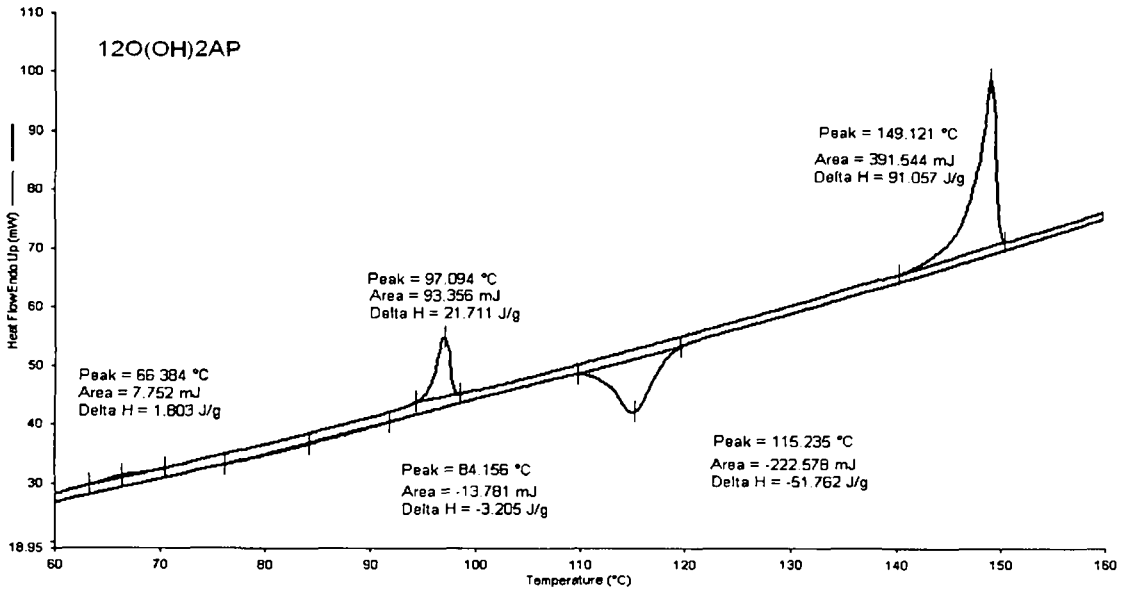

Figure 6.7.1. Differential scanning calorimetry profile of Schiff base ligand (L_3) derived from $C_{12}O(OH)CHO$ and 2-aminophenol.

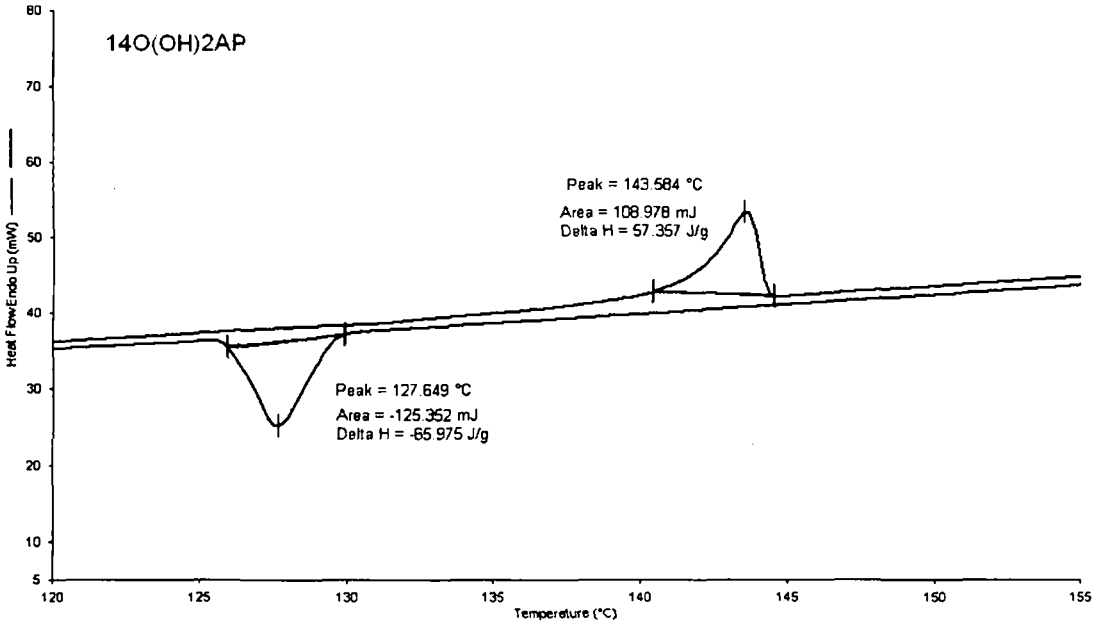

Figure 6.7.2. Differential scanning calorimetry profile of Schiff base ligand (L_4) derived from $C_{14}O(OH)CHO$ and 2-aminophenol.

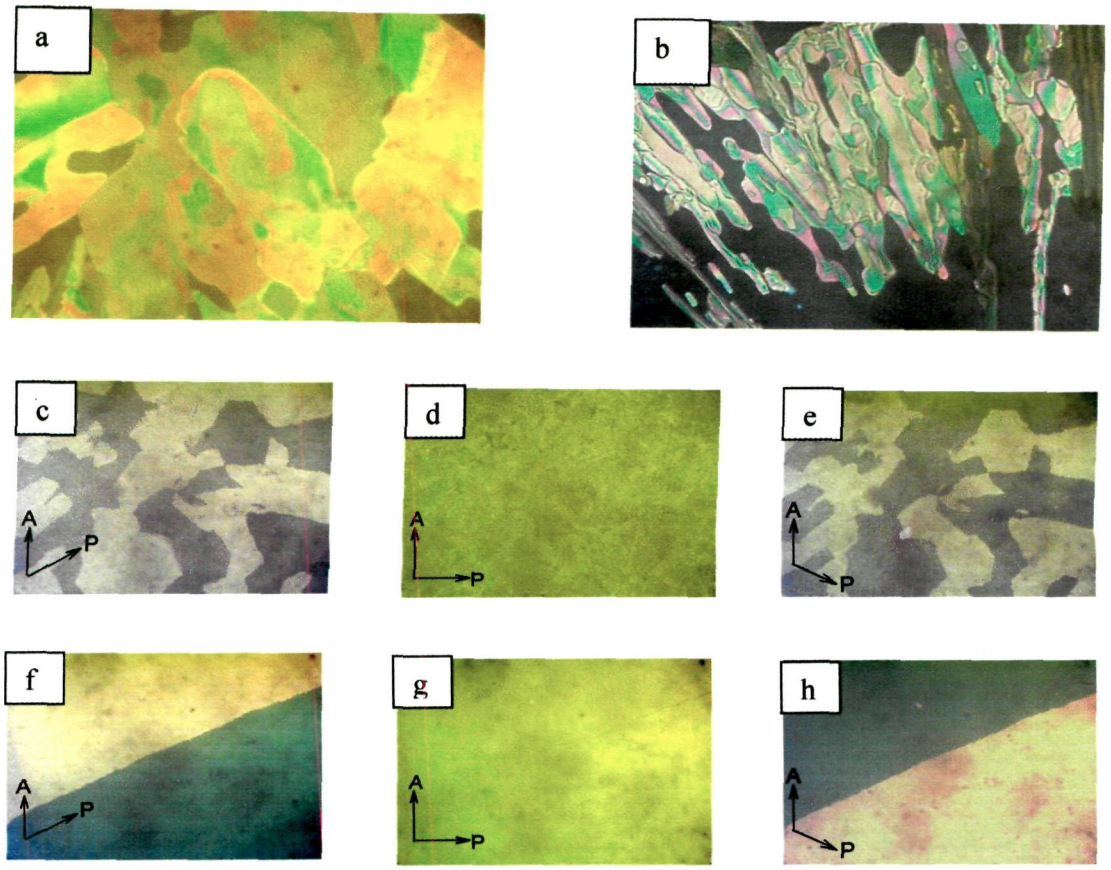

Figure 6.7.3. Optical micrograph of compound (a) L_1 at 162.1 ^{0}C (b) L_2 at 162.1 ^{0}C (c) L_1 at 146.2 ^{0}C (d) L_1 at 146.2 ^{0}C (e) L_1 at 146.2 ^{0}C (f) L_2 at 145.9 ^{0}C (g) L_2 at 145.9 ^{0}C (h) L_2 at 145.9 ^{0}C

interchanges depending on the sense of the decrossing direction, two domains were identified as chiral domains [228]. It was also observed that the size of the domains depends on the rate of cooling the sample. This kinds of optical property was reported in several bent core materials [229, 230]. Thus the possibility of the smectic X phase being a variant of B_2 phase may not be ruled out. XRD study is needed to confirm this. Analogous Schiff bases ($\mathbf{L_3'}$ and $\mathbf{L_4'}$) prepared from simple aniline(vide experimental) without any hydroxo group at the ortho position, however, are devoid of any mesogenicity. These compounds also lack any solid state chirality. This clearly suggests

the significance of the phenolic OH (of 2-aminophenol) group via intermolecular hydrogen bonding for the chiral mesogenic behaviour through stacking interaction.

The vanadyl and iron chloride complexes of the ligands L_3 and L_4 exhibited only crystal to isotropic (Cr→Iso) transition. The stronger interaction between square pyramidal V=O or Fe-Cl centre seemed to inhibit the formation of liquid crystallinity. Also the deprotonation of the ligand during complexation restricted the scope of intermolecular hydrogen bonding and this may be considered as an additional factors for the loss of mesogenicity.

6.9. Antimicrobial activity studies

The ligands $\mathbf{L_5}$ and $\mathbf{L_6}$ and their oxovanadium(IV) complexes were assayed for their *in vitro* antimicrobial activities at a concentration of 50 μg/ml against *Klebsiella pneumoniae, Staphylococcus aureus, Pseudomonas aeroginosa, Escherichia coli, Bacillus subtilis* and *Proteus vulgaris* using ethanol as solvent as well as control and tetracyclin as standard drug following the method described in experimental. The results are listed in **Table-10A**. It is apparent that the ligands containing phenolic hydroxy group ($\mathbf{L_5}$) are more active than those having aromatic carboxylic group ($\mathbf{L_6}$).

TABLE-10A. Antimicrobial effects of the ligands L_5 and L_6 and their complexes 10 and 16.

Compound	Microorganism (Inhibition zone [a] / mm)					
	K.pneumonia	*S.aureus*	*P.aeroginosa*	*E.coli*	*B.subtilis*	*P.vulgaris*
Control	N.O.	N.O.	N.O.	8	8	7
Tetracyclin	16.33±0.57	20.66±0.57	19.0±1.0	22.66±1.15	18.0±0.0	24.66±0.57
Ligand ($\mathbf{L_5}$)	7.66±0.57	10.0±1.0	7.66±1.15	14.0±1.0	12.66±1.15	8.33±0.57
Ligand ($\mathbf{L_6}$)	6.66±0.57	N.O.	N.O.	10.66±1.15	12.0±0.0	N.O.
$[VOL_5]_2.H_2O$(**10**)	10.0±1.0	13.66±0.57	11.0±0.0	13.0±1.0	10.33±0.57	14.33±1.15
$[VOL_6(H_2O)].H_2O$ (**16**)	N.O.	6.33±0.57	N.O.	N.O.	N.O.	6.33±0.57

[a] including disc diameter 4 mm, N.O.- not observed

Further the complex **10** showed much higher activity compared to the free ligand L_5. The enhancement in activity on complexation is related to transamination and racemization reaction in biological system [231, 232]. Upon chelation the lipophilic nature increases which favours its permeation through the lipid layer of the membrane and thus helps in crossing cell membrane of the microorganism and thereby enhances the biological utilization ratio and activity of the testing compound [233]. In our work we observed that the Schiff base L_5 exhibited maximum inhibitory activity against *E.coli* while its oxovanadium(IV) complex (**10**) showed promising inhibitory effect against *P.vulgaris* amongst the microorganism tested.

The ligands L_3 and L_4 and their iron(III) complexes (**5** and **6**) were also tested for their *in vitro* antimicrobial activities at a concentration of 50 μg/ml against *Klebsiella pneumoniae* and *Bacillus subtilis* using ethanol as solvent as well as control and kanamycin as standard drug. The results are presented in **Table-10B.**

TABLE- 10B. Antimicrobial activity of the ligands L_3 and L_4 and their iron(III) complexes.

Compound	Inhibition zone[a] (mm)	
	K. pneumoniae	*B. subtilis*
Control	Not observed	7.0±0.0
Kanamycin	16.33±0.57	17.66±0.57
Ligand (L_3)	8.0±1.0	Not observed
Ligand (L_4)	11.66±0.57	Not observed
$[FeL_3Cl]_2$ (**5**)	9.0±0.0	Not observed
$[FeL_4Cl]_2$ (**6**)	14.0±1.0	Not observed

[a] including disc diameter 4 mm

All the compounds were moderately active against *Klebsiella pneumoniae* while none showed any activity against *Bacillus subtilis*. Further, a significant increase in activity

against *Klebsiella pneumoniae* with increasing the chain length of alkoxy group in aldehyde part of the Schiff base is believed to be due to enhanced polarizability of the molecule [234].

6.10. Electrochemical behaviour

Electrochemical studies of the selected compounds were carried out by cyclic voltametry in anhydrous acetonitrile solution of ca 10^{-3} M concentration containing 0.1 M tetrabutyl ammonium perchlorate (TBAP) as supporting electrolyte in the potential range 1.2 to -1.2 V vs SCE at 100 mVs^{-1} scan rate unless stated otherwise. The redox potentials for the compounds are given in **Table-11** and corresponding voltamograms are presented in appendix 6. As can be seen from the voltamograms that the oxovanadium(IV) complexes **10**, **16** and **36** exhibited almost reversible oxidation behaviour one electron response assignable to VO(V)/VO(IV) couple. The iron(III) complex **34** also displayed a reversible one electron wave assignable to Fe(III)-Fe(II) redox process. The oxovanadium(IV) complexes **29**, **30**, **31** and **39** displayed a quasireversible one electron response with ΔE_p values greater than 100 mV and may be assigned to VO(V)/VO(IV) redox couple. The iron(III) complexes **9**, **15**, **17**, **18**, **19**, **20**, **21**, **24**, **25**, **26** and **38** also exhibited quasireversible (peak to peak separation > 100 mV) one electron response corresponding to Fe(III)/Fe(II) couple.

The half wave potential $E_{1/2}$ of all the complexes except **18**, **29**, **30** and **31** are negative and very small implying that these compounds can be easily oxidized or reduced. This feature would make them valuable as catalyst in redox reactions[235]. In addition, from the fact that the $E_{1/2}$ values are close to one another, it follows that all the Schiff base complexes would exhibit nearly identical redox activity. For the complexes **18**, **29**, **30** and **31**, the $E_{1/2}$ values being positive as well as large, suggest that these compounds can neither be easily oxidized nor can be reduced. Thus, in order to use them successfully in

redox reactions, some structural modifications to reduce the $E_{1/2}$ value may be required.

TABLE-11. Electrochemical data of the complexes in acetonitrile

Compounds	E_p^a (V)	E_p^c (V)	ΔE_p (V)	$E_{1/2}$ (V)
$[FeL_5Cl]_2$ (**9**)	-0.183	-0.738	0.555	-0.460
$[VOL_5]_2.H_2O$ (**10**)	-0.468	-0.525	0.057	-0.496
$[FeL_6Cl]$ (**15**)	-0.311	-0.688	0.377	-0.499
$[VOL_6(H_2O)].H_2O$ (**16**)	-0.357	-0.412	0.055	-0.384
$[FeL_7(acac)(EtOH)]$ (**17**)	0.682	-0.707	1.389	-0.012
$[FeL_8(acac)(EtOH)]$(**18**)	0.806	-0.691	1.497	0.0575
$[FeL_9(H_2O)_2]NO_3$ (**19**)	-0.448	-0.854	0.406	-0.651
$[FeL_{11}(H_2O)_2]NO_3$ (**20**)	-0.404	-0.763	0.359	-0.583
$[FeL_{12}(H_2O)_2]NO_3$ (**21**)	-0.326	-0.687	0.361	-0.506
$NH_4[FeL_9F_2]$ (**24**)	-0.253	-0.648	0.395	-0.450
$NH_4[FeL_9(NCS)_2]$ (**25**)	-0.152	-0.553	0.399	-0.351
$Na[FeL_9(N_3)_2]$ (**26**)	-0.433	-0.570	0.137	-0.501
$[VOL_9]H_2O$ (**29**)	0.735	0.529	0.206	0.632
$[VOL_{11}]H_2O$ (**30**)	0.982	0.640	0.342	0.811
$[VOL_{12}]H_2O$ (**31**)	0.735	0.646	0.089	0.690
$[FeL_{15}Cl_2]Cl$ (**34**)	-0.380	-0.447	0.067	-0.413
$[VOL_{15}]SO_4.H_2O$ (**36**)	-0.162	-0.209	0.047	-0.185
$FeL_{10}(H_2O)_2](NO_3)_3$ (**38**)	1.21	-1.38	2.59	-0.085
$[VOL_{10}]SO_4.H_2O$ (**39**)	-0.270	-0.564	0.294	-0.834

6.11. Thermal investigations

The thermal behaviour of the few selected complexes have been studied using TGA, DTG and DTA analysis (Appendix 7). The decomposition stages, temperature ranges, decomposition products as well as found and calculated weight loss percentages of the complexes are summerised in **Table 12A**. The DTA data of the complexes are presented in **Table 12B**.

TABLE-12A. T.G.A. and D.T.G. data of the complexes

Complex	T.G. plateau(^{0}C)	D.T.G (^{0}C)	Mass loss (%)		Process
			Expt	Calcd	
$[VO(L_2)_2]SO_4.H_2O$ **(4)**	94-833	193	91.43	92.99	loss of lattice water and final decomposition of the ligand.
$[VO(L_6)(H_2O)].H_2O$ **(16)**	40-128	48	4.29	5.59	loss of lattice water
	128-321	172	31.43	-	loss of coordinated water and partial decomposition of the ligand.
	321-435	365	11.71	-	partial decomposition of the ligand
	435-928	458	44.01	-	final decomposition of the ligand
$[Fe(L_7)(acac)(EtOH)]$ **(17)**	214-292	278	11.24	9.25	loss of ethanol
	464-535	515	21.87	21.64	loss of acetylacetone
	603-628	615	7.5	-	partial decomposition of the ligand
$[Fe(L_9)(H_2O)_2]NO_3$ **(19)**	171-235	225	34.37	-	Loss of NO_3, two coordinated water molecule and partial decomposition of the ligand
	300-321	313	19.37	-	partial decomposition of the ligand
	350-385	369	2.85	-	partial decomposition of the ligand
	471-500	486	4.29	-	partial decomposition of the ligand

Complex	T.G. plateau(^{0}C)	D.T.G (^{0}C)	Mass loss (%)		Process
			Expt	Calcd	
$[Fe(L_{12})(H_2O)_2]NO_3$ **(21)**	135-164	147	6.88	6.92	loss of two coordinated water molecule
	164-252	244	11.87	11.92	loss of NO_3
	252-664	643	28.75	-	partial decomposition of the ligand
$[Fe(L_{13})(NO_3)(H_2O)]$ **(24)**	103-214	198	13.34	13.74	Loss coordinated water and nitrate
	214-385	376	11.66	-	partial decomposition of the ligand
	385-532	503	9.45	-	partial decomposition of the ligand
	532-707	693	3.33	-	partial decomposition of the ligand
	707-1000	893	22.22	-	partial decomposition of the ligand
$[VO(L_{14})]H_2O$ **(31)**	40-72	70	2.86	3.10	Loss of lattice water
	72-671	231	85.72	85.66	final decomposition of the ligand
$[Fe(L_{10})(H_2O)_2](NO_3)_3$ **(38)**	128-192	177	7.63	7.22	loss of two molecules of coordinated water
	192-635	601	38.62	40.34	final decomposition of the ligand

The complex **4** undergoes decomposition mainly in a single stage in 94-833^{0}C range with DTG peak at 193^{0}C. The mass loss observed in this step is 91.43% against the calculated loss of 92.43% corresponding to dehydration and complete decomposition of the ligand. The complex **16** undergoes decomposition in four stages. The first stage takes place in the temperature range 40-128^{0}C with DTG peak at 48^{0}C corresponding to the release of loosely bound lattice water molecule [236]. The second stage in the

TABLE-12B. D.T.A. data of the complexes

Complex	Temperature range (^{0}C)	D.T.A. peaks (^{0}C)	ΔH (J/g)	Process
$[VO(L_2)_2]SO_4.H_2O$ (**4**)	-	-	-	-
$[VO(L_6)(H_2O)].H_2O$ (**16**)	110-190	139 endo	158.12	dehydration
	414-608	464 exo	1950.20	decomposition
$[Fe(L_7)(acac)(EtOH)]$ (**17**)	495-612	542 exo	1003.29	decomposition
$[Fe(L_9)(H_2O)_2]NO_3$ (**19**)	172-248	182 endo	15.21	dehydration
		230 endo	68.01	ionization
	294-352	317 endo	251.75	melting
$[Fe(L_{12})(H_2O)_2]NO_3$ (**21**)	100-185	150 exo	166.28	partial decomposition
	226-287	254 exo	64.25	partial decomposotion
$[Fe(L_{13})(NO_3)(H_2O)]$ (**24**)	291-422	382 exo	312.85	partial decomposition
$[VO(L_{14})]H_2O$ (**31**)	145-280	235 endo	148.36	melting
$[Fe(L_{10})(H_2O)_2](NO_3)_3$ (**38**)	-	-	-	-

temperature range 128-321^{0}C with DTG peak at 172^{0}C corresponds to the loss of coordinated water molecule [237] and partial decomposition of the ligand. The dehydration step is associated with endothermic change in 110-190^{0}C with DTA peak at 139^{0}C. The exothermic change in 414-608^{0}C with DTA peak at 464^{0}C is associated with decomposition of the ligand molecule. The T.G. curve of the complex **17** shows a weight loss of 11.24% (calcd. 9.25%), 21.87% (calcd 21.64%) and 7.5% in the temperature ranges 214-292, 464-535 and 603-628^{0}C with DTG peak at 278, 515 and 615 ^{0}C , respectively corresponding to elimination of ethanol, acetylacetone and partial decomposition of the ligand molecule. The exothermic change in 495-612^{0}C with DTA

peak at 542^{0}C is related to decomposition of the ligand molecule. The decomposition of the complex **19** in 171-235^{0}C with DTG peak at 225^{0}C corresponding to a weight loss of 34.37% is related to elimination of nitrate, two molecules of cooedinated water and partial loss of the Schiff base logand. Subsequent decomposition of the complex is attributed to partial decomposition of the ligand. The complex has endothermic change in the temperature range 172-248^{0}C with two DTA peaks at 182 and 230^{0}C. The first peak indicates dehydration while the second represents ionization of the complex. A sharp endothermic peak in 294-352^{0}C with DTA peak at 317^{0}C favours melting of the compound. The T.G. curve of the complex **21** shows a weight loss of 6.88% (calcd. 6.92%) in the temperature range 135-164^{0}C with d.t.g. peak at 147 ^{0}C corresponding to loss of two molecules of coordinated water. The second decomposition stage of the complex in 164-252^{0}C range having DTG peak at 244^{0}C. It brings a weight loss of 11.87% (calcd. 11.92%) that correlate with ionization of the complex leading to loss of nitrate ion. Partial decomposition of the complex is continued in 252-664^{0}C with d.t.g. peak at 643^{0}C showing weight loss of 28.75%. The exothermic obtained the 100-185 and 226-287^{0}C with DTA peak at 150 and 254^{0}C are associated with partial decomposition of the ligand. The complex **24** undergoes decomposition in five stages. The first stage of decomposition takes place in 103-214^{0}C range with DTG peak at 198^{0}C representing loss of coordinated water as well as nitrate. The weight loss observed in this step is 13.34% against the calculated value of 13.79%. This is followed by further decomposition of the complex in 214-385, 385-532, 532-797 and 707-1000^{0}C ranges with DTG peak at 376, 503, 693 and 893^{0}C attributable to partial decomposition of the ligand. Exothermic changes in 291-422^{0}C with DTA peak at 382^{0}C represents decomposition of the ligand moiety. The oxovanadium(IV) complex **31** shows a weight loss of 2.86% (calcd. 3.10%) and 85.72% (calcd. 85.66%) respectively in the

temperature ranges 40-72 and 72-671^{0}C with DTG peak at 70 and 231^{0}C representing release of lattice water and final decomposition of the ligand. The endothermic peak in the temperature range 145-280^{0}C with DTA peak at 235^{0}C indicates melting of the complex. The iron(III) complex **38** shows initial weight loss of 7.63% (calcd. 7.72%) in the temperature range 128-192^{0}C with DTG peak at 177^{0}C is associated with loss of two molecules of coordinated water. The subsequent weight loss of 38.62% (calcd. 40.34%) in 192-635^{0}C having DTG peak at 601^{0}C is related to final decomposition of the ligand.

6.12. Magnetic Properties

The characteristics of any magnetic material, whether it is hard, soft, or intermediate, are best described in terms of their hysteresis loop. The most common measurement method employed for hysteresis loop determinations at ambient temperature is the Vibrating Sample Magnetometer (VSM). Room temperature magnetic susceptibility measurements of the selected samples were conducted on Vibrating Sample Magnetometer. The magnetization vs magnetic field were examined in the range -20000 to +20000 Gauss and the corresponding curves were presented in appendix 8. The parameters extracted from the hysteresis loop that are most often used to characterize the magnetic properties of materials are the saturation magnetization (Ms), the remanence (Mr), the coercivity (Hc), the squareness ratio (SQR), the slope at Hc and the initial slope. The results are summerised in **Table 13**. When a ferromagnetic material is magnetized in one direction, the maximum remanent magnetization that a material can acquire is called **saturation magnetization**. Strong magnets have higher saturation. It will not relax back to zero magnetization when the imposed magnetizing field is removed. The amount of magnetization it retains at zero driving field is called its **remanence**. It must be driven back to zero by a field in the opposite direction; the

amount of reverse driving field required to demagnetize it is called its **coercivity**. Coercivity measures how permanent a magnet is. A soft magnet possess small coercivity while a hard magnet possess large coercivity. The **squareness ratio** (SQR) is given by the ratio of (Mr/Ms) and is essentially a measure of how square the hysteresis loop is. In general large SQR values are desired for recording devices. Magnetic materials are classified into two broad categories, soft or hard. Soft magnetic materials are characterized by large permeabilities and very small coercivities, typically less than 1 Oe. Hard magnetic materials are most often used in permanent magnet applications and are characterized by large saturation magnetizations, large coercivities, typically greater than 10 kOe, and also by large energy products (i.e., BH_{max}). Intermediate magnetic materials are generally characterized by coercivities on the order of 1 kOe, and these materials are usually used in magnetic media[238].

TABLE-13. Magnetic behaviour of the complexs

Complex	Saturation Magnetization(Ms) **emu/g**	Remanence (Mr) **emu/g**	Coercivity (Hc) **Gauss**	Squareness Ratio (SQR)	Slope at Hc **emu/(gG)**	Initial slope of magnetization **emu/(g G)**
$[Fe(L_2)_2(NO_3)_2]NO_3$ (**2**)	$34.865X10^{-3}$	$10.251X10^{-3}$	269.91	0.29403	$35.025X10^{-6}$	$14.649\ X10^{-6}$
$[FeL_5Cl]_2$ (**9**)	$434.851\ X10^{-3}$	$11.552\ X10^{-3}$	238.51	0.02656	$42.139\ X10^{-6}$	$19.167\ X10^{-6}$
$[VOL_5]_2.H_2O$ (**10**)	$14.186\ X10^{-3}$	$1.828\ X10^{-3}$	245.32	0.12891	$11.4\ X10^{-6}$	$0.607\ X10^{-6}$
$[VOL_6(H_2O)].H_2O$ (**16**)	Not reached	$7.789\ X10^{-3}$	338.04	-	$5.120X10^{-6}$	$3.796\ X10^{-6}$
$[FeL_{12}(H_2O)_2]NO_3$ (**21**)	$170.163\ X10^{-3}$	$12.461\ X10^{-3}$	179.53	0.07323	$91.287\ X10^{-6}$	$27.838\ X10^{-6}$
$[FeL_{14}NO_3H_2O]$ (**23**)	$710.082\ X10^{-3}$	$77.513\ X10^{-3}$	160.50	0.10915	$50.3\ X10^{-6}$	$19.169\ X10^{-6}$
$[VOL_9]H_2O$ (**29**)	$36.485\ X10^{-3}$	$3.932\ X10^{-3}$	313.45	0.10777	$11.712\ X10^{-6}$	$6.169\ X10^{-6}$
$[VOL_{12}]H_2O$ (**31**)	$274.591\ X10^{-3}$	$35.254\ X10^{-3}$	685.04	0.12837	$60.3\ X10^{-6}$	$8.234\ X10^{-6}$
$[FeL_{15}Cl_2]Cl$ (**34**)	$110.009\ X10^{-3}$	$27.758\ X10^{-3}$	650.73	0.2532	$47.8\ X10^{-6}$	$21.943\ X10^{-6}$
$FeL_{10}(H_2O)_2](NO_3)_3$ (**38**)	$343.562\ X10^{-3}$	$36.970\ X10^{-3}$	162.06	0.10761	$225.7\ X10^{-6}$	$76.740\ X10^{-6}$
$[VOL_{10}]SO_4.H_2O$ (**39**)	$12.993\ X10^{-3}$	$3.307\ X10^{-3}$	254.51	0.25404	$10.0\ X10^{-6}$	$9.126\ X10^{-6}$
$[FeL_9(H_2O)_2]$ (**40**)	$435.272\ X10^{-3}$	$13.400\ X10^{-3}$	186.81	0.03078	$89.867X10^{-6}$	$26.757\ X10^{-6}$

The magnetic moment of the complexes is calculated from the initial slope of a hysteresis experiment as follows. The initial slope of magnetization in emu/(gG) will give the gram magnetic susceptibility (χ_g).

Molar magnetic susceptibility (χ_m) = (χ_g) x M, where M= molecular mass of the substance.

The effective magnetic moment (μ_{eff}) is then calculated using the relation

$\mu_{eff} = 2.827x\sqrt{(\chi'_m xT)}$,

$\chi'_m = \chi_m - \chi_{dia}$, where χ_{dia} is diamagnetic correction. The diamagnetic corrections are calculated by summing the contributions from the atoms, ions and bonds of the molecule [239]. These group contributions are known as Pascal's constants.

Calculation of the effective magnetic moment (μ_{eff})

(1) $[Fe(L_2)_2(NO_3)_2]NO_3$ (**2**)

gram magnetic susceptibility (χ_g) = 14.649×10^{-6}

Molar susceptibility (χ_m) = $\chi_g \times M$

$= 14.649 \times 10^{-6} \times 1018$

$= 14912.682 \times 10^{-6}$ emu mol^{-1}

$\chi'_m = \chi_m - \chi_{dia}$

$= (14912.682 \times 10^{-6}) - (-544.22 \times 10^{-6})$

$= 15456.902 \times 10^{-6}$ emu mol^{-1}

$\mu_{eff} = 2.827 \times \sqrt{(\chi'_m \times T)}$

$= 2.827 \times \sqrt{(15456.902 \times 10^{-6} \times 300)}$

= 6.08 B.M.

(2) $[FeL_5Cl]_2$ (**9**)

gram magnetic susceptibility (χ_g) = 19.167×10^{-6}

Molar susceptibility (χ_m) = $\chi_g \times M$

$= 19.167 \times 10^{-6} \times 561$

$= 10752.687 \times 10^{-6}$ emu mol^{-1}

$\chi'_m = \chi_m - \chi_{dia}$

$= (10752.687 \times 10^{-6}) - (-249.7 \times 10^{-6})$

$= 11002.387 \times 10^{-6}$ emu mol^{-1}

$\mu_{eff} = 2.827 \times \sqrt{(\chi'_m \times T)}$

$= 2.827 \times \sqrt{(11002.387 \times 10^{-6} \times 300)}$

$= 5.36$ B.M.

(3) $[VOL_5]_2.H_2O$ (**10**)

gram magnetic susceptibility (χ_g) $= 0.607 \times 10^{-6}$

Molar susceptibility (χ_m) $= \chi_g \times M$

$= 0.607 \times 10^{-6} \times 530$

$= 321.71 \times 10^{-6}$ emu mol^{-1}

$\chi'_m = \chi_m - \chi_{dia}$

$= (321.71 \times 10^{-6}) - (-214.5 \times 10^{-6})$

$= 536.21 \times 10^{-6}$ emu mol^{-1}

$\mu_{eff} = 2.827 \times \sqrt{(\chi'_m \times T)}$

$= 2.827 \times \sqrt{(536.21 \times 10^{-6} \times 300)}$

$= 1.13$ B.M.

(4) $[VOL_6(H_2O)].H_2O$ (**16**)

gram magnetic susceptibility (χ_g) $= 3.796 \times 10^{-6}$

Molar susceptibility (χ_m) $= \chi_g \times M$

$= 3.796 \times 10^{-6} \times 320$

$= 1214.72 \times 10^{-6}$ emu mol^{-1}

$\chi'_m = \chi_m - \chi_{dia}$

$= (1214.72 \times 10^{-6}) - (-135.58 \times 10^{-6})$

$= 1350.3 \times 10^{-6}$ emu mol^{-1}

$\mu_{eff} = 2.827 \times \sqrt{(\chi'_m \times T)}$

$= 2.827 \times \sqrt{(1350.3 \times 10^{-6} \times 300)}$

= 1.79 B.M.

(5) $[FeL_{12}(H_2O)_2]NO_3$ (**21**)

gram magnetic susceptibility (χ_g) = 27.838×10^{-6}

Molar susceptibility (χ_m) $= \chi_g \times M$

$= 27.838 \times 10^{-6} \times 520$

$= 14475.76 \times 10^{-6}$ emu mol^{-1}

$\chi'_m = \chi_m - \chi_{dia}$

$= (14475.76 \times 10^{-6}) - (-258.48 \times 10^{-6})$

$= 14734.24 \times 10^{-6}$ emu mol^{-1}

$\mu_{eff} = 2.827 \times \sqrt{(\chi'_m \times T)}$

$= 2.827 \times \sqrt{(14734.24 \text{ X} 10^{-6} \times 300)}$

= 5.94 B.M.

(6) $[FeL_{14}NO_3H_2O]$ (**23**)

gram magnetic susceptibility (χ_g) = $19.169 \text{ X} 10^{-6}$

Molar susceptibility (χ_m) = $\chi_g \times M$

$= 19.169 \times 10^{-6} \times 630$

$= 12076.47 \times 10^{-6}$ emu mol^{-1}

$\chi'_m = \chi_m - \chi_{dia}$

$= (12076.47 \times 10^{-6}) - (-309.12 \times 10^{-6})$

$= 12385.59 \times 10^{-6}$ emu mol^{-1}

$\mu_{eff} = 2.827 \times \sqrt{(\chi'_m \times T)}$

$$=2.827\times\sqrt{(12385.59\times10^{-6}\times300)}$$

$$= 5.45 \text{ B.M.}$$

(7) $[VOL_9]H_2O$ (**29**)

gram magnetic susceptibility (χ_g) = $6.169 X10^{-6}$

Molar susceptibility (χ_m) = $\chi_g \times M$

$$= 6.169\times10^{-6}\times307$$

$$= 1893.883\times10^{-6} \text{ emu mol}^{-1}$$

$$\chi'_m = \chi_m - \chi_{dia}$$

$$= (1893.883\times10^{-6}) - (-119.14\times10^{-6})$$

$$= 2013.023\times10^{-6} \text{ emu mol}^{-1}$$

$$\mu_{eff} = 2.827\times\sqrt{(\chi'_m\times T)}$$

$$=2.827\times\sqrt{(2013.023\times10^{-6}\times300)}$$

$$= 2.19 \text{ B.M.}$$

(8) $[VOL_{12}]H_2O$ (**31**)

gram magnetic susceptibility (χ_g) = $8.234 X10^{-6}$

Molar susceptibility (χ_m) = $\chi_g \times M$

$$= 8.234\times10^{-6}\times451$$

$$= 3713.534\times10^{-6} \text{ emu mol}^{-1}$$

$$\chi'_m = \chi_m - \chi_{dia}$$

$$= (3713.534\times10^{-6}) - (-216.08\times10^{-6})$$

$$= 3929.614\times10^{-6} \text{ emu mol}^{-1}$$

$$\mu_{eff} = 2.827\times\sqrt{(\chi'_m\times T)}$$

$$=2.827\times\sqrt{(3929.614\times10^{-6}\times300)}$$

$$= 3.06 \text{ B.M.}$$

(9) $[FeL_{15}Cl_2]Cl$ (**34**)

gram magnetic susceptibility (χ_g) = 21.943 $X10^{-6}$

Molar susceptibility (χ_m) $= \chi_g \times M$

$= 21.943 \times 10^{-6} \times 630.5$

$= 13835.061 \times 10^{-6}$ emu mol^{-1}

$\chi'_m = \chi_m - \chi_{dia}$

$= (13835.061 \times 10^{-6}) - (-342.92 \times 10^{-6})$

$= 14177.981 \times 10^{-6}$ emu mol^{-1}

$\mu_{eff} = 2.827 \times \sqrt{(\chi'_m \times T)}$

$= 2.827 \times \sqrt{(14177.981 \times 10^{-6} \times 300)}$

= 5.83 B.M.

(10) $FeL_{10}(H_2O)_2](NO_3)_3$ (**38**)

gram magnetic susceptibility (χ_g) = 76.740 $X10^{-6}$

Molar susceptibility (χ_m) $= \chi_g \times M$

$= 76.740 \times 10^{-6} \times 466$

$= 35760.84 \times 10^{-6}$ emu mol^{-1}

$\chi'_m = \chi_m - \chi_{dia}$

$= (35760.84 \times 10^{-6}) - (-176.22 \times 10^{-6})$

$= 35937.06 \times 10^{-6}$ emu mol^{-1}

$\mu_{eff} = 2.827 \times \sqrt{(\chi'_m \times T)}$

$= 2.827 \times \sqrt{(35937.06 \times 10^{-6} \times 300)}$

= 9.28 B.M.

(11) $[VOL_{10}]SO_4.H_2O$ (**39**)

gram magnetic susceptibility (χ_g) = 9.126 $X10^{-6}$

Molar susceptibility (χ_m) $= \chi_g \times M$

$= 9.126 \times 10^{-6} \times 369$

$= 3367.494 \times 10^{-6}$ emu mol^{-1}

$\chi'_m = \chi_m - \chi_{dia}$

$= (3367.494 \times 10^{-6}) - (-136.1 \times 10^{-6})$

$= 3503.594 \times 10^{-6}$ emu mol^{-1}

$\mu_{eff} = 2.827 \times \sqrt{(\chi'_m \times T)}$

$= 2.827 \times \sqrt{(3503.594 \times 10^{-6} \times 300)}$

$= 2.89$ B.M.

(12) $[FeL_9(H_2O)_2]$ (**40**)

gram magnetic susceptibility $(\chi_g) = 26.757 \times 10^{-6}$

Molar susceptibility $(\chi_m) = \chi_g \times M$

$= 26.757 \times 10^{-6} \times 314$

$= 8401.698 \times 10^{-6}$ emu mol^{-1}

$\chi'_m = \chi_m - \chi_{dia}$

$= (8401.698 \times 10^{-6}) - (-145.64 \times 10^{-6})$

$= 8547.338 \times 10^{-6}$ emu mol^{-1}

$\mu_{eff} = 2.827 \times \sqrt{(\chi'_m \times T)}$

$= 2.827 \times \sqrt{(8547.338 \times 10^{-6} \times 300)}$

$= 4.52$ B.M.

The magnetic moment of the iron(III) complexes **2**, **21**, **23** and **34** lie in the range 5.45-6.08 B.M. indicating the presence of five unpaired electrons consistent with a high spin Fe(III) octahedral complex. The magnetic moment of the binuclear Fe(III) complex **9** is much lower than expected for a high spin d^5 configuration. This is due to antiferromagnetic interactions between the pair Fe^{3+} ions [240]. The complex **40** is

found to have effective magnetic moment of 4.52 B.M. that corresponds to four unpaired electrons and thus consistent with high spin Fe(II) octahedral complex having d^6 configuration. The mononuclear oxovanadium(IV) complex **16** and **29** have magnetic moments little higher than expected for a d^1 system. The higher values of magnetic moment is due to orbital contribution [241]. Unusual high values of magnetic moment for the Fe(III) complex **38** and VO(IV) complexes **31** and **39** is probably due to dimerization and ferromagnetic interaction.

6.13. DFT study

Quantum chemical DFT calculations were performed on selected compounds using B3LYP/6-31G* functional implemented in commercially available Gaussian 03 program suite [242] without imposing symmetry constraints. The optimized structure of the compounds are presented in Figure 6.12.a - 6.12.j and significant structural data are summerised in **Table 14**. The thermochemical properties of the complexes **19**, **24**, **25** and **26** is also computed and listed in **Table-15**.

It is seen from the optimized structure of the ligand $\mathbf{L_3}$, $\mathbf{L_4}$ and $\mathbf{L_3'}$ that hydrogen atom of the OH group at ortho position of the aldehyde moiety is intramolecularly hydrogen bonded to azomethine nitrogen. Further, the orientation of the two phenyl rings across the C=N bond is quite different in the Schiff base compounds obtained from 2-amino phenol ($\mathbf{L_3}$ and $\mathbf{L_4}$) and those with anilines ($\mathbf{L_3'}$). This may as well be responsible for the difference in chiral behaviour. The optimised geometry of the binuclear complex **6** and **7** reveals that the coordination environment around metal centre is square pyramidal with the oxo group in complex **6** and chloro group in complex **7** are projected along axial direction. The optimized structure of the complex **17** showed the geometry around the metal centre is distorted octahedral with metal-oxygen (ethanol) distance of 2.576 Å. The optimized structure of the complexes **19**, **24**, **25** and **26** reveals that the

TABLE-14. Selected bond lengths and bond angles for the ligands L_3, L_4, L_3' and complexes **6, 7, 19, 24, 25, 26.**

Compounds	Bond lengths	(Å)	Bond angles	(^{0})
Schiff base (L_3)	C(4)-O(10)	1.366	C(5)- C(4)-O(10)	120.7
	C(4)-C(5)	1.430	C(4)- C(5)-C(11)	121.5
	C(5)-C(11)	1.441	C(5)- C(11)-N(15)	122.5
	O(10)-H(14)	1.011	C(11)-N(15))-(17)	122.9
	C(11)-N(15)	1.309	N(15))-C(17)-(36)	116.4
	C(17)-N(15)	1.414	C(17)-C(36)-(41)	121.1
	C(17)-C(36)	1.413		
	O(41)-H(42)	0.979		
	C(36)-O(41)	1.383		
Schiff base (L_4)	C(4)-O(10)	1.367	C(5)- C(4)-O(10)	120.7
	C(4)-C(5)	1.430	C(4)- C(5)-C(11)	121.5
	C(5)-C(11)	1.441	C(5)- C(11)-N(15)	122.5
	O(10)-H(14)	1.011	C(11)-N(15))-(17)	122.9
	C(11)-N(15)	1.309	N(15))-C(17)-(36)	116.4
	C(17)-N(15)	1.414		
	C(17)-C(36)	1.414		
	O(41)-H(42)	0.981		
	C(36)-O(41)	1.382		
Schiff base (L_3')	C(4)-O(10)	1.361	C(5)- C(4)-O(10)	120.7
	C(4)-C(5)	1.432	C(4)- C(5)-C(11)	121.0
	C(5)-C(11)	1.442	C(5)- C(11)-N(15)	121.9
	O(10)-H(14)	1.020	C(11)-N(15))-(17)	122.9
	C(11)-N(15)	1.307		
	C(17)-N(15)	1.416		
	C(17)-C(36)	1.407		

Compounds	Bond lengths	(Å)	Bond angles	(^{0})
$[FeL_4Cl]_2$ (**6**)	Fe(23)–N(28)	2.073	N(28)-Fe(23)-O(22)	79.64
	Fe(23)–O(22)	2.113	N(28)-Fe(23)-O(24)	91.24
	Fe(23)–O(24)	1.989	O(24)-Fe(23)-O(16)	99.07
	Fe(23)–O(16)	2.147	O(16)-Fe(23)-O(22)	77.53
	Fe(23)–Cl(44)	2.459		
	Fe(17)–N(13)	2.077	N(13)-Fe(17)-O(16)	79.34
	Fe(17)–O(16)	2.102	N(13)-Fe(17)-O(10)	90.62
	Fe(17)–O(10)	1.997	O(10)-Fe(17)-O(22)	102.57
	Fe(17)–O(22)	2.167	O(22)-Fe(17)-O(16)	77.32
	Fe(17)–Cl(43)	2.475		
$[VOL_3]_2$ (7)	V(23)–N(28)	2.191	N(28)-V(23)-O(22)	75.89
	V(23)–O(22)	2.177	N(28)-V(23)-O(24)	85.16
	V(23)–O(24)	2.044	O(24)-V(23)-O(16)	96.27
	V(23)–O(16)	2.166	O(16)-V(23)-O(22)	75.81
	V(23)–O(44)	1.818		
	V(17)–N(13)	2.191	N(13)-V(17)-O(16)	75.16
	V(17)–O(16)	2.175	N(13)-V(17)-O(10)	84.68
	V(17)–O(10)	2.059	O(10)-V(17)-O(22)	102.64
	V(17)–O(22)	2.199	O(22)-V(17)-O(16)	75.17
	V(17)–O(43)	1.820		
$[Fe(L_7)(acac)(EtOH)]$ (**17**)	Fe(1)-N(1)	2.122	N(1)-Fe(1)-O(1)	87.4
	Fe(1)-O(1)	2.034	N(1)-Fe(1)-O(2)	79.6
	Fe(1)-O(2)	2.091	O(1)-Fe(1)-O(3)	97.2
	Fe(1)-O(3)	2.075	O(2)-Fe(1)-O(3)	95.5
	Fe(1)-O(4)	2.143	N(1)-Fe(1)-O(4)	95.3
	Fe(1)-O(5)	2.576	N(1)-Fe(1)-O(5)	91.6

Compounds	Bond lengths	(Å)	Bond angles	(^{0})
$[FeL_9(H_2O)_2]NO_3$ (**19**)	Fe(1)–N(1)	1.931	N(1)-Fe(1)-N(2)	85.6
	Fe(1)–N(2)	1.931	O(1)-Fe(1)-O(2)	90.8
	Fe(1)–O(1)	1.893	N(1)-Fe(1)-O(1)	92.3
	Fe(1)–O(2)	1.893	N(2)-Fe(1)-O(2)	92.3
	Fe(1)–O(3)	1.988		
	Fe(1)–O(4)	1.988		
$NH_4[FeL_9F_2]$ (**24**)	Fe(1)–N(1)	1.940	N(1)-Fe(1)-N(2)	86.1
	Fe(1)–N(2)	1.940	O(1)-Fe(1)-O(2)	86.5
	Fe(1)–O(1)	1.943	N(1)-Fe(1)-O(1)	93.7
	Fe(1)–O(2)	1.943	N(2)-Fe(1)-O(2)	93.7
	Fe(1)-F(1)	1.843		
	Fe(1)-F(2)	1.844		
$NH_4[FeL_9(NCS)_2]$ (**25**)	Fe(1)–N(1)	1.937	N(1)-Fe(1)-N(2)	85.8
	Fe(1)–N(2)	1.937	O(1)-Fe(1)-O(2)	86.7
	Fe(1)–O(1)	1.925	N(1)-Fe(1)-O(1)	93.7
	Fe(1)–O(2)	1.925	N(2)-Fe(1)-O(2)	93.8
	Fe(1)–N(3)	1.941		
	Fe(1)–N(4)	1.941		
$Na[FeL_9(N_3)_2]$ (**26**)	Fe(1)–N(1)	1.943	N(1)-Fe(1)-N(2)	85.9
	Fe(1)–N(2)	1.943	O(1)-Fe(1)-O(2)	86.3
	Fe(1)–O(1)	1.927	N(1)-Fe(1)-O(1)	93.9
	Fe(1)–O(2)	1.928	N(2)-Fe(1)-O(2)	94.0
	Fe(1)–N(3)	1.985		
	Fe(1)–N(4)	1.985		

TABLE-15. Thermochemical properties of the complexes 19, 24, 25 and 26.

Compounds	Dipole moment (Debye)	Ionozation potential ($kJmol^{-1}$)	Electron affinity ($kJmol^{-1}$)
$[FeL_9(H_2O)_2]NO_3$ (**19**)	2.0482	1023.3	-390.2
$NH_4[FeL_9F_2]$ (**24**)	5.3973	291.9	414.8
$NH_4[FeL_9(NCS)_2]$ (**25**)	4.6815	381.7	180.6
$Na[FeL_9(N_3)_2]$ (**26**)	8.1044	327.1	277.7

geometry around the metal center is slightly distorted octahedral with aquo, fluora, thiocyanato and azido groups along the axial direction. Intramolecular hydrogen bonding between the pair of atoms O1-H19 and O2-H21 are seen in the optimized structure of $[Fe(L)(H_2O)_2]NO_3$ complex (**19**). The data showed that Fe-N (azomethine) bond length is nearly same in all the complexes while Fe-O bond length significantly differs. The largest Fe-O bond distance was noticed when the axial position was occupied by the highest electronegative fluoride and the smallest for labile water molecule occupancy. When bond angles of different complexes are compared, it was observed that (N1-Fe1-N2) angle differs negligibly while a large variation in (O1-Fe1-O2), (N1-Fe1-O1) and (N2-Fe1-O2) bond angles was noticed. The ionization potential of the complex **19** is very high while its electron affinity being negative, presumably due to cationic nature of the complex ion.

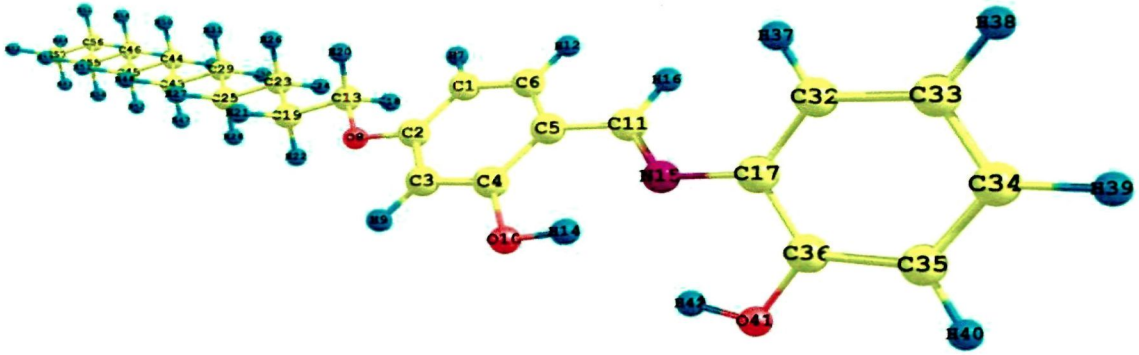

Figure 6.12.a. B3-LYP/6-31G* optimized geometry of the Schiff base L_3.

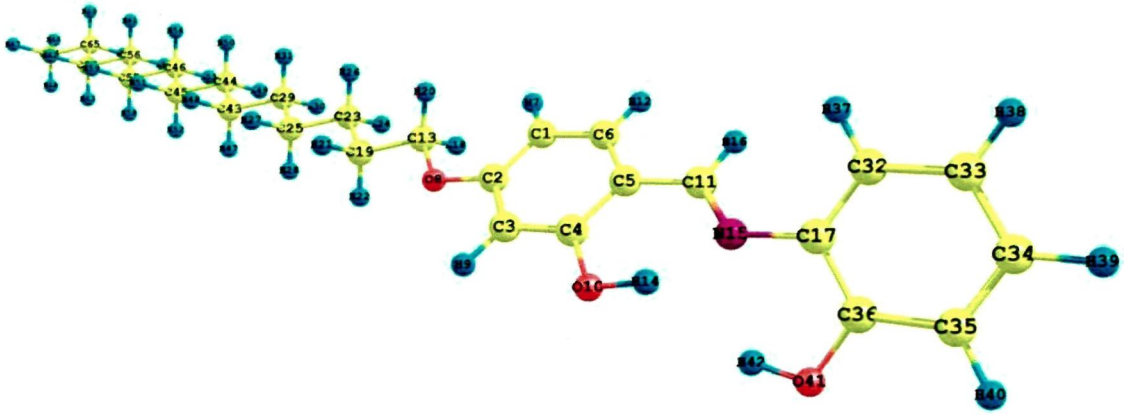

Figure 6.12.b. B3-LYP/6-31G* optimized geometry of the Schiff base L_4.

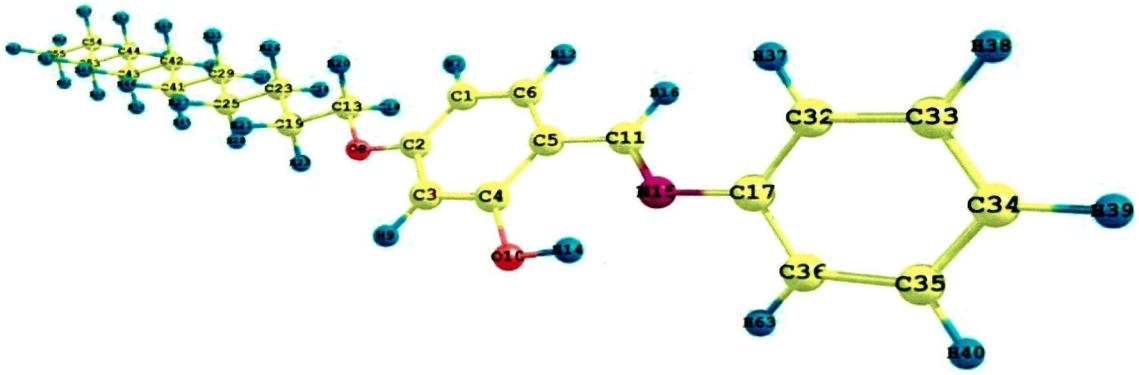

Figure 6.12.c. B3-LYP/6-31G* optimized geometry of the Schiff base L_3'.

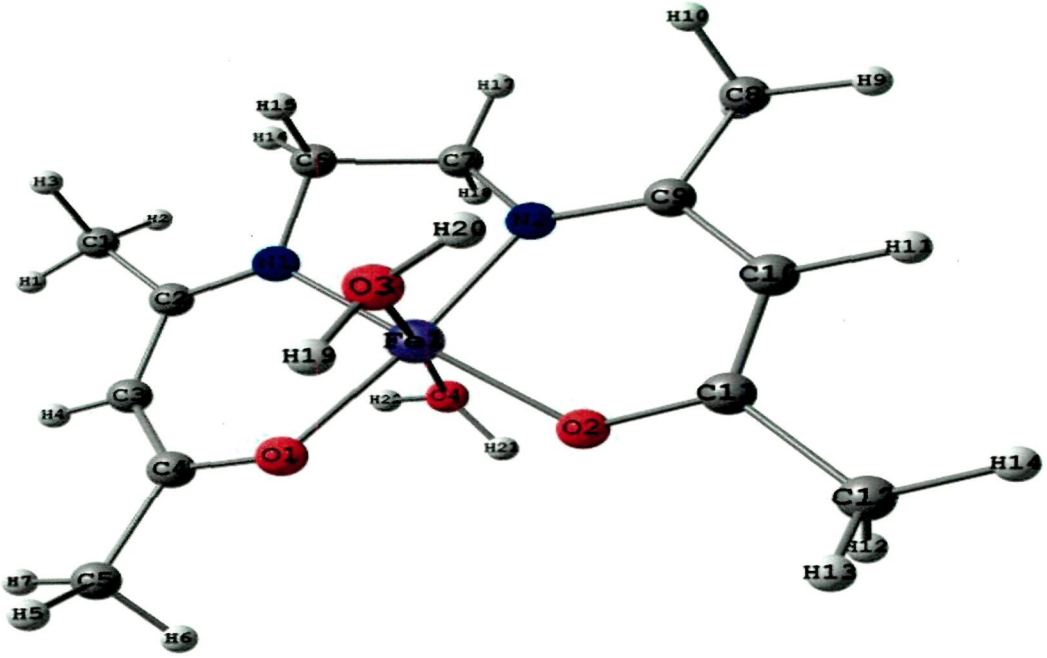

Figure 6.12.d. B3-LYP/6-31G* optimized geometry of the complex $[FeL_9(H_2O)_2]NO_3$ (**19**).

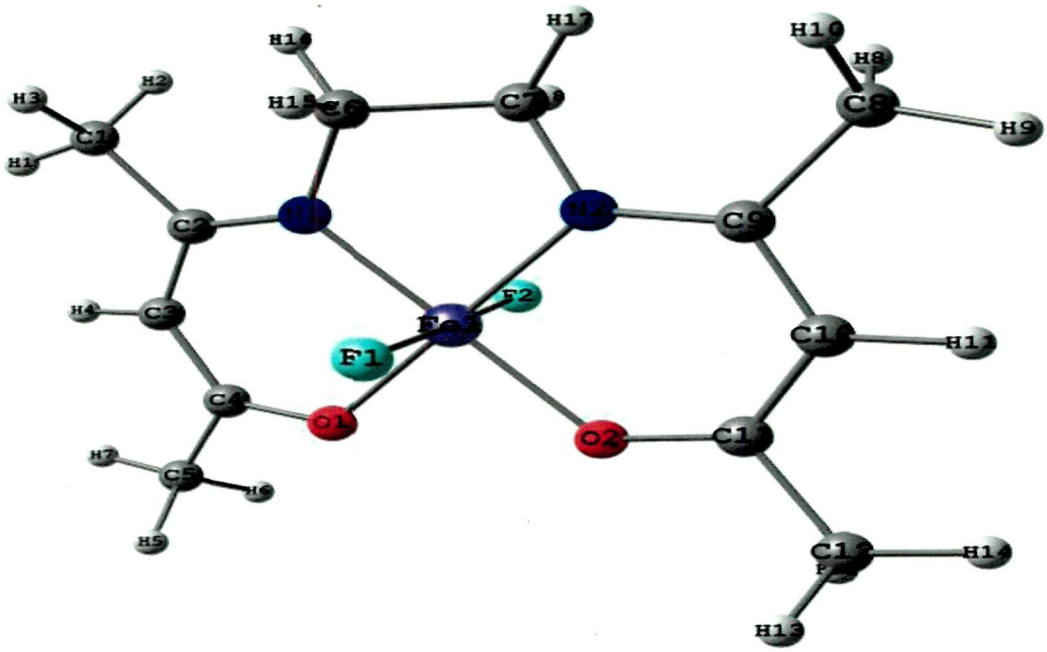

Figure 6.12.e. B3-LYP/6-31G* optimized geometry of the complex $NH_4[FeL_9F_2]$ (**24**).

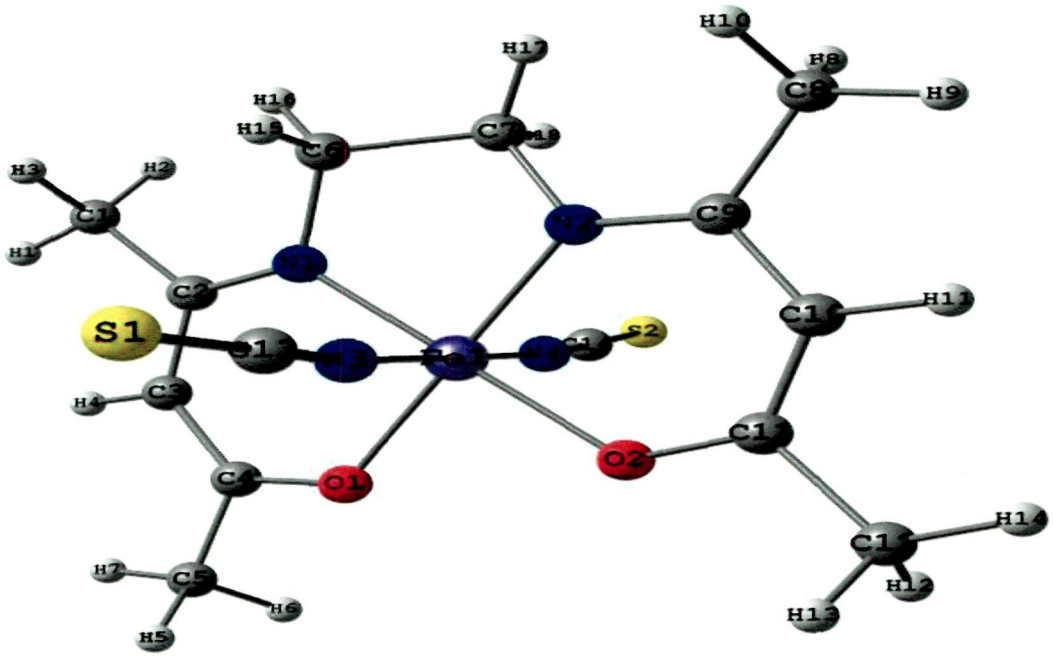

Figure 6.12.f. B3-LYP/6-31G* optimized geometry of the complex $NH_4[FeL_9(NCS)_2]$ **(25)**.

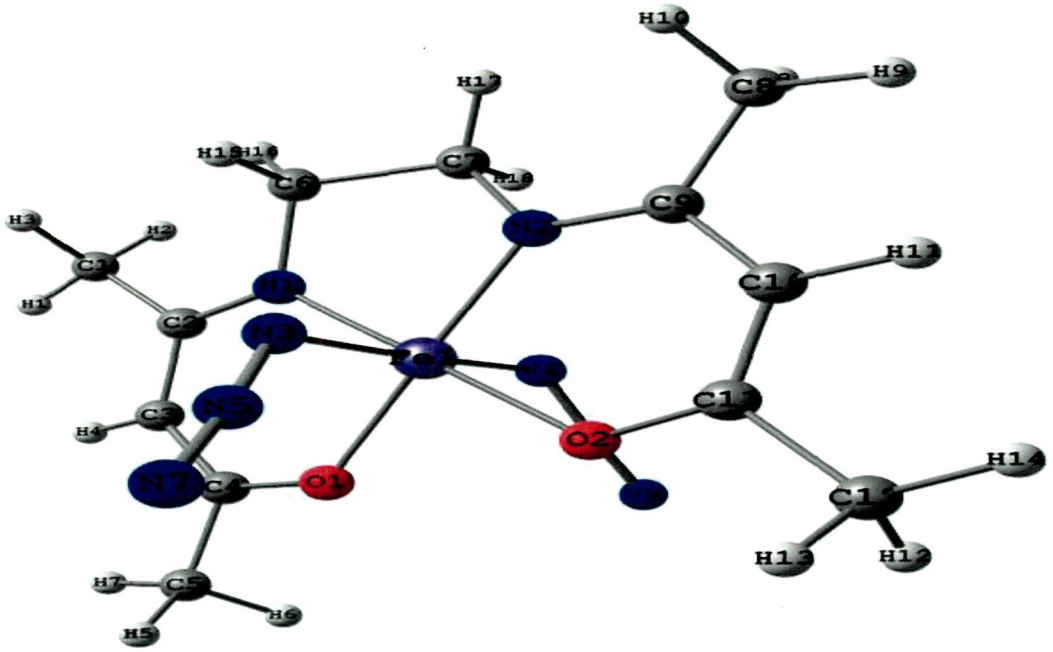

Figure 6.12.g. B3-LYP/6-31G* optimized geometry of the complex $Na[FeL_9(N_3)_2]$ **(26).**

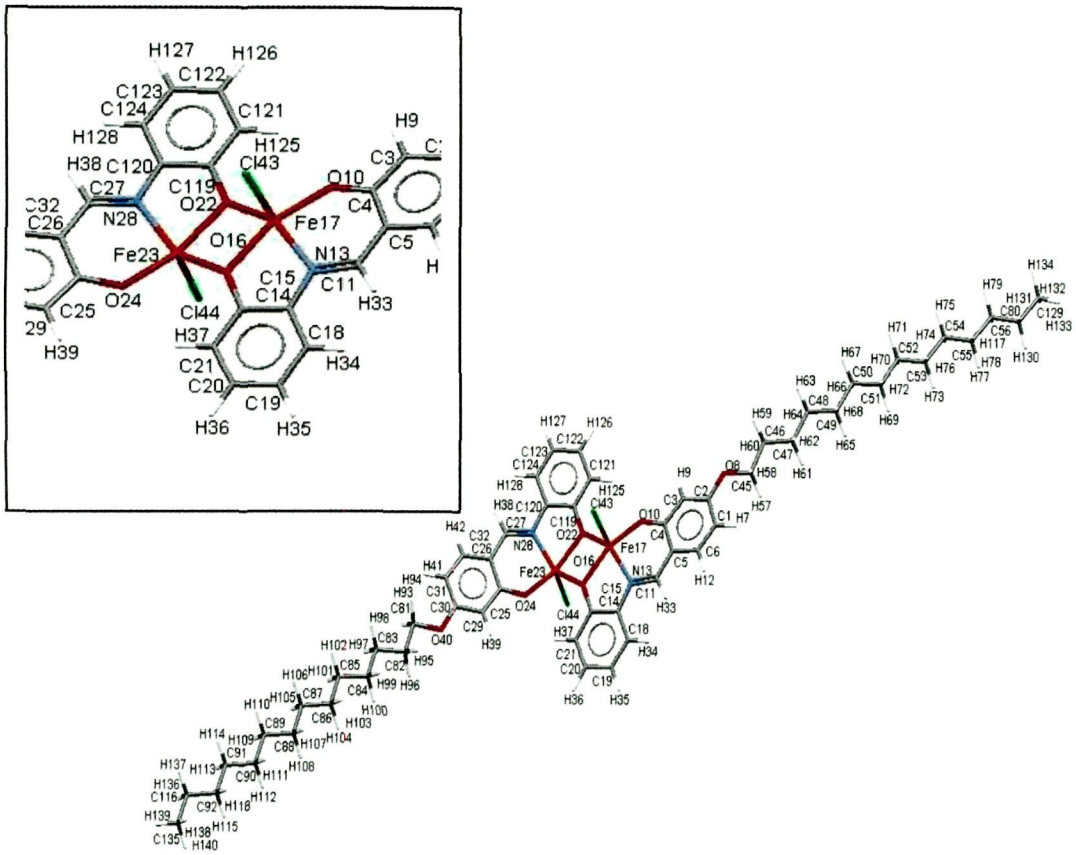

Figure 6.12.h. B3-LYP/6-31G* optimized geometry of the complex $[FeL_4Cl]_2$ (**6**).

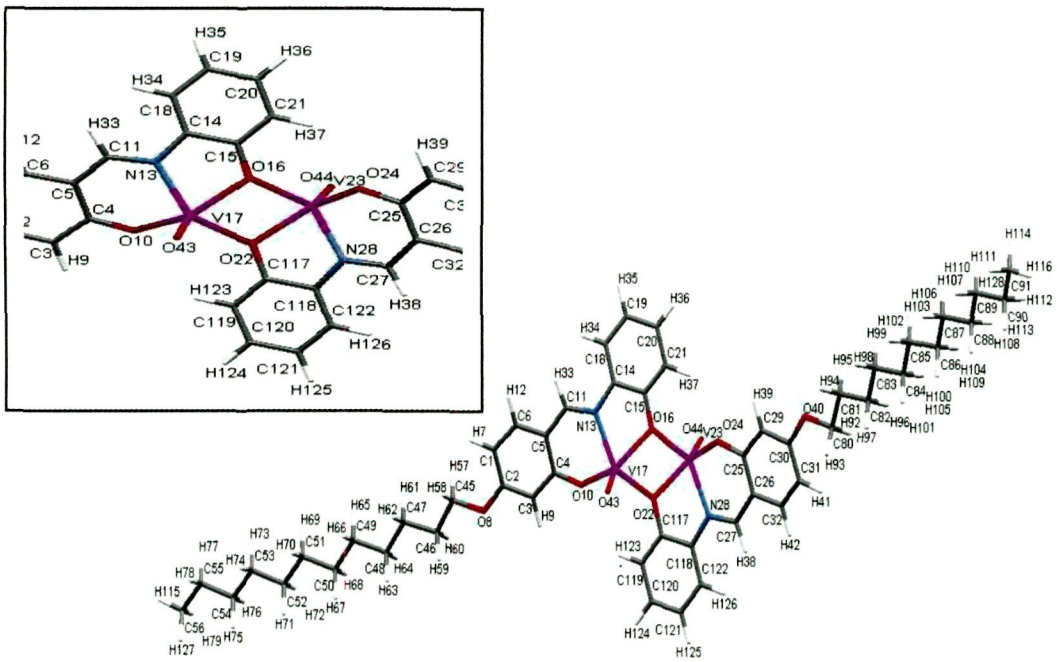

Figure 6.12.i. B3-LYP/6-31G* optimized geometry of the complex $[VOL_3]_2$ (**7**).

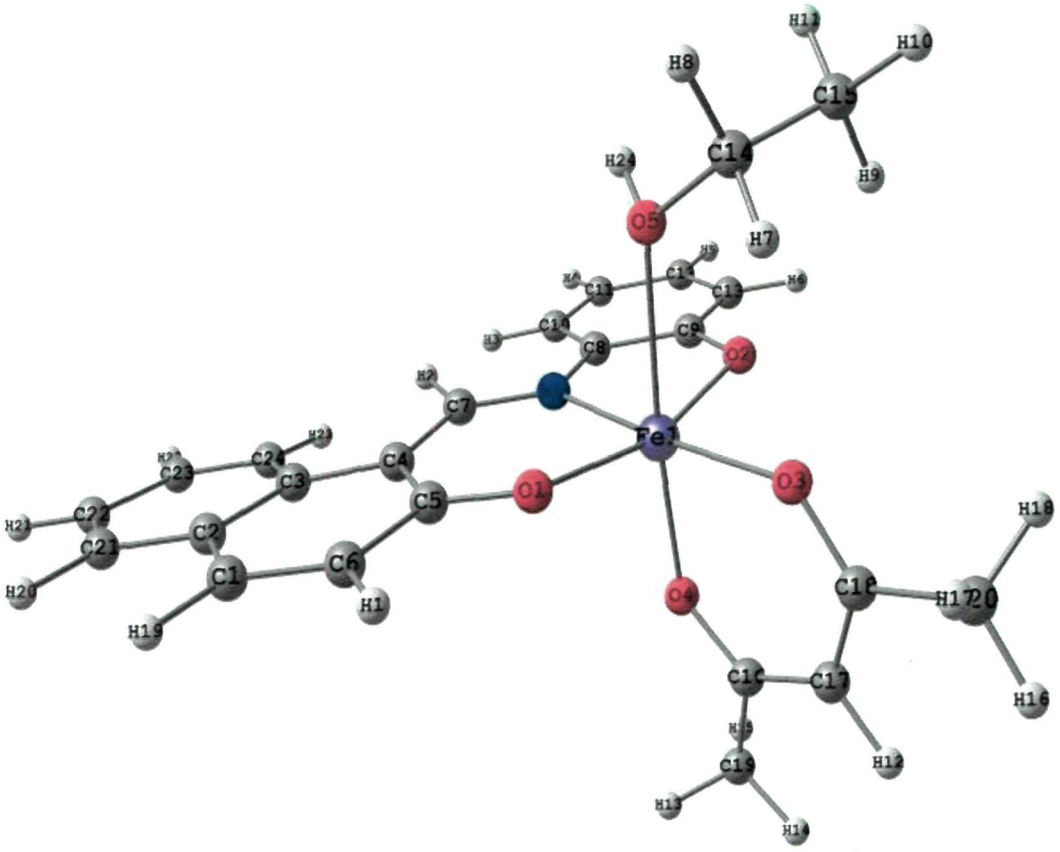

Figure 6.12.j. B3-LYP/6-31G* optimized geometry of the complex [FeL7(acac)(EtOH) (**17**).

The harmonic vibrational frequencies of the compounds were also computed theoretically by DFT methods (**Table 16** and **17**) and the results are compared with the experimental ones. It is observed that the empirically scaled harmonic vibrational frequencies are very similar and in fairly good agreement with the experimental ones [243]. The large deviation observed in $\mathbf{L_3}$ and $\mathbf{L_4}$ for O(41)-H(42) stretching may be attributed to the intermolecular hydrogen bonding that was ignored in DFT studies.

TABLE-16. B3LYP optimized harmonic vibrational frequencies of the compounds L_3 and L_4.

Assignments	Stretching frequency (cm^{-1})	
	L_3	**L_4**
O(41)-H(42)	3614(3431)	3614(3446)
O(10)-H(14)	2998 (2953)	2997 (2956)
C-H $_{sym}$ (-CH_2)	3025(3024)	3025(3024)
C-H $_{asym}$(-CH_2)	3081(3083)	3082(3085)
C(17)-N(15)	1648(1636)	1648(1636)
C(36)-O(41)	1289(1270)	1289(1270)
C(4)-O(10)	1178(1158)	1178(1159)

values in parenthesis indicates corresponding experimental ones.

TABLE-17. B3LYP optimized harmonic vibrational frequencies of the compound 19, 24, 25 and 26.

Assignment	**19**	**24**	**25**	**26**
Fe(1)-O(1)	440 (435)	442(431)	474 (435)	434 (438)
Fe(1)-N(1)	475 (453)	456 (484).	489 (483)	466 (486)
Fe(1)-N(3)	-	-	416 (414)	419
Fe(1)-F(1)	-	624 (652)	-	-
C(4)-O(1)	1281 (1274)	1503 (1508)	1484 (1420)	1492 (1508)
C(2)=N(1)	1569 (1573)	1631 (1627)	1625 (1569)	1631 (1590)
C(11)-S(1)	-	-	774 (771)	-
C(13)-N(3)	-		2077 (2073) 2086 (2049)	-
N(3)-N(5)-N(7)	-	-	-	2046 (2344) 2060 (2366)

values in parenthesis indicates corresponding experimental ones.

Little deviations of the others from the observed values arises due to neglect of anharmonicity in B3LYP method and also due to relatively large size of the molecule [244, 245]. It is to be mentioned here that the average error for frequencies calculated with B3LYP functional was reported to be of the order of 40-50 cm^{-1} [246].

CONCLUSIONS

Various Schiff base ligands of bi, tri and tetradentate nature were synthesized and their complexes with Fe(II), Fe(III) and VO(IV) were prepared. Structural characterization of the synthesized compounds were done by elemental analysis and spectral technique viz. IR, UV-VIS, ^{1}H NMR, ^{13}C NMR, magnetic susceptibility measurements and mass spectroscopy. Single crystal of one of the Schiff bases was obtained successfully and characterized by X-ray diffraction technique. Few Fe(III) complexes containing loosely bound solvent molecule were used successfully to access newer mixed ligand complexes. The reaction of the aquated iron(III)-Schiff base complex of the type $[FeL(H_2O)_2]NO_3$ with anionic ligand ammonium bifluoride, ammonium thiocyanate or sodium azide in 1:2 molar ratio afforded hitherto unreported mixed-ligand complexes of the type $A^{+}[FeL(X)_2]^{-}$ ($A=NH_4$; X=F, NCS and A=Na ; $X=N_3$) (Scheme 5.3.b). Similar type reaction with neutral donors, imidazole and pyridine led to the formation of mixed-ligand complexes of the type $[FeL(X)_2]NO_3$ (X=Im or Py). Reaction of binuclear Fe(III)

complex of the type $[Fe(L_5)Cl]_2$ with imidazole and triphenyl phosphine in 1:1 molar ratio also afforded mixed ligand complexes of the type $[Fe(L_5)(X)Cl]_2$ (X= Im or PPh_3). The mesogenic behavior of the compounds were investigated by Polarizing Optical Microscope and Differential Scanning Calorimetry. Schiff bases ($\mathbf{L_3}$ and $\mathbf{L_4}$) derived from condensation of 4-substituted long chain alkoxy salicyldehyde and 2-aminophenol displayed liquid crystalline property with smectic-X phase having chiral domain. This mesogenic behaviour was lost on complexation with iron(III) and oxovanadium(IV). The stronger interaction between square pyramidal V=O or Fe-Cl centre seemed to inhibit the formation of liquid crystalline phase.

Few selected compounds were screened for their *invitro* antimicrobial activities against various gram-positive and gram-negative bacteria. The Schiff base L_5 and its oxovanadium(IV) complex were found to have pronounced activity against *Klebsiella pneumoniae, Staphylococcus aureus, Pseudomonas aeroginosa, Escherichia coli, Bacillus subtilis* and *Proteus vulgaris* while the other compounds examined showed only moderate activity.

The redox behaviour of the compounds were examined by cyclic voltammetric technique. Most of the complexes exhibited a quasi-reversible response. The half wave potential of almost all the complexes are negative and very small implying that present Schiff base complexes of iron(III) and oxovanadium(IV) can be easily oxidized or reduced. This characteristics feature would make them a valuable catalyst in redox reactions.

Thermal behaviour of the complexes were studied by TGA, DTG and DTA technique. Weight loss at different temperature ranges was explained satisfactorily with the help of proposed structure.

Magnetic susceptibility of the few complexes were studied using Vibrating Sample Magnetometer at room temperature against variable field sirength. The magnetic properties of the compounds were characterized by the parameters saturation magnetization (Ms), the remanence (Mr), the coercivity (Hc), the squareness ratio (SQR), the slope at Hc and the initial slope. The saturation magnetization and coercivities of the compounds are neither very high nor very low and thus these are characterized as intermediate magnetic material. These materials are usually used in magnetic media. The magnetic moment of mononuclear Fe(III) complexes and VO(IV) complexes are consistent with high spin d^5 and d^1 system while much lower values of magnetic moment in binuclear complexes is due to antiferromagnetic interaction. Unusual high values of magnetic moment for the Fe(III) complex **38** and VO(IV) complex **31** and **39** is probably due to dimerization and subsequent ferromagnetic interaction.

The structure of the selected compounds were optimized by Quantum Chemical Density Functional Theory using B3LYP functional and 6-31G* basis set implemented in GAUSSIAN 03 package and structurally significant geometrical parameters were computed. Harmonic vibration frequencies as calculated theoretically was found comparable with those of experimental ones.

In all, condensation of appropriately selected aldehyde and amines led to quite a large number of Schiff base ligands which depending on metal : ligand stoichiometry, metal source, reaction condition, solvent used led to neutral or anionic, mononuclear or dinuclear, simple or mixed-ligand Schiff base complexes. The solvated complexes have been demonstrated to be suitable synthons for accessing newer complexes via ligand exchange reactions.Though efforts to obtain single crystals of the complexes did not prove successful, choice of appropriate technique is anticipated to afford single crystals

suitable for structure determinations. This is also expected to render unambiguous proof of the molecular structures proposed based on spectral data. Some complexes which were were obtained as solvated ones, in particular, may serve as catalyst for many organic transformation reactions. Appending a long alkyl or alkoxy group at suitable position of the Schiff base ligand can generate interesting supramolecular arrangements which in turn may lead to mesogenicity, NLO activity etc.

Supplementary materials

Crytallographic data for the structural analysis of the ligand have been deposited with the Cambridge Crystallographic Data Centre, CCDC No. 262373 A copy of this information may be obtained free of charge from The Director, CCDC, 12 Union Road, Cambridge, Cb2 1EZ, UK (fax: +44 1223 336 033; e-mail: deposit@ccdc.cam.ac.uk or www: http://www.ccdc.ac.uk).

REFERENCES

[1] H. Schiff, **Ann. Suppl.** 1864, **3**, 343.

[2] K.N. Campbell, H. Sommers and B.K. Campbell, **J. Am. Chem. Soc.** 1944, **66**, 82.

[3] J. Hine and C.Y. Yeh, **J. Am. Chem. Soc.** 1967, **89**, 2669.

[4] C.M. Brewster, **J. Am. Chem. Soc.** 1924, **46**, 2463.

[5] C. Munir, S.M. Yousaf and N. Ahmed, **J. Chem. Soc. Pak.** 1985, **7(4)**, 301.

[6] E. Brand and S.M. Berg, **Org. Synth. Coll.** 1943, **2**, 49.

[7] E. Dane, F. Dress, P. Konard and T. Dockner, **Angew. Chem.** 1962, **74**, 873.

[8] J.C. Sheehan and V.J. Grinda, **J. Am. Chem. Soc.** 1962, **84**, 2417.

[9] A.A. Alemi and B. Sabani, **Acta. Chim. Slov.** 2000, **47**, 363.

[10] M. Shamsipur, A.R. Ghiasvand, H. Shargi and H. Naeimei, **Anal. Chim. Acta.** 2000, **408**, 271.

[11] P. Buhlman, E. Prestsch, E. Bakker, **Chem. Rev.** 1998, **98**, 1593.

[12] E. Bakker, P. Buhlman, E. Prestch, **Chem. Rev.** 1997, **97**, 3083.

[13] M. Shamsipur, S. Sadegi, H. Naeimi and H. Sharghi, **Pol. J. Chem.** 2000, **74**, 231.

[14] N. Alizadeh, S. Ershad, H. Naeimi, H. Shargi, M. Shamsipur and J. Freshenius, **J. Anal. Chem.** 1999, **365**, 511.

[15] E.J. Jacobsen, W. Zhang and M.L. Guler, **J. Am. Chem. Soc.** 1991, **113**, 6703.

[16] G.J. Kim and J.H. Shin, **Catal. Lett.** 1999, **63**, 83.

[17] H. Shargi and H. Naeimi, **Bull. Chem. Soc. Jpn.** 1999, **72**, 1525.

[18] J.O. Kennet, J.W. Shiow and J.B. Cynthia, **Tetrahedron Lett.** 1992, **33**, 1001.

[19] C. Sasaki, K. Nakajima and M. Kojima, **Bull. Chem. Soc. Jpn.** 1991, **64**, 1318.

[20] H. Sigel, **Metal Ions in Biological Systems**, Marcel Dekker, New York, 1973.

[21] N. Sari, S. Arslan, E. Logoglu and I. Sakiyan, **G.U. Journal of Science**, 2003, 283.

[22] A.S. Rathod, B.N. Berad and A.G. Doshi, **Orient. J. Chem**. 2000, **16**, 549.

[23] W.M. Singh and B.C. Dash, **Pesticides**, 1988, **22**, 33.

[24] S.P. Rajendran and R. Karvembu, **Indian J. Chem. Sect. B**, 2002, **41**, 222; **Chem. Abstr.** 2002, 136, 366043h.

[25] U. Calis, M, Yarim, M. Koksal and M. Ozalp, **Arzneimittel – Forschung**, 2002, 52, 778; **Chem. Abstr**. 2003, **138**, 201550w.

[26] M. Nagatsuka, H. Ishida and S, Tanaka, **Jpn. Kokai Tokkyo Koho,** JP, 2002, **128**, 610; **Chem. Abstr.** 2002, **136**, 365280t.

[27] S.N. Pandeya, D. Sriram, G. Nath and E. De, **Pharmaco**, 1999, **54**, 624.

[28] K.A. Shaikh, M.A. Baseer and N.A. Mote, **Ashian. J. Chem**. 2001, **13**, 496.

[29] M.D. Deshmuk and A.G. Doshi, **Orient. J. Chem**. 1995, **11**, 85; Chem. Abstr. 1995, **1236**, 256269g.

[30] S.K. Sridhar, S.N. Pandeya, J.P. Stables and A. Ramesh, **Eur. J. Pharm. Sci.** 2002, **16**, 129; **Chem. Abstr**. 2003, **138**, 162966t.

[31] S.K. Sridhar, S.N. Pandeya and E. De Clercq, **Bolletino Chimoco Farmaceutico,** 2001, **140**, 302 ; **Chem. Abstr**. 2002, **136**, 263052c.

[32] S.K. Sridhar and A. Ramesh, **Indian Drugs**, 2001, **38**, 174 ; **Chem. Abstr**. 2002, **137**, 226351z.

[33] V.E. Kuz'min, V.P. Lozitsky, G.L. Kamalov, R.N. Lozitskaya, A.I. Zheltvay, A.S. Fedtchouk and D.N. Kryzanhovsky, **Acta Biochiimoca Polonica**, 2000, **47**, 867.

[34] G. Georgiev, **Dokl. Bolg. Akad. Nauk**, 1981, **34(2)**, 189.

[35] G.H. Schmid, " **Organic Chemistry**" Mosby, New York, 1996, p.624.

[36] F.A. Carry, " **Organic Chemistry**", Mc-Graw Hill, 2nd edition, 1992, p.695.

[37] F. Basolo and R.C. Johnson, " **Coordination Chemistry : The Chemistry of Metal complexes**". W.A. Benjamin, INC, 1964, 8.

[38] H. Schiff, **Ann. Chem.. Pharm**. 1869, **150**, 193.

[39] H.Schiff, **Ann. Chem.. Pharm**. 1869, **151**, 186.

[40] M. Delpine, Bull. Soc. Chim. Franch. 1899, **21**, 943.

[41] P. Pfeiffer, E. Buccholz and O. Baver, **J. Prakt. Chem.** 1931, **129**, 163.

[42] P. Pfeiffer, E. Breith, E. Lubbe, T. Tsumaki, **Ann. Chem. Pharm**. 1933, **503**, 84; P. Pfeiffer and H. Pfitzinger, **J. Prakt. Chem.** 1936, **145**, 243; P. Pfeiffer, T. Hesse, H. Pfitzinger, W. Schol and H. Thielertl, **J. Prakt. Chem.** 1937, **149**, 217.

[43] F. Zetzsche, H. Silberman and G. Vieli, **Helv. Chim. Acta**. 1925, **8**, 596.

[44] U.P. Singh, S. Singh and S.M. Singh, **Metal Based Drugs**, 1998, **5**, 35 ; **Chem. Abstr.** 1998, **129**, 48732z.

[45] Z.H. Liu, C.Y. Duan, J.Hu, **Inorg. Chem**. 1999, **38**, 1719.

[46] Y.P. Tian, C.Y. Duan, C.Y. Zhao, X.Z. You, T.C.W. Mak, Z.Y. Zhang, **Inorg. Chem.** 1997, **36**, 1247.

[47] D.X. West, A.E. Liberta, S.B. Padhye, R.C. Chikate, P.B. Sonawane, A.S. Kumbhar, R.G. Yerande, **Coord. Chem. Rev**. 1993, **123**, 49.

[48] N.C. Kasuga, K. Sekino , M. Ishikawa, A. Honda, M. Yokoyama, S. Nakano, N. Shimada, C. Koumo, K. Nomiya , **J .Inorg. Biochem**. 2003, **96**, 298.

[49] K.A. Crouse, K.B. Chew, M.T.H. Tarafder, A. Kasbollah, A.M. Ali, B.M. Yamin, H.K. Fun , **Polyhedron**, 2004, **23**, 161.

[50] K.A. Crouse, K.B. Chew, B.Y. Yamin, S.W. Ng, M.T.H. Tarafder, **Acta. Crystallogr. Sect.E**, 2003, **59**, 148.

[51] A.E. Liberta, D.X. West, **BioMetals**. 1992, **5**, 121.

[52] I.H. Hall, K.G. Rajendran, D.X. West, A.E. Liberta, **Anticancer Drugs**, 1993, **4**, 231.

[53] J. Costamagna, J. Vargas, R. Lattorre, A. Alvarado, G. Mena, **Coord. Chem. Rev**. 1992, **119**, 67.

[54] A.D. Garnovskii, A.L. Nivorozhkin, V.I. Minkin, **Coord. Chem. Rev**. 1993, **126**,1.

[55] P. Guerriero, **Coord. Chem. Rev**. 1995, **139**, 17.

[56] H. Luo, P.E. Franwick, M.A. Green, **Inorg. Chem**. 1998, **37**, 1127.

[57] R. Hasanov, M. Sadıkoğlu, S. Bilgic, **Applied Surface Science**, 2007, **253(8)**, 3913.

[58] M.M.T. khan, S. Shukla and J. Shark, J. **Mol. Catal**. 1990, **57**, 301.

[59] D.E. Fenton, **Chem. Soc. Rev**. 1999, **28**, 159.

[60] A. Vander Bergen, K.S. Murray, M.J. O'Connor, N. Rehak and B.O. West. **Aust. J. Chem.** 1968, **21**, 1505.

[61] J. Davices and B.M. Gatehouse. **Chem. Commun**. 1970, 1166.

[62] M. Gerloch, J. Lewis, F.F. Mabbs and A. Richards. **J.Chem. Soc. (A)**, 1968, 112.

[63] M. Gerloch and F.E. Mabbs. **J.Chem. Soc. (A)**, 1967, 1559.

[64] M. Gerloch and F.E. Mabbs. **J.Chem. Soc. (A)**, 1967, 1900.

[65] A. Nabei, T. Kuroda-Sowa, T.Okubo, M. Maekawa, M. Munakata, **Inorg. Chim. Acta**. 2008, **361**, 3489.

[66] D. Rehder, **Inorg. Chem. Commun**. 2003, **6**, 604.

[67] K. Elvingson, A.G. Baro´ and L. Petterson, **Inorg. Chem**. 1996, **35**, 3388

[68] A. Syamal, **Coord. Chem. Rev**. 1975, **16**, 309.

[69] A. Sayamal and I.J. Theriot, **J. Coord. Chem.** 1973, **2**, 193.

[70] A. Sayamal and K.S. Kale, **J. Ind. Chem. Soc.** 1978, 55, 606.

[71] I.G. Vanquickenborne and S.P. McGlynn, **Theor. Chem. Acta.** 1968, **9**, 390.

[72] R.P. Mathur, P. Mathur and R.K. Mehta, **Curr. Sci.** 1983, **52**, 481.

[73] R.L. Dutta and M.M. Hossain, **Ind. J. Chem. Sec. A.** 1982, **21**, 746.

[74] T. Ghosh and C. Bandyopadhyay, **Trans. Met. Chem.** 2004, **29**, 444.

[75] T. Ghosh, **Trans. Met. Chem.** 2006, **31**, 560.

[76] Saeed Rayati, Marjan Koliaei, Fatemeh Ashouri, Sajjad Mohebbi, Andrzej Wojtczak, Anna Kozakiewicz, **Applied Catalysis A: General**, 2008, **346**, 65.

[77] R. H. Hoim, G. W. Everett, Jr and A. Chakraborty, **Prog. Inorg. Chem.** 1966, **7**, 83.

[78] A. Nishinaga, T. Yamada, H. Fujisawa and K. Ishizaki, **J. Mol. Catal.** 1988, **48**, 249.

[79] H. Chakraborty, N. Paul and M. L. Rahman, **Trans. Met. Chem.** 1994, **19**, 524.

[80] Y. D. Zhao, D. W. Pang, Z. Zong, J.K. Cheng, Z. F. Luo, C. J. Feng, H. Y. Shen and X. C. Zhung, **Chem. Abstr.** 1998, **128**, 252661.

[81] R. Sreekala and K. K. Yusuff, **Chem. Abstr.** 1999, **130**, 115551.

[82] P.G. Cozzi. **Chem. Soc. Rev.** 2004, **33**, 410. ; S.K. Edulji and S.T. Nguyen., **Organometallics,** 2009, **22**, 3374. ; J.A. Miller, W. Jin and S.T. Nguyen. **Angew. Chem. Int. Edit.**, 2002, **41**, 2953.

[83] M. Bagherzadeh and M. Amini. **Inorg. Chem. Commun.** 2009, **12**, 21.

[84] K. Shanker, P.M. Reddy, R. Rohini, Y. Ho and V.Ravinder. **J. Coord. Chem.** 2009, **62**, 2388.

[85] S. Rayati, S. Zakari, M. Koliaei, A. Wojtczak, A. Kozakiewicz, **Inorg. Chem. Commun**. 2010, **13**, 203.

[86] K. C. Gupta and A. K. Sutar, **J. Mol. Catal. A : Chemical**, 2007, **272**, 64.

[87] S. Rayati, N. Sadeghzadeh and H. R. Khavasi, **Inorg. Chem. Commun**. 2007, **10**, 1545.

[88] C. G. Saxena and S. V. Shrivastava, **J. Ind. Chem. Soc.** 1987, **64**, 685.

[89] C. N. Bhardwaj and V. R. Singh, **Indian J. Chem**. 1994, **33A**, 423.

[90] R. Chohan, H. Zahid and S. Kausar, **J. Chem. Soc. Pak.** 2001, **23**, 163 ; **Chem. Abstr**. 2002, **136,** 410591.

[91] D. M. Kar, S. K. Sahu, D. Pradhan, G. K. Dash and P. K. Mishra, **J. Teach. Res. Chem**. 2003, **10**, 20 ; Chem. Abstr. 2004, 141, 23376.

[92] A. Cukurovali, I. Yilmaz, Z. Ozmen and M. Ahmedzade, Trans. Met. Chem. 2002, 27, 171.

[93] S. Gaur, Asian J. Chem. 2003, 15, 250 ; Chem. Abstr. 2003, 138, 264728.

[94] S. Zhang, Y, Jiang and M. Chen, Chem. Abstr. 2005, 142, 347400.

[95] J. Patole, D. Shingnapurkar, S. Padhye and C. Ratledge, **Bio-Org. Med. Chem. Lett.** 2006, **16**, 1514.

[96] B. Dash, P. K. Mahapatra, P. Panda and J. M. Patnaik, **J. Indian Chem. Soc.** 1984, **61**, 1061.

[97] N. R. Rao. P. V. Rao, G. V. Reddy and M. C. Ganorkar, **Indian J. Chem.** 1987, **26A**, 887.

[98] P. Mishra, P. N. Gupta and A. K. Shakaya, **J. Indian Chem. Soc.** 1991, **68**, 539.

[99] R. Dhakrey and G. Sexena, **J. Indian Chem. Soc.** 1987, **64**, 685.

[100] R. V. Singh, N. Gupta and N. Fahmi, Indian J. Chem. 1999, 38A, 1150.

[101] K. M. Patel, N. H. Patel, K. N. Patel and M. N. Patel, **Synth. React. Inorg. Met-Org. Chem.** 2000, **30**, 1953.

[102] Y. Dang, X. Bao, X. Zhu and C. Wang, **Chem. Abstr.** 2004, **140**, 398771.

[103] M. M. Omar, G. G. Mohamed and A. A. Ibrahim, **Spectrochim. Acta Part A : Molecular and Bio-molecular**, 2009, **73**, 358.

[104] A. B. Mirzabdullaev, D. K. Ashlanova and F. I. Ershov, **Chem. Abstr.** 1984, **99**, 22191.

[105] F. Meng, Q. Zhao, M. Li and Y. Xin, **Chem. Abstr.** 2003, **138**, 330746.

[106] M. J. Haem, M. H. Cynamom, M. F. Chen, R. Chopins, J. Davis, H. Kong, A. Noble, B. Sekine, M. S. Terrot, D. Trombino, M. Thai, E. R. Webster and R. Wilson, **Eur. J. Med. Chem.** 2009, **44**, 4109.

[107] K. S. Siddiqi, R. I. Kureshi, N. H. Khan, S. Tabassum and S. Zaidi, **Inorg. Chim. Acta.** 1988, **151**, 95.

[108] N. S. Kozlov, G. P. Korotyshova, N. G. Rozhkova and E. I. Andreeva, **Chem. Abstr.** 1987, **106**, 155955.

[109] L. Zhu, N. Chen, H. Li, F. Song and X. Zhu, **Chem. Abstr.** 2004, **141**, 374026.

[110] Y. Wang, X. Yu, B. Lu and W. Ye, **Chem. Abstr.** 2002, **136**, 247530.

[111] X. Song, Z. Wang, Y. Wang, Z. Zhang and C. Chen, **Chem. Abstr.** 2005, **143**, 367252.

[112] L. Hadjipavlu, J. Dimitra and A. Athina, **Drug Des. Discovery** 1998, **15**, 199.

[113] B. De and G. V. S. Ramasharma, **Indian Drugs**, 1999, **36**, 583.

[114] X. Luo, J. Zhao, Y. Ling and Z. Liu, **Chem. Abstr.** 2003, **138**, 247927.

[115] B. S. Jayashree, J. Jerald and K. N. Venugopala, **Orient. J. Chem.** 2004, **20**, 123.

[116] Y. Zhou, M. Zhao, Y. Wu, C. Li, J. Wu, M. Zhong, L. Peng and S. Peng, **Bio-Inorg. Med. Chem.** 2010, **18**, 2165.

[117] Z. Guo, R. Xing, S. Liu, H. Yu, P. Wang, C. Li and P. C. Li, **Bio-Org. Med. Chem. Lett**. 2005, **15**, 4600.

[118] K. P. Latha, V. P. Vaidya and J. Keshavayya, **J. Teach. Res. Chem**. 2004, **11**, 39.

[119] L. Cheng, J. Tang, H. Luo, X. Jin, F. Dai, J. Yang, Y. Quien, X. Li and B. Zhau, **Bio-Inorg. Med. Chem. Lett**. 2010, **In press**, Available online 11 March/2010.

[120] A. Begum, S. Saha, M. Netaji and A. R. Chakraborty, **J. Inorg. Biochem**. 2010, **104**, 477.

[121] P. Prasad, P. K. Sasmol, R. Mazumder, R. R. Didhe and A. R. Chakraborty, **Inorg. Chim. Acta**, 2010, **In press**, Available online 12 March/2010.

[122] A. A. Nejo, G. A. Kolawole, A. R. Opoku, J. Wolowska and P. O. Brien, **Inorg. Chim. Acta**. 2009, **362**, 3993.

[123] R. K. Parashar, R. C. Sharma and G. Mohan, **Biol. Trace. Ele. Res**. 1989, **23**, 145.

[124] Y. Gaowen, X. Xiaping, T. Huan and Z. Chenxue, **Chem. Abstr**. 1995, **123**, 101089.

[125] K. P. Sharma, V. S. Jolly and P. Pathak, **Chem. Abstr.** 1999, **130**, 346977.

[126] L. Xu and X. Xu, **Chem. Abstr**. 2001, **134**, 4833.

[127] X. U. Dongfang, M. A. Shuzhi, D. U. Guangying, H. E. Quzhuang and S. Dazhi, **J. Rare earth**, 2008, **26**, 643.

[128] R. S. George, R. Joseph and K. E. George, **Int. J. Polym. Mater**. 1993, **23**, 17.

[129] I. Y. Levitin, A. L. Sigan, N. N. Sazikova, E. I. Pisarenko, M. S. Tsarkova and O. A. Chumak, **Chem. Abstr**. 2005, **143**, 153521.

[130] M. W. Sabba, R. R. Mohamed and E. H. Oraby, **Eur. Poly. J**. 2009, **45**, 3072.

[131] J. Dehnert and W. Juchemann, **Chem. Abstr.** 1985, **103**, 106288 ; U. Bergmann and Hansen, **Chem. Abstr.** 1985, **103**, 7731.

[132] A. Fakhari, R. Afsin and H. Naeim, **Talanta**, 2005, **66**, 813.

[133] G. C. Ferrerira, P. J. Neame and H. A. Dailey, **Protein Sci.** 1993, **2**, 1959.

[134] M. N. Ibrahim and S. A. Sarif, **E-Journal. Chem.** 2007, **4**, 531.

[135] Y. M. Hijji, B. Barare, A. P. Kennedy and R. Butcher, **Sensors and Actuasis B : Chemical**, 2009, **136**, 297.

[136] S. Wang, G. Men, L. Zhao, Q. Hou and S, Jhiang, **Sensors and Actuasis B : Chemical**, 2010, **145**, 826.

[137] N. N. Negm and M. F. Zaki, **Colloids and Surfaces A : Physicochemical and Engineering Aspects**, 2008, **322**, 97.

[138] H. Fujii, T. Kurahashi, T. Ogura. **J. Inorg. Biochem.** 2003, **96**, 133.

[139] R.B. Bedfort, D.W. Bruce, R.M. Frost, J.W. Goodby, M. Hird. **Chem. Commun.** 2004, 2822.

[140] K.P. Bryliakov, E.P. Talsi. **Angew. Chem. Int. Edit.** 2004, **43**, 5288.

[141] T. Katsuki. **Chem. Soc. Rev.** 2004, **33**, 437.

[142] C.T. Brewer, G. Brewer, G.B. Jameson, P. Kamaras, L. May, M. Rapta. **J. Chem. Soc. Dalton Trans.** 1995, 37.

[143] H. Olmez, F. Arslan, H. Icbudak. **J. Therm. Anal. Cal.** 2004, **76**, 793.

[144] R. Carballo, A. Casti_eiras, S. Balboa, B. Covelo, J. Niclós. **Polyhedron**, 2002, **21**, 2811.

[145] J.B. Vincent, T. Hui-Lún, A.B. Blackman, E.B. Lobkovsky, D.N. Hendrickson, G. Christoug. **J. Am. Chem. Soc.** 1993, **115**, 2353.

[146] C. Kaes, A. Katz, M.W. Hosseini. **Chem. Rev.** 2000, **100**, 3533.

[147] G. Psomas, C. Dendrinou-Samara, P. Philippakopoulos, V. Tangoulis, C.P. Raptopoulou, E. Samaras, D.P. Kessissoglou. **Inorg. Chim. Acta.** 1998, **272**, 24.

[148] P. Losier, M.J. Zaworotka. **Angew. Chem. Int. Edit. Engl.** 1996, **35**, 2779.

[149] A. Saxena, J.K. Koacher, J.P. Tandon. **Inorg. Nucl. Chem. Lett.** 1981, **17,** 229.

[150] P.G. Cozzi. **Chem. Soc. Rev.** 2004, **33**, 410.

[151] S.K. Edulji, S.T. Nguyen. Organometallics, 2009, **22**, 3374.

[152] J.A. Miller, W. Jin, S.T. Nguyen. Angew. Chem. Int. Edit, 2002, **41**, 2953.

[153] J. Legros, C. Bolm, **Angew. Chem. Int. Ed.** 2003, **42**, 5487.

[154] M. Bagherzadeh, M. Amini, **Inorg. Chem. Commun**. 2009, **12**, 21.

[155] K. Takeda, K. Isobe, Y. Nakamura, S. Kawaguchi, **Bull. Chem. Soc. Jpn**.1976, 49.

[156] F.A. Cotton, G. Wilkinson, **Advanced Inorganic Chemistry**, 5th ed., Wiley Eastern, New York, USA, 1988; N.N. Greenwood, E. Earnshaw, **Chemistry of Elements**, 1st ed., Pergmon Press, Oxford, 1984; R.C. Mehrotra, R. Bohra, D.F. Gaur, **Metal β-Diketonates and Allied Derivatives**, Academic Press, London, 1978.

[157] I. Harvey, J. M. Arber, R. R. Eady, B. E. Smith, C. D. Garner and S. S. Hasnain, **Biochem. J.** 1990, **266**, 929 ; J. Chen, J. Christiansen, R. C. Tittsworth, B. J. Hales, S. J. George, D. Coucouvanis and S. P. Cramer, **J. Am. Chem. Soc.** 1993, **115**, 5509.

[158] N. Bharti, Shailendra, M. T. G. Garza, D. E. Cruz-Vega, J. C. Garza, K. Saleem, F. Naqvi, M. R. Maurya and A. Azam, **Bioorg. Med. Chem. Lett.** 2002, **12**, 869 ; M. R. Maurya, S. Khurana, A. Azam, W. Zhang and D. Rehder, **Eur. J. Inorg. Chem.** 2003, 1966.

[159] J. M. Arber, E. de Boer, C. D. Garner, S. S. Hasnain and R. Wever, **Biochemistry**, 1989, **28**, 7968.

[160] M. R. Maurya, **Coord. Chem. Rev.** 2003, **237,** 163.

[161] R. Ando, S. Mori, M. Hayashi, T. Yagyu and M. Maeda, **Inorg. Chim. Acta**. 2004, **357**, 1177.

[162] Y. Maeda, N. Kakiuchi, S. Matsumura, T. Nishimura, T. Kawamura and S. Uemura, **J. Org. Chem.** 2002, **67,** 6718 ; Y. Maeda, N. Kakiuchi, S. Matsumura, T. Nishimura, T. Kawamura and S. Uemura, **Tetrahedron Lett.** 2001, **42,** 8877.

[163] M. R. Maurya, A. Kumar, **J. Mol. Catal. A: Chem.**, 2006, **250**, 190.

[164] S. Rayati, N. Torabi, A. Ghaemi, S. Mohebbi, A. Wojtczak and A. Kozakiewicz, **Inorg. Chim. Acta**, 2008, **361,** 1239 ; S. Rayati, N. Sadeghzadeh, H. R. Khavasi, **Inorg. Chem. Comm**. 2007, **10,** 1545.

[165] M. R. Maurya, A. K. Chandrakar and S. Chand, **J. Mol. Catal. A: Chem**. 2007, **274**, 192 ; M. R. Maurya, A. K. Chandrakar and S. Chand, **J. Mol. Catal. A: Chem.** 2007, **270**, 225.

[166] A. A. Nejo, G. A. Kolawole, A. R. Opoku, C. Muller and J. Wolowska. **J. Coord. Chem.** 2009, **62**, 3411.

[167] M. Melchior, K.H. Thompson, J.M. Jong, S.J. Rettig, E. Shuter, V.G. Yuen, Y. Zhou, J.H. McNeill, C. Orvig, **Inorg. Chem**. 1999, **38**, 2288.

[168] C. Gruning, H. Schmidt, D. Rehder, **Inorg. Chem. Commun**. 1999, **2**, 57.

[169] G. Asgedom, A. Sreedhara, J. Kivikoski, E. Kolehmainen, C.P. Rao, **J. Chem. Soc. Dalton. Trans**. 1996, 93.

[170] H. Schmidt, D. Rehder, **Inorg. Chim. Acta.** 1998, **267**, 229.

[171] M. R. Maurya, **Coord. Chem. Rev**. 2003, **237**, 163.

[172] J. M. Lehn In **Supramolecular Chemistry: Concepts and Perespectives**, 1995, VHC, Weinhein.

[173] D. S. Kumar and V. Alexander, **Polyhedron,** 1999, **18** 1561.

[174] D. K. Cabiness and D. W. Margerum, **J. Am. Chem. Soc**. 1969, **91** 6540.

[175] V. D. Campbell, E. J. Parsons and W. T. Permington, **Inorg. Chem.** 1993, **32** 1173.

[176] S. Chandrashekhar , W. L. Waltz , L. Prasad and J. W. Quail, **Can. J. Chem. 75** 1363.

[177] G, Cand and R. Guilard, **J. Micro. Chem**. 1996, **53**, 109.

[178] T. L. Karaseva , A. S. Yovoskii , V. L. Pavlovsky and Z. N. Tsapenkka **Ukr. Biochem. Zh.** 1993, **65,** 95.

[179] J. H. Jeong , M. W. Chun and W. K. Chung, **Korean. J. Med. Chem**. 1996, **6** 47.

[180] V. Comblin , D. Gilsoul , M. Herman , V. Humblet , V. Jaques , M. Masbahi , C. Sauvage and J. F. Desreeux, **Coord. Chem. Rev.** 1999, **185,** 451.

[181] X. Sun, M. Wuest, G. R. Weismen, E. H. Wong, D. P. Reed, C. A. Bosewell, R. Motekaitis, A. E. Martell, M. J. Wekch and C. J. Anderson **J. Med. Chem**. 2002, **45** 469.

[182] G. A. Melson In **Coordination Chemistry of Macrocyclic Compounds**, 1979, Plenum Press, New York.

[183] K. Harada, in " **The Chemistry of carbon-nitrogen double bond**" ed. S. Patai; Interscience, New York, 1970, p255.

[184] J.E. Badwin, F.J. Urban, R.D.G. Cooper and F.L. Jose, **J. Am. Chem. Soc**. 1973, **95**, 2401.

[185] R. J. Morath and G.W. Stacy in " **The Chemistry of carbon-nitrogen double bond**" ed. S. Patai; Interscience, New York, 1970, p327.

[186] H. Bonme and M. Haake, in " **Iminium Salts in Organic Chemistry**" Part-I, ed. H. Bohme and H.G. Viehe, **Vol 9**, ' Advances in Organic Chemistry' ed. E.C. Taylor, Interscience, New York, 1970, p107.

[187] Y. Ogata and A. Kawasaki, **J. Chem. Soc**. 1971, 325.

[188] F. Dardoize, J.L. Moreau and M. Gaudemer, **Bull. Soc. Chim. France.** 1972, 3841 ; 1973, 1668.

[189] A. J. Speziale, C.C. Tung, K.W. Ratts and A. Yaho, **J. Am. Chem. Soc**. 1965, **87**, 3460.

[190] J.P. Anselmc, in " **The Chemistry of carbon-nitrogen double bond**" ed. S. Patai; Interscience, New York, 1970, p299 ; A.P. Marehand, in " **The Chemistry of Double Bonded Fuinctional Groups**" ed. S. Patai, Interscience, New York, 1977, Suppl. A, Part-I, p 612.

[191] P. Baret, H. Buffet and J.L. Pierre, **Bull. Soc. Chim. Fr.** 1972, 825.

[192] F. Duran and L. Ghosez, **Tetrahedron Lett.** 1970, 245.

[193] H.W. Moore, L. Harnendez and A. Singh, **J. Am. Chem. Soc**. 1976, **98**, 3728.

[194] E. Schmitz, **Adv. Heterocycl. Chem.** 1963, **2**, 104 ; P.M. Henry and G.L. Lange, in " **The Chemistry of Double Bonded Functional Groups** " ed. S. Patai, Interscience, New York, 1977, Suppl. A, Part-II, p 1067.

[195] S.E. Dinizo and D.S. Watt, **J. Am. Chem. Soc**. 1975, **97**, 6900.

[196] A. Catoo, F. Corbani, B. Rindone and C. Seolastico, **Tetrahedron Lett**. 1973, 2723.

[197] R.N. Butler, F.L. Scott and T.A.F. O'Mahony, **Chem. Rev**. 1973, **73**, 93.

[198] K.N. Mehrotra and B.P. Giri, **Synthesis**, 1977, 489.

[199] R.L. Augustine, in " **Catalytic Hydrogenation**", Dekker, New York, 1965,81.

[200] K. Horoda and K. Matsumoto, **Bull. Chem. Soc**, Jpn. 1971, **44**, 1068. [43] E. Frainnet, P. Braquet and F. Moulines, **Compt. Rend**. 1971, **272**, 1435.

[201] I. Ojima, T. Kogure and Y. Nagai, **Tetrahedron Lett**. 1973, 2475.

[202] N. Raman, S. Johnson Raja, A. Sakthivel, **J. Coord. Chem**. 2009, **62**, 691.

[203] A. D. Garnovskii, I. S. Vasil'chenko, D. A. Garnovskii, A. S. Burlov and A. I. Uraev, **Russian J. Gen. Chem**. 2009, **79**, 2776.

[204] K.C. Gupta and A.K. Sutar, **Coord. Chem. Rev**. 2008, **252**, 1240.

[205] F. Faridbod , M. R. Ganjali, R. Dinarvand , P. Norouzi and S. Riahi, **Sensors**. 2008, **8**, 1645.

[206] A. A. Soliman and W. Linert, **Monatshefte fur chemie**. 2007, **138**, 175.

[207] W. R. Paryzek, V. Patroniak and J. Lisowski, **Coord. Chem. Rev**. 2005, **249**, 2156.

[208] S. Brooker, **Coord. Chem. Rev**. 2001, **222**, 33.

[209] C. Glidewell, "Metal acetylacetonate complexes: preparation and characterization" In J. Woolins Ed. Inorganic Experiments, 2nd Edition, Wiley-VCH, Weinheim, 2003.

[210] C. K. Lai , Y. F. Leu. **Liq. Cryst.** 1998, **25**, 689.

[211] K.C. Gupta, H.K. Abdulkadir, S. Chad, **Journal Applied Polymer Sci.** 2003, **90**, 1398.

[212] P.R. Athapan and G. Rajagopal, **Polyhedron**, 1990, **15**, 527.

[213] K. Sakata, M. Hashimoto, T. Hamada and S. Matsuno, **Polyhedron**, 1996, **15**, 967.

[214] S.M. Annigeri, A.D. Naik, U.B. Gangadharnath, V.K. Revankar and V.B. Mahale, **Transition Met. Chem**., 2002, **27**, 316.

[215] K. Nakamoto, **Infrared Spectra of Inorganic and Coordination Compounds,** Wiley Interscience, Newyork, 1970.

[216] Tumer M, Koksal H and Serin S. **Synth. React. Inorg. Met-Org. Chem.** 1997, **27**, 775.

[217] N. Raman, S. Ravichandran and C. Thangaraja. **J. Chem. Sci.** 2004, **116**, 215.

[218] M. M. Abd-Elzahar, **J. Chin. Chem. Soc.** 2001, **48(2),** 153.

[219] M.X. Li, G.Y. Xie, Y.D. Gu, J. Chen and P.J. Zheng. **Polyhedron.** 1995, **14**, 1235.

[220] J.B. Vincent, K. Folting, J.C. Huffman and G. Christou, **Inorg. Chem.** 1986, **25,** 996; S.T. Lutta and S.M. Kagwanja, **Transit. Met. Chem**. 2000, **25**, 415; A. Panja, N. Shaikh, S. Gupta, R.J. Butcher and P. Banerjee, **Eur. J. Inorg. Chem**. 2003, 1540.

[221] S.N. Rao, K.N. Munshi, N.N. Rao, M.M. Bhadbhade and E. Suresh, **Polyhedron,** 1999, **18**, 2491.

[222] N. J. Long, D. G. Parker, P. R. Speyer, A. J. P. White and D. J. Williams. **J. Chem. Soc. , Dalton Trans.** 2002, 2142.

[223] A. Altomare, G. Cascarano, C. Giacovazzo and A. Gualaradi. **J. Appl. Cryst.** 1993, **26,** 343.

[224] G. M. Sheldrick, SHELXL 97 Program for the Solution of Crystal Structure, University of Göttingen, Germany, **1997**.

[225] A. L. Spek, **J. Appl. Cryst.** 2003, **36**, 7.

[226] G. M. Sheldrick, SHELXS 97, Program for the Solution of Crystal Structure, University of Göttingen, Germany, **1997**.

[227] L. J. Farrugia. WinGX - A Windows Program for Crystal Structure Analysis. **J. Appl. Crystallogr.** 1999, **32**, 837.

[228] H. Takezoe and Y. Takanishi. **Japanese Journal of Applied Physics.**, 2006, **45**, 597.

[229] J. Thisayukta, Y. Nakayama, S. Kawauchi, H. Takezoe and J. Watanabe. **J. Am. Chem. Soc.** 2000, **122**, 7441.

[230] G. Dantlgraber, A. Eremin, S. Diele, H. Hauser, H. Kresse, G. Pelzl and C. Tschierske. **Angew. Chem., Int. Ed.** 2002, **41**, 2408.

[231] K. Y. Lau, K. Mayr and K. K. Cheung, **Inorg. Chim.Acta,** 1999, **285**, 525.

[232] P. P. Dholakiya and M. N. Patel, **Synth. React. Inorg. Met-Org. Chem.** 2004, **34**, 553.

[233] Z. H. Chohan, M. Arif, A. Aktar and C. T. Supuran, **Bioinorganic Chemistry and Application**, 2006, 1.

[234] Z. H. Chohan. **Applied Organometallic Chem.** 2002, **16**, 17.

[235] F. R. Perez, L. Basaez , J. Belmar and P. Vanysek. **J. Chil. Chem. Soc.** 2005, **50**, 575.

[236] S. A. Sallam. **Trans. Met. Chem.** 2006, **31**, 46.

[237] K. H. Mostaga, M. H. Repat and A. A. Mohamed. **Monatsch. Chem.** 1991, **122**, 829.

[238] W.F. Brown In: Condon and Odishaw (Ed) Magnetic Materials, Chapter 8 in the Handbook of Chemistry and Physics, McGraw-Hill (1958)

[239] Gordon A. Bain, John F. Berry "Diamagnetic Corrections and Pascal's Constants" **Journal of Chemical Education**, 2008, **85**, 532.

[240] M. R. Truter, **Chem. Brit.** 1971, **7**, 203.

[241] A. Bajpai and S. Rai. **J. App. Pol. Sc.**, 1998, **69**, 751.

[242] M. J. Frisch, G.W. Trucks, H.B. Schlegel, G.E. Scuseria, M.A. Robb, J.R. Cheeseman, J.A. Montgomery Jr,T. Vreven, K.N. Kudin, J.C. Burant, J.M.

Millam, S.S. Iyengar, J. Tomasi, V. Barone, B. Mennucci, M. Cossi, G. Scalmani, N. Rega, G.A. Petersson, H. Nakatsuji, M. Hada, M. Ehara, K. Toyota, R. Fukuda, J. Hasegawa, M. Ishida, T. Nakajima, Y. Honda, O. Kitao, H. Nakai, M. Klene, X. Li, J.E. Knox, H.P. Hratchian, J.B. Cross, C. Adamo, J. Jaramillo, R. Gomperts, R.E. Stratmann, O. Yazyev, A.J. Austin, R. Cammi, C. Pomelli, J.W. Ochterski, P.Y. Ayala, K. Morokuma, G.A. Voth, P. Salvador, J.J. Dannenberg, V.G. Zakrzewski, S. Dapprich, A.D. Daniels, M.C. Strain, O. Farkas, D.K. Malick, A.D. Rabuck, K. Raghavachari, J.B. Foresman, J.V. Ortiz, Q. CuiA, G. Baboul, S. Clifford, J. Cioslowski, B.B. Stefanov, G. Liu, A. Liashenko, P. Piskorz, I. Komaromi, R.L. Martin, D.J. Fox, T. Keith, M.A. Al-Laham, C.Y. Peng, A. Nanayakkara, M. Challacombe, P.M.W. Gill, B. Johnson, W. Chen, M.W. Wong, C. Gonzalez, J.A. Pople, **Gaussian 03**, Revision D.01; Gaussian: Wallingford, CT, 2004.

[243] T. D. Klots. **Spectrochim. Acta, Part A.** 1998, **54**, 1481.

[244] N. Sundaraganesan, B. W. Joshua, C. Meghanathan and S. Sebastian. **Ind. J. Chem.** 2008, **47**, 821.

[245] D. Kalita, R. C. Deka and N. S. Islam. **Inorg. Chem.Comm.** 2007, **10**, 45.

[246] I. Bytheway and M. W. Wong. **Chem. Phys. Lett.** 1998, **282**, 219.

PUBLICATIONS

1. C R Bhattacharjee, **P Goswami**, S Neogi and S Dhibar. *Transition metal complexes of a neutral $[N_2O_2]$ donor Schiff base derived from furfuraldehyde and hydrazine hydrate : Synthesis, characterization and redox behaviour.* **Assam Univ. J. Sc. Tech.** 2010, **5**, 81.
2. C R Bhattacharjee, **P Goswami** and P Mondal. *Synthesis, structural characterization and DFT studies of new mixed ligand iron(III) Schiff base complexes.* **J. Coord. Chem.** 2010, Accepted.
3. C R Bhattacharjee, **P Goswami** and M Sengupta. *Mono and binuclear iron(III) and oxovanadium(IV) complexes of [ONO] donor tridentate Schiff base ligands – synthesis, electrochemical and antimicrobial studies.* **J. Coord. Chem.** (Communicated).
4. C R Bhattacharjee and **P Goswami**. *Synthesis, characterization, electrochemical and magnetic studies of 12-membered tetraimine macrocyclic Schiff base ligands and their iron(III) and oxovanadium(IV) complexes.* **J. Chem. Sci.** (communicated)
5. C R Bhattacharjee, **P Goswami,** H A R Pramanik and P. Mondal. *Reactivity of tris (acetylacetonato) iron(III), $[Fe(acac)_3]$ as an access to new mixed-ligand tridentate [ONO]- donor Schiff base Complexes.* **Inorg. Chem. Commun.** (communicated)
6. C R Bhattacharjee, **P Goswami** and P Mondal. *Synthesis, spectroscopic characterization and dft studies of mixed ligand coordination complexes of iron (III) with a tetradentate [NNOO] donor Schiff base ligand incorporating aquo, fluoro, thiocyanato and azido group.* **Procedings on International Conference on Coordination and Organic Chemistry**, Bharatiar University, Coimbatore, India, 18-20 March, 2009.

7. C R Bhattacharjee, **P Goswami**, M Sengupta and B Chakraborty. *Synthesis and antimicrobial activity of a new binuclear vanadyl complex of a tridentate [ONO] donor Schiff base.* **Proceedings on National Conference on Recent Progresses in Physical Sciences**, Karimganj College, Karimganj, India, 20-21 December, 2008.

APPENDIX 1

Infrared spectra of the compounds

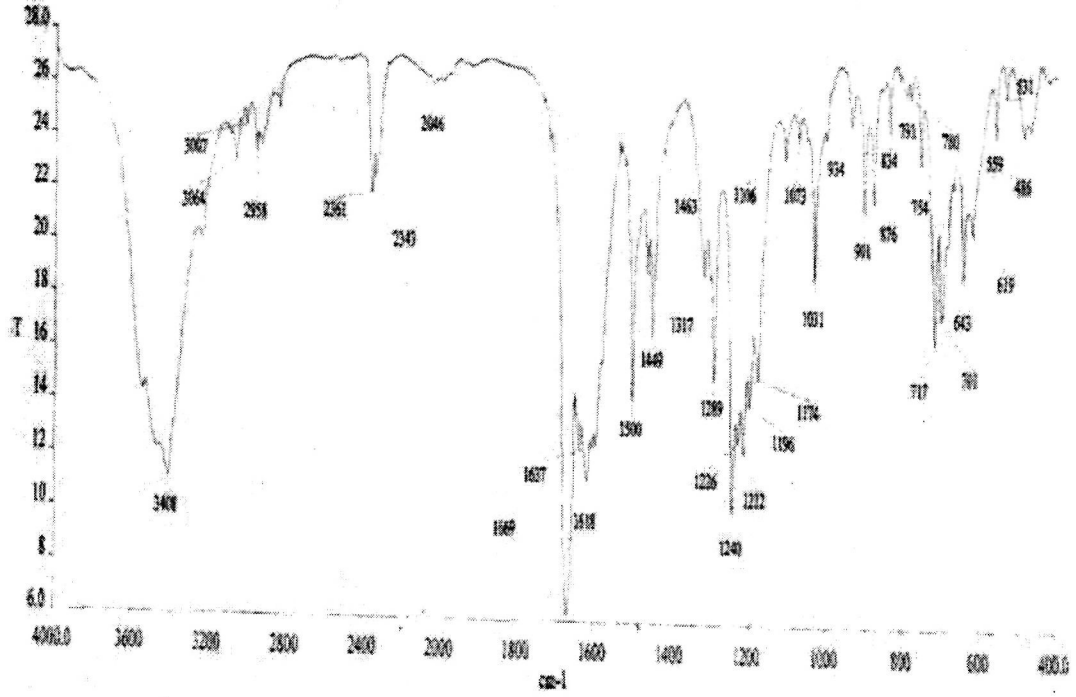

Infrared spectra of the Schiff base L_1

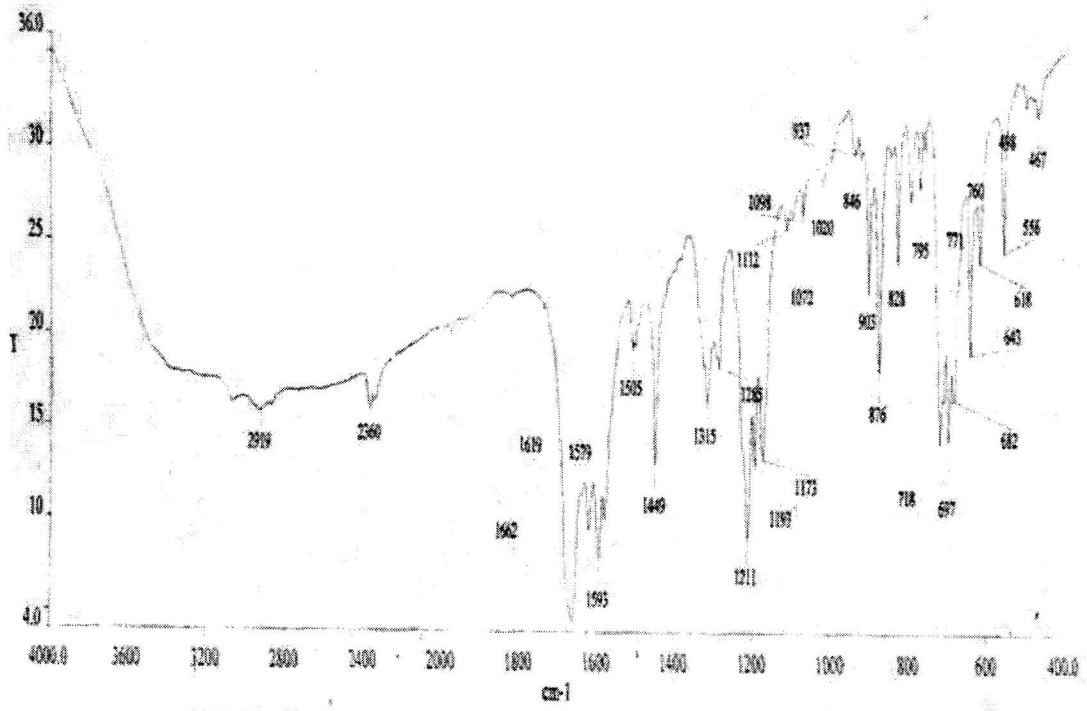

Infrared spectra of the Schiff base L_2

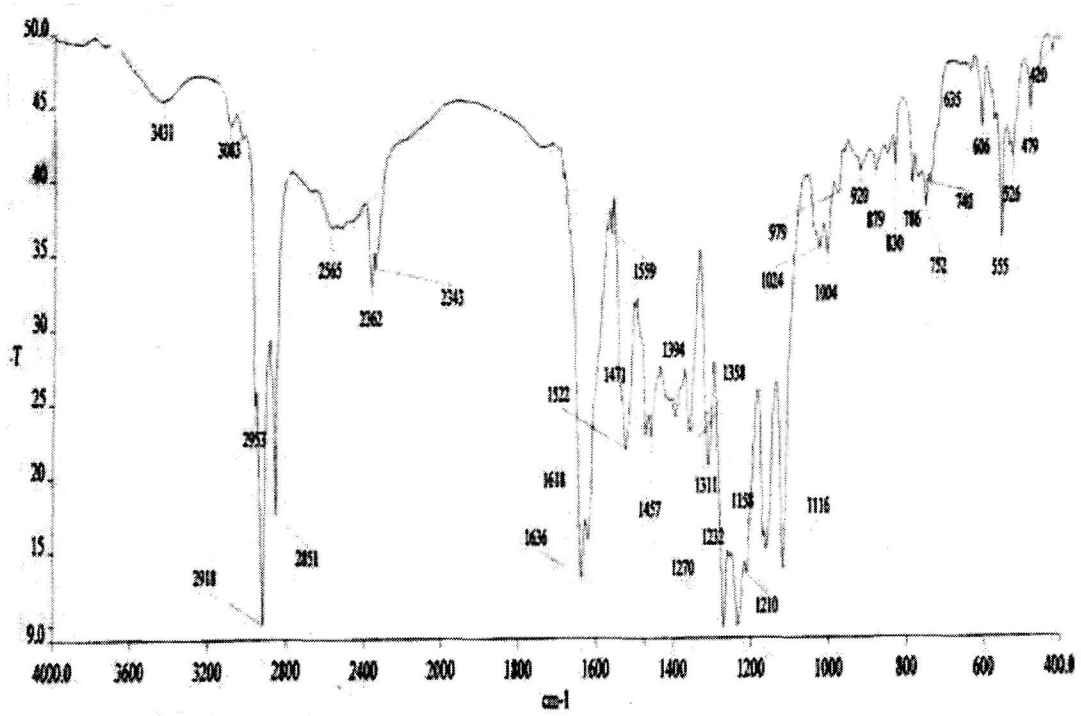

Infrared spectra of the Schiff base L_3

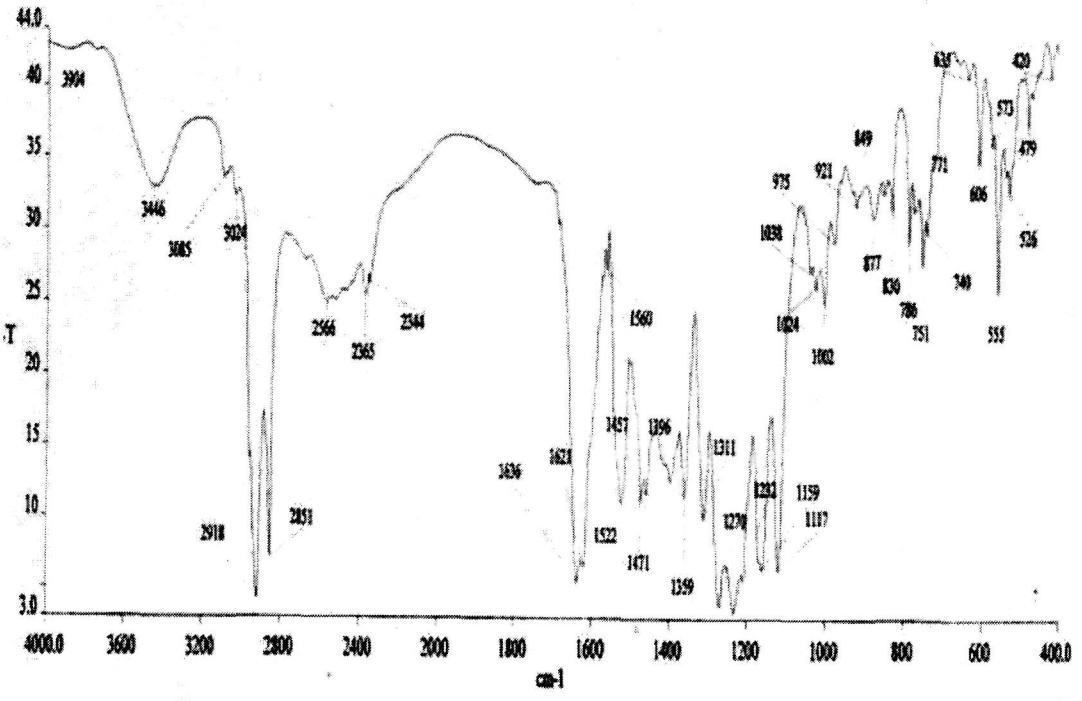

Infrared spectra of the Schiff base L_4

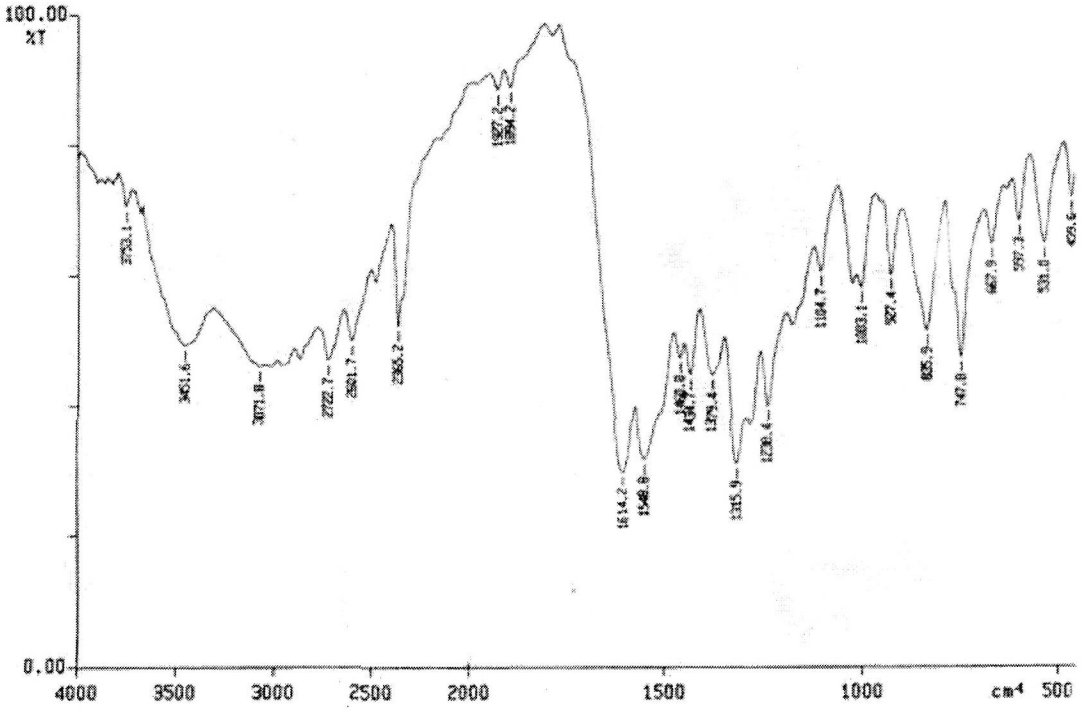

Infrared spectra of the Schiff base L_5

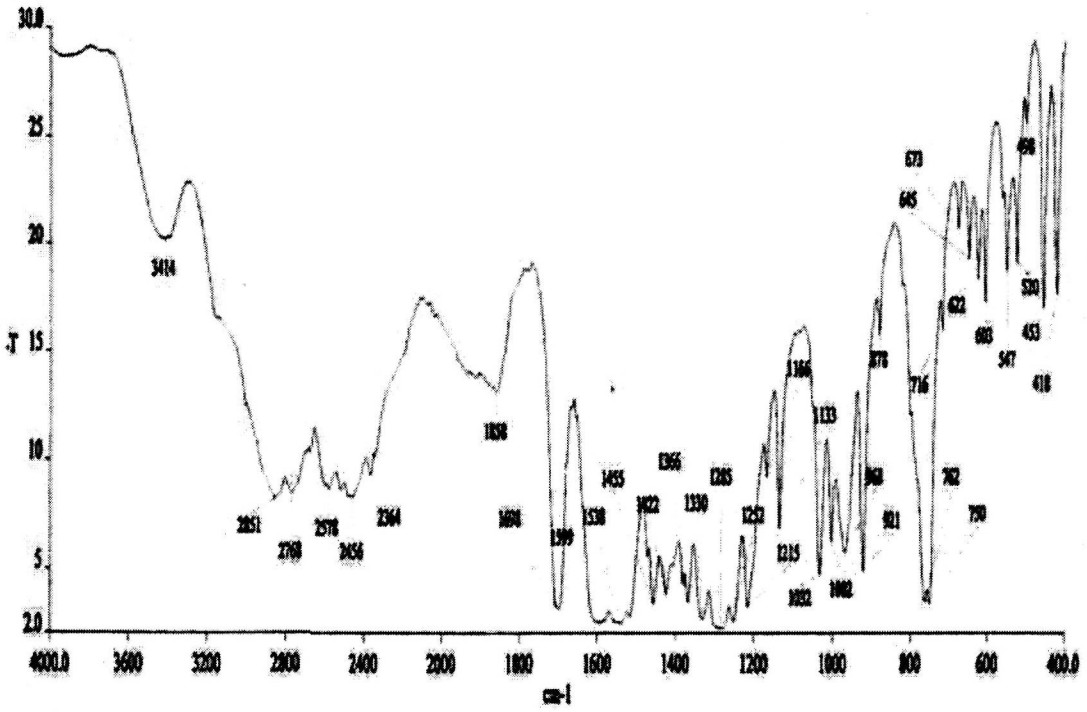

Infrared spectra of the Schiff base L_6

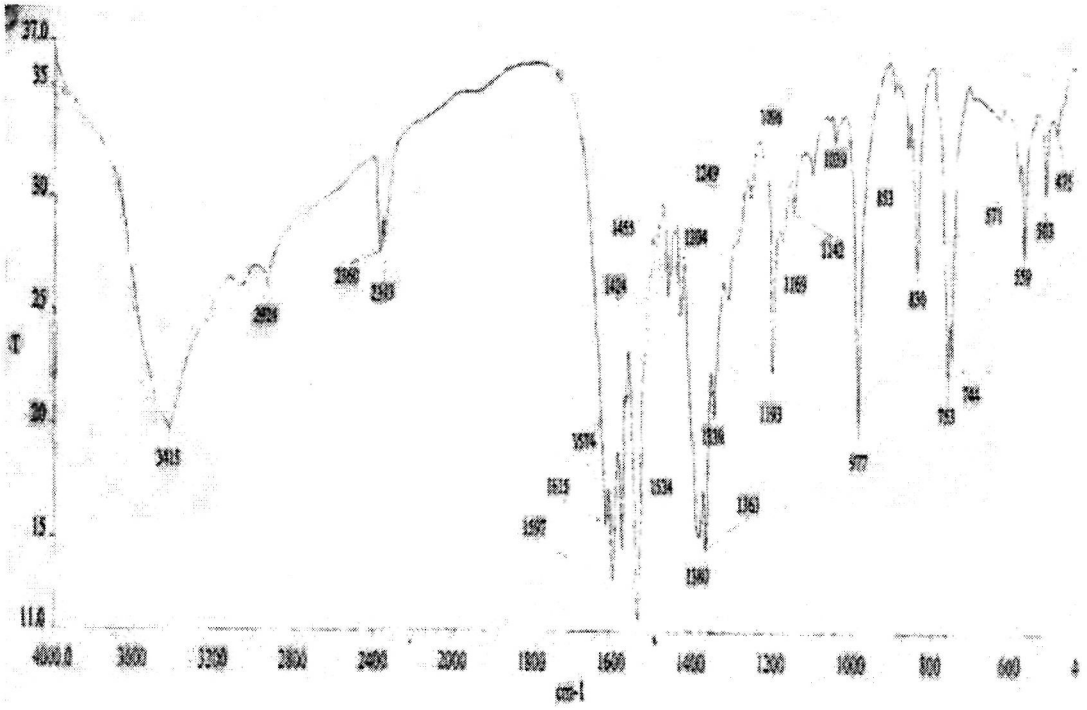

Infrared spectra of the Schiff base L_7

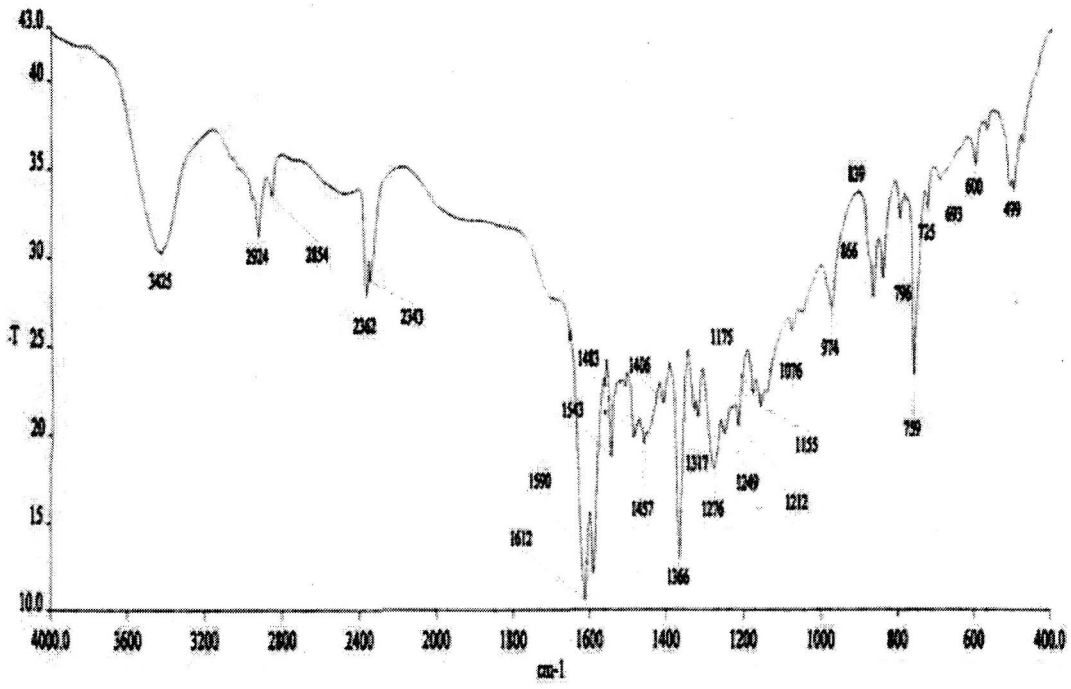

Infrared spectra of the Schiff base L_8

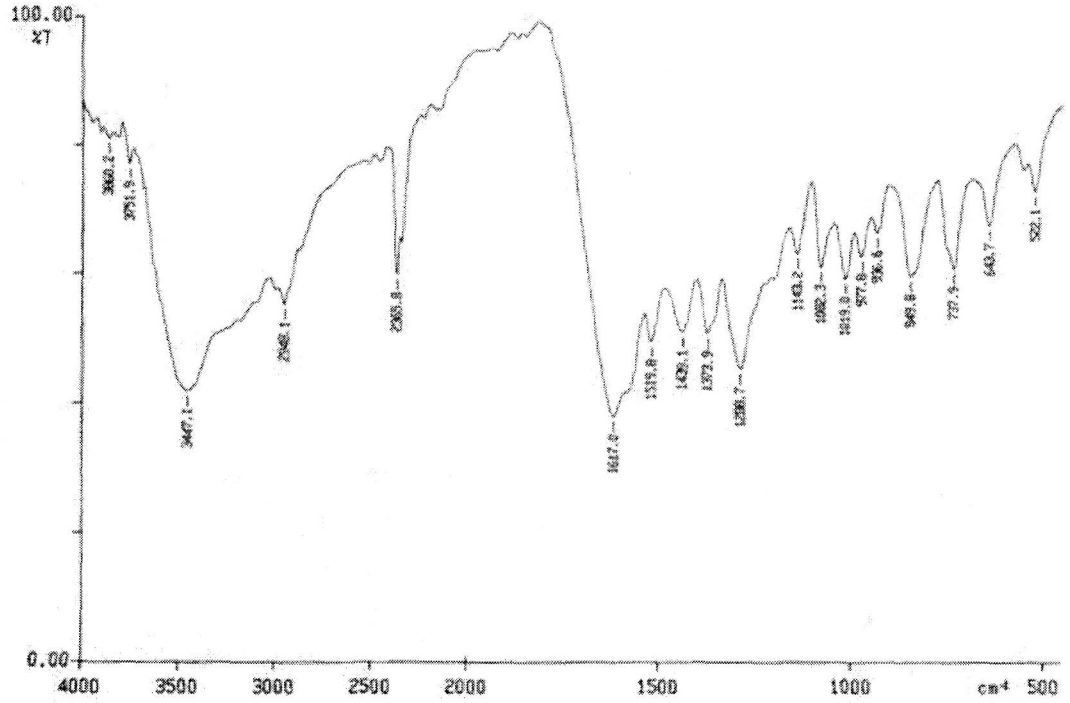

Infrared spectra of the Schiff base L_9

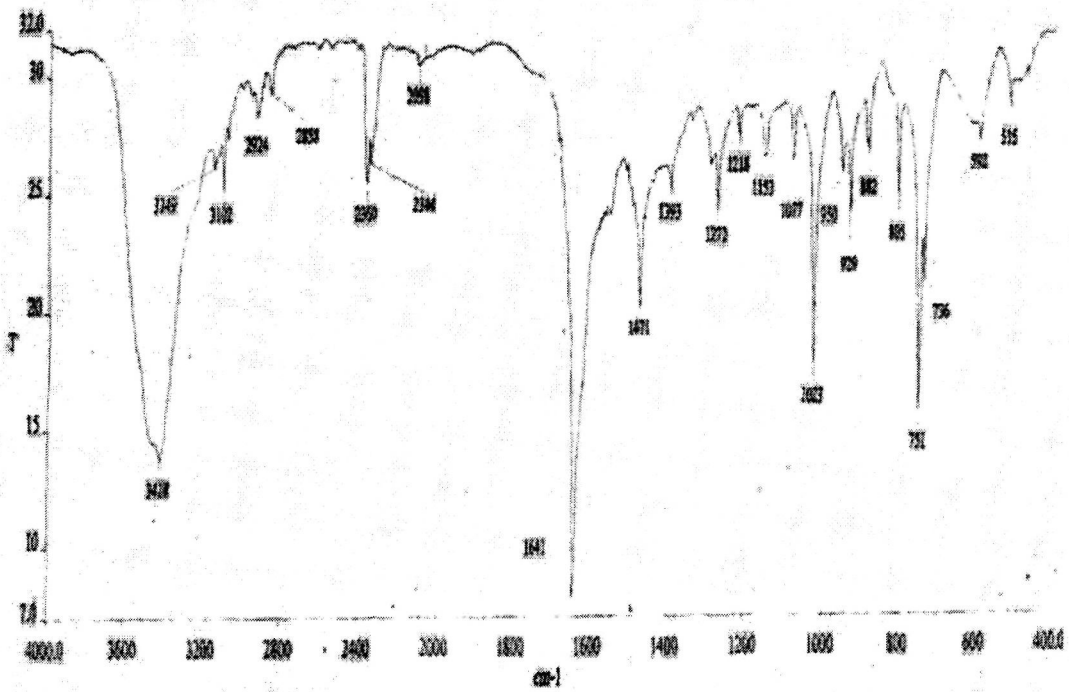

Infrared spectra of the Schiff base L_{10}

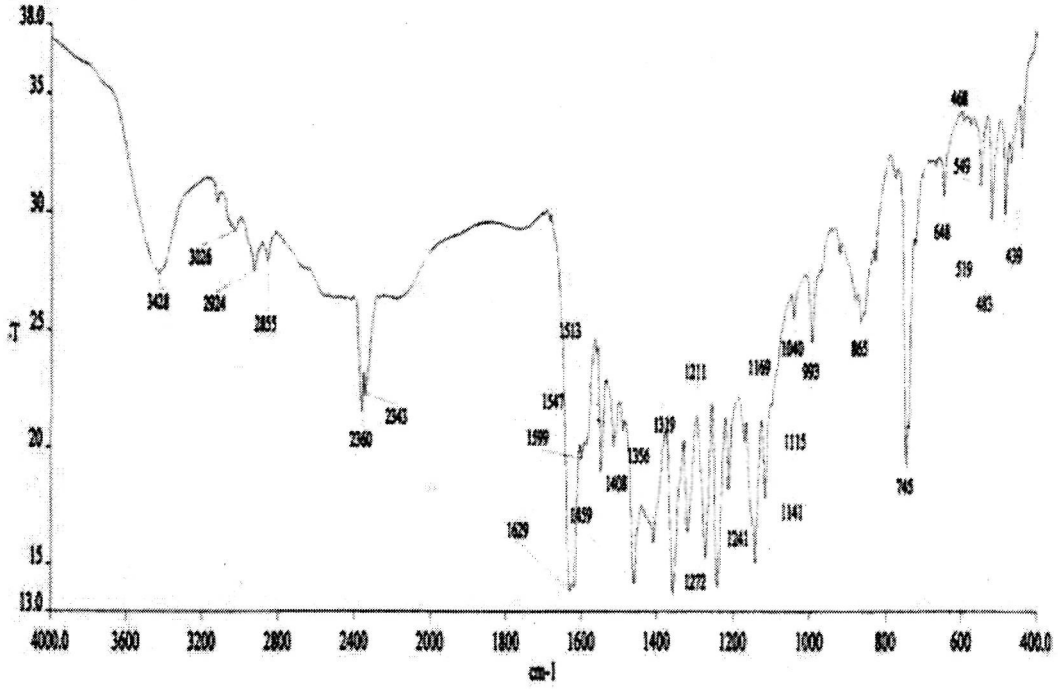

Infrared spectra of the Schiff base L_{11}

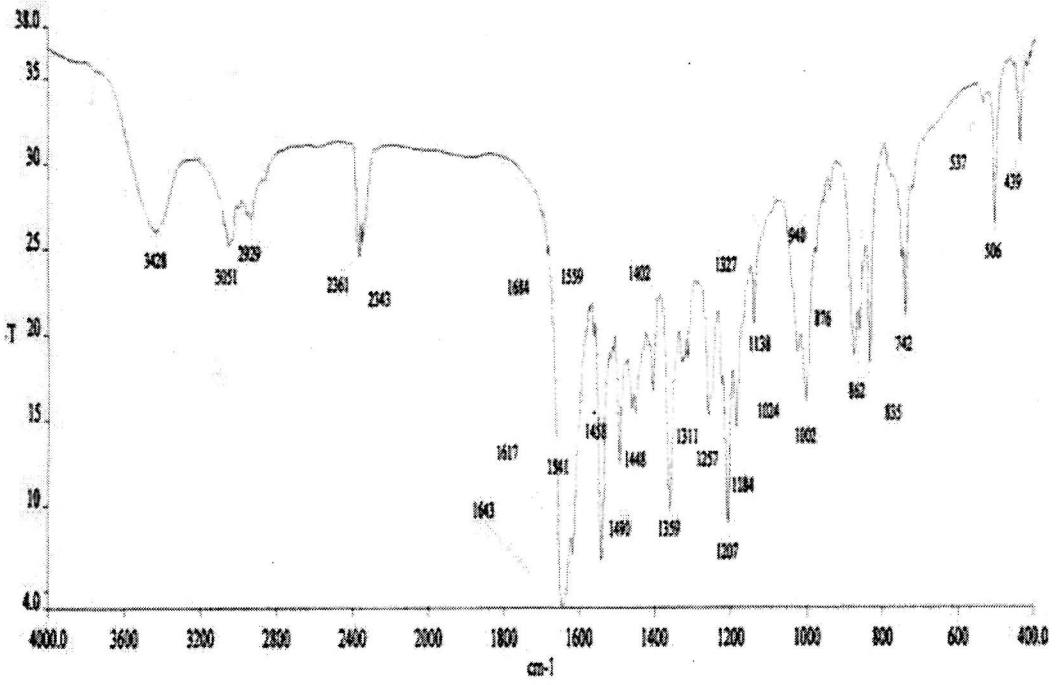

Infrared spectra of the Schiff base L_{12}

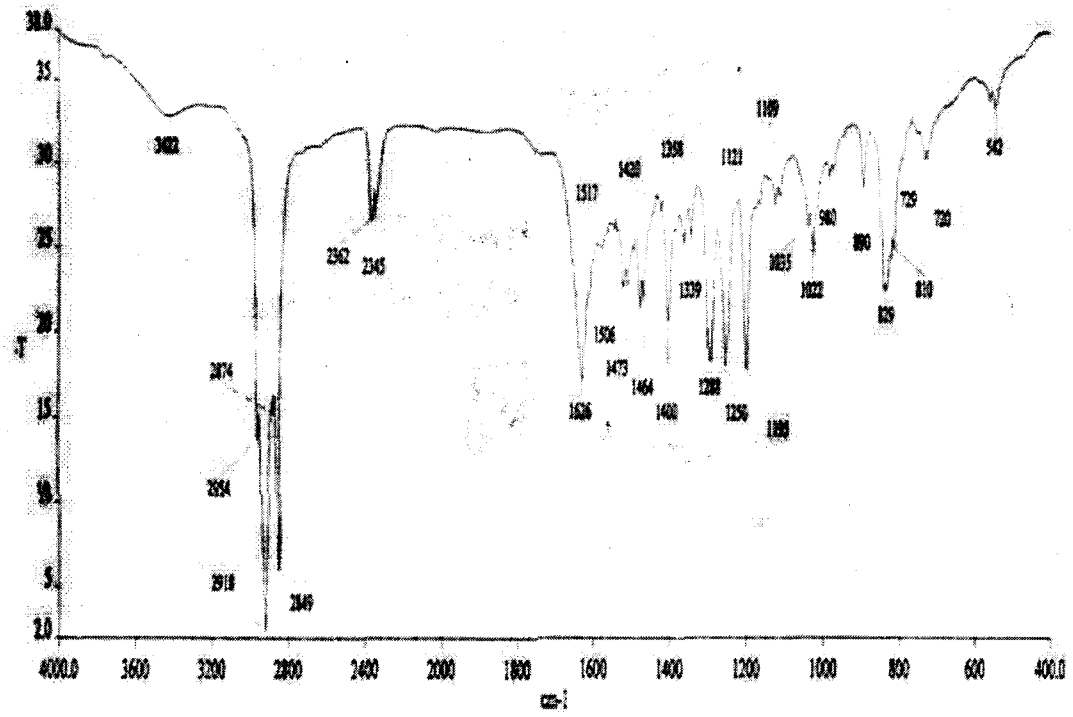

Infrared spectra of the Schiff base L_{13}

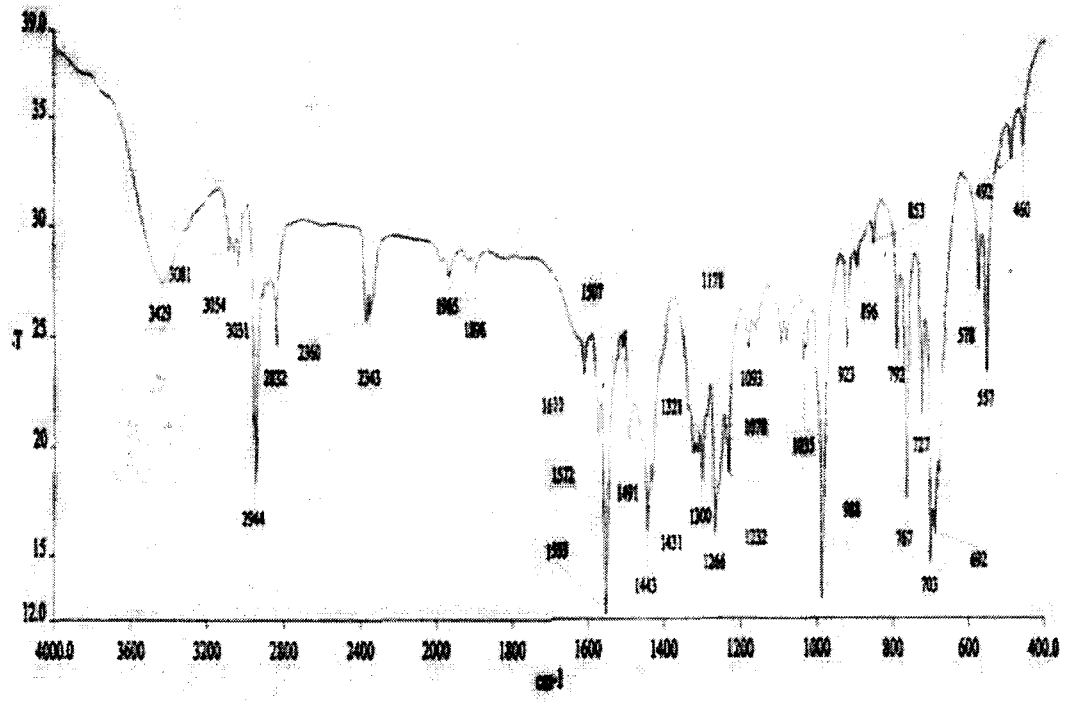

Infrared spectra of the Schiff base L_{14}

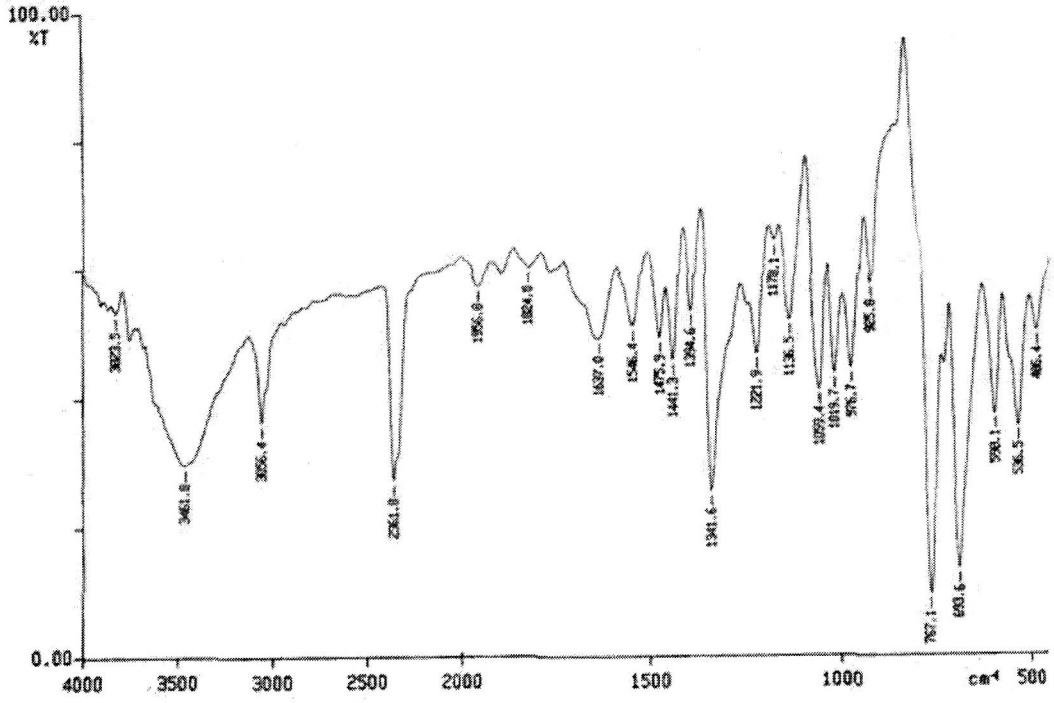

Infrared spectra of the Schiff base L_{15}

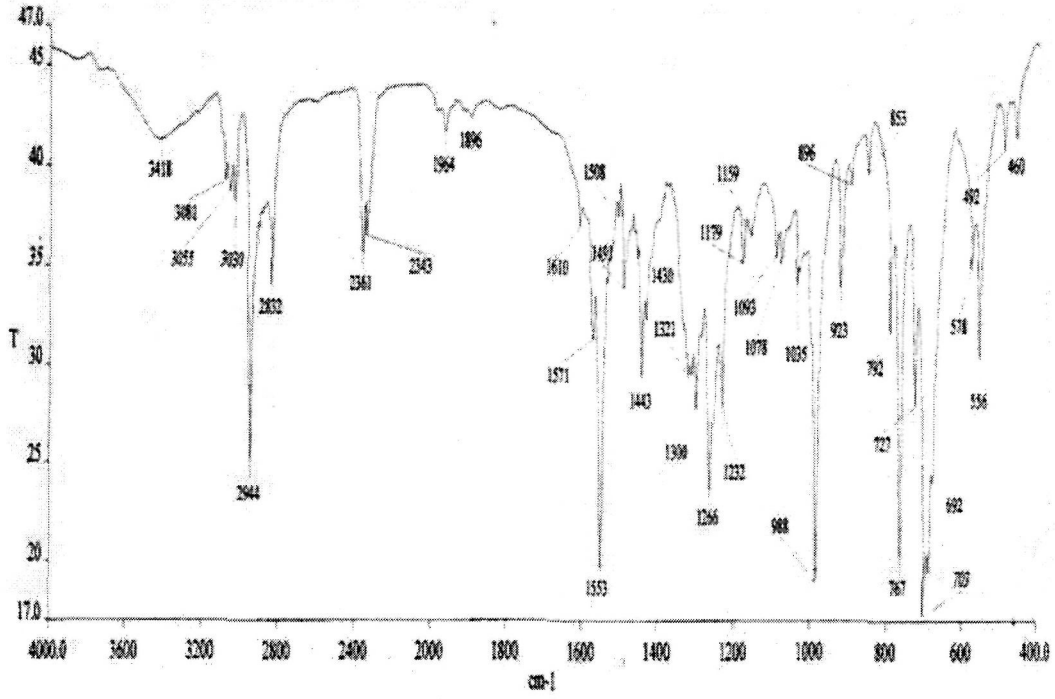

Infrared spectra of the Schiff base L_{16}

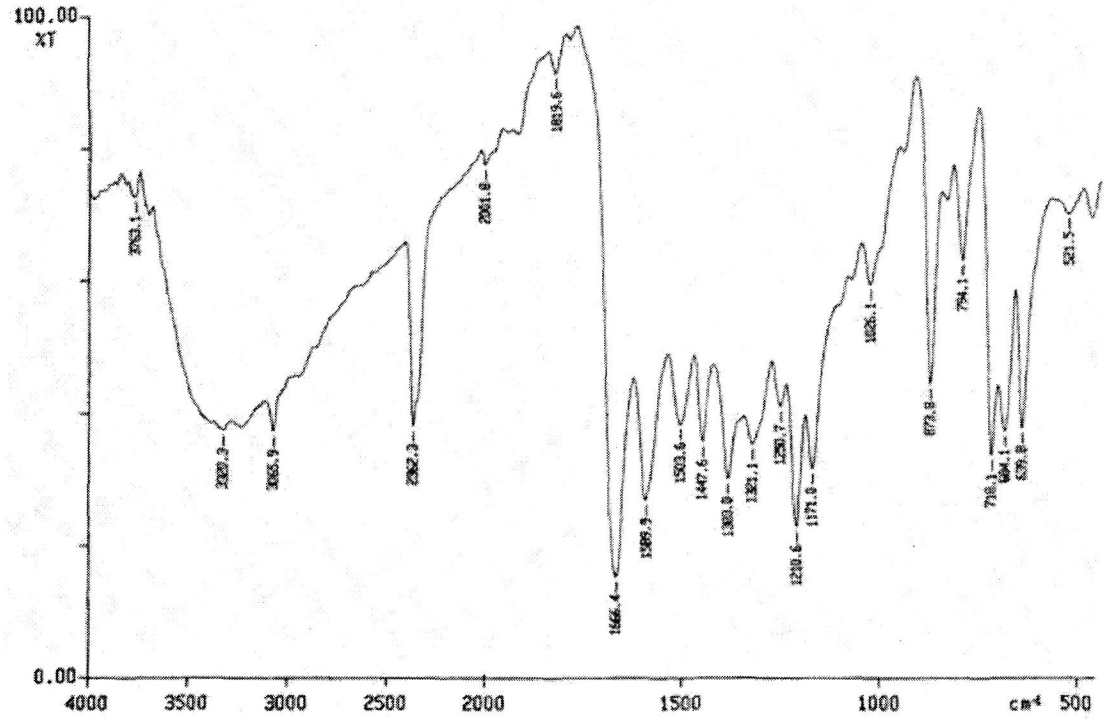

Infrared spectra of the complex **$[Fe(L_1)_2(NO_3)_2]NO_3$ (1)**

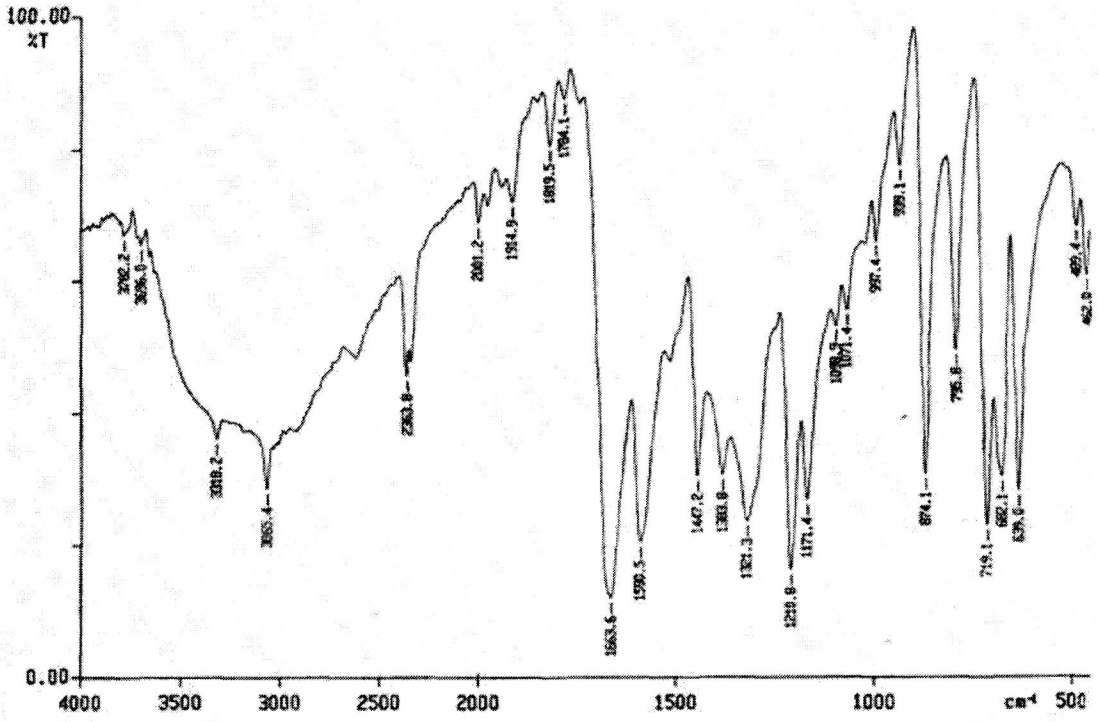

Infrared spectra of the complex **$[Fe(L_2)_2(NO_3)_2]NO_3$ (2)**

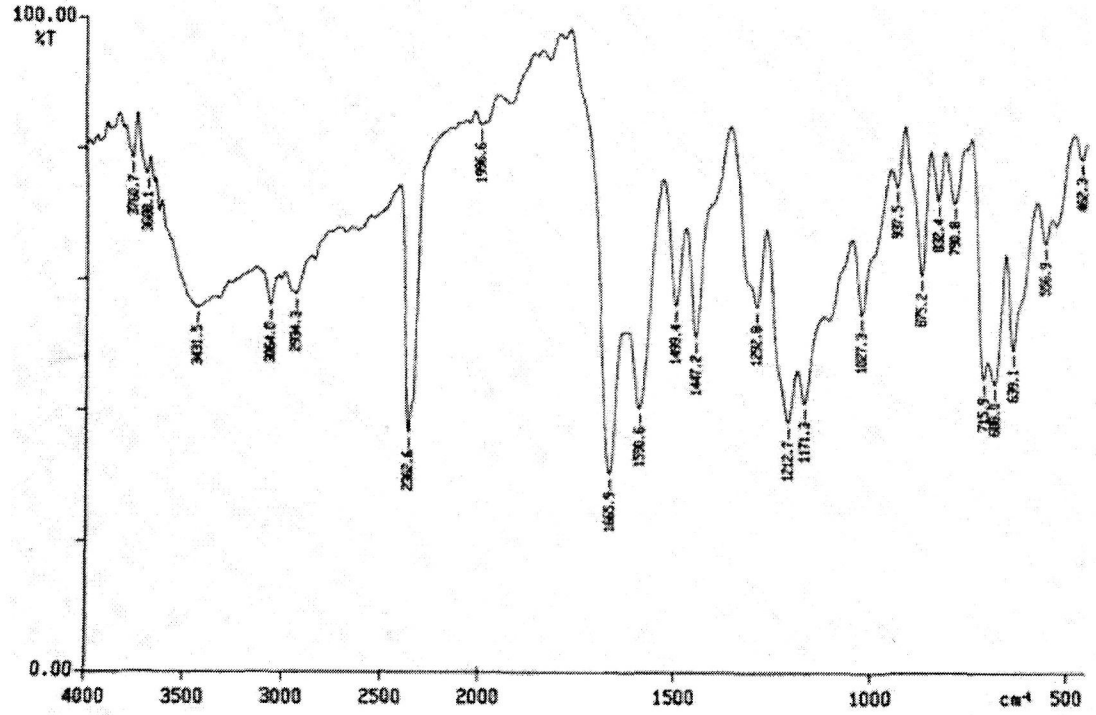

Infrared spectra of the complex $[VO(L_1)_2]^{2+}SO_4^{2-}.H_2O$ (3)

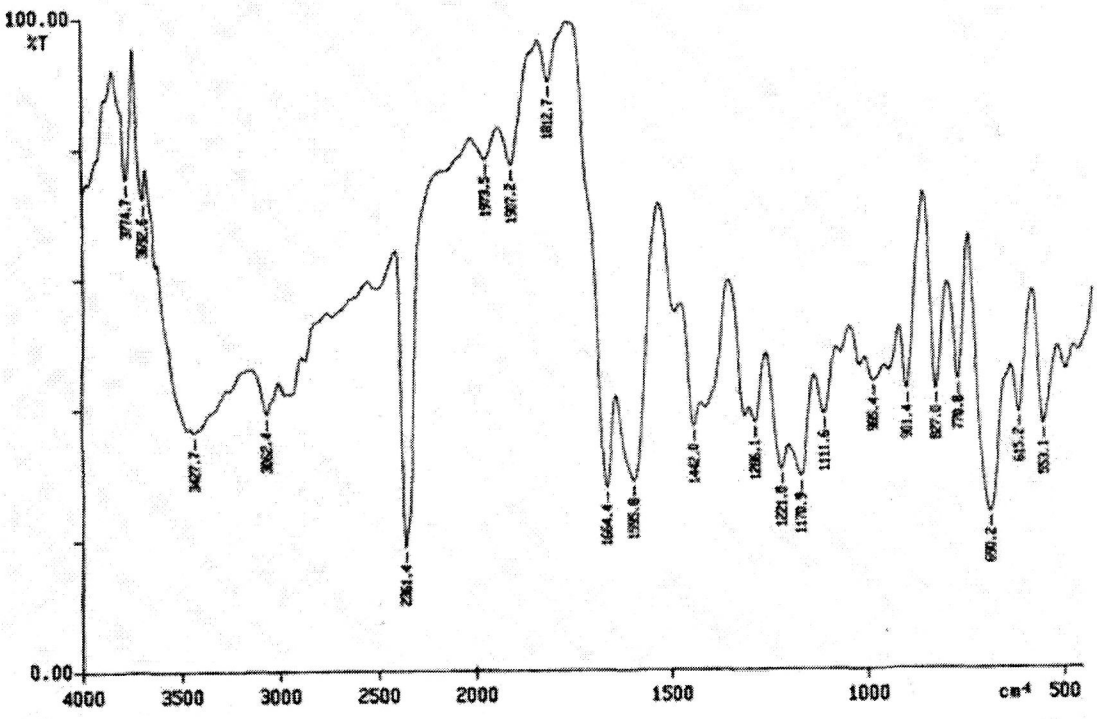

Infrared spectra of the complex $[VO(L_2)_2]^{2+}SO_4^{2-}.H_2O$ (4)

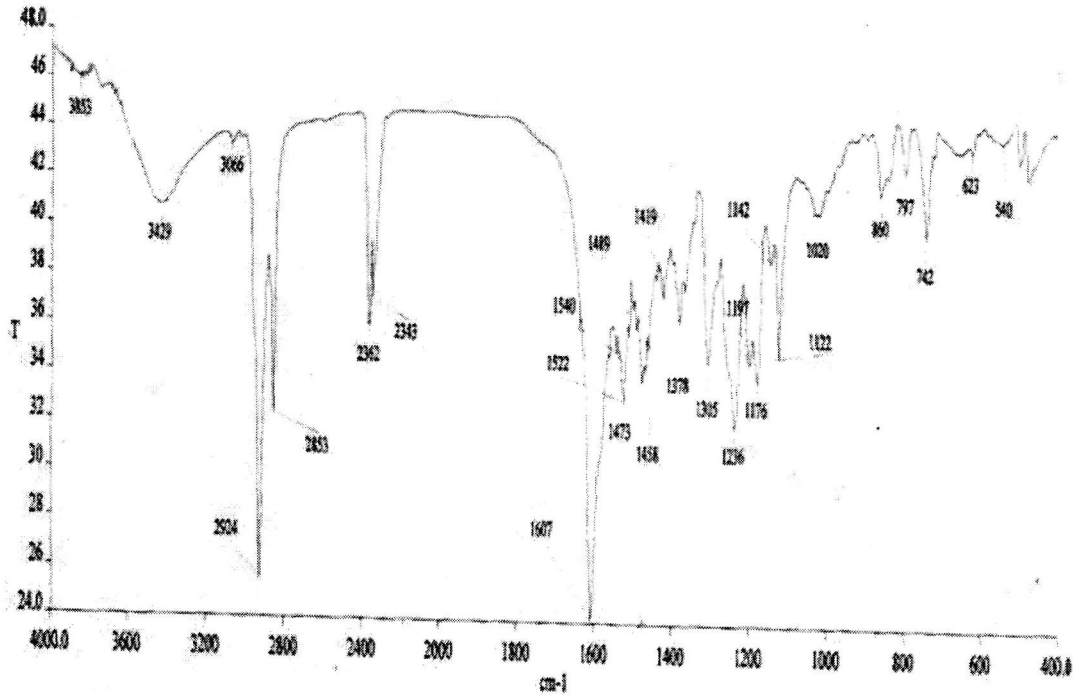

Infrared spectra of the complex $[Fe(L_3)Cl]_2$ **(5)**

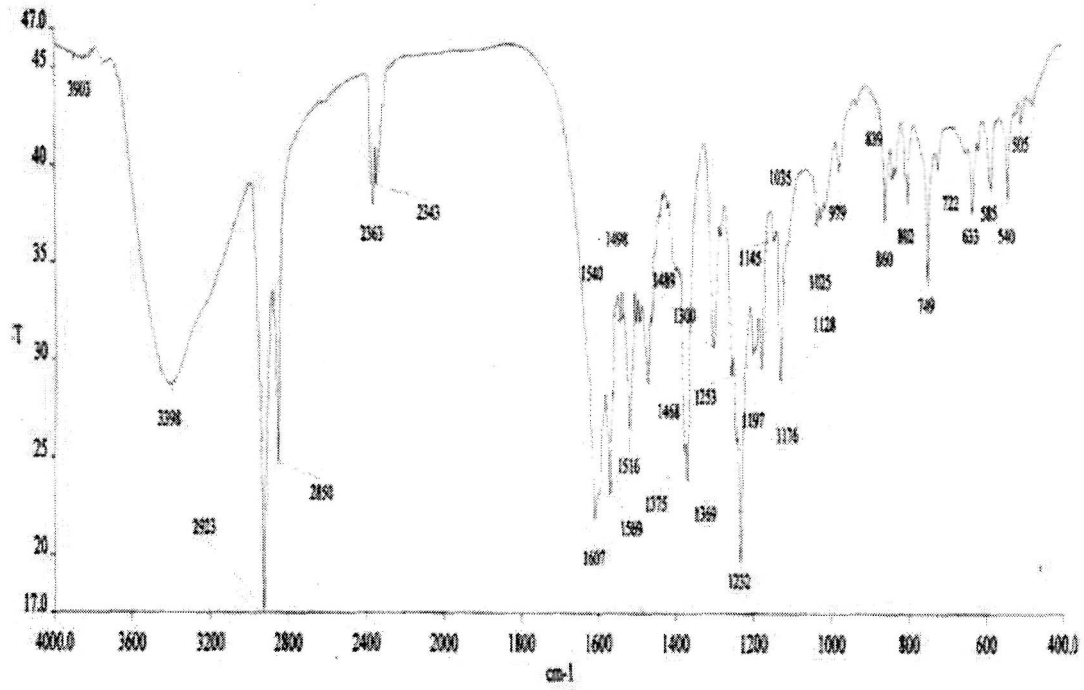

Infrared spectra of the complex $[Fe(L_4)Cl]_2$ **(6)**

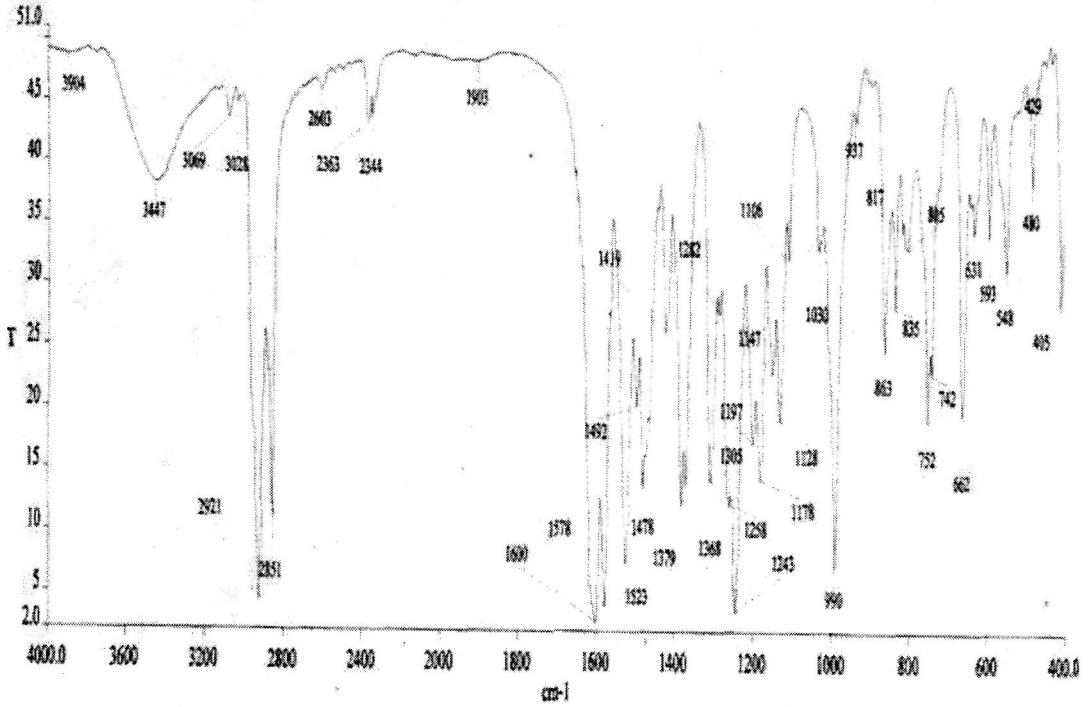

Infrared spectra of the complex **[VO(L$_3$)]$_2$ (7)**

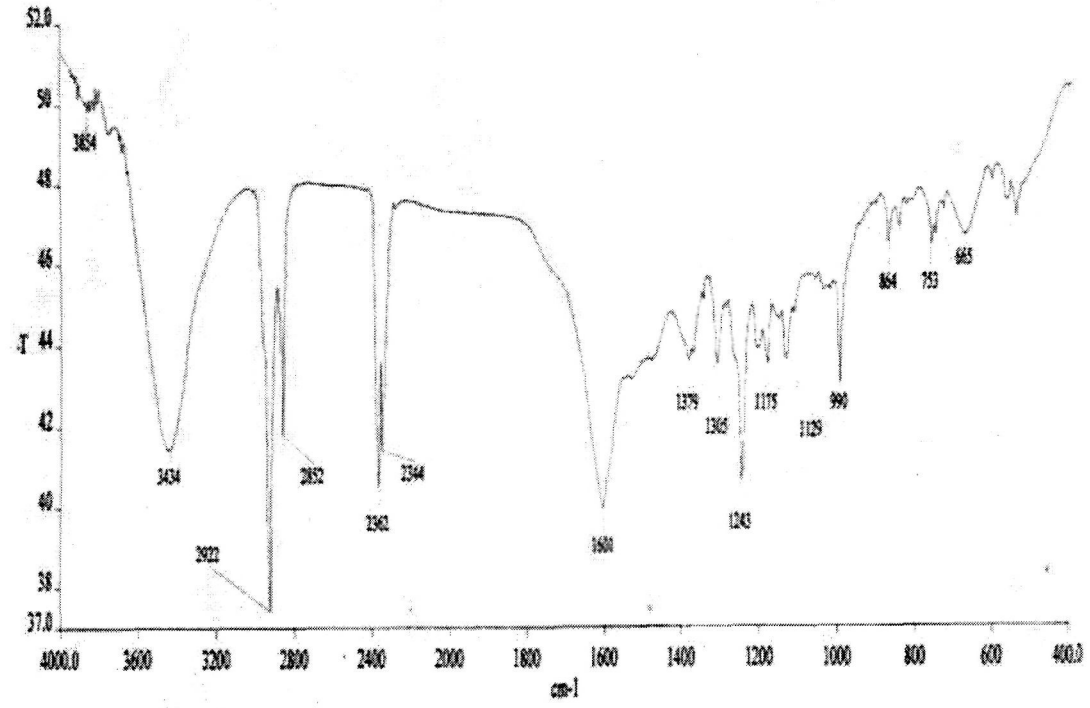

Infrared spectra of the complex **[VO(L$_4$)]$_2$ (8)**

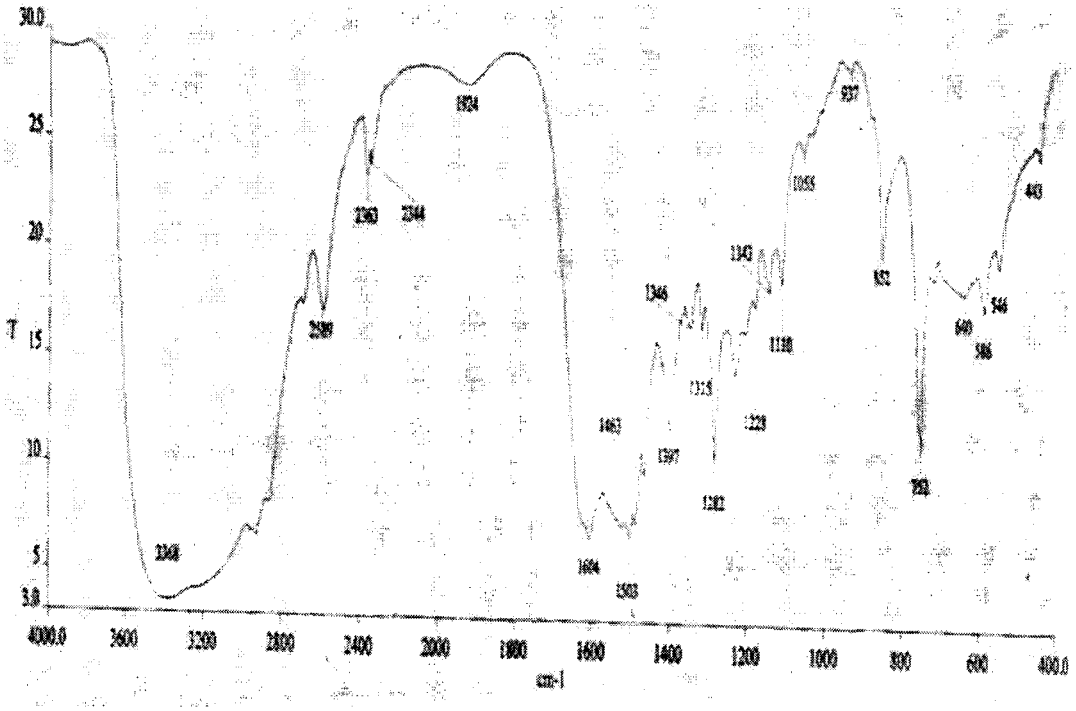

Infrared spectra of the complex $[Fe(L_5)Cl]_2$ **(9)**

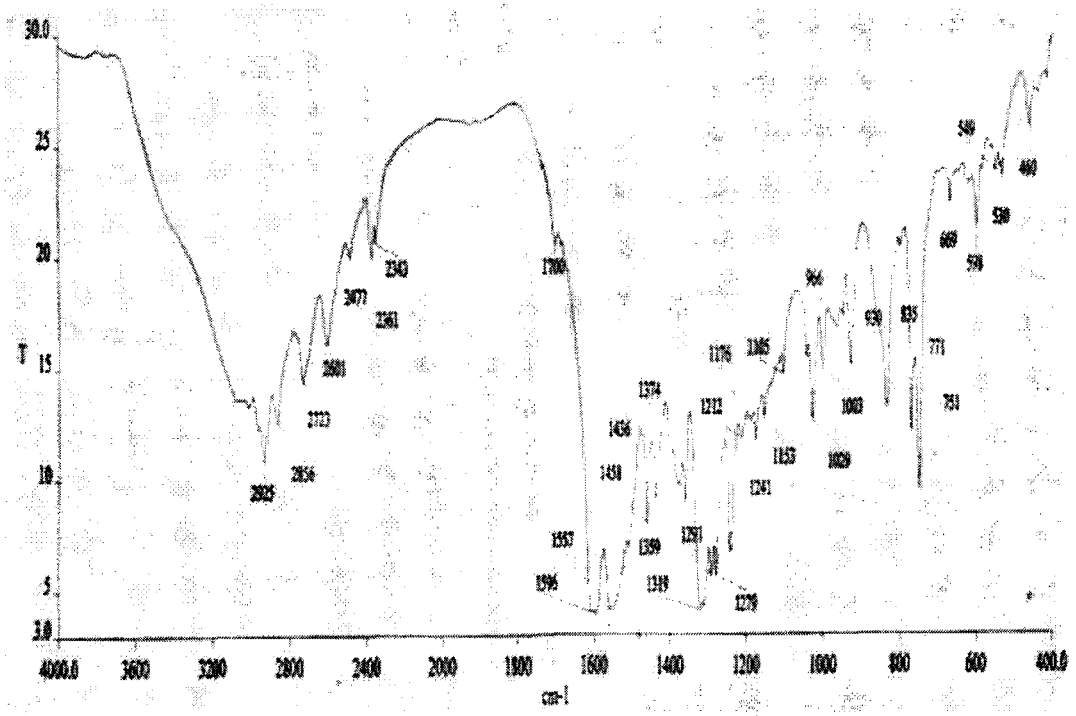

Infrared spectra of the complex $[VO(L_5)]_2.H_2O$ **(10)**

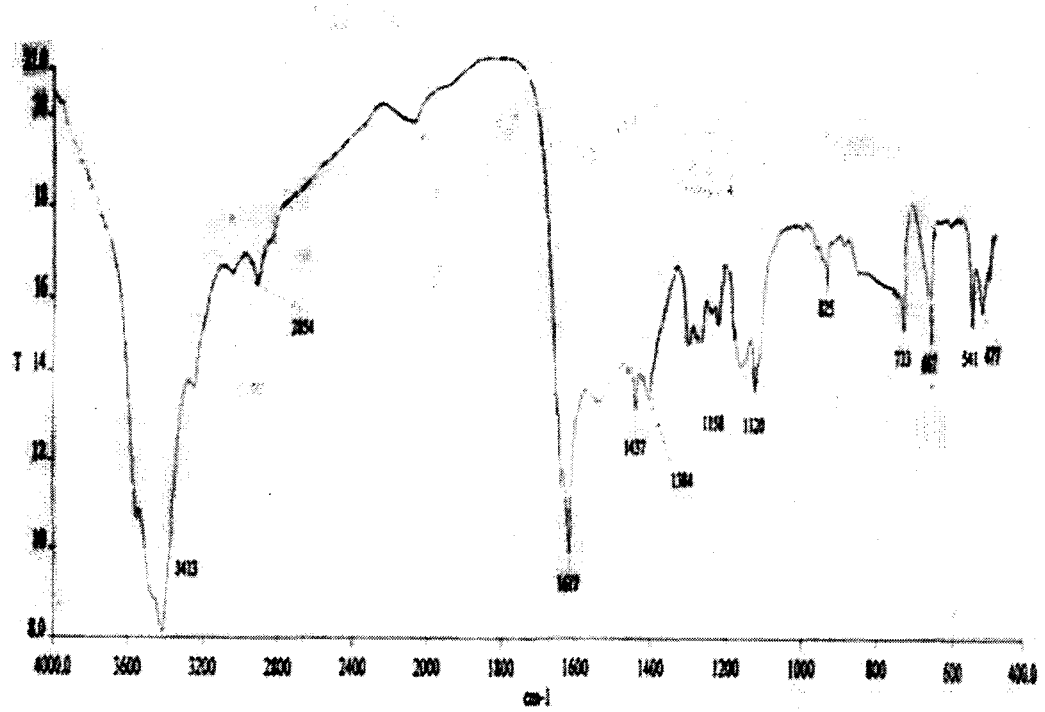

Infrared spectra of the complex $[Fe(L_5)Cl(PPh_3)]_2$ (11)

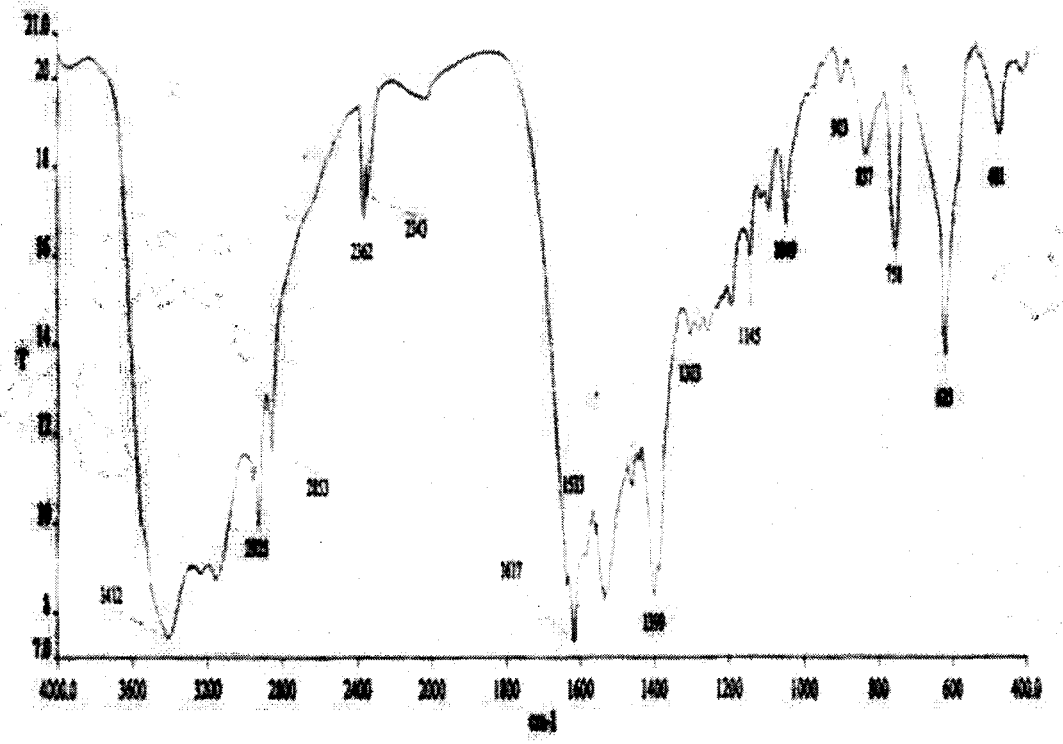

Infrared spectra of the complex $[Fe(L_5)Cl(Imz)]_2$ (12)

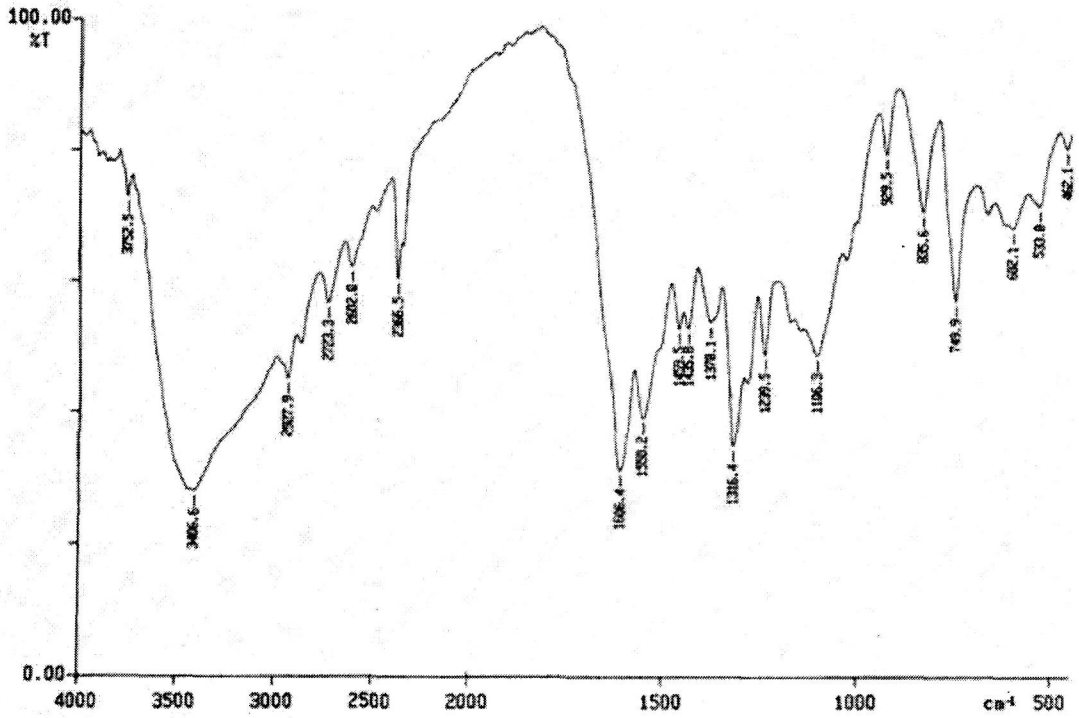

Infrared spectra of the complex **$[FeL_5(H_2O)]_2$ (13)**

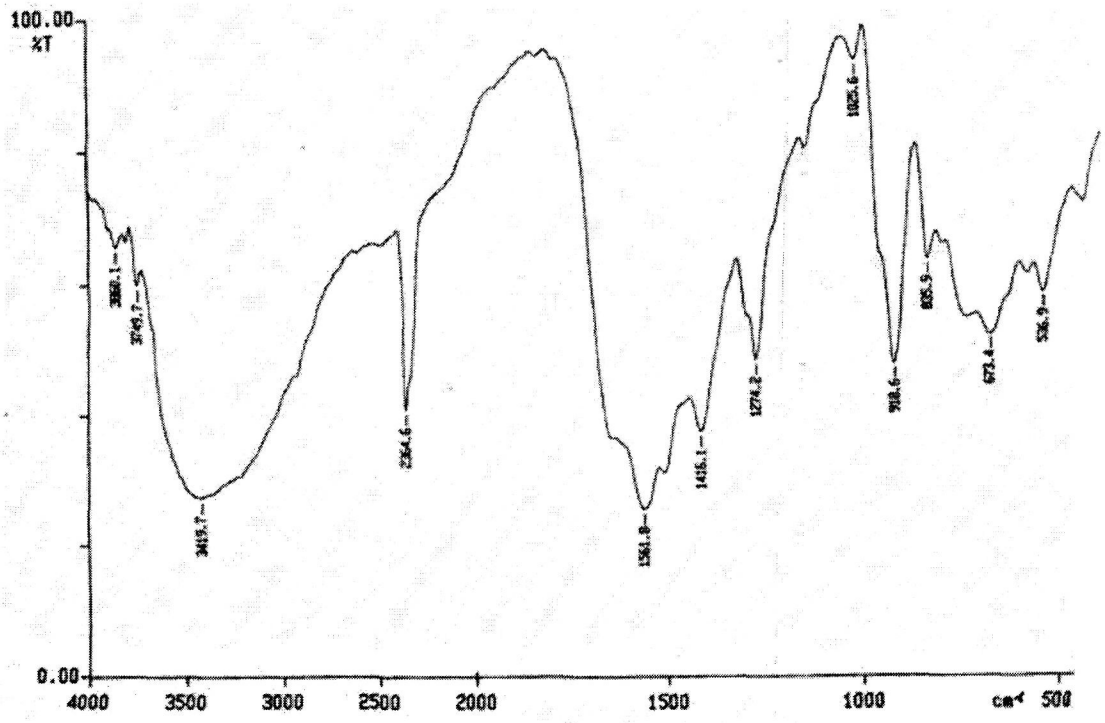

Infrared spectra of the complex **$Na[VO_2(L_5)]$ (14)**

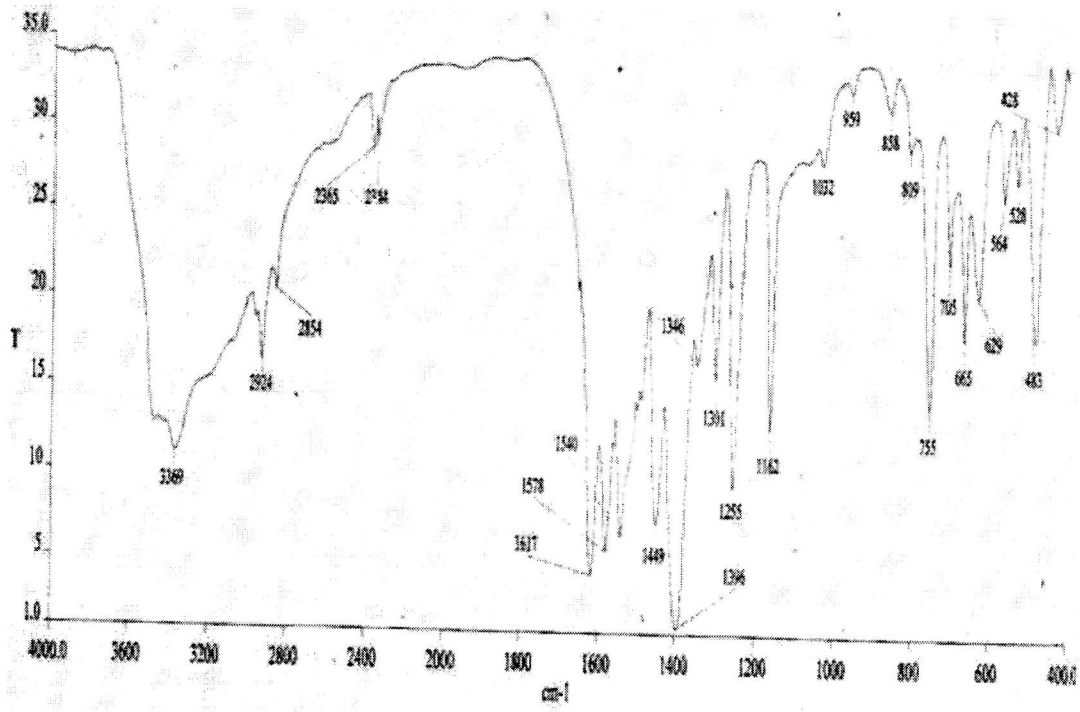

Infrared spectra of the complex **[Fe(L_6)Cl] (15)**

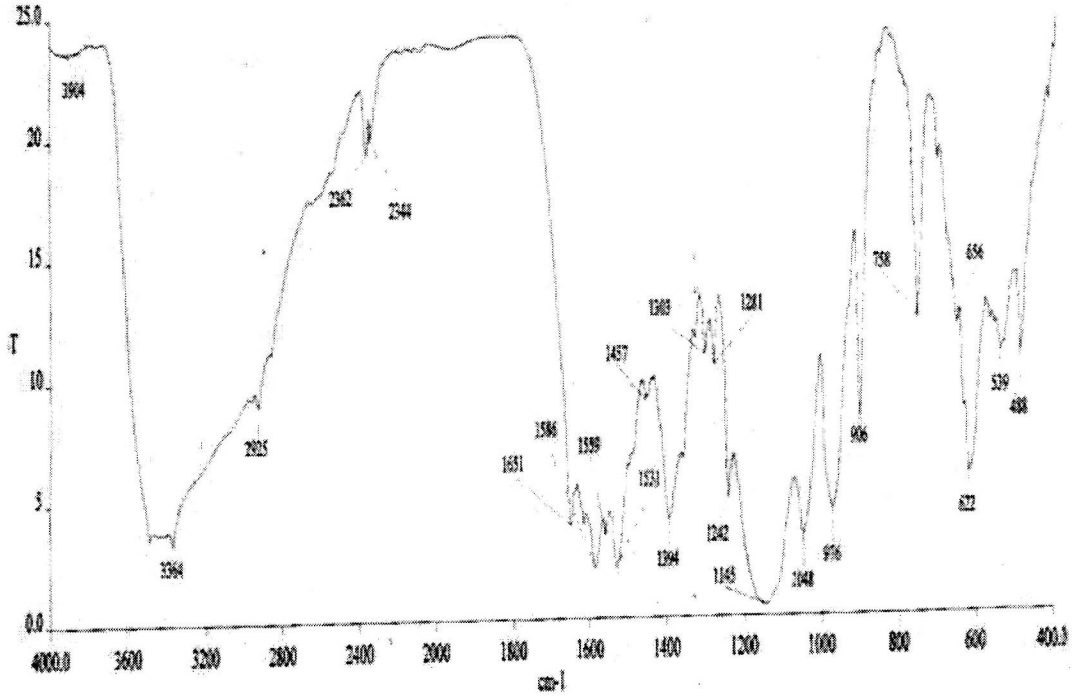

Infrared spectra of the complex **[VO(L_6)(H_2O)].H_2O (16)**

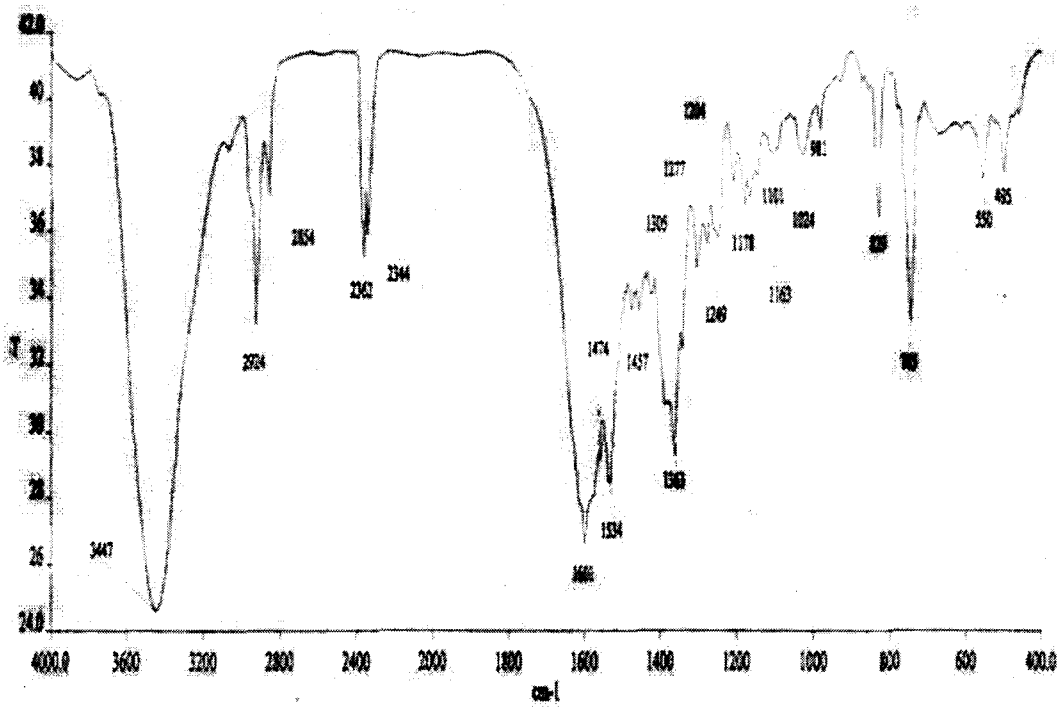

Infrared spectra of the complex **[Fe(L_7)(acac)(EtOH)] (17)**

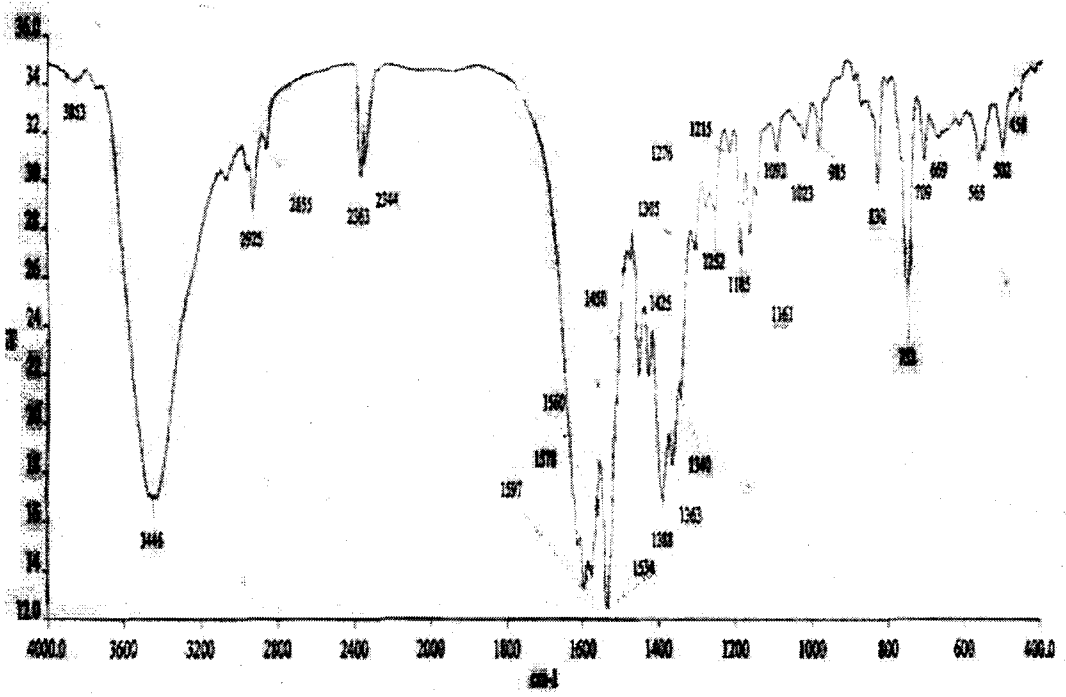

Infrared spectra of the complex **[Fe(L_8)(acac)(EtOH)] (18)**

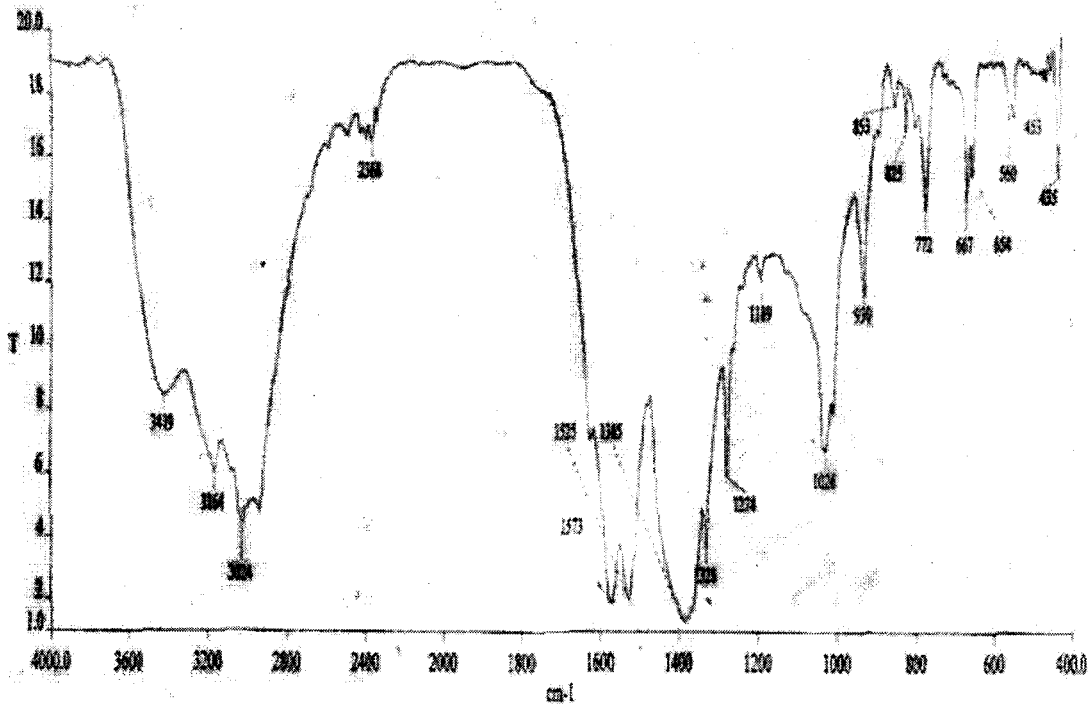

Infrared spectra of the complex $[Fe(L_9)(H_2O)_2]NO_3$ **(19)**

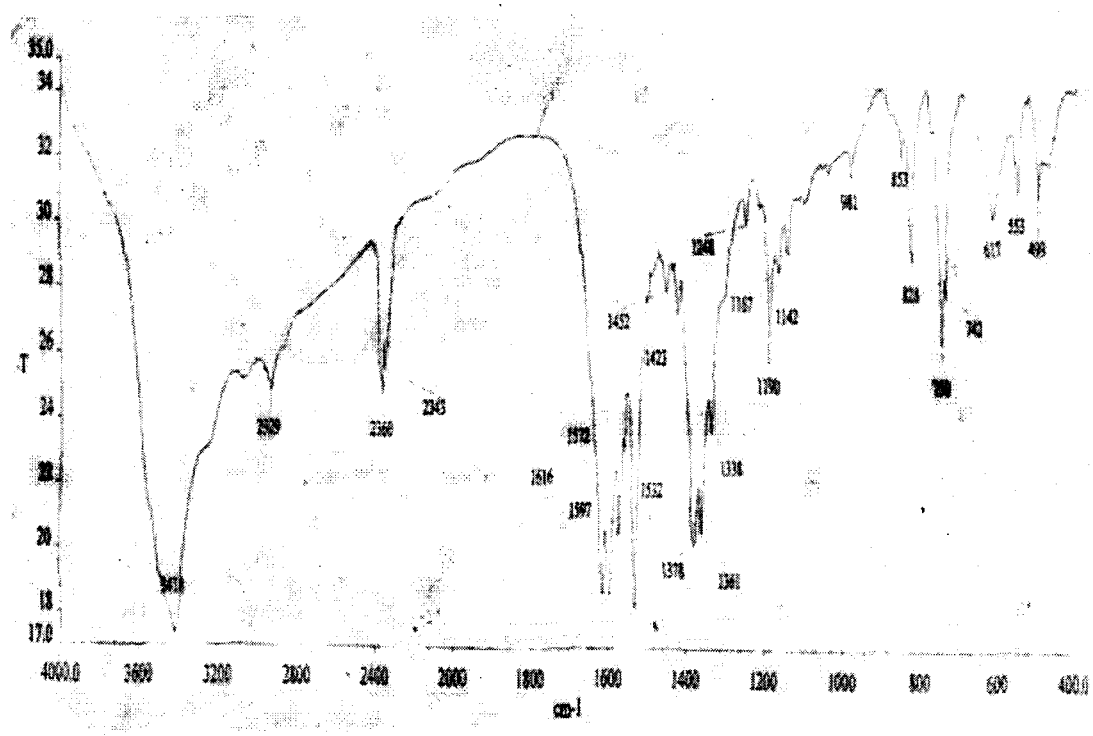

Infrared spectra of the complex $[Fe(L_{11})(H_2O)_2]NO_3$ **(20)**

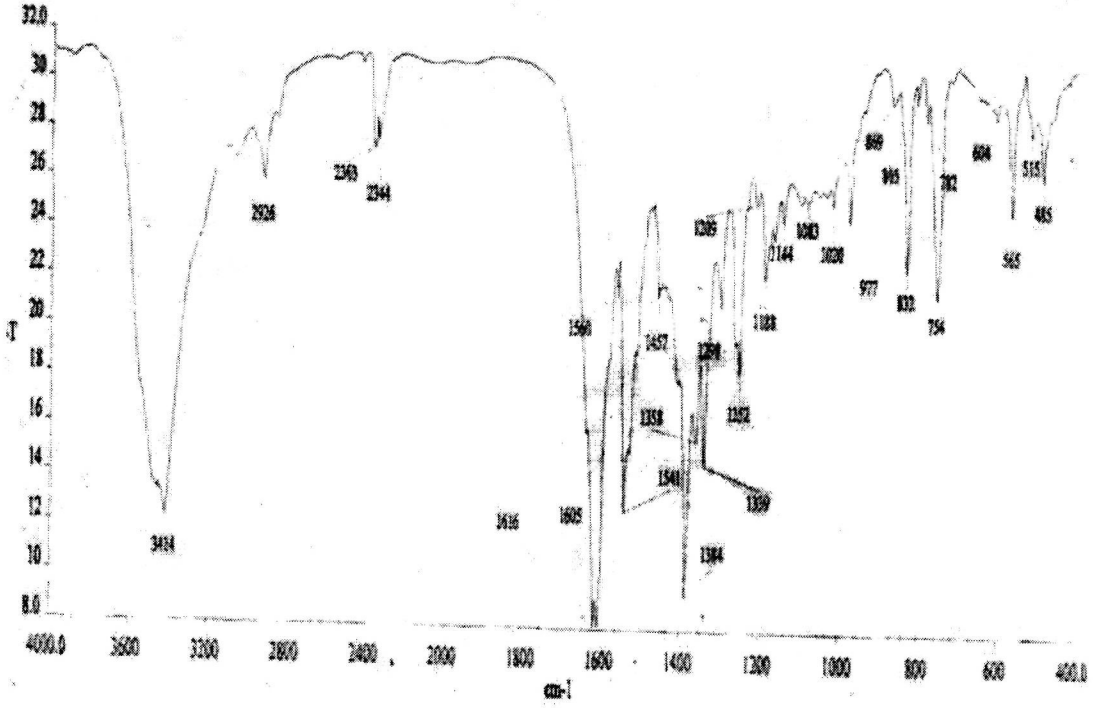

Infrared spectra of the complex $[Fe(L_{12})(H_2O)_2]NO_3$ (21)

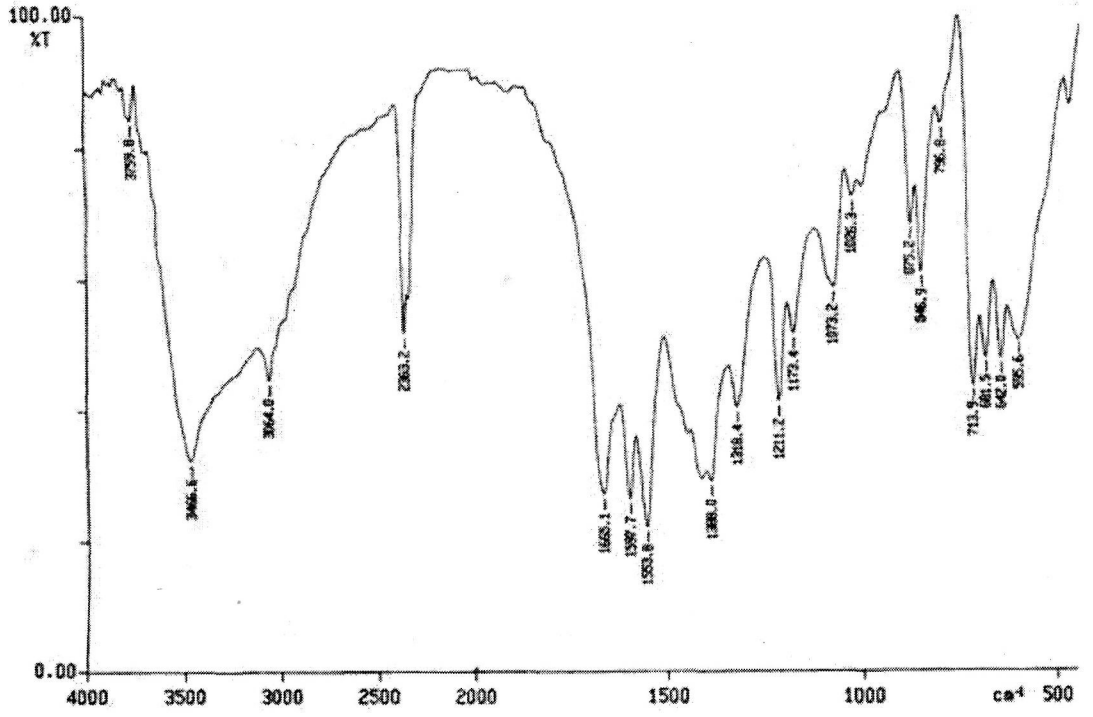

Infrared spectra of the complex $[Fe(L_{13})(NO_3)(H_2O)]$ (22)

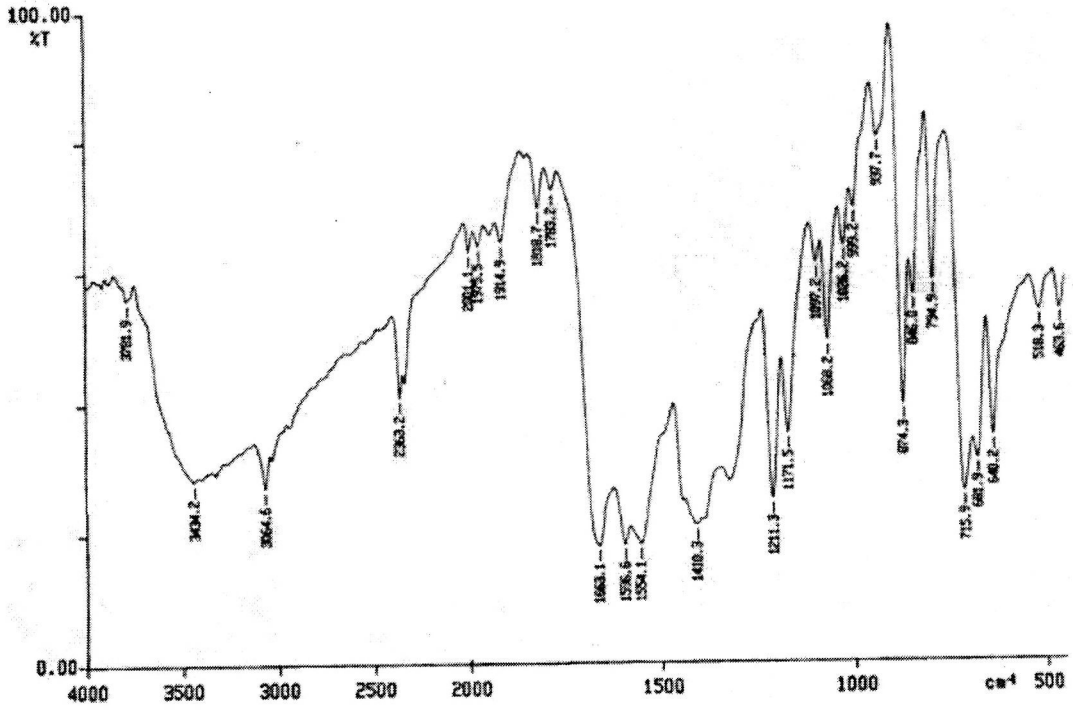

Infrared spectra of the complex **$[Fe(L_{11})(NO_3)(H_2O)]$ (23)**

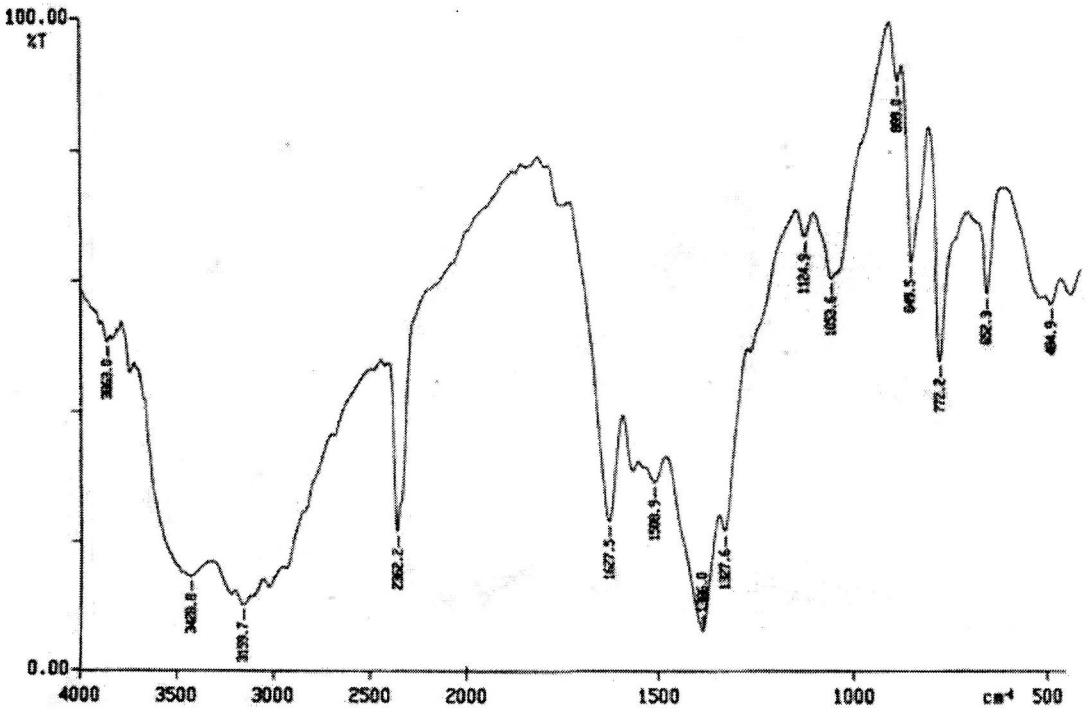

Infrared spectra of the complex **$NH_4[Fe(L_9)F_2]$ (24)**

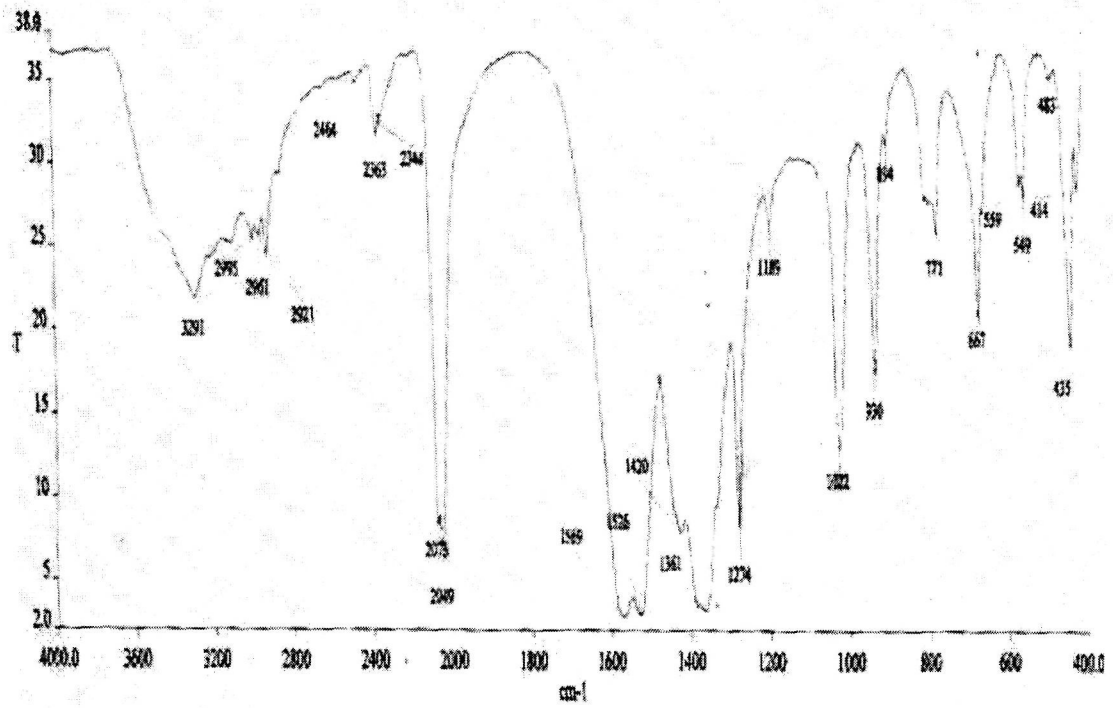

Infrared spectra of the complex $NH_4[Fe(L_9)(NCS)_2]$ (25)

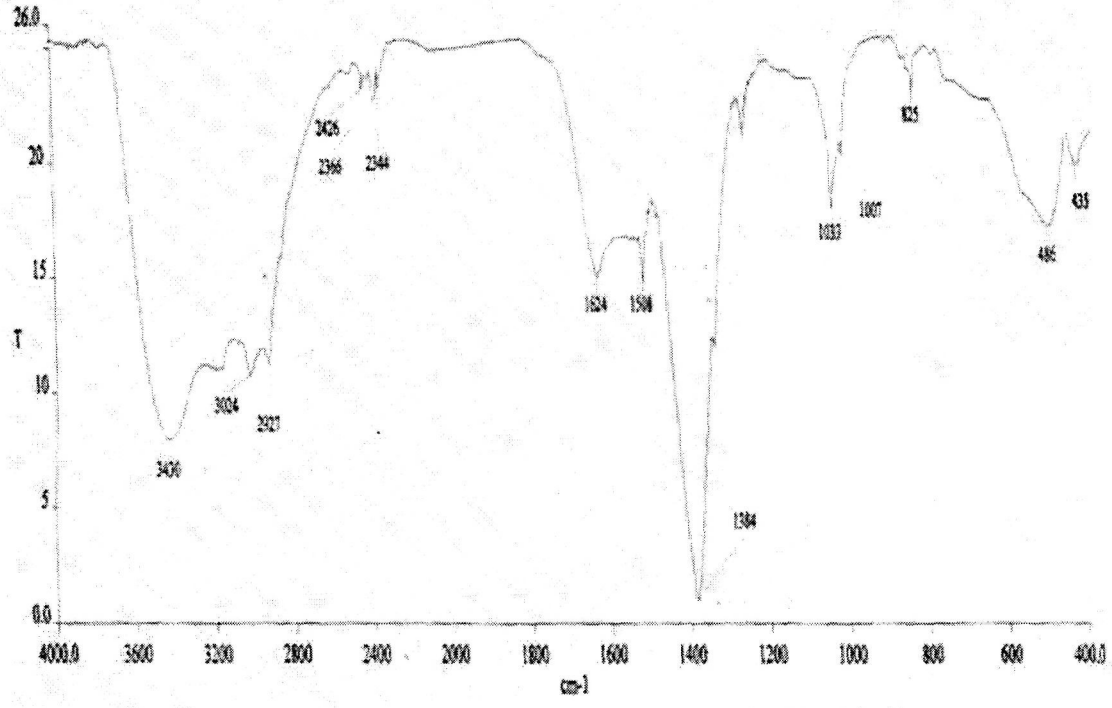

Infrared spectra of the complex $Na[Fe(L_9)(N_3)_2]$ (26)

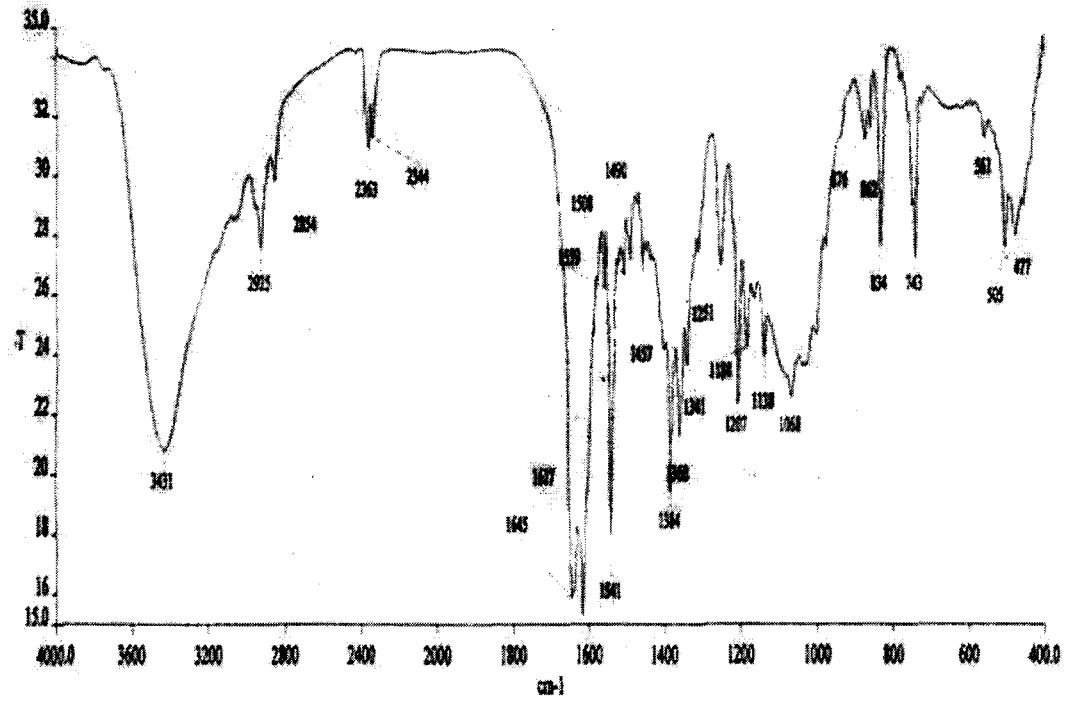

Infrared spectra of the complex $[Fe(L_{12})(Imz)_2]NO_3$ (27)

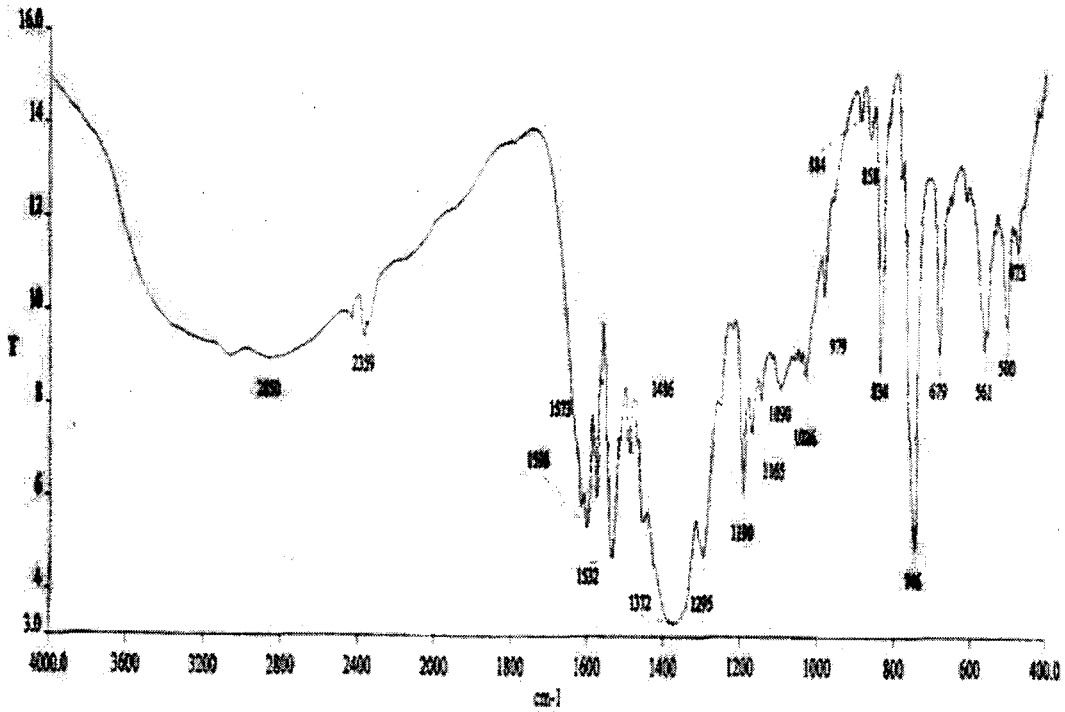

Infrared spectra of the complex $[Fe(L_{12})(Py)_2]NO_3$ (28)

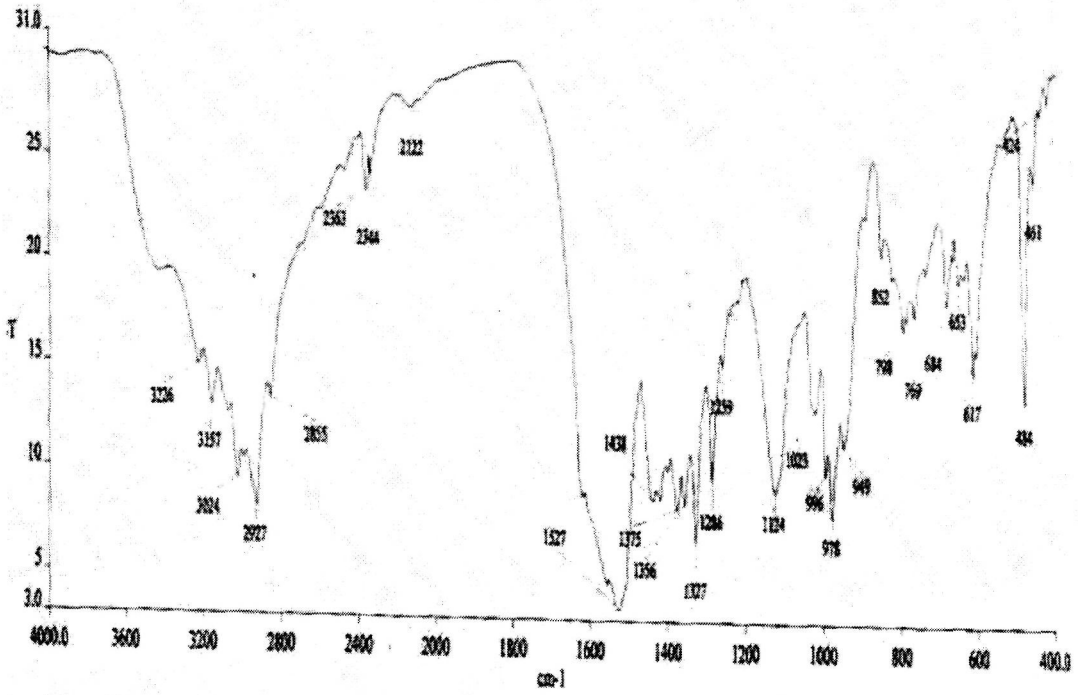

Infrared spectra of the complex **[VO(L_9)].H_2O (29)**

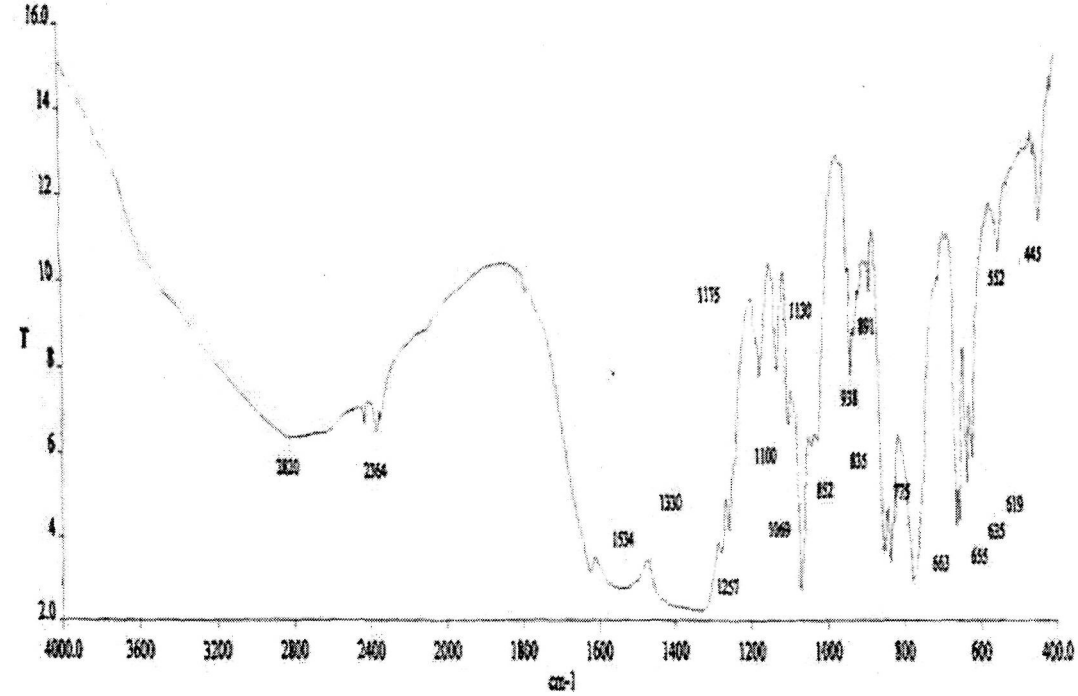

Infrared spectra of the complex **[VO(L_{11})].H_2O (30)**

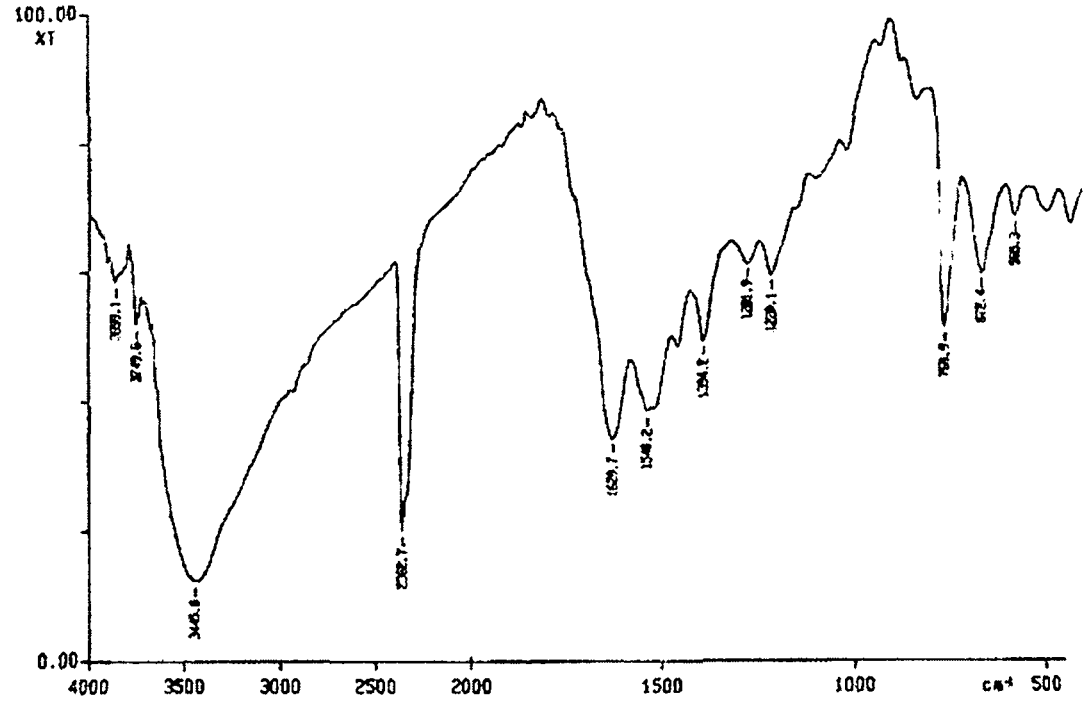

Infrared spectra of the complex $[Fe(L_{16})Cl_2]Cl$ (35)

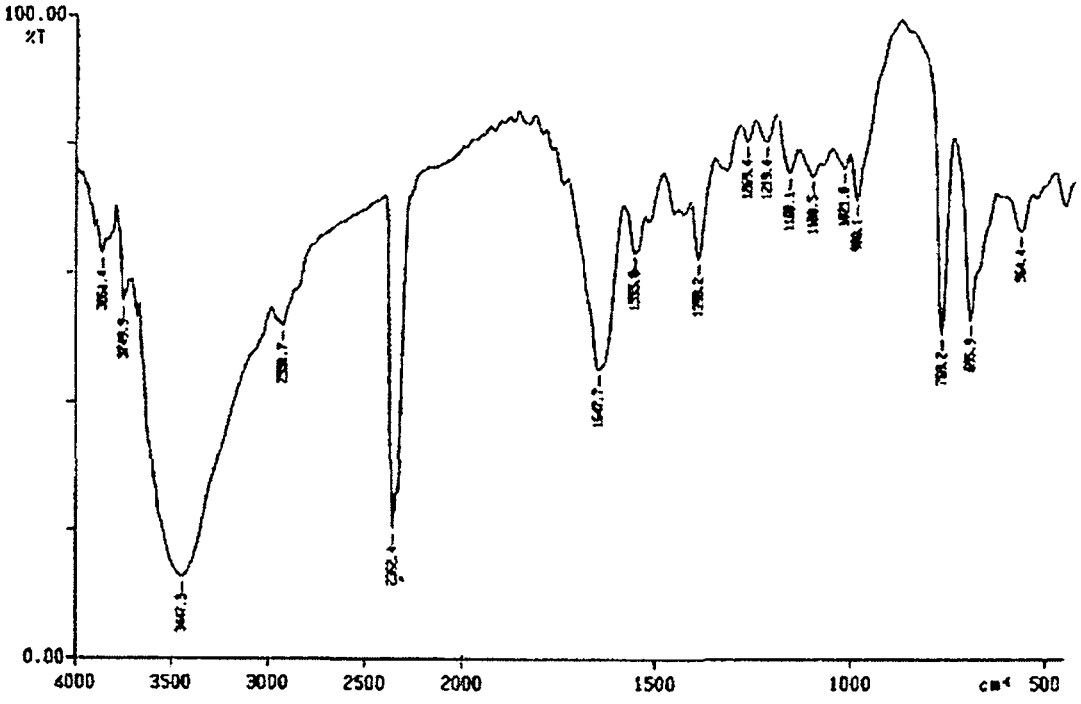

Infrared spectra of the complex $[VO(L_{15})]SO_4.H_2O$ (36)

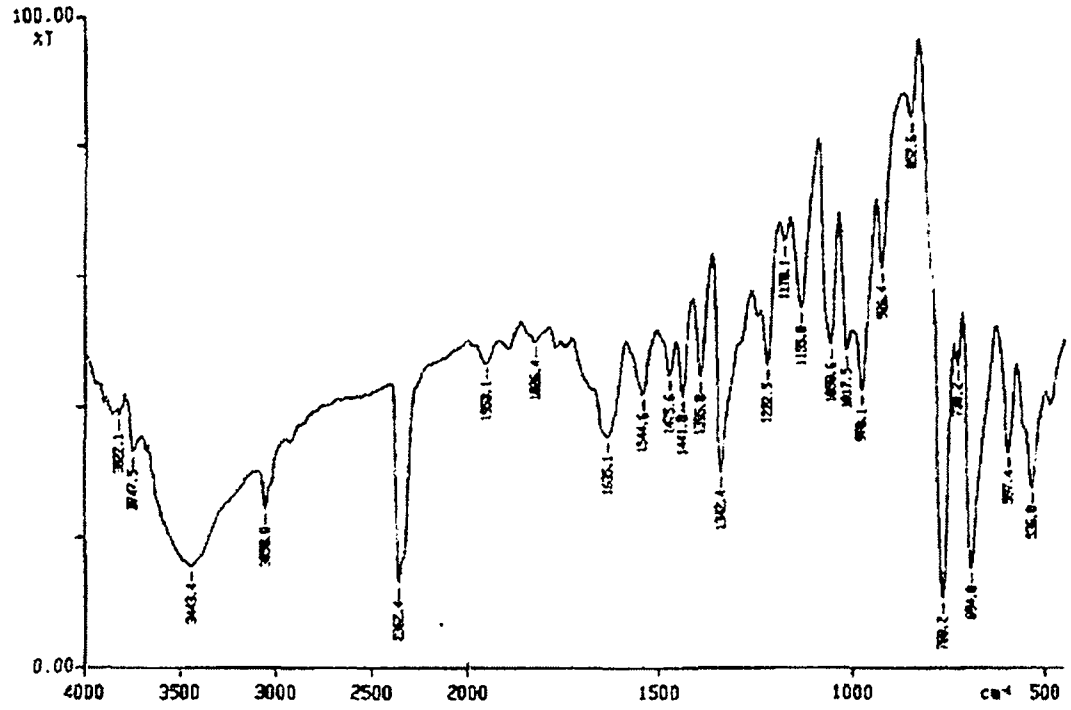

Infrared spectra of the complex $[VO(L_{16})]SO_4.H_2O$ (37)

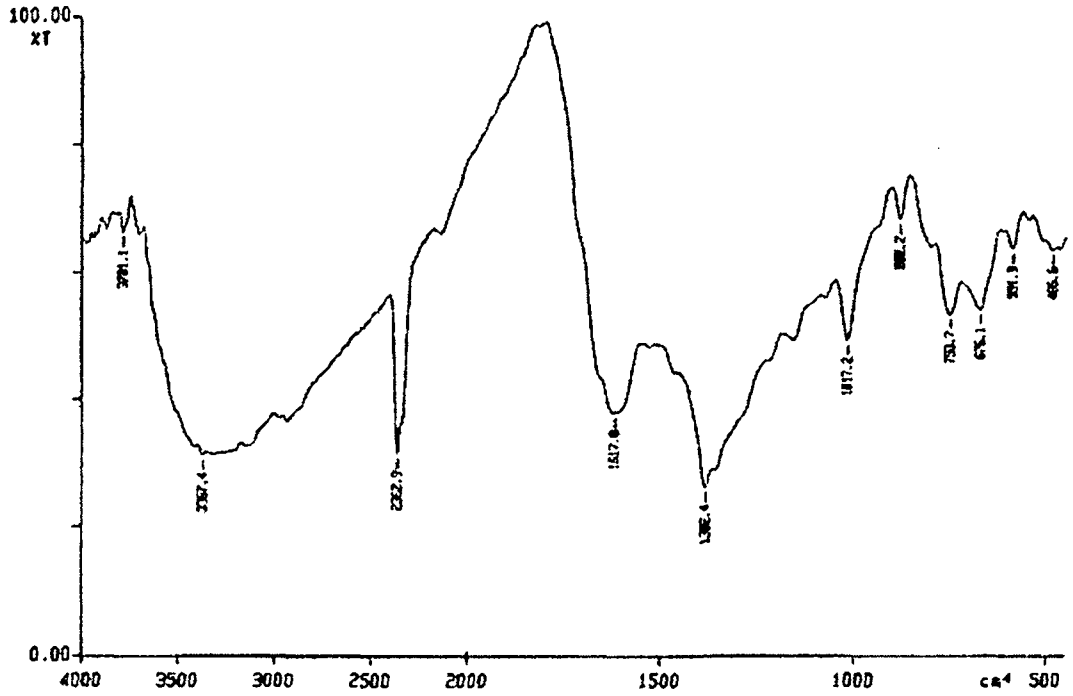

Infrared spectra of the complex $[Fe(L_{10})(H_2O)_2](NO_3)_3$ (38)

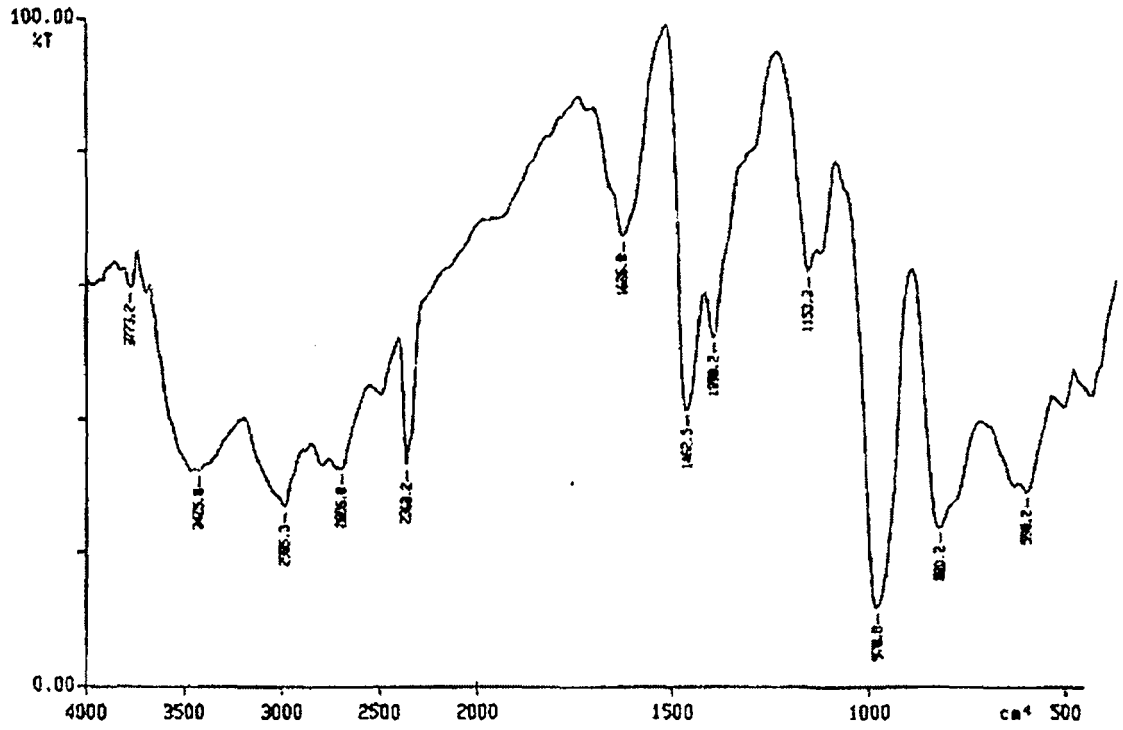

Infrared spectra of the complex $[VO(L_{10})]SO_4.H_2O$ (39)

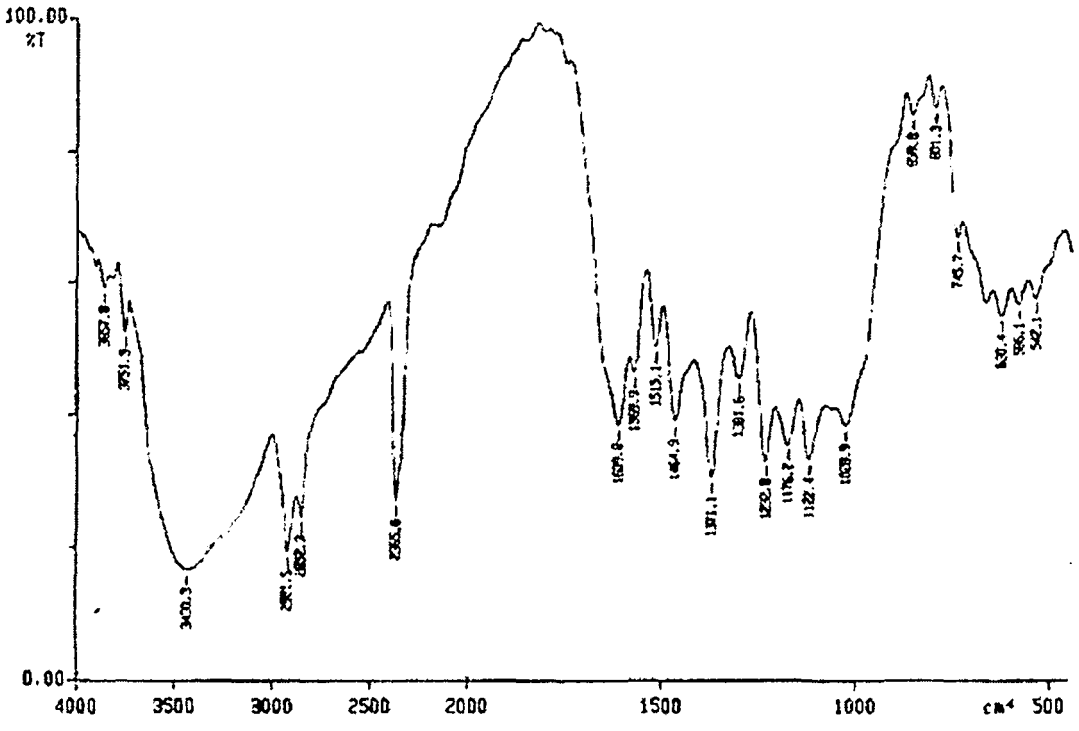

Infrared spectra of the complex $[Fe(L_9(H_2O)_2]$ (40)

APPENDIX 2

UV-VIS spectra of the compounds

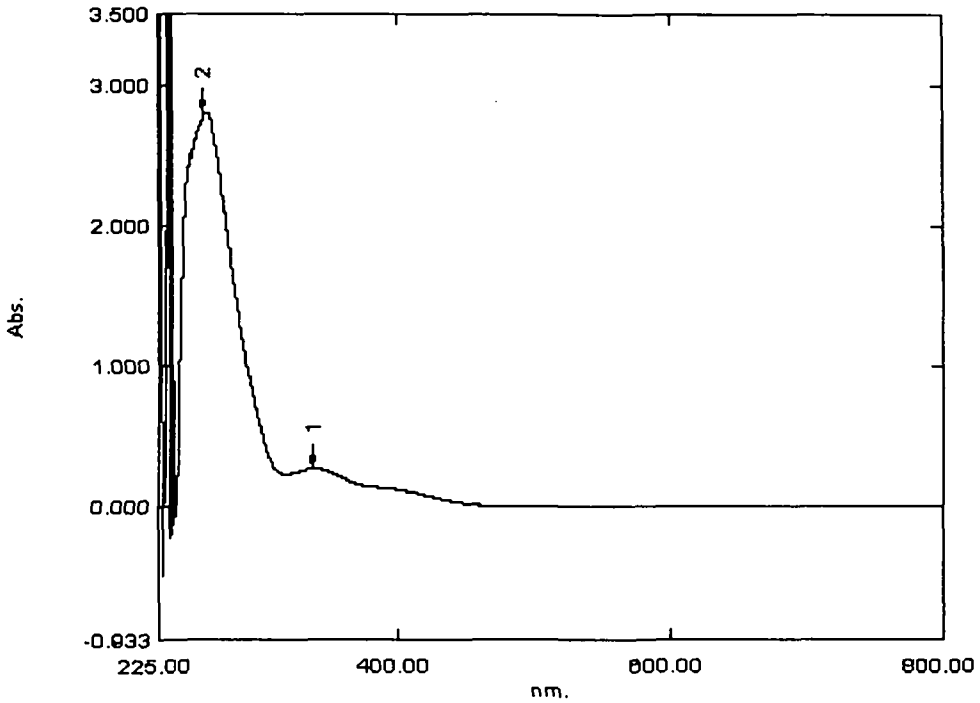

UV-VIS spectra of the Schiff base $\mathbf{L_1}$

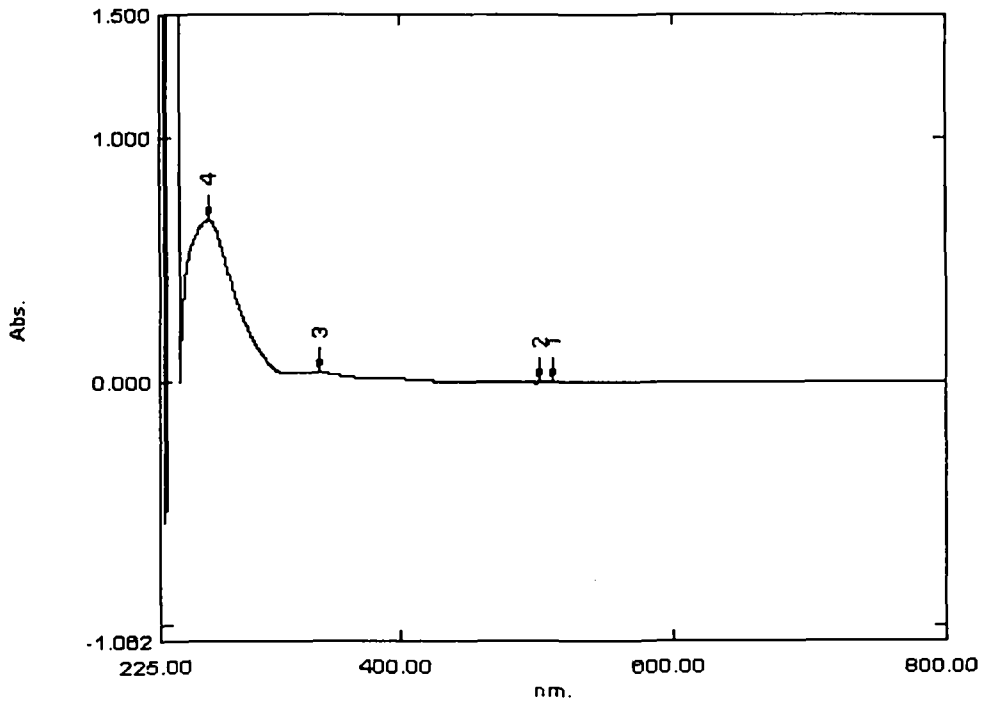

UV-VIS spectra of the Schiff base $\mathbf{L_2}$

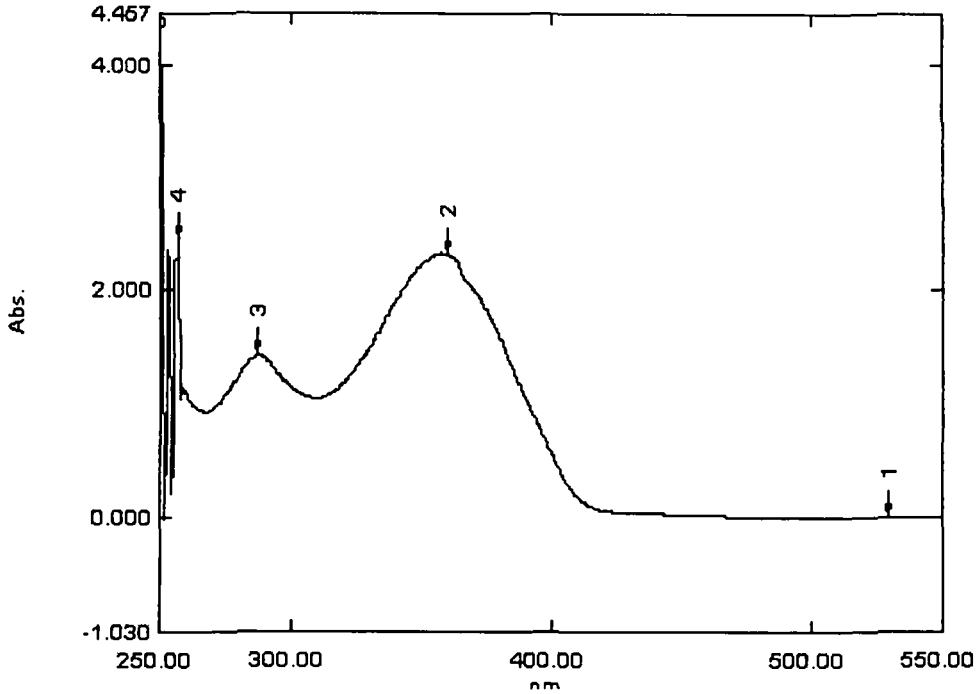

UV-VIS spectra of the Schiff base L_3

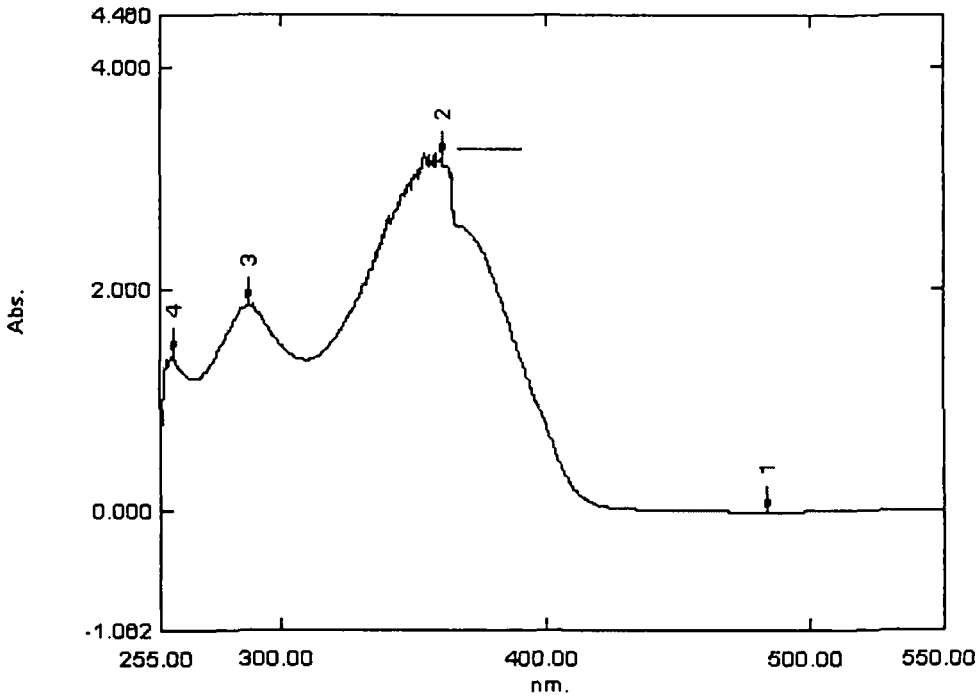

UV-VIS spectra of the Schiff base L_4

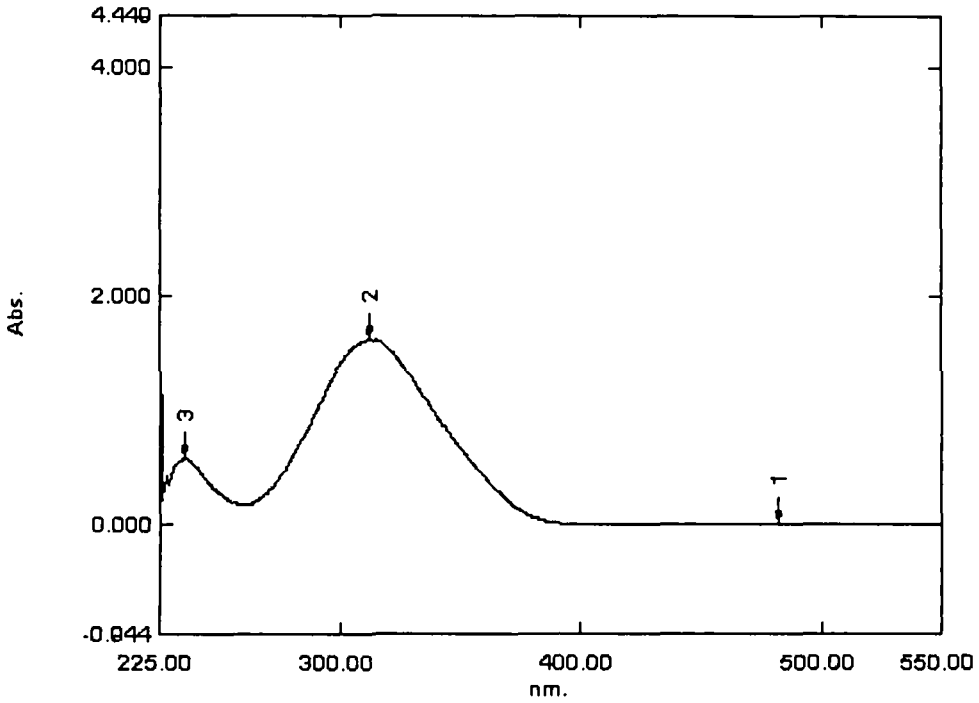

UV-VIS spectra of the Schiff base L_5

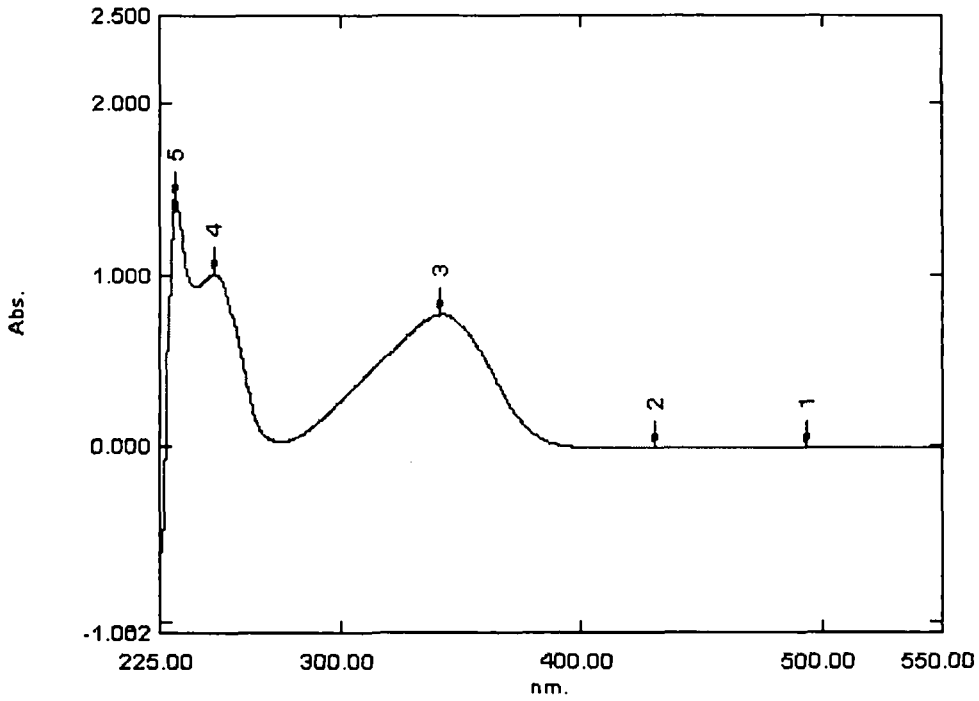

UV-VIS spectra of the Schiff base L_6

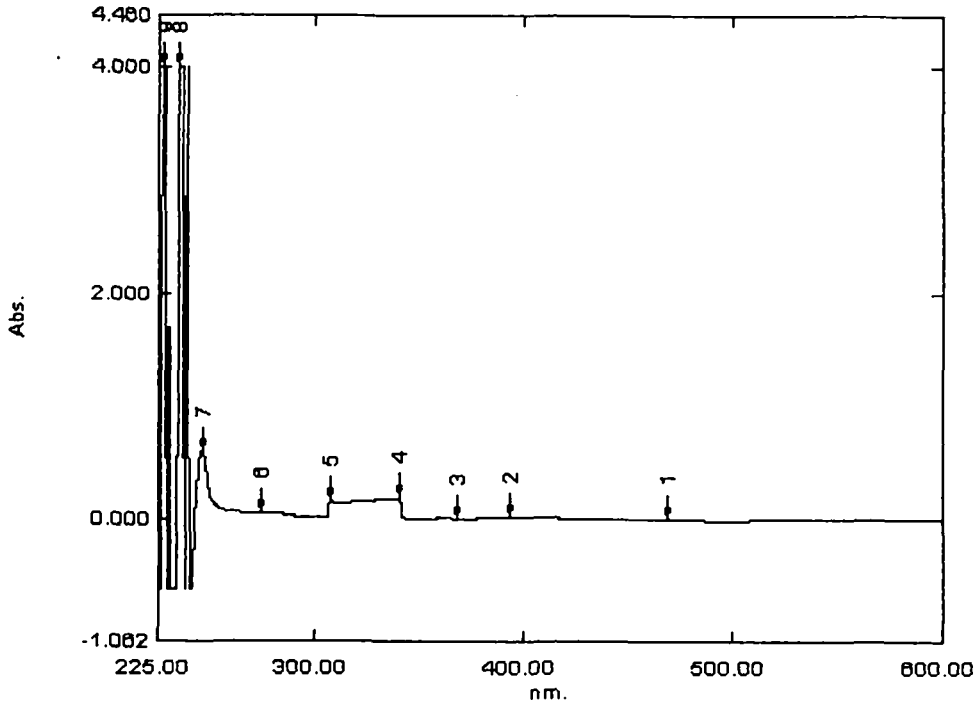

UV-VIS spectra of the Schiff base $\mathbf{L_7}$

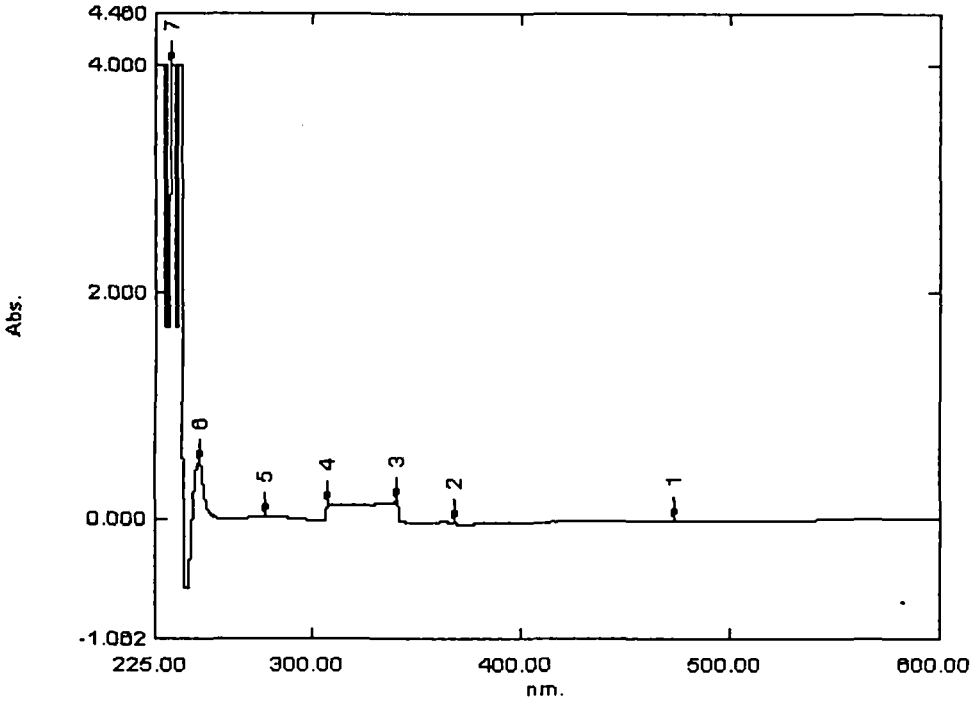

UV-VIS spectra of the Schiff base $\mathbf{L_8}$

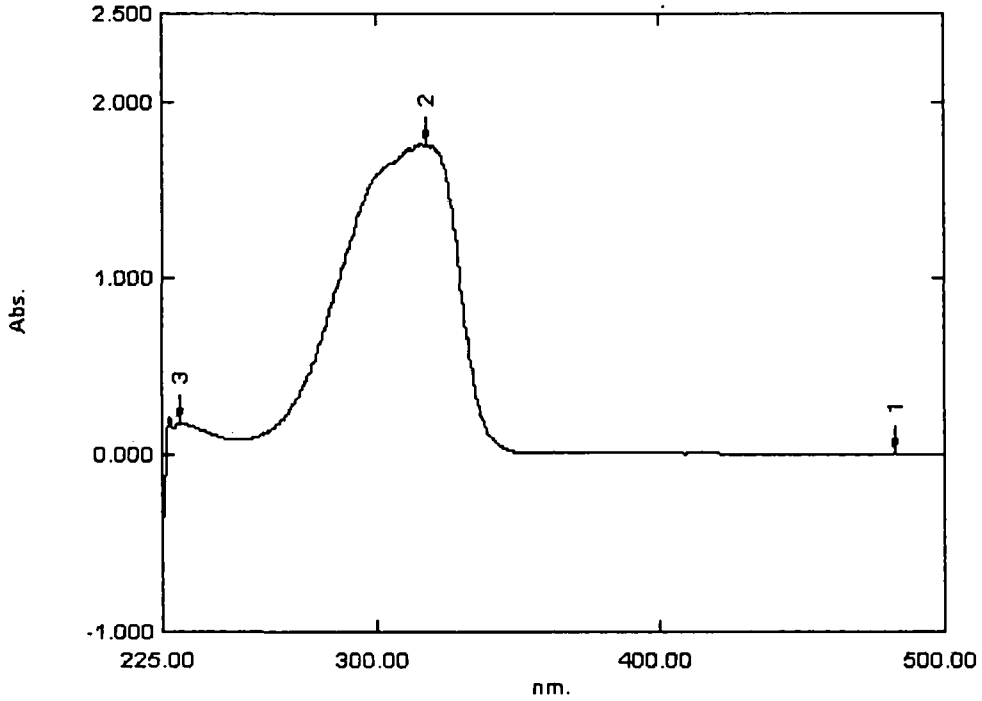

UV-VIS spectra of the Schiff base L_9

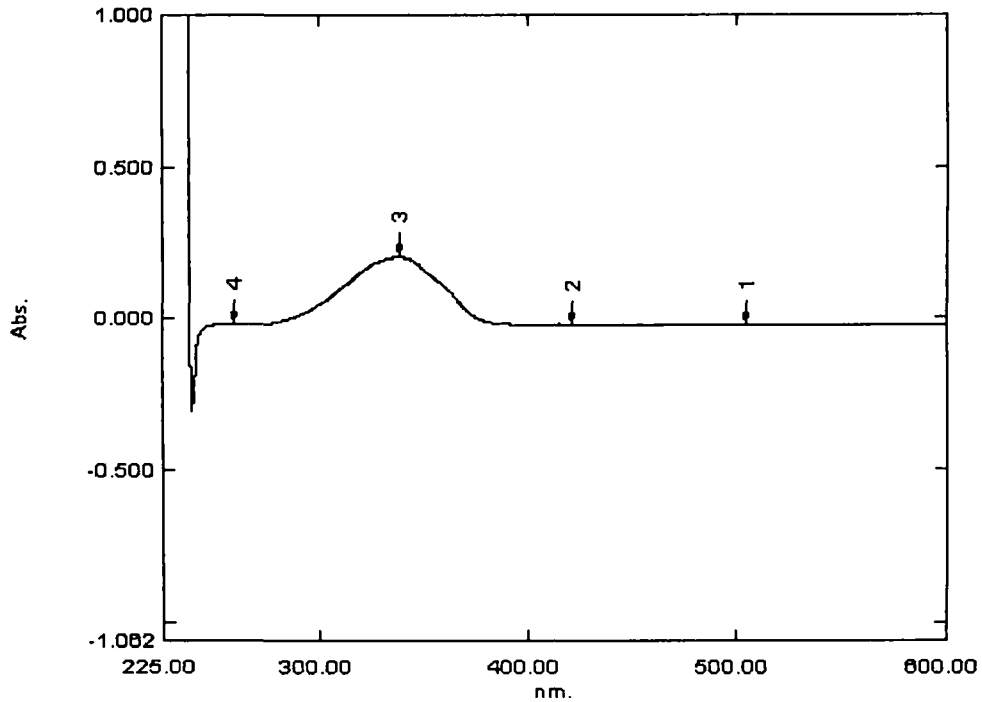

UV-VIS spectra of the Schiff base L_{10}

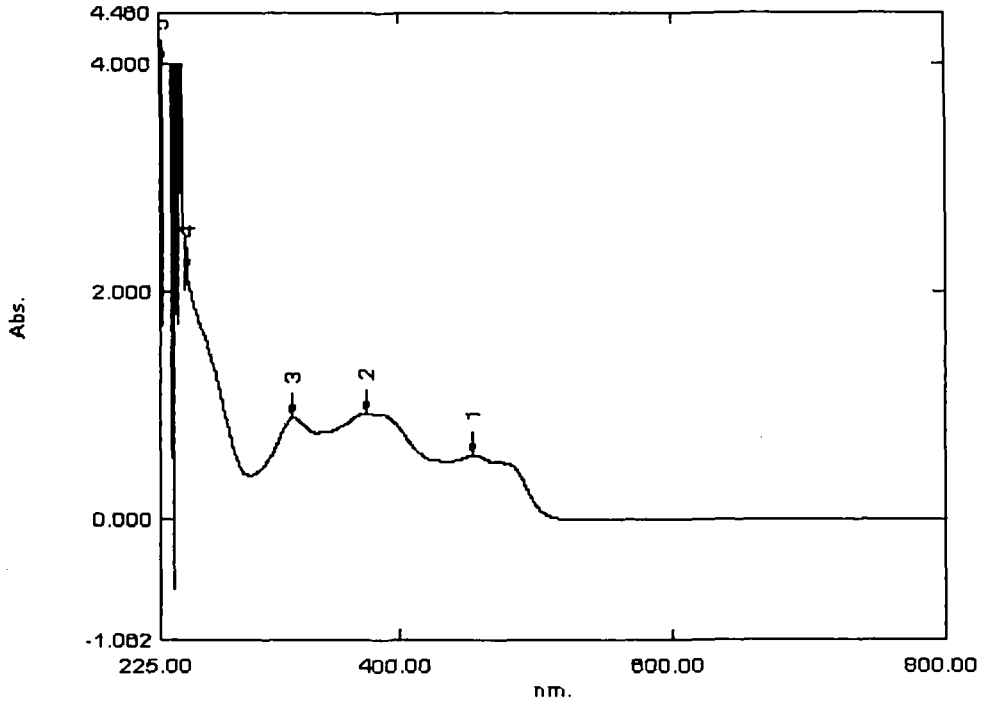

UV-VIS spectra of the Schiff base L_{11}

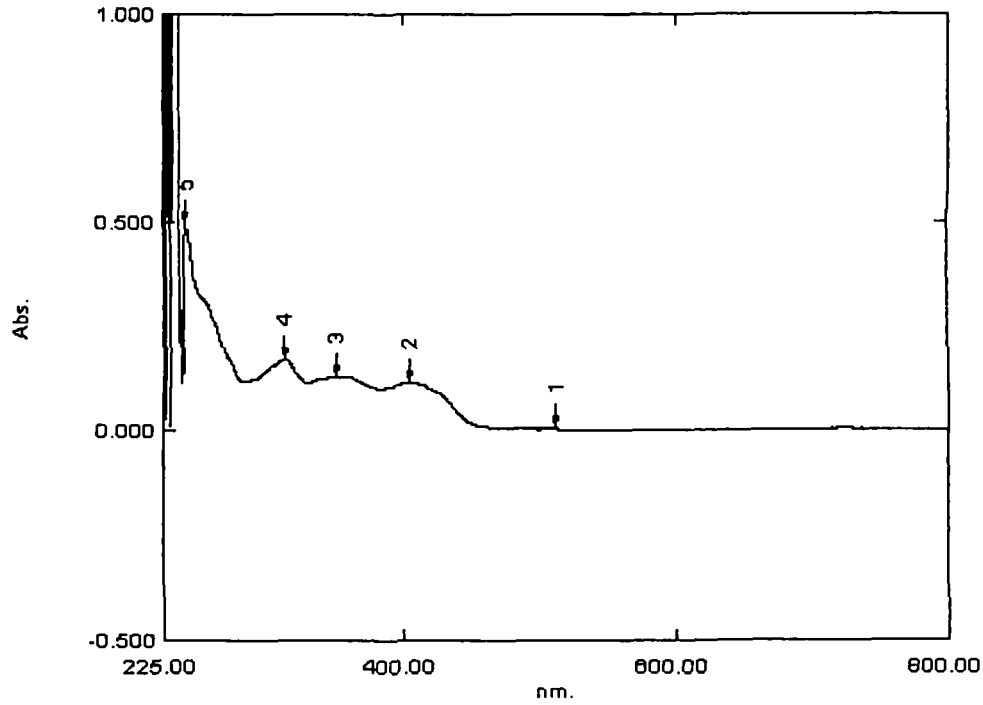

UV-VIS spectra of the Schiff base L_{12}

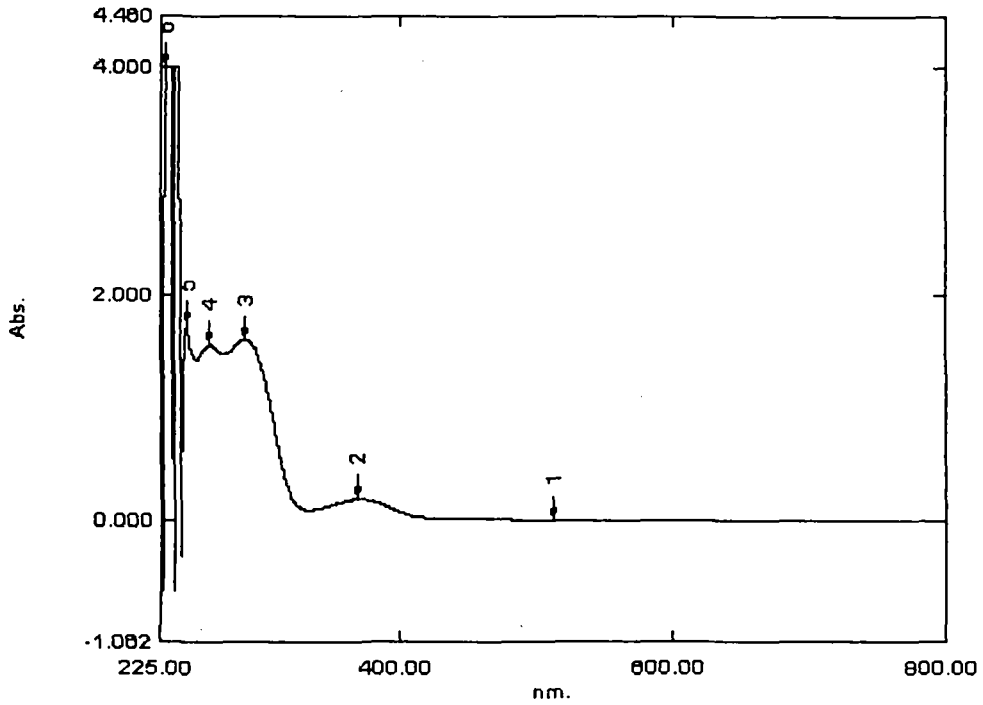

UV-VIS spectra of the Schiff base L_{13}

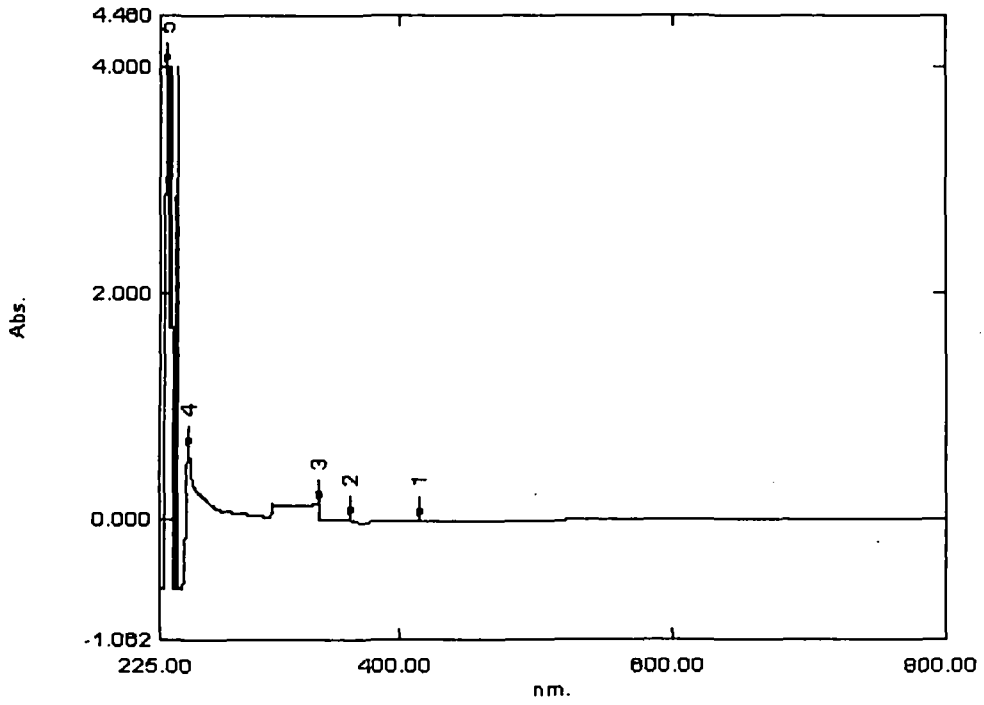

UV-VIS spectra of the Schiff base L_{14}

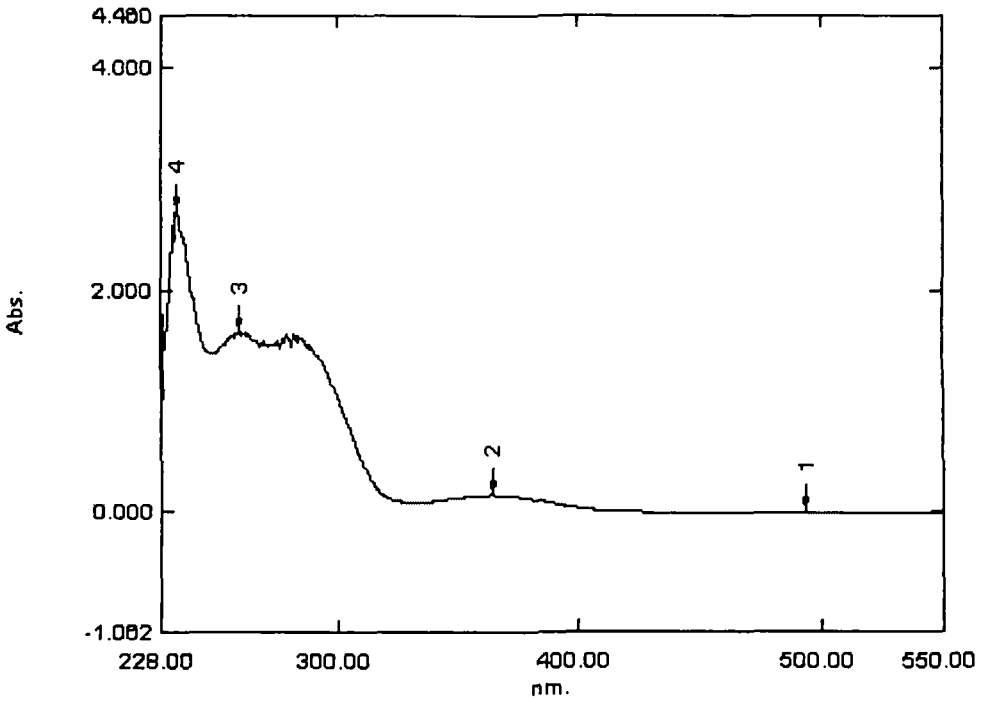

UV-VIS spectra of the Schiff base L_{15}

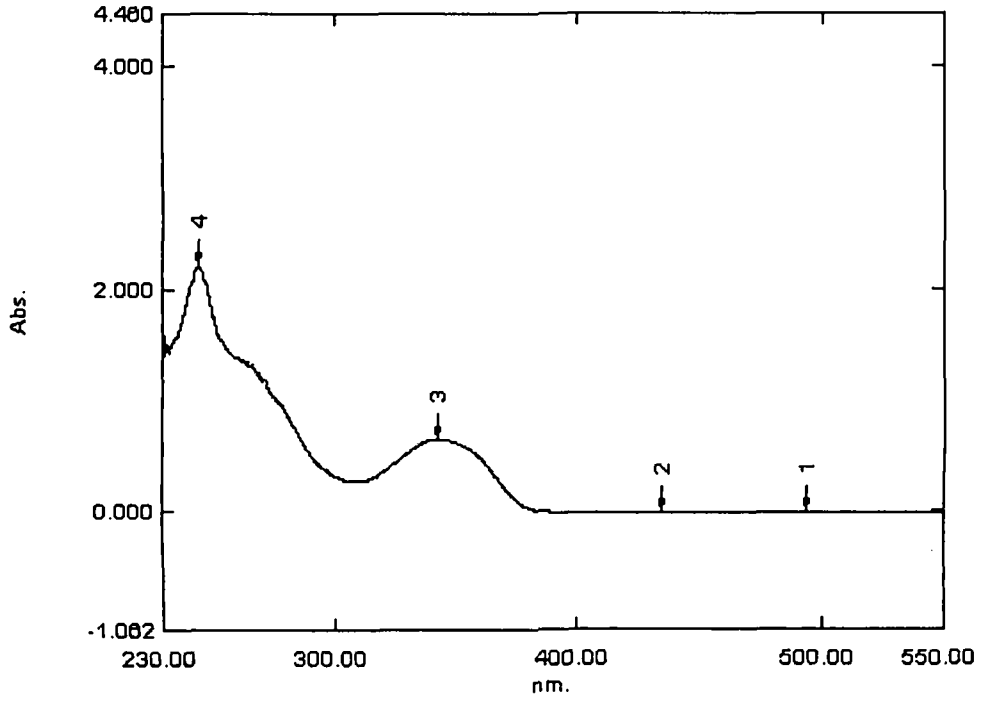

UV-VIS spectra of the Schiff base L_{16}

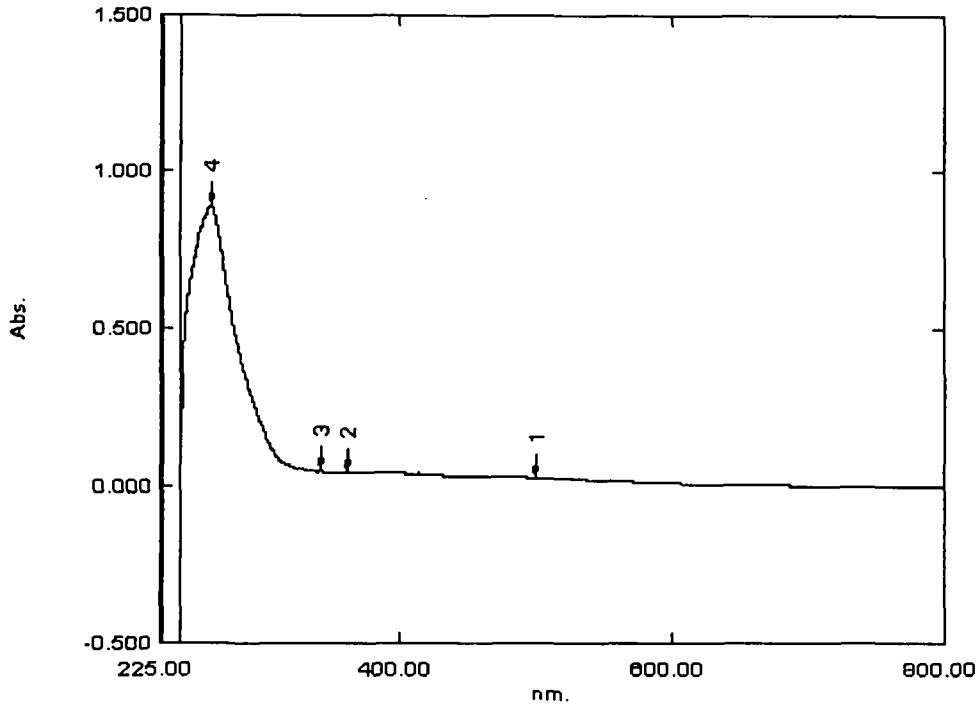

UV-VIS spectra of the complex $[Fe(L_1)_2(NO_3)_2]NO_3$ **(1)**

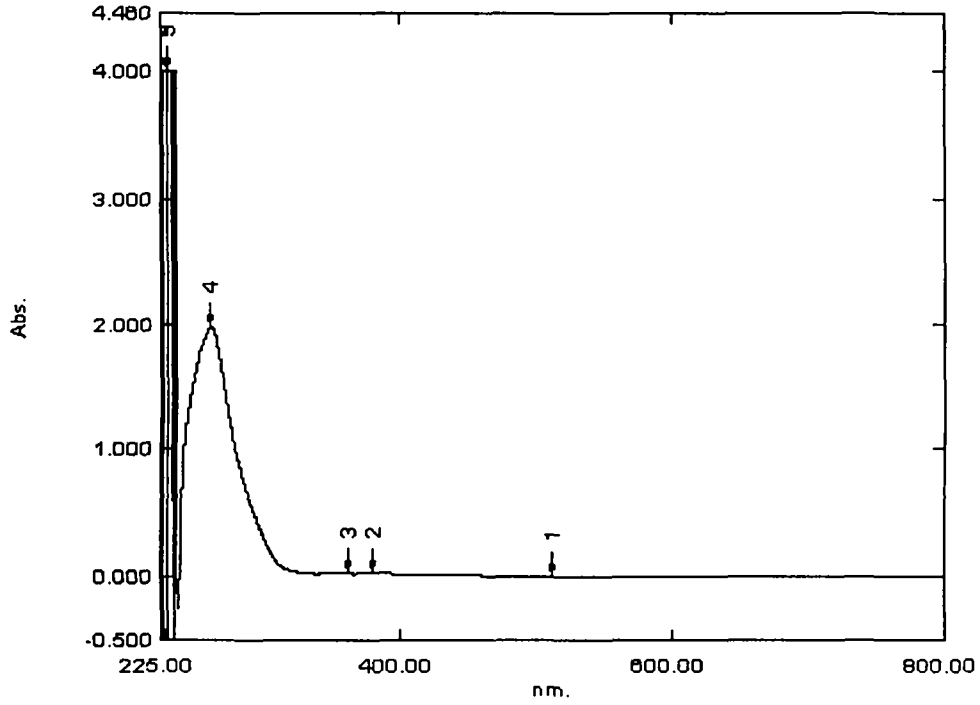

UV-VIS spectra of the complex $[Fe(L_2)_2(NO_3)_2]NO_3$ **(2)**

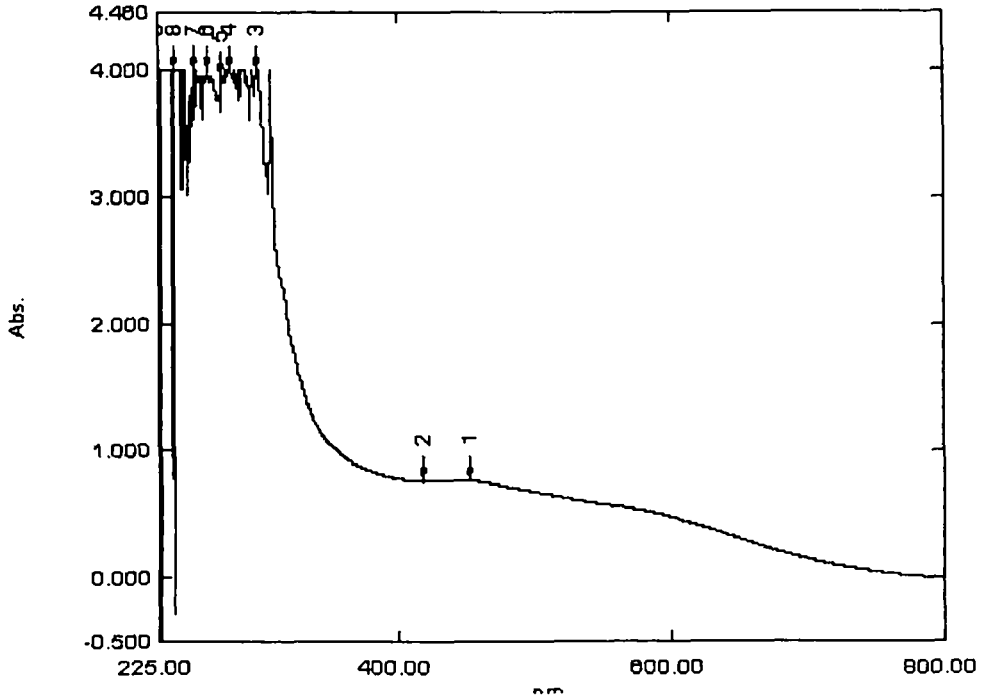

UV-VIS spectra of the complex $[VO(L_1)_2]SO_4.H_2O$ (3)

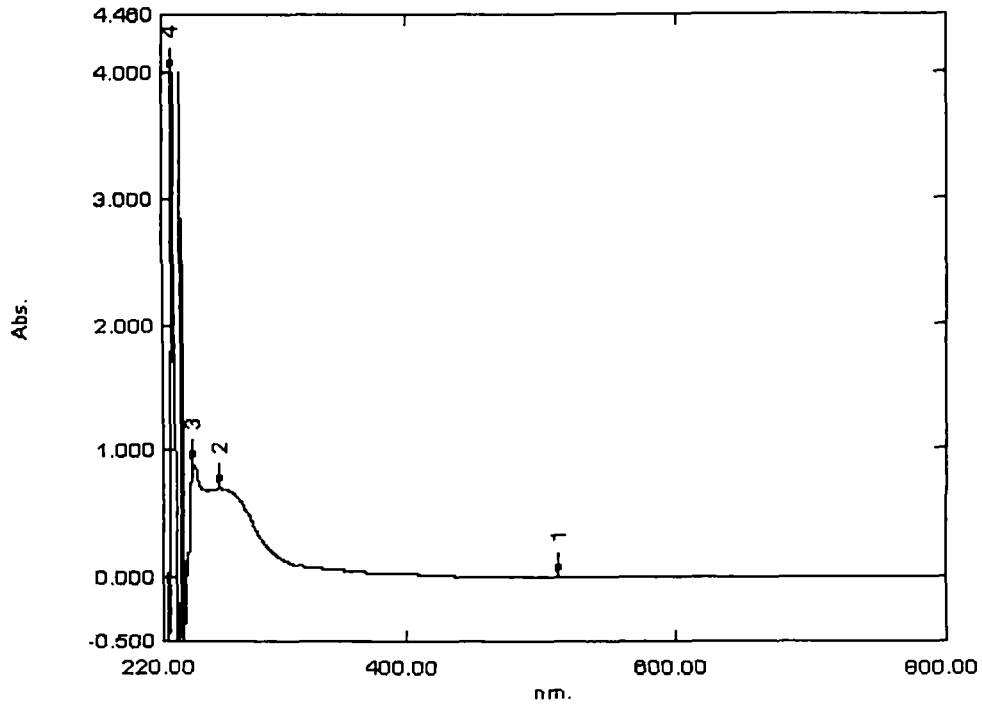

UV-VIS spectra of the complex $[VO(L_2)_2]^{2+}SO_4^{2-}.H_2O$ (4)

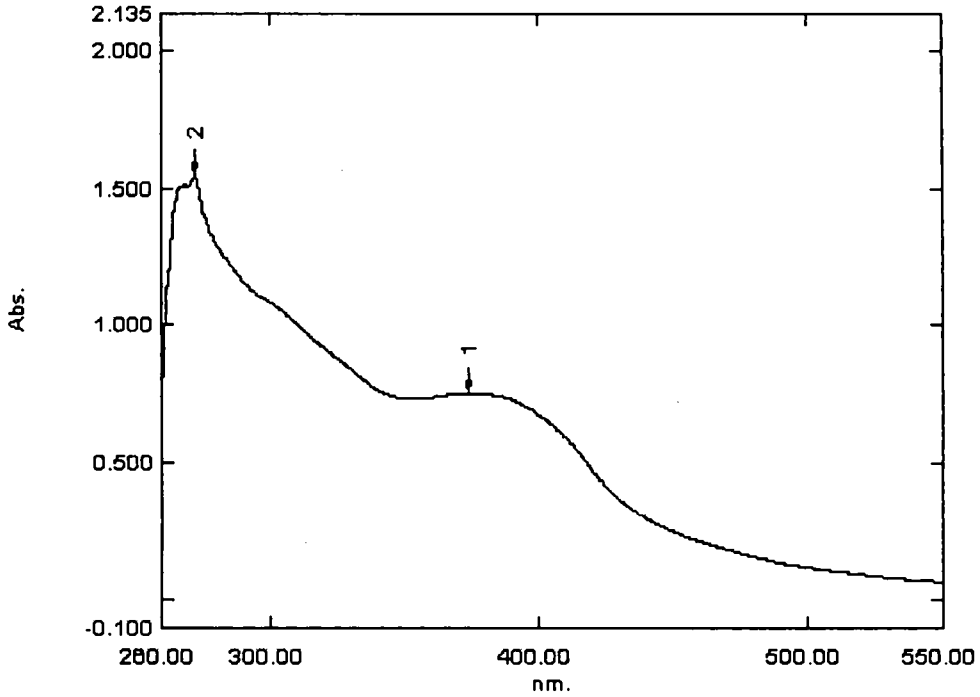

UV-VIS spectra of the complex $[Fe(L_3)Cl]_2$ (5)

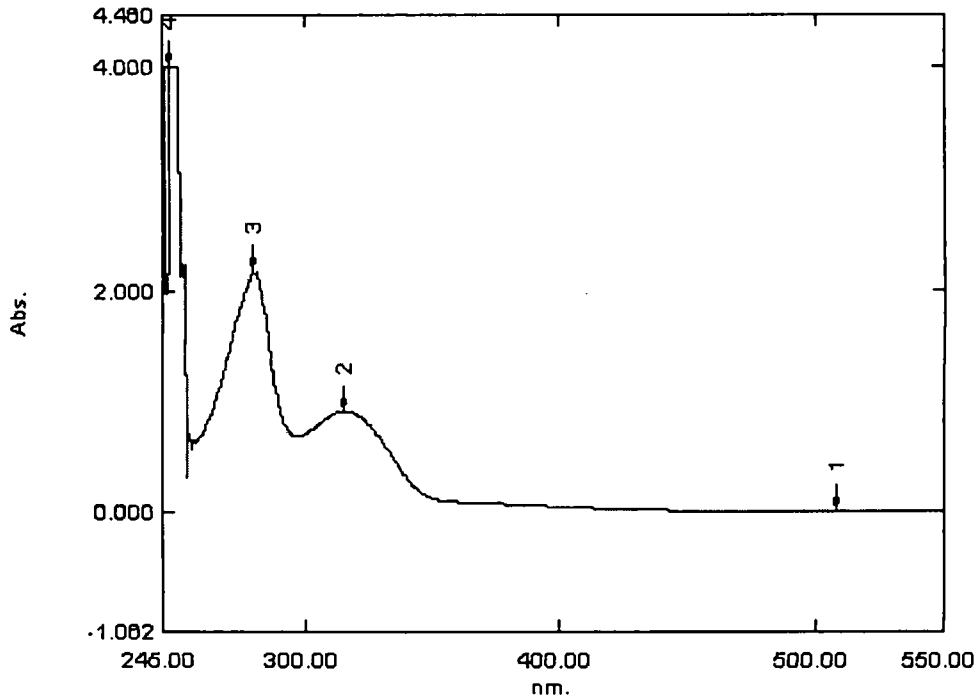

UV-VIS spectra of the complex $[Fe(L_4)Cl]_2$ (6)

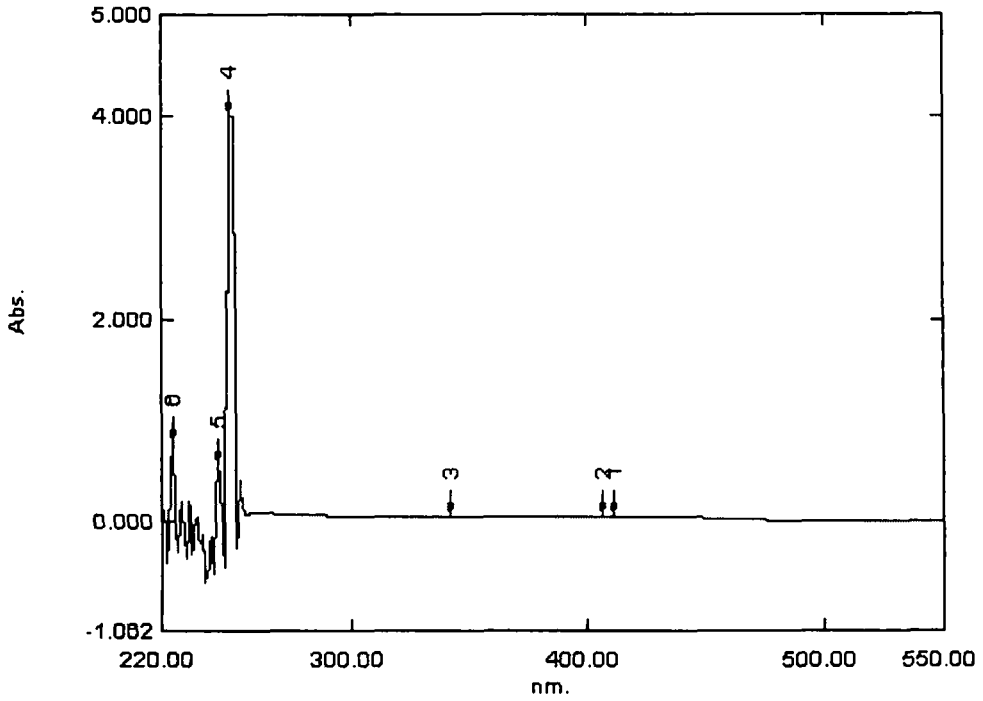

UV-VIS spectra of the complex $[VO(L_3)]_2$ (7)

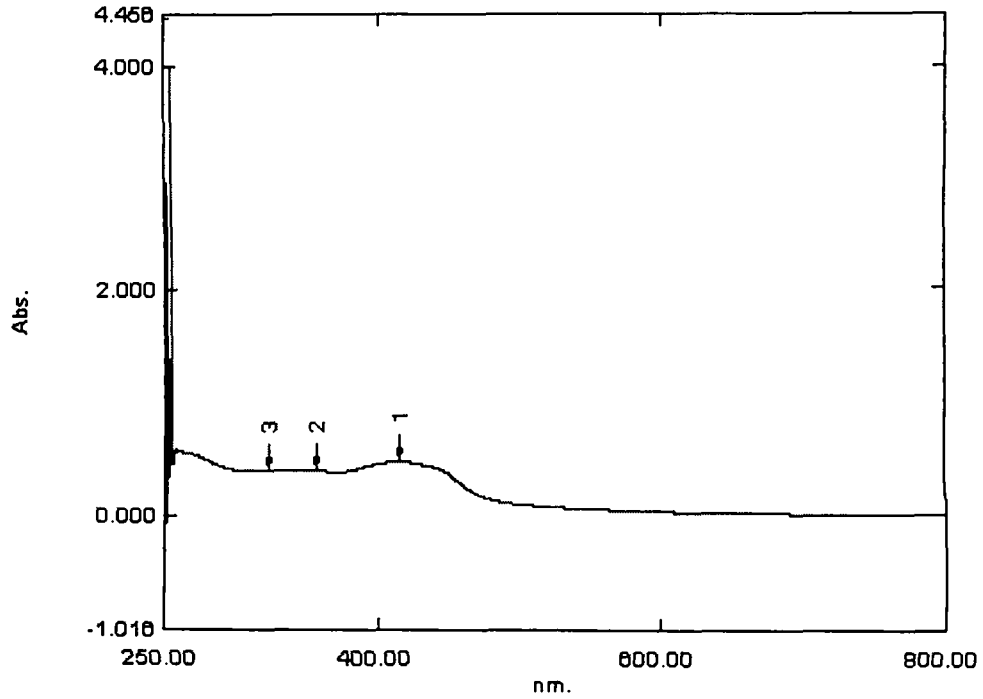

UV-VIS spectra of the complex $[VO(L_4)]_2$ (8)

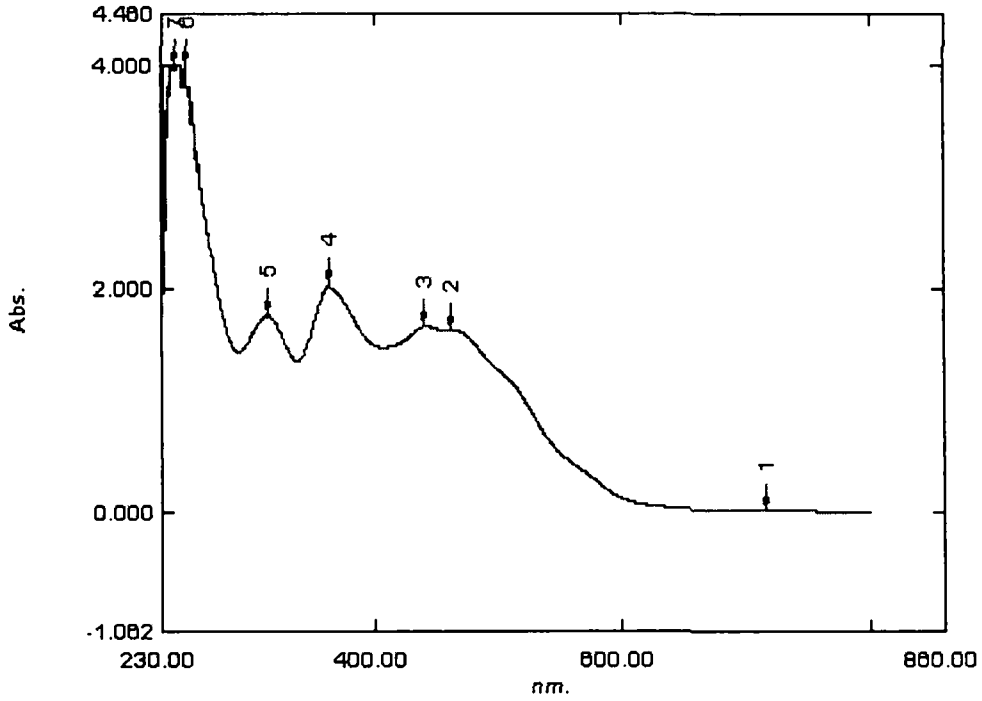

UV-VIS spectra of the complex $[Fe(L_5)Cl]_2$ **(9)**

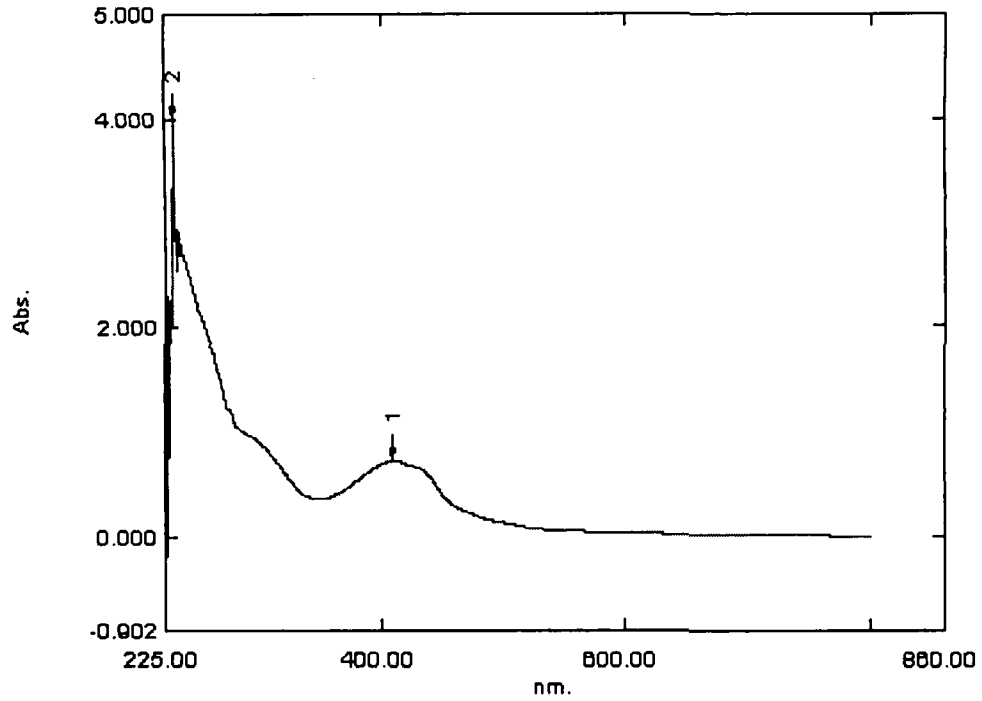

UV-VIS spectra of the complex $[VO(L_5)]_2.H_2O$ **(10)**

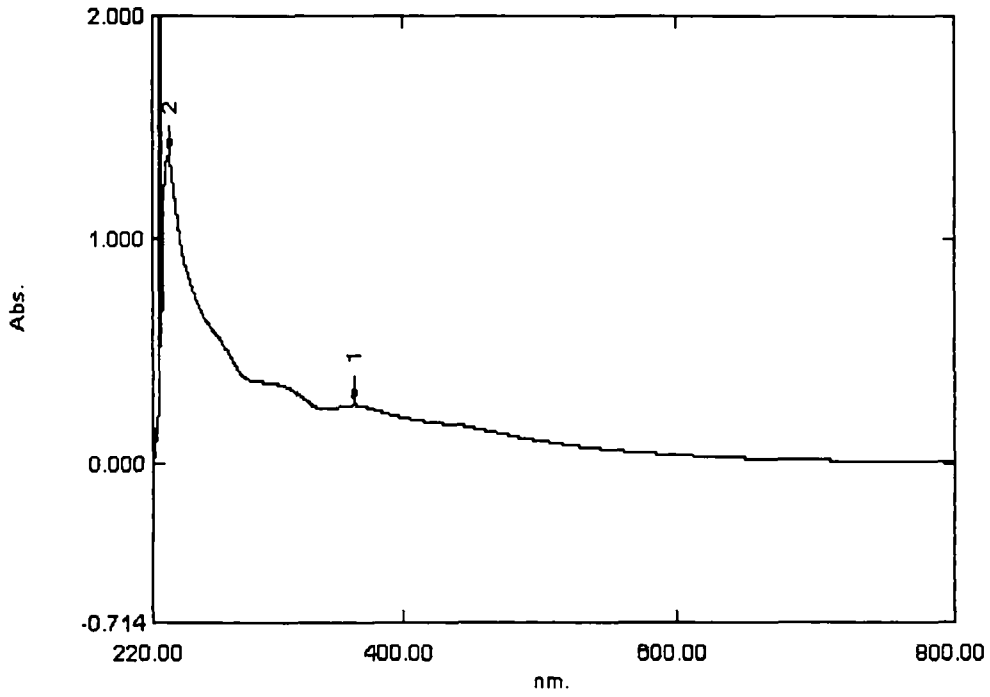

UV-VIS spectra of the complex **[Fe(L_5)Cl(PPh_3)] (11)**

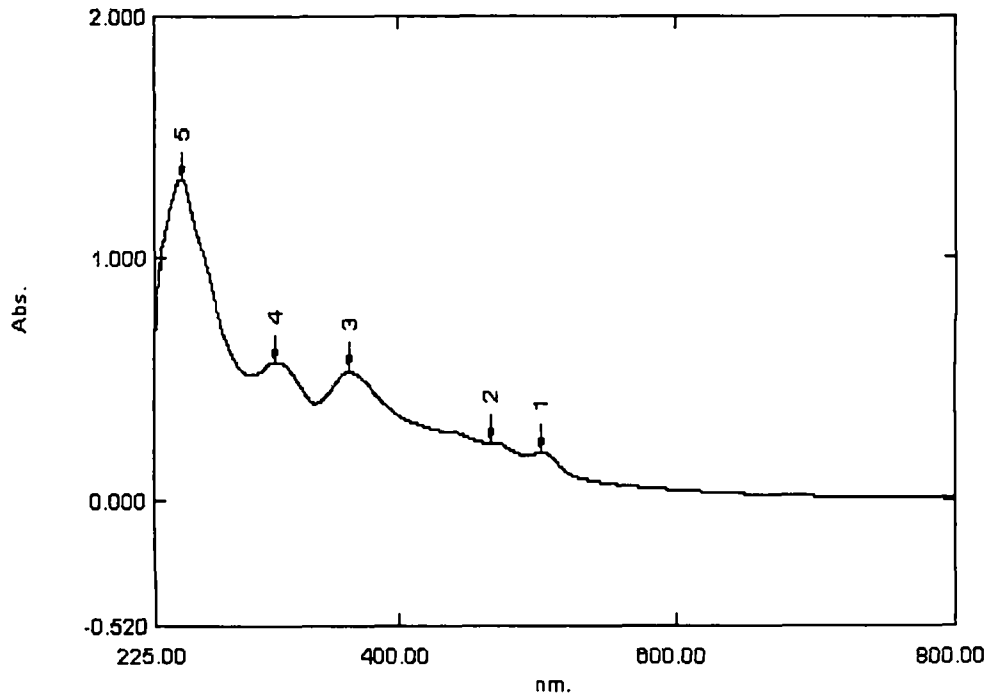

UV-VIS spectra of the complex **[Fe(L_5)Cl(Imz)] (12)**

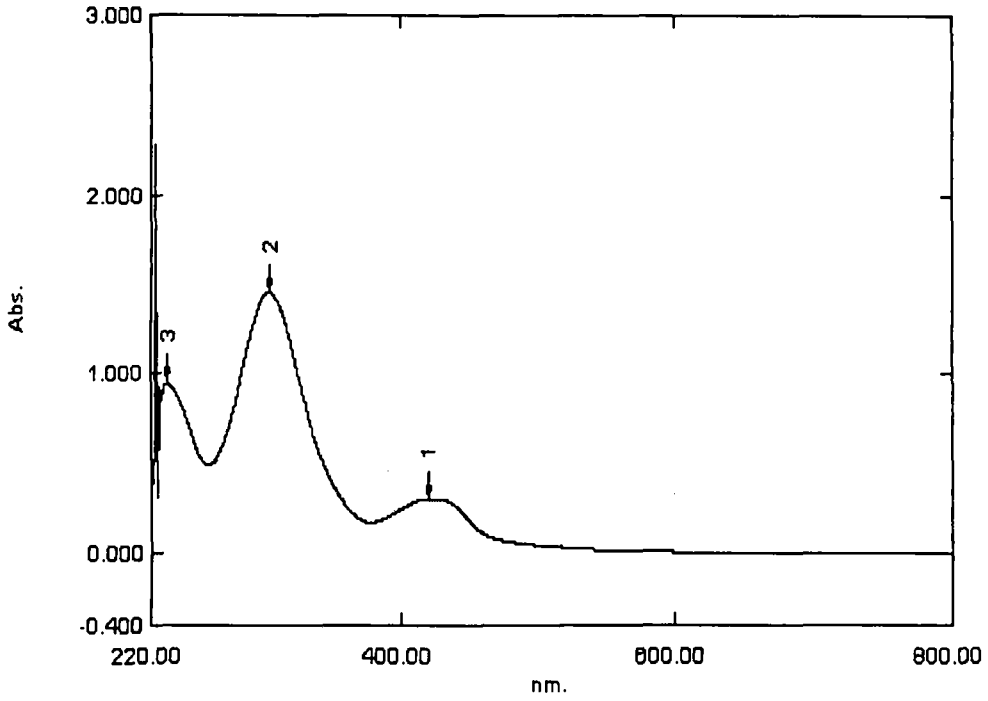

UV-VIS spectra of the complex $[Fe(L_5)(H_2O)]_2$ **(13)**

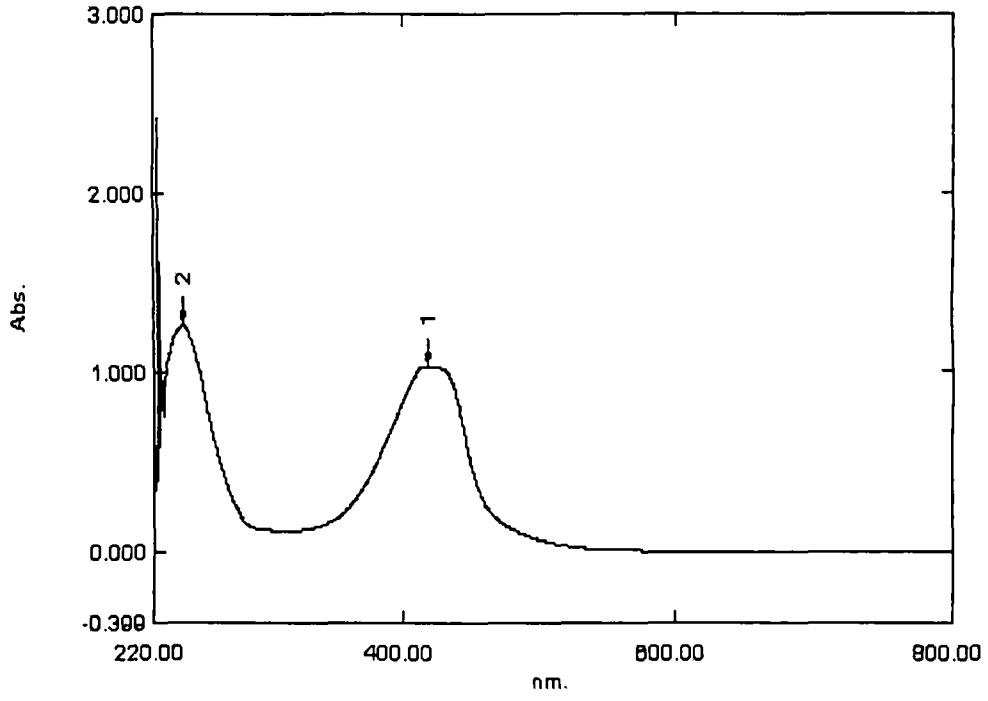

UV-VIS spectra of the complex $Na[VO_2(L_5)]$ **(14)**

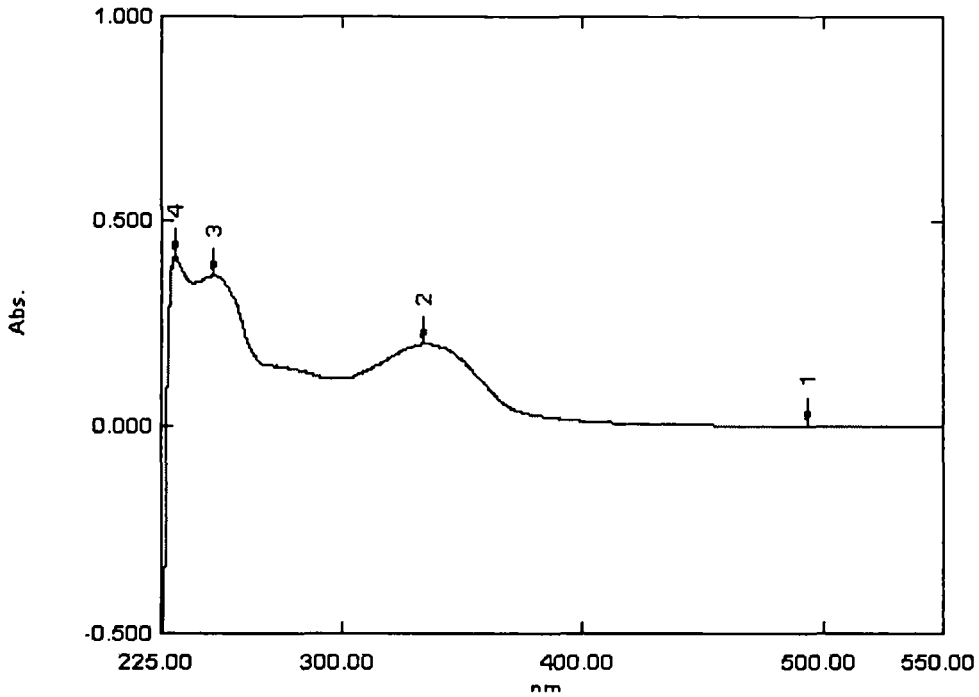

UV-VIS spectra of the complex **$Fe(L_6)Cl$ (15)**

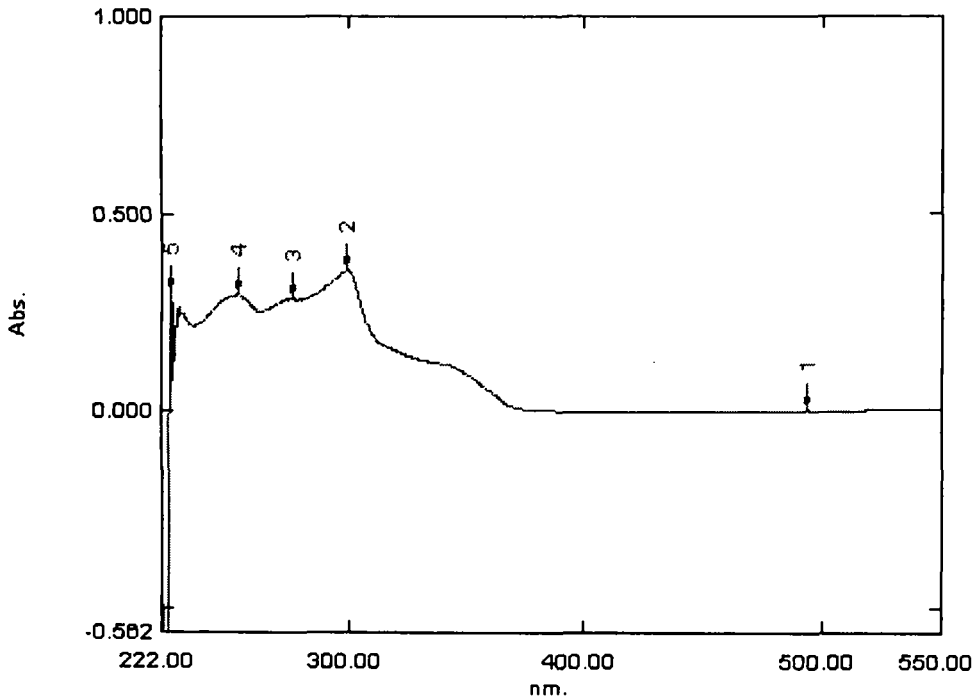

UV-VIS spectra of the complex **$[VO(L_6)(H_2O)].H_2O$ (16)**

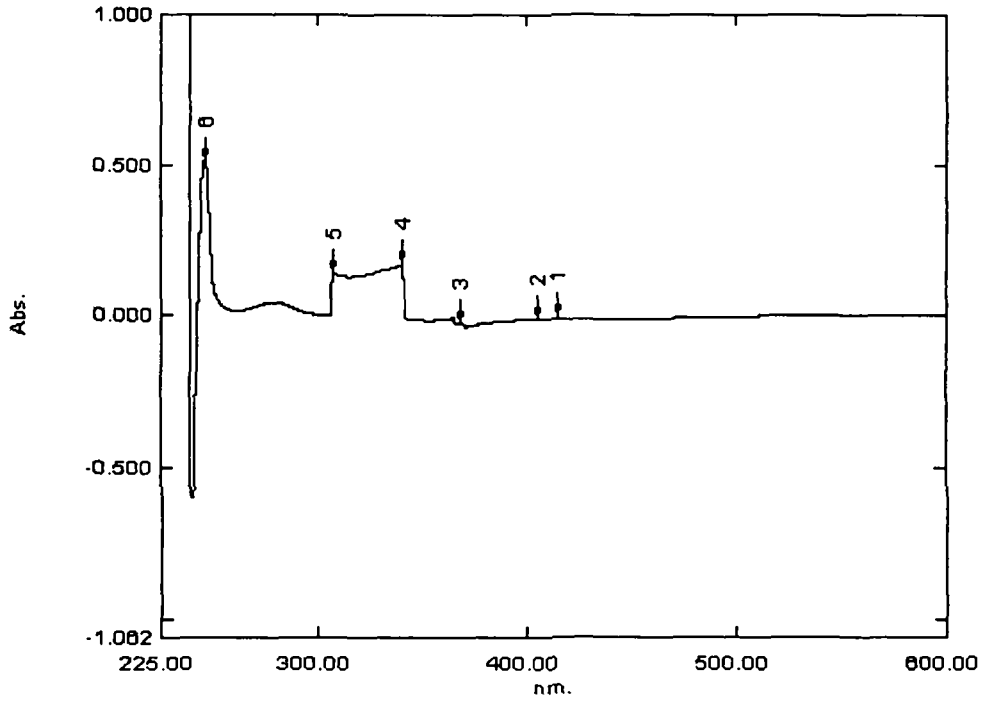

UV-VIS spectra of the complex **[Fe(L_7)(acac)(EtOH)] (17)**

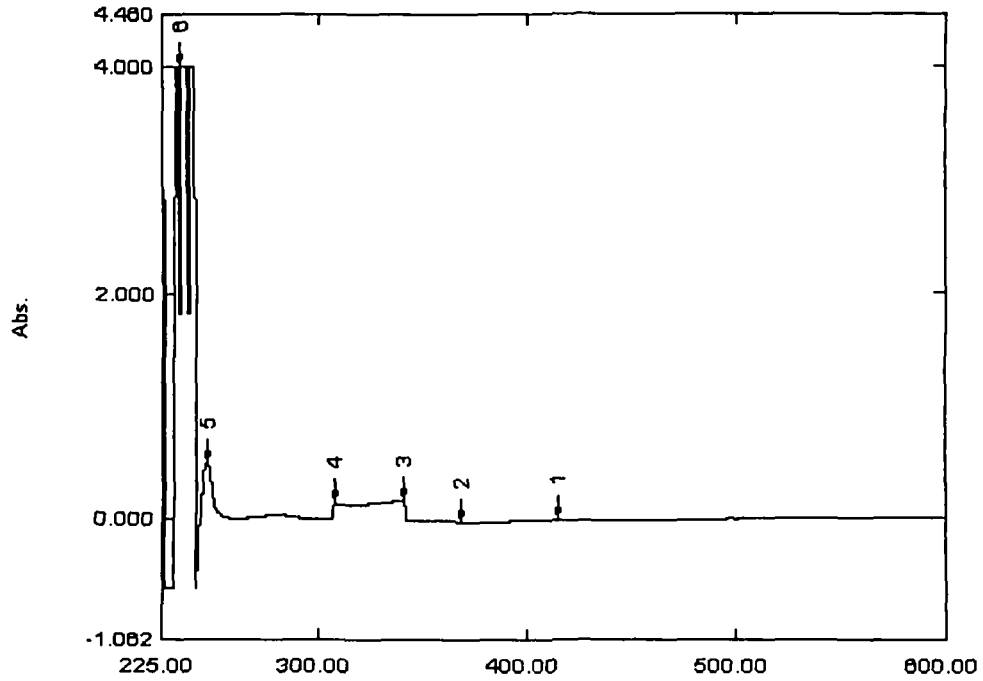

UV-VIS spectra of the complex **[Fe(L_8)(acac)(EtOH) (18)**

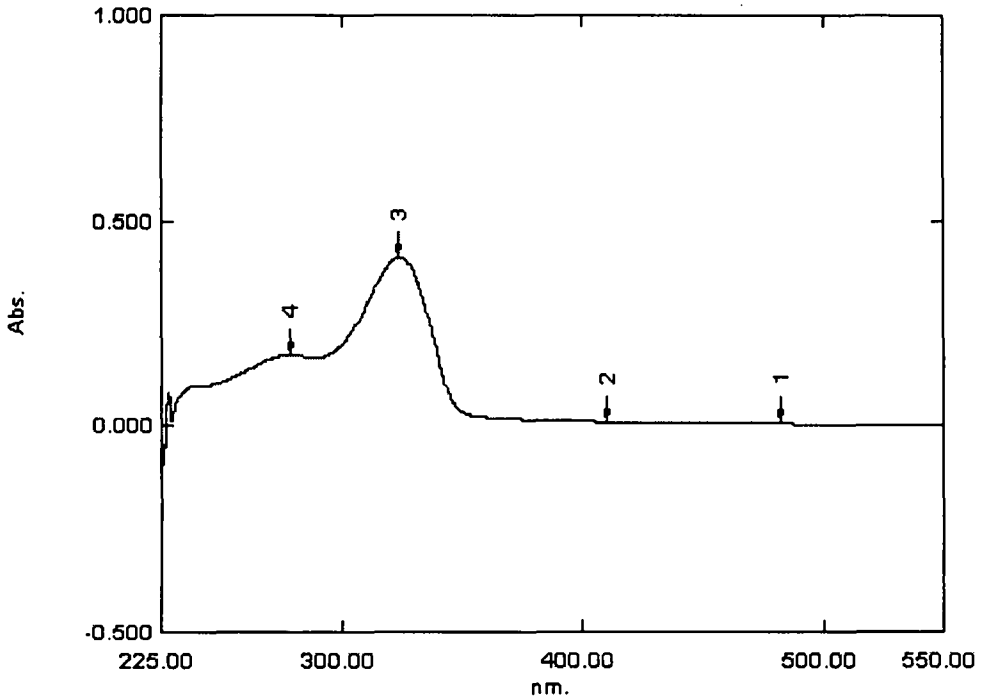

UV-VIS spectra of the complex $[Fe(L_9)(H_2O)_2]NO_3$ (19)

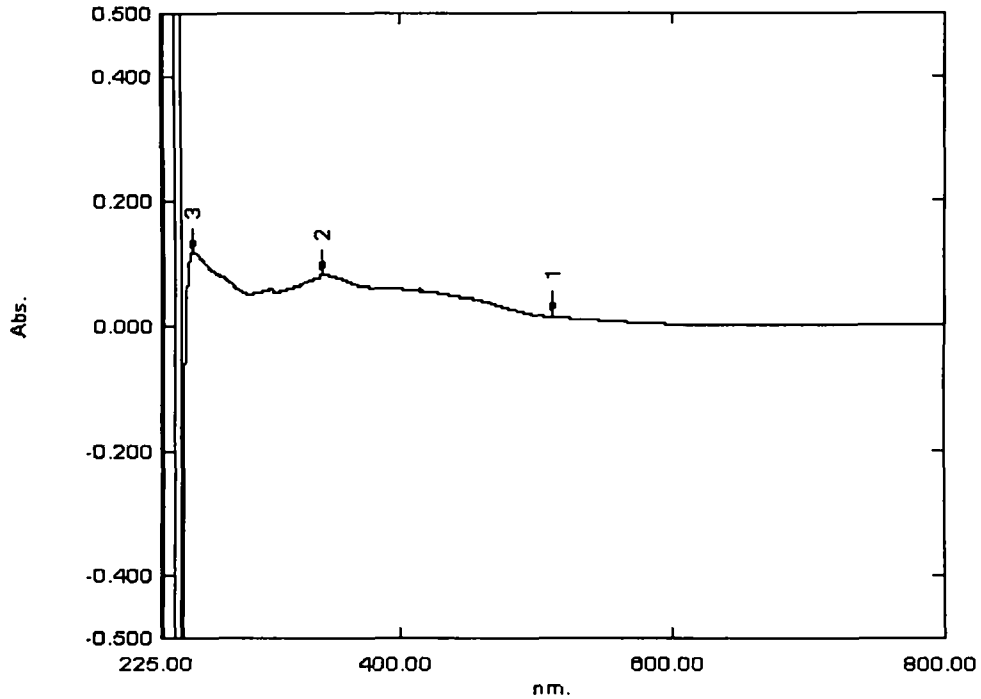

UV-VIS spectra of the complex $[Fe(L_{11})(H_2O)_2]NO_3$ (20)

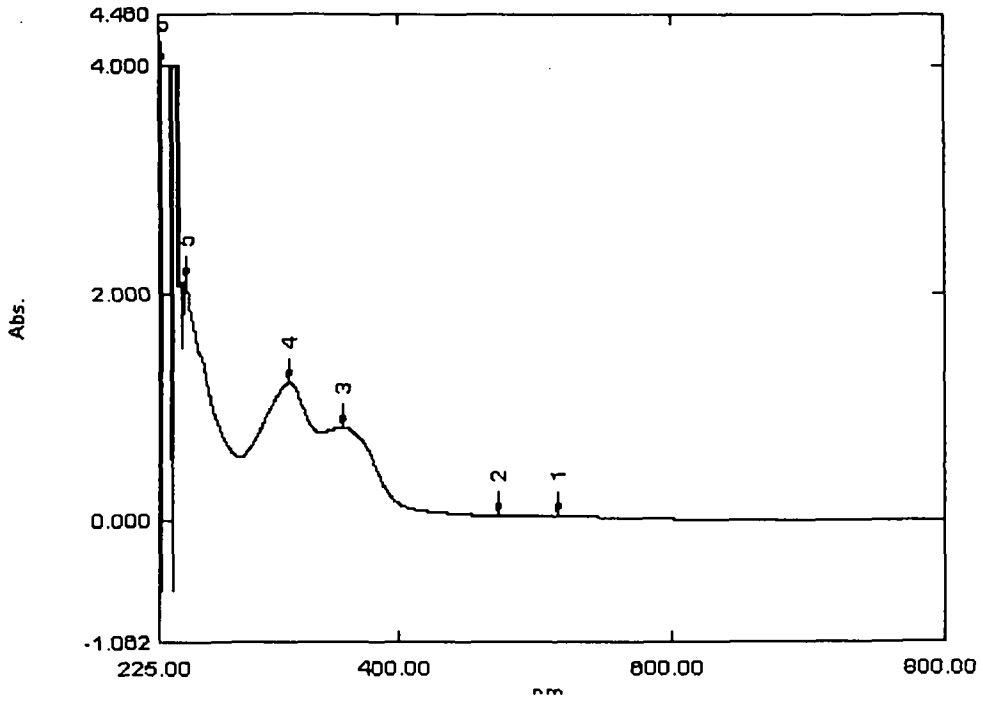

UV-VIS spectra of the complex $[Fe(L_{12})(H_2O)_2]NO_3$ (21)

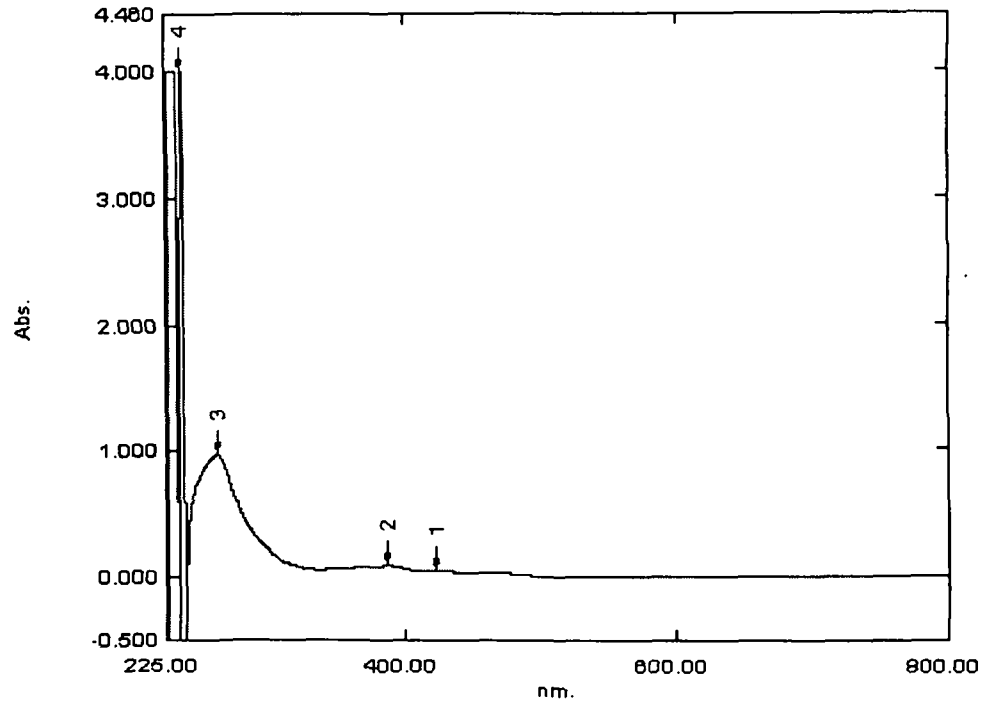

UV-VIS spectra of the complex $[Fe(L_{13})(NO_3)(H_2O)]$ (22)

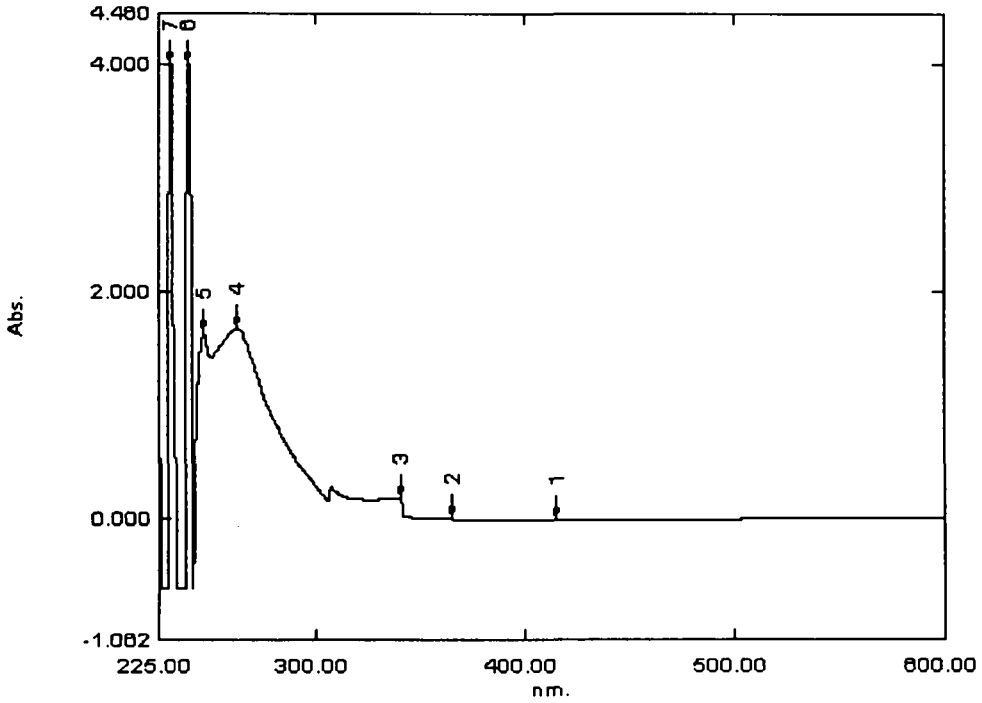

UV-VIS spectra of the complex **$[Fe(L_{14})(NO_3)(H_2O)]$ (23)**

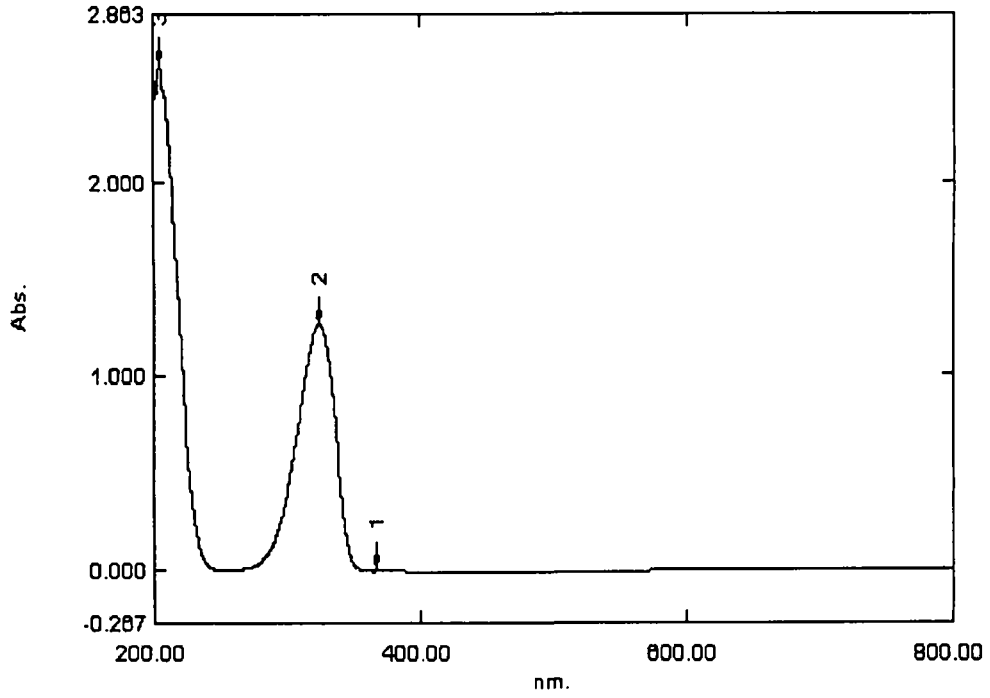

UV-VIS spectra of the complex **$NH_4[Fe(L_9)F_2]$ (24)**

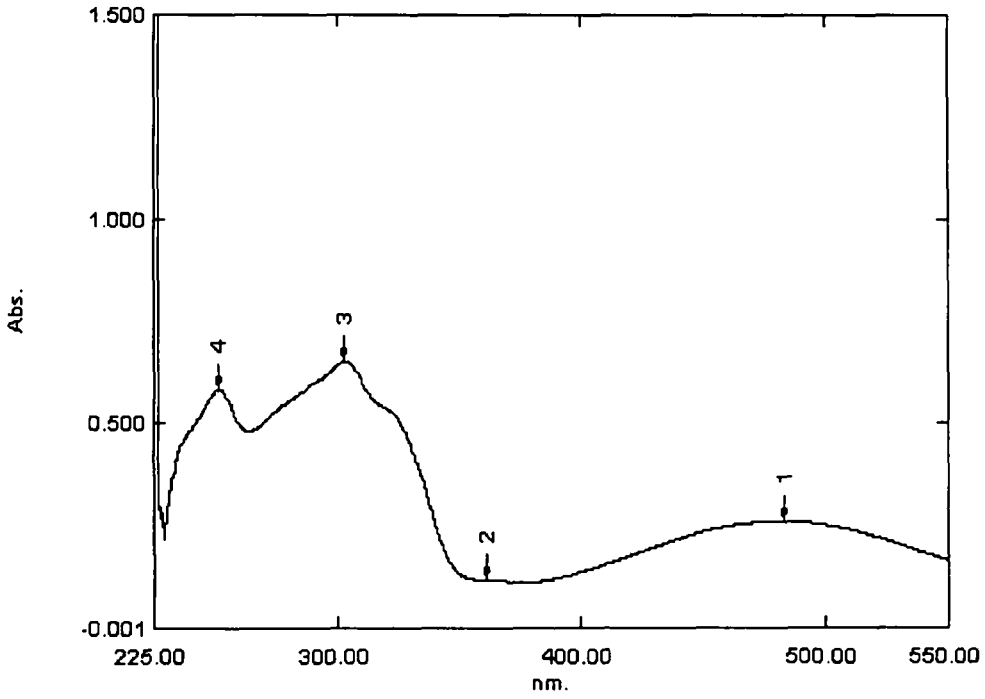

UV-VIS spectra of the complex $NH_4[Fe(L_9)(NCS)_2]$ **(25)**

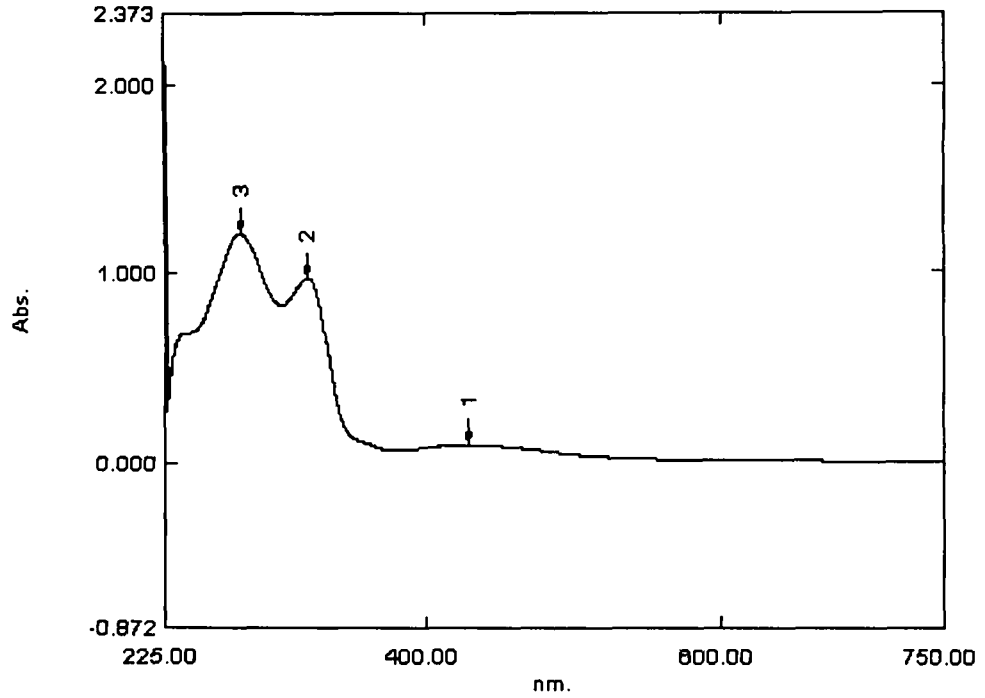

UV-VIS spectra of the complex $Na[Fe(L_9)(N_3)_2]$ **(26)**

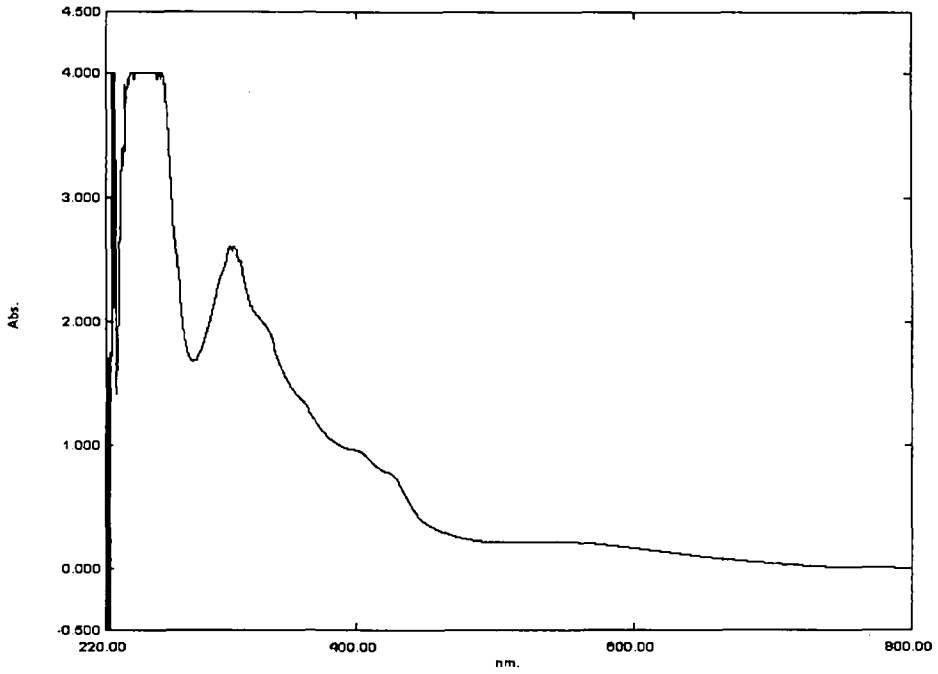

UV-VIS spectra of the complex $[Fe(L_{12})(Im)_2]NO_3$ (27)

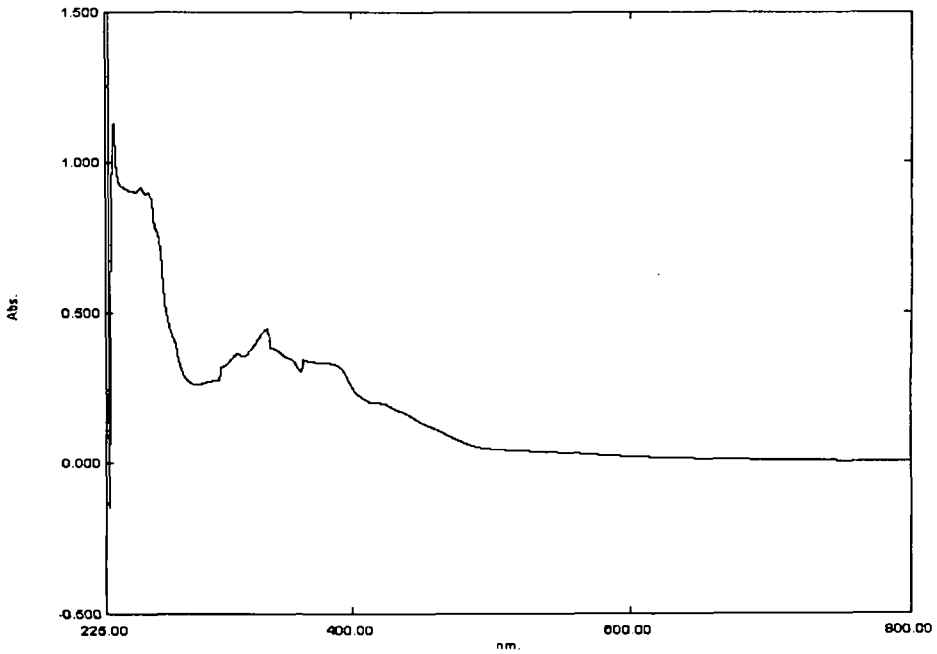

UV-VIS spectra of the complex $[Fe(L_{12})(Py)_2]NO_3$ (28)

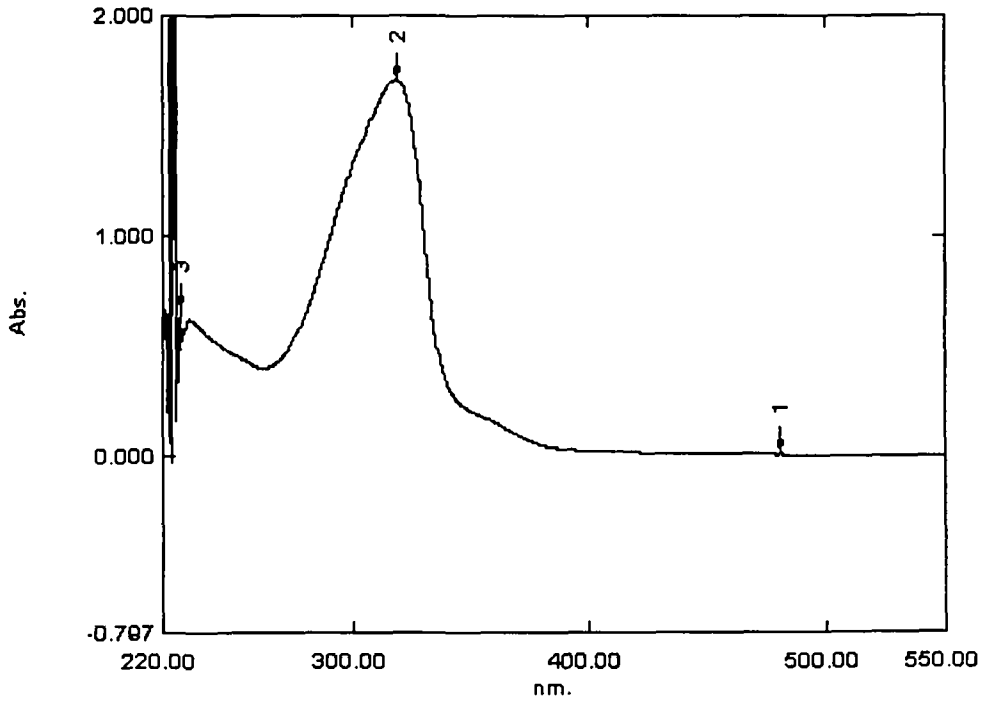

UV-VIS spectra of the complex $[VO(L_9)].H_2O$ (29)

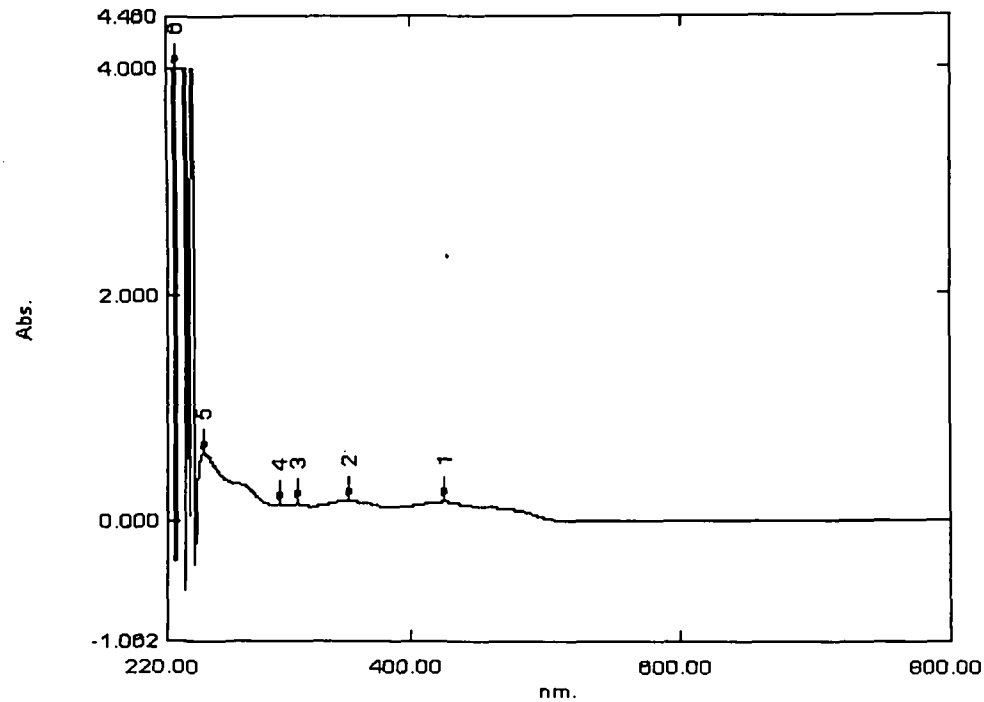

UV-VIS spectra of the complex $[VO(L_{11})].H_2O$ (30)

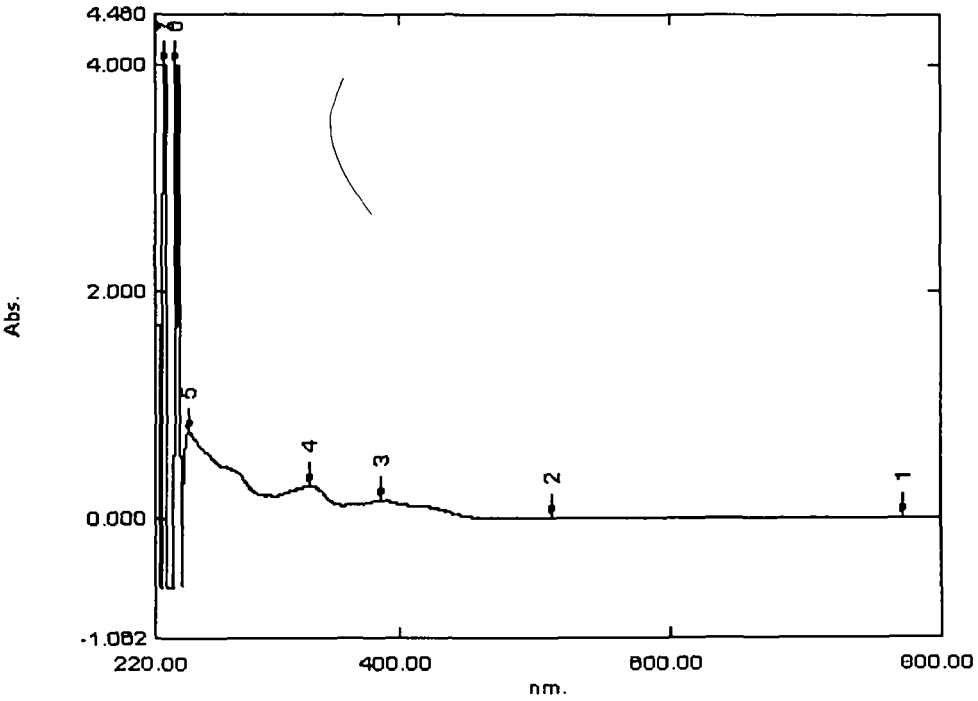

UV-VIS spectra of the complex $[VO(L_{12})].H_2O$ (31)

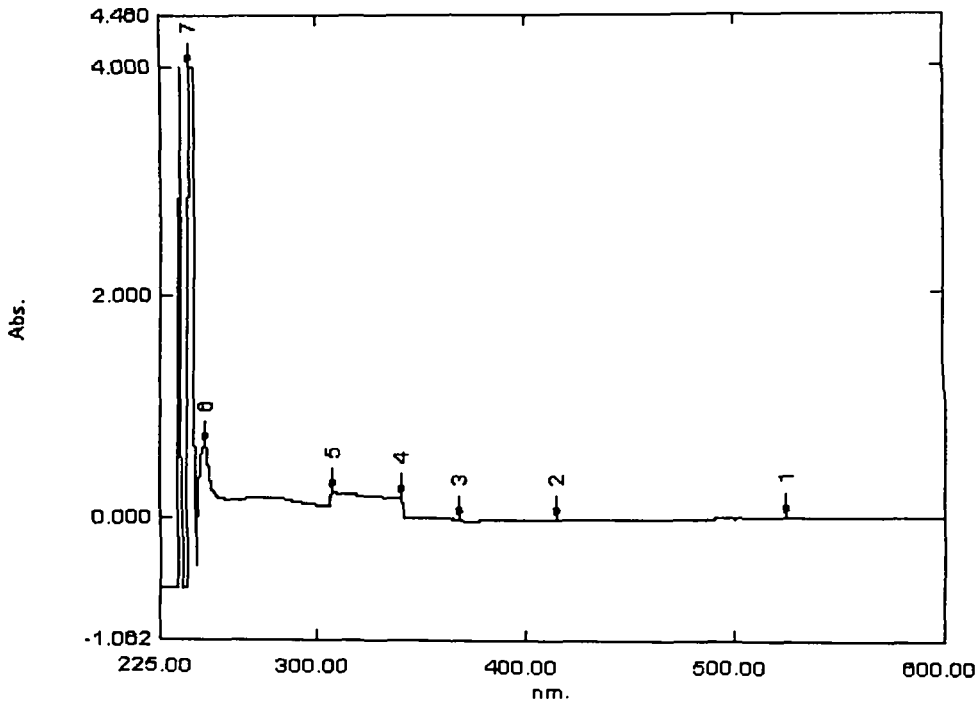

UV-VIS spectra of the complex $[VO(L_{13})].H_2O$ (32)

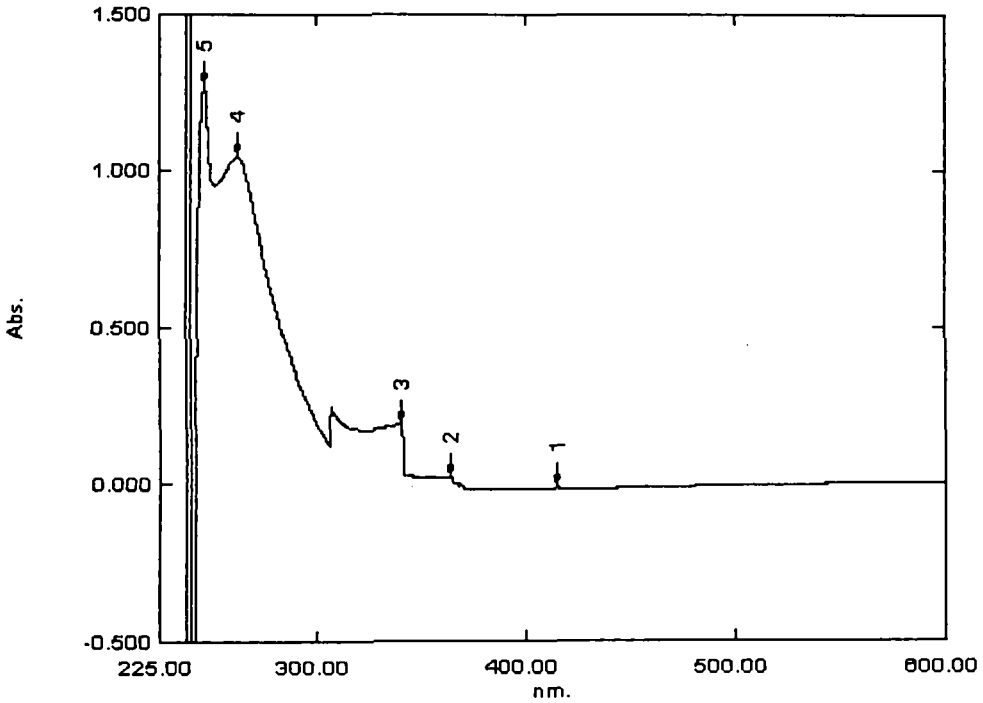

UV-VIS spectra of the complex $[VO(L_{14})].H_2O$ **(33)**

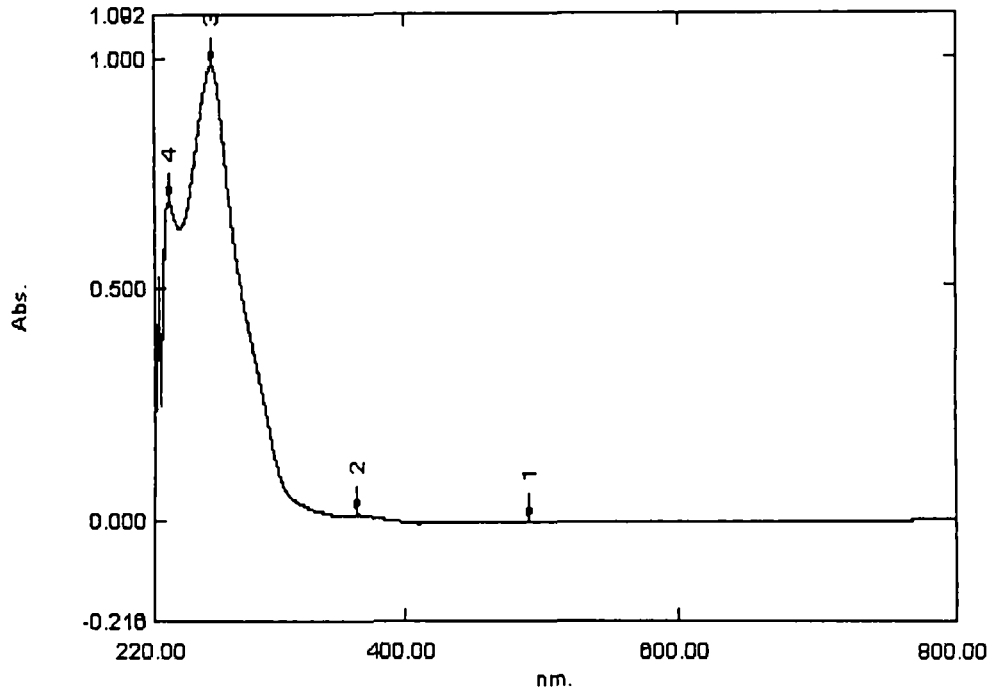

UV-VIS spectra of the complex $[Fe(L_{15})Cl_2]Cl$ **(34)**

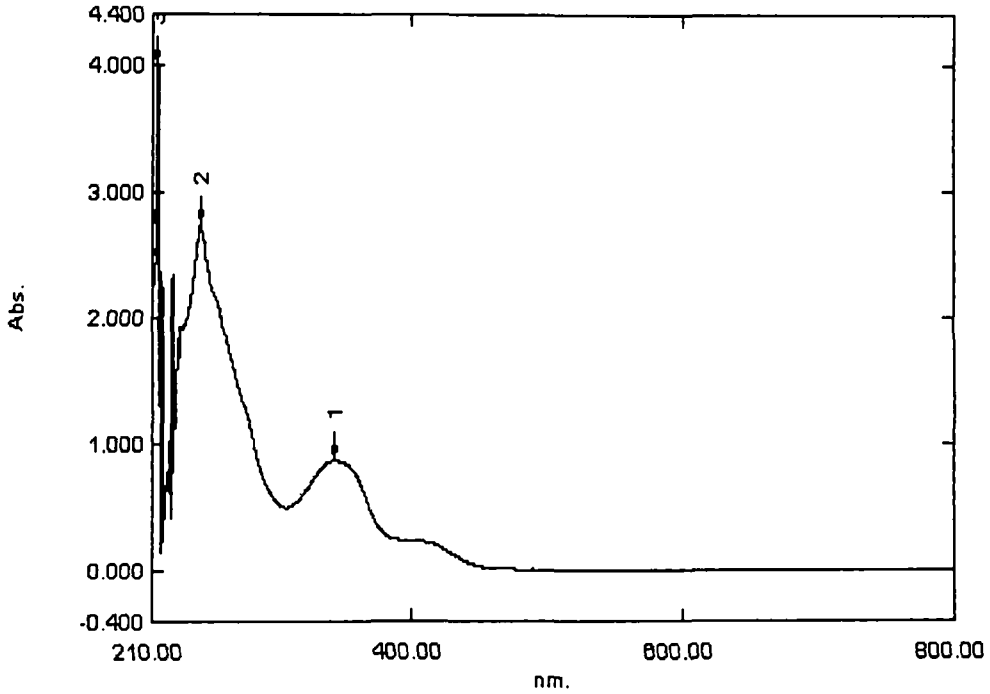

UV-VIS spectra of the complex $[Fe(L_{16})Cl_2]Cl$ **(35)**

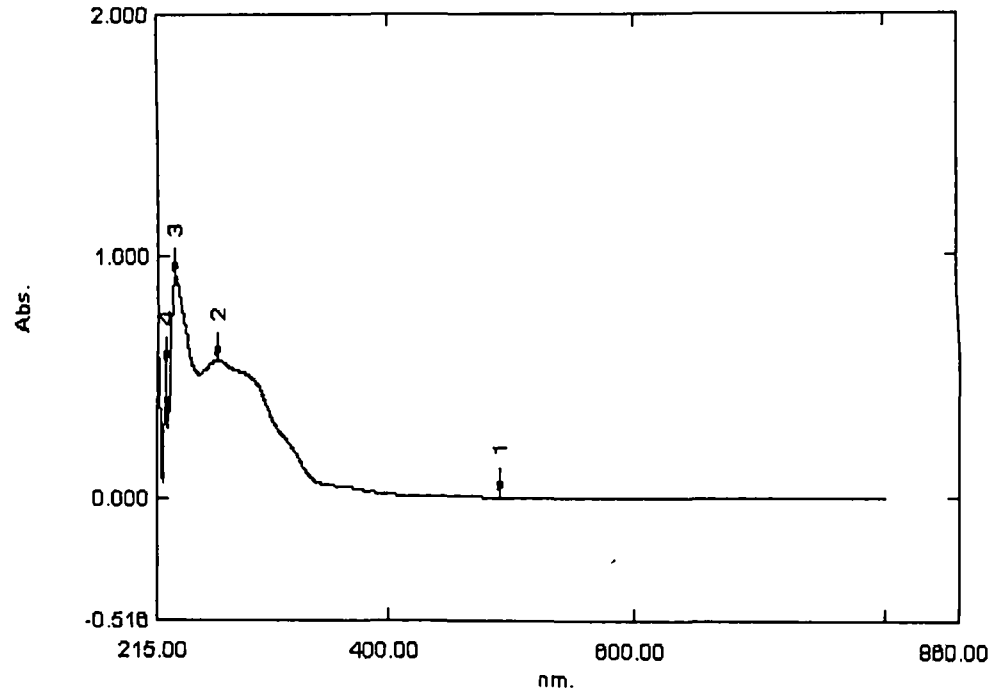

UV-VIS spectra of the complex $[VO(L_{15})]SO_4.H_2O$ **(36)**

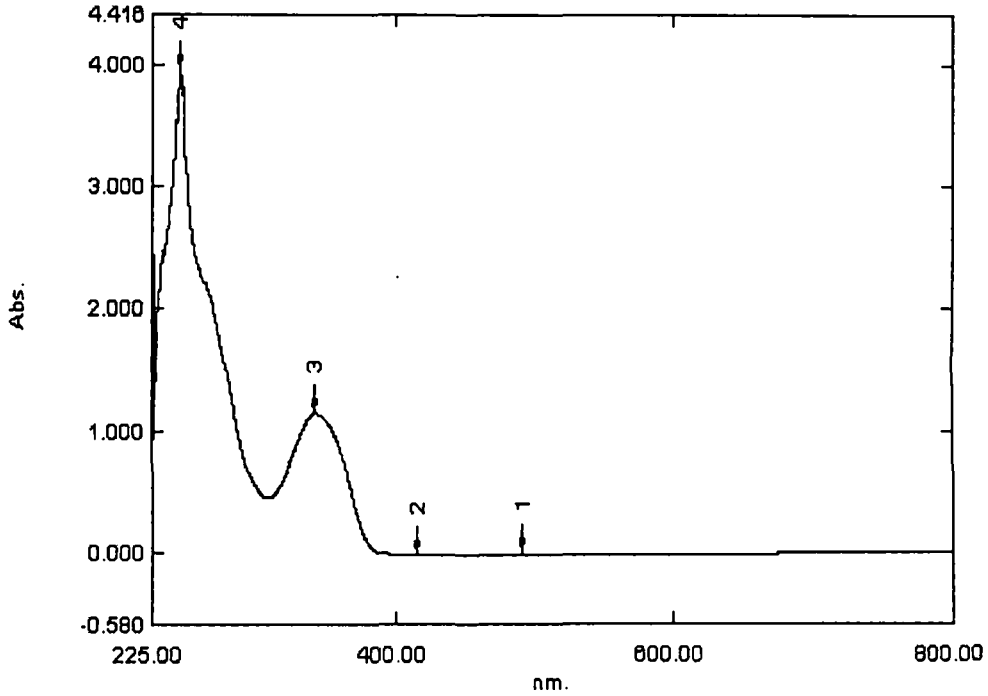

UV-VIS spectra of the complex $[VO(L_{16})]SO_4.H_2O$ (37)

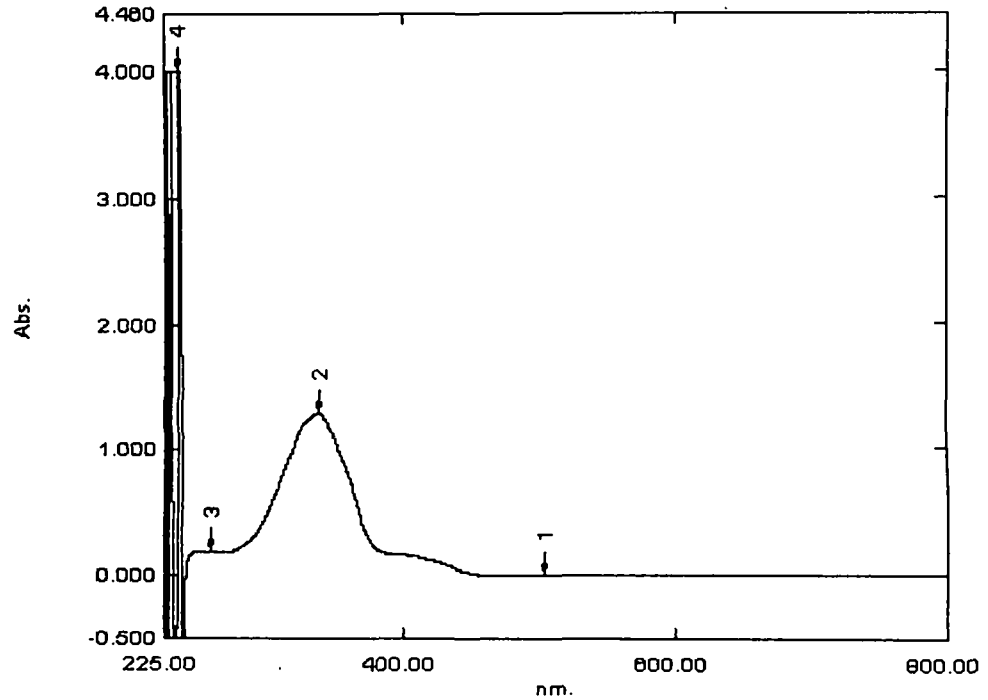

UV-VIS spectra of the complex $[Fe(L_{10})(H_2O)_2](NO_3)_3$ (38)

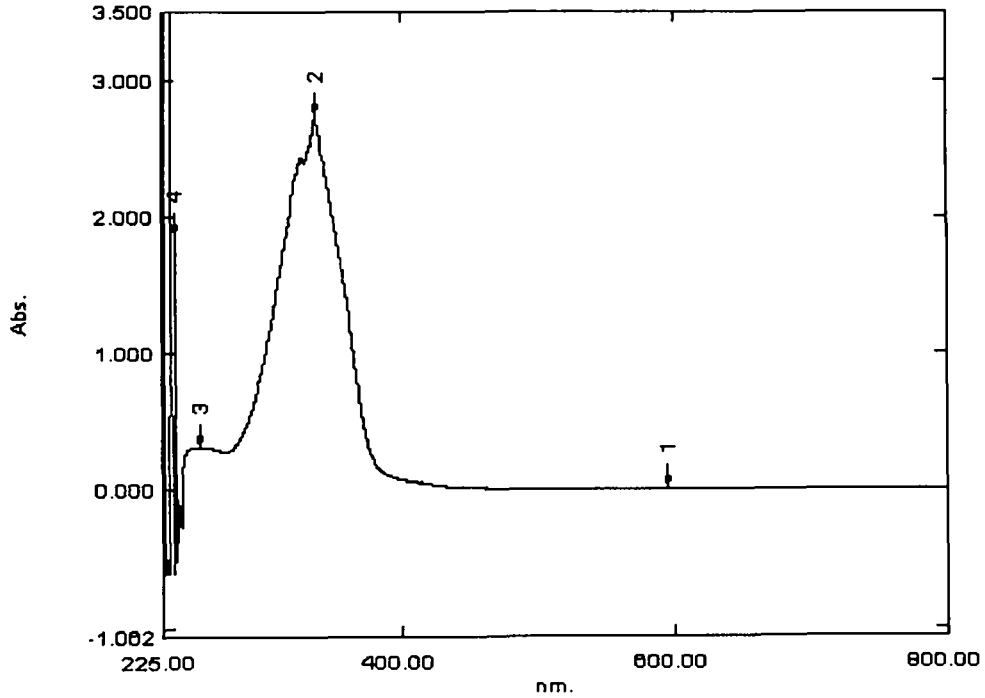

UV-VIS spectra of the complex $[VO(L_{10})]SO_4.H_2O$ (39)

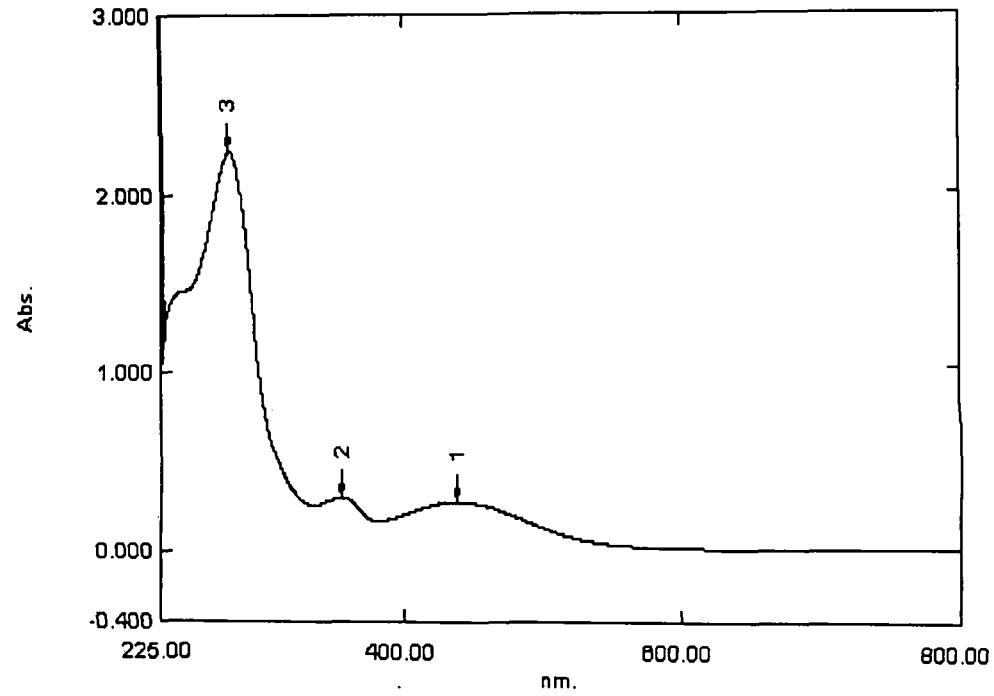

UV-VIS spectra of the complex $[Fe(L_9)(H_2O)_2]$ (40)

APPENDIX 3

^{1}H NMR spectra of the compounds

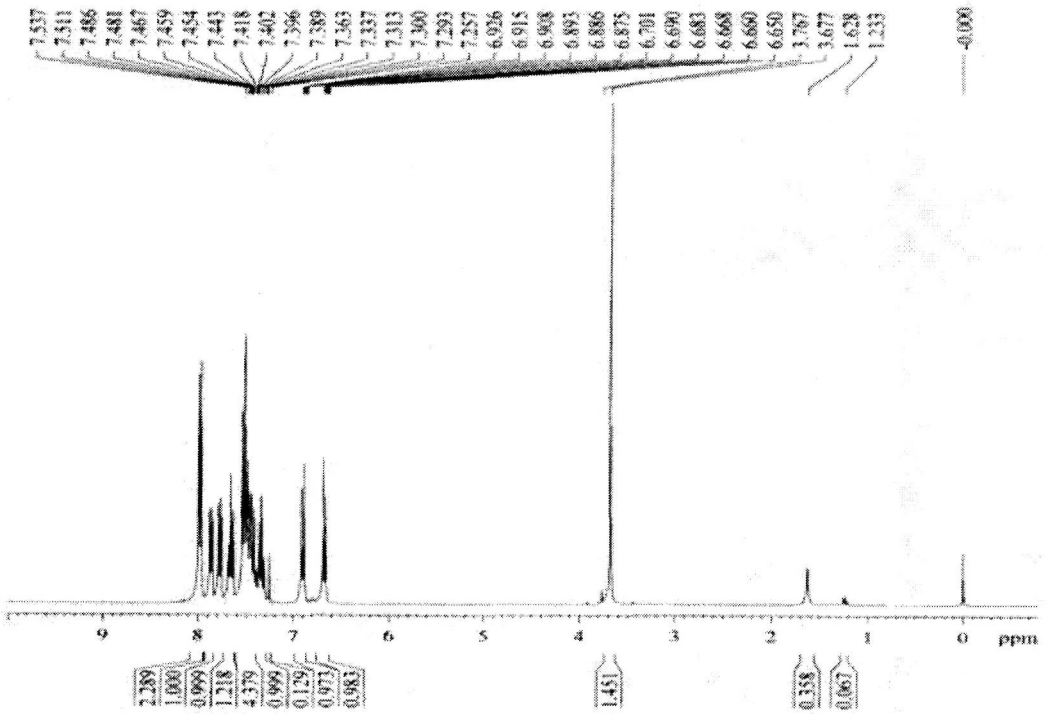

^{1}H NMR spectra of the Schiff base $\mathbf{L_1}$

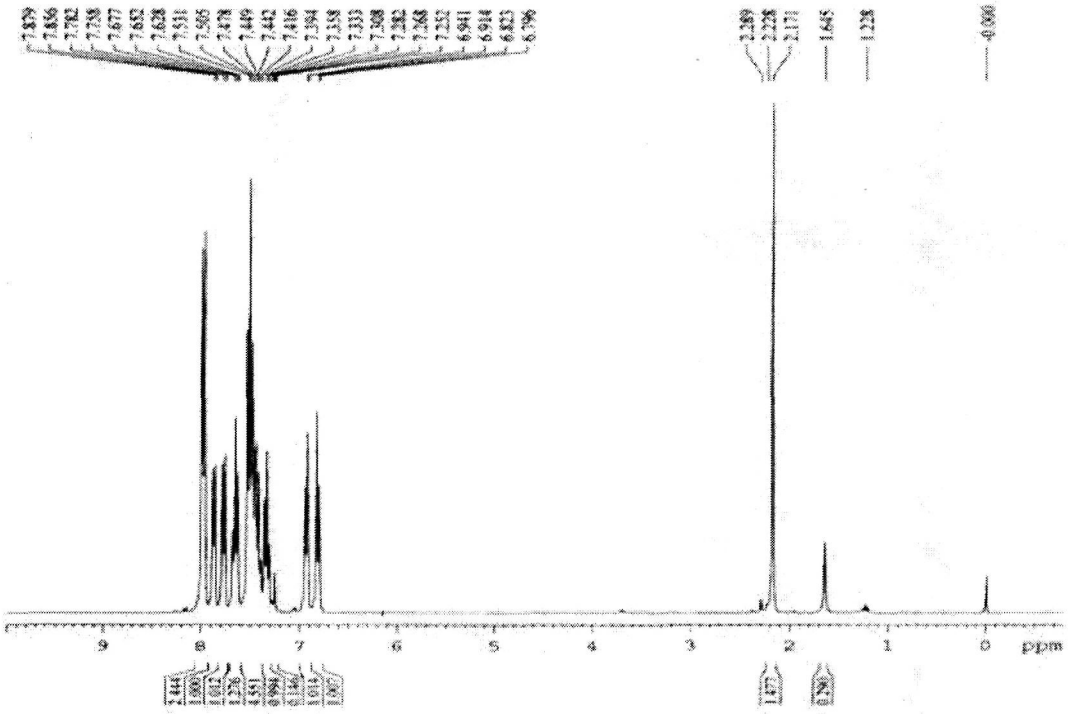

^{1}H NMR spectra of the Schiff base $\mathbf{L_2}$

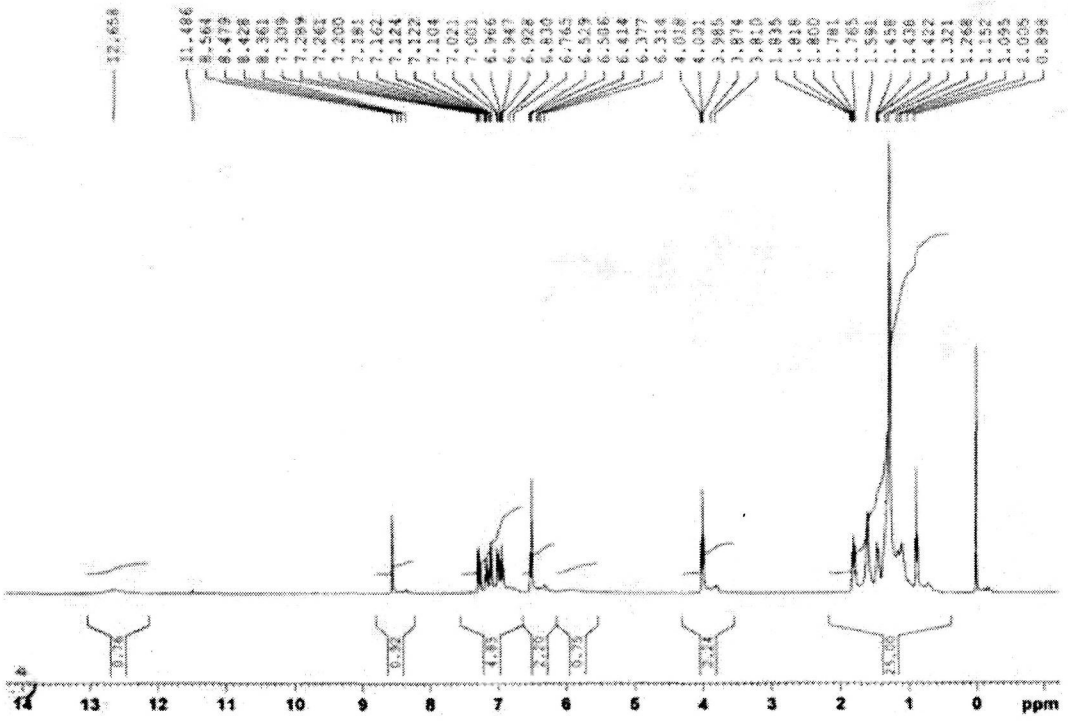

^{1}H NMR spectra of the Schiff base L_3

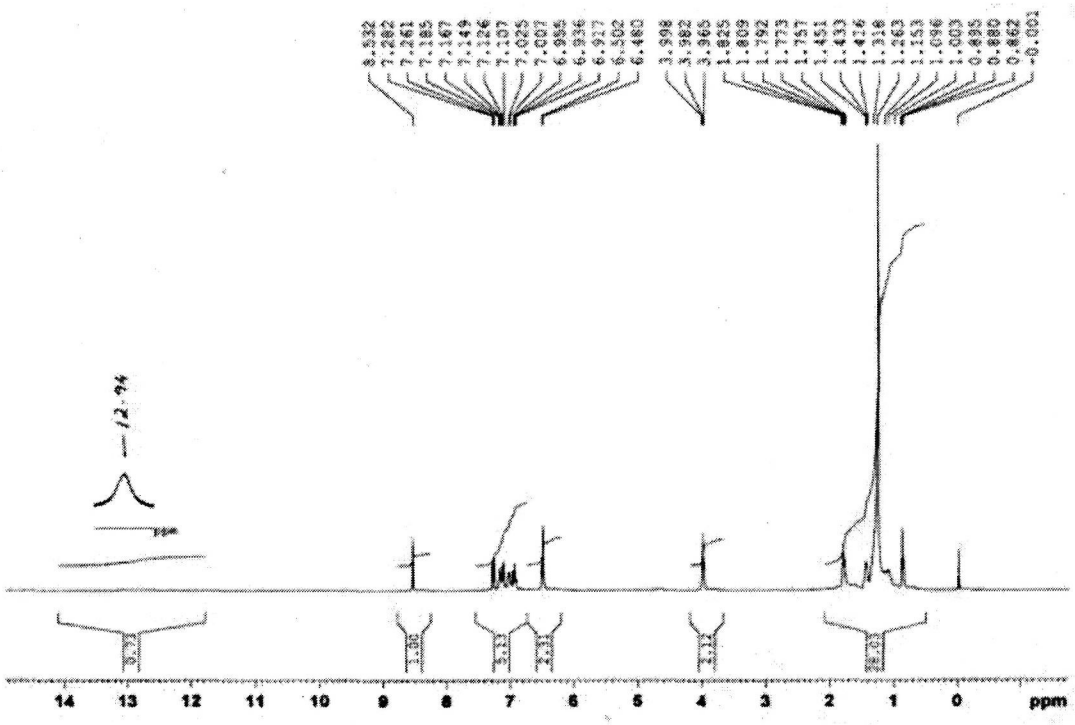

^{1}H NMR spectra of the Schiff base L_4

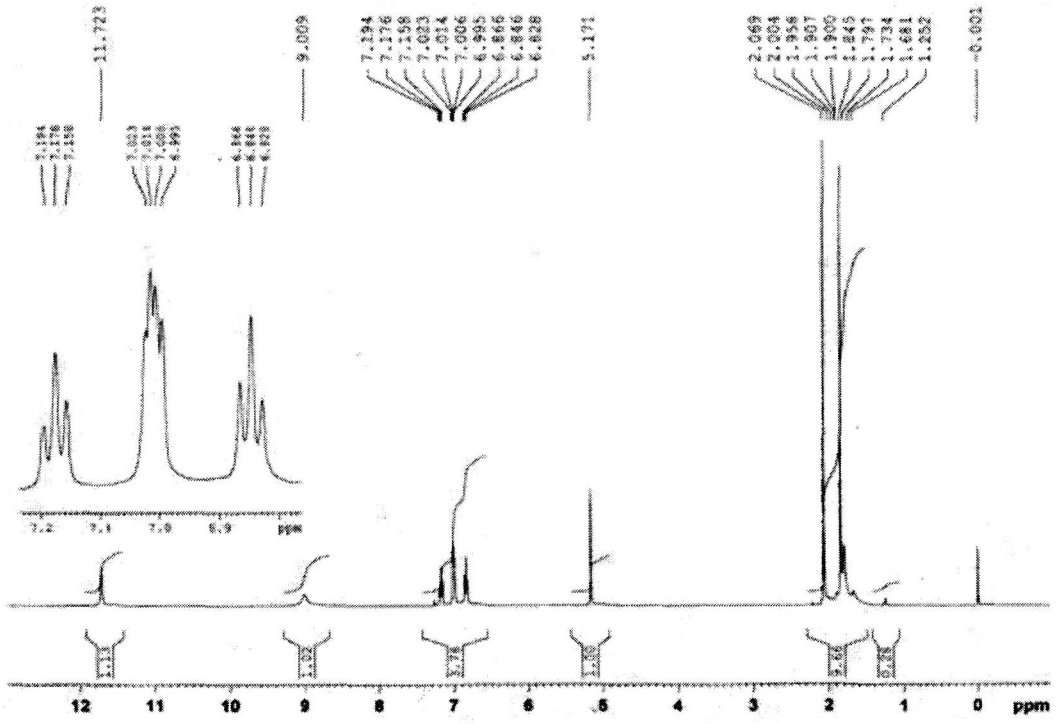

^{1}H NMR spectra of the Schiff base L_5

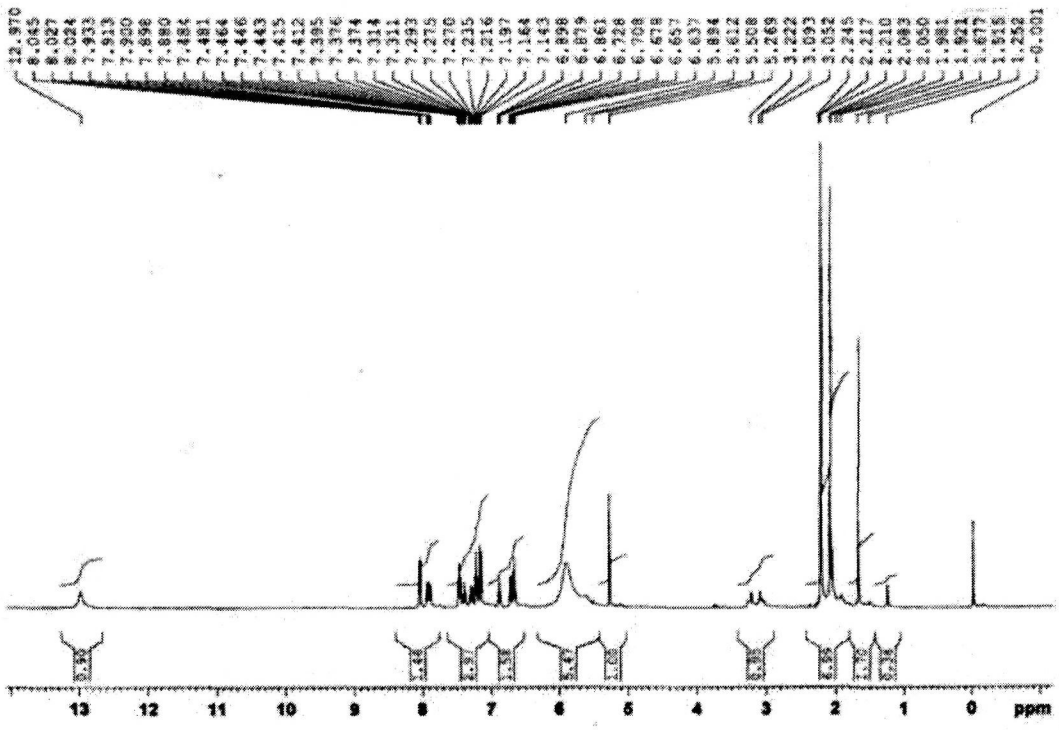

^{1}H NMR spectra of the Schiff base L_6

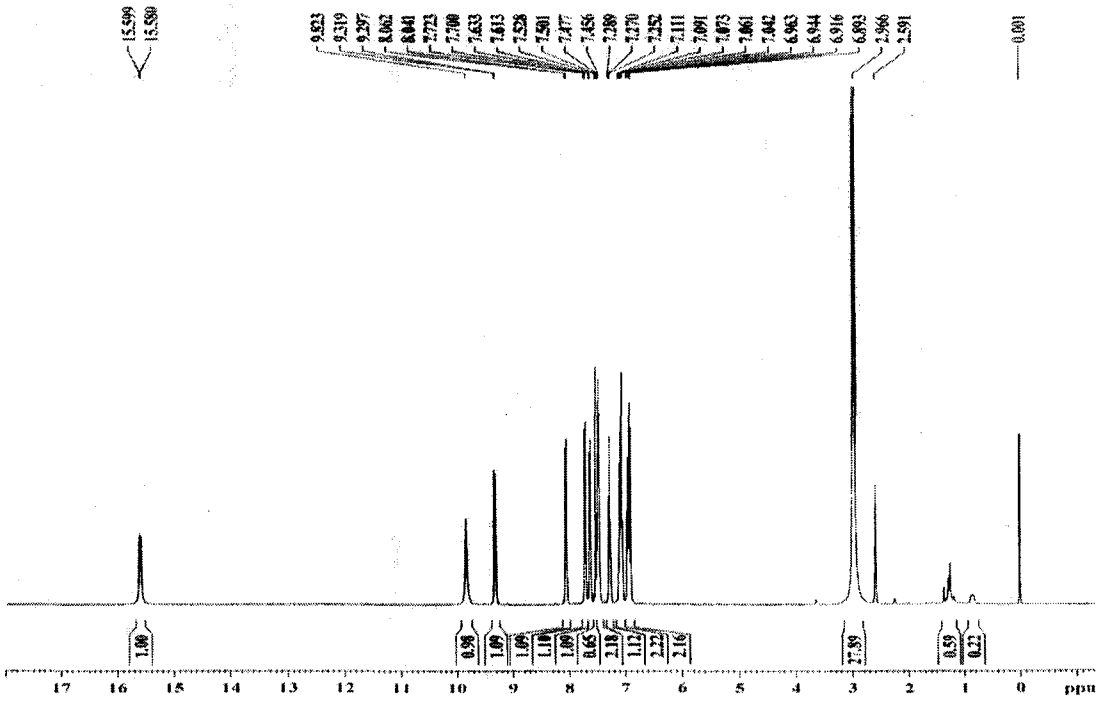

^{1}H NMR spectra o the Schiff base $\mathbf{L_7}$

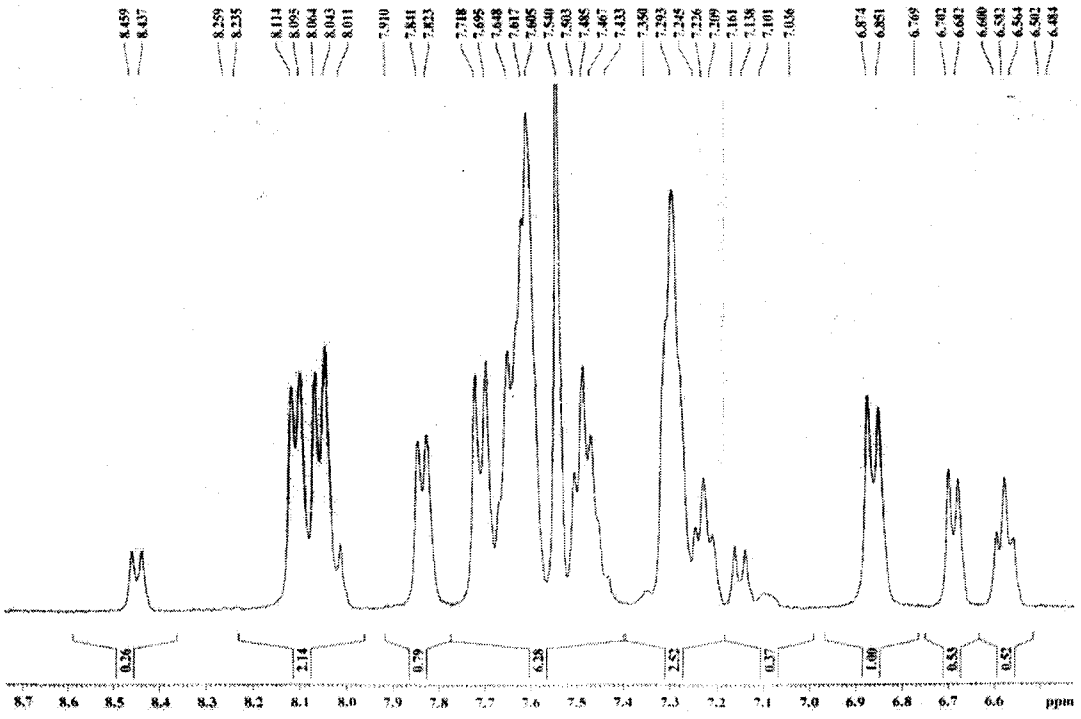

^{1}H NMR spectra of the Schiff base $\mathbf{L_8}$

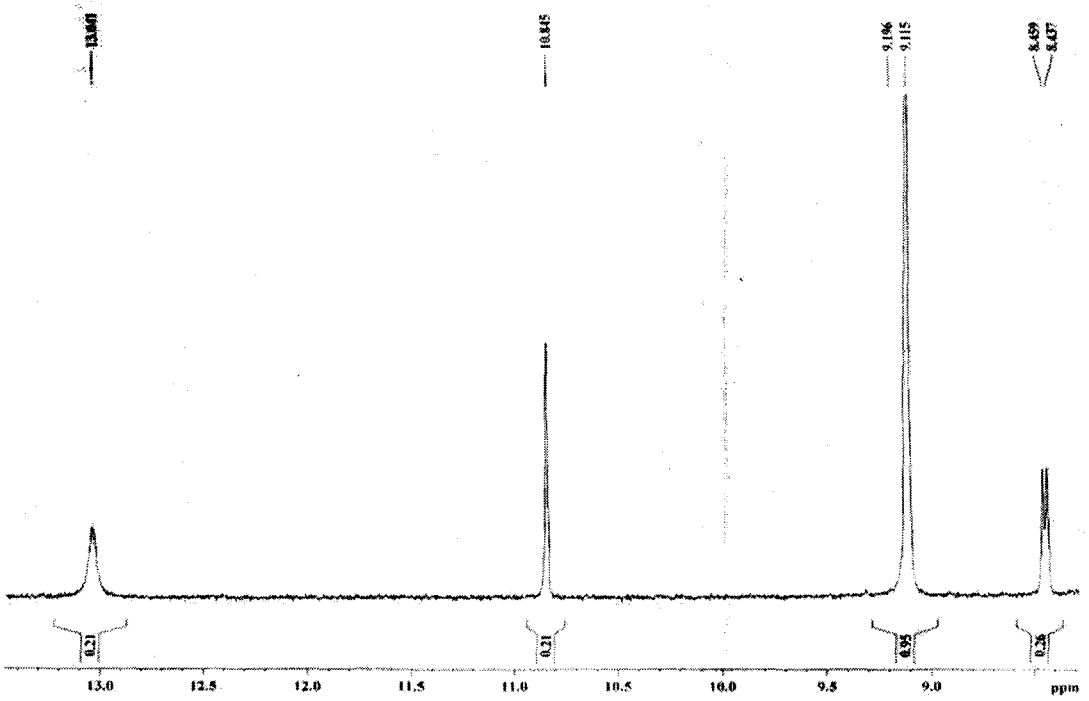

^{1}H NMR spectra of the Schiff base $\mathbf{L_8}$

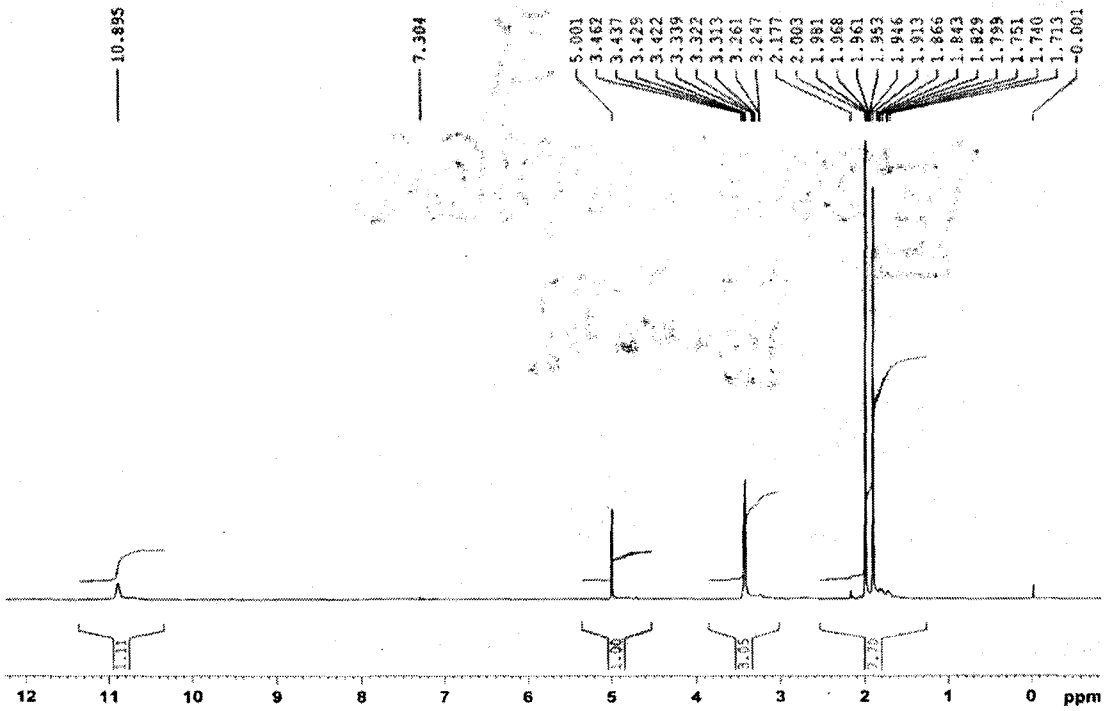

^{1}H NMR spectra of the Schiff base $\mathbf{L_9}$

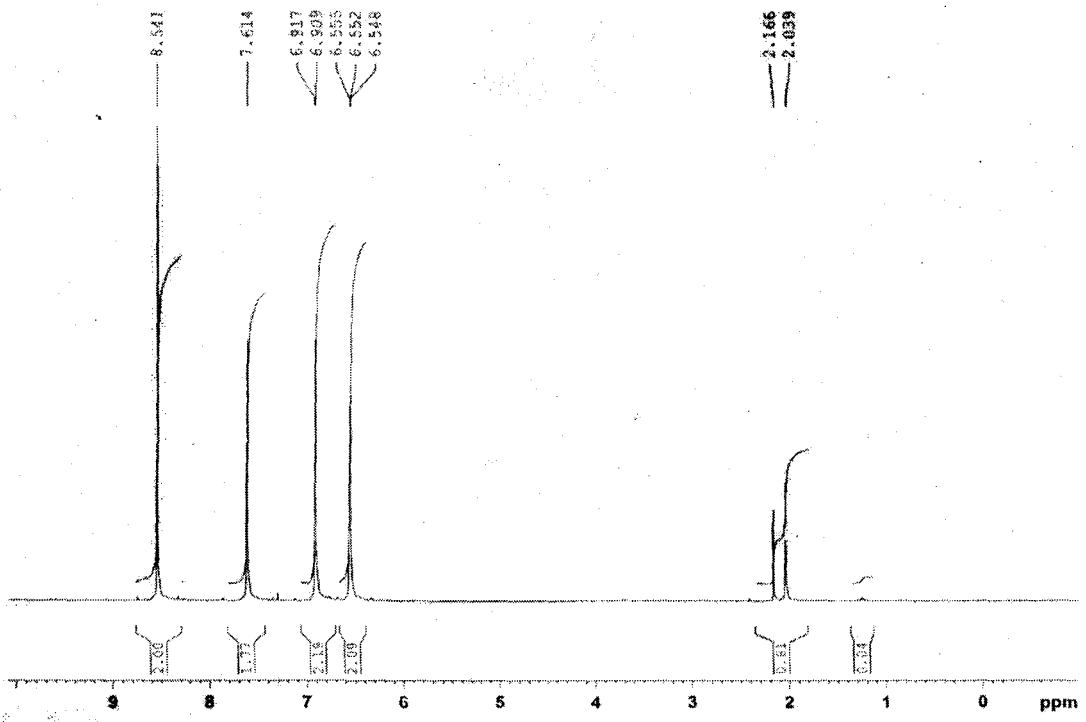

^{1}H NMR spectra of the Schiff base $\mathbf{L_{10}}$

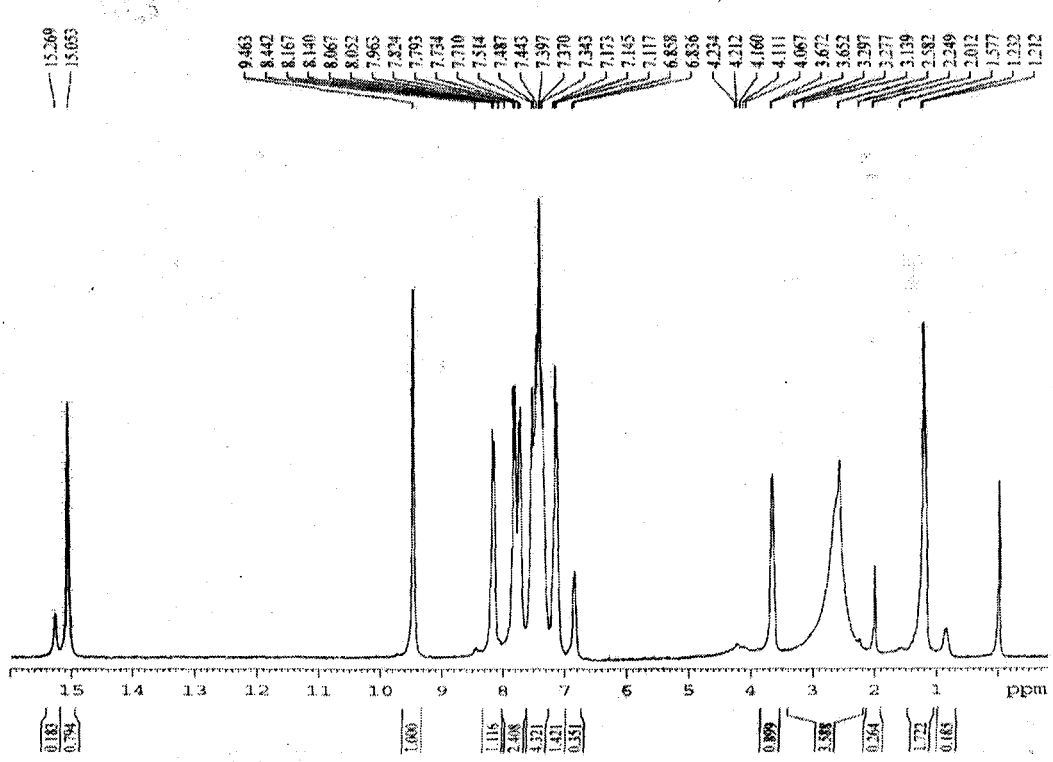

^{1}H NMR spectra of the Schiff base $\mathbf{L_{11}}$

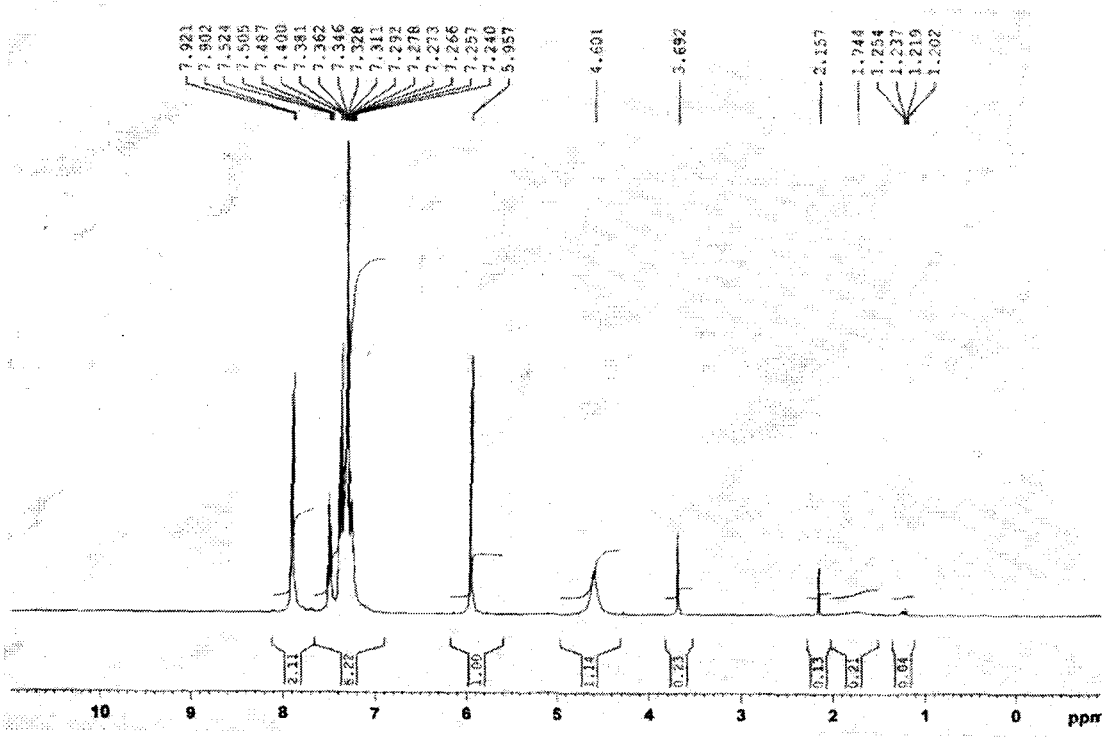

^{1}H NMR spectra of the Schiff base $\mathbf{L_{13}}$

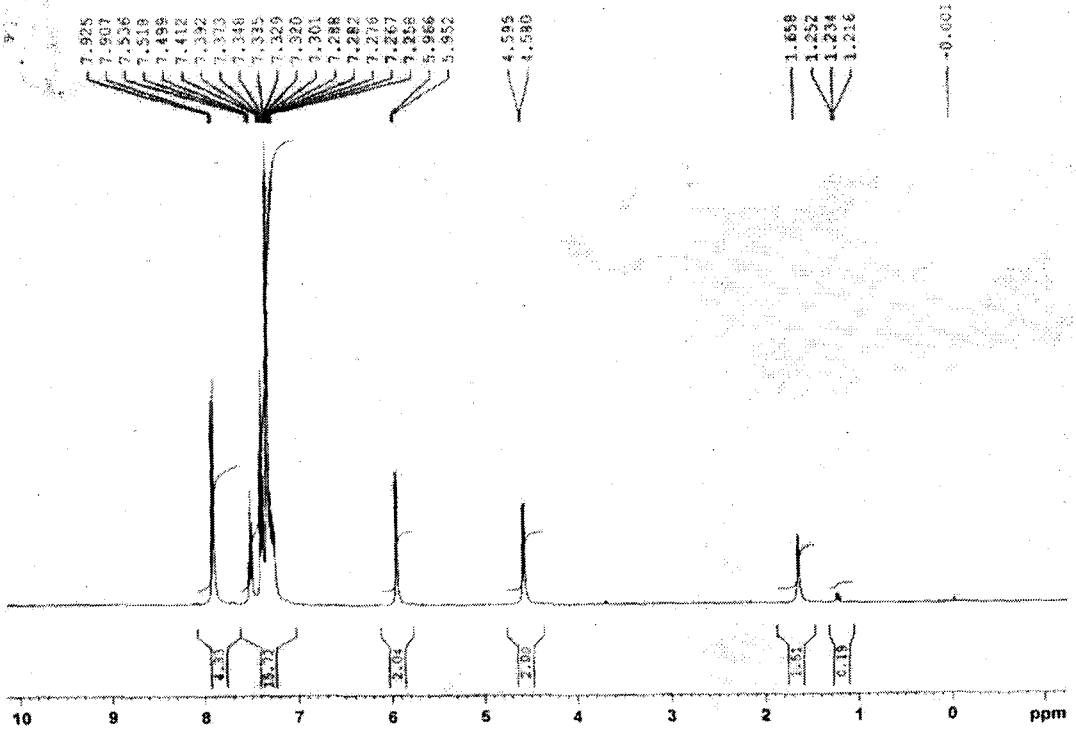

^{1}H NMR spectra of the Schiff base $\mathbf{L_{14}}$

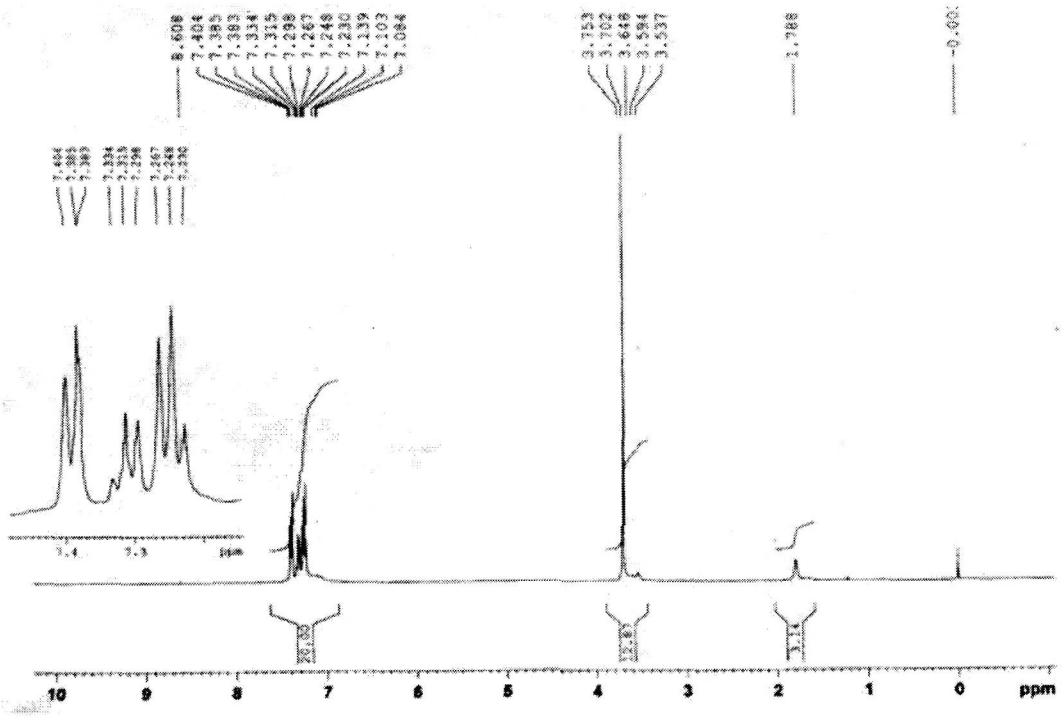

^{1}H NMR spectra of the Schiff base L_{15}

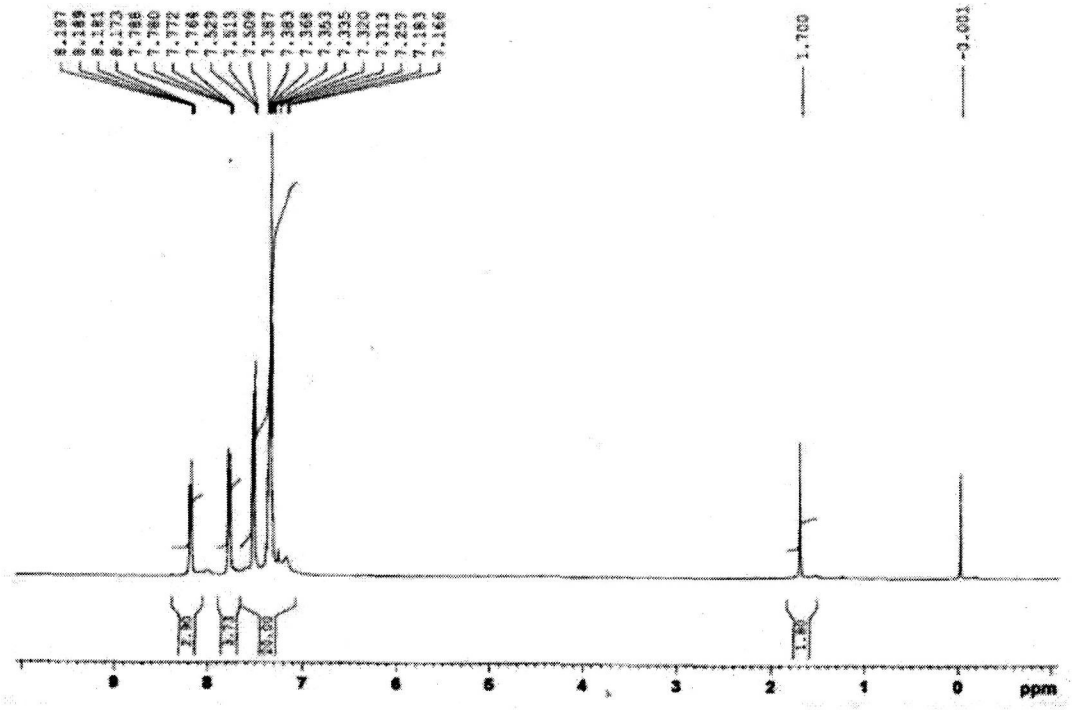

^{1}H NMR spectra of the Schiff base L_{16}

APPENDIX 4

^{13}C NMR spectra of the compounds

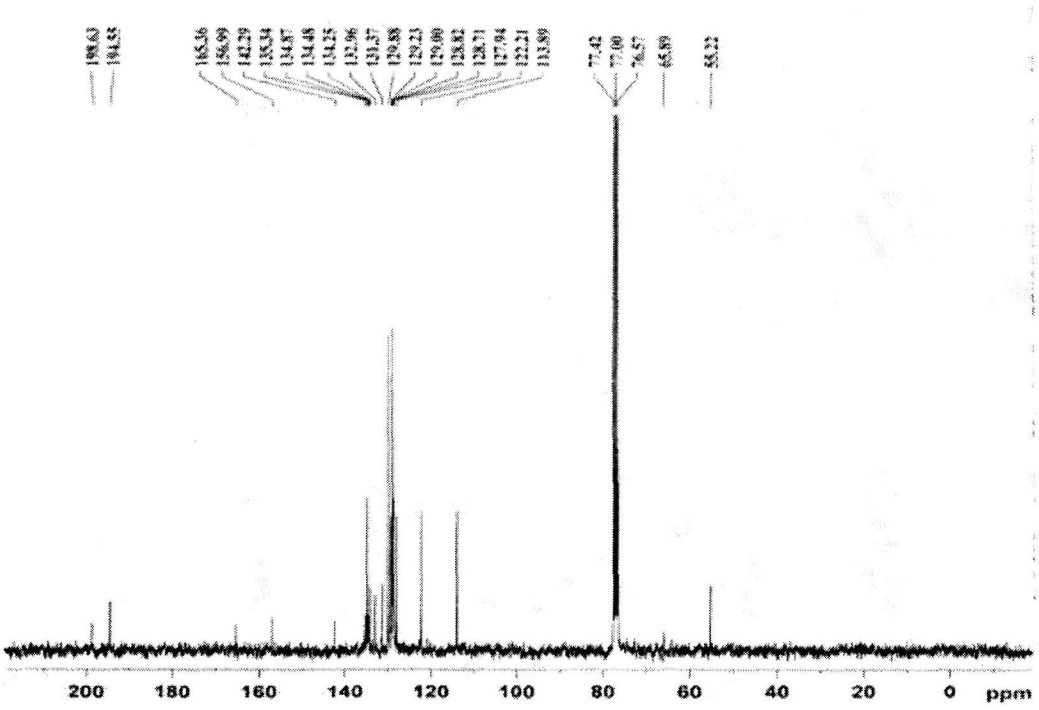

^{13}C NMR spectra of the Schiff base L_1

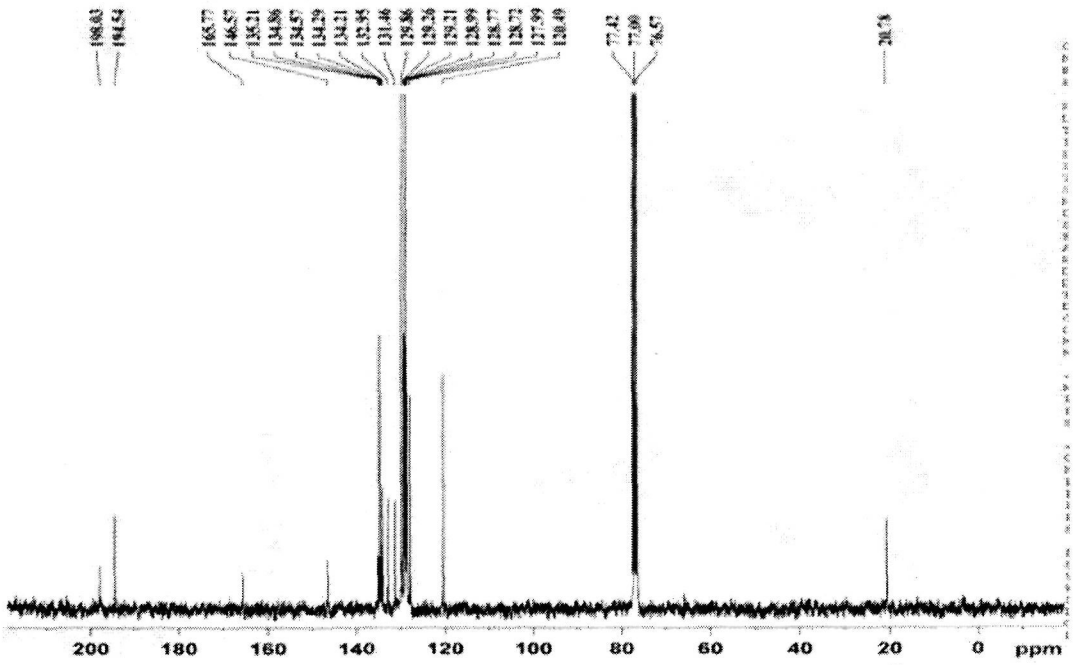

^{13}C NMR spectra of the Schiff base L_2

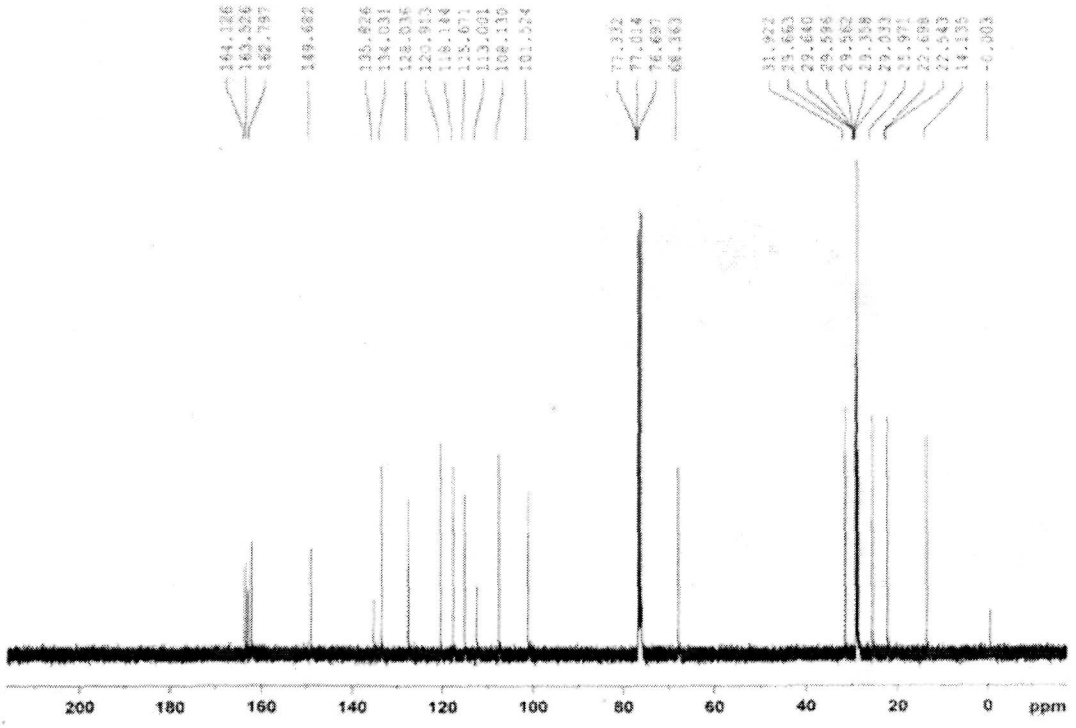

^{13}C NMR spectra of the Schiff base L_3

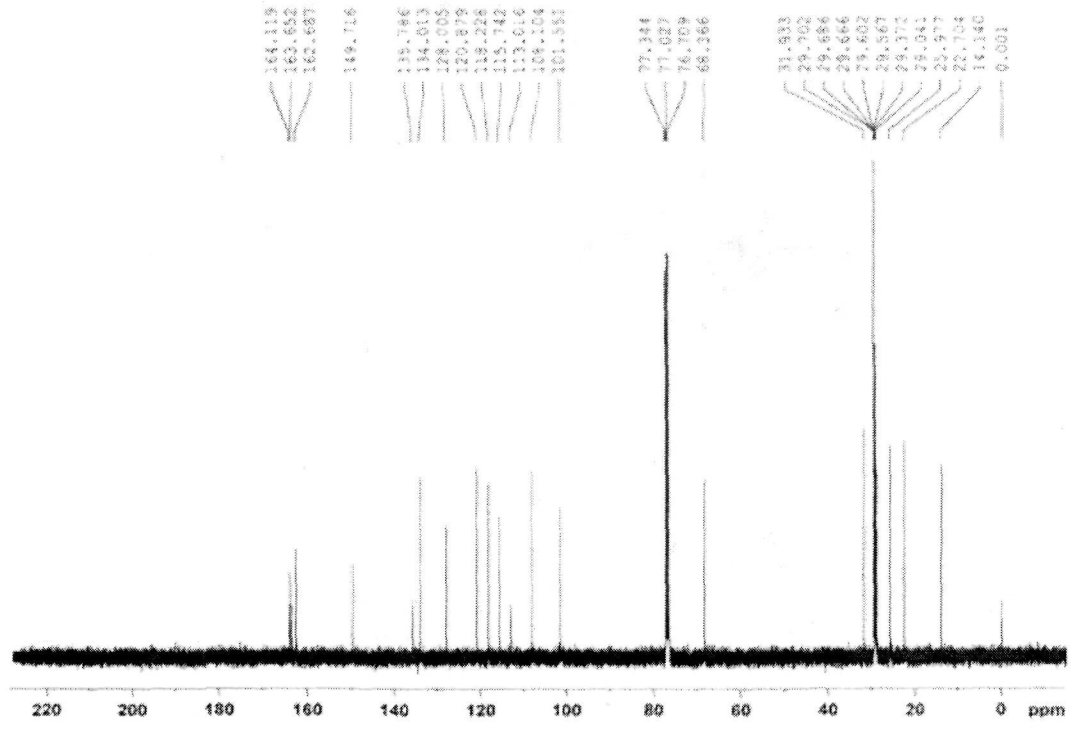

^{13}C NMR spectra of the Schiff base L_4

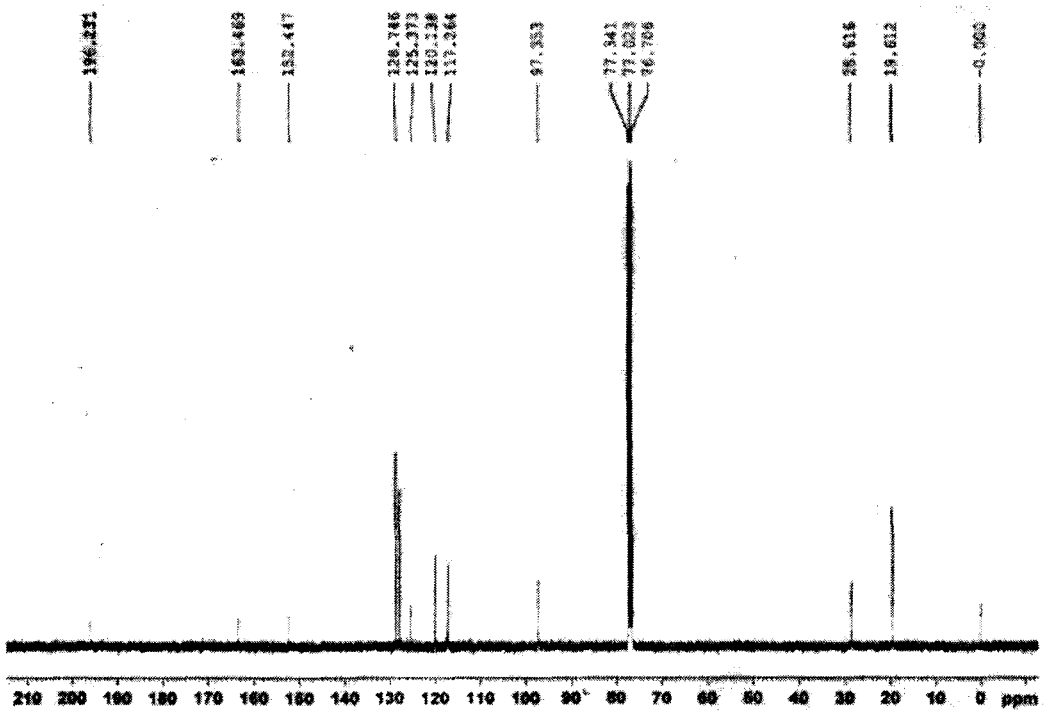

^{13}C NMR spectra of the Schiff base L_5

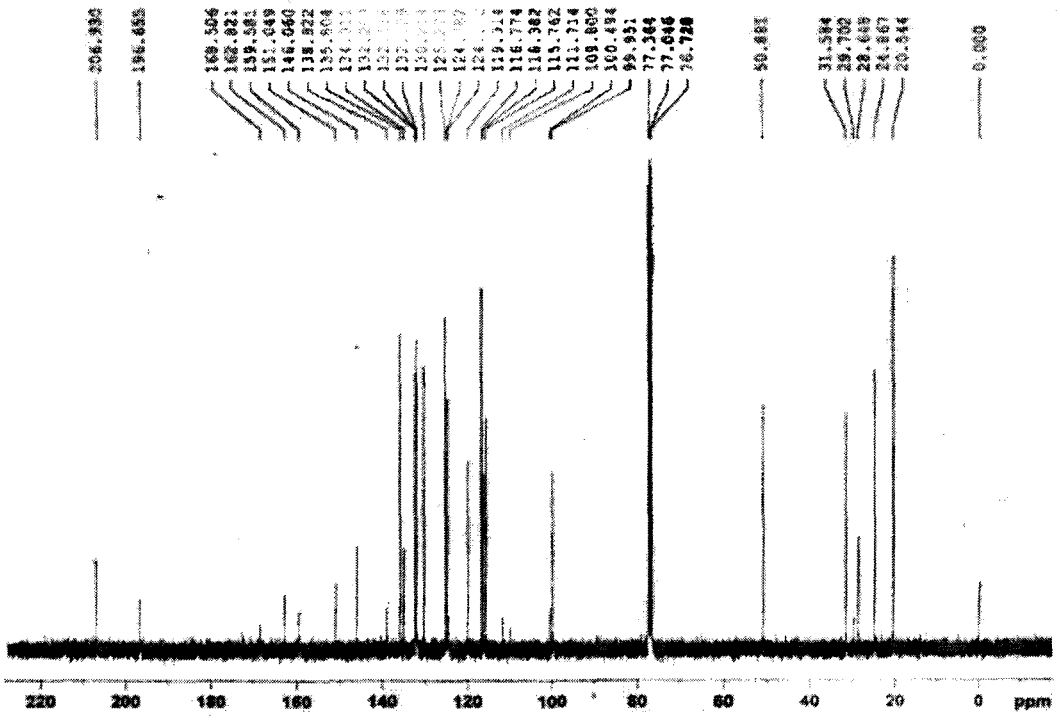

^{13}C NMR spectra of the Schiff base L_6

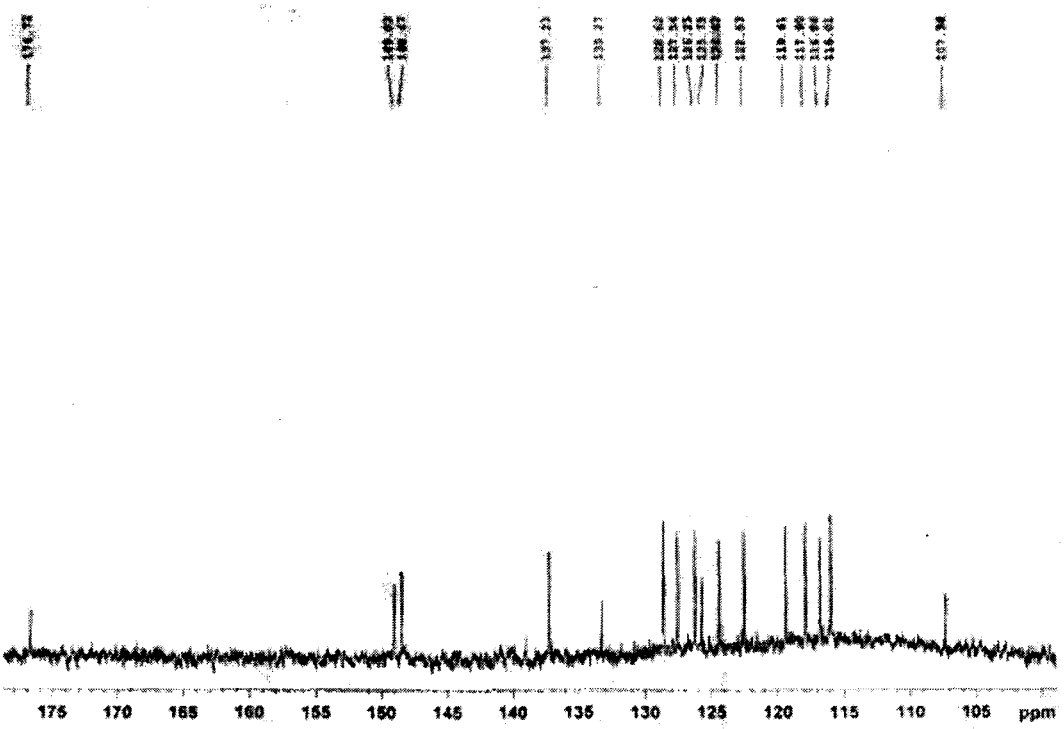

^{13}C NMR spectra of the Schiff base L_7

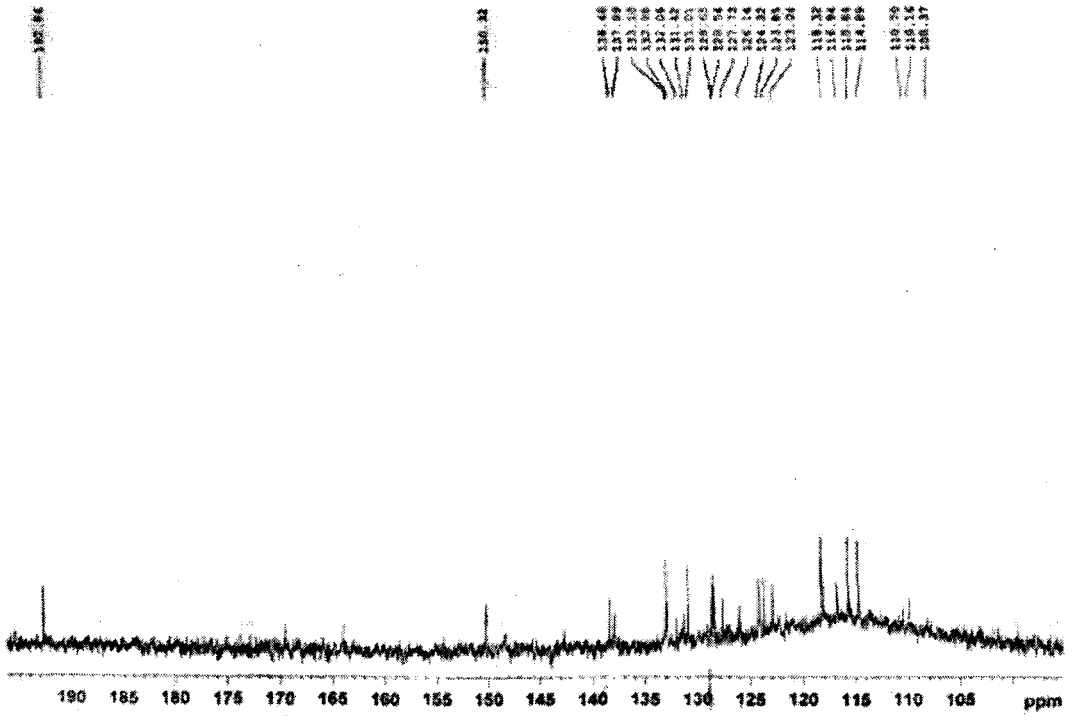

^{13}C NMR spectra of the Schiff base L_8

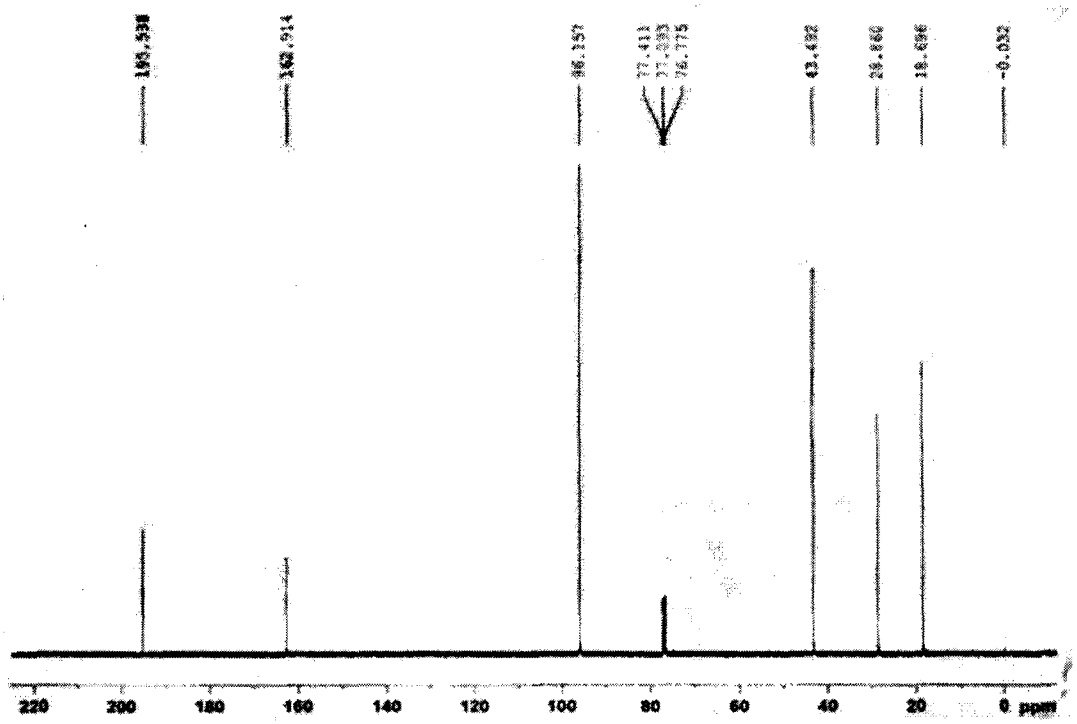

^{13}C NMR spectra of the Schiff base L_9

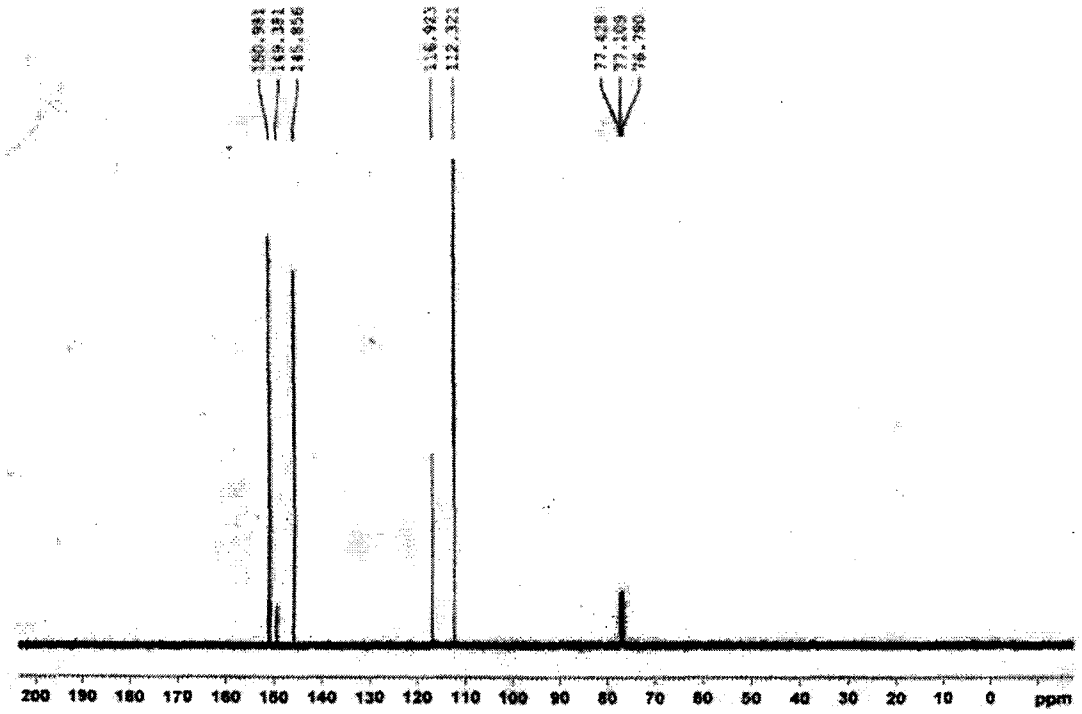

^{13}C NMR spectra of the Schiff base L_{10}

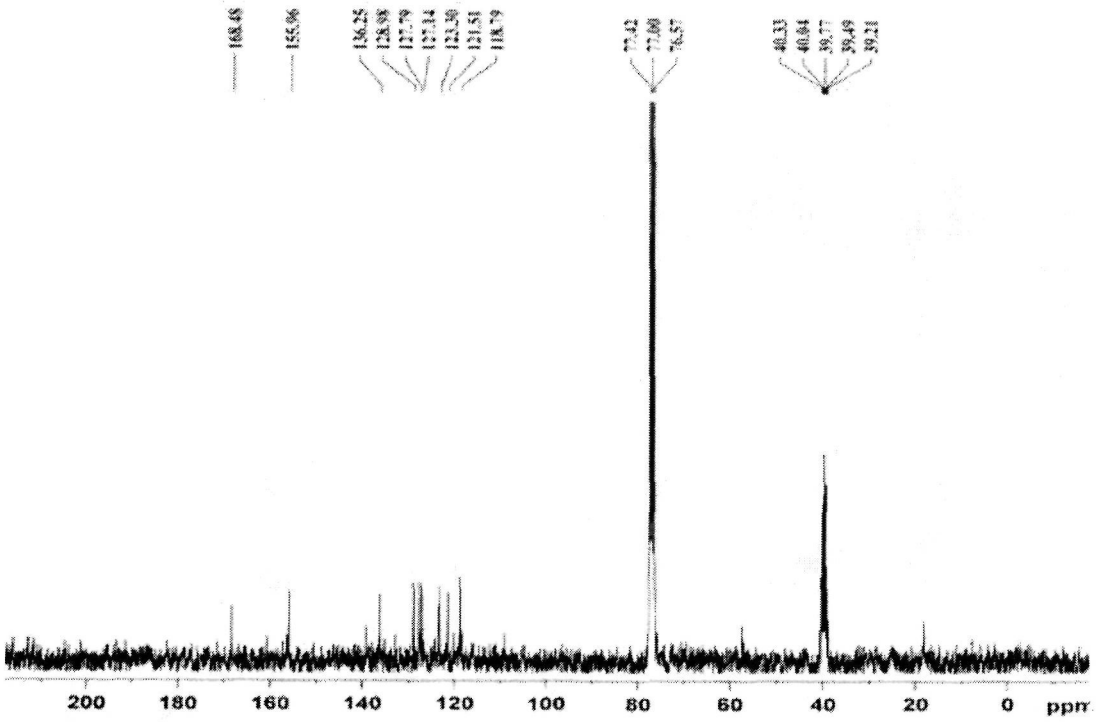

^{13}C NMR spectra of the Schiff base $\mathbf{L_{11}}$

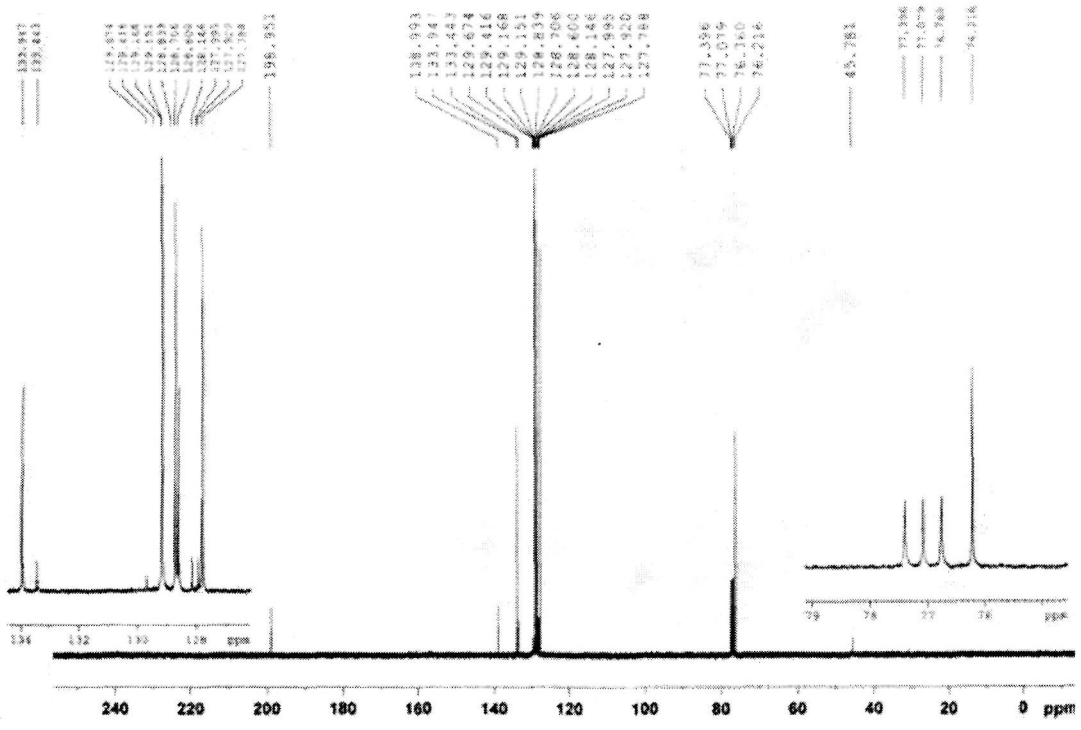

^{13}C NMR spectra of the Schiff base $\mathbf{L_{13}}$

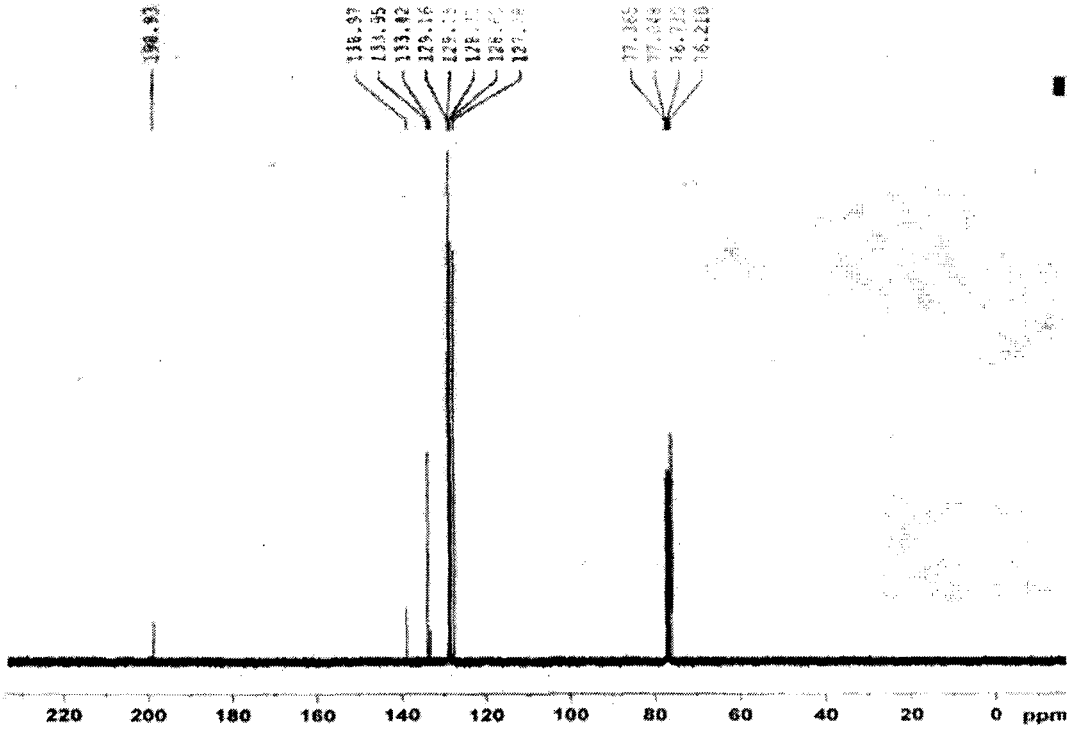

^{13}C NMR spectra of the Schiff base L_{14}

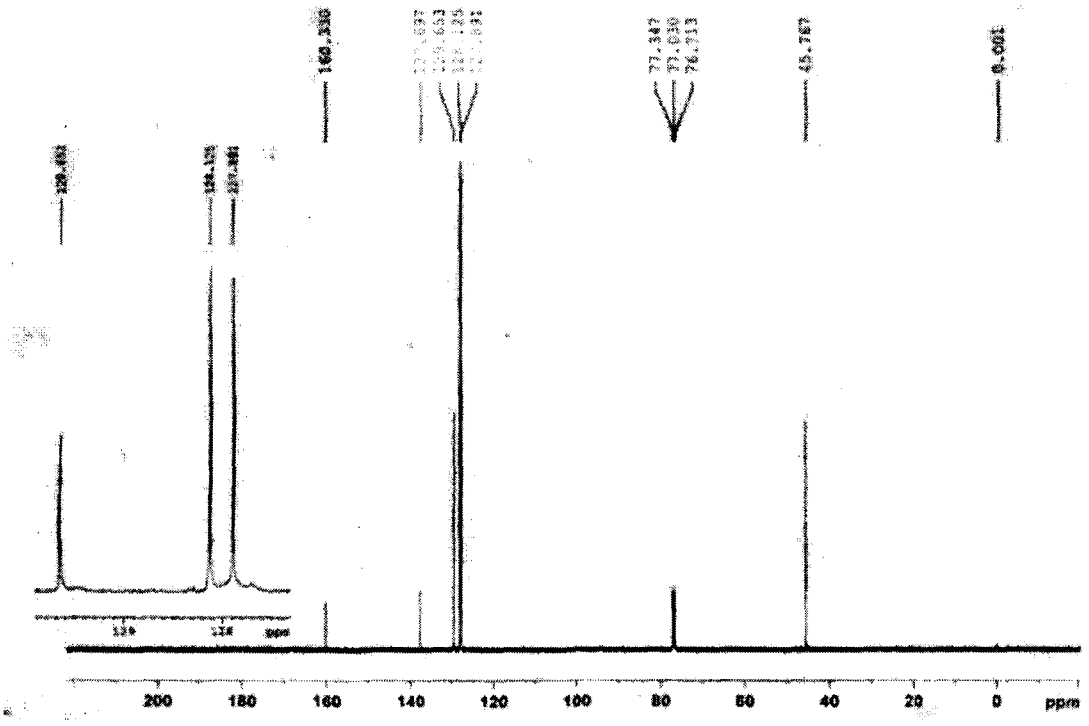

^{13}C NMR spectra of the Schiff base L_{15}

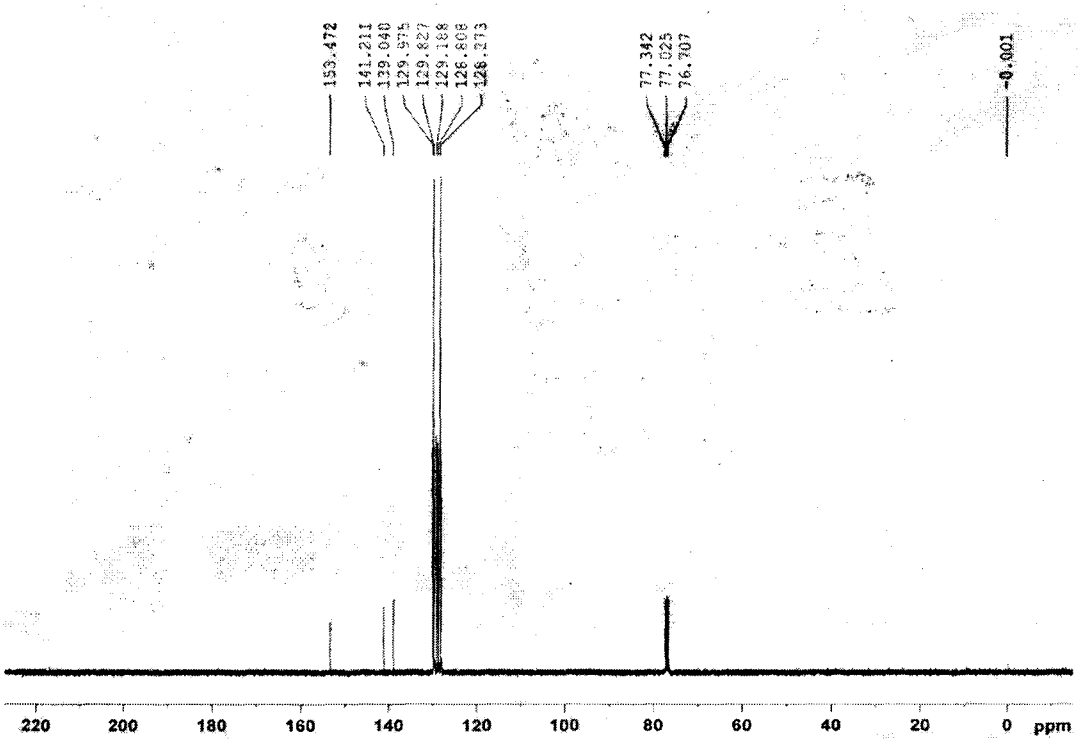

^{13}C NMR spectra of the Schiff base $\mathbf{L_{16}}$

APPENDIX 5

Mass spectra of the compounds

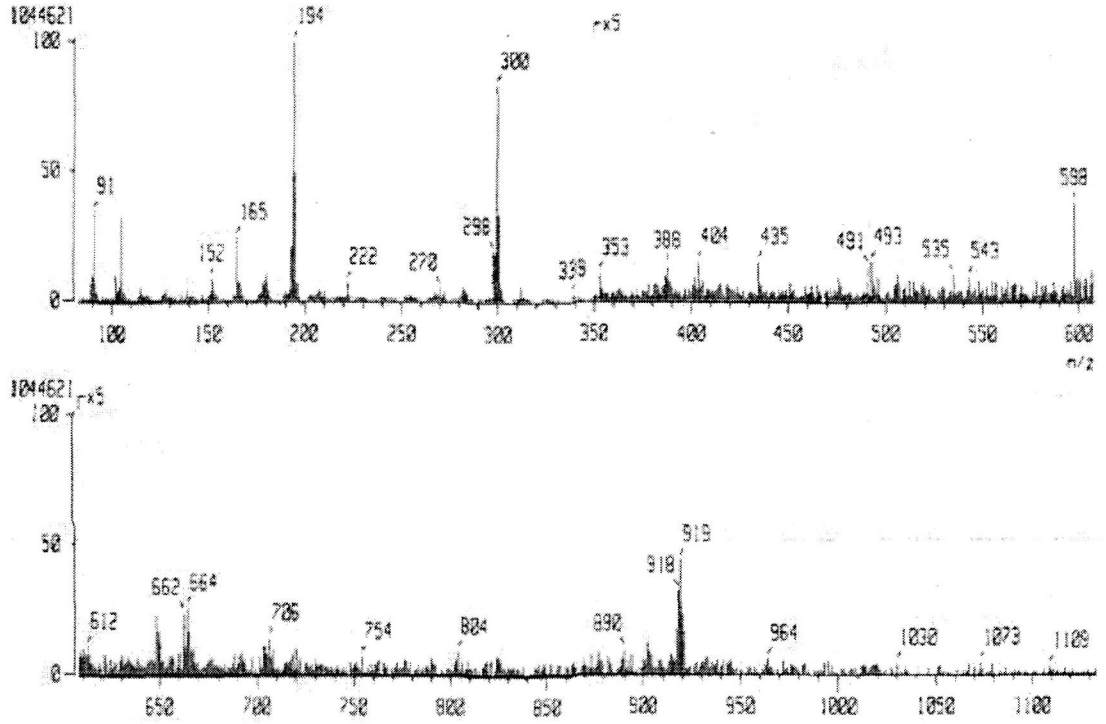

Mass spectra of the ligand L_2

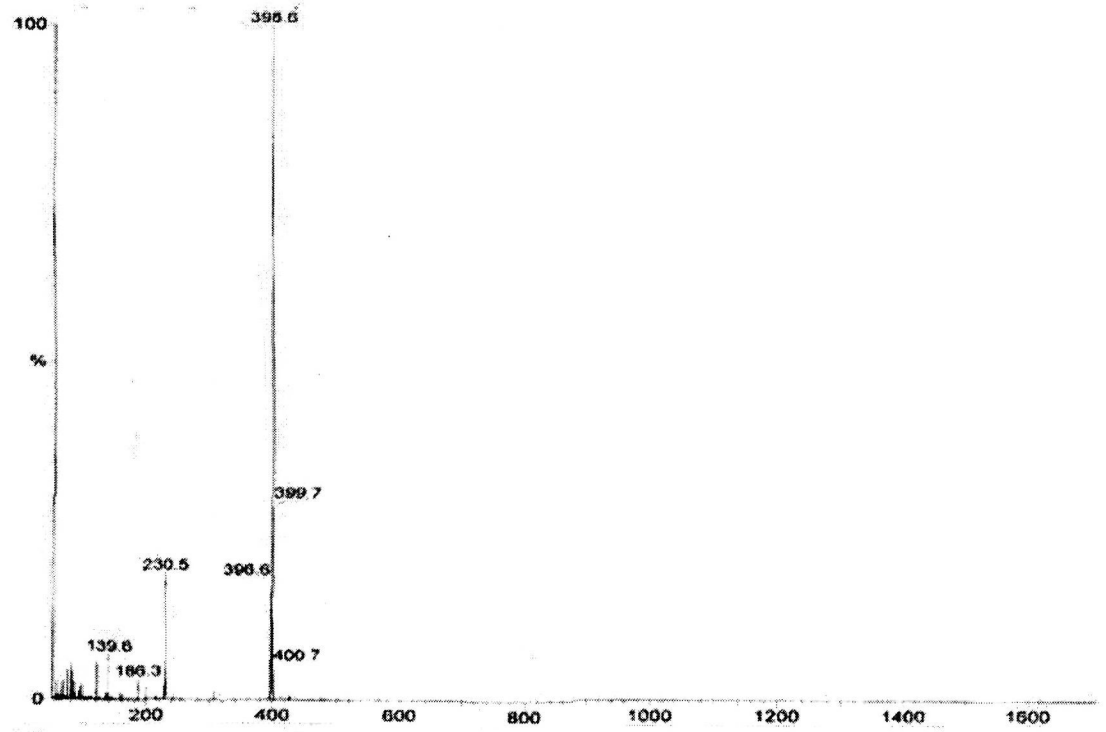

mass spectra of the ligand L_3

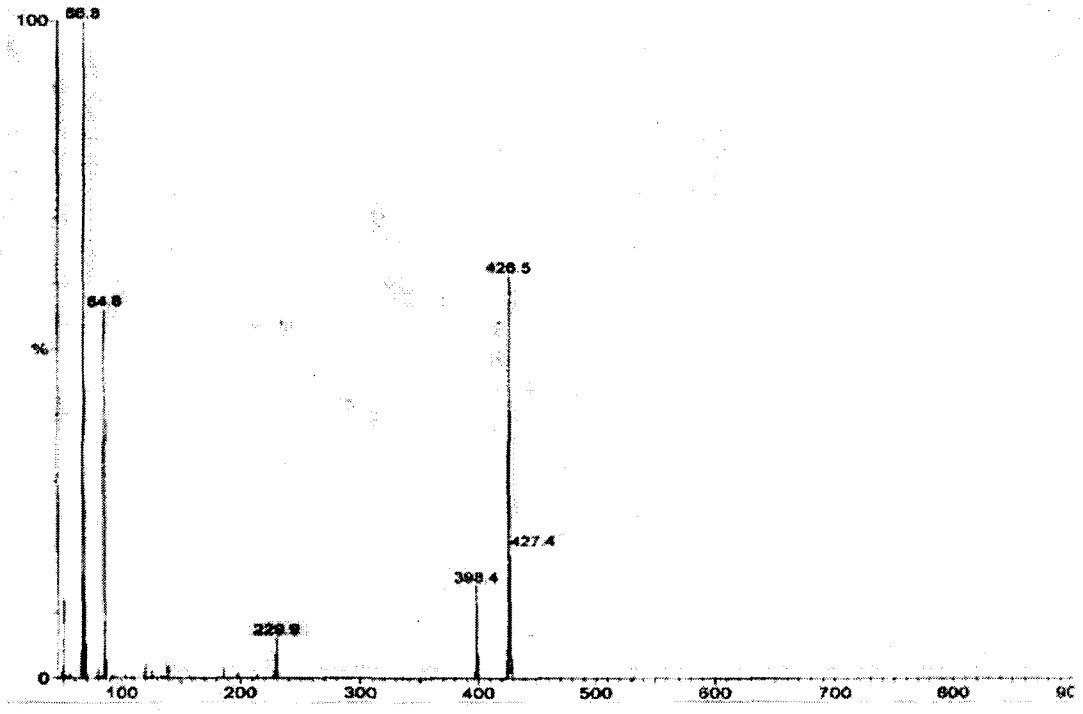

mass spectra of the ligand L_4

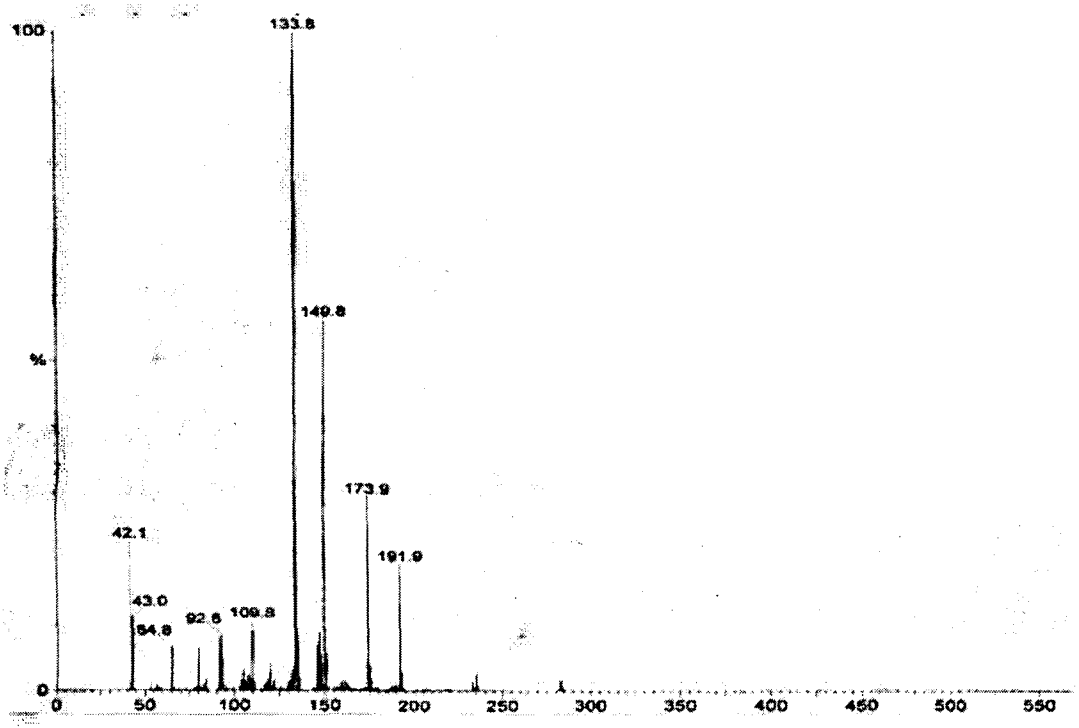

mass spectra of the ligand L_5

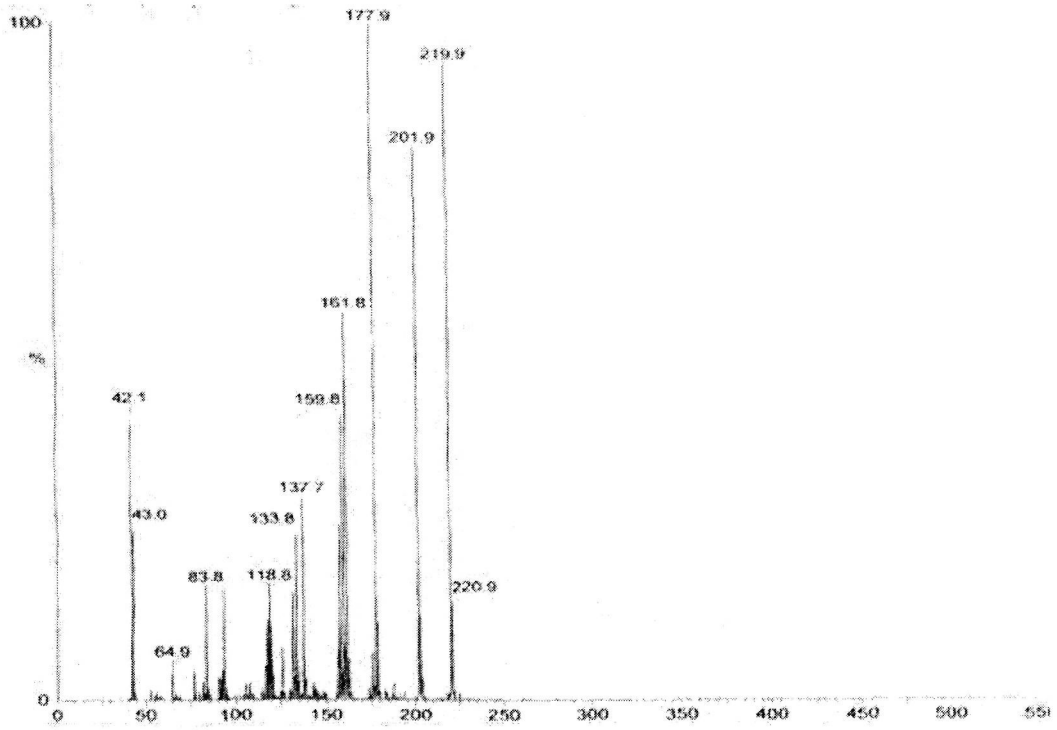

mass spectra of the ligand L_6

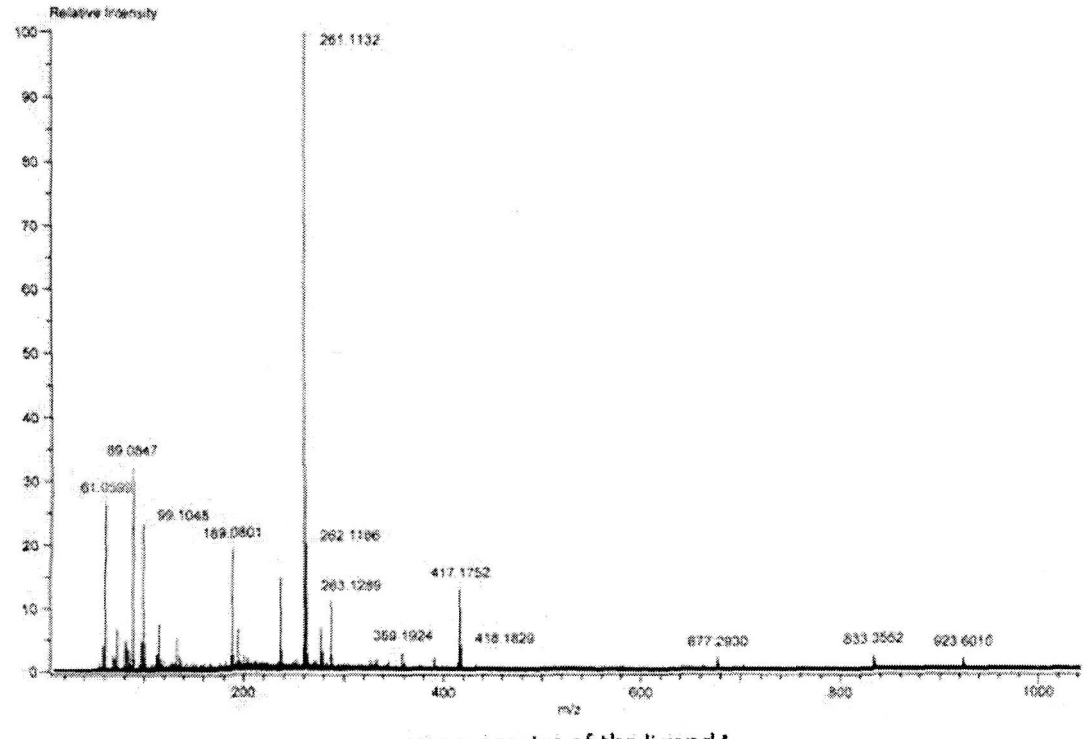

mass spectra of the ligand L_7

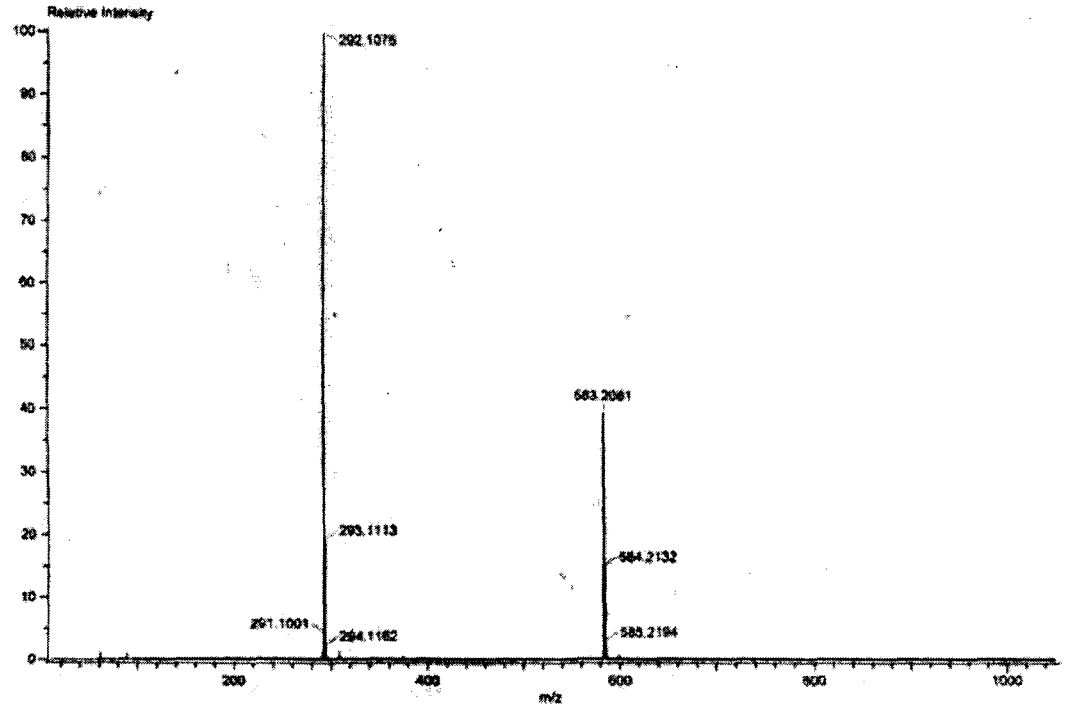

mass spectra of the ligand L_8

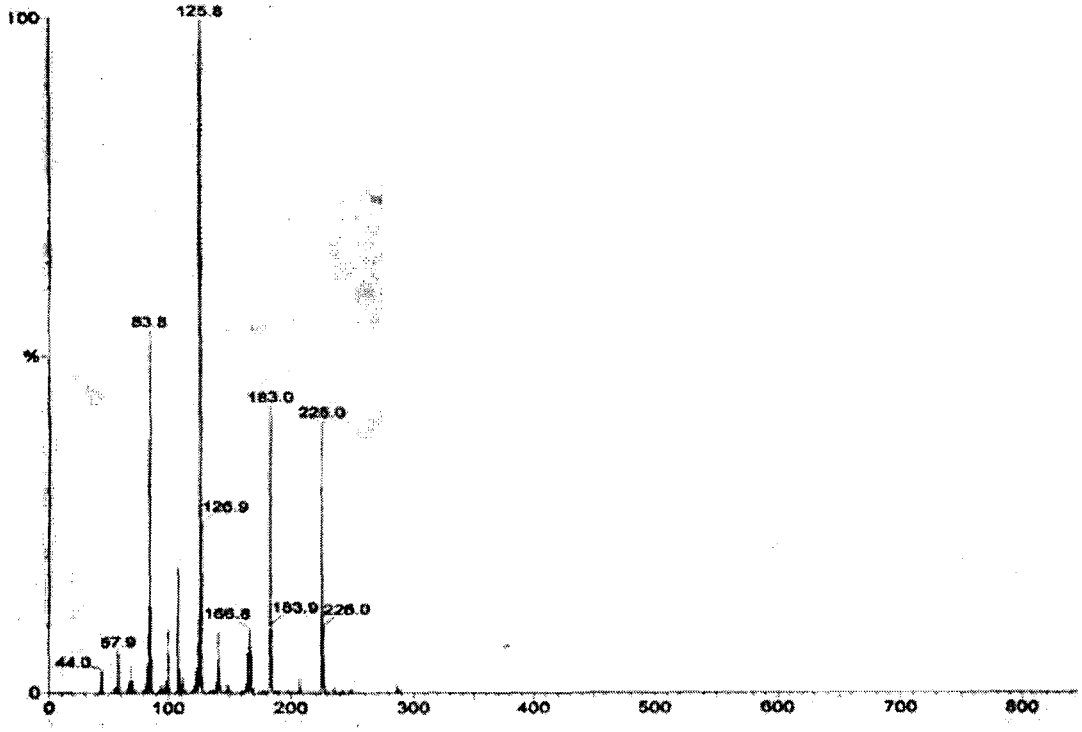

mass spectra of the ligand L_9

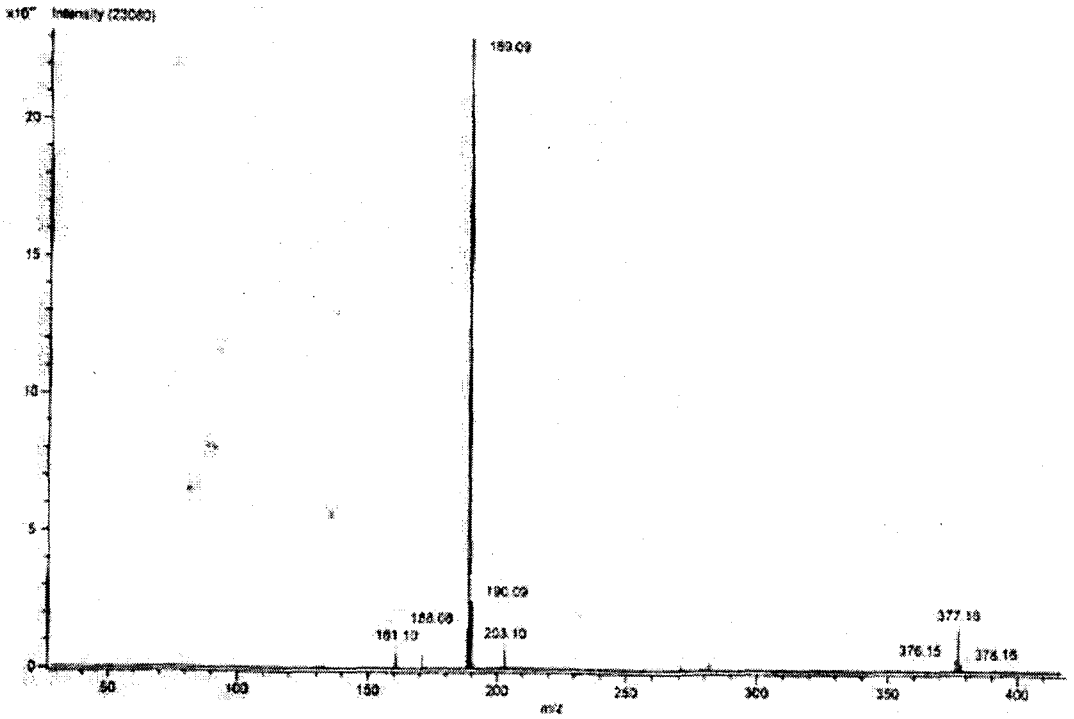

mass spectra of the ligand L_{10}

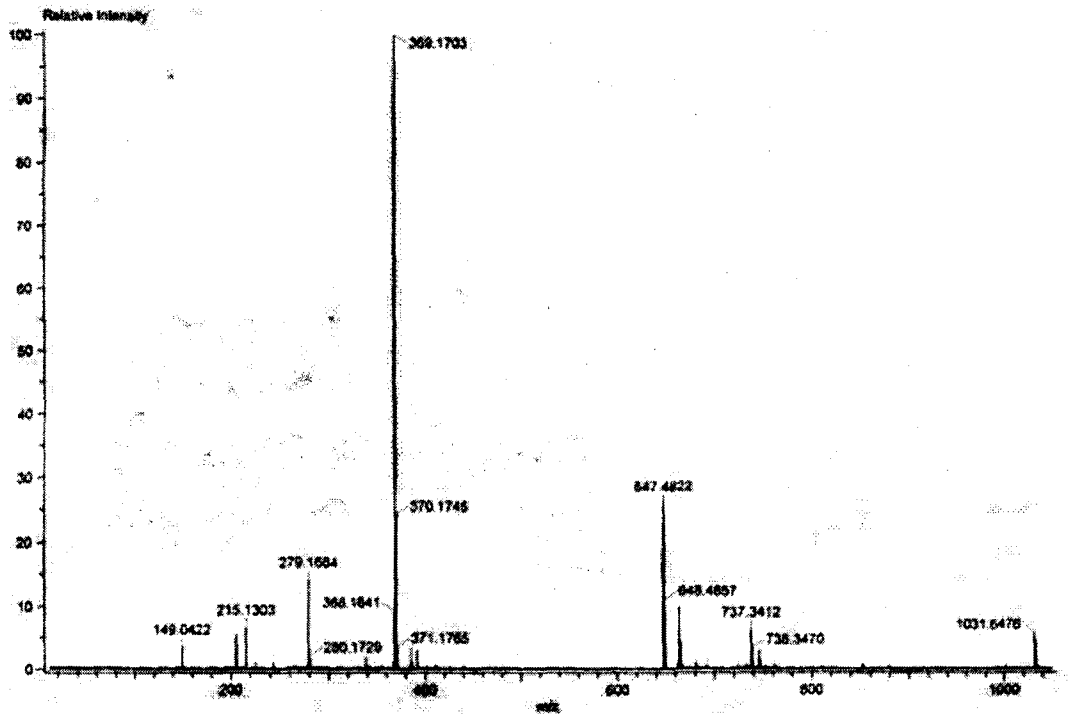

mass spectra of the ligand L_{12}

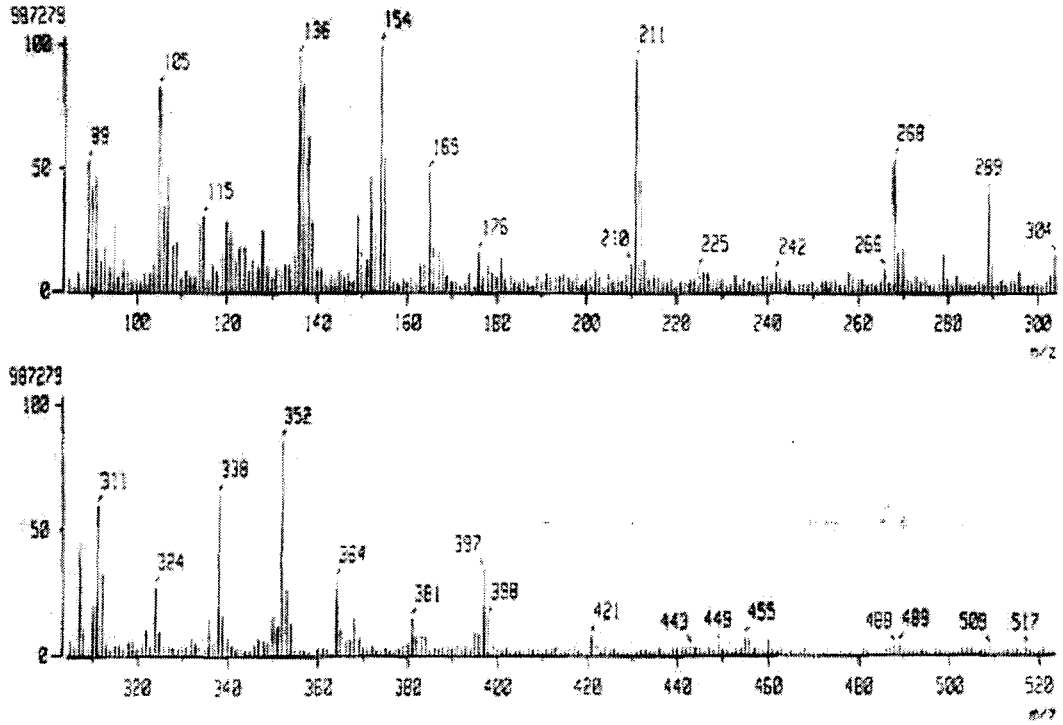

mass spectra of the ligand L_{13}

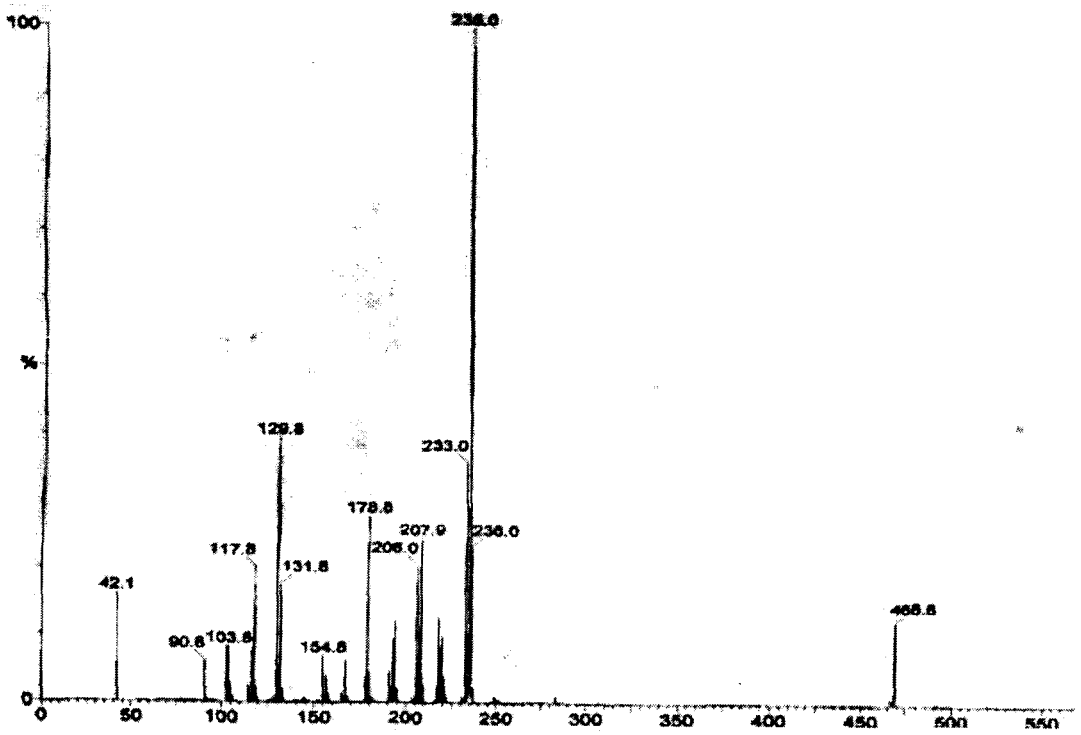

mass spectra of the ligand L_{15}

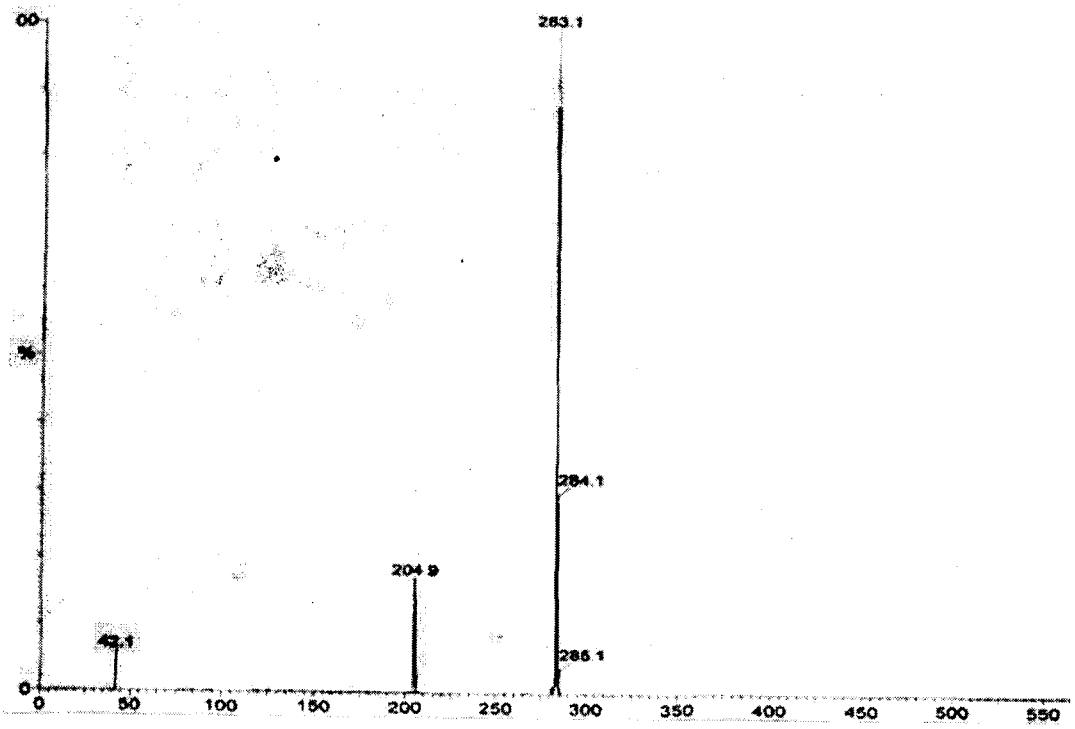

mass spectra of the ligand L_{16}

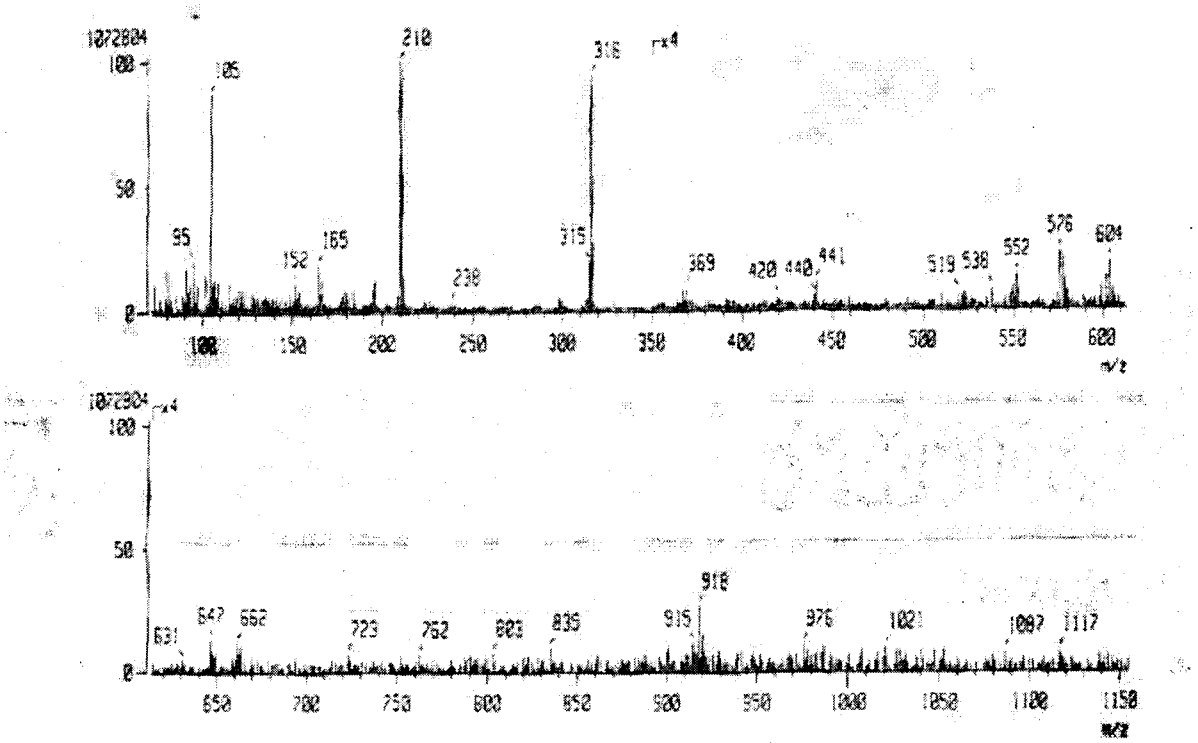

mass spectra of the complex $[VO(L_1)_2]^{2+}SO4^{2-}.H_2O$ (3)

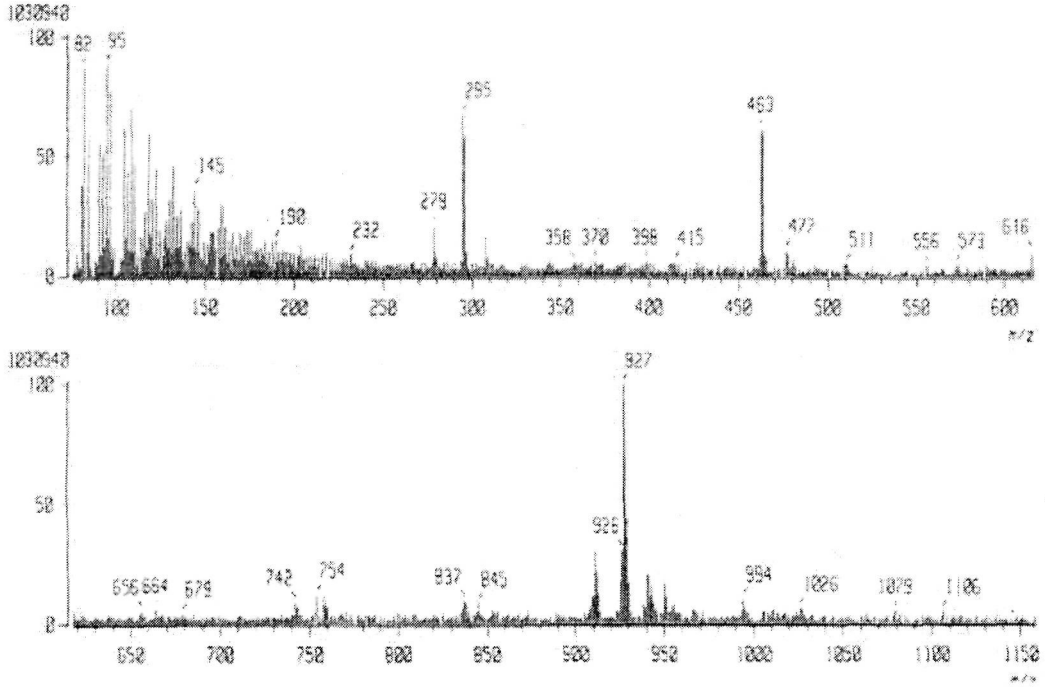

Mass spectra of the complex **$[VO(L_5)]_2$ (7)**

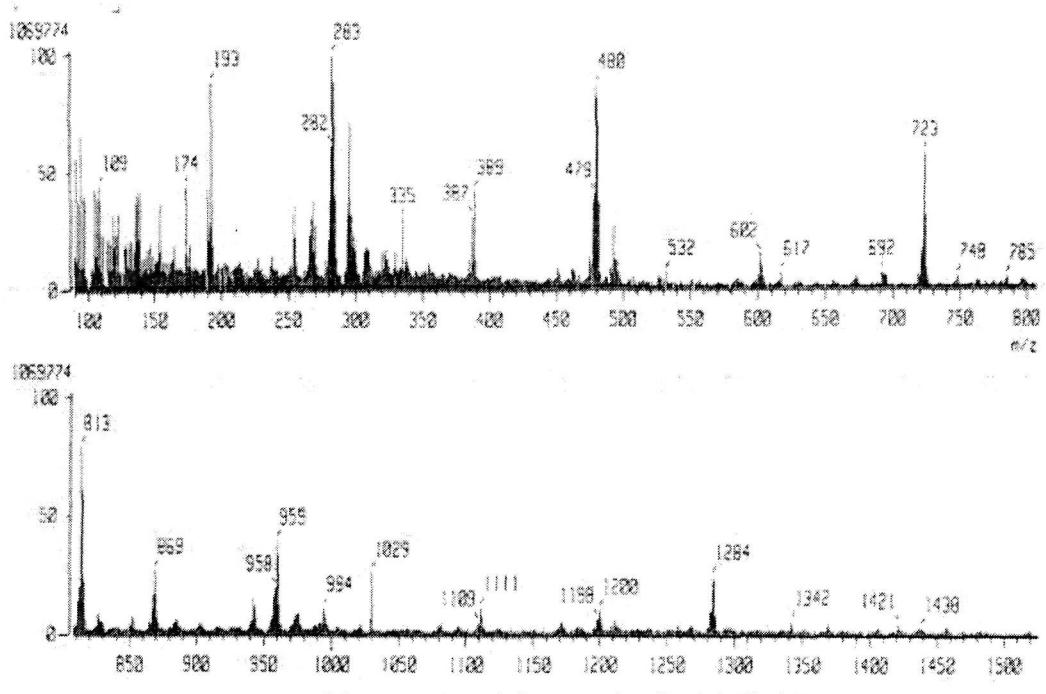

Mass spectra of the complex **$[Fe(L_4)Cl]_2$ (6)**

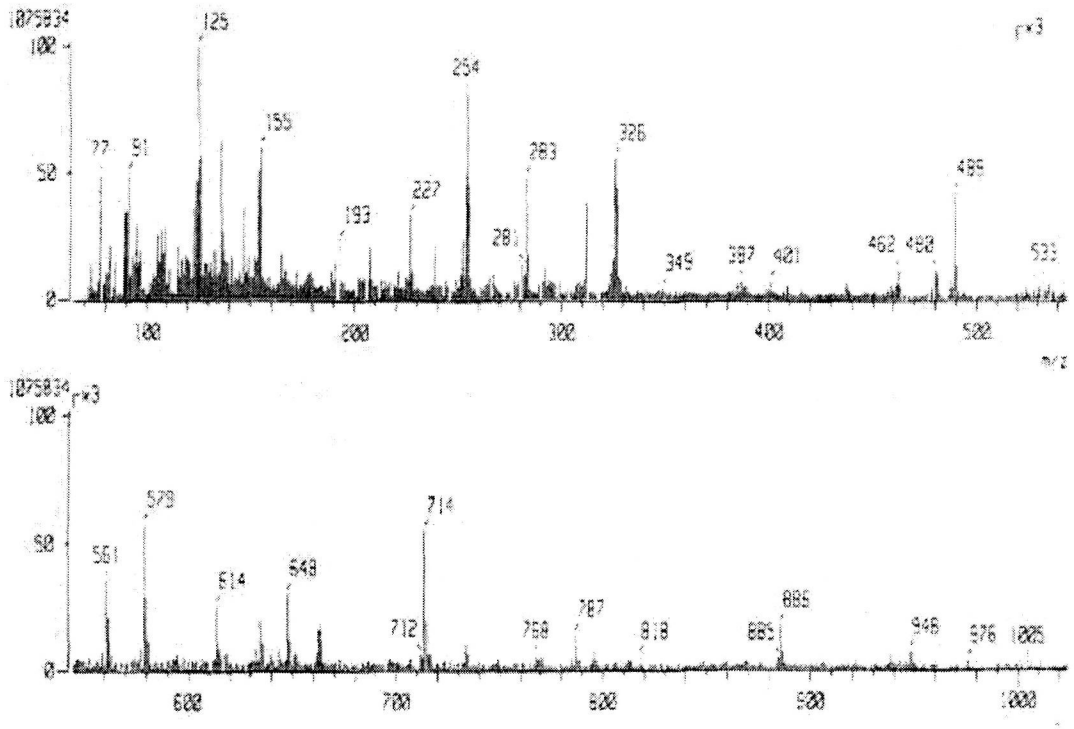

Mass spectra of the complex **$[Fe(L_5)Cl]_2$ (9)**

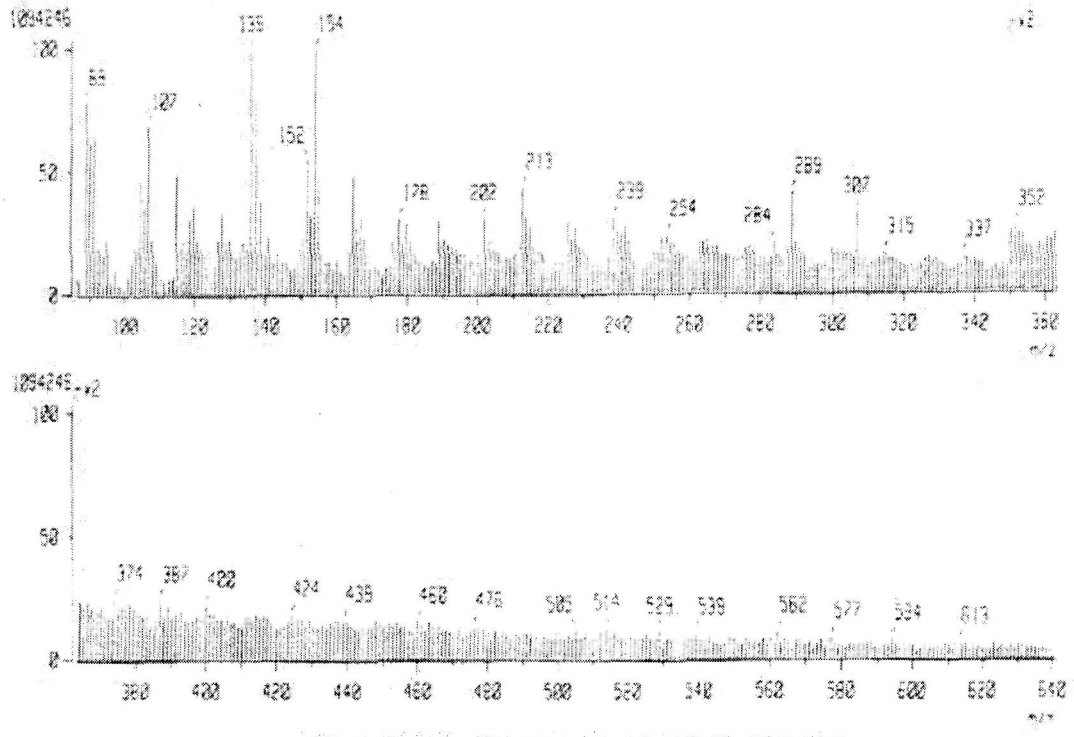

Mass spectra of the complex **$[VO(L_5)]_2.H_2O$ (10)**

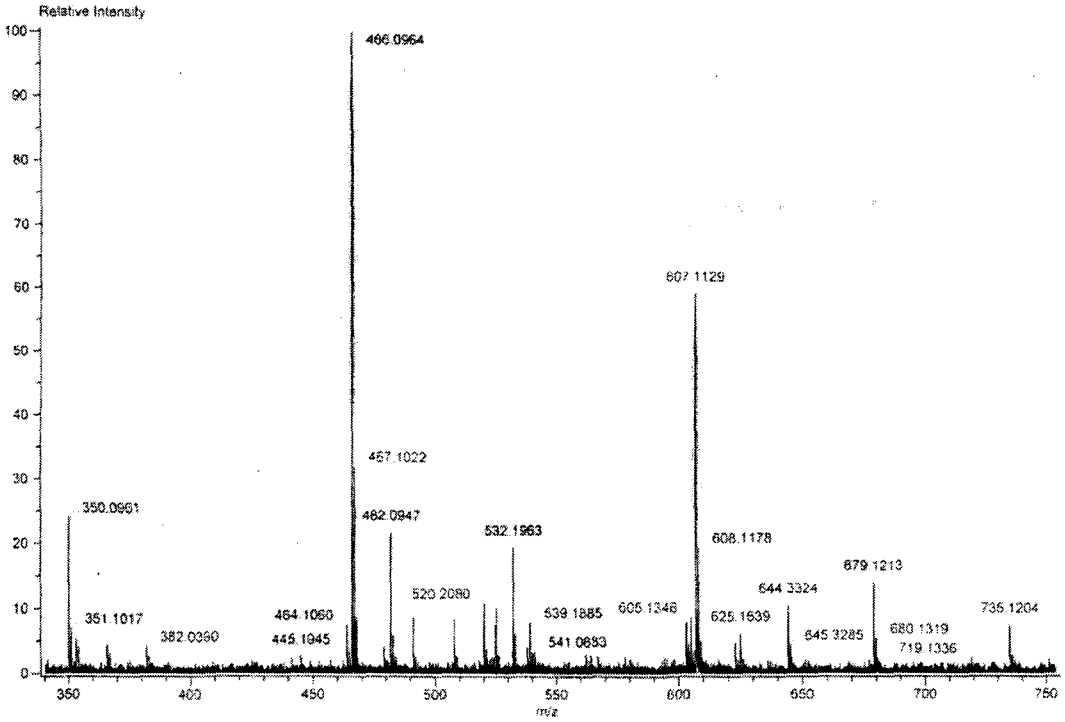

Mass spectra of the complex **[Fe(L_7)(acac)(EtOH)] (17)**

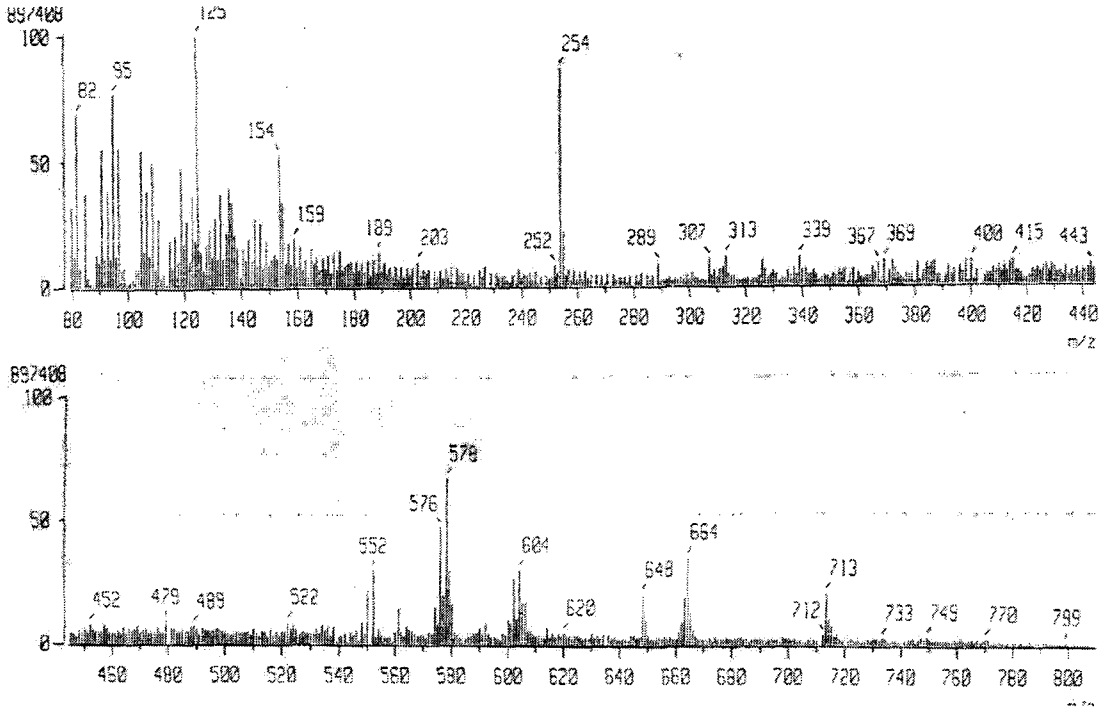

Mass spectra of the complex **[Fe(L_8)(acac)(EtOH)] (18)**

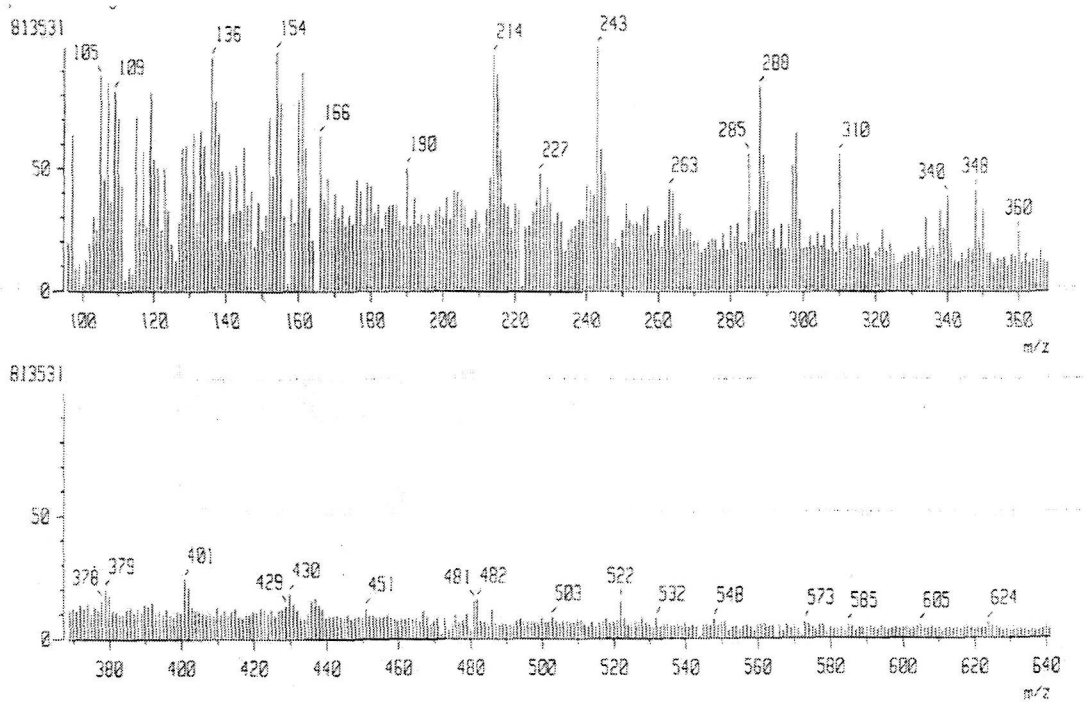

Mass spectra of the complex $[Fe(L_9)(H_2O)_2]NO_3$ (19)

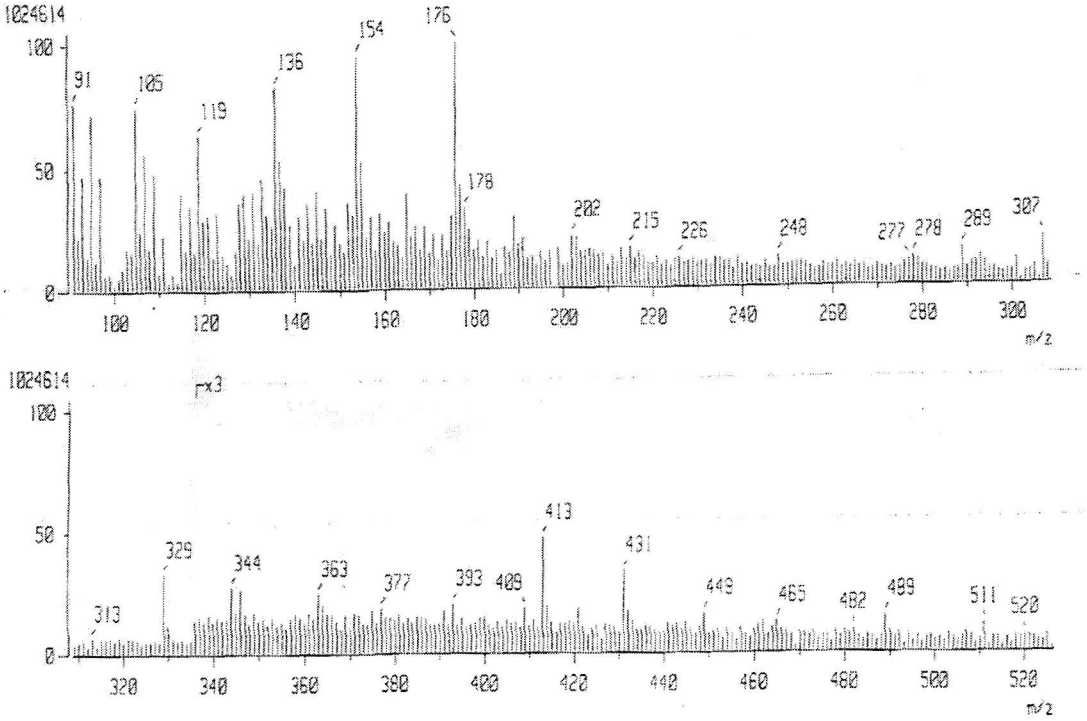

Mass spectra of the complex $NH_4[Fe(L_9)(NCS)_2]$ (25)

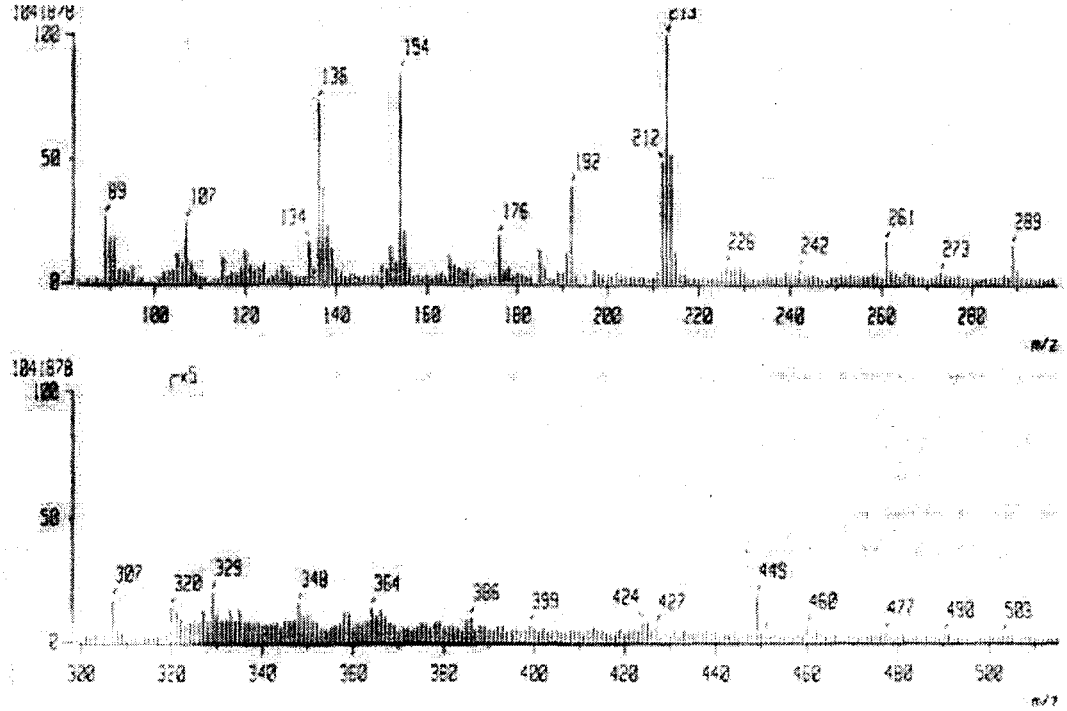

Mass spectra of the complex **Na[Fe(L_9)(N_3)$_2$] (26)**

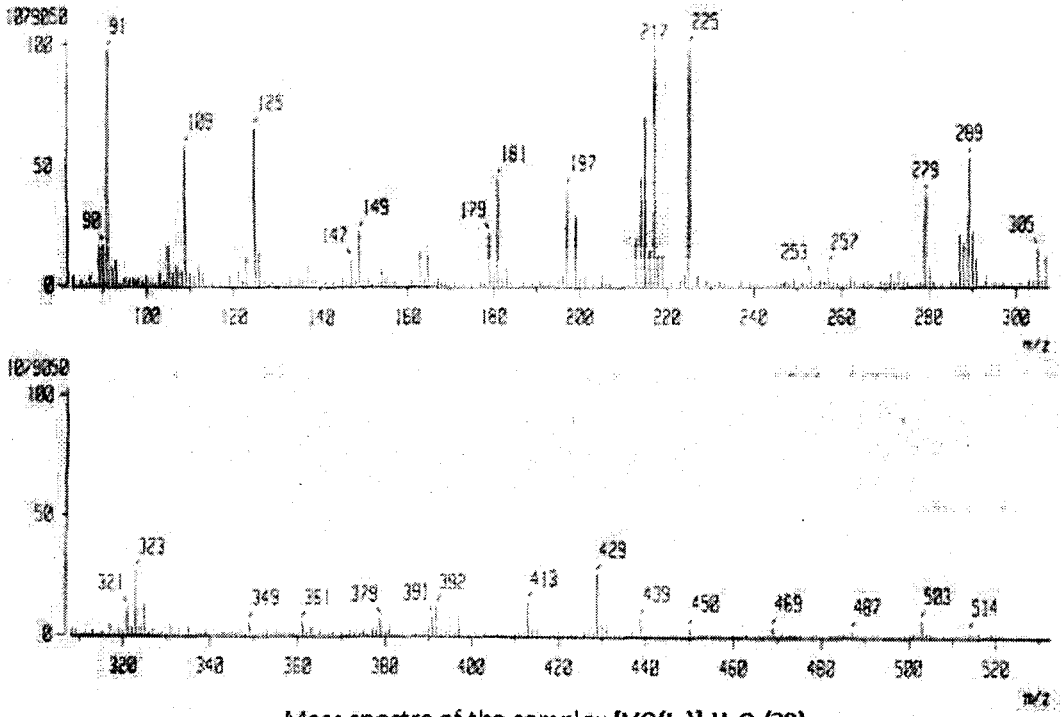

Mass spectra of the complex **[VO(L_9)].H_2O (29)**

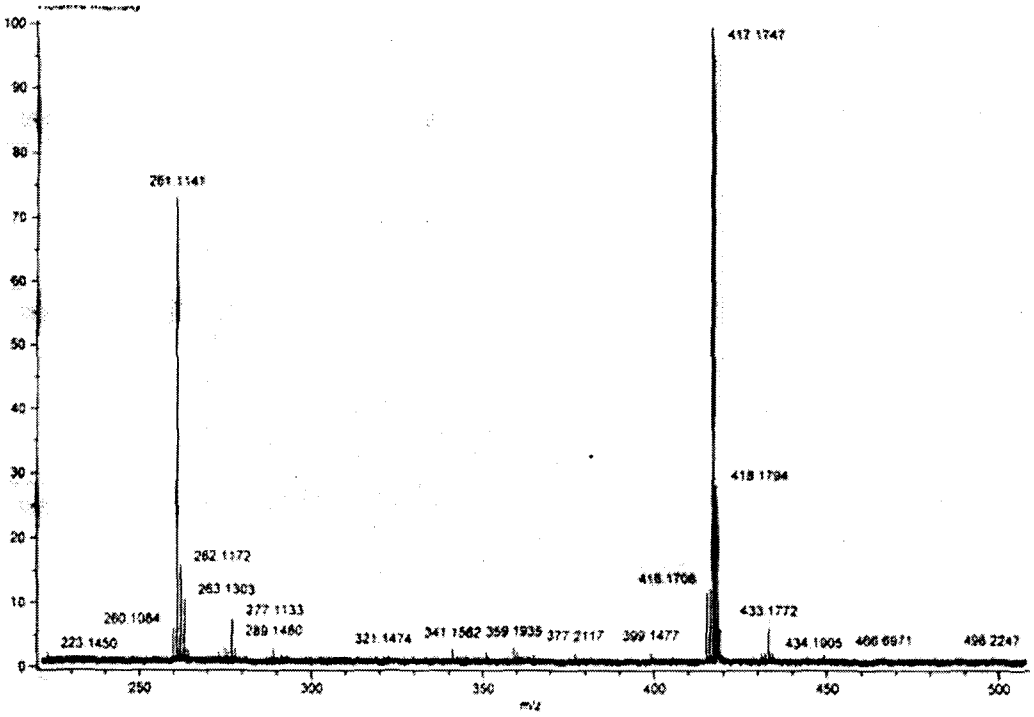

Mass spectra of the complex **[VO(L_{11})].H_2O (30)**

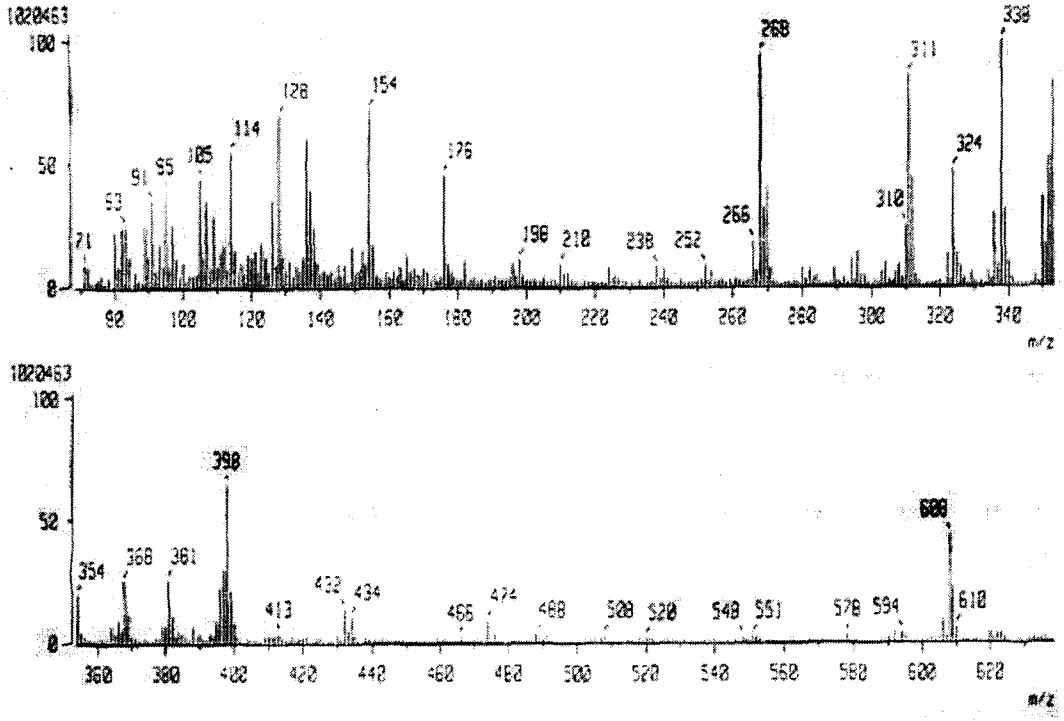

Mass spectra of the complex **[Fe(L_{13})(NO_3)(H_2O)] (22)**

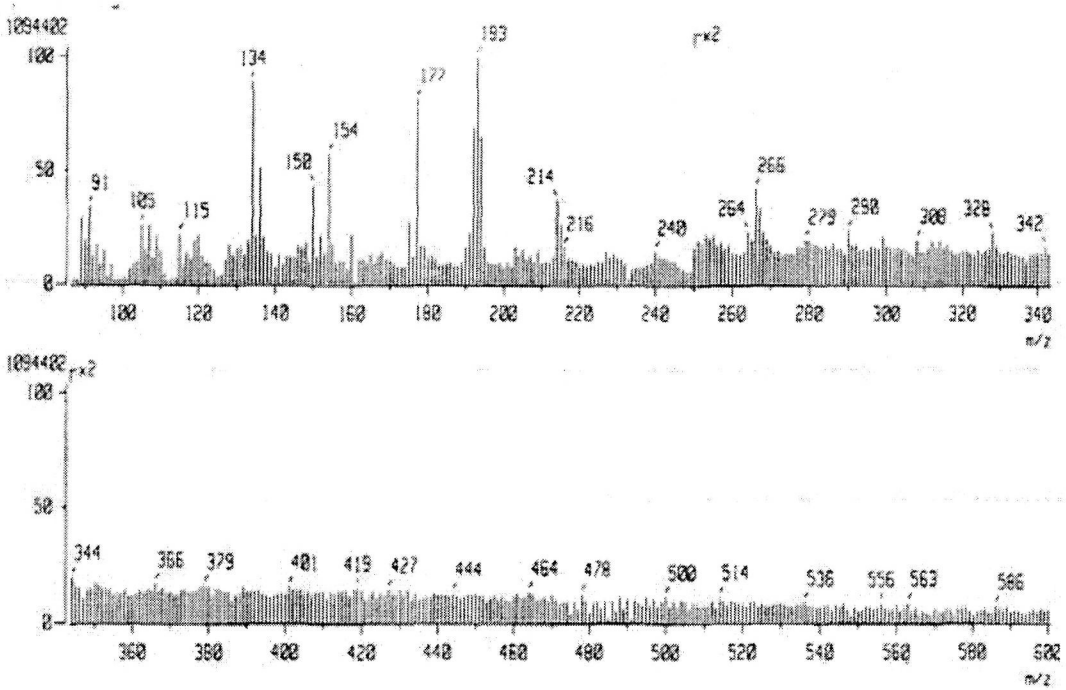

Mass spectra of the complex **[[VO(L_{13})(H_2O)] (32)**

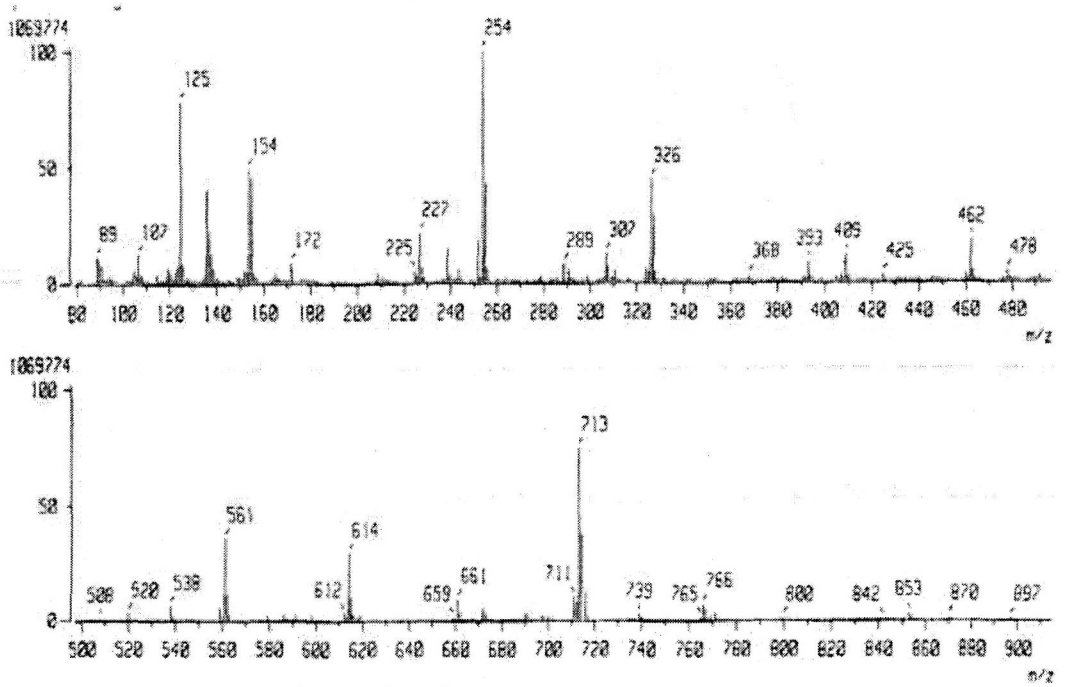

Mass spectra of the complex **[[VO(L_{14})(H_2O)] (33)**

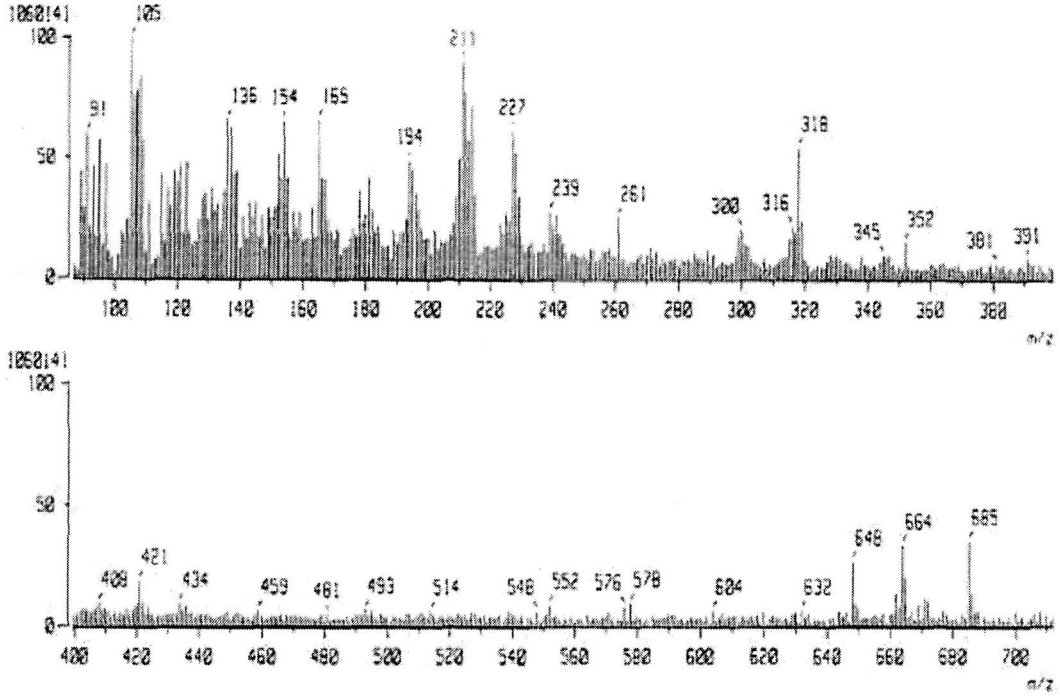

Mass spectra of the complex **[[VO(L_{15})]SO_4.H_2O (36)**

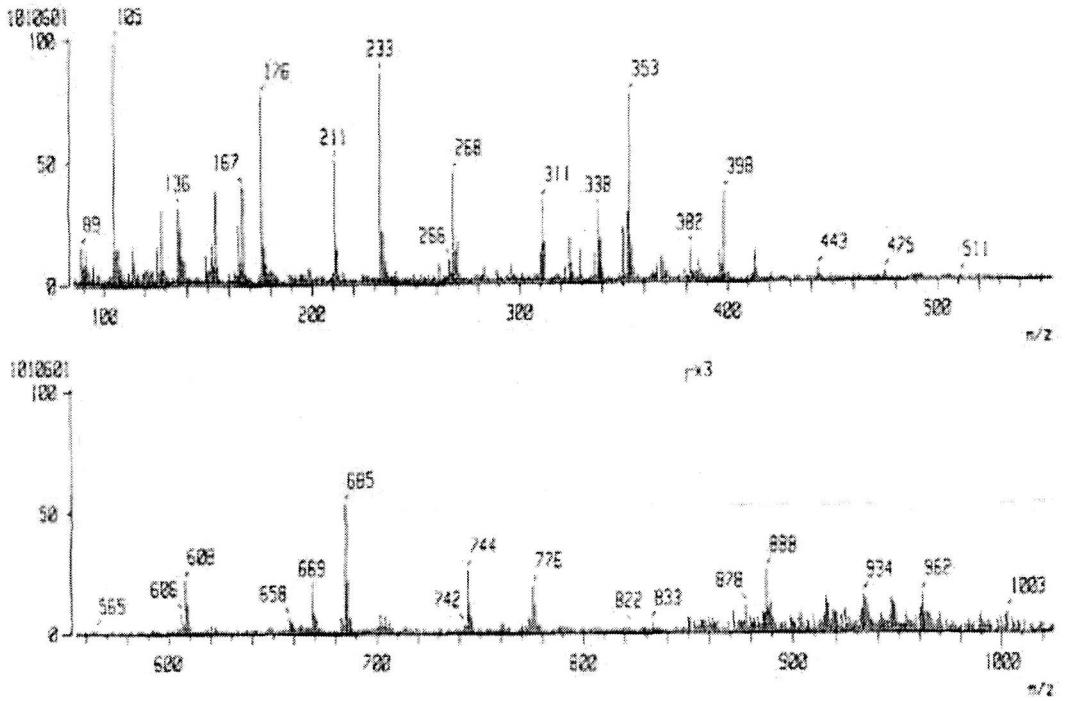

Mass spectra of the complex **[[VO(L_{16})]SO_4.H_2O (37)**

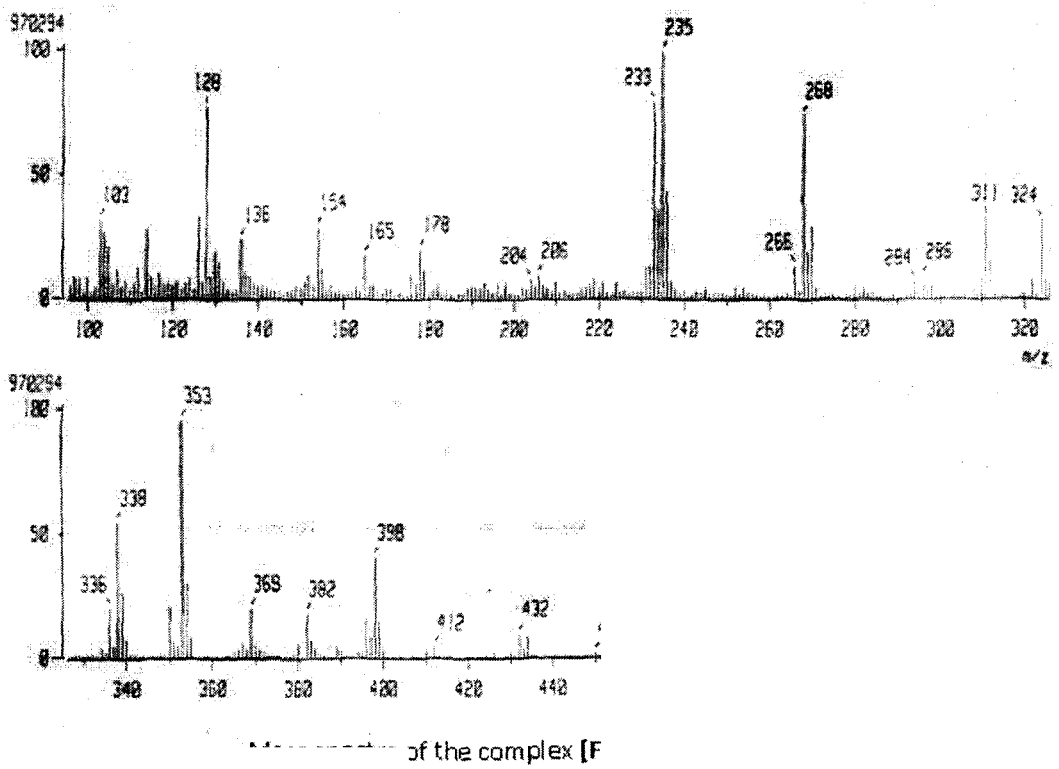

of the complex [F

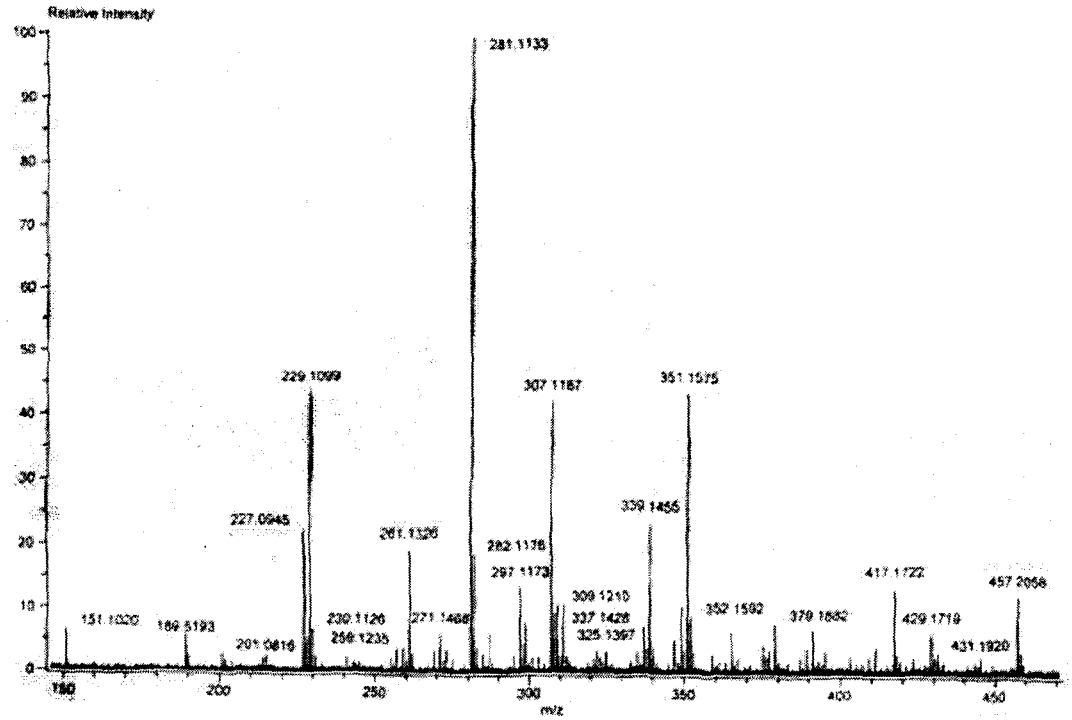

Mass spectra of the complex **[[VO(L_{10})]SO_4.H_2O (39)**

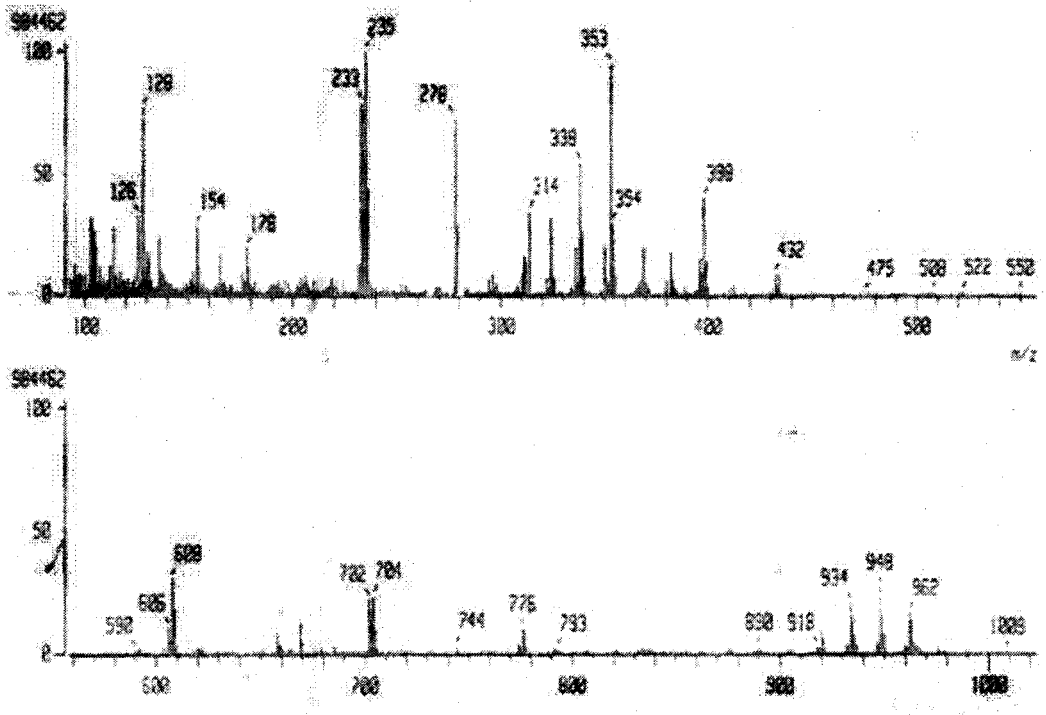

Mass spectra of the complex **$[Fe(L_9)(H_2O)_2]$ (40)**

APPENDIX 6

Cyclic voltammogram of the complexes

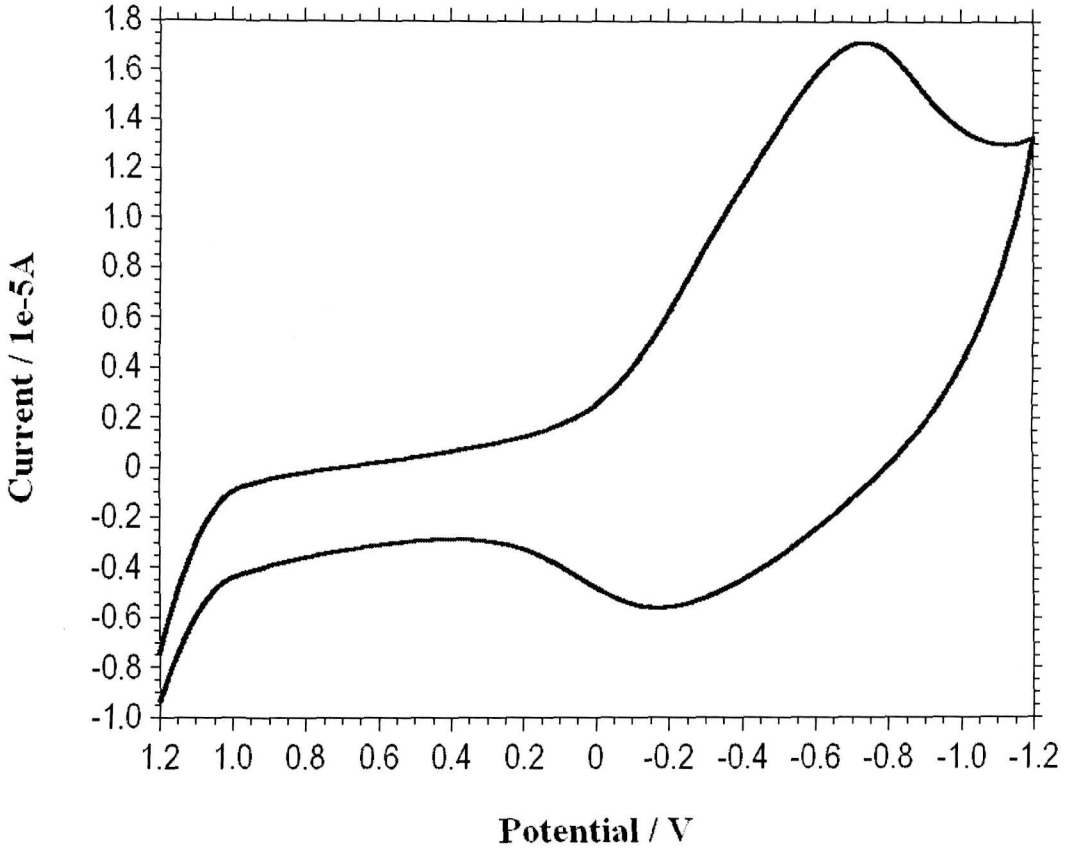

Cyclic voltamogram of the complex **9**

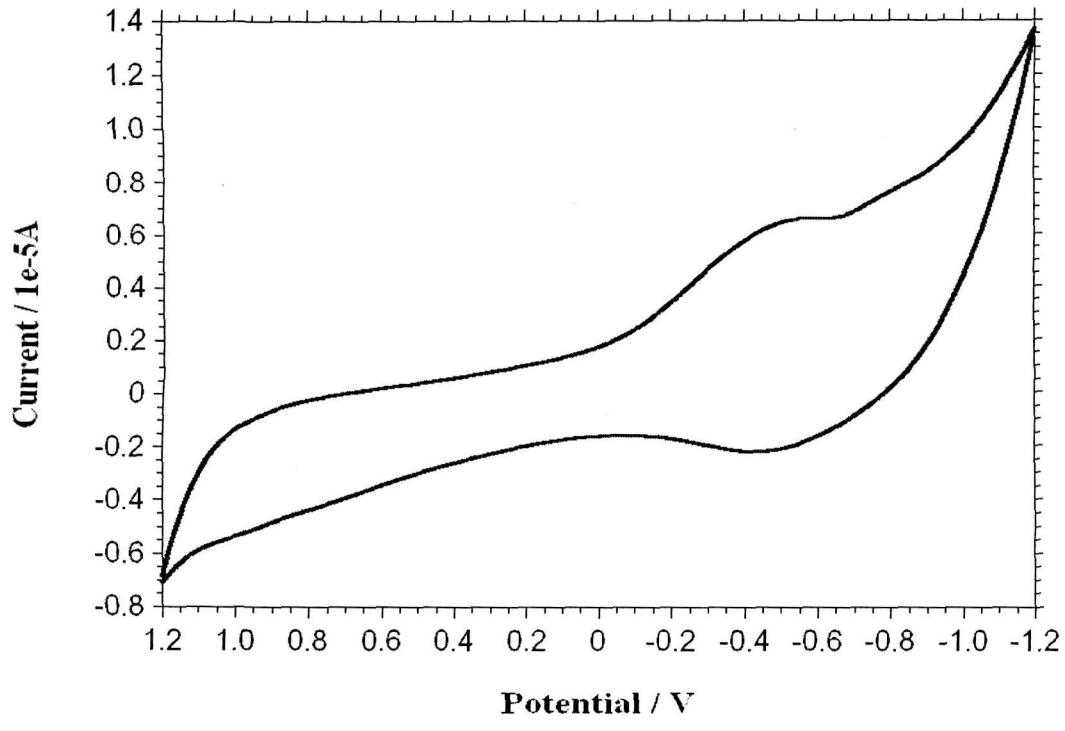

Cyclic voltamogram of the complex **10**

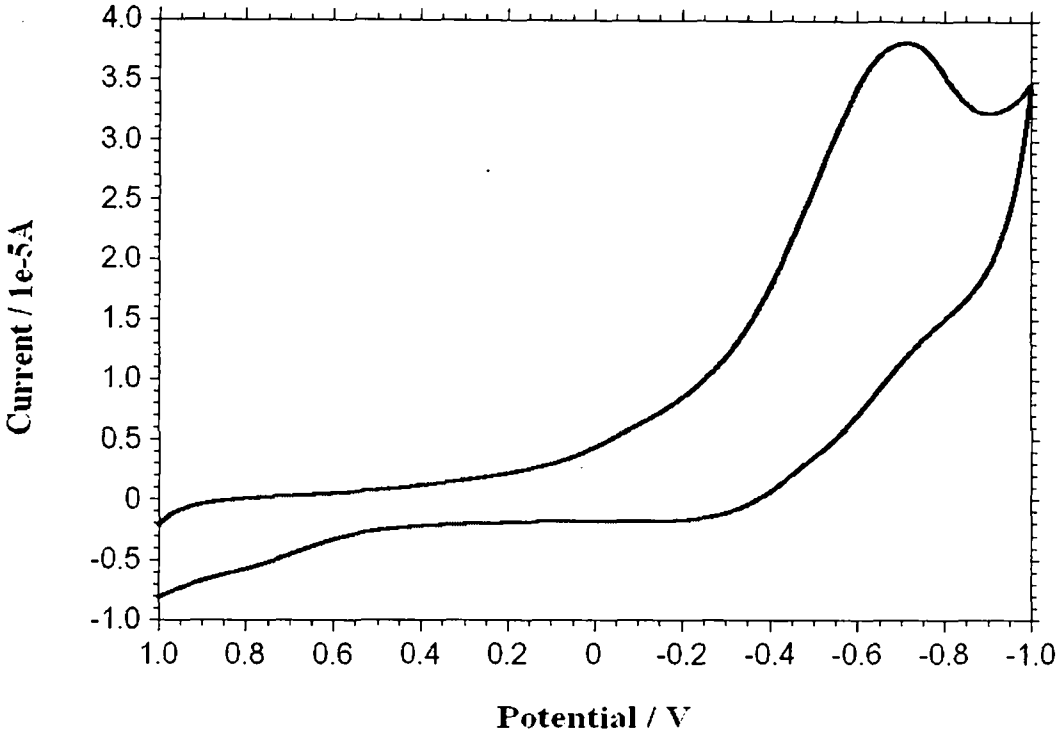

Cyclic voltamogram of the complex **15**

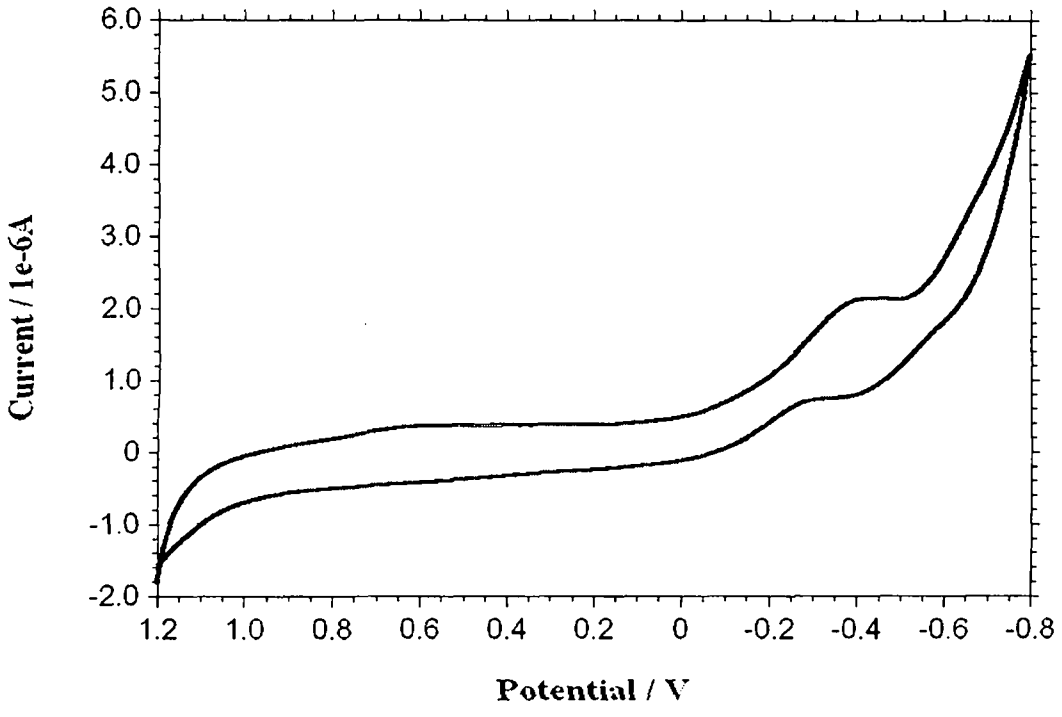

Cyclic voltamogram of the complex **16**

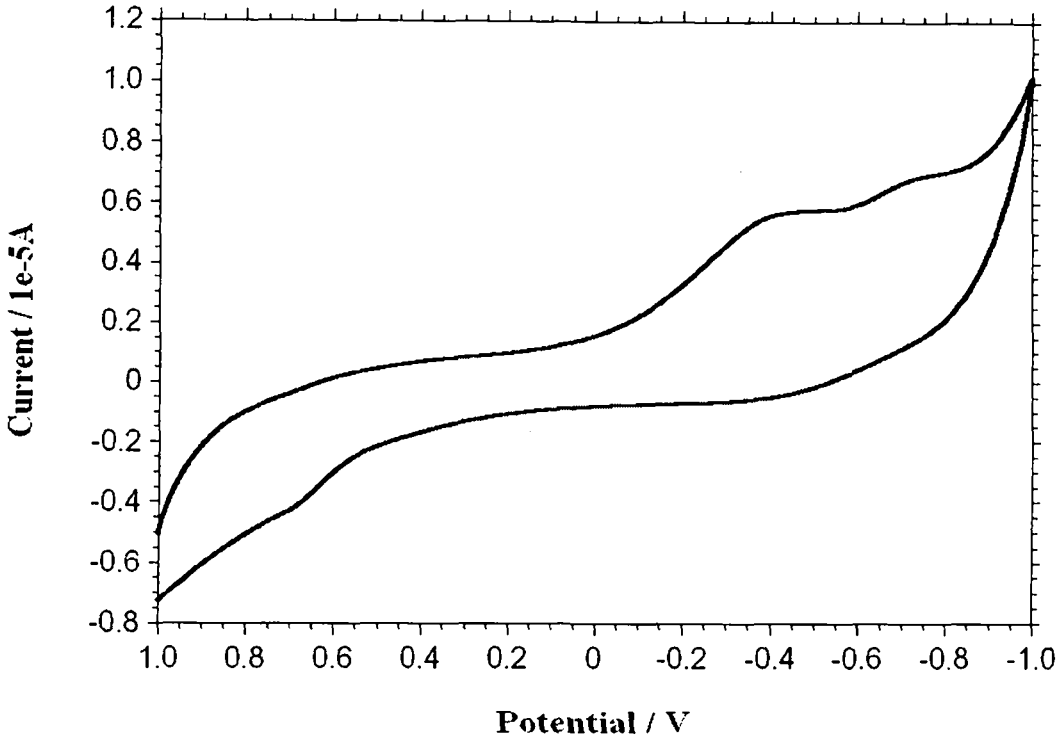

Cyclic voltamogram of the complex **17**

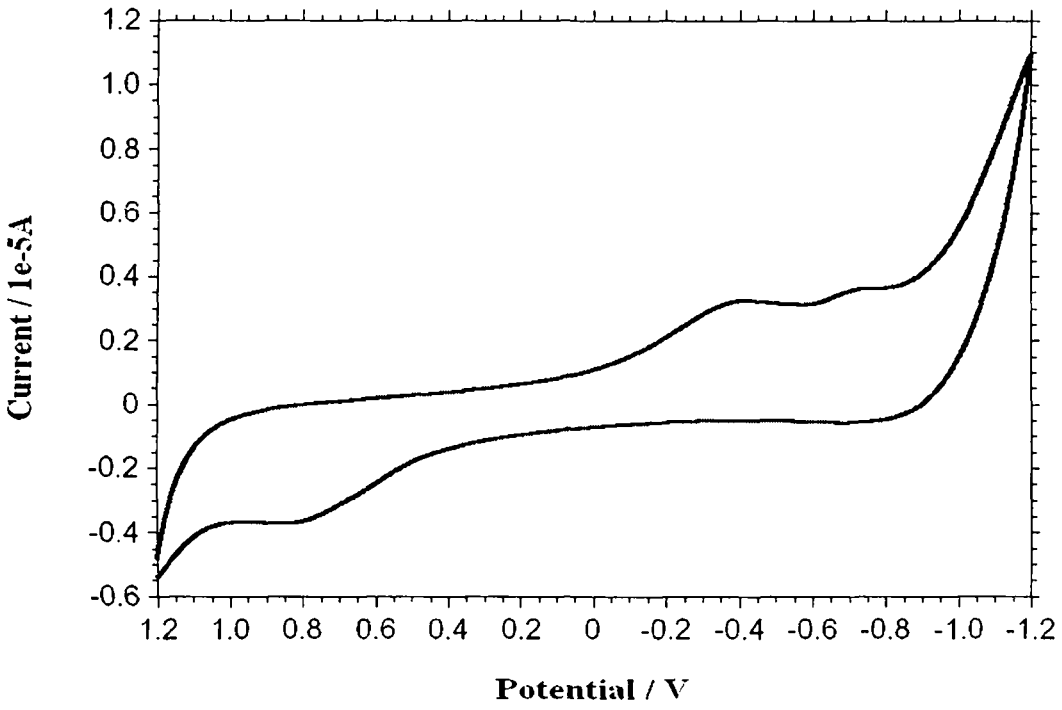

Cyclic voltamogram of the complex **18**

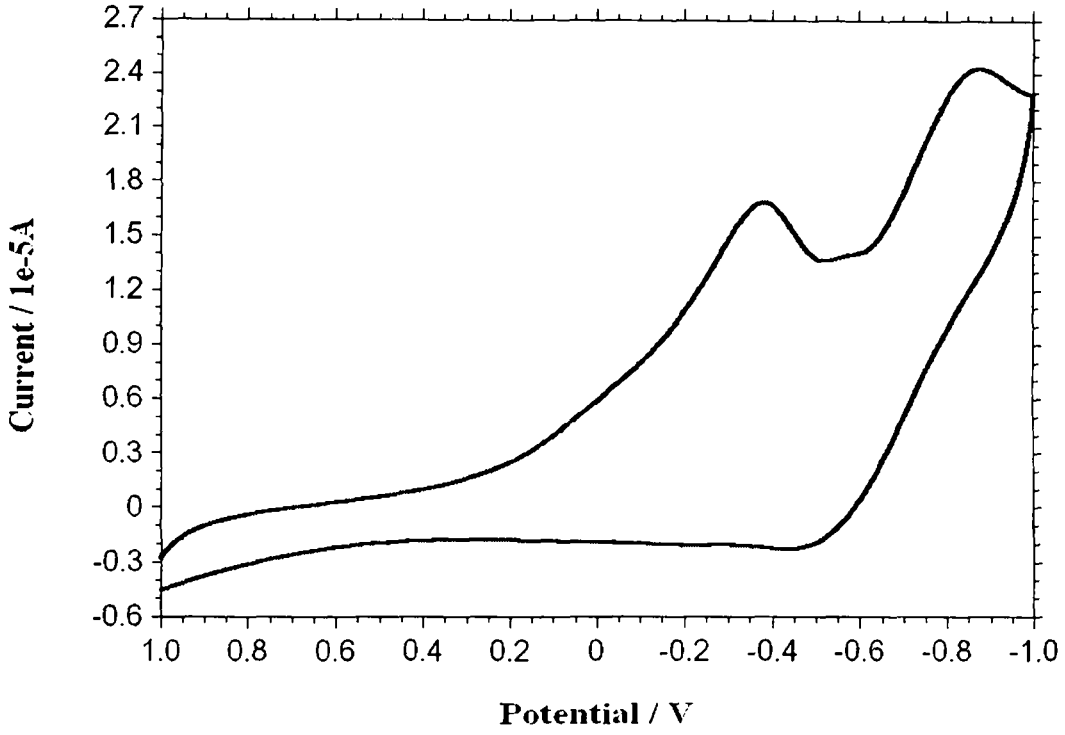

Cyclic voltamogram of the complex **19**

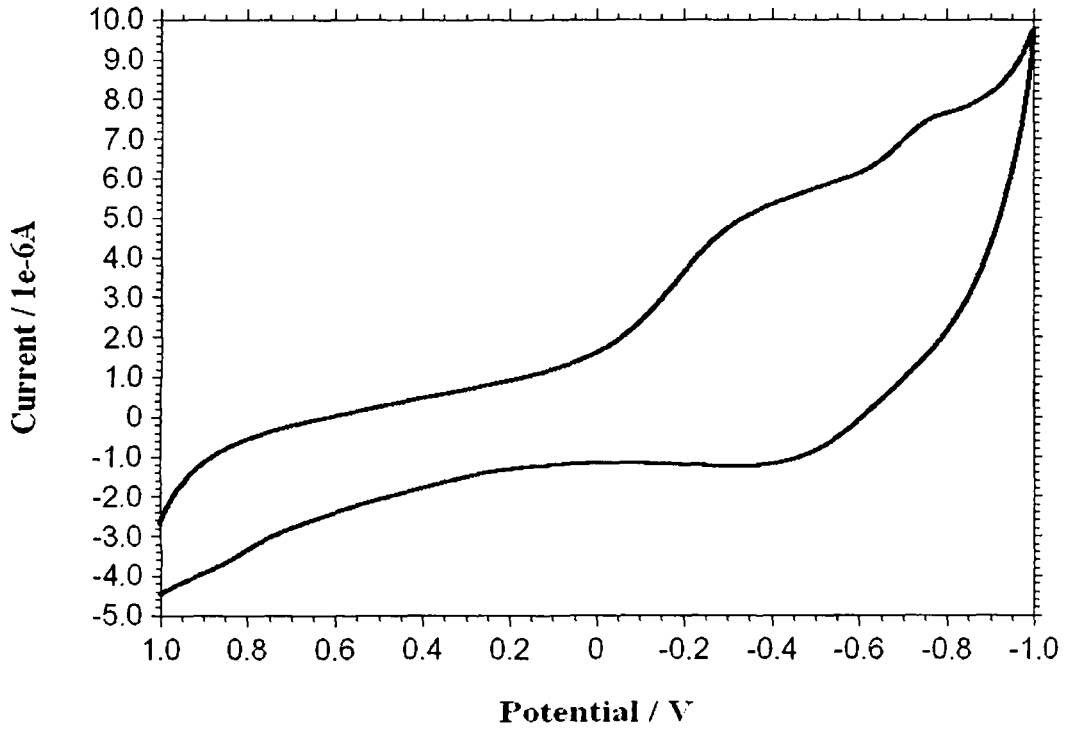

Cyclic voltamogram of the complex **20**

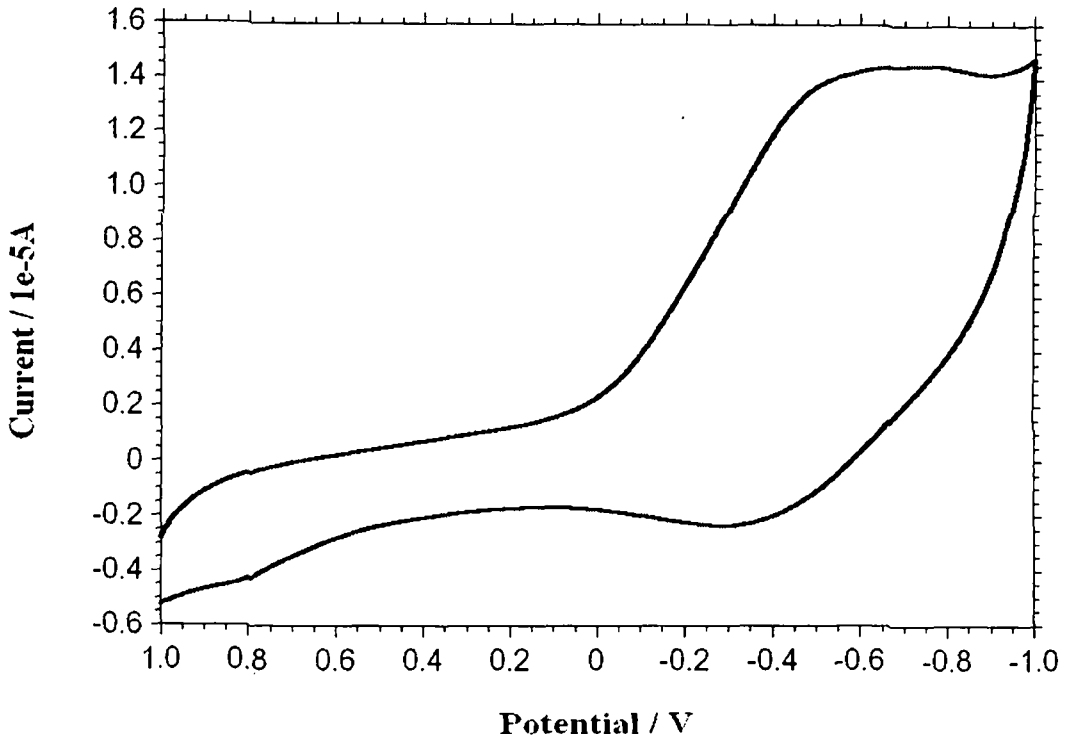

Cyclic voltamogram of the complex **21**

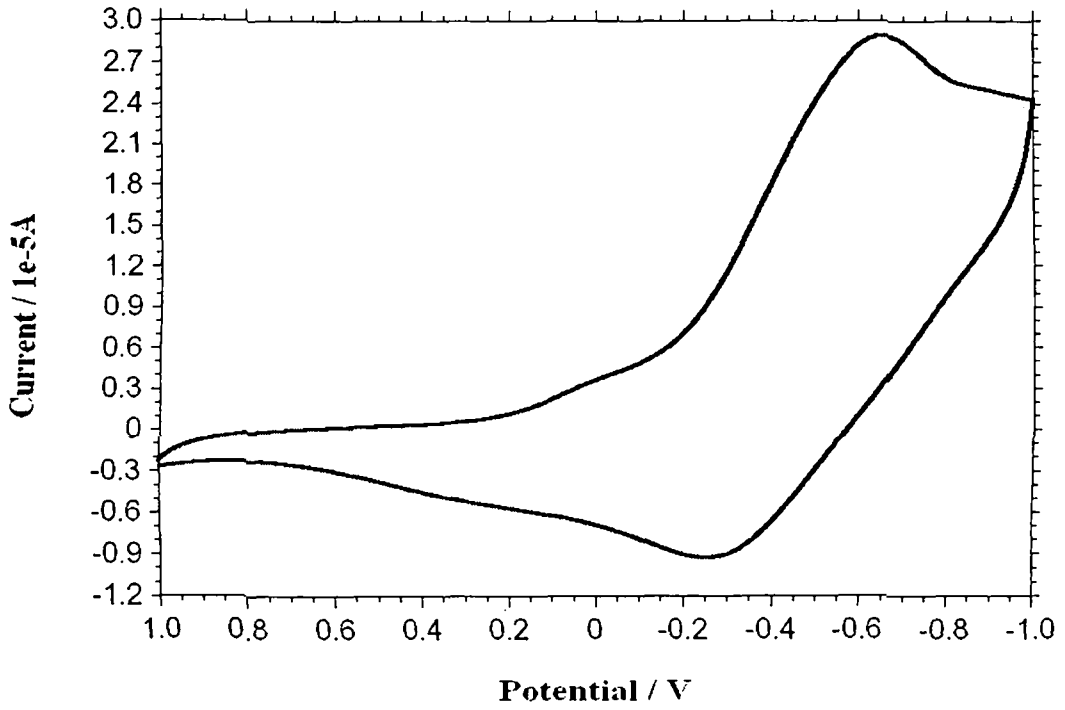

Cyclic voltamogram of the complex **24**

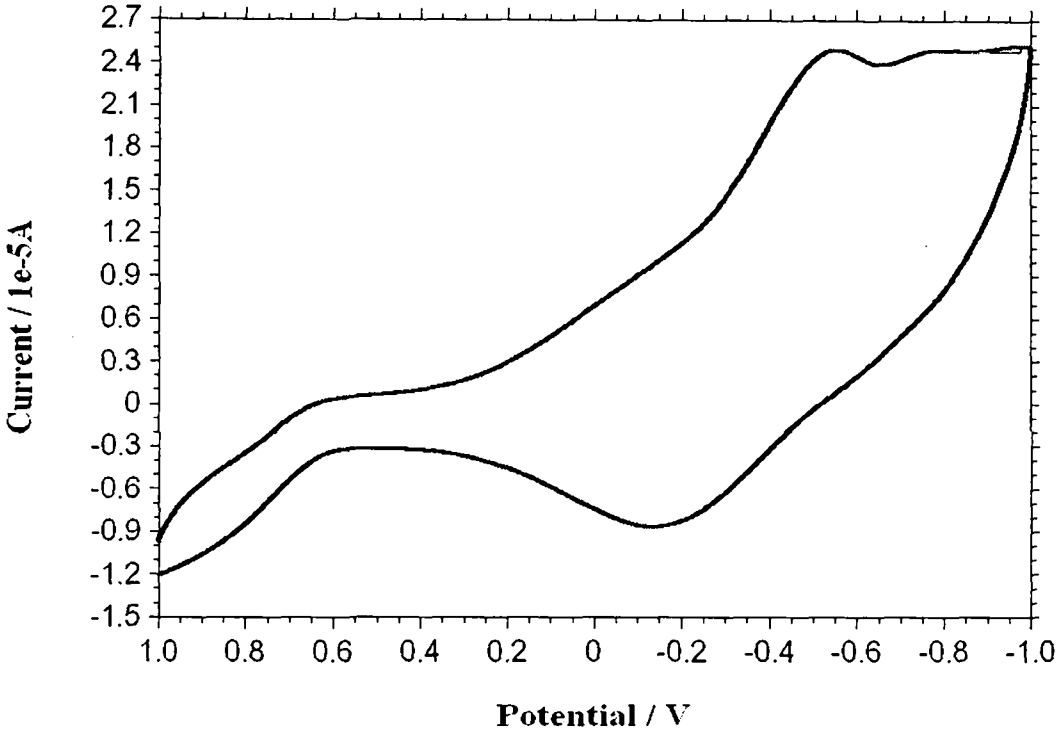

Cyclic voltamogram of the complex **25**

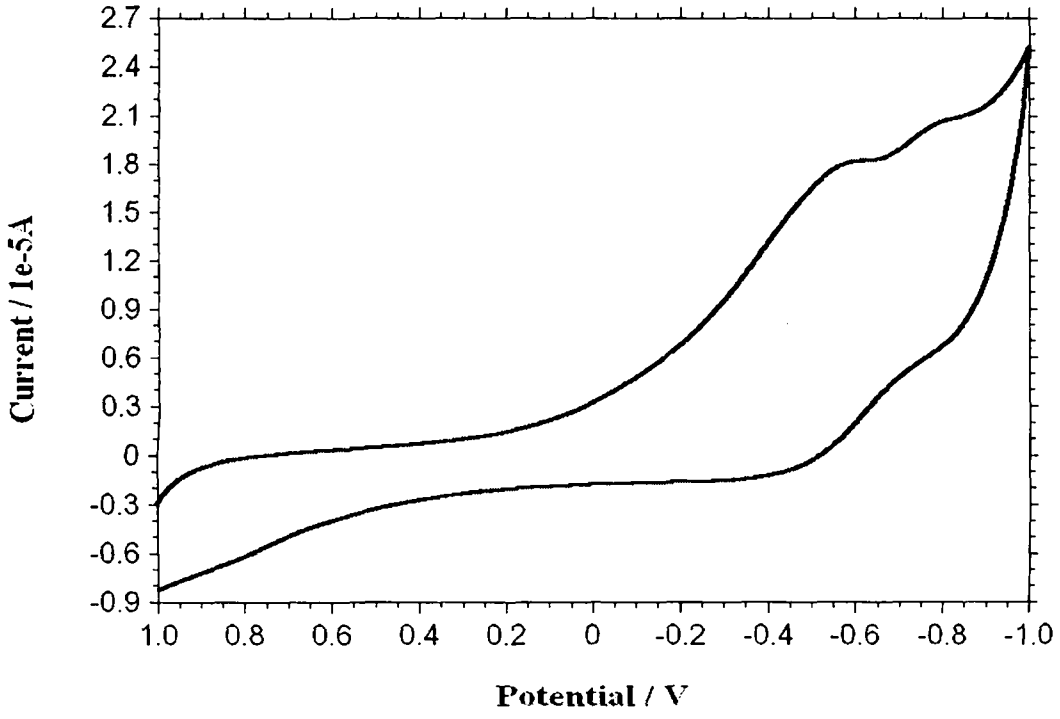

Cyclic voltamogram of the complex **26**

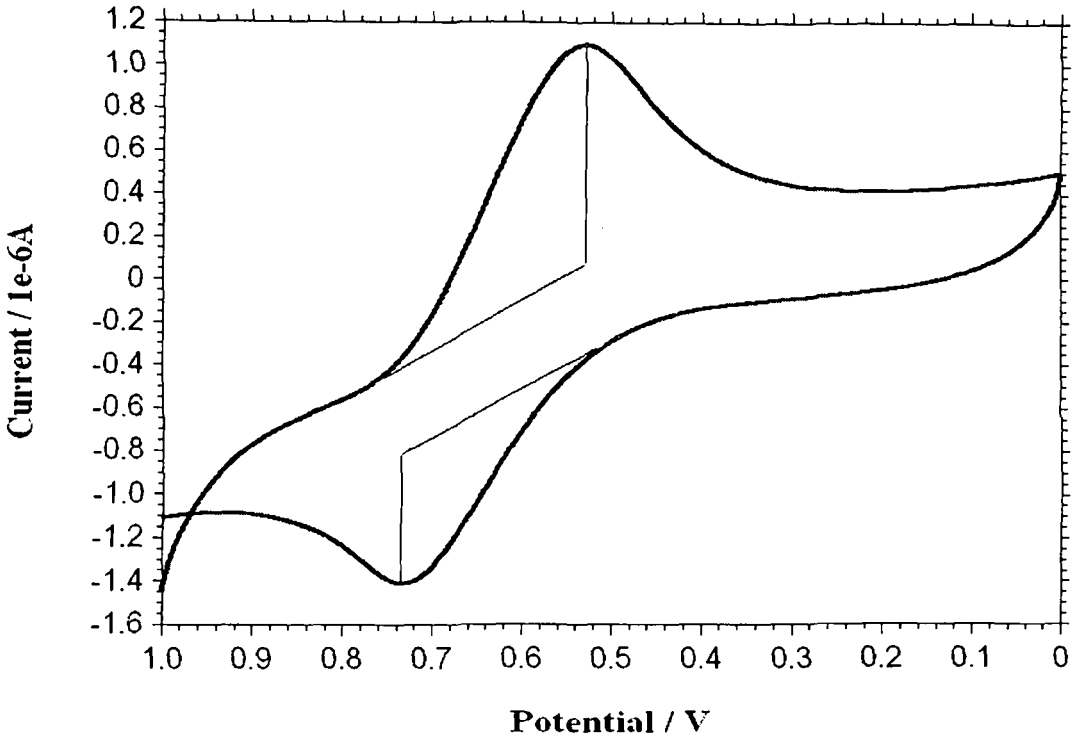

Cyclic voltamogram of the complex **29**

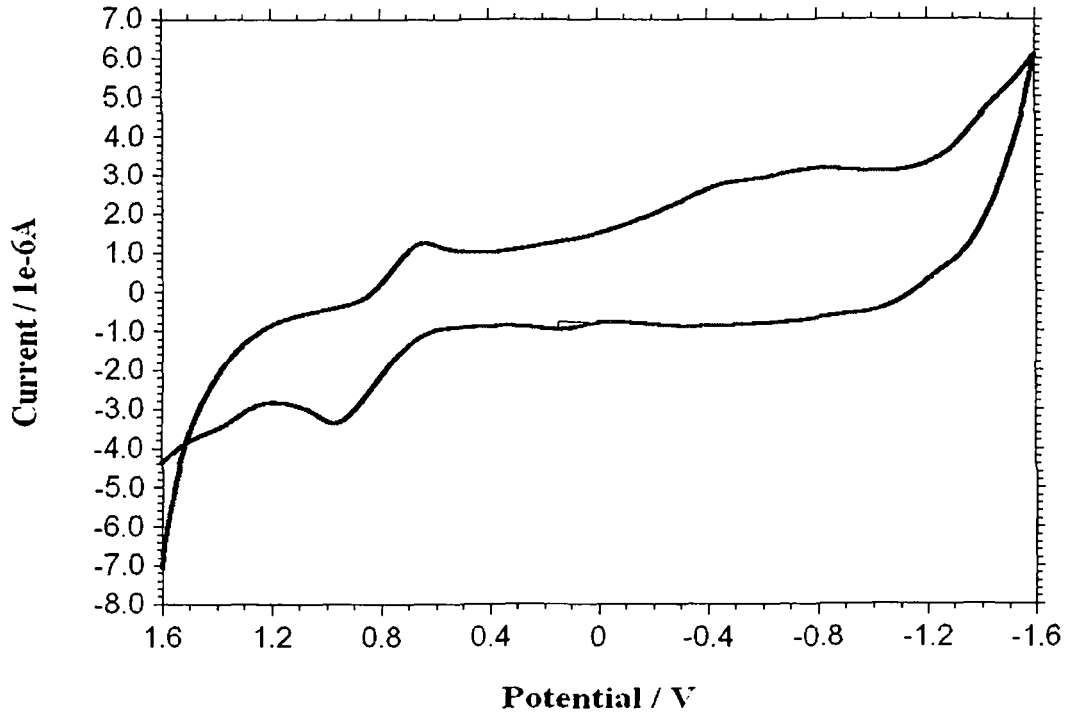

Cyclic voltamogram of the complex **30**

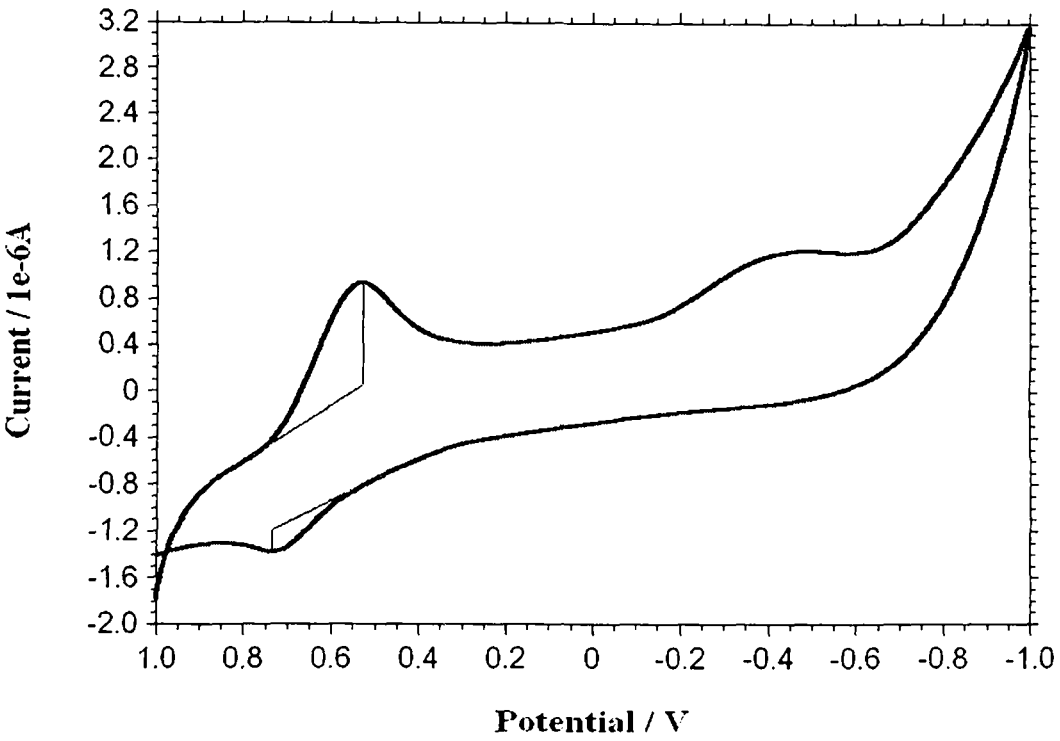

Cyclic voltamogram of the complex **31**

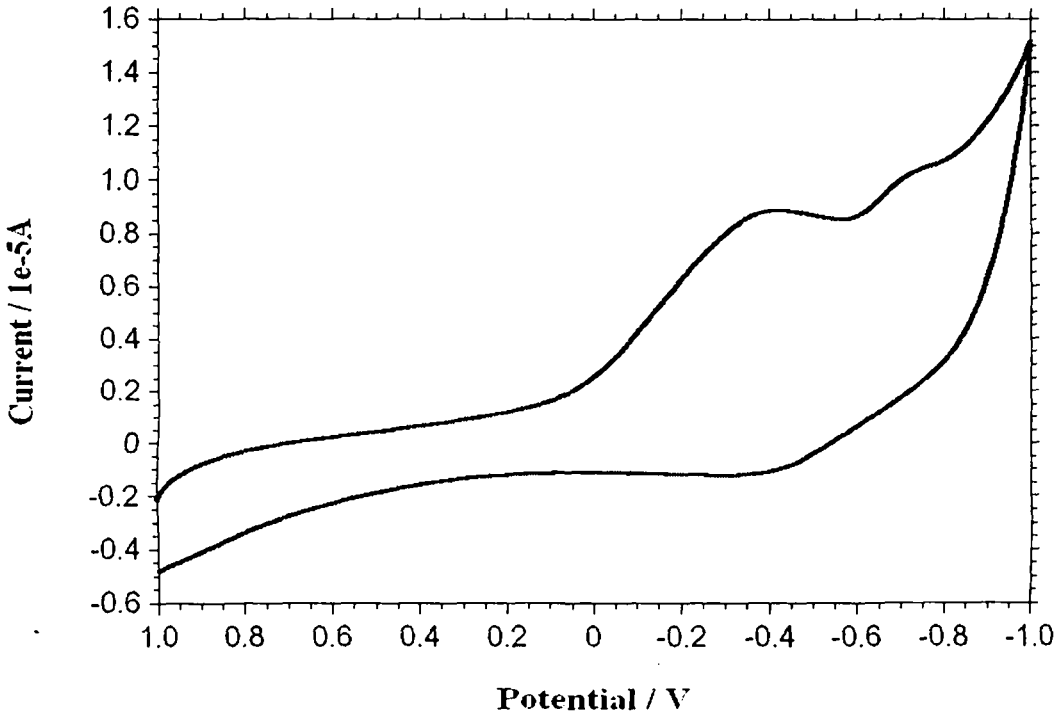

Cyclic voltamogram of the complex **34**

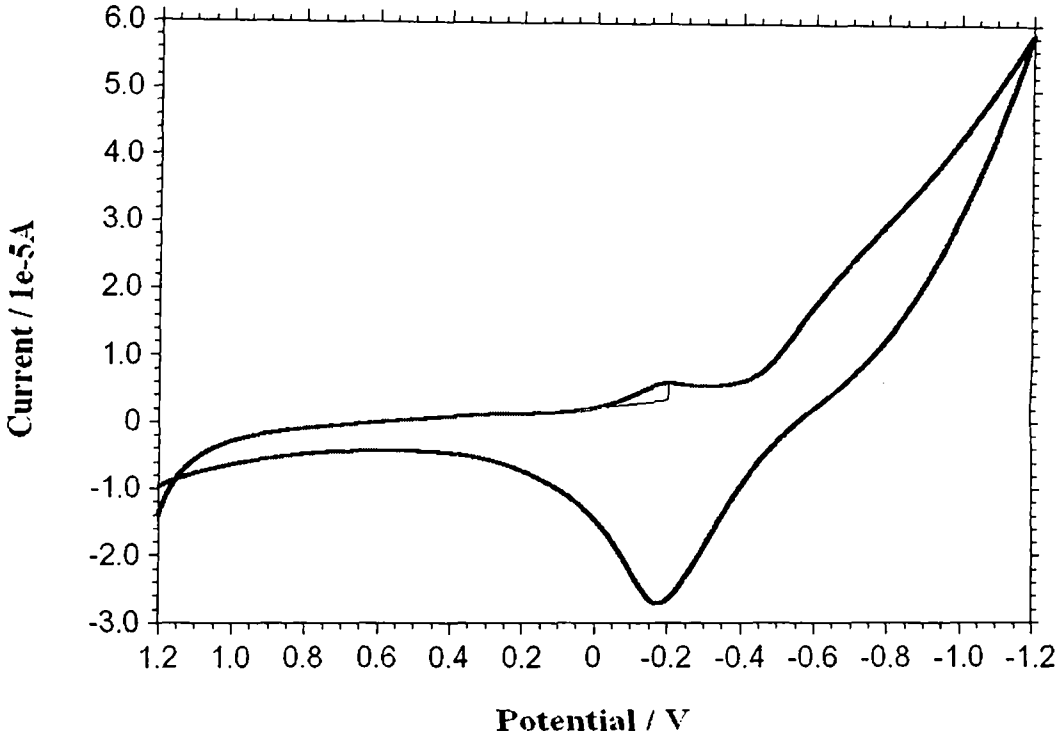

Cyclic voltamogram of the complex **36**

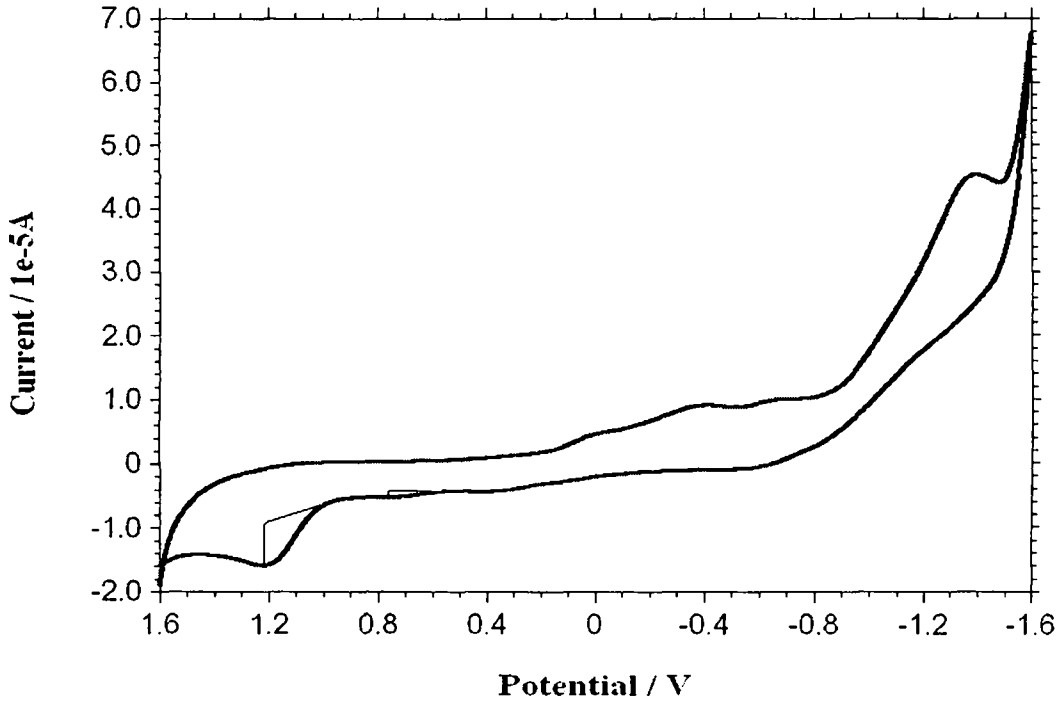

Cyclic voltamogram of the complex **38**

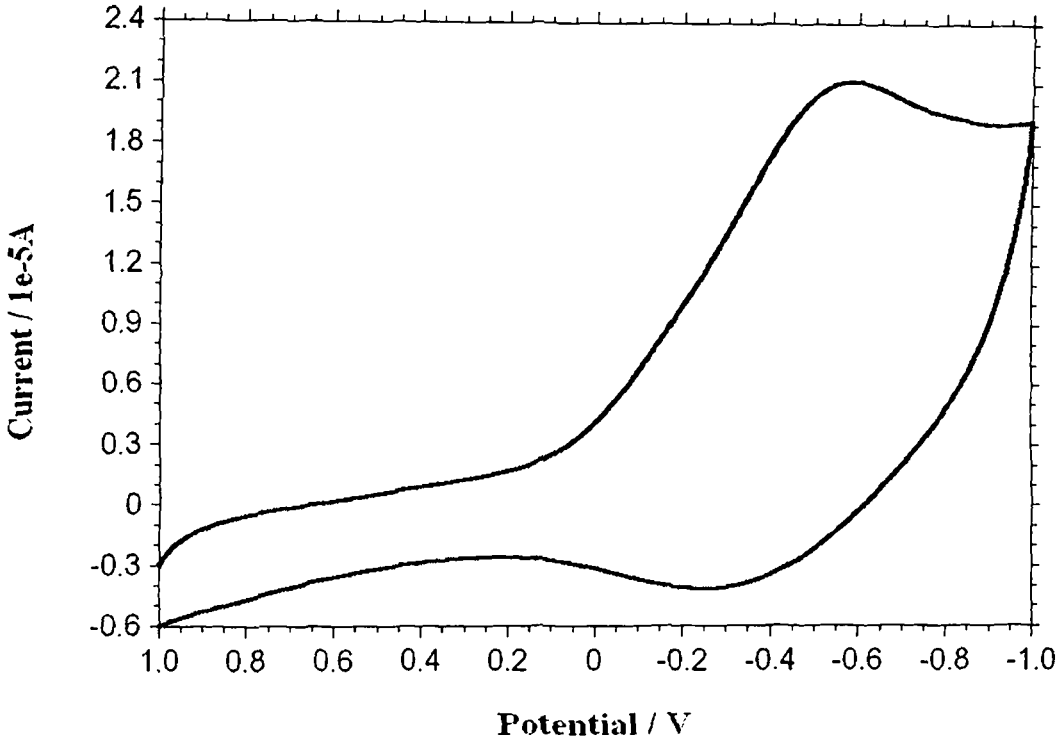

Cyclic voltamogram of the complex **39**

APPENDIX 7

TGA and DTA graph of the complexes

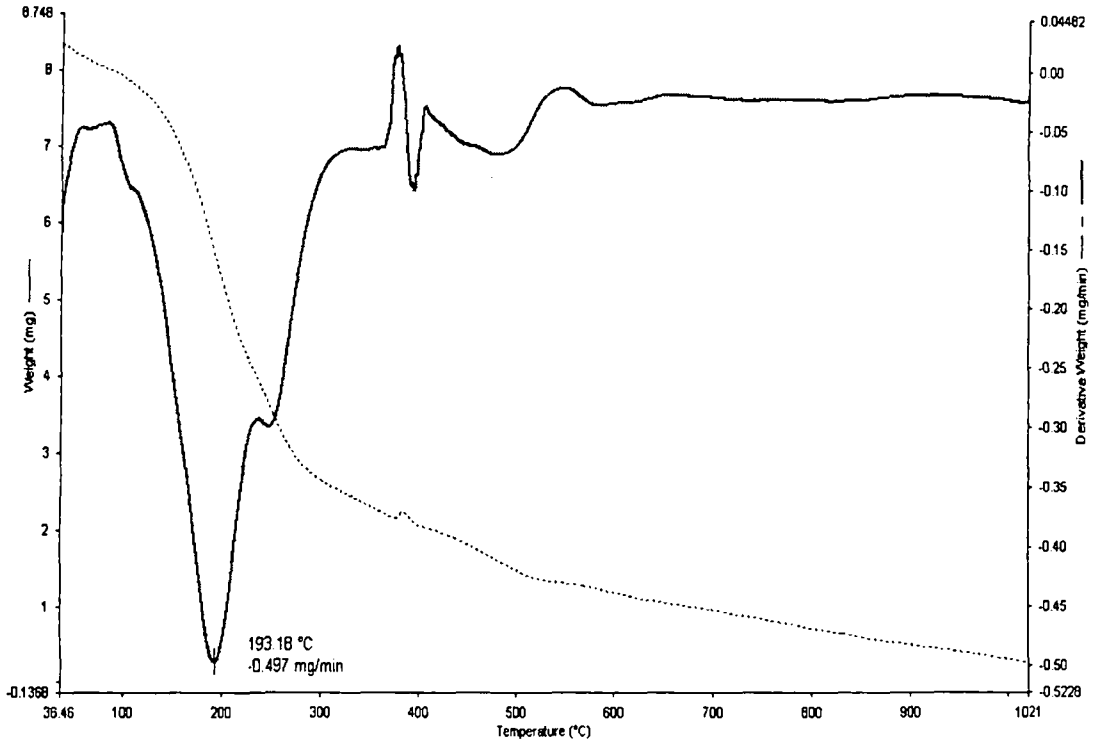

TGA graph of the complex $[VO(L_2)_2]SO_4.H_2O$ (**4**)

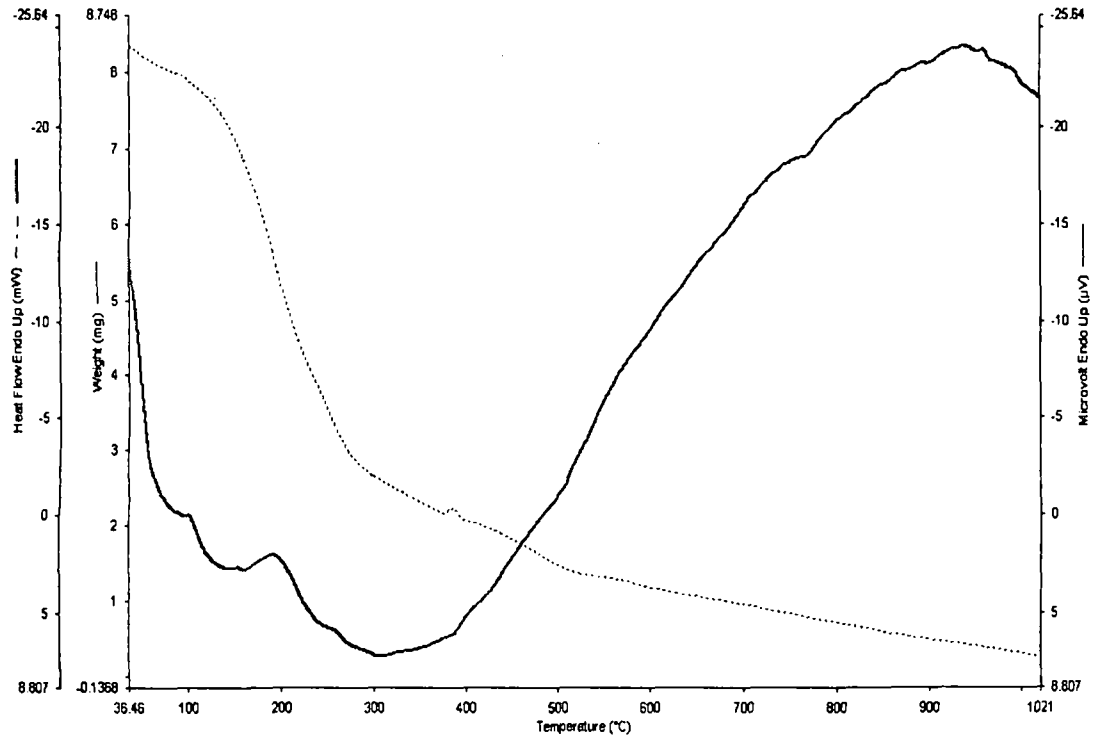

DTA graph of the complex $[VO(L_2)_2]SO_4.H_2O$ (**4**)

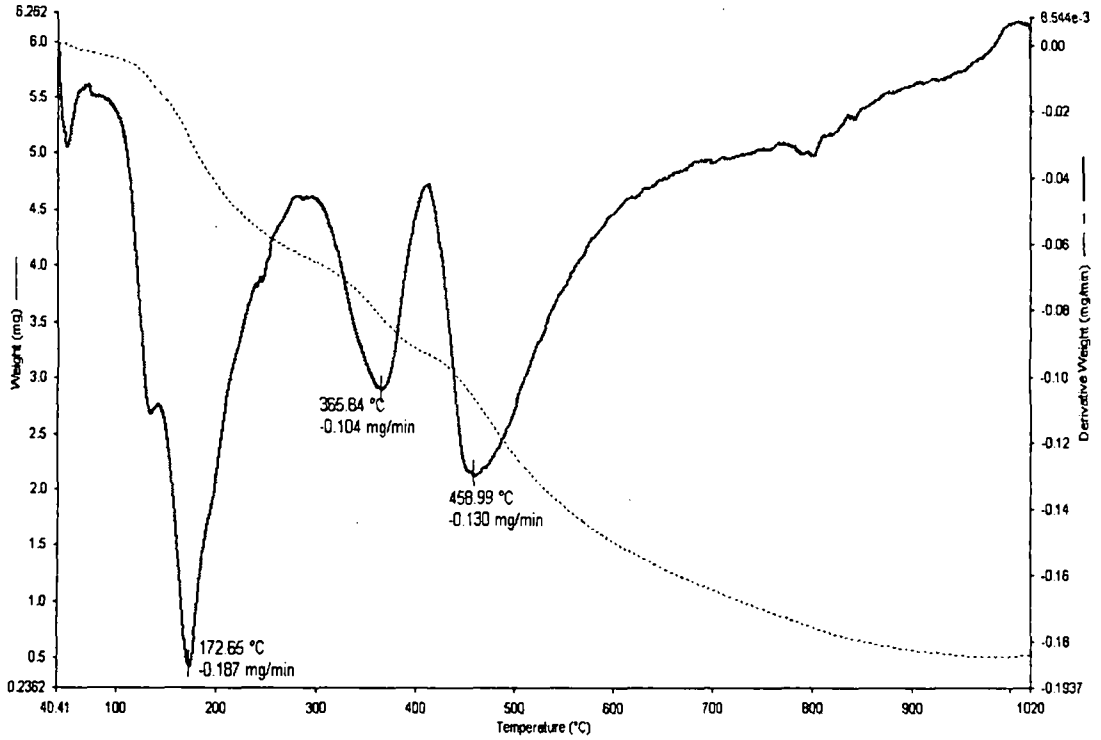

TGA graph of the complex $[VOL_6(H_2O)].H_2O$ (**16**)

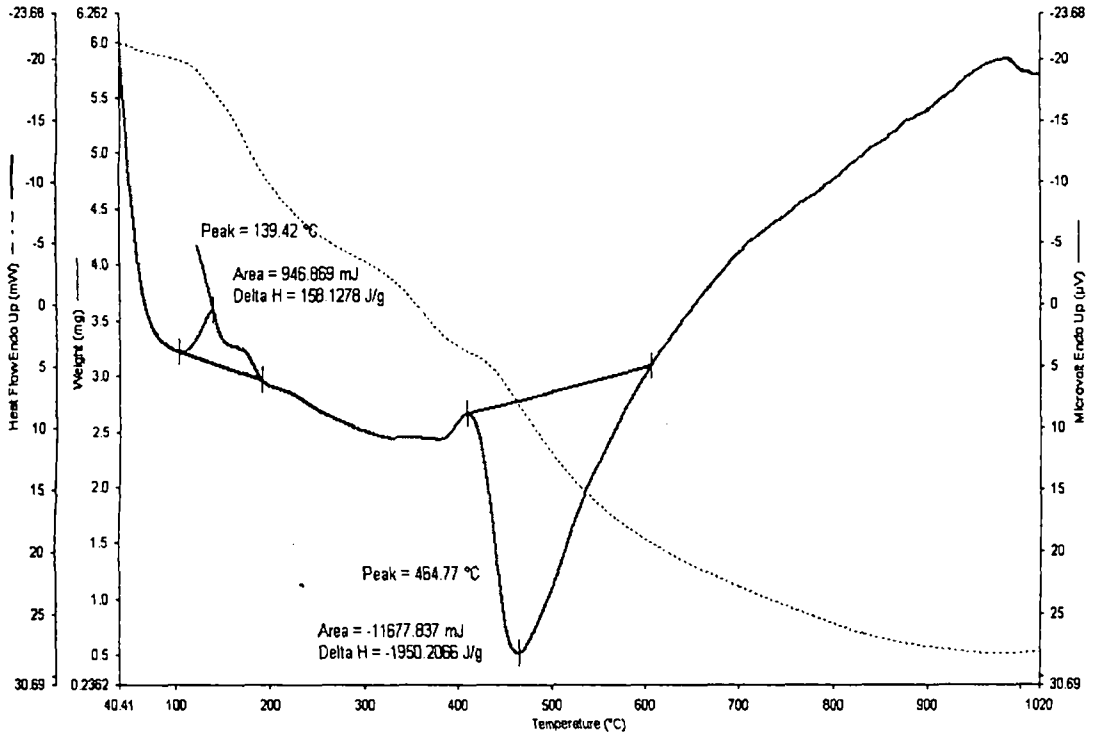

DTA graph of the complex $[VOL_6(H_2O)].H_2O$ (**16**)

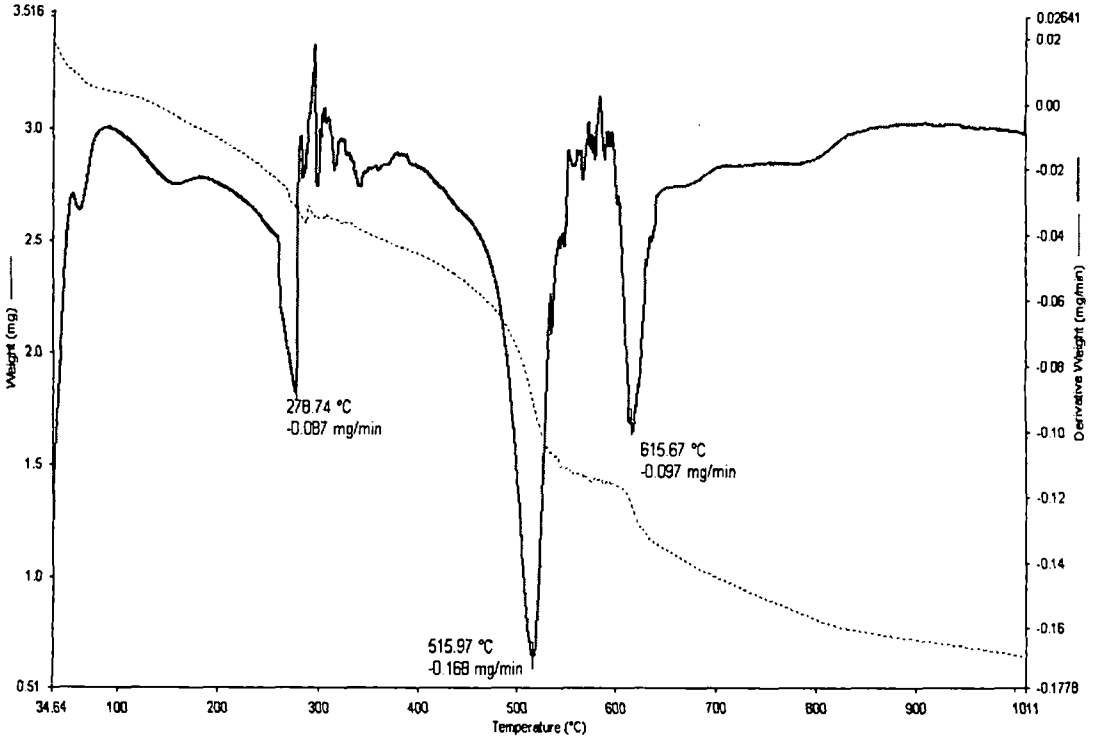

TGA graph of the complex $[FeL_7(acac)(EtOH)]$ (**17**)

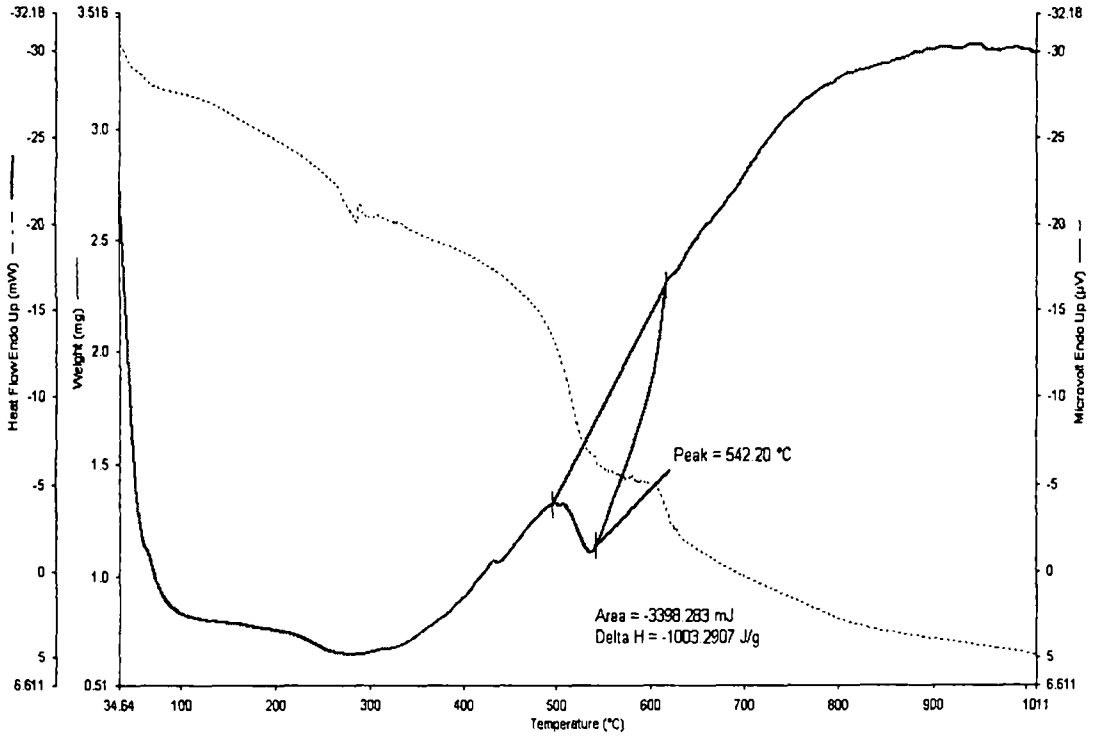

DTA graph of the complex $[FeL_7(acac)(EtOH)]$ (**17**)

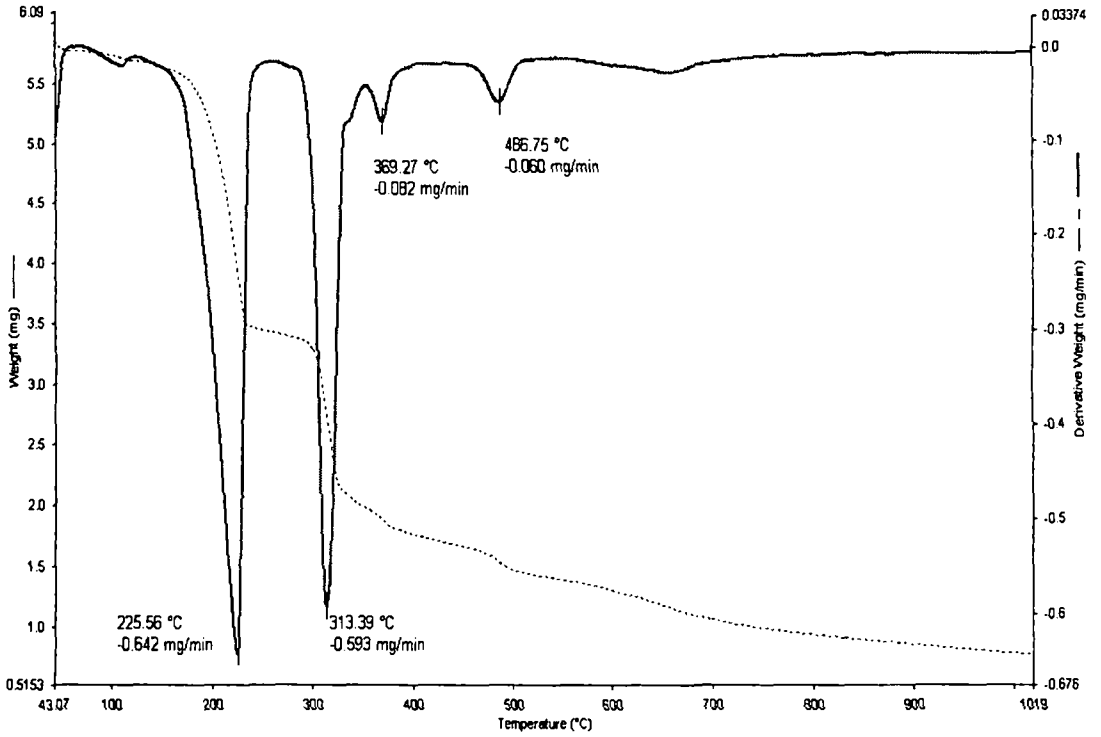

TGA graph of the complex $[FeL_9(H_2O)_2]NO_3$ (**19**)

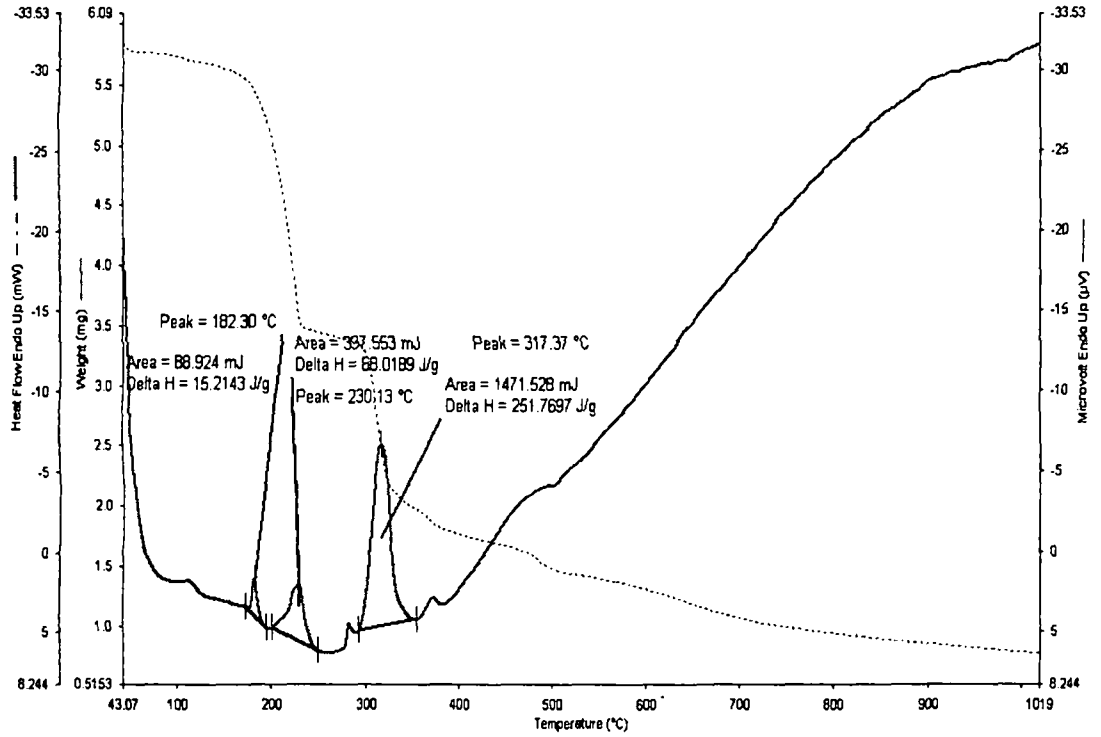

DTA graph of the complex $[FeL_9(H_2O)_2]NO_3$ (**19**)

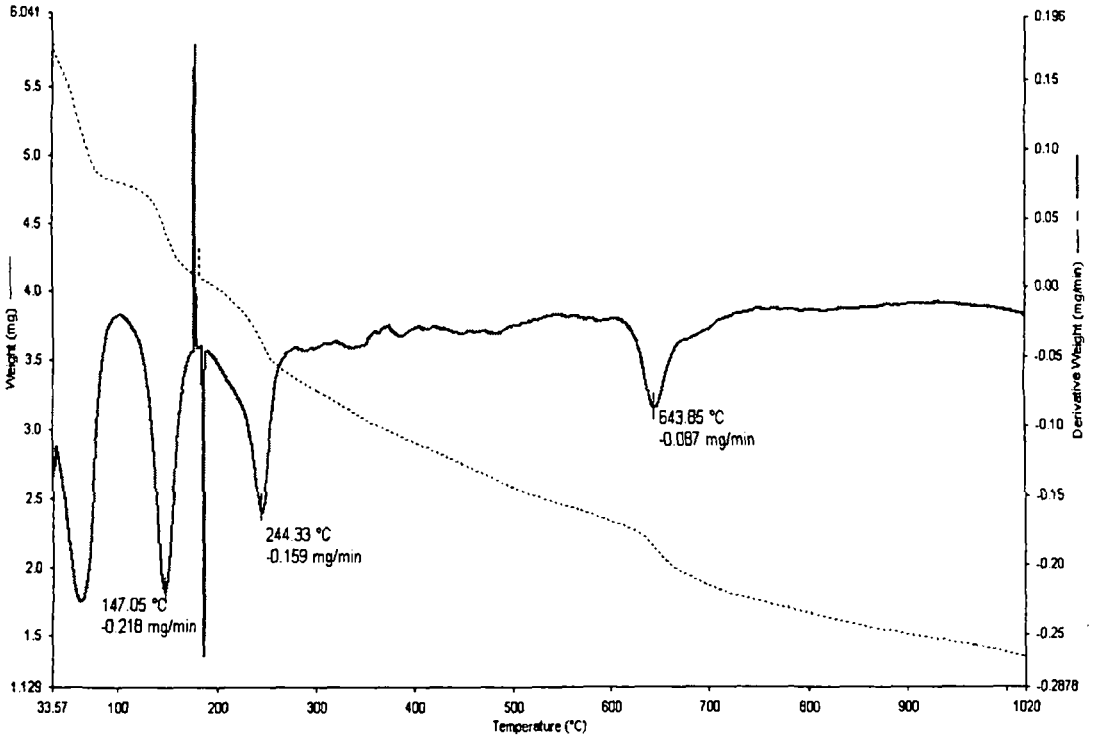

TGA graph of the complex $[FeL_{12}(H_2O)_2]NO_3$ (**21**)

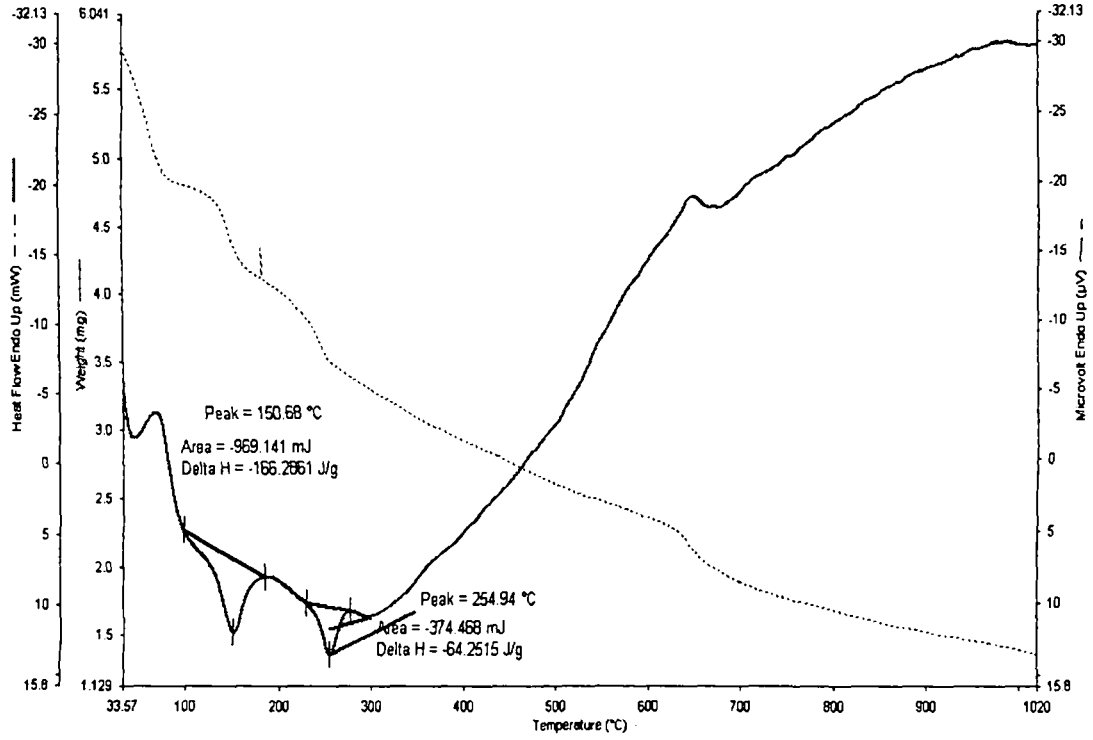

DTA graph of the complex $[FeL_{12}(H_2O)_2]NO_3$ (**21**)

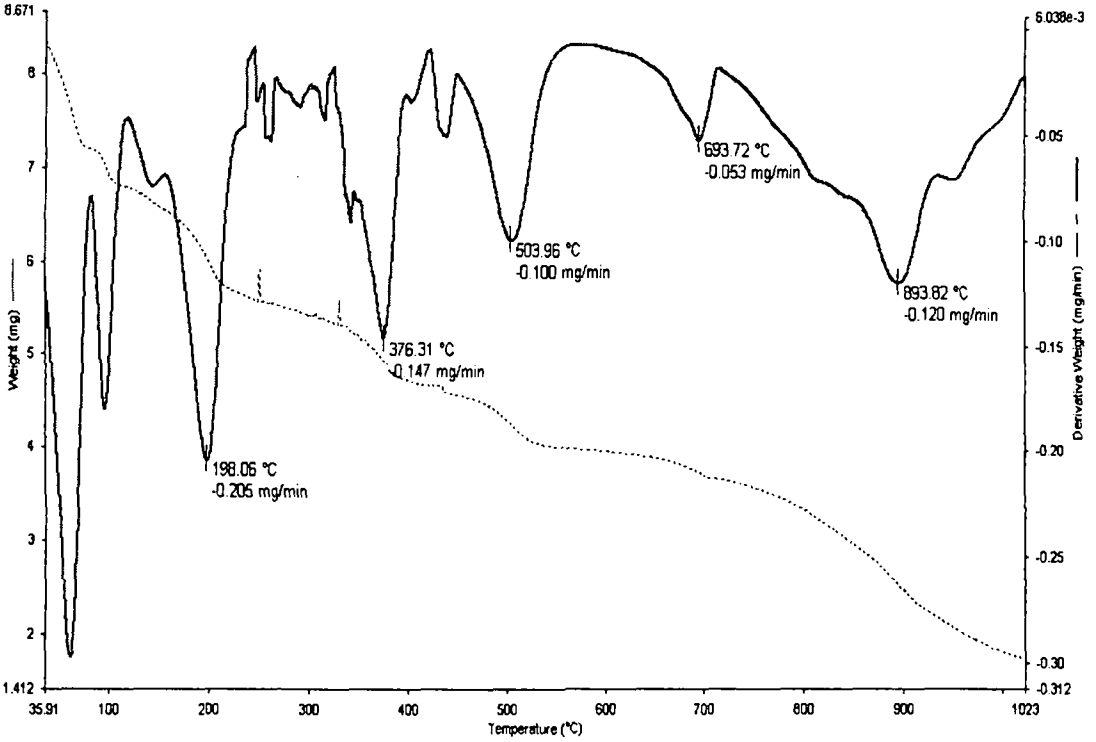

TGA graph of the complex $NH_4[FeL_9F_2]$ (**24**)

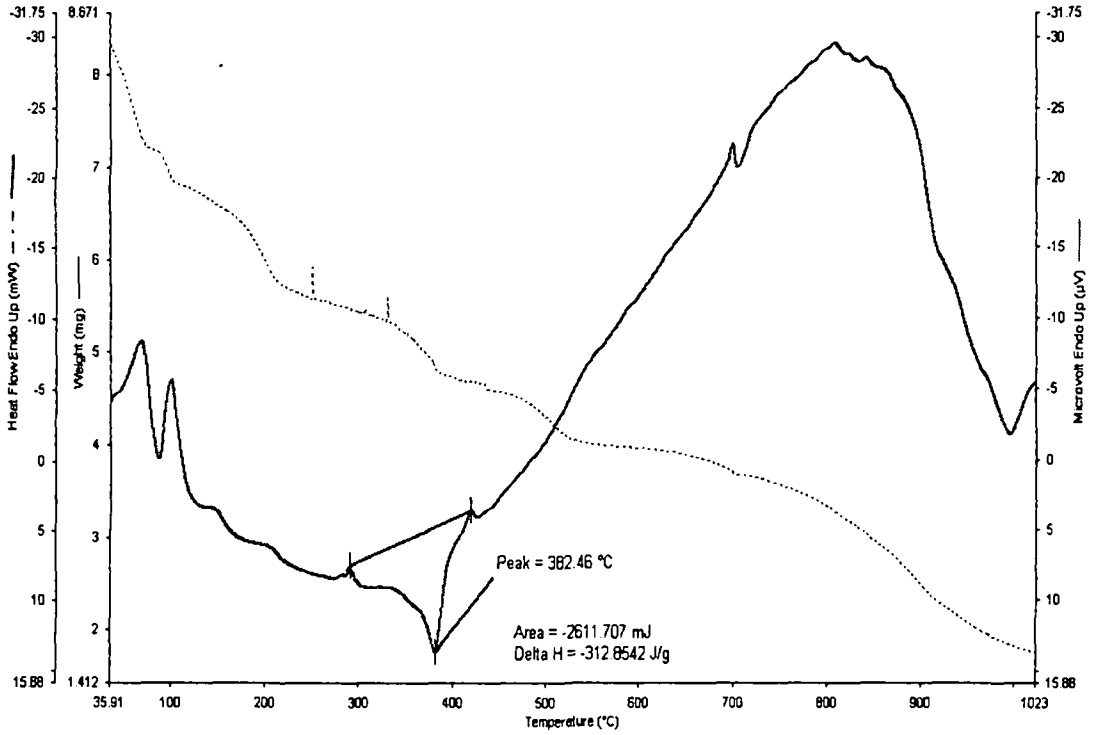

DTA graph of the complex $NH_4[FeL_9F_2]$ (**24**)

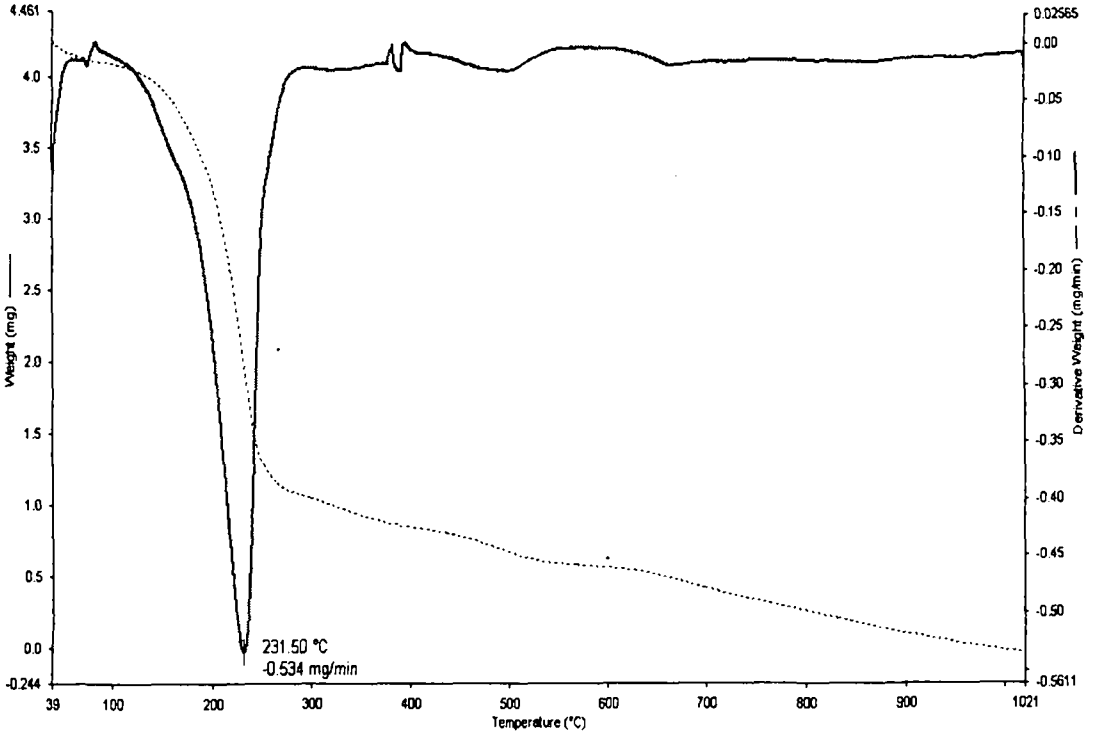

TGA graph of the complex $[VOL_{12}]H_2O$ (**31**)

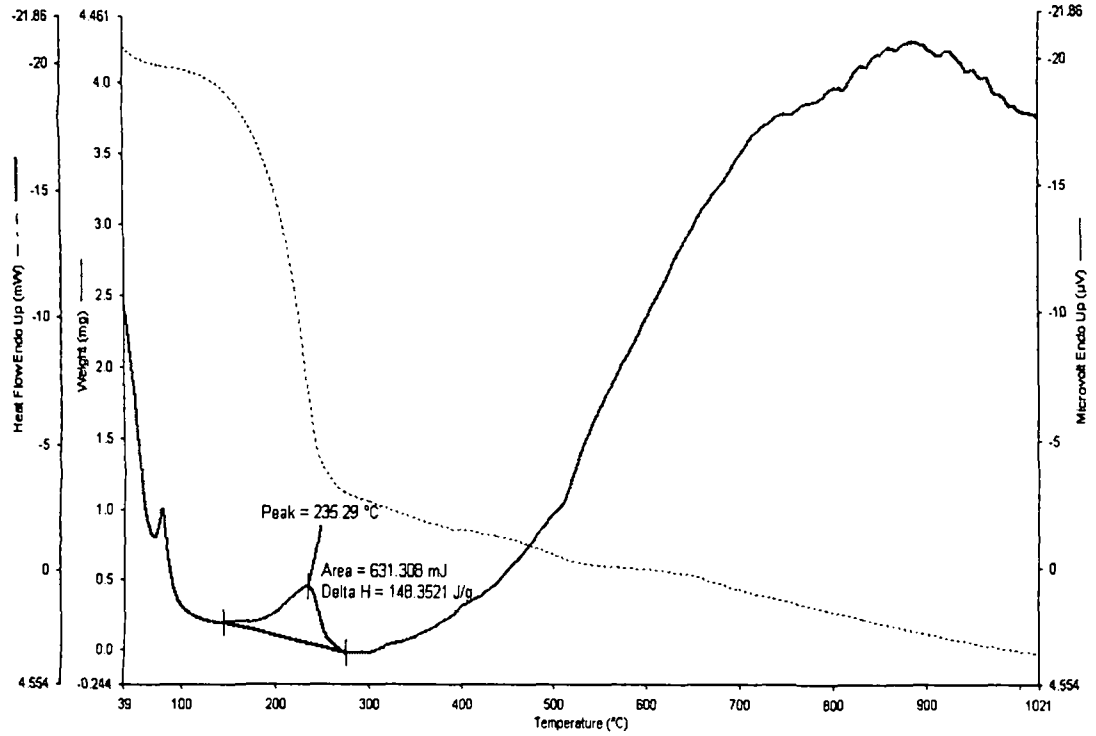

DTA graph of the complex $[VOL_{12}]H_2O$ (**31**)

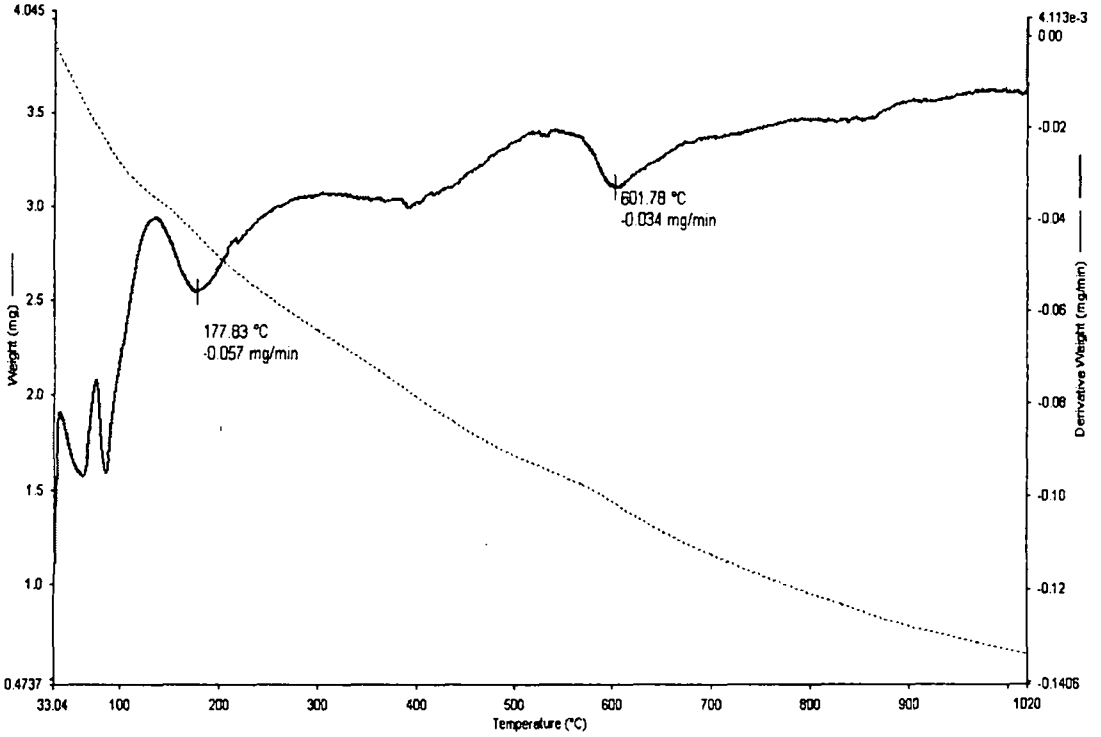

TGA graph of the complex $FeL_{10}(H_2O)_2](NO_3)_3$ (**38**)

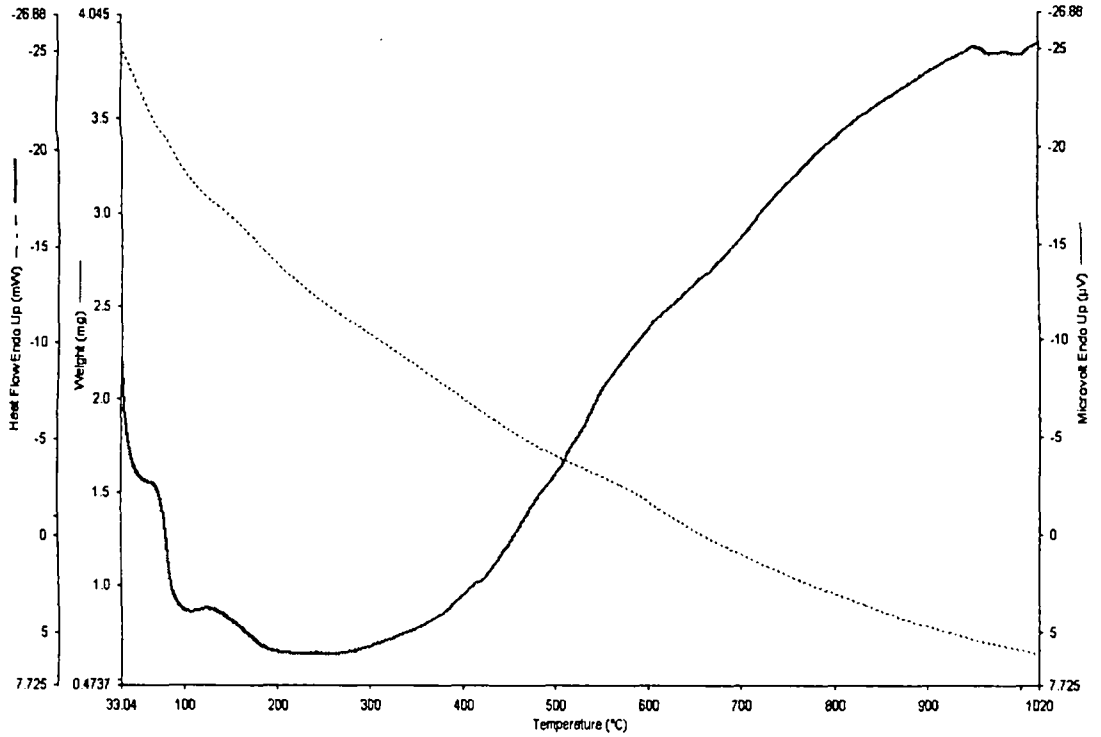

DTA graph of the complex $FeL_{10}(H_2O)_2](NO_3)_3$ (**38**)

APPENDIX 8

Hysteresis curve of the complexes

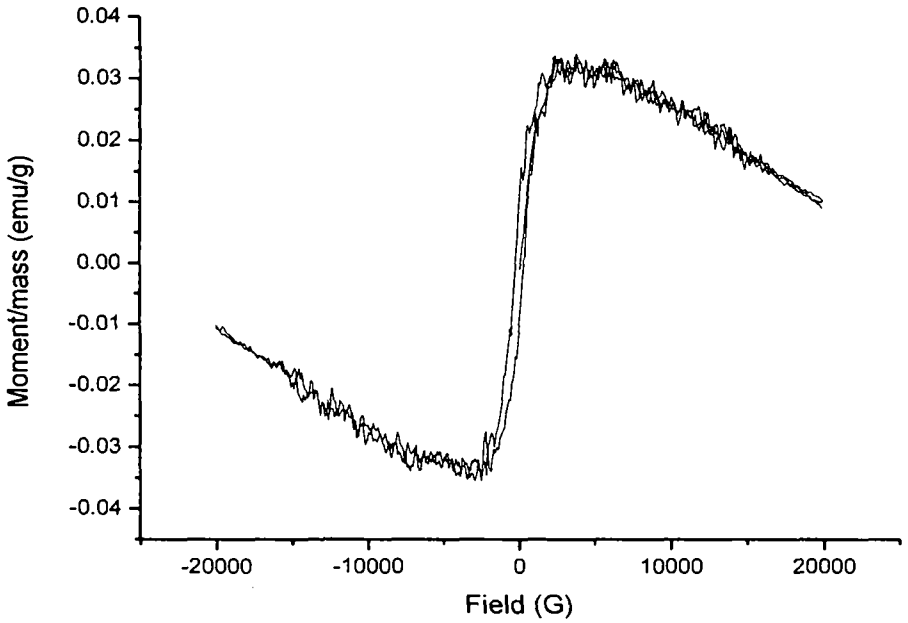

Field dependence of magnetization for the complex

$[Fe(L_2)_2(NO_3)_2]NO_3$ (**2**)

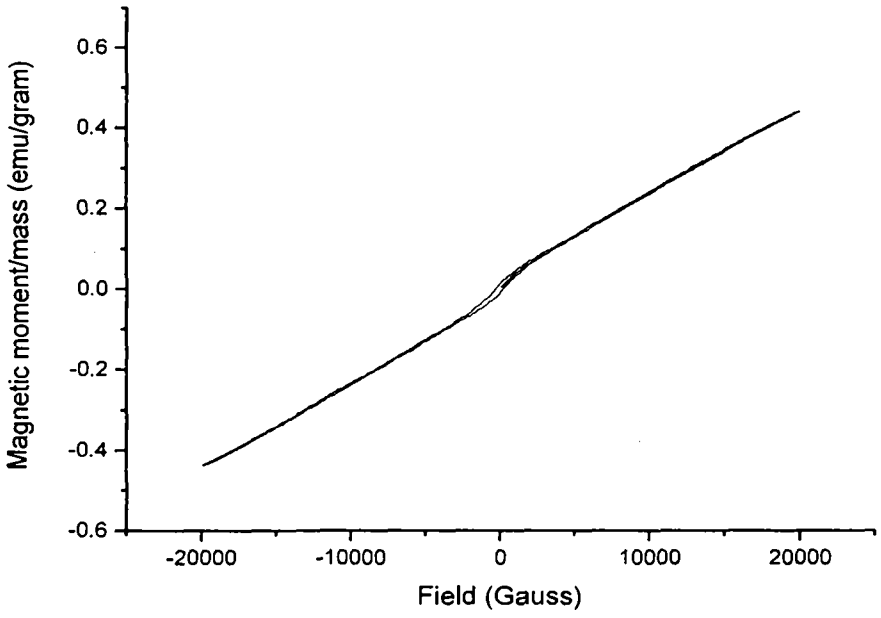

Field dependence of magnetization for the complex

$[FeL_5Cl]_2$ (**9**)

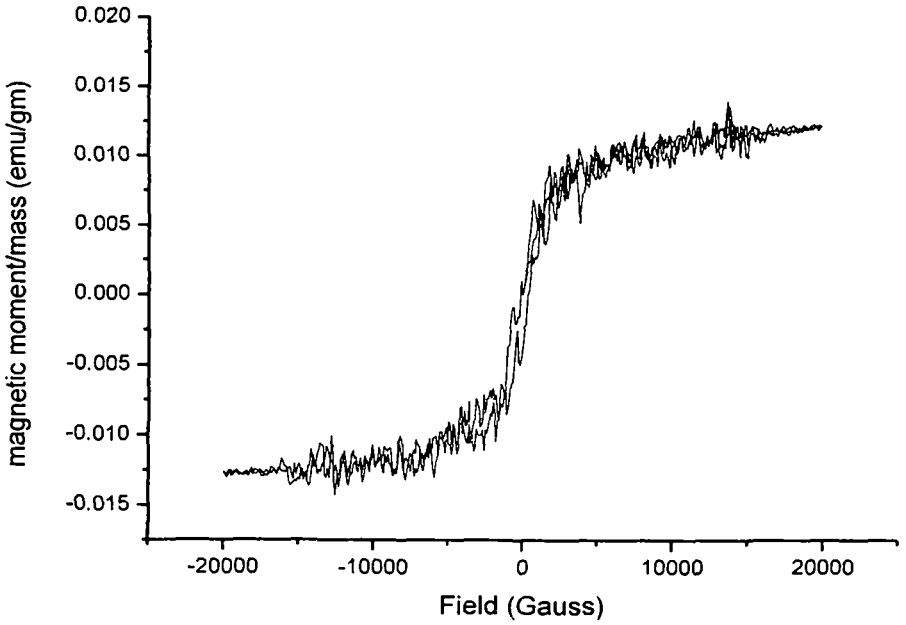

Field dependence of magnetization for the complex $[VOL_5]_2.H_2O$ (**10**)

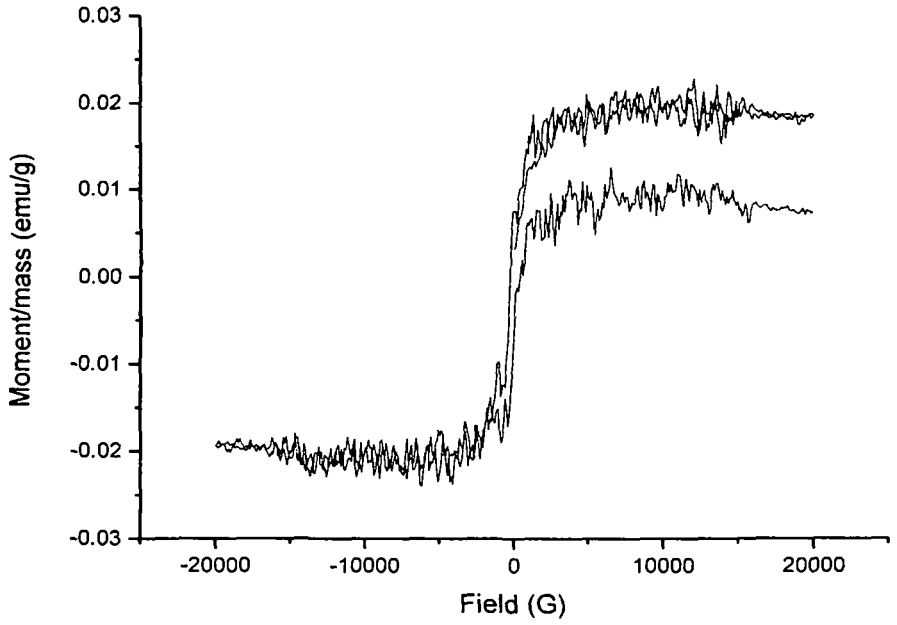

Field dependence of magnetization for the complex $[VOL_6(H_2O)].H_2O$ (**16**)

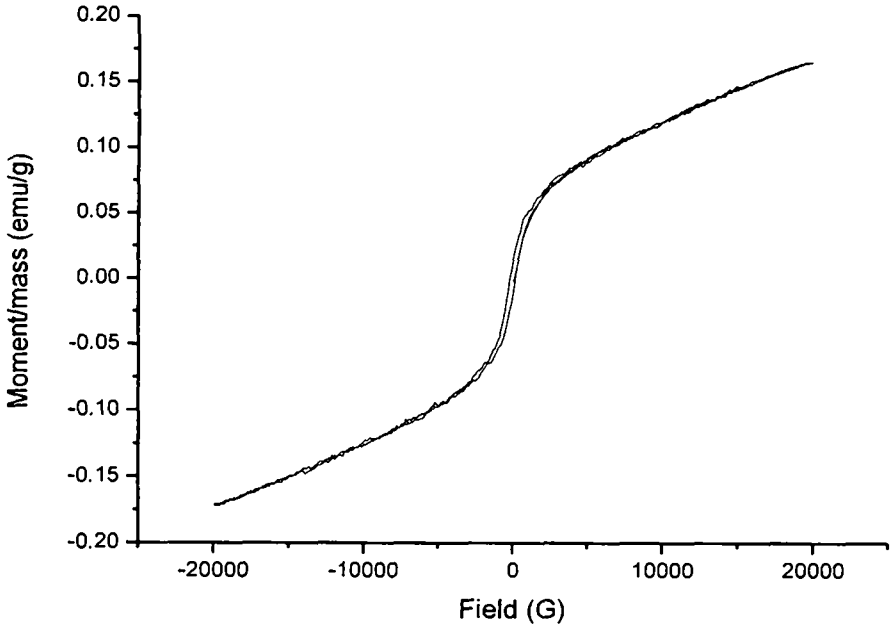

Field dependence of magnetization for the complex $[FeL_{12}(H_2O)_2]NO_3$ (**21**)

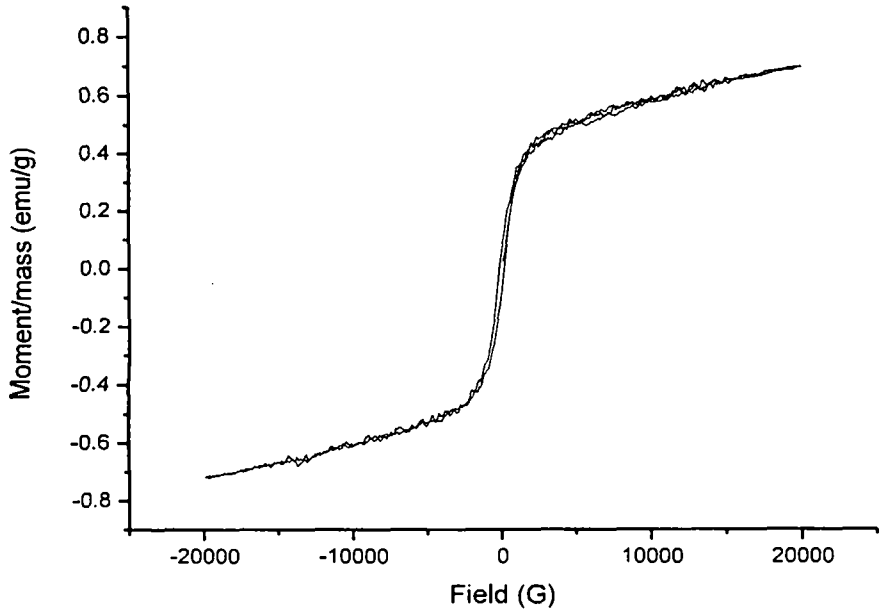

Field dependence of magnetization for the complex $[FeL_{14}NO_3H_2O]$ (**23**)

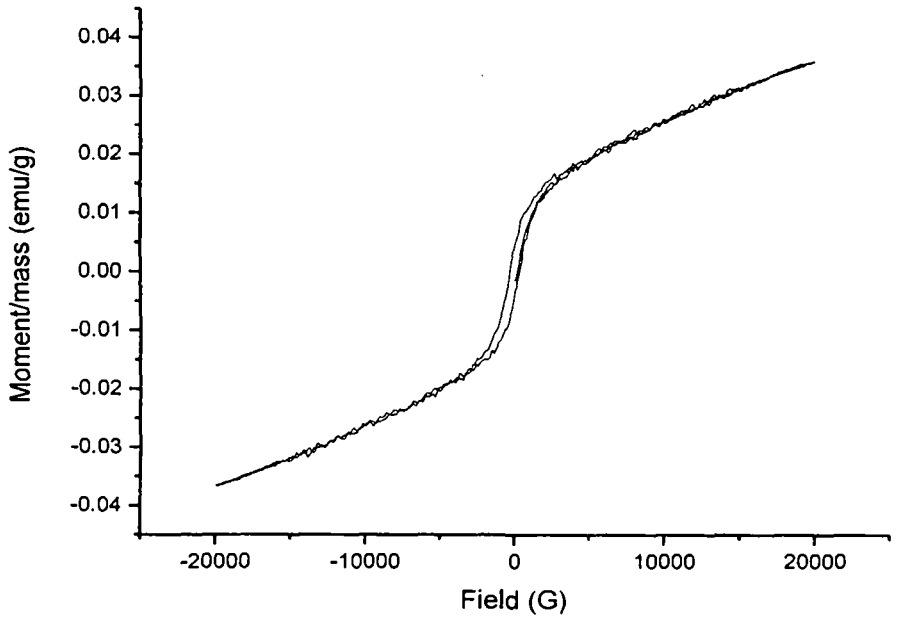

Field dependence of magnetization for the complex $[VOL_9]H_2O$ (**29**)

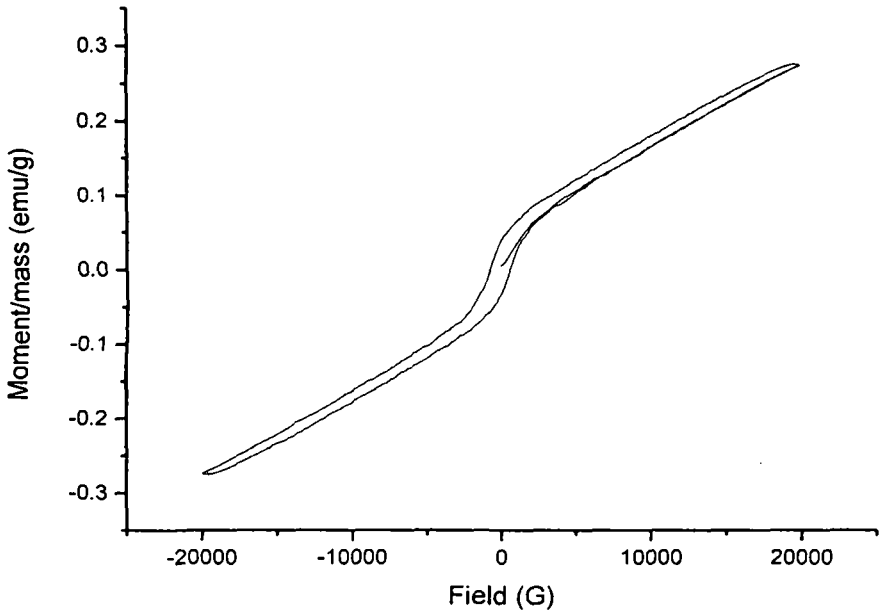

Field dependence of magnetization for the complex $[VOL_{12}]H_2O$ (**31**)

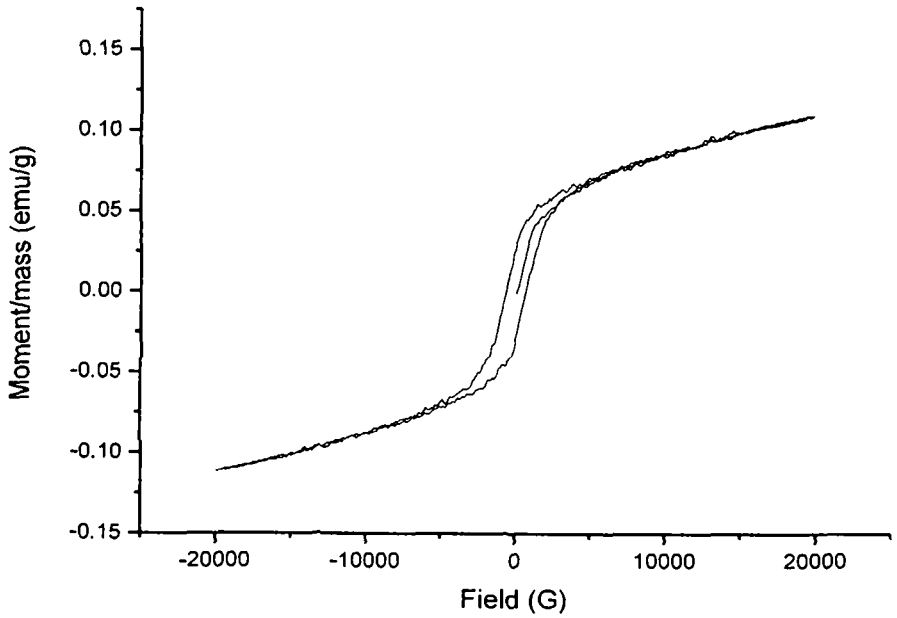

Field dependence of magnetization for the complex $[FeL_{15}Cl_2]Cl$ (**34**)

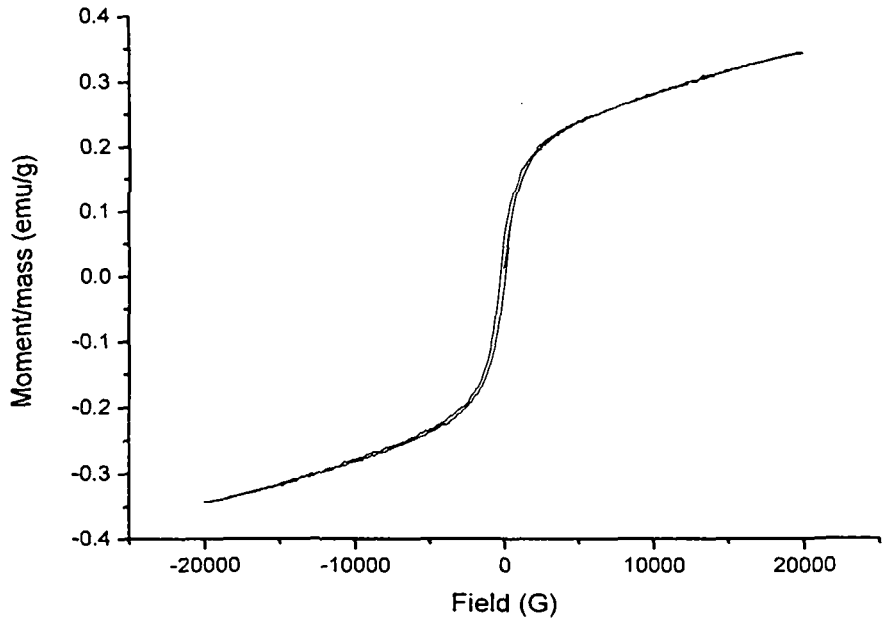

Field dependence of magnetization for the complex $[FeL_{10}(H_2O)_2](NO_3)_3$ (**38**)

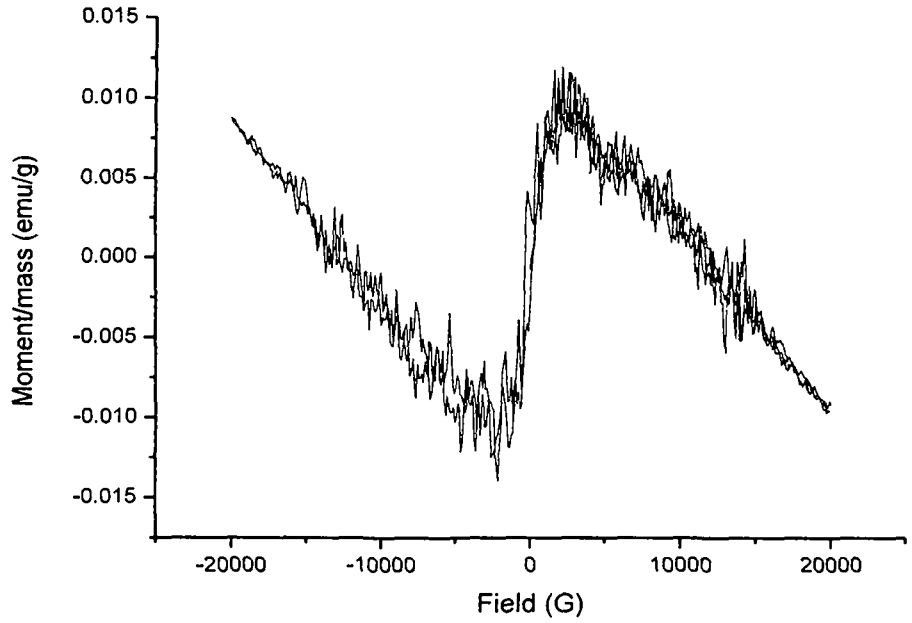

Field dependence of magnetization for the complex $[VOL_{10}]SO_4.H_2O$ (**39**)

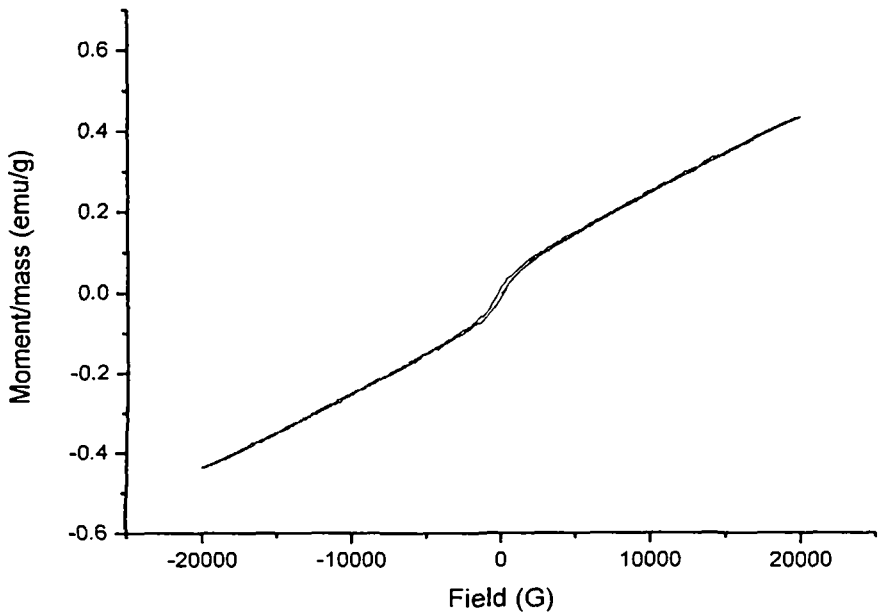

Field dependence of magnetization for the complex $[FeL_9(H_2O)_2]$ (**40**)

Assam University Journal of Science &
Technology : Physical Sciences and Technology
Vol. 5 Number II
81-87, 2010

Transition Metal Complexes of a Neutral $[N_2O_2]$ Donor Schiff Base Derived from Furfuraldehyde and Hydrazine Hydrate : Synthesis, Characterization and Redox Behaviour

Chira R Bhattacharjee[1], Pankaj Goswami[2], Sankar Neogi[3] and Saptarshi Dhibar[1]

[1]Department of Chemistry, Assam University, Silchar 788011, Assam, India
[2]Department of Chemistry, Silchar Polytechnic, Silchar 788015, Assam, India
[3]Department of Chemistry, Haflong Govt. College, Haflong, Assam, India
[2] corresponding author Tel : +919435175671 Fax : +913842270803
Correspondence; [1]e-mail : crbhattacharjee@rediffmail.com

Abstract

Neutral $[N_2O_2]$ donor tetradentate Schiff base derived from furfuraldehyde and hydrazine hydrate and its complexes with VO(IV), Fe(III), Co(II), Ni(II), Cu(II) and Zn(II) have been prepared and characterized by physical, spectral and analytical studies. The complexes have a stoichiometry $[ML(H_2O)_n]X_m$ (M=VO, Fe, Co, Ni, Cu and Zn ; n=0 or 2 ; X=SO_4, NO_3 or CH_3COO ; m=1, 2 or 3). An octahedral geometry were proposed for the Fe(III) and Co(II) complexes and a square pyramidal geometry for the VO(IV) complex. While Ni(II), Cu(II) and Zn(II) complexes were conjectured to possess a square planar geometry. The redox behaviour of the complexes were examined by cyclic voltammatric studies.

Key words: Tetradentate Schiff Base, Hydrazine Hydrate, Furfuraldehyde.

Introduction

Compounds containing imines have not only found extensive application in organic synthesis, but several of these molecules display significant biological activity (Miyaura *et. al.* 1995, Baleizno *et. al.* 2004, Bandini *et al.* 2002, Canali and Sherrington, 1999). In the last decade Schiff base ligands have received extensive attention mainly because of their wide application in the field of catalysis and due to their antimicrobial (Chouhan and Sheazi, 1999), anti-tuberculosis (Jayabalakrishnan and Natarajan, 1999), and antitumour activity (Jeeworth *et al.* 2000). They easily form stable complexes with most transition metal ions. Schiff base complexes derived from heterocyclic compounds have found increased interest in the context of bioinorganic chemistry (Chaviara *et al.* 2004, Ciller *et al.* 2009, Agarwal and Hingorani, 1990). Heterocyclic compounds such as pyridine, 2, 2′-bipyridine and related molecules are good ligands due to the presence of one or more ring nitrogen atoms with a localized pair of electrons. The application potential has led to the formation of series of novel Schiff base compounds with a wide range of physical, chemical and biological properties (Maurya *et. al.* 1993, Bassett *et al.* 1978, Tarcero *et al.* 2003, Milvoic *et al.* 2003), spanning a broad spectrum of reactivity and stability. Though anionic Schiff base ligands have been exploited for complexation, those with neutral Schiff base ligands have not been adequately studied.

Accordingly we report herein, synthesis and characterization of some new complexes of VO(IV), Fe(III), Co(II), Ni(II), Cu(II) and Zn(II) with a neutral N_2O_2 donor Schiff base derived from furfuraldehyde with hydrazine hydrate. Cyclic voltammetry of VO(IV) and Fe(III) complexes showed typical quasireversible electrochemical response.

Materials and Methods

Reagents and solvents

All the chemicals and solvents used were of analytical grade. The metal salts (E. Merck) were commercially available pure samples. Furfuraldehyde obtained from Qualigens fine chemicals was distilled before use and hydrazine hydrate was used as received. Ethanol was dried over activated lime.

Physical measurements

Microanalytical (C, H, N) data were obtained with a Perkin-Elmer Model 240C elemental analyzer. Infrared spectra were determined by using KBr pellets on a FT-IR spectrophotometer in the region 400-4000 cm^{-1}. Electronic spectra were recorded in dichloromethane solution on a Shimadzu 1600-PC UV-VIS spectrophotometer in 200-800 nm range. Nuclear magnetic resonance spectra (^1H and ^{13}C) were acquired from Bruker Advance 300 MHz FT NMR Spectrometer using $CDCl_3$ as solvent and TMS as internal standard. Mass spectra were recorded on a DART-MS spectrometer with ESI ionization mode. Electrochemical behaviour of the complexes were investigated by cyclic voltametric method at room temperature in acetonitrile for ca. 1 X 10^{-3} mol dm^{-3} using n-Bu_4NClO_4 as supporting electrolyte under a dry N_2 atmosphere on a PC controlled CHI model 660C electrochemistry system. A Pt disk, a Pt wire auxiliary electrode and an aqueous saturated calomel electrode (SCE.) were used in a three electrode configuration.

Synthesis of ligand (L)

Hydrazine hydrate (0.01 mol, 0.50 g) was dissolved in dry ethanol and then added to an ethanolic solution of furfuraldehyde (0.02 mol, 1.92 g) containing few drops of acetic acid and the mixture was refluxed for 4 hours. The solvent was then removed on rotary evaporator and the residue crystallized at room temperature. The yellow crystals so obtained was recrystallised from ethanol to obtain the pure Schiff base compound (Fig.1).

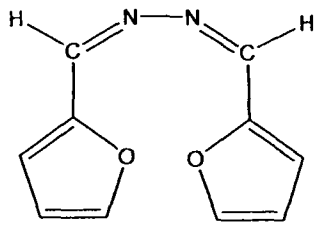

Schiff base (**L**)

Figure 1. The molecular structure of the Schiff base.

Synthesis of complexes(1-6)

General procedure

Warm ethanolic solution (20 cm^3) of Schiff base (1 mmol) was added to a magnetically stirred solution of the respective metal salts (1 mmol) in ethanol (20 cm^3). Vanadyl sulphate, iron (III) nitrate, cobalt (II) nitrate, nickel (II) acetate, copper (II) acetate and zinc (II) acetate were used as metal source. The mixture was refluxed for 1 hour and cooled to room temperature. On cooling, precipitates of the desired metal complexes were formed, which were filtered, washed with ethanol and dried. Recrystallization from ethanol afforded the pure metal complexes. The yield recorded were *ca* 65%.

Results and discussions

The tetradentate Schiff base is devoid of any ionisable proton and serve as neutral ligand forming cationic complexes. The complexes (**1-6**) were all obtained as coloured microcrystalline solids stable to air and moisture. Following an elicit reaction strategy (Scheme 1), the complexes were accessed by direct interaction of the ligand (L) and the metal ion in ethanolic medium.

$$M(NO_3)_x \text{ or } M(OAc)_2 \text{ or } M(SO_4)_2 + L \xrightarrow[\text{Reflux, 1h}]{\text{Ethanol}} [ML]X_n$$

(X=NO_3, OAc or SO_4 ; n=1, 2 or3

Scheme - 1

The analytical data of the ligand and complexes along with some physical properties are summarized in Table 1. The elemental analysis of the complexes correspond well with the proposed formulae (Fig 2).

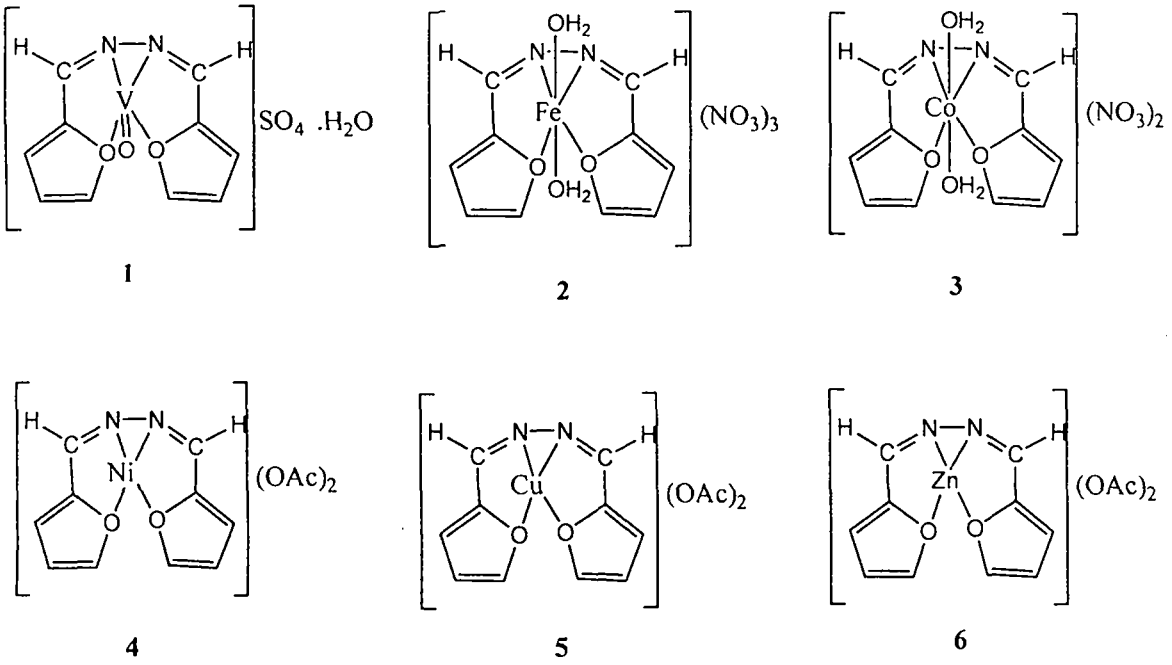

1 2 3

4 5 6

Figure 2. Proposed structure of the Schiff base complexes, 1-6.

IR spectra

The IR spectra of the ligand and complexes feature absorption bands characteristics of various bond types providing information regarding the formation of the ligand and its coordination mode in the complexes. The structurally relevant IR bands with their assignments are shown in Table2.

The ligand showed characteristic azomethine (C=N) band at *ca* 1640 cm^{-1}. Shifting of this band to lower wave numbers in the spectra of the complexes suggested coordination of the azomethine nitrogen during complexation (Tas *et. al.* 1998). Two distinct bands in the region 434–592 cm^{-1} in the complexes assignable to M–N and M-O stretch provide compelling evidence for the coordinated metal ion in the ligand framework (Thomas et. al. 1995) The vanadyl complex exhibited an additional band at *ca* 980 cm^{-1} attributed to the V=O stretching (Xiu et. al. 1996). In addition, the broad bands at *ca* 3425 cm^{-1} in the vanadyl complexes assignable to ν (O-H) of the lattice water molecule. Coordination of water molecule to the vanadyl centre may not, however, be ruled out. The characteristics ν ($S\text{-}O_{assy}$) of uncoordinated sulphate was observed at *ca* 1120 cm^{-1} (Nakamoto, 1986). Iron(III) and cobalt(II) complexes showed sharp band at *ca* 1385 cm^{-1} which corresponds to ν $N\text{-}O_{(asy)}$ of uncoordinated nitrate (Kunchandy and Indrasenan1990). The coordinated water molecules in iron(III) and cobalt(II) complex was evidenced by the appearance of broad bands in the range 3367-3407 and weak bands at *ca* 880 and 590 cm^{-1}, owing to ν(O-H), $\rho_{rock}(H_2O)$ and $\rho_{wagg}(H_2O)$, respectively (Nakamoto, 1986). The aquo groups occupy the axial positions completing six coordination. The C-O stretching vibration of the free acetate ion was observed at *ca* 1600 cm^{-1} in Ni(II), Cu(II) and Zn(II) complexes (Wang, 2007) in conformity with their occurrence as counter anion.

Table 1. Physical and analytical data of the Schiff base ligand and its complexes, 1-6

Compound	Molecular composition	Colour	Yield (%)	Found (Calcd) (%)		
				C	H	N
Ligand (L)	$C_{10}H_8N_2O_2$ MW=188	yellow	70	63.5(63.8)	4.4(4.3)	15.2(14.9)
Complex **1**	$VC_{10}H_{10}N_2O_2S$ MW=369	red	65	32.1(32.5)	2.9(2.7)	7.4(7.6)
Complex **2**	$FeC_{10}H_{12}N_5O_{13}$ MW=466	red	60	26.0(25.8)	2.7(2.6)	14.9(15.0)
Complex **3**	$CoC_{10}H_{12}N_4O_{10}$ MW=407	red	60	29.9(29.5)	3.1(2.9)	13.5(13.8)
Complex **4**	$NiC_{14}H_{14}N_2O_6$ MW=364.5	light yellow	55	46.0(46.1)	4.0(3.8)	8.1(7.7)
Complex **5**	$CuC_{14}H_{14}N_2O_6$ 369.5	brown	60	45.3(45.5)	4.1(3.8)	7.6(7.6)
Complex **6**	$ZnC_{14}H_{14}N_2O_6$ MW=371.5	dirty white	65	45.4(45.2)	3.5(3.8)	7.2(7.5)

Table 2. Characteristic IR bands (cm^{-1}) for the ligand and the complexes, 1-6.

Compounds	ν(C=N)	ν(M–N)	ν(M–O)	ν(V=O)	ν (O-H/H_2O)	ν(S-O)	ν (N-O)
Ligand (L)	1641	-	-	-	-	-	-
Complex 1	1626	470	434	978	-	1120	3425
Complex 2	1617	530	486	-	3367 882(ρ_r) 591(ρ_w)	-	1382
Complex 3	1638	588	512	-	3407 882(ρ_r) 588(ρ_w	-	1386
Complex 4	1577	592	515	-	-	-	
Complex 5	1577	592	515	-	-	-	
Complex 6	1576	592	515	-	-	-	

Electronic absorption spectra

The electronic absorption spectra of the Schiff base ligand and its complexes (1-6) were recorded in dichloromethane at room temperature. The absorption regions of the compounds are given in Table 3. The appearance of d→d transition peaks in all UV-VIS spectra of the complexes is compatible with the presumed geometry. Further, the ligand as well as complexes exhibited bands with high molar extinction coefficients assignable to intraligand charge transfer n→π*and π →π* transition in the expected region.

NMR spectrum

The ^1H and ^{13}C NMR spectral data of the ligand is summarized in Table 4. Multiplet at 6.548-6.917 δ is attributable to ring protons. A sharp singlet at 8.541 δ assignable to azomethine proton (-CH = N-) confirms the formation of the ligand as proposed.

The ^{13}C NMR spectrum of the ligand showed the presence of five magnetically non-equivalent carbons and thus provide an additional evidence for the proposed structure of the ligand.

Table 3. Electronic spectral data of the compounds

Compounds	Absorption (nm)	Molar extinction coefficient (ε, $M^{-1}cm^{-1}$)	Band assignment	Geometry
Ligand (L)	337 259	20300 1800	n →π* π →π*	-
Complex 1	596 337 253 234	60 27370 3130 18510	d→d Intraligand Intraligand Intraligand	Square pyramidal
Complex 2	505 338 259 235	210 25760 3960 4300	d→d Intraligand Intraligand Intraligand	Octahedral
Complex 3	334 247 236	25530 2440 3600	Intraligand Intraligand Intraligand	Octahedral
Complex 4	496 308 267	120 23400 1740	d→d Intraligand Intraligand	Square planar
Complex 5	669 369 286	170 27000 2440	d→d Intraligand Intraligand	Square planar
Complex 6	505 332 308	100 21660 17430	d→d Intraligand Intraligand	Square planar

Table 4. The ^1H NMR spectral data and their assignment.

^1H		^{13}C	
δ (ppm)	Assignment	δ (ppm)	Assignment
6.548-6.917(6H, m)	Ring proton	112.32, 116.92, 145.85, 149.38,	Ring carbon
8.541 (1H, s)	-CH=N-	150.98	-CH=N-

Mass Spectra

The mass spectrum of the ligand recorded in ESI^+ ionization mode showed molecular ion peak at 188 m/z. Further the peaks at m/z 190 and 191 are assignable to [M+H] and [M+2H] fragments, respectively thus confirming the stoichiometry of the ligand as proposed.

Electrochemical studies

The redox behaviour of the complexes 1 and 2 were examined by cyclic voltammetry in anhydrous acetonitrile solution of ca 10^{-3} M concentration containing 0.1 M tetrabutyl ammonium perchlorate (TBAP) as supporting electrolyte in the potential range 1.6 to -1.6 V vs SCE at 100 mVs^{-1} scan rate. The redox potentials for the compounds are given in Table 5 and corresponding voltammograms are presented in figure 3. The cyclic voltammogram of the complexes showed a well defined redox process corresponding to the formation of Fe(III)/Fe(II) and VO(V)/VO(IV) couple, respectively suggesting a quasi-reversible (ΔEp > 100 mV) electrochemical response.

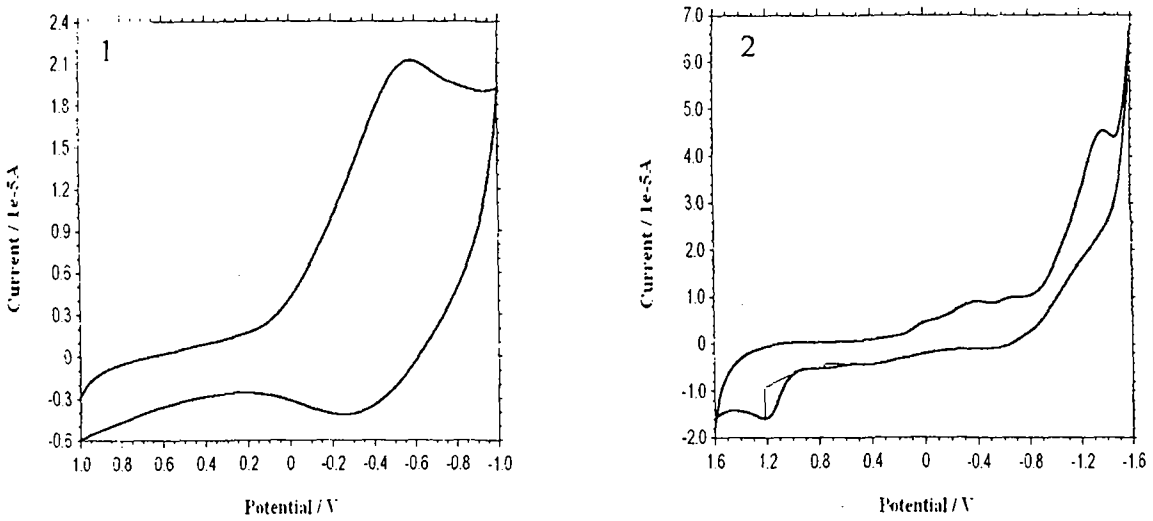

Figure 3. Cyclic voltammograms of the complex 1 and 2

Table 5. Electrochemical data of the complexes 1 and 2.

Compounds	E_p^a (V)	E_p^c (V)	? E_p (V)	$E_{1/2}$ (V)
Complex 1	-0.270	-0.564	0.294	-0.834
Complex 2	1.21	-1.38	2.59	-0.085

The half wave potential $E_{1/2}$ of the complexes is negative implying their redox susceptibility. This feature would make them valuable as catalyst in redox reactions (Perez *et al.* 2005).

Conclusion

In this work N_2O_2 donor neutral tetradentate Schiff base (derived from condensation of furfuraldehyde with hydrazine hydrate) and its oxovanadium(IV), iron(III), cobalt(II), nickel(II), copper(II) and zinc(II) complexes were synthesized and characterized by spectral and analytical data. Square pyramidal structure for complex 1 and octahedral structure for 2 and 3 and square planer for the rest, 4-6 has been proposed. The redox behaviour of the iron (III) and oxovanadium(IV) complexes were investigated by cyclic voltammetry. Based on half wave potential values, the iron complex appeared to be easily oxidizable or reducible. This characteristic feature render such compounds a potential catalyst in many reactions.

Acknowledgements

The authors express their sincere thanks to the SAIF, NEHU, Shillong and SAIF, CDRI, Lucknow, India for providing analytical and spectral results

References

Agarwal, B. V. ; Hingorani, S. (1990). Characteristics IR and electronic spectral studies on novel mixed ligand complexes of copper(II) with thiosemicarbazones and heterocyclic bases. *Synth. React. Inorg. Met-Org. Chem.* 20 :123-132

Baleizno, C. ; Gigante, B. ; Garcia, H. ; Corma, A. (2004). Vanadyl salen complexes covalently anchored to single wall carbon nanotubes as heterogeneous catalyst for the cyanasilylation of aldehydes. *J.Catal.* 221 : 77-84

Bandini, M. ; Cozzi, P. G. ; Umani-Ronichi, A. (2002). [Cr(Salen)] as a bridge between asymmetric catalysts, Lewis acids and redox processes. *Chem. comun.* : 919-927

Bassett, J. ; Denney, R. C. ; Jaffery, G. H. ; Mendham, J. (1978). *Vogel's Textbook of quantitative Inorganic Analysis Including Instrumental Analysis*. ELBS and Longman Group Ltd. London

Canali, L. ; Sherrington, D. C. (1999). Utilisation of homogeneous and supported chiral metal salen complexes in asymmetric catalysis. *Chem. Soc. Rev.* 28. : 85-94

Chaviara, A. T. ; Cox, P. J. ; Repana, K. H. ; Papi R. M.; Papazisis, K. T. ; Zambouli, D. ; Kortsaris, A. H. ; Kyriakidis, D. A. ;. Bolos C. A. (2004). Copper(II) Schiff base coordination compounds of dien with heterocyclic

aldehydes and 2-amino-5-methyl-thiazole: synthesis, characterization, antiproliferative and antibacterial studies. Crystal structure of CudienOOCl$_2$. *J. Inorg. Biochem.* 98(8): 1271-1283

Chohan, Z. H. ; Sherazi, S. K. A. (1999). Synthesis and characterization of some Co (II) and Ni(II) complexes with nicolinyl hydrazine derivatives and their biological role of metal and anions (SO_4^{-2}, NO_3^-, $C_2O_4^{-2}$ and CH_3COO^-) on the antibacterial properties. *Synth. React. Inorg. Met-Org. Chem.* 29 : 105-118

Cíller, J. A. ; Seoane, C ; Soto, J. L. ; Yruretagoyena, B. (2009). Synthesis of heterocyclic compounds. Schiff bases of ethyl 2-aminofurancarboxylates. *J. Heterocyclic. Chem.* 23(5) : 1583-1586

Jayabalakrishnan, C. ; Natarajan, K. (2001). Synthesis, characterization and biological activities of ruthenium (II) carbonyl complexes containing bifunctional tridentate Schiff bases. Synth. React. Inorg. Met –Org. Chem. 31 : 983-995

Jeeworth, T.; Wah, H. L. K. ; Bhoeon, M.G. ; Ghoorhoo, D. ; Babooram, K. (2000). Synthesis and antibacterial/ catalytic properties of Schiff bases and Schiff base metal complexes derived from 2, 3-diaminopyridine. Synth. React. Inorg. Met –Org. Chem. 30 : 1023-1038

Kunchandy, S.; Indrasenan, P. (1990). Synthesis and IR spectral studies of some lanthanide nitrate complexes with 4-benzyl-3-methyl-1-phenylpyrazol-5-one. Polyhedron. 9(6): 765-799

Maurya, R. C.;Mishra, D. D. ; Jain, S. ; Jaiswal, M.(1993). Synthesis and characterization of some mixed ligand complexs of copper (II) and cobalt(II) with Schiff bases and heterocyclic organic compounds. *Synth. React. Inorg. Met-Org. Chem.* 23: 1335-1349

Milvoic, N. M. ; Dutca, L. M. ; Kostic, N. M. (2003). Combined use of platinum (II) complexes and palladium(II) complexes for selective cleavage of peptides and proteins. *Inorg. Chem.* 42 : 4036-4045

Miyaura, N.; Suzuki, A. (1995). Palladium catalyzed cross coupling reactions of organoboron compounds. *Chem. Rev.* 95 : 2457-2483

Nakamoto, K. (1986). *Infrared and Raman Spectra of Inorganic and Coordination Compounds.* John Wiley and Sons. INC, New York

Perez, F. R. ; Basaez, L. ; Belmar, J. ; Vanysek, P. (2005). Cyclic voltametry of 1-(n-hexyl)-3-methyl-5-pyrazolone based enamines and their chloromanganese(III) and nitridomanganese(V) complexes. *J. Chil. Chem. Soc.* 50 : 575-580

Tarcero, J. M. ; Matilla, A. ; Sanjuan, M. A. ; Moreno, C.F. ; Martin, J. D. ; Walmsley, J. A. (2003). Synthesis, characterization, solution equilibria and DNA binding of some mixed ligand palladium(II) complexes. Thermodynamic models for carboplatin drugs and analogous compounds. *Inorg. Chim. Acta.* 342 : 77-87

Tas, E. ; Cukurovali, A. ; Kaya, M. (1998). Synthesis of a new glyoxime derivative, characterization and investigation of its complexes with Ni(II), Co(II), Cu(II) and UO_2(VI) metals. *J. Coord. Chem.* 44 : 109-117

Thomas, M. ; Nair, M. K. M. ; Radhakrishnan, P. K. (1995). Rare earth iodide complexes of 4-(2',4'-dihydroxyphenylazo) antipyrene. Synth. React. Inorg. Met.-Org. Chem. 25 : 471-479

Wang, C. (2007). Synthesis, characterization and crystal structure of a novel acetate bridged polynuclear Schiff base Cu(II) complex. *Synth. React. Inorg. Met.-Org. Chem.* 37(7) 573-576

Xiu, R. B.; Mintz, E. A.; You, X. Z. (1996). Synthesis and characterization of vanadyl complexes with unsymmetrical bis-Schiff base ligands containing a cis-N_2O_2 coordinate chromophore . *Polyhedron.* 15 : 4585-4591

Journal of Coordination Chemistry
Accepted article

Taylor & Francis
Taylor & Francis Group

Synthesis, structural characterization and DFT studies of new mixed-ligand iron(III) Schiff base complexes.

Chira R Bhattacharjee[1*], Pankaj Goswami[2] and Paritosh Mondal[1]

[1]Department of Chemistry, Assam University, Silchar 788011, Assam, India.

[2]Department of Chemistry, Silchar Polytechnic, Silchar 788015, Assam, India

* corresponding author Tel : +919435175671 Fax : +913842270803
E-mail address : crbhattacharjee@rediffmail.com

Abstract

Cationic Iron(III) Schiff base aquo complex of the type $[FeL(H_2O)_2]NO_3$ (L= $C_{12}H_{18}N_2O_2$) was accessed from an interaction of $Fe(NO_3)_3.9H_2O$ with the $[N_2O_2]$ donor Schiff base. Reaction of the aquated complex with bifluoride (HF_2^-), thiocyanate (SCN^-) or azide (N_3^-) in 1:2 molar ratio in methanolic medium led to the synthesis of anionic mixed-ligand complexs, $[FeLX_2]^{n-}$ (L=$C_{12}H_{18}N_2O_2$, X=F, NCS, N_3). The tetradentate Schiff base ligand was prepared from condensation of acetylacetone and ethylenediamine following literature method and characterized by spectroscopic and single crystal XRD technique. The complexes were characterized using elemental analysis, FT-IR, UV-VIS, mass spectroscopy and solution electrical conductivity studies. The magnetic susceptibility measurements suggested occurrence of high spin Fe(III) in the complexes. The electronic structures of the compounds were extensively analyzed by DFT method using B3LYP/6-31G(d,p) functional and overall, very good agreement between theoretical expectations and experimental data was achieved. The electrochemical behaviour of the complexes were examined by cyclic voltametric method.

Key words : Schiff base; mixed-ligand iron(III) complex; dft; acetylacetone; ethylenediamine.

1. Introduction

Metal-Schiff base complexes have continued to enjoy extensive interest owing to their synthetic proclivity, structural diversity and potential application in pharmacology and catalysis. The design, synthesis and characterization of iron complexes with Schiff base ligand, however, play a relevant role in the coordination chemistry of iron due to their importance as synthetic models for the iron containing enzymes [1,2], oxidation catalysts [3-5] and bistable molecular materials based on temperature, pressure or light induced spin crossover behaviour [6-9]. Considerable attention has been devoted in recent years to the study of mixed-ligand complexes of transition metals containing nitrogen donor ligands [10-12]. Their potential applications like separation materials, catalysis precursors, potential models of the catalyse enzymes [13-16]) and their interesting structures [17-19] has spurred extensive research in this field. The mixed-ligand complexes containing N, O, and/or S donor atoms are important owing to their significant antifungal, antibacterial, and anticancer activity [20]. Use of iron-Schiff base complexes in different catalytic reactions have been dealt with in some recent works [21-23]. Although quite a large number of metal-$[N_2O_2]$ compounds are on record [25-28], reports on corresponding Fe(III) complexes are rather scarce. A scrutiny of related literature reveals that mostly divalent metal ions have been used for complexation with Schiff bases having $[N_2O_2]$ core [29-31]. Recent studies showed iron(III) tridentate Schiff base complex as efficient catalyst for oxidation of sulfides to sulfoxides by urea hydrogen peroxide [32]. Similarly, $[N_2O_2]$ donor Schiff base complexes of palladium(II) have been used as catalyst for reduction of organic substrates under mild conditions [33]. Further, oxovanadium(IV)-$[N_2O_2]$ Schiff base complexes have been shown to exhibit insulin-mimetic activity [34]. $[N_2O_2]$ donor planar tetradentate ligands with four coordinating site render two axial site open to

ancillary ligands. For instance, iron(III) complexes of $[N_2O_2]$ donor tetradentate Schiff base ligands, $[FeL(Im)_2].BPh_4$ (L=salen, acacen) have been shown to posses interesting magnetic behaviour [35,36]. Coordination of varying donor ligands at the axial site is a synthetic challenge and also allow tunability to physical properties. Complexes of VO(II), Ni(II), Co(II) and Cu(II) with unsymmetrical $[N_2O_2]$ donor Schiff base derived from 2,4-pentanedione/ 1-phenyl-1,3-butanedione and ethylenediamine have recently been reported [37].

Accordingly, we report herein the synthesis and structural characterization of mixed-ligand iron(III) complexes with N_2O_2 donor tetradentate Schiff base derived from condensation of acetylacetone with ethylenediamine incorporating aquo, fluoro, thiocyanato or azido group. In addition, density functional theory (DFT) methods have been used to model the most stable equilibrium geometry of the complexes. The electrochemical behaviour of the complexes are also studied.

2. Experimental

2.1. *Materials*

Reagent grade and HPLC grade solvents and chemicals were used. Acetylacetone, ethanol, methanol and other solvents were distilled prior to their use. Ethylenediamine, ammonium bifluoride, ammonium thiocyanate, sodium azide and ferric nitrate were obtained from E. Merck. India Ltd. and were used as received.

2.2. *Measurements*

Microanalytical (C, H, N) data were obtained with a Perkin-Elmer Model 240C elemental analyzer. Infrared spectra were obtained by using KBr pellets on a Spectrum BX series FT-IR spectrophotometer in the region 400-4000 cm^{-1}. Electronic spectra were recorded in DCM on a Shimadzu 1600-PC UV-VIS spectrophotometer in 200-800 nm range. Nuclear magnetic resonance spectra (^1H and ^{13}C) were

acquired from Bruker Advance 300 MHz FT NMR Spectrometer using $CDCl_3$ as solvent and TMS as internal standard. Mass spectra were recorded on a Jeol SX-102 spectrometer with fast atom bombardment. Magnetic susceptibilities of the complexes were measured at room temperature on a Sherwood scientific susceptibility balance using $Hg[Co(SCN)_4]$ as calibrant. Molar conductances of complexes were determined in DMSO (ca. 10^{-3} M) at room temperature using a Toa CM 405 conductivity meter. Electrochemical behaviour of the complexes were investigated by cyclic voltammetric method in CHI 660C Electrochemical Workstation in dicholoromethane solution versus SCE electrode at room temperature in the potential range -1.0 to 1.0 V.

3. Synthesis

3.1. ***Synthesis Schiff base ligand, $C_{12}H_{20}N_2O_2$ (H_2L)***

The ligand was prepared from condensation of acetylacetone and ethylenediamine in 2:1 molar ratio according to the reported method [38]. Acetylacetone (0.02 mol, 2.0 g) and ethylenediamine (0.01 mol, 0.06 g) in 60 cm^3 dry ethanol were refluxed for two hours in presence of few drops of acetic acid and cooled in a refrigerator. The resulting compound was precipitated, filtered and recrystallized from methanol.

Elem. anal. (%) Calcd C (64.29), H (8.93) and N (12.50). Found C (64.22), H (8.84) and N (12.45). FTIR (KBr pallets, v cm^{-1}) 1143 (C-O), 1617 (C=N), 3447 (O-H). UV-VIS (CH_2Cl_2, λ_{max} nm) 231, 317. ^1H NMR (300 MHz, δ ppm, from TMS in $CDCl_3$) 10.89 (s, 2H, OH), 5.00 (s, 2H, -CH=C), 3.42 (t, 4H, $-CH_2-$), 2.17 (s, 6H, CH_3), 1.91 (s, 6H, CH_3). ^{13}C NMR (300 MHz, δ ppm, from TMS in $CDCl_3$) 195.5, 162.9, 96.1, 43.4, 28.8, 18.6. MS(FAB, m/z) 225$[M+H]^+$.

3.2. ***Synthesis of iron (III) complex $[FeL(H_2O)_2]NO_3$***

The ligand, H_2L (0.005 mol, 1.12g) dissolved in methanol (20 cm^3) and added to a methanol solution (20 cm^3) of $[Fe(NO_3)_3].9H_2O$ (0.005 mol, 2.02g) and the mixture

was stirred for 4 h. On cooling to room temperature dark brown microcrystalline solid was obtained which was washed with cold absolute ethanol and then dried at air. Yield 68%. Elem. anal. (%) calcd C (38.30), H (5.85), and N (11.17). Found C (38.23), H (5.88), and N (11.25). FT IR (KBr pellets, $\nu\,cm^{-1}$) 435 (Fe-O), 453 (Fe-N), 654 ($\rho_{wagg}H_2O$), 930 ($\rho_{rock}H_2O$), 1274 (C-O), 1385 (N-O), 1573 (C=N), 3419 (O-H). UV-VIS (CH_2Cl_2, λ_{max} nm) 278, 323, 410, 482. MS (FAB, m/z) 376$[M]^+$.

3.3. *Synthesis of iron (III) complex $NH_4[FeLF_2]$*

The complex $[FeL(H_2O)_2]NO_3$ (0.001 mol, 0.376g) was dissolved in 10 cm^3 of methanol and to this a methanol solution (10 cm^3) of $NH_4F{\cdot}HF$ (0.002 mol, 0.112g) was added with continuous stirring and the mixture further stirred for 1 h. On standing overnight the compound so precipitated was collected, washed with ethanol and then dried in open air. Yield 63%.

Elem. anal. (%) calcd C (43.11), H (6.59), and N(12.66). Found C (43.18), H (6.52), and N (12.66). FTIR (KBr pellets, $\nu\,cm^{-1}$) 431 (Fe-O), 484 (Fe-N), 652 (Fe-F), 1508 (C-O), 1627 (C=N). UV-VIS (CH_2Cl_2) 365, 323. MS (FAB, m/z) 334$[M]^+$.

3.4. *Synthesis of iron (III) complex $NH_4[FeL(NCS)_2]$*

The complex was prepared by a procedure similar to that of the complex $NH_4[FeLF_2]$ with the difference that NH_4SCN was added instead of $NH_4F{\cdot}HF$. Yield 70%.

Elem. anal. (%) calcd C (40.78), H (5.34), and N (19.99). Found C (40.85), H (5.39), and N (20.02). FT IR (KBr pellets, $\nu\,cm^{-1}$) 414 (Fe-NCS), 435 (Fe-O), 483 (Fe-N), 771 (C-S), 1420 (C-O), 1569 (C=N), 2073 (C-N sym), 2049 (C-N asym). UV-VIS (CH_2Cl_2, λ_{max} nm) 251, 303, 361, 482. MS (FAB, m/z) 412$[M]^+$.

3.5. *Synthesis of iron (III) complex $Na[FeL(N_3)_2]$*

The complex was prepared by a procedure similar to that of the complex $NH_4[FeLF_2]$ with the difference that NaN_3 was added instead of $NH_4F{\cdot}HF$. Yield 64%.

Elem. anal. (%) calcd C (37.40), H (4.68), and N (29.09). Found C (37.36), H (4.62), and N (29.15). FT IR (KBr pellets, ν cm^{-1}) 425 (Fe-N_3), 438 (Fe-O), 486 (Fe-N), 1260 (C-O), 1624 (C=N), 2344 (N-N-N), 2366 (N-N-N). UV-VIS (CH_2Cl_2, λ_{max} nm) 276, 320, 429, 699. MS (FAB, m/z) 385$[M]^+$.

4. Results and discussion

4.1. *Chemistry*

A condensation reaction occurred between acetylacetone and ethylenediamine in 1:2 molar ratio yielding a pale yellow Schiff base bis(acetylacetonato)ethylenediamine in weakly acidic medium (scheme 1). The formation of Schiff base was confirmed by FT IR, UV-VIS, ^1H NMR, ^{13}C NMR, mass spectroscopy and single crystal XRD study. The compound is soluble in polar solvents like methanol, ethanol, chloroform, dichloromethane etc but insoluble in nonpolar solvents.

Iron (III) complexes were prepared in good yield by the reaction of iron(III)nitrate and the ligand in 1 : 1 molar ratio (scheme 2). Two molecules of water were found to be coordinated to the metal center as supported by microanalysis and spectral data. The complex reacts with ammonium bifluoride, ammonium thiocyanate or sodium azide in 1:2 molar ratio to give mixed-ligand complexes of the type $NH_4[FeLF_2]$, $NH_4[FeL(NCS)_2]$ and $NH_4[FeL(N_3)_2]$, respectively. The two axial aquo groups were replaced by fluoro, thiocyanato or azido groups (Scheme 3). Pertinent here is to mention that insertion of isothiocyanato (NCS) group in the coordination sphere of iron centre has been earlier exploited as probe for Surface Enhanced Raman Spectroscopy (SERS) and functionalisation of metal nano particle [39,40].

4.2. *IR spectra*

The free ligand showed stretching modes attributed to C=N, C–O and O–H at 1617, 1143 and 3447 cm^{-1}, respectively. On complexation, the C=N band was shifted to

lower wave number indicating coordination through of the azomethine nitrogen to the central metal ion [41]. The bands due to ν(O-H) were absent in the complexes, indicating coordination through deprotonated ligand. The participation of enolate

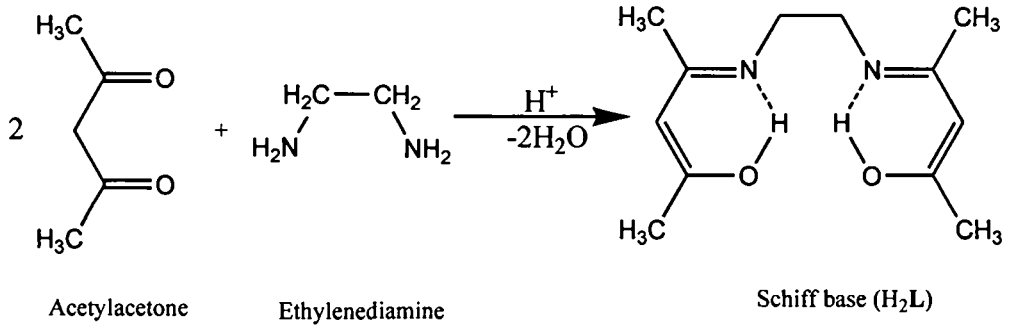

Scheme 1. Synthesis of the ligand H_2L

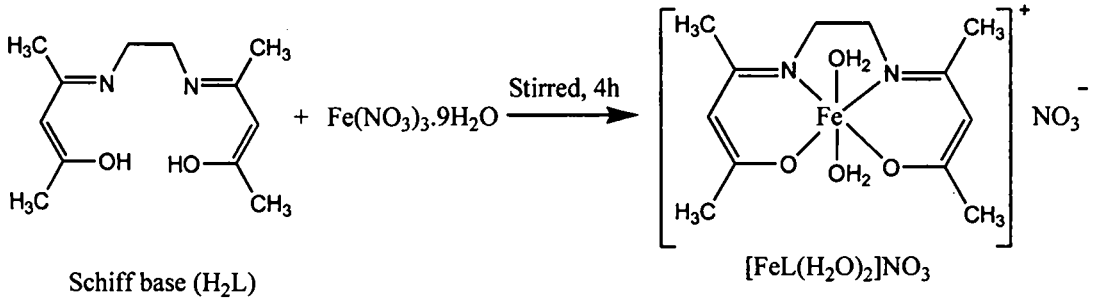

Scheme 2. Synthesis of Fe(III) complex with Schiff base H_2L.

oxygen and azomethine nitrogen in the complexes is further supported by the appearance of prominent IR peaks for ν(Fe–O) and ν(Fe–N) at 435–442 cm^{-1} and 454–483 cm^{-1}, respectively [42]. The presence of coordinated water molecules in the complex $[FeL(H_2O)_2]NO_3$ was confirmed by the appearance of a broad band at ca 3420 cm^{-1} for ν(O-H) together with a weak band at ca 650 and 930 cm^{-1} attributable to wagging and rocking modes of coordinated water, respectively [43]. A sharp band at 1385 cm^{-1} assignable to $\nu NO_{(asy)}$ is typical of uncoordinated nitrate ion. Occurrence of a strong doublet band at 2049 and 2073 cm^{-1} alongwith a medium intensity band at ca 770 cm^{-1} in $NH_4[FeL(NCS)_2]$ attributed, respectively, to ν(C-N) and ν(N-C-S)

mode suggested the presence of nitrogen bonded terminal NCS^- group [44]. The peaks at 2344 and 2366 cm^{-1} in the complex $Na[FeL(N_3)_2]$ are attributable to the characteristics vibration of azido group.

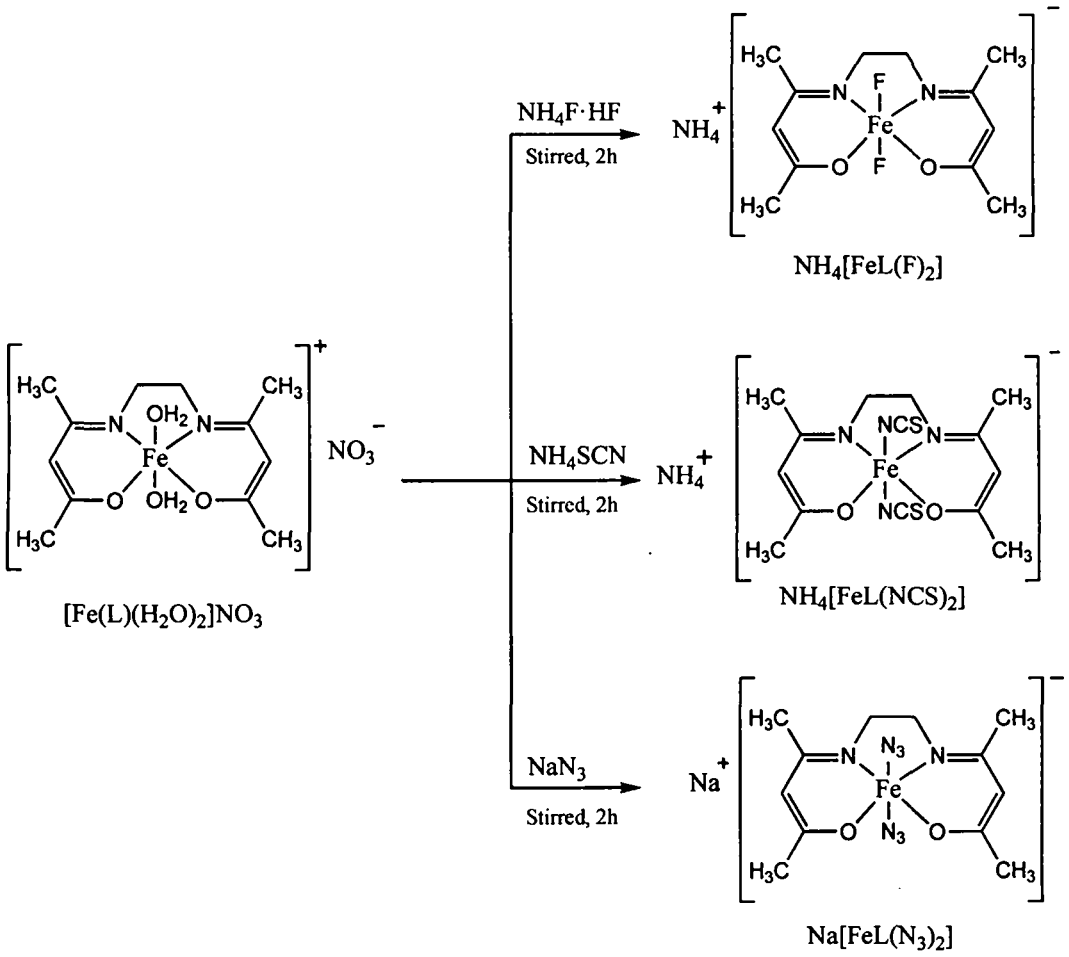

Scheme 3. Reactivity of the complex $[FeL(H_2O)_2]NO_3$

4.3. *Electronic spectra*

The UV–VIS spectra of complexes recorded in dichloromethane solution showed a very weak d–d band at ca 480 nm while for azido complexes the same appeared at ca 700 nm. An absorption band at ca 320 nm in aquo, fluoro or azido complexes is attributed to a ligand (p_π) → iron(III) (d_σ*) charge transfer transition [45,46].The higher energy bands in the region 250- 280 nm has been attributed to intraligand $\pi \rightarrow \pi$ * transitions [47].

4.4. *NMR spectra*

The ^{1}H NMR spectra of the ligand revealed a singlet at 10.89 ppm, for the enolic proton. The signals for methylene protons (-N-CH_2-CH_2-N-), olefinic proton (-CH=C<) and methyl protons (-CH_3) were located at 3.42, 2.17 and 1.91 ppm, respectively [48].

The ^{13}C NMR spectra showed resonances at six different positions concordant with six different type of carbon. The peak at 18.69 and 28.66 ppm is due to carbon atom of the magnetically nonequivalent methyl groups, while azomethine carbon showed resonances at 62.91 ppm. The peak at 43.49, 96.15 and 195.53 is attributable to carbon atom of the –CH_2, -CH= and =C-OH groups, respectively.

4.5. *Mass spectra*

The mass spectra of the compounds were recorded in FAB^+ ionization mode.The molecular ion peak of the ligand appeared at m/z 225$[M+H]^+$. The molecular formula $C_{12}H_{22}N_3O_7Fe$, $C_{12}H_{22}N_3O_2F_2Fe$, $C_{14}H_{22}N_5O_2S_2Fe$ and $C_{12}H_{18}N_8O_2FeNa$ suggested for the complexes were confirmed by their mass spectra. The peak observed at m/z 378 (ca 376), 334 (ca 334), 413 (ca 412) and 386 (ca 385), respectively corresponds to molecular mass of the complexes. The peak at m/z 360 and 340 observed for the $[FeL(H_2O)_2]NO_3$ complex is attributed to $[M-H_2O]^+$ and $[M-2H_2O]^+$ species arising from the loss of coordinated water molecules. Complexes $Na[FeL(N_3)_2]$ and $NH_4[FeL(NCS)_2]$ showed peak corresponding to the complex anionic species at m/z 364 (ca 362) and 393 (ca 394), respectively.

4.6. *Magnetic susceptibility*

The magnetic moment values of the complexes $[FeL(H_2O)_2]NO_3$, $NH_4[FeLF_2]$, $NH_4[FeL(NCS)_2]$ and $NH_4[FeL(N_3)_2]$ at room temperature were found to be 5.97,

6.54, 6.00 and 6.45 B.M., respectively, supporting high spin (d^5, S=6) octahedral geometry for the complexes A rather high value of magnetic moment is presumably due to orbital contributions [49].

4.7. *Molar conductance*

The molar conductances of the complexes $[FeL(H_2O)_2]NO_3$, $NH_4[FeLF_2]$, $NH_4[FeL(NCS)_2]$ and $NH_4[FeL(N_3)_2]$ in DMSO solution (ca 10^{-3} M) were 53.8, 47.2, 50.8 and 51.4 $\Omega^{-1}cm^2mol^{-1}$ suggesting 1:1 electrolytic nature of the complexes [50].

4.8. *Single crystal XRD*

Single crystal X-ray diffraction study of the ligand showed the existence of intramolecular O-H...N hydrogen bonds between the pair of atoms H_1-N_2 and H_2-N_1 (Figure 1). Crystal/refinement data: Empirical formula C_{12} H_{20} N_2 O_2, M = 224.30. Triclinic, P-1 (No. 2), a = 7.1158(5), b = 10.4490(8), c = 10.4810(8) Å, α = 62.589(5), β = 78.531(6), γ = 75.900(6) ^{0} V = 667.55(9) $Å^3$. D_c (Z = 2) = 1.116g cm^{-3}. μ_{Mo} = 0.076 mm^{-1}; specimen: 0.06 x 0.60 x 0.80 mm; 'θ' Min-Max = 2.2 - 27.5 ^{0}; $N_{(total)}$ = 9466 , $N_{(unique)}$ = 3057 (R_{int} = 0.091), N_o ($I > 2\sigma(I)$) = 1079 ; R_1 = 0.0842, wR2 = 0.2622. S = 0.94.

4.9. *DFT study*

As efforts to obtain single crystal of the complexes failed, quantum chemical DFT calculations were performed using B3LYP/6-31G(d,p) functional implemented in commercially available Gaussian 03 program suite [51] without imposing symmetry constraints. The optimized structure of the complexes are presented in Figure 2 and significant structural data are summerised in Table 1. The geometry around the metal center is slightly distorted octahedral with aquo, fluoro, thiocyanato or azido groups along the axial direction. Intramolecular hydrogen bonding between the pair of atoms O1-H19 and O2-H21 are seen in the optimized structure of $[Fe(L)(H_2O)_2]NO_3$

complex. The data showed that Fe-N (azomethine) bond length is nearly same in all the complexes while Fe-O bond length significantly differs. The largest Fe-O bond distance was noticed when the axial positions were occupied by the highest electronegative fluoride and the smallest when the axial positions were occupied by the labile water molecules. When bond angles of different complexes are compared it was seen that (N1-Fe1-N2) angle differs negligibly while a large variation in (O1-Fe1-O2), (N1-Fe1-O1) and (N2-Fe1-O2) bond angles was noticed. The harmonic vibrational frequencies of the complexes were also computed theoretically by DFT methods (Table 2) using 0.9664 as scaling factor [52] and the results are compared with the experimental ones. It was observed that the empirically scaled harmonic vibrational frequencies are in fairly good agreement with the experimental ones. Little deviations from the observed values are due to neglect of anharmonicity in B3LYP method [53,54]. It is to be mentioned here that the average error for frequencies calculated with B3LYP functional was reported to be of the order of 40-50 cm^{-1}[55].

4.10. ***Electrochemical behaviour***

The electrochemical behaviour of the compounds were studied by cyclic voltametry at room temperature in dichloromethane solution of *ca* 10^{-3} M concentration containing 0.1 M tetrabutyl ammonium perchlorate as supporting electrolyte in the potential range -1.0 to 1.0 V versus SCE electrode at a scan rate of 100 mV s^{-1}. The redox potential of the compounds are given in Table 3 and a representative voltammogram is presented in Figure 3. The complexes displayed a quasireversible one electron wave with $\Delta E > 100$ mV, assignable to Fe(III)/Fe(II) redox couple. The half wave potential, $E_{½}$ obtained for the complexes are negative and small indicating ready redox susceptibility of the compounds. These feature render the complexes as valuable catalyst for redox reactions [56]. The free ligand did not show any responses in the

potential range of -1.0 to 1.0 V under similar experimental condition, implying their redox innocent character.

5. Conclusion

Aquated iron(III)-Schiff base complex, $[FeL(H_2O)_2]NO_3$ was prepared by the reaction of H_2L and $Fe(NO_3)_3.9H_2O$ in 1 : 1 molar ratio. The reaction of the complex with ammonium bifluoride, ammonium thiocyanate or sodium azide in 1:2 molar ratio afforded hitherto unreported mixed-ligand complexes of the type $A^+[FeL(X)_2]^-$ ($A=NH_4$; X=F, NCS and A=Na; $X=N_3$) . The crystal structure of the ligand indicated the existence of intramolecular hydrogen bonding in its enolic form. The distorted octahedral structures of the complexes were conjectured from analytical and spectral data. The B3LYP/6-31G(d,p) DFT study also showed the geometry around iron(III) center to be octahedral with two axially oriented aquo, fluoro, thiocyanato or azido group in trans configuration. The thermochemical parameter and harmonic vibrational frequencies of the complexes computed by DFT method using B3LYP/6-31G(d,p) functional matches well with the experimental. All the complexes showed quasireversible redox behaviour with small and negative $E_{1/2}$ values suggesting their potential as catalyst in redox reactions. The synthetic strategy may serve as a paradigm for accessing newer mixed ligand Schiff base complexes. The complexes reported herein may be used as stabilizing agents for synthesis of metal nano particles.

Acknowledgement

The authors express sincere thanks to SAIF, NEHU, Shillong and SAIF, CDRI, Lucknow, India for providing analytical and spectral results.

Supplementary materials

Crytallographic data for the structural analysis of the ligand have been deposited with the Cambridge Crystallographic Data Centre, CCDC No. 262373 A copy of this

information may be obtained free of charge from The Director, CCDC, 12 Union Road, Cambridge, CB2 1EZ, UK (fax: +44 1223 336 033; e-mail: deposit@ccdc.cam.ac.uk or www: http://www.ccdc.ac.uk).

References

[1] V.K. Subramanian, M. Ganesan, S. Rajagopal, R. Ramaraj. *J. Org. Chem.*, **67**, 1506 (2002).

[2] H. Fujii, T. Kurahashi, T. Ogura. *J. Inorg. Biochem.*, **96**, 133 (2003).

[3] R.B. Bedfort, D.W. Bruce, R.M. Frost, J.W. Goodby, M. Hird. *Chem. Commun.*, 2822 (2004).

[4] K.P. Bryliakov, E.P. Talsi. *Angew. Chem. Int. Edit.*, **43**, 5288 (2004).

[5] T. Katsuki. *Chem. Soc. Rev.*, **33**, 437 (2004).

[6] M.M. Bhadbhade, D. Srinivas. *Polyhedron* , **17**, 2669 (1998).

[7] S. Hayami, K. Inoue, Y. Maeda. *Mol. Cryst. Liq. Cryst.*, **334**, 1285 (1999).

[8] W. Chiang, D. Vanengan, M.E. Thompson. *Polyhedron*, **15**, 2369 (1996).

[9] C.T. Brewer, G. Brewer, G.B. Jameson, P. Kamaras, L. May, M. Rapta. *J. Chem. Soc. Dalton Trans.*, 37 (1995).

[10] H. Olmez, F. Arslan, H. Icbudak. *J. Therm. Anal. Cal.*, **76**, 793 (2004).

[11] D. Czakis-Sulikowska, J. Radwa_ska-Doczekalska, A. Czylkowska, J. Go_uchowska. *J. Therm. Anal. Cal.*, **78**, 501 (2004).

[12] R. Carballo, A. Casti_eiras, S. Balboa, B. Covelo, J. Niclós. *Polyhedron*, **21**, 2811 (2002).

[13] J.B. Vincent, T. Hui-Lún, A.B. Blackman, E.B. Lobkovsky, D.N. Hendrickson, G. Christoug. *J. Am. Chem. Soc.*, **115**, 2353 (1993).

[14] C. Kaes, A. Katz, M.W. Hosseini. *Chem. Rev.*, **100**, 3533 (2000).

[15] G. Psomas, C. Dendrinou-Samara, P. Philippakopoulos, V. Tangoulis, C.P. Raptopoulou, E. Samaras, D.P. Kessissoglou. *Inorg. Chim. Acta.*, **272**, 24 (1998).

[16] P. Losier, M.J. Zaworotka. *Angew. Chem. Int. Edit. Engl.*, **35**, 2779 (1996).

[17] R. Kruszynski, B. Kuznik, T.J. Bartczak, D. Czakis-Sulikowska. *J. Coord. Chem.*, **58**, 165 (2005).

[18] Jian-Min Li, Yu-Gen Zhang, Jing-Hua Chen, Lei Rui, Quan-Ming Wang, Xin-Tao Wu. **Polyhedron**, **19** 1117 (2000).

[19] J.H. Liao, S.H. Chehg, C.T. Su. *Inorg. Chim. Commun.*, **5**, 761 (2002).

[20] A. Saxena, J.K. Koacher, J.P. Tandon. *Inorg. Nucl. Chem. Lett.*, **17**, 229 (1981).

[21] P.G. *Cozzi. Chem. Soc. Rev.*, **33**, 410 (2004).

[22] S.K. Edulji, S.T. Nguyen., *Organometallics*, **22**, 3374 (2009)

[23] J.A. Miller, W. Jin, S.T. Nguyen. *Angew. Chem. Int. Edit.*, **41**, 2953 (2002).

[24] C. Celic, M. Tumer, S. Serin. *Synth. React. Inorg. Met-Org. Chem.* **32**, 1839 (2002).

[25] M.T. Kaczmarck, I. Pospieszna-Markiewick, W. Radecka-Paryzek, *J. Incl. Phenom. Macro. Chem.*, **49**, 115 (2004).

[26] S. Ilhan, H. Temel, A. Kilic, E. Tas. *J. Cord. Chem.*, **61**, 1443 (2008).

[27] S. Chandra, R. Kumar. *Synth. React. Inorg. Met-Org. Chem.* **35**, 161 (2005).

[28] S. Ilhan, H. Temel, I. Yilmaz, A. Kilic. *Trans. Met. Chem.*, **32**, 344 (2007).

[29] S.K. Gupta, P.B. Hitchcock, Y.S. Kushwah. *J. Coord. Chem.*, **55**, 1401, (2002).

[30] C. Che, J. Huang. *Coord. Chem. Rev.*, **247**, 97 (2003).

[31] F. Marchetti, C. Pettinary, R. Pettinary, A. Cingolari, D. Leonesi, A. Lorenzotti. *Polyhrdron.*, **18**, 3041 (1999).

[32] M. Bagherzadeh, M. Amini. *Inorg. Chem. Commun.*, **12**, 21 (2009).[

[33] K. Shanker, P.M. Reddy, R. Rohini, Y. Ho, V.Ravinder. *J. Coord. Chem.*, **62**, 2388 (2009).

[34] A.A. Nejo, G.A. Kolawole, A.R. Opoku, C. Muller, J. Wolowska. *J. Coord. Chem.*, **62**, 3411 (2009).

[35] Y. Nishida, S. Oshio, S. Kida. Chem. Lett. 79, (1975).

[36] Y. Nishida, S. Oshio, S. Kida. Bull. Chem. Soc. Jpn. 50, 119 (1975).

[37] G.A. kolawole, A.A. Osowok. *J. coord. Chem.*, **62**, 1437 (2009).

[38] K.C. Gupta, H.K. Abdulkadir, S. Chad. *J. App. Pol. Sc.*, **90**, 1398 (2003).

[39] C.R. Mayer, G. Cucchiaro, J. Jullien, F. Dumur, J. Marrot, E. Dumas, F. Secheresse. *Eur. J. Inorg. Chem.*, 3614 (2008).

[40] G. Hu, Z. Feng, J. Li, G. Jia, D. Han, Z. Liu, C. Li. *J. Phy. Chem.*, **111**, 11267 (2007).

[41] B. Chiswell, J.P. Crawford, E.J. O'reilly. *Inorg. Chim. Acta.*, **49**, 223 (1980).

[42] N. Nawar, N.M. Hosny. *Trans. Met. Chem.*, **25**, 1 (2000).

[43] N. Raman, S. Ravichandran, C. Thangaraja. *J. Chem. Sci,*. **116**, 215 (2004).

[44] M.X. Li, G.Y. Xie, Y.D. Gu, J. Chen, P.J. Zheng. *Polyhedron*, **14**, 1235 (1995).

[45] M.S. Shongwe, B.A. Al-Rashdi, H. Adams, M.J. Morris, M. Mikuriya, G.R. Hearne. *Inorg. Chem.*, **46**, 9558 (2007).

[46] M.I. Davis, A.M. Orville, F. Neese, J.M. Zaleski, J.D. Lipscomb, E.I.J. Solomon, *J. Am. Chem. Soc.*, **124**, 602 (2002).

[47] S.N. Rao, K.N. Munshi, N.N. Rao, M.M. Bhadbhade, E. Suresh. *Polyhedron*, **18**, 2491 (1999).

[48] G. Prabusankar, G. Ashok, N. Sengottuvelan, D. Saravanakumar, V. Narayanan, M. Kandaswamy. *Indian J. Chem. Tech.*, **9**, 9 (2002).

[49] A. Bajpai, S. Rai. *J. App. Pol. Sc.*, **69**, 751 (1998).

[50] W.J. Geary. *Coord. Chem. Rev.*, 7, 81 (1971).

[51] M.J. Frisch, G.W. Trucks, H.B. Schlegel, G.E. Scuseria, M.A. Robb, J.R. Cheeseman, J.A. Montgomery Jr, T. Vreven, K.N. Kudin, J.C. Burant, J.M. Millam, S.S. Iyengar, J. Tomasi, V. Barone, B. Mennucci, M. Cossi, G. Scalmani, N. Rega, G.A. Petersson, H. Nakatsuji, M. Hada, M. Ehara, K. Toyota, R. Fukuda, J. Hasegawa, M. Ishida, T. Nakajima, Y. Honda, O. Kitao, H. Nakai, M. Klene, X. Li, J.E. Knox, H.P. Hratchian, J.B. Cross, C. Adamo, J. Jaramillo, R. Gomperts, R.E. Stratmann, O. Yazyev, A.J. Austin, R. Cammi, C. Pomelli, J.W. Ochterski, P.Y. Ayala, K. Morokuma, G.A. Voth, P. Salvador, J.J. Dannenberg, V.G. Zakrzewski, S. Dapprich, A.D. Daniels, M.C. Strain, O. Farkas, D.K. Malick, A.D. Rabuck, K. Raghavachari, J.B. Foresman, J.V. Ortiz, Q. CuiA, G. Baboul, S. Clifford, J. Cioslowski, B.B. Stefanov, G. Liu, A. Liashenko, P. Piskorz, I. Komaromi, R.L. Martin, D.J. Fox, T. Keith, M.A. Al-Laham, C.Y. Peng, A. Nanayakkara, M. Challacombe, P.M.W. Gill, B. Johnson, W. Chen, M.W. Wong, C. Gonzalez, J.A. Pople, Gaussian 03, Revision D.01; Gaussian: Wallingford, CT, 2004.

[52] C.J. Cramer. *Essentials of Comput. Chem.*, John Wiley and Sons, West Sussex, England (2004).

[53] N. Sundaraganesan, B.W. Joshua, C. Meghanathan, S. Sebastian. *Ind. J. Chem.*, **47**, 821 (2008).

[54] D. Kalita, R.C. Deka, N.S. Islam. *Inorg. Chem. Commun.*, **10**, 45 (2007).

[55] I. Bytheway, M.W. Wong. *Chem. Phys. Lett.*, **282**, 219 (1998).

[56] F.R. Perez, L. Basaez, J. Belmar, P. Vanysek. *J. Chil. Chem. Soc.*, **50** 575 (2005).

Table 1. DFT [B3LYP/6-31G(d,p)] optimized significant structural data of the complexes.

Parameters	$[Fe(L)(H_2O)_2]^+$	$[Fe(L)(F)_2]^-$	$[Fe(L)(NCS)_2]^-$	$[Fe(L)(N_3)_2]$
bond distance in angstrom and bond angles in degrees				
r(Fe1–N1)	1.931	1.940	1.937	1.943
r(Fe1–N2)	1.931	1.940	1.937	1.943
r(Fe1–O1)	1.893	1.943	1.925	1.927
r(Fe1–O2)	1.893	1.943	1.925	1.928
r(Fe1–O3)	1.988	-	-	-
r(Fe1–O4)	1.988	-	-	-
r(Fe1–F1)	-	1.843	-	-
r(Fe1–F2)	-	1.844	-	-
r(Fe1–N3)	-	-	1.941	1.985
r(Fe1–N4)	-	-	1.941	1.985
a(N1-Fe1-N2)	85.6	86.1	85.8	85.9
a(O1-Fe1-O2)	90.8	86.5	86.7	86.3
a(N1-Fe1-O1)	92.3	93.7	93.7	93.9
a(N2-Fe1-O2)	92.3	93.7	93.8	94.0
Thermochemical properties				
Dipole moment (Debye)	2.0482	5.3973	4.6815	8.1044
Ionozation potential ($kJmol^{-1}$)	1023.3	291.9	381.7	327.1
Electron affinity ($kJmol^{-1}$)	-390.2	414.8	180.6	277.7

Table 2. B3LYP optimized (experimental) selected harmonic vibrational frequencies in cm^{-1}.

Assignment	$[Fe(L)(H_2O)_2]^+$	$[Fe(L)(F)_2]^-$	$[Fe(L)(NCS)_2]^-$	$[Fe(L)(N_3)_2]^-$
ν Fe-O	440 (435)	431 (431)	474 (435)	434 (438)
ν Fe-N	475 (453)	456 (484)	489 (483)	466 (486)
ν Fe-N (NCS)	-	-	416 (414)	-
ν Fe-N (N_3)	-	-	-	419 (425)
ν Fe-F	-	624 (652)	-	-
ν C-O	1281 (1274)	1503 (1508)	1484 (1420)	1292 (1260)
ν C=N	1569 (1573)	1631 (1627)	1625 (1569)	1631 (1624)
ν C-S	-	-	774 (771)	-
ν C-N	-		2077 (2073) 2086 (2049)	-
ν N-N-N	-	-	-	2346 (2344) 2360 (2366)

Table 3. Electrochemical data of the complexes

Compound	E_p^a (V)	E_p^c (V)	ΔE (V)	$E_{1/2}$ (V)
$[Fe(L)(H_2O)_2]NO_3$	-0.448	-0.854	0.406	-0.651
$NH_4[Fe(L)F_2]$	-0.253	-0.648	0.395	-0.450
$NH_4[Fe(L)(NCS)_2]$	-0.152	-0.553	0.399	-0.351
$Na[Fe(L)(N_3)_2]$	-0.433	-0.570	0.137	-0.501

Figure captions

Figure 1. XRD structure of the ligand H_2L.

Figure 2(a). DFT [B3LYP/6-31G(d,p)] optimized structure of $[FeL(H_2O)_2]^+$

Figure 2(b). DFT [B3LYP/6-31G(d,p)] optimized structure of $[FeLF_2]^-$

Figure 2(c). DFT [B3LYP/6-31G(d,p)] optimized structure of $[FeL(NCS)_2]^-$

Figure 2(d). DFT [B3LYP/6-31G(d,p)] optimized structure of $[FeL(N_3)_2]^-$

Figure 3. Cyclic voltammogram of the complex $NH_4[FeLF_2]$

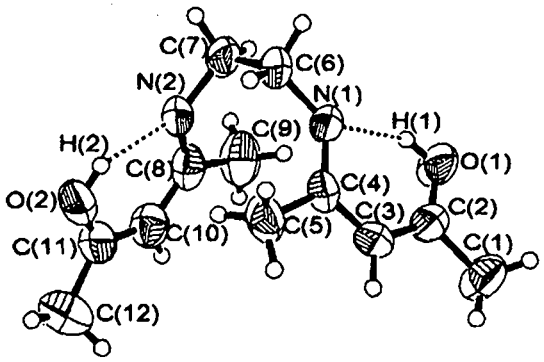

Figure 1

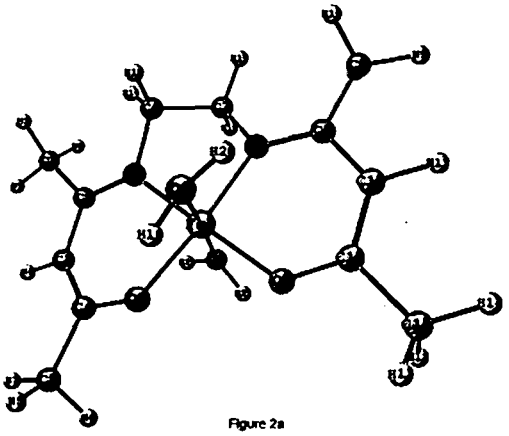

Figure 2a

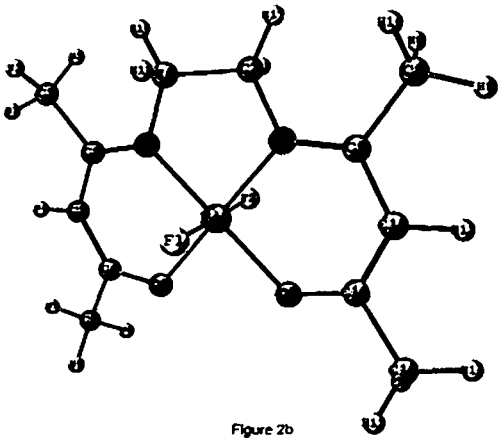

Figure 2b

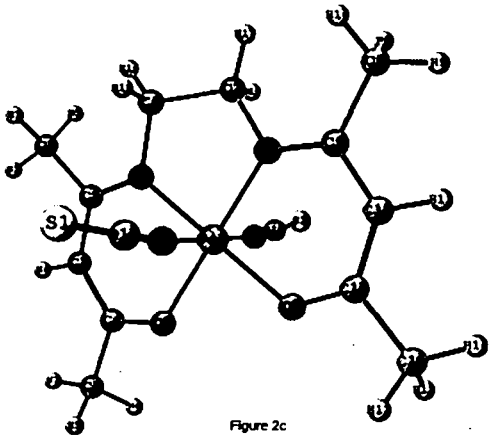

Figure 2c

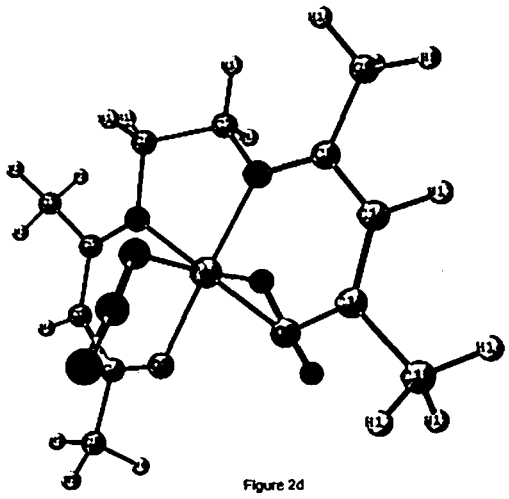

Figure 2d

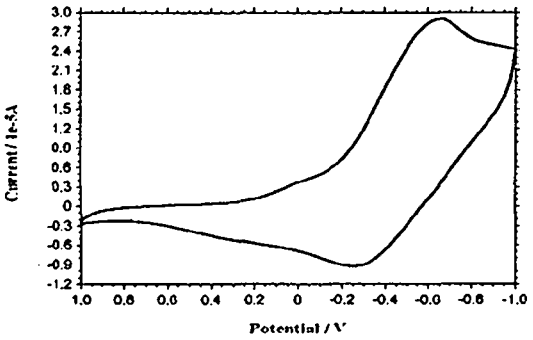

Figure 3